(2)

AFAPL-TR-77-63

AIRCRAFT HYDRAULIC SYSTEMS DYNAMIC ANALYSIS

MCDONNELL AIRCRAFT COMPANY
MCDONNELL DOUGLAS CORPORATION
ST. LOUIS, MISSOURI 63166

OCTOBER 1977

TECHNICAL REPORT AFAPL-TR-77-63
Final Report– March 1974 - February 1977

AIR FORCE AERO PROPULSION LABORATORY
AIR FORCE SYSTEMS COMMAND
WRIGHT-PATTERSON AIR FORCE BASE, OHIO 45433

NOTICE

When Government drawings, specifications, or other data are used for any purpose other than in connection with a definitely related Government procurement operation, the United States Government thereby incurs no responsibility nor any obligation whatsoever; and the fact that the government may have formulated, furnished, or in any way supplied the said drawings, specifications, or other data, is not to be regarded by implication or otherwise as in any manner licensing the holder or any other person or corporation, or conveying any rights or permission to manufacture, use, or sell any patented invention that may in any way be related thereto.

This report has been reviewed by the Information Office (OI) and is releasable to the National Technical Information Service (NTIS). At NTIS, it will be available to the general public, including foreign nations.

This technical report has been reviewed and is approved for publication.

Paul D. Lindquist
Project Engineer

Kenneth E. Burns
Acting Technical Area Manager

FOR THE COMMANDER

Stephen P. Condon

STEPHEN P. CONDON, Major, USAF
Chief, Vehicle Power Branch

"If your address has changed, if you wish to be removed from our mailing list, or if the addressee is no longer employed by your organization please notify AFAPL/POP, W-PAFB, OH 45433 to help us maintain a current mailing list".

Copies of this report should not be returned unless return is required by security considerations, contractual obligations, or notice on a specific document.

UNCLASSIFIED

SECURITY CLASSIFICATION OF THIS PAGE *(When Data Entered)*

REPORT DOCUMENTATION PAGE

READ INSTRUCTIONS BEFORE COMPLETING FORM

1. REPORT NUMBER: AFAPL-TR-77-63	2. GOVT ACCESSION NO.
3. RECIPIENT'S CATALOG NUMBER	
4. TITLE (and Subtitle): AIRCRAFT HYDRAULIC SYSTEMS DYNAMIC ANALYSIS. FINAL REPORT	5. TYPE OF REPORT & PERIOD COVERED: Final Report. Mar 74 - Feb 77,
6. PERFORMING ORG. REPORT NUMBER: 18	
7. AUTHOR(s): G. E. Amies, J. B. Greene, R. J. Levek, N. J. Pierce	8. CONTRACT OR GRANT NUMBER(s): F33615-74-C-2016
9. PERFORMING ORGANIZATION NAME AND ADDRESS: McDonnell Douglas Corporation, P O Box 516, St. Louis, Missouri 63166	10. PROGRAM ELEMENT, PROJECT, TASK AREA & WORK UNIT NUMBERS: 3145-30-18 17 39
11. CONTROLLING OFFICE NAME AND ADDRESS: Air Force Aero Propulsion Laboratory, Air Force Systems Command, Wright-Patterson Air Force Base, Ohio 45433	12. REPORT DATE: Oct 77
	13. NUMBER OF PAGES: 461 12 464 p.
14. MONITORING AGENCY NAME & ADDRESS *(if different from Controlling Office)*	15. SECURITY CLASS. *(of this report)*: Unclassified
	15a. DECLASSIFICATION/DOWNGRADING SCHEDULE

16. DISTRIBUTION STATEMENT *(of this Report)*

Approved for public release, distribution unlimited.

DDC RECEIVED MAR 8 1978 B

17. DISTRIBUTION STATEMENT *(of the abstract entered in Block 20, if different from Report)*

18. SUPPLEMENTARY NOTES

19. KEY WORDS *(Continue on reverse side if necessary and identify by block number)*

Hydraulic System	Transient Thermal Response
Transient Response	Final Report
Frequency Response	Computer Program Verification
Steady State	Test Results

20. ABSTRACT *(Continue on reverse side if necessary and identify by block number)*

This report describes the development and verification of four computer programs used to simulate hydraulic systems under dynamic conditions. The programs were developed by McDonnell Douglas Corp. under contract with the Air Force. The Hydraulic Systems Frequency Response (HSFR) program predicts the ripple in the flow from piston-type pumps and shows how it is transmitted and attenuated through the system. It predicts the resonant frequencies and the locations and amplitudes of the standing waves of the oscillatory flow

DD FORM 1 JAN 73 1473 EDITION OF 1 NOV 65 IS OBSOLETE

UNCLASSIFIED

SECURITY CLASSIFICATION OF THIS PAGE *(When Data Entered)*

403 111

20. ABSTRACT

and pressure. The Steady-State Flow Analysis (SSFAN) program defines the system flow and pressure distribution resulting from the simultaneous operation of actuator devices under any combinations of loads and rates. The Hydraulic Transient Analysis (HYTRAN) program simulates the dynamic response of a system to sudden changes in load flow demand. The typical input to the system is a valve motion from which pressure and flow disturbances propagate through the system, causing pump and component responses. The Hydraulic Transient Thermal Analysis (HYTTHA) program predicts the effects of system heat generation and dissipation of the temperatures and performance of a hydraulic system.

The Air Force has made the programs available to all prospective users and has rendered technical assistance. User manuals and programs were first made available to industry in September 1974, and updated versions were disseminated at the final oral presentation in February 1977.

PREFACE

This final report was prepared by the McDonnell Aircraft Company, Design Engineering Power and Fluid Subsystem Department, McDonnell Douglas Corporation under contract F33615-74-C-2016.

The effort was sponsored by the Air Force Aero Propulsion Laboratory, Air Force Systems Command, Wright-Patterson AFB, Ohio under Project No. 3145-30-18 with AFAPL/POP/, and was under the direction of Paul Lindquist and William Kinzig.

The final report covers work conducted from 7 March 1974 through 18 February 1977. At McDonnell, Neil Pierce directed the program and Gerry Amies was the principal investigator. Special acknowledgement is also given to J. B. Greene , R. J. Levek, D. A. Struessel, and R. E. Young.

ABSTRACT

This report describes the development and verification of four computer programs used to simulate hydraulic systems under dynamic conditions. The programs were developed by McDonnell Douglas Corp. under contract with the Air Force. The Hydraulic Systems Frequency Response (HSFR) program predicts the ripple in the flow from piston-type pumps and shows how it is transmitted and attenuated through the system. It predicts the resonant frequencies and the locations and amplitudes of the standing waves of the oscillatory flow and pressure. The Steady-State Flow Analysis (SSFAN) program defines the system flow and pressure distribution resulting from the simultaneous operation of actuator devices under any combinations of loads and rates. The Hydraulic Transient Analysis (HYTRAN) program simulates the dynamic response of a system to sudden changes in load flow demand. The typical input to the system is a valve motion from which pressure and flow disturbances propagate through the system, causing pump and component responses. The Hydraulic Transient Thermal Analysis (HYTTHA) program predicts the effects of system heat generation and dissipation of the temperatures and performance of a hydraulic system.

The Air Force has made the programs available to all prospective users and has rendered technical assistance. User manuals and programs were first made available to industry in September 1974, and updated versions were disseminated at the final oral presentation in February 1977.

TABLE OF CONTENTS

LIST OF ILLUSTRATIONS

LIST OF ILLUSTRATIONS (Continued)

LIST OF ILLUSTRATIONS (Continued)

LIST OF ILLUSTRATIONS (Continued)

LIST OF ILLUSTRATIONS (Continued)

LIST OF ILLUSTRATIONS (Continued)

LIST OF ILLUSTRATIONS (Continued)

LIST OF ILLUSTRATIONS (Continued)

LIST OF ILLUSTRATIONS (Continued)

LIST OF ILLUSTRATIONS (Continued)

LIST OF TABLES

SECTION I
INTRODUCTION

This report describes the work performed under the Aircraft Hydraulic System Performance Analysis contract.

The task was to develop and verify computer programs to simulate aircraft hydraulic systems. Four digital computer programs were developed.

The Hydraulic System Frequency Response (HSFR) predicts how oscillatory flows and pressures caused by the acoustical energy content of a pump output are transmitted through the lines and components of a hydraulic system.

The program predicts the pump speeds at which major resonances occur, and defines the amplitude and location of the oscillatory pressure and flow standing waves. The description of the system being simulated is easily changed to investigate various practical system modifications for the attenuation and/or relocation of the major resonant conditions. This capability allows potential problems related to hydraulic acoustic energy to be eliminated during the design stage.

The user describes the system to be simulated by means of punched data cards. The description includes the type and physical characteristics of each of the elements of the circuit. An element may be a pump, a section of line, a fitting, a component, or a branch.

The user completes the problem statement by specifying the range of pump speed and the harmonic of interest, the locations at which flow, pressure, impedance, and/or energy levels are to be plotted, the fluid type, the fluid temperature, and the steady state pump output pressure.

The program calculates the oscillatory pressures and flows at the input to system elements. Standing wave characteristics produce large variations in pressure amplitude along the length of a line. Division of a length of line into small elements may be required to allow this standing wave pattern to be examined to ensure that an excessive pressure amplitude is not being ignored.

Acoustic analysis can be performed on the pressure side or on both the pressure and return sides of a system.

The Hydraulic Transient Analysis (HYTRAN) predicts the dynamic response of a system to sudden changes in load flow demands. The input to the system is normally a servo valve or solenoid valve motion from which pressure and flow disturbances propagate through the system, causing pump and component responses.

The program simulates the complete system and calculates the value of all the flows, pressures and state variables, throughout the system.

HYTRAN is composed of five basic parts, input, steady state calculation, line simulation, component simulation, and output.

The designer inputs data describing the lines, components and system configuration.

The steady state section of the program balances the pressures and flows in the system and calculates the initial values for all the system state variables. Once the initial values are established at zero time, the program starts by calculating for a small change in time (delta T), new flows and pressures in the lines.

Once the new pressures and flows have been established for the lines the program calculates new values for the state variables of all the components, and the flows and pressures at the junctions between the components and the lines.

The program continues to march forward in time (delta T) intervals, first calculating the line and then the component variables.

The output part of the program selects the variables that are required as output of output plots, at specified time steps. When the program calculations are completed, the output is then printed and plotted.

The output is essentially a time history of selected system variables which have been disturbed by the controlling input.

Since the program actually advances in discrete time steps, it can be integrated into other simulations.

The Steady State Flow Analysis (SSFAN) Program predicts the steady state flows and pressures in a closed loop aircraft hydraulic system.

It uses a building block approach so that new elements or components can be added with minimum change to the rest of the program. A matrix method is used to compute the steady state flows throughout the system line network.

The program corrects viscosities for pressure, determines whether flow is laminar, transitive or turbulent to apply appropriate resistance factors; and corrects reservoir pressure for altitude.

Some of the outputs of SSFAN can be predicted values of flow rate, surface rate, pressure drop, pressure, or subsystem operating time. The program can also be used to predict steady-state motor speeds and actuator rates under varying load conditions.

The Hydraulic Transient Thermal Analysis (HYTTHA) Program predicts the effects of system heat generation and dissipation of the temperature and performance of an aircraft hydraulic system.

The program can simulate complete closed loop systems. It calculates flows, pressures, state variables, component temperatures, fluid temperatures, and line wall temperatures throughout the system.

The program is composed of four basic parts; input, steady state calculations, thermal line and component calculations, and output.

The designer inputs data describing the lines, ambient thermal conditions components, and system configuration.

The steady state part of the program balances the pressures and flows in the system, and calculates for all the system state variables. Once the initial values are established at zero time, the program calculates new temperatures throughout the system for a small change in time (DELT).

The program continues the calculations at DELT intervals, first calculating the system flows pressures and state variables and then calculating the line and component temperatures.

SECTION II

TEST METHODS

Test conditions for transient and frequency response tests were altered as testing progressed to minimize testing of components which showed no significant dynamic effects. For components which showed significant dynamic effects (pump, check valve, etc.) test conditions were expanded to further investigate these effects.

Standard test temperature range was 70°F to 210°F, which was attainable on the component test bench set-up without requiring elaborate temperature conditioning equipment.

Testing was accomplished with both MIL-H-5606B and MIL-H-83282 hydraulic fluids. The range of flows investigated was from zero to 157 CIS. The dissolved air content of the fluid in the test bench for all the data runs was less than 1% by volume. Test conditions that deviated from the above are noted.

Each test run was assigned a unique number. The run number definition is explained in Figure 1.

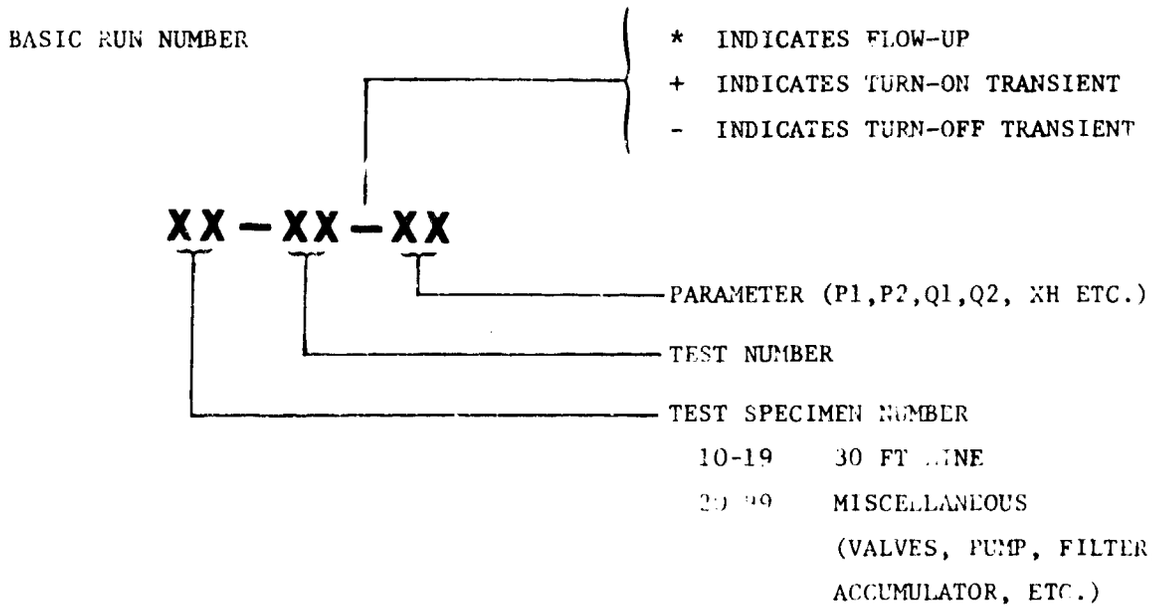

FIGURE 1 - TEST RUN NUMBER DEFINITION

1. FREQUENCY RESPONSE TESTS

Frequency response tests were required for verifying the frequency domain (HSFR) pump model, and model/system interaction. Test conditions established the pump frequency characteristics with steady state flows from laminar to turbulent conditions. The effects of temperature were investigated. For each test condition, amplitude and phase data of the pump inlet and outlet pressures and flows were recorded, and harmonic analysis was performed at system resonance points. Time domain data was also recorded at several speeds for pump internal and boundary parameters.

2. TRANSIENT TESTS

a. Test Benches and Conditions - The time domain component standard test series determined the effects of the test specimen on system transient response.

The test specimen inlet pressure range depended on whether it was tested as a pressure side or return side component. Hyd aulic power for the transient test was provided by the pump via an F-15 JFS accumulator. Transient flow demands were generated by opening and closing a fast response control valve, with data recorded during both portions of the cycle.

Data was required for transient flow changes to and from two peak flow levels at each of two temperature levels, one peak flow value in the laminar flow range, and one in the turbulent flow range.

Peak steady-state flow and test specimen inlet pressure were preset before the transient test using the pressure or return load valve with the transient control valve open and the flow control servovalve at full signal. This recharged the JFS accumulator prior to each transient discharge.

Transient pressure and flow on both sides of the specimen were recorded during the opening and closing transients. Temperatures were stabilized and recorded during the flow calibration.

Some of the component tests dictated that configuration changes be made to the basic test bench. These components included the F-15 instrumented pump, two stage relief valve, and two pump tests. These changes are explained with the discussion of the data.

Tests were run to study cavitation waves downstream of a fast closing valve. The effects of different valve closing rates and temperatures were monitored at different system air contents.

The effects of varying system pressure from 1500 to 3750 psi were tested to verify the computer program for that range of pressures.

The F-15 iron bird's utility speedbrake system was tested to verify a simple system with the HYTRAN computer program.

b. Test Problems

(1) Fast Control Valve - A good deal of effort was required to develop a fast operating control valve that would provide the transients for the test system. Desired valve closing time was about 2 milliseconds from a maximum flow rate of 40 GPM. Solenoid valves were ruled out as being to slow and not providing a sharp cutoff characteristic. Commercial solenoid operated poppet valves could handle the desired flow rates, but the closing times were too slow. It was felt that with a few changes, a commercial poppet valve could produce the required operating times.

A Victor SV 41S-9021 solenoid operated poppet valve was chosen for modification. The standard valve incorporates a balanced poppet design which accounts for its high flow ability at high pressure. The poppet was directly actuated by the solenoid. In the modified version of the valve the solenoid was removed and the poppet displaced by a spring and push rod arrangement.

A servovalve driven piston was connected to the opposite side of the spool as shown in Figure 2.

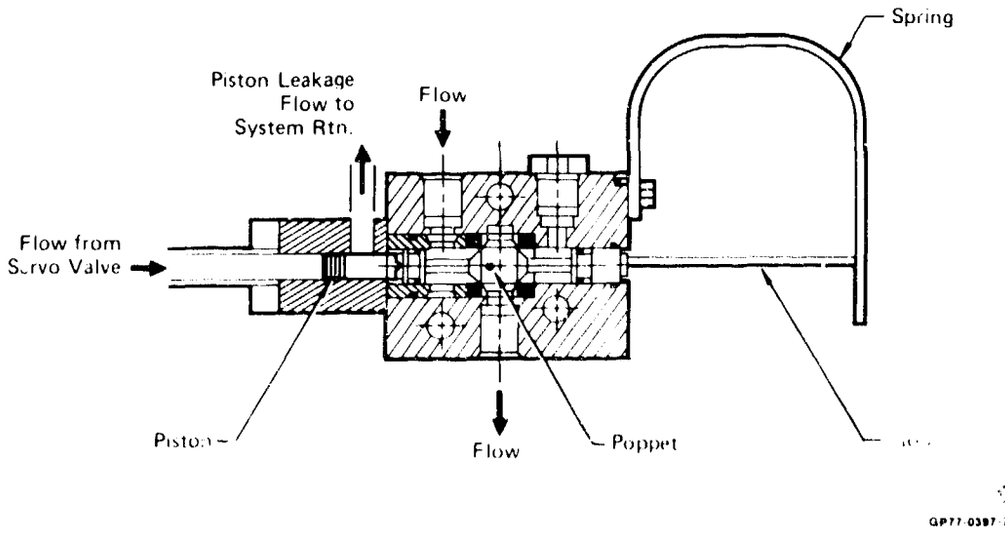

FIGURE 2. MODIFIED VICTOR SOLENOID VALVE
(SHOWN IN PRESSURE OPENED SPRING CLOSED CONFIGURATION)

Much time and effort was spent perfecting the valve operation. Even after this was accomplished, many problems with the valve plagued the verification test efforts. These problems included poppet bounce on closing, premature closing due to poppet flow forces, and lack of adequate poppet rate control.

(2) Mechanical Vibration - Trouble was encountered from reflections in the system when using a long line test configuration (see Figure 3). For example, small amplitude high frequencies can be seen on P_3 in Figure 4. These reflections were determined timewise to have occurred at the 180° bends. The reflected wave from the fast closing valve travelled down the surface of the tube faster than in the fluid because of the differences between the velocity of sound in the two mediums.

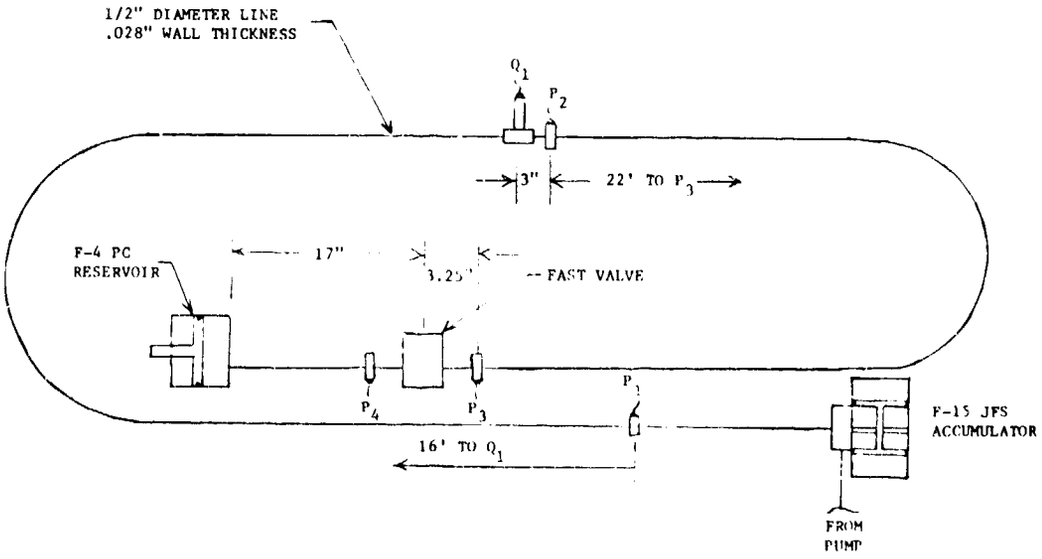

FIGURE 3. LONG LINE TEST CONFIGURATION

The lines were then clamped at approximately 18" intervals to simulate the amount of mechanical damping that actually occurs in an aircraft hydraulic system. P_3 in Figure 5 shows that the effect of clamping greatly reduces the mechanical vibration and the excessive reflections when compared with P_3, Figure 4. Since it was desired that an adequate line model be verified, it was necessary to eliminate as much of the mechanical movement as possible to ride the system of these internal reflections. Thus the line system was further weighted and clamped down.

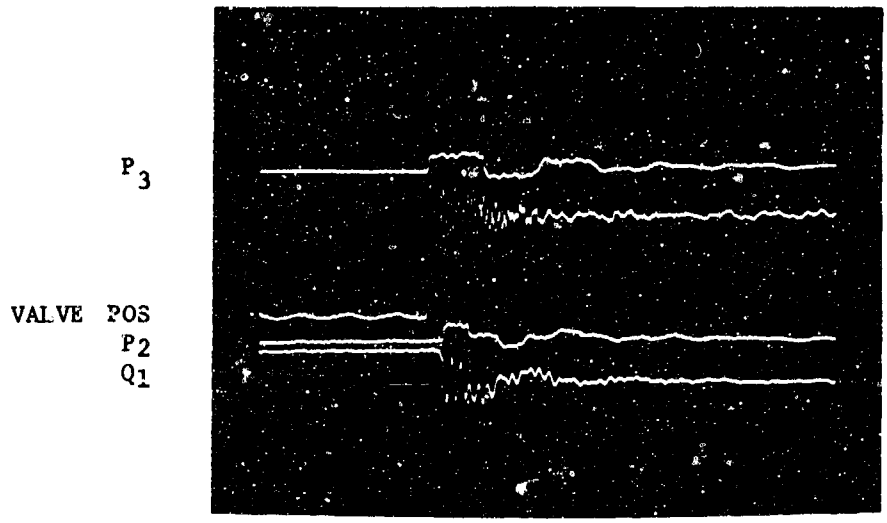

Flow Rate: 19.25 CIS
Temperature: 125°
Time Scale: 20 msec/cm
Date: 16 May 1975
Condition: Turn-off Transient

FIGURE 4. UNDAMPED LINE MECHANICAL VIBRATIONS

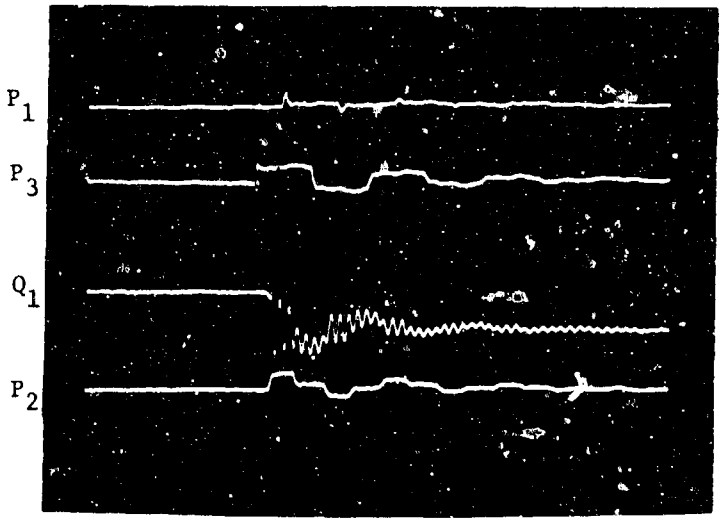

Flow: 17.25 CIS
Temp: 125°F
Time Scale: 20 msec/cm
Date: 23 May 1975
Flow Condition: Turn-off Transient

FIGURE 5. DAMPED LINE MECHANICAL VIBRATIONS

The differences in P_2 and P_3 pressure traces for the clamped and unclamped lines are shown in Figures 6 and 7, respectively, for the 1/2" diameter tube with a turn-on transient.

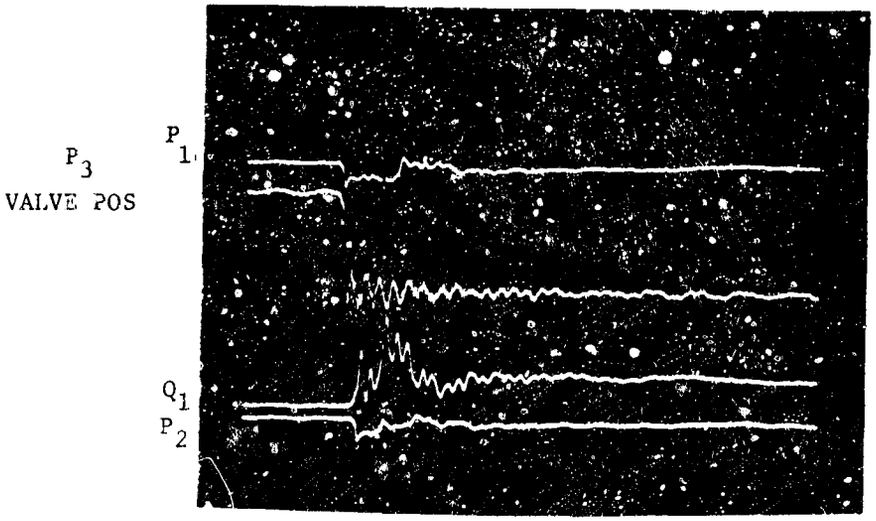

Flow: 17.25 CIS
Temp: 125°F
Time Scale: 20 msec/cm
Date: 16 May 1975
Flow Condition: Turn-on Transient

FIGURE 6. LINES UNCLAMPED

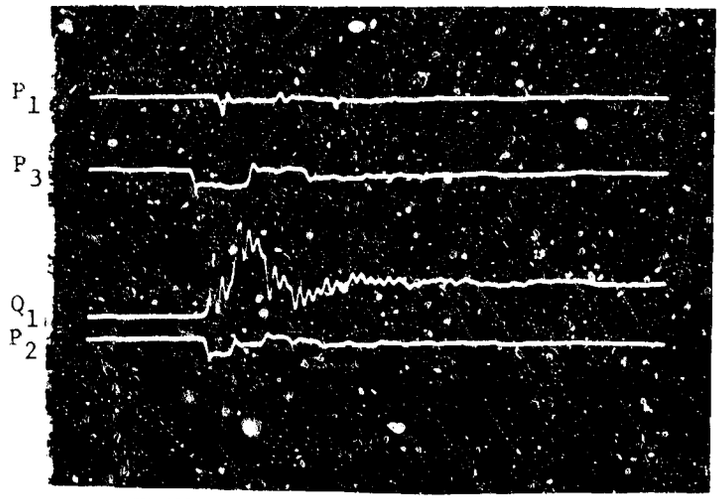

FLOW: 17.25 CIS
Temp: 125°F
Time Scale: 20 msec/cm
Date: 23 May 1975
Flow Condition: Turn-on Transient

FIGURE 7. LINES CLAMPED

(3) Pump Test Problems - The turn-off transients caused an abnormal oscillation in the hanger position data (XH) during the first two pump test series runs. Figures 8 and 9 show that the LVDT was not properly tracking the hanger movement. The transducer was originally installed so that the probe shaft extended into the pump case and rested on the actuator spring piston. The probe shaft was spring loaded to eliminate slop and to overcome the forces resulting from case pressures. However it appears that this preload was not adequate to track the response of the hanger. Different preload springs were tried without much success. The spring was removed from the LVDT and pressurized nitrogen was used to force the probe against the actuator spring piston. The gas pressure exerted a more constant pressure on the LVDT probe over its full range of travel and thus it was able to accurately track the hanger as shown in Figure 10.

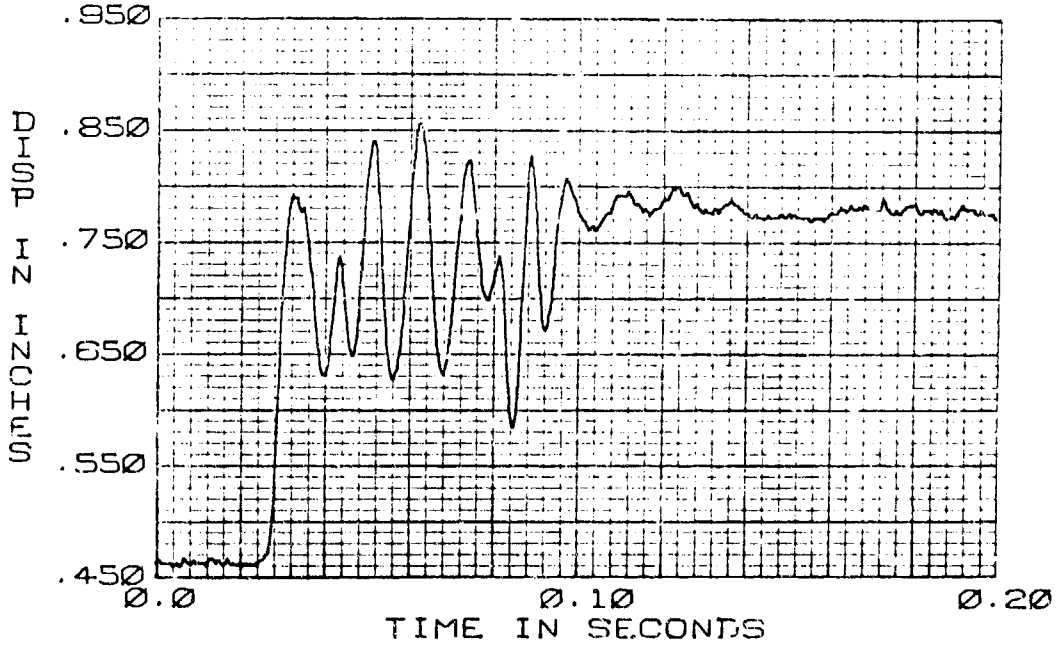

F-15 HYDRAULIC PUMP
63-03-XH TURN-OFF TRANSIENT
77 CIS 130 F

FIGURE 8.

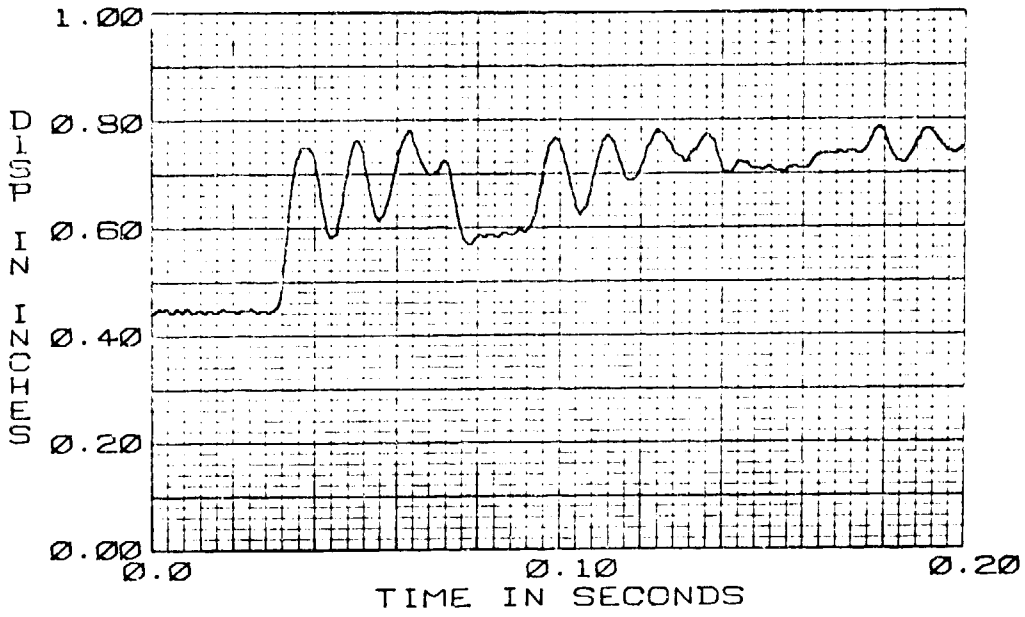

F-15 HYDRAULIC PUMP
64-03-XH TURN-OFF TRANSIENT
77 CIS 130 F

FIGURE 9.

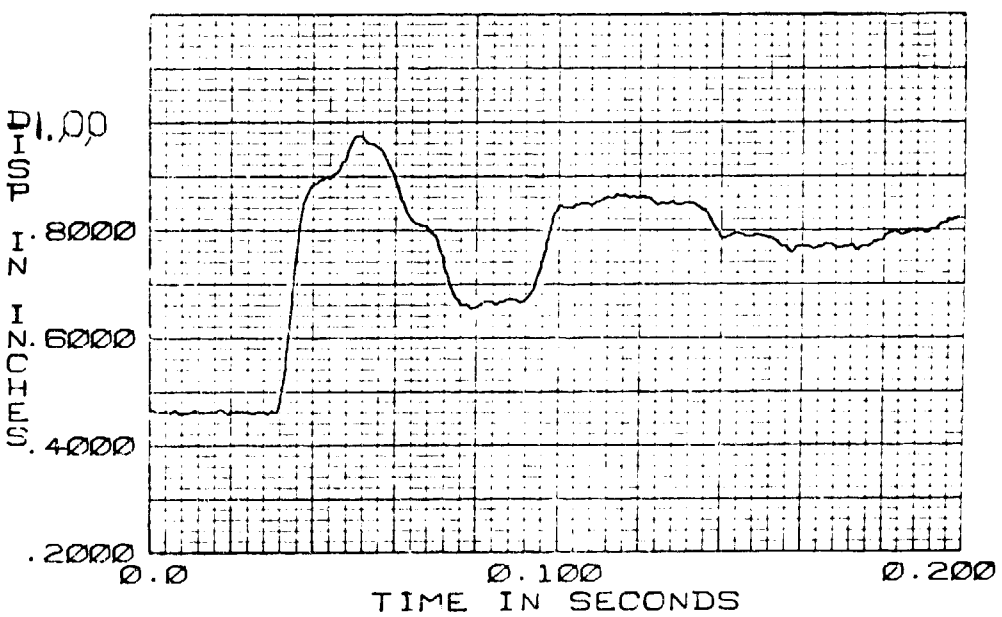

F-15 HYDRAULIC PUMP
65-03-XH TURN-OFF TRANSIENT
77 CIS 130 F

FIGURE 10.

(4) Operational Life of Hot Film Anemometer Probes - The first two Thermal Systems Incorporated hot film probes failed after 50 hours of operation. These were mechanical failures caused by a separation of the connecting wire from the film surface. Separation occurred because of strain cracks that developed in the epoxy insulating the probe tip from the anemometer case. Additional efforts were made to locate the probes in acoustically quiet areas in the system (i.e. not at the peak of a pressure standing wave). This coupled with improved probe construction by the manufacturer appreciably extended the useful life of the hot film probes.

3. STEADY STATE TESTS

The flow domain test series provides steady-state pressure drop and flow data on the component test specimen. Data was recorded as the steady-state flow was varied from zero to a maximum value and back to zero again. The maximum flow depended on the test specimen and downstream test bench flow resistance, instrumentation operating limits, and pump capacity.

4. THERMAL TESTS

Thermal testing was performed on the test bench and the F-15 iron bird's utility speedbrake system. Thermal properties of steady state and transient operating hydraulic systems were investigated.

Steady state testing on the test bench consisted on running the system at a constant temperature and flow and recording the heat transfer through each component. Transient test temperatures were monitored from start-up ambient temperature until the system stabilized at some specified operating condition.

The utility system oil on the F-15 iron bird was heated by cycling an actuator in the system. The speedbrake subsystem remained near ambient temperature during this period. The speedbrake selector valve was cycled to operate the speedbrake and the subsystem warm-up characteristics were measured. Data was recorded for opening, closing, and reversal.

SECTION III
INSTRUMENTATION

Accurate test data was essential for the development and verification of the Aircraft Hydraulic Systems Performance Analysis Computer Programs. As with any test program choosing and setting up the proper instrumentation to measure the data must be done painstakingly and correctly to assure reasonable accuracy. Proper selection of test equipment and test procedures can contribute greatly to the effectiveness and accuracy of the element model verification.

The development and verification of component models required special care in the selection of the variables to be measured and how they were measured. For a general model this required monitoring the variables at all the external connections. Because of the complex nature of fluid behavior in the individual components caused by a system disturbance (e.g., a valve closing) the mathematical representation in the computer program becomes quite sophisticated. Therefore the key variables must be recorded for the proper model verification of a component. The effort in the Hydraulic Dynamics Laboratory refined the procedures and techniques needed to evaluate the operating characteristics of hydraulic system components.

1. HYDRAULIC PERFORMANCE ANALYSIS FACILITY

The Hydraulic Performance Analysis Facility (HPAF) was built to provide an improved means for obtaining dynamic test data on hydraulic components and systems. Program verification is accomplished by comparing results obtained from the computer analyses with actual data obtained in the test facility.

a. Description - The major items which make up the HPAF are a pump drive system, a fluid deaeration unit, a test bench, and an instrumentation and data handling system. The following paragraphs present some of the defining requirements for these items as well as their general descriptions. Figure 11 is a photograph showing the layout of the facility.

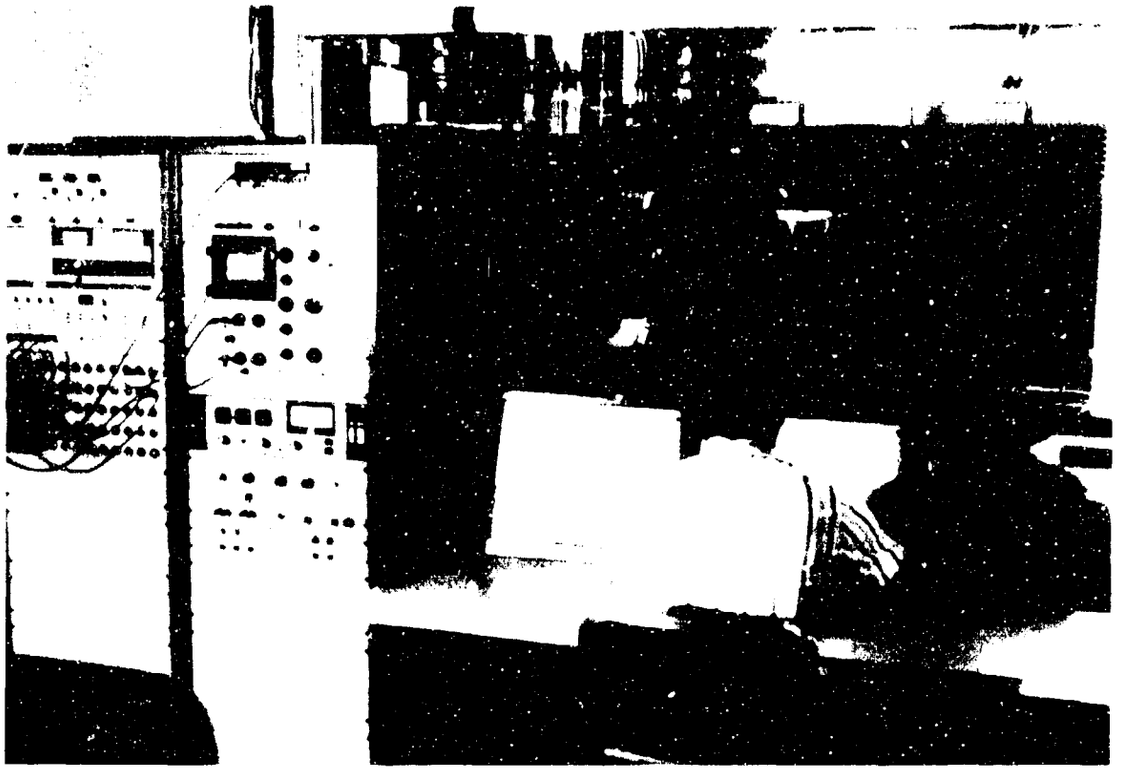

FIGURE 11. HYDRAULIC PERFORMANCE ANALYSIS FACILITY

b. Pump Drive System - The requirement for tes ing fast response hydraulic pumps such as those employed on the F-15 aircraft provided one of the primary justifications for the HPAF. Conventional laboratory drives do not provide adequate speed control or "dynamic stiffness" to maintain a constant pump speed as transient flow loads are applied. As a result, pump performance data is often obscured by speed variations and in some cases erroneous data results because the speed variations cause abnormal pump operation. The pump drive system (Figure 12) in the HPAF is a direct drive 200 horsepower unit of the adjustable frequency AC type capable of speeds up to 7000 RPM. It eliminates significant speed variations under changing load conditions by sensing output speed and torque and adjusting motor drive frequency accordingly. The direct drive feature eliminates elements which could introduce backlash or compliance to allow dynamic testing of high response pumps.

FIGURE 12. PUMP DRIVE SYSTEM

c. Fluid Deaeration System - One of the variables which affects the dynamic performance of a hydraulic system is the amount of dissolved air in the fluid. Air content in a system can vary significantly depending on filling and bleeding procedures, and operating pressures. It was concluded that a means of controlling dissolved air content was required. Further, it was decided that to obtain baseline data the best approach for dealing with the dissolved air problem was to reduce the air content to an insignificant level. To accomplish this, a deaeration system (Figure 13) was fabricated. This unit has the capability of maintaining the air content within the system at less than 1% by volume. An air measuring system allows verification of the reduced air content. Control and verification at higher levels [illegible] when performance at these levels is to be investigated.

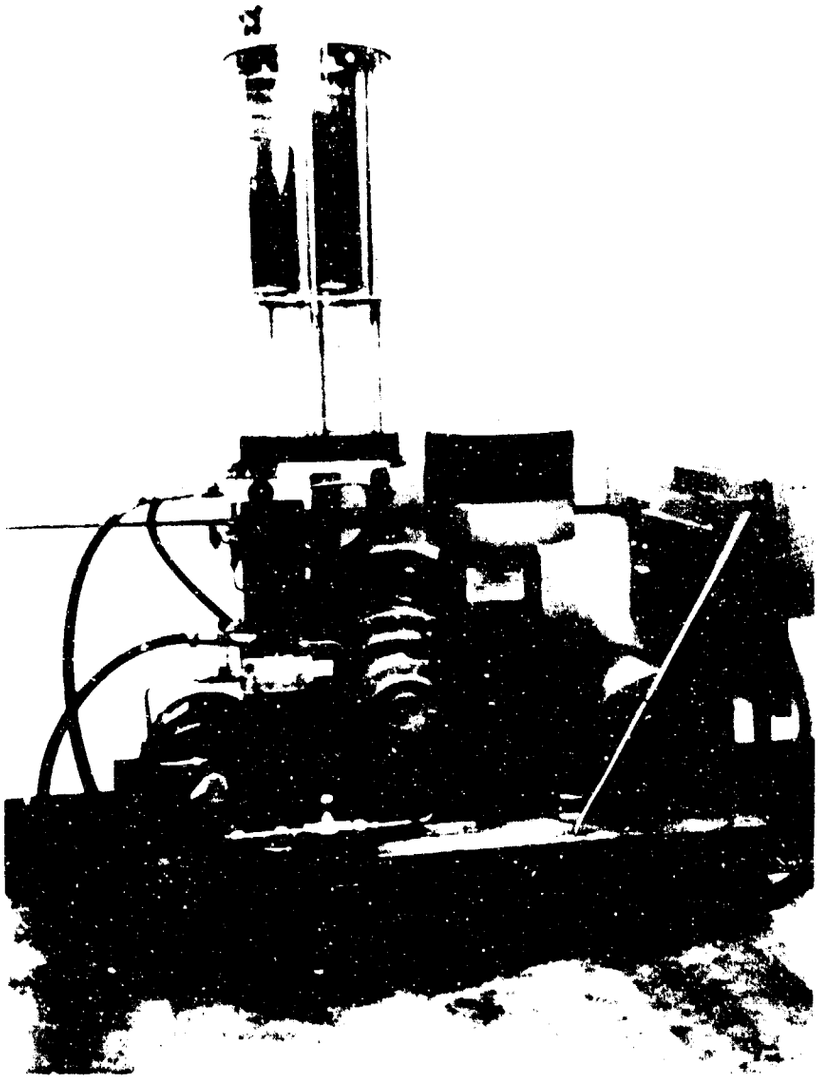

FIGURE 13 FLUID DEAERATION SYSTEM

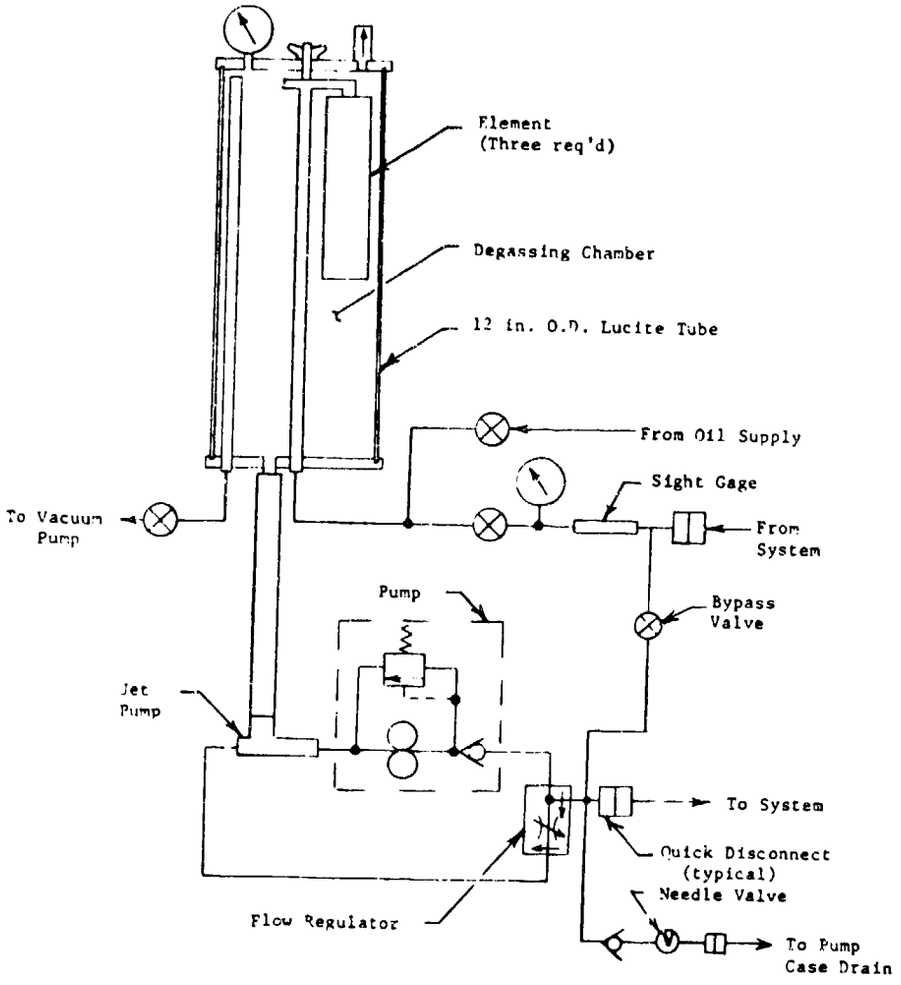

FIGURE 14. DEAERATION UNIT HYDRAULIC SCHEMATIC

Figure 14 shows the hydraulic schematic for the hydraulic fluid degassing unit. The MCAIR built unit is capable of degassing and storing a quantity of oil. Oil can be circulated through the test system from the degassing unit power supply, which also supplies power to operate the jet pump.

The unit is capable of initially evacuating the test system with or without operation of the system pump, loading previously degassed oil into the system, degassing oil at a high rate while in series or parallel with the system, and receiving and storing degassed oil from the system before test specimen changeover.

d. Test Bench - The test table was designed to accommodate most specimen configurations with minimum changeover effort. In addition to providing a location for the specimen and instrumentation, the table included the equipment for generating transient hydraulic flows. Transients were generated with the specially developed fast control valve which had operating times on the order to two milliseconds.

The test bench and instrumentation schematic is shown in Figure 15 for component transient tests. Steady state flow rate was controlled by the load valve downstream of the test station. Transient flow demands were generated by opening and closing the fast response solenoid control valve. Pressures and flows were recorded on both sides of the test specimen during the opening and closing transients. The basic power supply consisted of a hydraulic pump, a commercial PULSCO hydraulic acoustic noise attenuator, pressure filter, case drain filter, and system relief valve. Hoses and quick disconnects at the pump permitted hookup of the oil degassing unit with or without the pump in the circuit. The case drain quick disconnect was required to pressurize the pump case from degassor power when the system was degassed with the pump connected. Test specimen temperature was controlled by stabilizing test bench temperatures with an industrial type heat exchanger in the pump suction line. A pressure hose permitted movement of the pressure side of the set-up to accommodate various test specimen envelopes. A flow control servo valve in the pressure supply line permitted remote control cycling of flow rates for steady-state flow domain tests. The F-4 bootstrap reservoir was strategically located at the termination of the straight test section to minimize dynamic reflections at the test specimen. Reservoir bootstrap pressure control was independent and variable. The reservoir pressure relief valve prevented overpressurization, and allowed safe operation slightly over normal reservoir pressure. The suction line was large to preclude pump cavitation during normal test conditions.

The test section consisted of an accumulator for transient power supply and additional source noise attenuation, solenoid control and load valves, and upstream/downstream instrumentation across the test specimen.

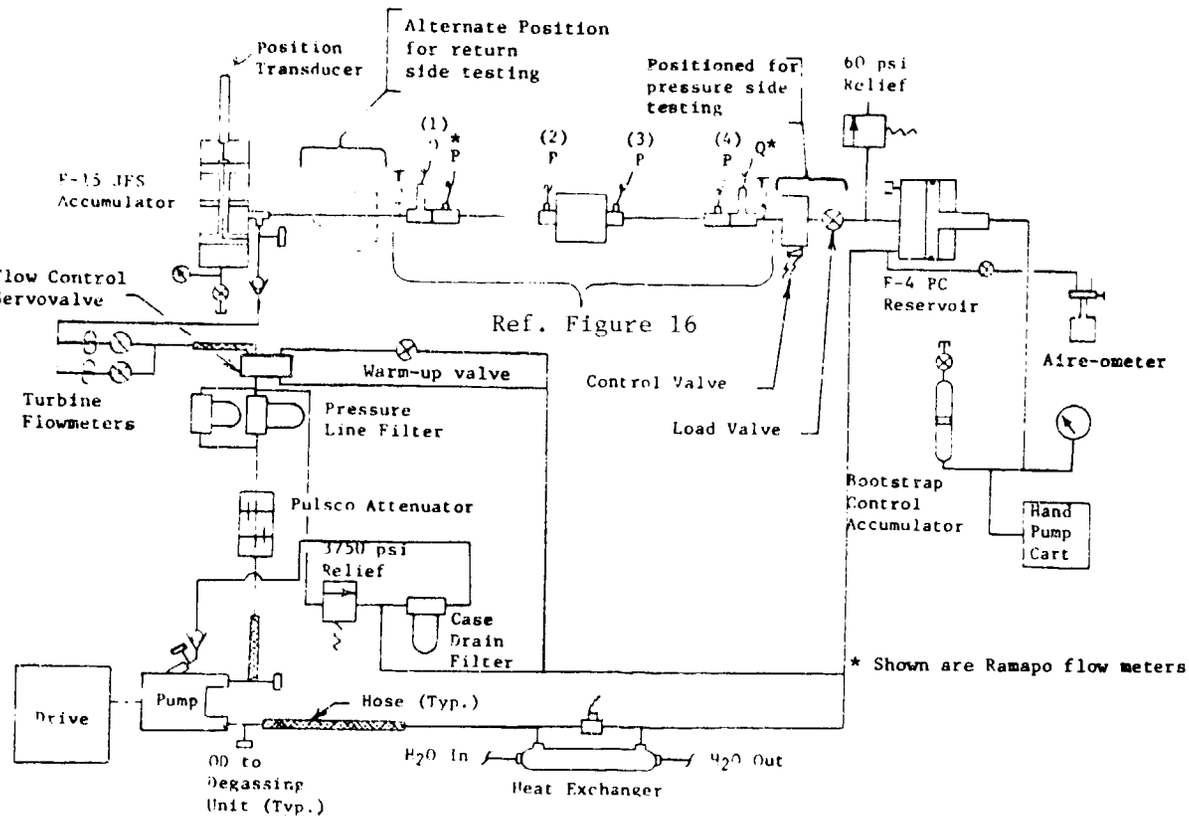

FIGURE 15. STEADY STATE AND TRANSIENT TEST BENCH HYDRAULIC SCHEMATIC

The test section was the highest point in the circuit to minimize fluid loss and air absorption during specimen changeover.

e. Instrumentation and Data Handling System - One common problem is the installation of a transducer itself on the dynamic performance of the system. Several approaches are employed to reduce this effect in the HPAF. These include the use of Clamp-on pressure transducers and hot wire anemometer flowmeters.

Figure 16 shows a cross section of the instrumented section of the test bench, upstream of the test specimen, for flow/time domain tests. The downstream instrumented section was identical to the upstream section.

The instrumented sections were designed to minimize flow disturbances. Split blocks were clamped over the tube section with matching block-to-tube holes for temperatures and flow probes, and pressure transducers. Fittings were drilled out to match tubing inside diameters where fitting wall thickness permitted. Pressure transducers were installed as near to the flow stream as possible, without protruding into the stream.

o Upstream section shown, downstream and size identical but reverse sequence

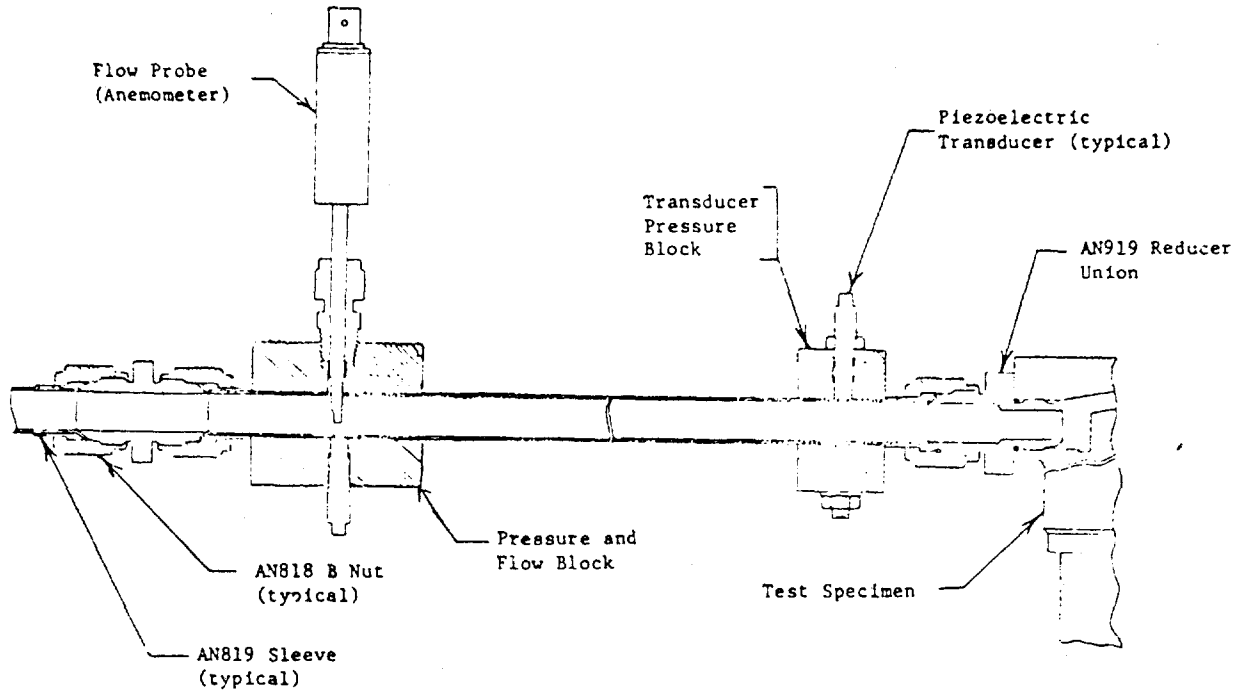

FIGURE 16. INSTRUMENTATION SECTION - COMPONENT MODEL VERIFICATION, STEADY STATE AND TRANSIENT

The primary element in the data handling system was a Wang 2200B programmable calculator. This calculator, with its optional thermal printer and X-Y plotter was capable of outputting measured data in report format. Transient data was input into the calculator under program control via a 4-channel transient recorder which accepted the analog transducer outputs, converted them to digital form, and stored them. The Wang system was also used as a terminal for direct communication with a general purpose digital computer when expanded capabilities were required. Figure 17 is a photograph showing the calculator system.

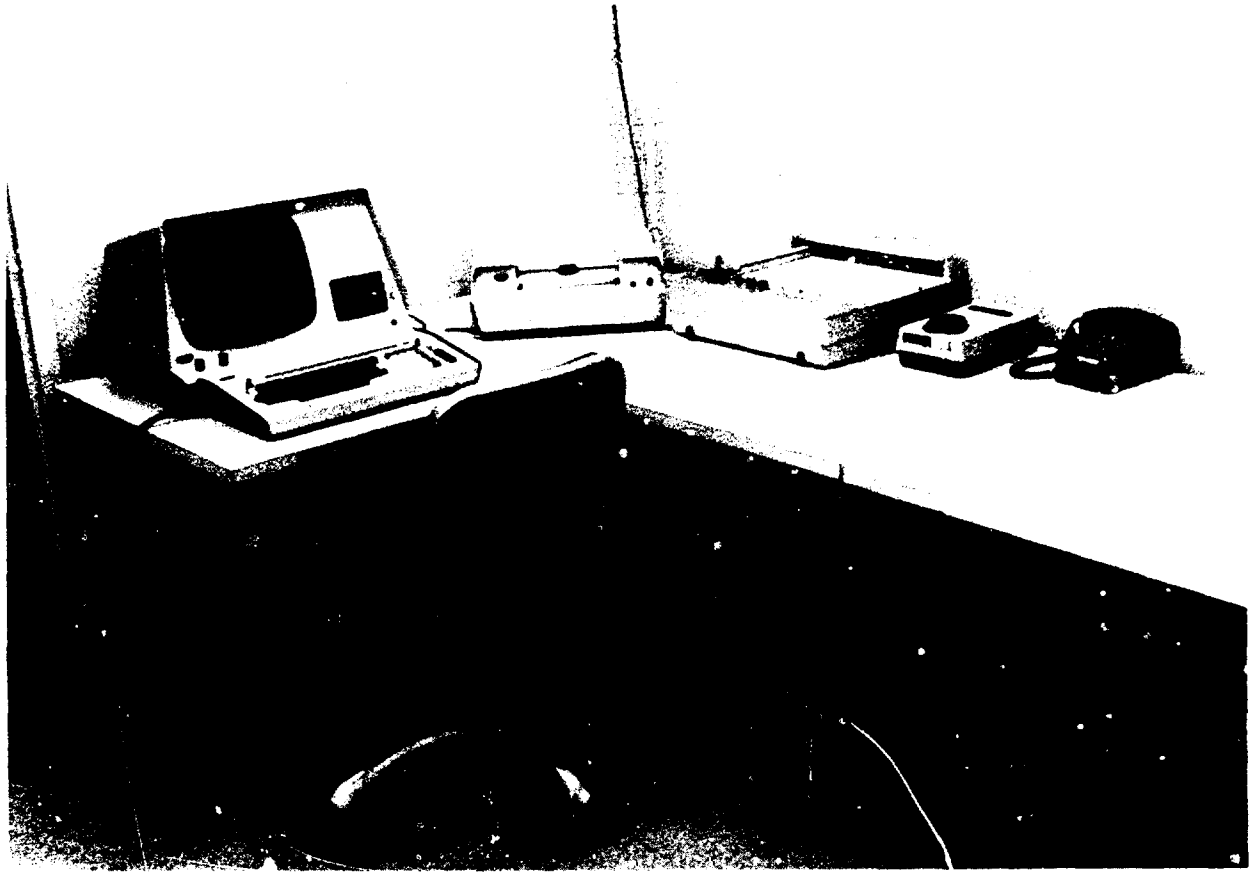

FIGURE 17. WANG 2200B PROGRAMMABLE CALCULATOR SYSTEM

2. DATA RECORDING AND PROCESSING

Figure 18 shows a block flow diagram of the instrumentation and data recording facilities. The data was taken via transducers, strain gages, flowmeters, thermocouples, etc., through their respective electronics to the patch panel. Data from the panel routed to a 14-track intermediate band FM magnetic tape recorder and to a 4-channel waveform recorder. The waveform recorder manufactured by Biomation Corporation was capable of recording 1000 points of data for each channel with a channel resolution of 10 binary bits per data word. Response of the data system, including the tape recorder, was from DC to 10,000 Hz. Recorder accuracy was 1% or better.

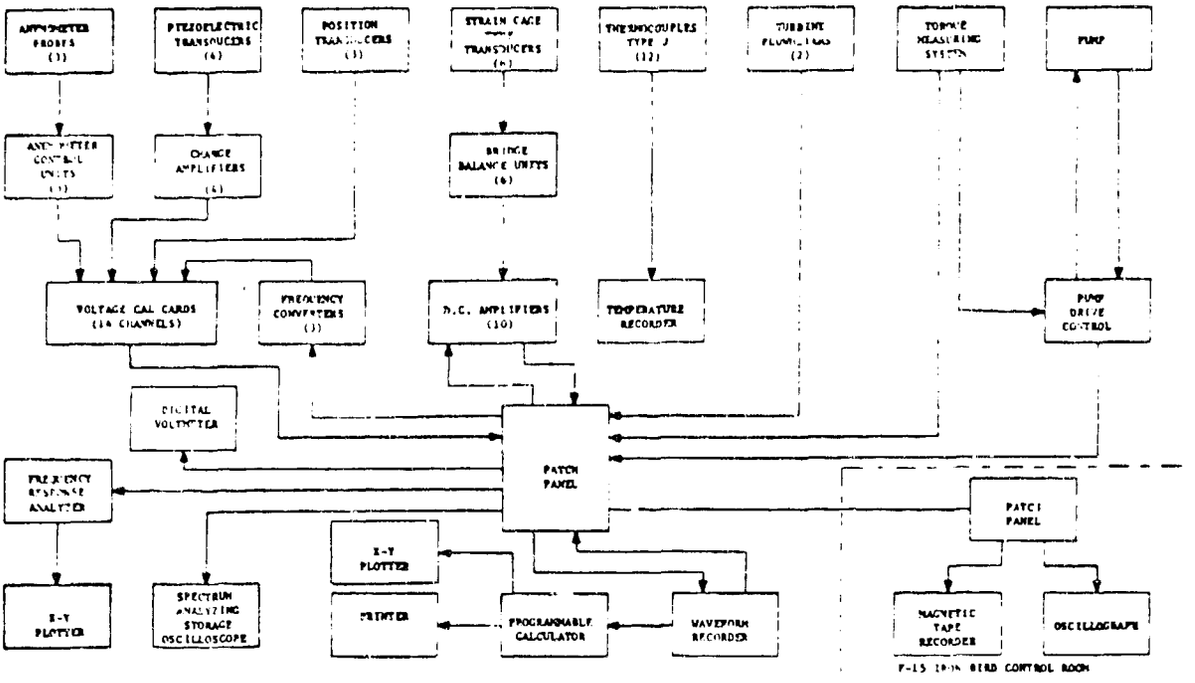

FIGURE 18. INSTRUMENTATION AND DATA FLOW BLOCK DIAGRAM COMPONENT MODEL VERIFICATION

The processing of the data began with mounting the appropriate data tape on the recorder and playing back four data channels at a time to the Biomation. These recorded analog signals were digitized (converted to a binary representation) by the Biomation waveform recorder. In this process some of the data was lost to tape noise and flutter. A $\pm$ .5% tolerance on the data was considered good resolution. However, for a 4000 psi pressure pulse, $\pm$ 20 psi can cause the steady state portion of the computer simulation to be in error. See Section 3 for a further discussion.

The data taken from the Biomation was stored on cassette tape through a Wang 2200 programmable calculator. Calibration factors for scaling, temperature and flow conditions were also stored on tape. One thousand data points per channel were recorded on the cassette.

From the tape the data was plotted on the Wang X-Y plotter or output on a thermal printer. The Wang calculator was interfaced with the CDC 6500 disk files through a telecommunications link. Data was transferred to a file where it was merged with the computer programs.

3. PRESSURE MEASUREMENT

For a transient analysis, knowing the initial steady state boundary conditions was important to starting the computer solution procedure. The problem of trying to measure steady state data with transient recording instruments was significant to this procedure. The pressure transducers being used were Statham thin film strain gage transducers with a range of 0-5000 psia and a natural frequency of 70000 Hz in air. The best that they could be calibrated to was $\pm$ 20 psia. A 5000 psia transducer cannot mechanically perform better, and further processing of the pressure signal through the electronic system ($\pm$ 1/2% was typical of tape noise) induced more error in the pressure reading. For the computer simulation this would sometimes cause errors in the calculated steady state flow resulting in erroneous pressure distributions.

The pressure transducers were calibrated for zero and maximum values provided by electronic circuitry, for every set of runs that were made. Each transducer was calibrated to give a linear relationship between voltage and pressure. Due to nonlinearities in the measuring equipment the transducers drifted in both zero and scale calibrations giving significant errors in pressure measurements. When necessary the pressure data was averaged to find a mean value for the steady state pressure, and all the other pressures were corrected to this mean value in order that meaningful verification effort could be accomplished. This method gave acceptable steady state starting and stopping conditions without drastically affecting the data. The technique involved was electronically equivalent to using one transducer as the standard and referencing the others to it through a gain factor.

Clamp-on pressure transducers were also used in the transient and frequency testing. These Piezo-electric transducers were Kistler 205 H2's. They have a resolution of .1 psi/rms with a sensitivity of .5 mv/psi. The maximum pressure measurable is 10000 psi and the transducers have a natural frequency of 250000 Hz.

4. FLOW MEASUREMENTS

A main area of concern that developed in testing was the measurement of transient flows in a simple line system. The inability to adequately measure a flow reversal hampered the computer simulation verification of the HYTRAN line model.

Although adequate pressure data can be obtained for the computer verification, meaningful transient flow data is very difficult to record during a water-hammer experiment.

The first transducer used to measure flow data was a Ramapo flowmeter. Figure 19 presents a schematic of the flowmeter. In actual laboratory testing the Ramapo flowmeter exhibited very poor damping characteristics when hit by a transient. The flowmeter oscillated at about 360 Hz, which is its natural frequency. Figure 20 shows typical results. The dynamic fluid flow force is sensed as a drag force on a specially contoured body of revolution suspended in the flow stream. The flow force is transmitted via a lever rod to a strain gage bridge. The drag force is proportional to the flow rate squared. When the drag element is hit by a transient wave, the cantilever beam arrangement of the meter overreacts to the flow forces and begins to oscillate at its natural frequency.

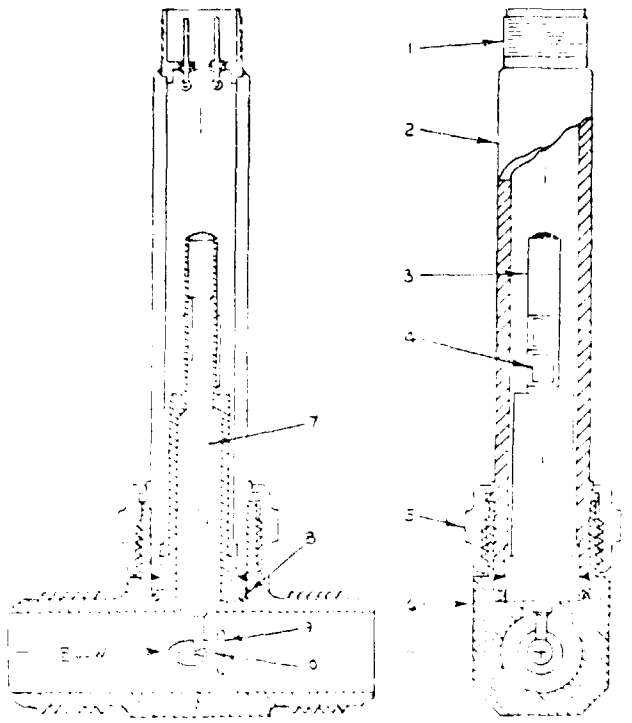

1. Electrical Connector
2. Case
3. Sensing Tube
4. Bonded Strain Gage Bridge
5. Retaining Nut
6. Housing
7. Lever Rod
8. "O" Ring Seal
9. Flow Sensor
10. Set Screw

FIGURE 19. RAMAPO FLOWMETER SCHEMATIC DIAGRAM

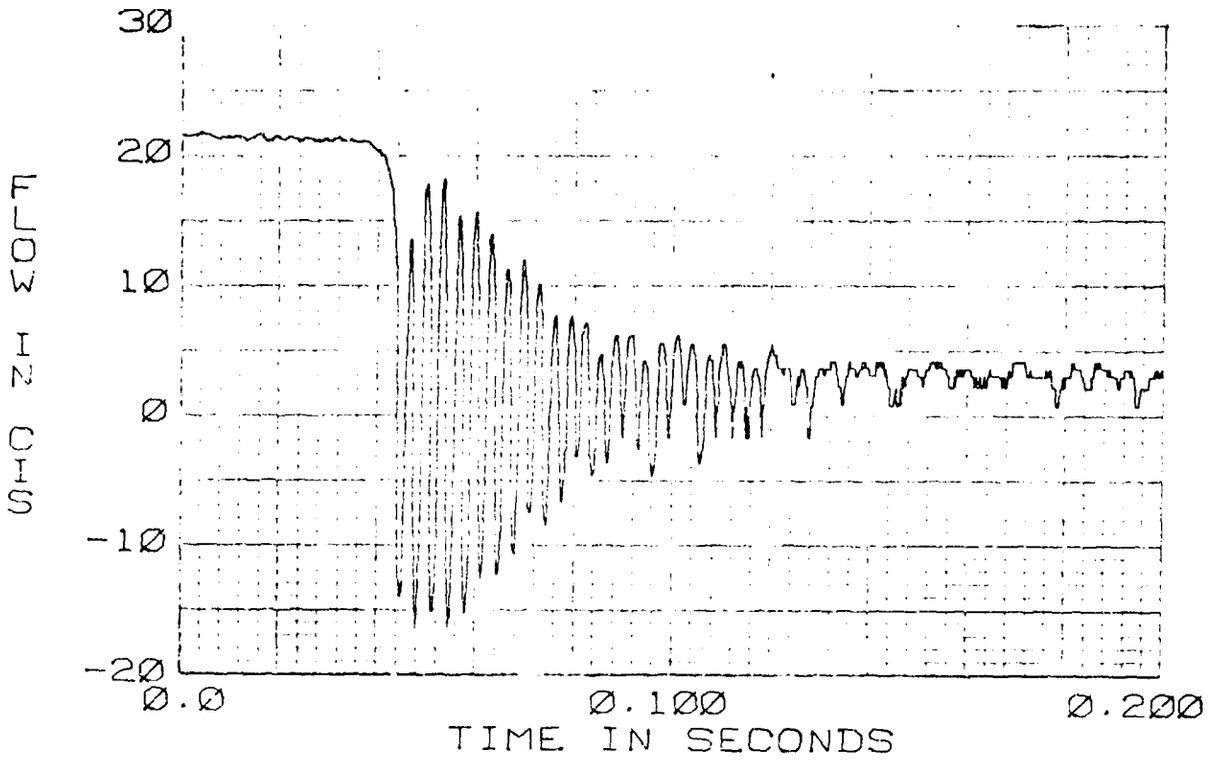

FIGURE 20. F4 PC FILTER HOUSING
Q2 TURN-OFF TRANSIENT
125°F

After analyzing the test data from Task 1A, it was originally believed that the flowmeters were placed at critical reflection points in the system. The test setup was expanded to locate a flowmeter in a different position. The configuration is shown in Figure 21. From this setup it was confirmed that the Ramapo flowmeter was oscillating at its natural frequency, and not being driven by internal reflections.

Figure 22 is an oscilloscope trace of the data points sampled by the Biomation waveform recorder for P_2, P_3, Q_1 and valve position. Q_1 is the data trace of the Ramapo flowmeter before a square law relationship was applied to the data to convert it to a direct representation of the flow transient as measured.

This flow data could not be used in the compute. program for model verification, because of the underdamped condition exhibited by the Ramapo flowmeter. It was hoped that better data would be obtained from hot film anemometers.

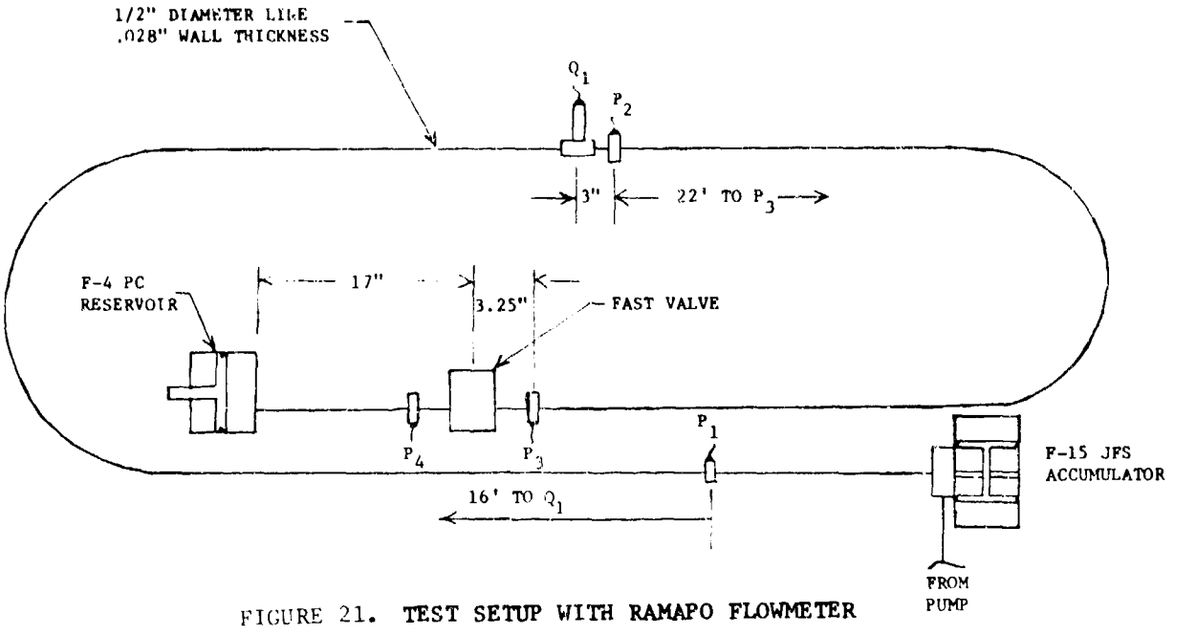

FIGURE 21. **TEST SETUP WITH RAMAPO FLOWMETER AT Q_1**

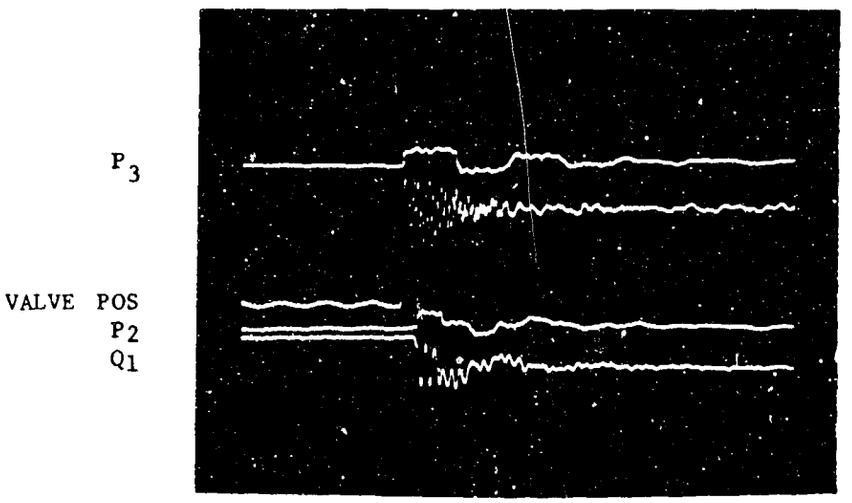

FIGURE 22. TURN-OFF TRANSIENT WITH RAMAPO FLOW METER IN NEW TEST SETUP

Flow Rate:	19.25 CIS
Temperature:	125°F
Time Scale:	20 msec/cm
Date:	16 May 1975
Condition:	Turn-off Transient

a. Hot Film Anemometer Flow Measurement Development- The hot film anemometer was installed in approximately the same position as the Ramapo flowmeter in Figure 21. The pressure transducer was located directly opposite the anemometer. The probe tip was inserted so that the center of the film was approximately in the centerline of the tube. The hot film probe is a Thermal System Inc., Model 1229 as shown in Figure 23. The hot film system uses a bridge balance network to supply current to the sensor to keep it at a constant temperature. The amount of current needed is a measure of the flow rate.

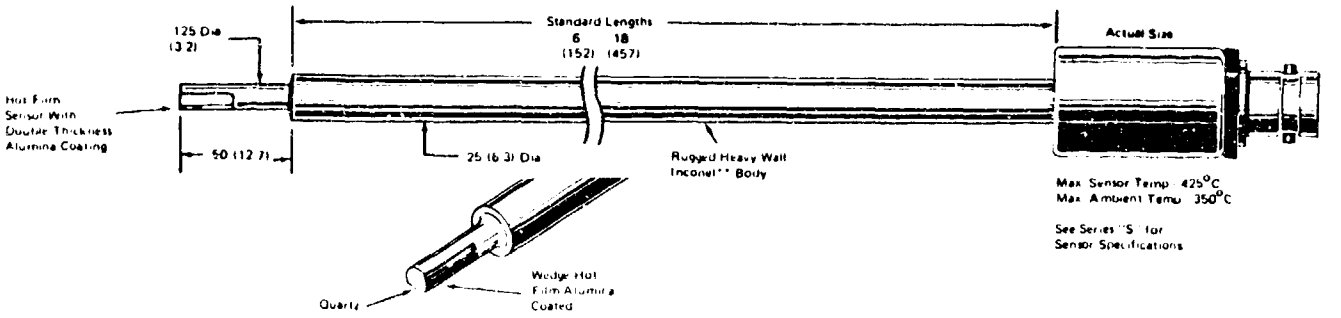

FIGURE 23. MODEL 1229 HOT FILM PROBE - SIDE FLOW WEDGE

The hot film sensors were chosen over hot wire sensors because of the following advantages:

1. Less suceptible to fouling and easier to clean - helpful in the high temperature ranges to reduce the effects of any possible oil degradation.
2. Excellent frequency response
3. More flexibility in sensor configuration
4. Lower heat conduction of the film to its supports which allows a smaller sensor to minimize effects on the fluid flow.

The basic anemometer voltage is related to flow approximately as follows:

$$E^2 = [A + B\ (\rho V)^{1/M}]\ \ (ts - ts) \qquad (1)$$

where A, B = constants depending on fluid properties

ρ = fluid density

V = velocity

M = exponent that varies with range and fluid (usually 2)

ts = sensor operating temperature

te = fluid or environmental temperature

This relation illustrates the non-linearity of the anemometer output as well as the relationship with density, velocity and temperature.

A test run was made with the probe tip in the location shown in Figure 24 and the oscilloscope trace of the pressure directly opposite the hot film probe and the anemometer output voltage is shown in Figure 25. The protrusion into the flow steam was chosen to place the sensor in approximately the centerline of the tube.

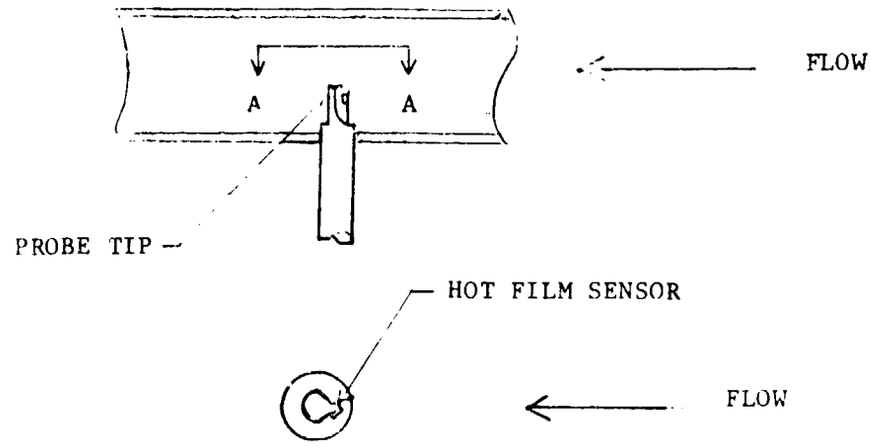

SECTION A-A

FIGURE 24. PLACEMENT OF SENSOR IN 1/2" LINE

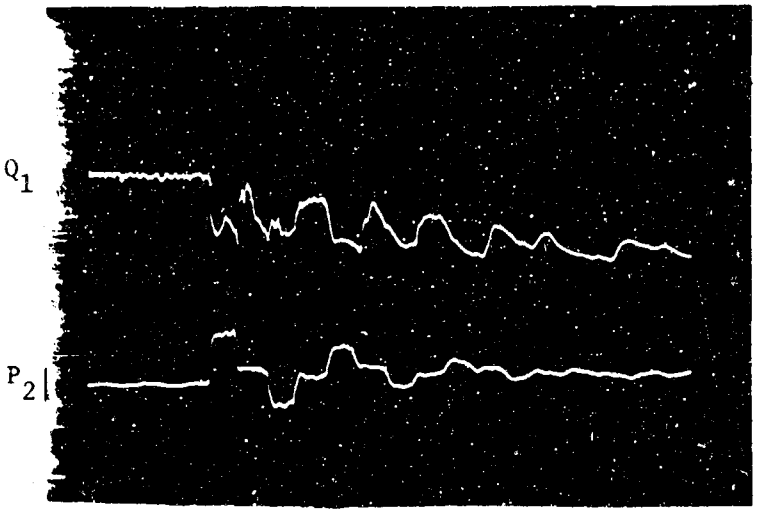

Flow: 27.6 CIS
Temp: 125°F
Time Scale: 20 msec/cm
Date: 24 May 75
Condition: Turn-off transient

FIGURE 25. HOT FILM SENSOR DATA IN 1/2" LINE

The Q_1 trace indicated much better flow data than was obtainable with the Ramapo flowmeter. Unfortunately, negative flow measurements were not accurate because of the direction in which the probe tip was placed.

The next step was to rotate the wedge shaped probe tip ninety degrees to the flow direction (Figure 26). Since there is an equal amount of exposed hot film on either side of the wedge, it was believed that the anemometer could adequately measure the flow in both directions. Figure 27 is an oscilloscope trace of the data run which shows significant improvement.

From basic waterhammer theory it is known that after the fast control valve is closed a positive wave propagates at acoustic velocity back along the pipe until it reaches the accumulator. The fluid behind the wave is at zero velocity and at a pressure higher than the accumulator. After the pressure wave reaches the accumulator, the higher pressure in the pipe causes the fluid in the pipe to flow back into the accumulator. The indicated flows in Figure 27 are all positive because the hot film probe cannot sense flow direction, it can only measure flow magnitude. The first flow peak is a negative and so is every alternate peak.

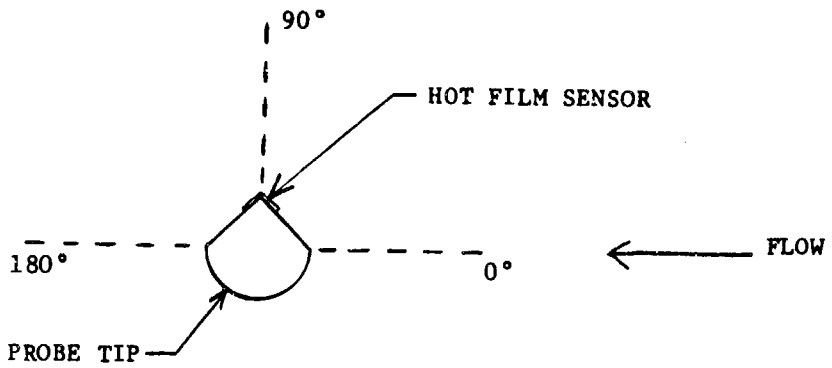

FIGURE 26. HOT FILM SENSOR ROTATED 90°

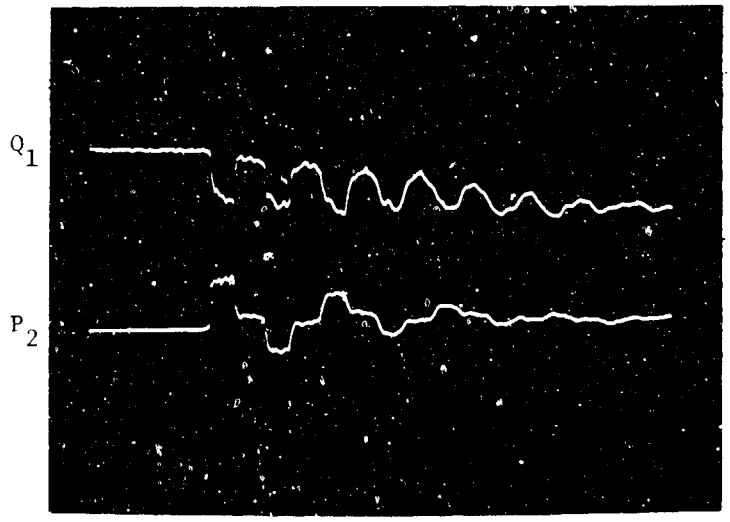

FIGURE 27. HOT FILM SENSOR DATA IN 1/2" LINE ROTATED 90° TO FLOW DIRECTION

Flow: 27.6 CIS
Temp: 130°F
Time Scale: 20 msec/cm
Date: 30 May 75
Condition: Turn off transient

An interesting observation on the anemometer data is the residual flow at the first flow reversal and its gradual decay. This is more prevalent in the oscilloscope photograph Figure 28 which covers a significantly longer time period. The probe location was the same as that in Figure 25. The initial response of the probe to the turn-off transient should show a flow drop to zero. The small flow measured by the probe in the position chosen shows the inability to measure zero mean flow in the velocity profile for that position.

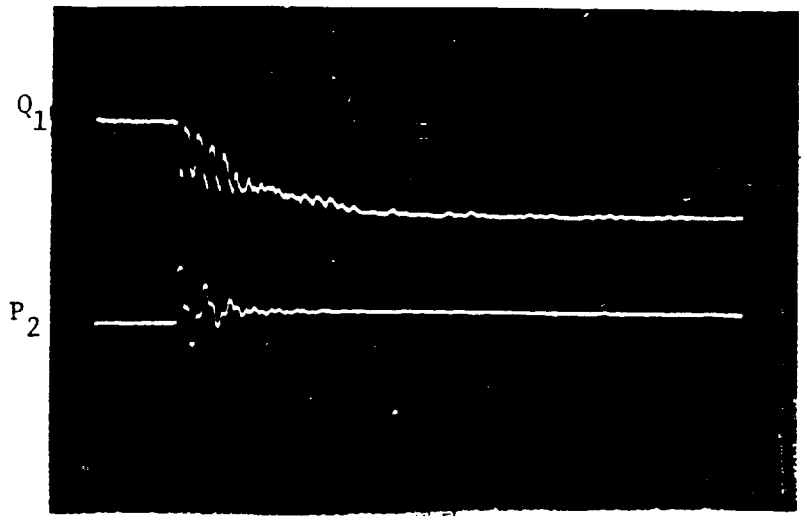

FIGURE 28. HOT FILM SENSOR DATA IN 1/2" LINE

Flow:	27.6 CIS
Temp:	125°F
Time Scale:	100 msec/cm
Date:	24 May 75
Condition:	Turn-off transient

b. Baseline Setup and Anemometer Usage Calibration/Optimization - Assured that the anemometer data gave reasonable answers the baseline 30 ft 1/2" dia tube was set up in the dynamics laboratory (Figure 15). Two 18" test stations were located up and downstream of the test specimen. Each station had an anemometer and two pressure transducers.

The first step was to perfectly align the anemometers 90° to the flow direction. This was accomplished dynamically by running a turn-off transient, observing the flow trace on an oscilloscope, and then adjusting the Q_1 anemometer position until decreasing square waves were measured. Figures 29, 30, and 31 illustrate an example of this. In Figure 29 the Q_1 probe was rotated greater than 90° to the flow direction, in Figure 30 Q_1 was less than 90°, and Figure 31 contains the final calibration curve for Q_1.

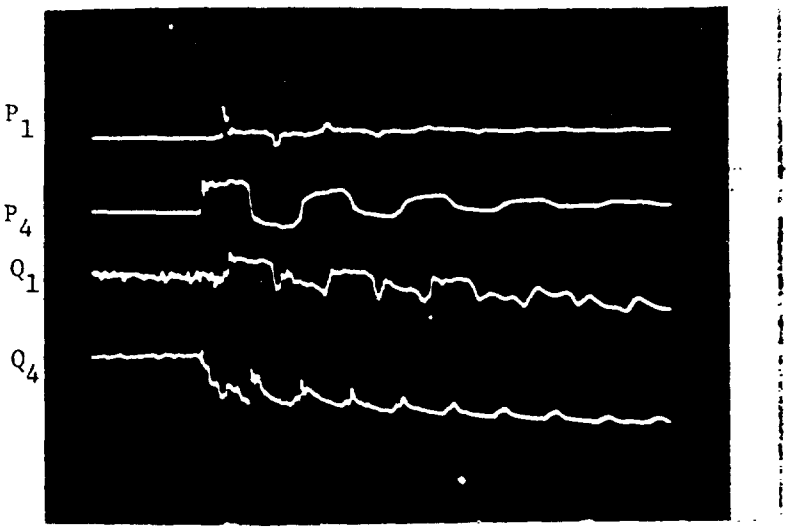

FIGURE 29 HOT FILM SENSOR DATA IN 1/2" LINE
BASELINE 30 FT TUBE
Q_1 ROTATED GREATER THAN 90°

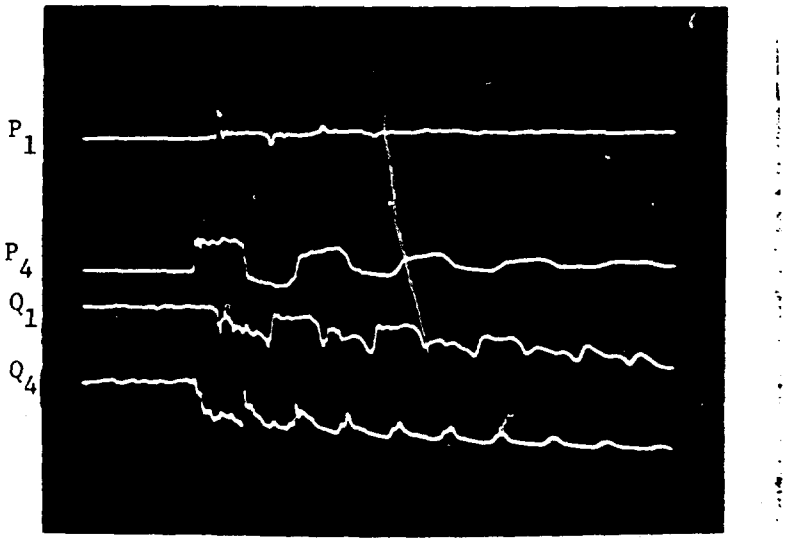

FIGURE 30 HOT FILM SENSOR DATA IN 1/2" LINE
BASELINE 30 FT TUBE
Q_1 ROTATED LESS THAN 90°

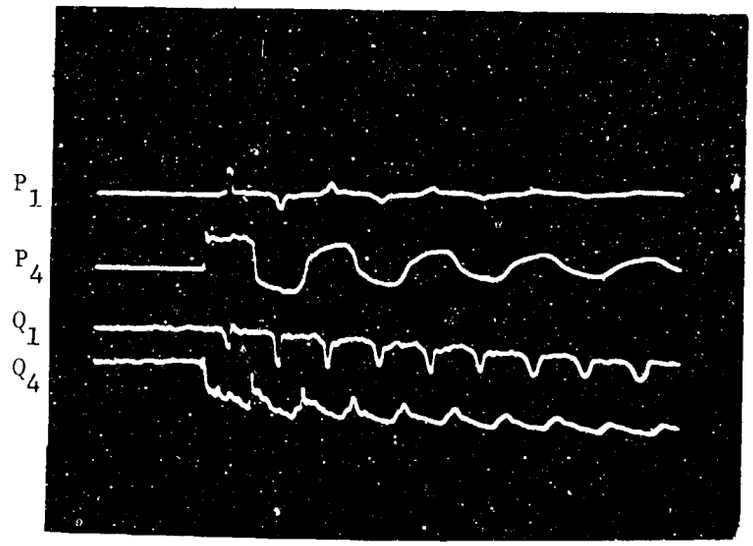

FIGURE 31. HOT FILM SENSOR DATA IN 1/2" LINE
BASELINE 30 FT TUBE
TIP 90° TO FLOW DIRECTION

Because the short line length between the fast valve and anemometer resulted in shorter reflection times (Figure 15), this procedure could not be accurately followed for the Q_4 anemometer. The entire Q_4 test station was relocated at the upstream test station for calibration and then returned to its original position.

A steady state calibration was performed on the hot film anemometer. A turbine flow meter was used for the flow data along with the anemometer bridge output voltage to generate a flow vs voltage calibration curve for the anemometer. The values of voltage and the turbine meter output of frequency were plotted on an X-Y plotter. The graph is shown in Figure 32. A dip was noted in the transition region from laminar to turbulent flow.

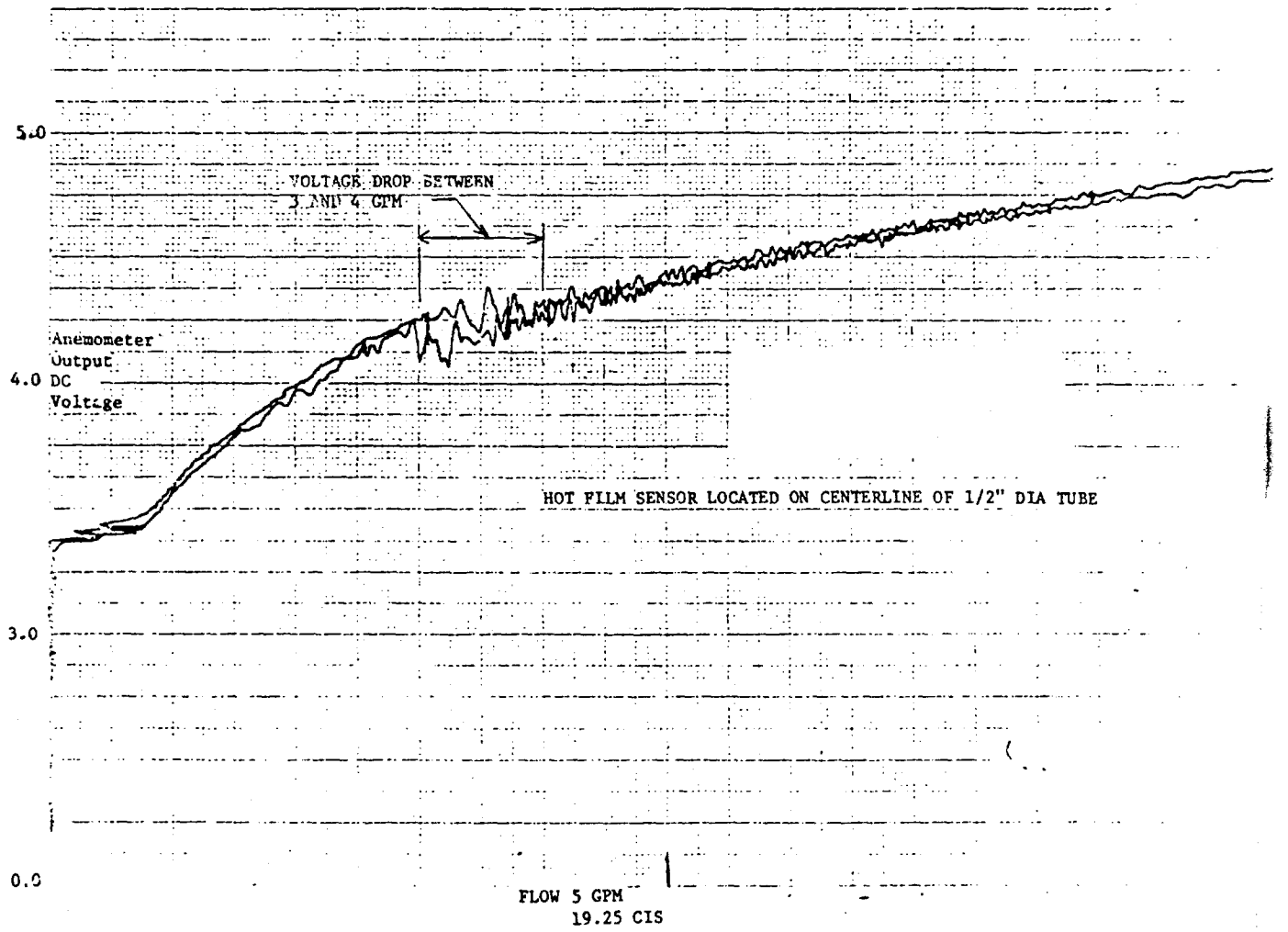

FIGURE 32. CALIBRATION OF Q_1 ANEMOMETER

TEMP 125°F

R. G. Leonard in his doctoral thesis on "A Simplified Model For A Fluid Transmission Line" (Pennsylvania State University Graduate School of Mechanical Engineering, June 1970), gave predicted variation in the fluid velocity at three different locations in a line as a function of

time following the valve closure in a waterhammer experiment. Figure 33 reproduced from Dr. Leonard's thesis shows that the fluid in the region near the tube wall responds much faster (in that it reverses sooner) to the reversal of the pressure gradient, than does the fluid in the central portion of the flow where the inertial effects are more dominant. i.e. reverse flows occur near the wall while in the central region, flow persists toward the valve. Thus the hot film probe was shifted laterally in the tube to obtain a better mean velocity measurement. Moving this probe tip from the tube centerline helped to remove the dip from the steady state calibration in Figure 32 to the curve in Figure 34. The calibration curve clearly indicates the nonlinearity characteristics of the anemometer. Figure 35 shows the results of moving the probe too far out of the flowstream. The transition region now begins to rise.

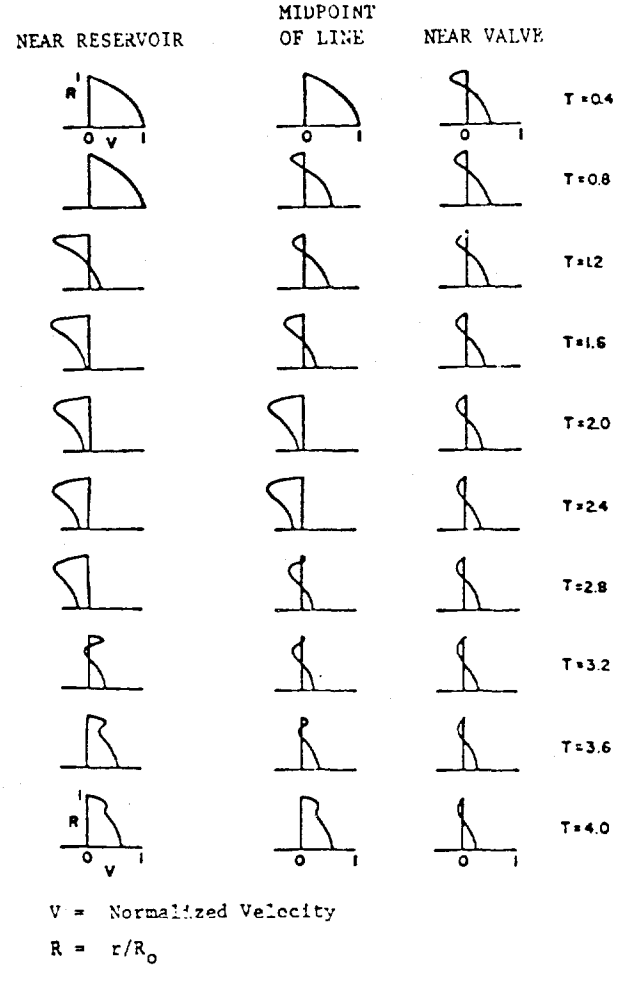

FIGURE 33. PREDICTED VELOCITY TRANSIENTS AT THREE LOCATIONS IN A LINE DURING A WATER HAMMER EXPERIMENT

After moving the probes, they were aligned 90° to the flow direction before a calibration run was made. Once a smooth calibration curve can be established, an equation was fitted to the curve and the actual data flow rates were calculated from this relationship.

The calibration was acccomplished by varying the load valve in Figure 15 from 0 to 38.5 CIS flow and back down again. If the system temperature was allowed to vary by more than 5 degrees a definite temperature hysteresis effect could be observed on the calibration curve. Figure 36 is an excellent example. If the temperature is kept relatively constant, there is no problem in the calibration curve. For fast transients there is little effect due to temperature variations on the flow measurements.

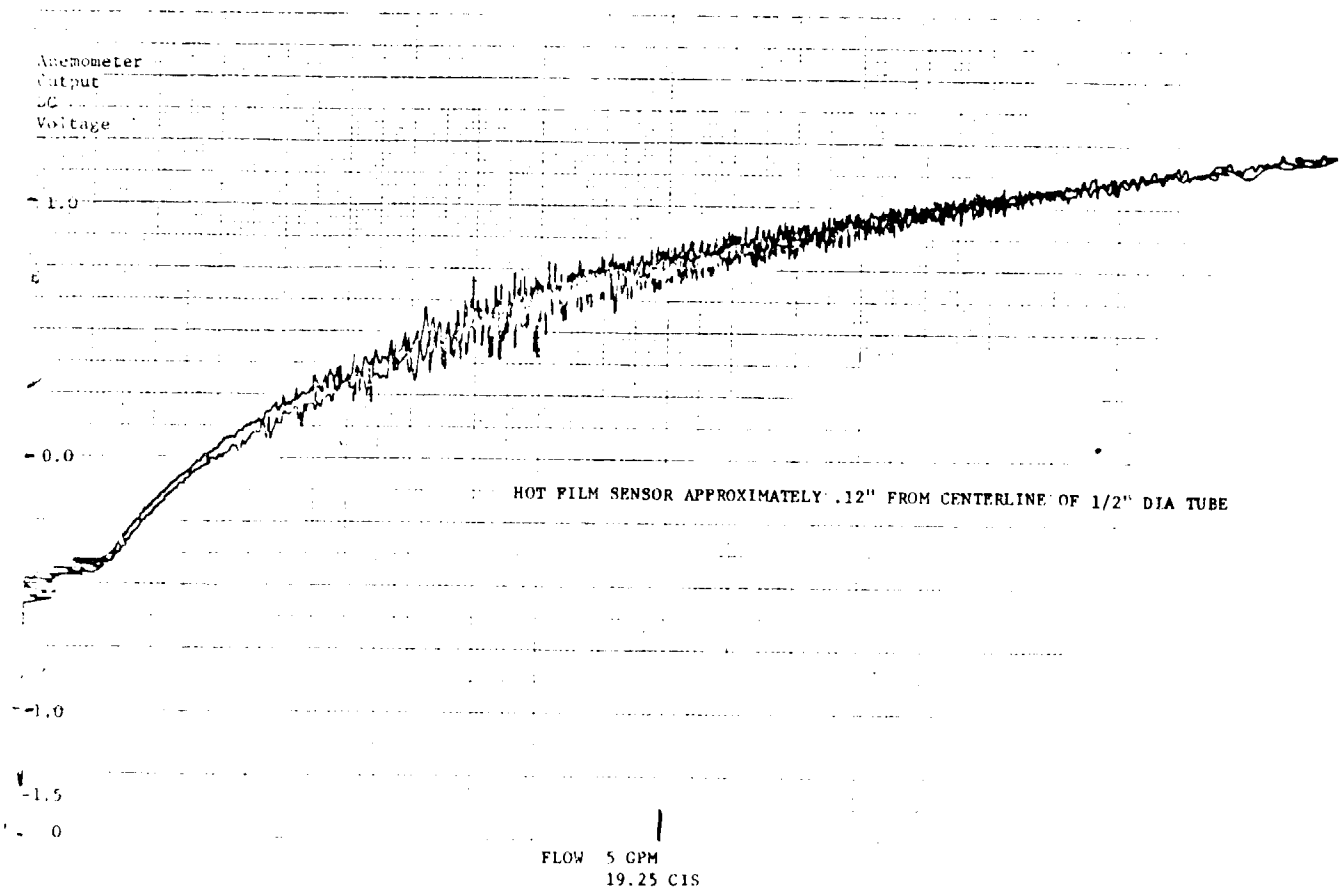

FIGURE 36. CALIBRATION OF Q_1 ANEMOMETER
TEMP 125°F

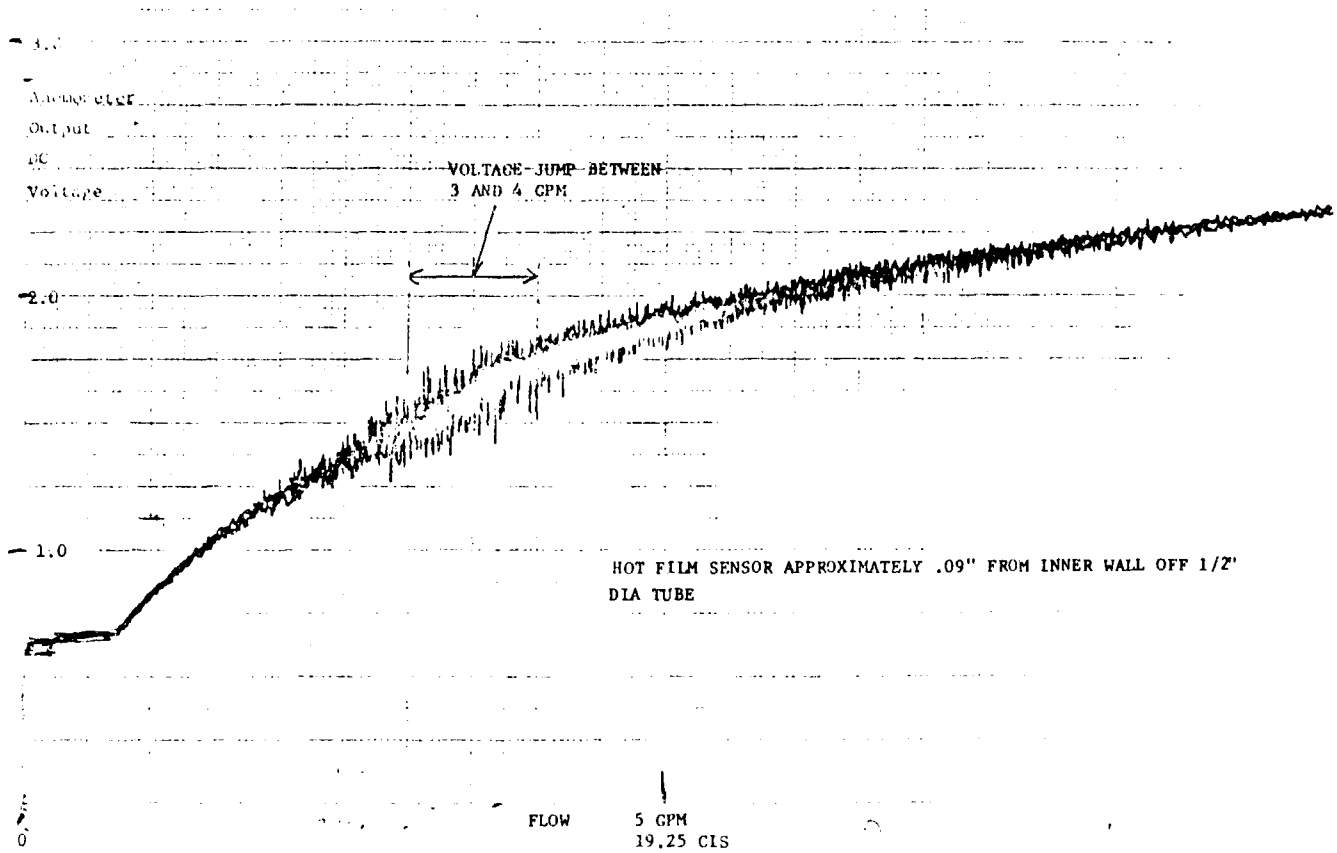

FIGURE 35. CALIBRATION OF Q_1 ANEMOMETER
TEMP 125°F

After the probes were aligned and calibrated, a 125°F turn-off transient was then run on the system. Figures 37 and 38 show the plotted results of the flow data, Q_1 and Q_4.

The flow signal is extremely noisy for the intial steady state flow and gradually dampens as the flow settles to zero. In Figure 37 the flow reversals shown by the first, third, fifth, etc., peaks have a definite flow decay, while the forward flows in the even numbered peaks indicate a flatter response.

These transient flow data were the best recorded to date. Although it may not be the most optimal for correlation to computer output plots of flow, it is definitely better than any flow data we measured previously, and was used in the verification of the element models.

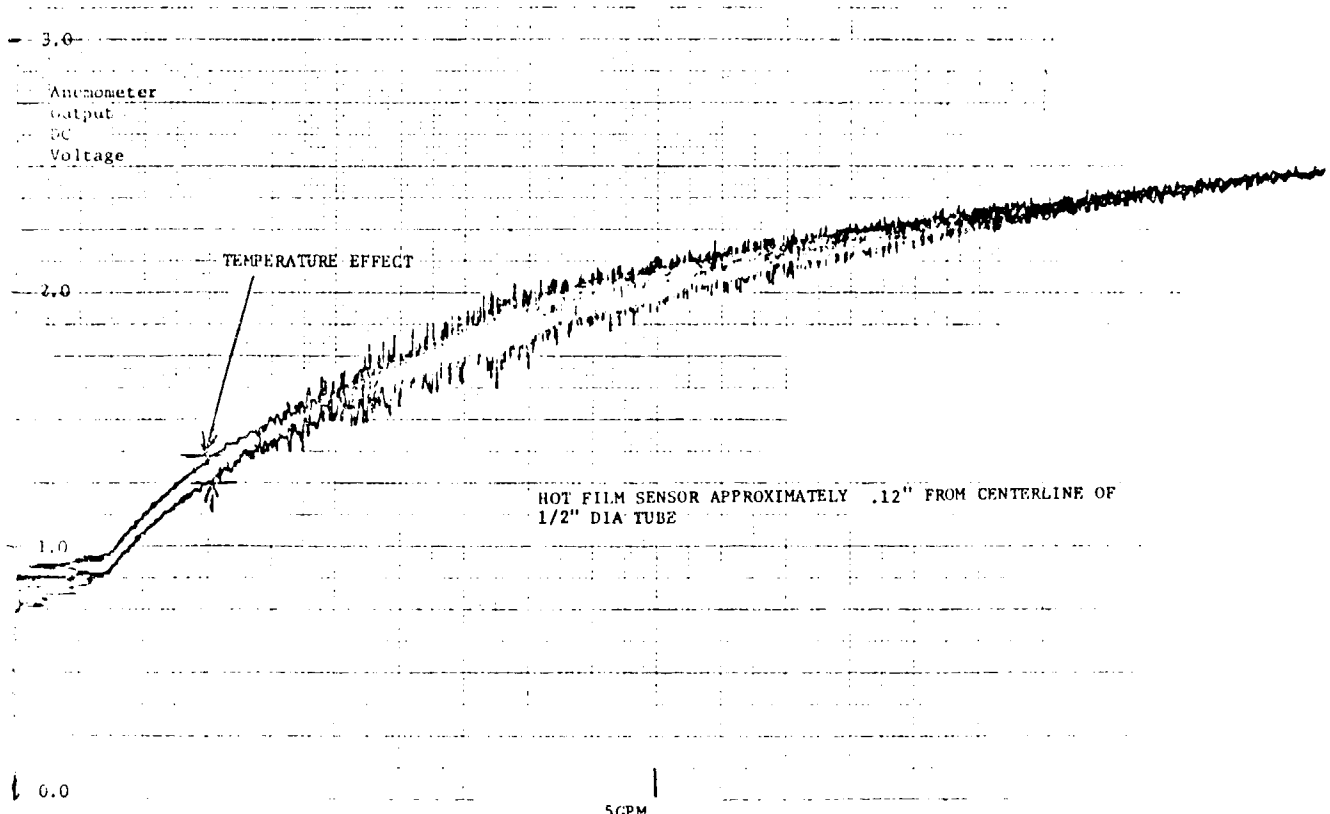

FIGURE 36. CALIBRATION OF Q ANEMOMETER

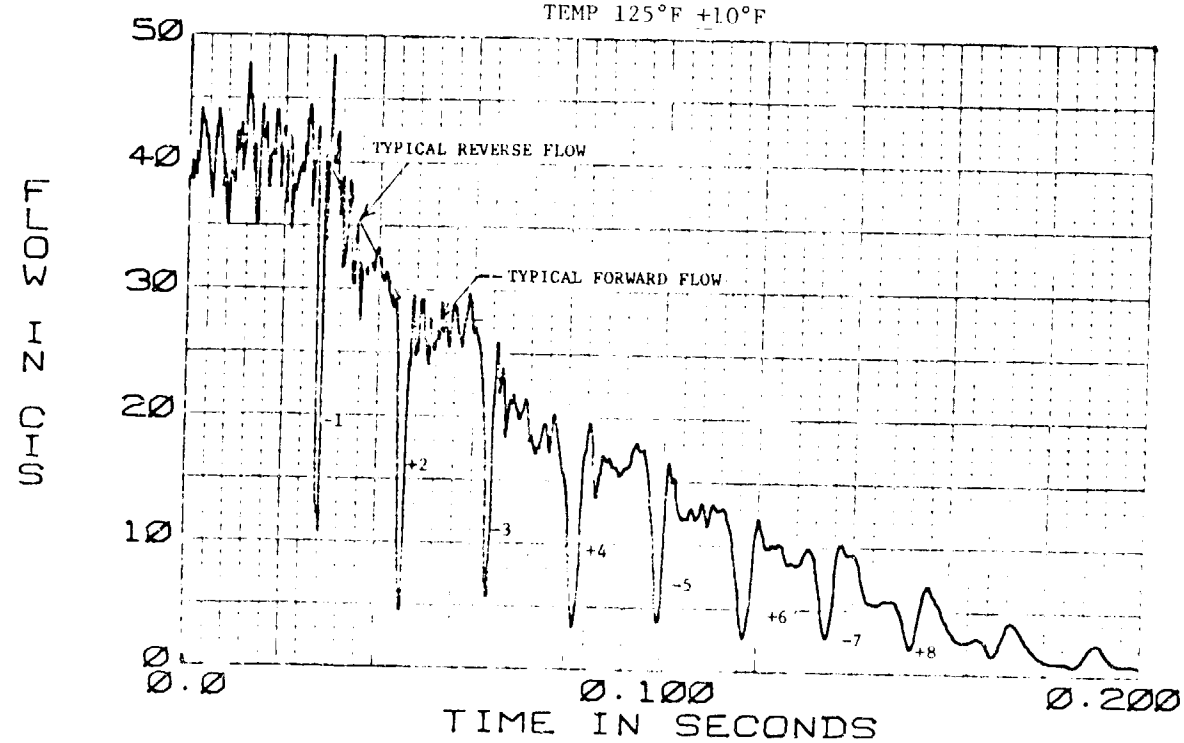

FIGURE 37. .5 DIA TUBE X 30 FT
ANEM-Q1 TURN-OFF TRANSIENT
38.5 CIS 125 DEG F

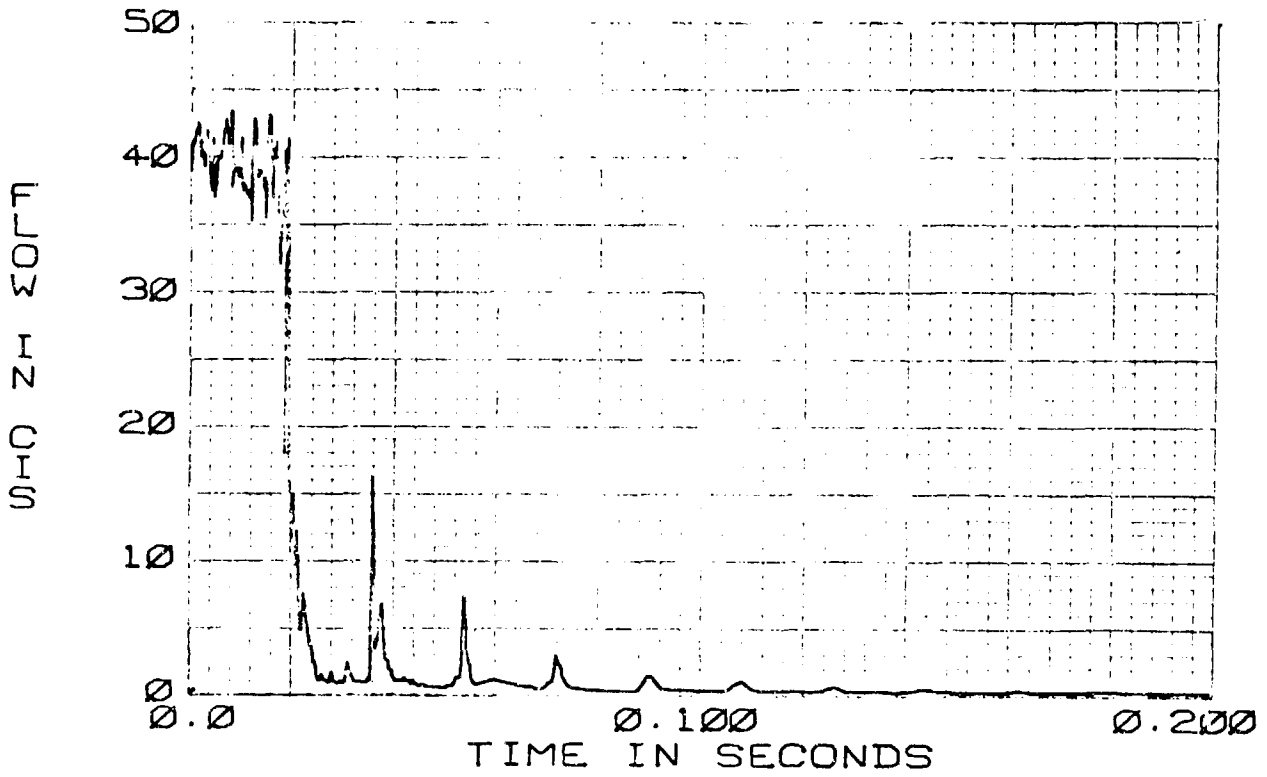

FIGURE 38. .5 DIA TUBE X 30 FT
ANEM-Q4 TURN-OFF TRANSIENT
38.5 CIS 125 DEG F

5. ANCILLARY INSTRUMENTATION

The pump instrumentation consists of two Standard Controls Inc. model 210-10-060-09 pressure transducers for control pressure (PC) and pump outlet pressure (PP). These units are temperature compensated, low volume, strain gage type pressure transducers with a pressure range from 0 to 10,000 psi. The control spool position (XC) is monitored using a variable impedance transducer having a linear range of 0.05 inches. The unit is manufactured by Kaman Measuring Systems. The model number of the sensor is KD 2300-15. The hanger position (XH) is measured using an SRL model KBJ00 LVDT with a rated linear range of $\pm$ .50 inches.

Turbine flowmeters incorporating a free-moving suspended rotor and a signal pickoff were used to measure the steady state flows on the test bench.

Other major instrumentation used included:

Aire-ometer - Measured the precent of dissolved air in the system.

Torque monitor - A strain gage device used to measure pump drive torque.

Biomation waveform recorder - A digital sampler used to process the data.

Bafco - Processed amplitude and phase data.

Spectrum Analyzer - Performed harmonic analysis at test system resonance points.

SECTION IV

FREQUENCY RESPONSE VERIFICATION TESTS

Development and verification efforts on the HSFR computer program during the contract period are covered in this section.

Development work on the HSFR computer program consisted of considerable work on the PUMP subroutine to improve and extend its capabilities. Steady state balancing of hanger angle with computed outlet flow, inlet acoustic flow/pressure analysis, and hanger torque analysis sections were developed. Hanger torque studies aided in the development of an accurate pump model for the transient analysis computer program (HYTRAN).

All HSFR subroutines were generalized to allow a common method of inputing data for the pump and all simulated circuit components and lines. The subroutines (WHEQUT) for a Quincke tube resonator was revised. A similar subroutine was developed to simulate a hydraulic system acoustic filter available commercially from the PULSCO division of the American Air Filter Co. Miscellaneous changes were made to the executive or main program to add acoustic energy analysis, and allow user selection of the harmonic of interest and the number of pumping pistons. The CDC program was also run on the IBM 360 system with minor changes to literal data formats.

Program verification tests consisted of operation of an F-15 hydraulic pump in a short (9 feet), straight, 1 inch steel line circuit terminated by a load valve. This baseline system provided data for combined verification of the main program, and models for the line, the pump, and valve/circuit termination. The dynamic interaction between the pump and system load is a basic part of HSFR program. A variable length circuit was also used in the tests. Tests were run at 130°F and 210°F fluid temperatures with MIL-H-5606B and MIL-H-83282A fluids. Steady state flow was varied from 0 to 20 gpm.

Original plans for component level model verification called for measuring dynamic pressure/flow magnitude and phase relationships at the component inlet and outlet. However, dynamics flow measurements were not accurate enough to permit pressure/flow phase measurements of sufficient quality for routine component model verification. Component verification therefore consisted of mapping circuit dynamic pressures with the component installed in the straight baseline test circuit. The F-15 pump was used as the acoustic source throughout the tests. Test data were obtained for two different component locations in the test circuit.

Total circuit length was held constant, regardless of the component being tested or its location in the circuit.

Test data was compared directly to computed results by plotting standing pressure waves and/or the peak pressure amplitude at a location (pump speed) of circuit resonance.

1. BASIC HSFR PROGRAM AND PUMP MODEL VERIFICATION

This section describes the development and verification of the basic Hydraulic System Frequency Response (HSFR) computer program. Development and verification of the HSFR pump model is also included since the dynamic interaction between the pump and system load is a basic part of the program.

Program verification encompassed operation of the instrumented F-15 hydraulic pump in a simple, straight-line test circuit terminated by a load valve. Verification also included the addition of a single closed end branch line to a straight line circuit.

Test results are discussed and analyzed for the three circuit/fluid combinations tested.

MIL-H-5606B/9 Ft. System
MIL-H-83282A/9 Ft. System
MIL-H-83282A/Trombone System

Analog plots of selected test data are included.

Development and use of the HSFR program and pump model to study pump hanger torque characteristics is discussed. This activity aided in the development of an accurate pump model for the transient analysis computer program (HYTRAN).

Verification tests for components modeled in the HSFR program are covered in subsequent sections.

a. HSFR Program Development

The following summarizes changes and additions made to the HSFR computer program during the contract period, Feb. 1974 - Feb. 1977.

(1) Generalized PUMP and WHEQUT Subroutines

The PUMP was originally modeled using programmed data. The PUMP subroutine was later generalized to allow the required data to be inputed along with other circuit component, line, and control input data. The same type of generalization was also applied to the WHEQUT

(Quincke tube) subroutine. With these changes, input data for all HSFR program models of system elements are input in the same generalized manner.

(2) Return System, Pump Inlet, and Hanger Torque Analysis

The HSFR program and HSFR pump subroutine were utilized to study pump hanger torque characteristics in order to improve the HYTRAN pump model in this area. Calculation of the return system dynamic loads was necessary, to study the effect of pump inlet load on pump outlet/ pressure system dynamics and hanger torque.

This effort resulted in a major expansion of the basic HSFR program and pump subroutine to allow resonant frequency analysis of a hydraulic return system, and pump hanger torque/actuator pressure analysis. Use of these capabilities is described in the HSFR user's manual. The HSFR technical description manual describes these model changes in detail. The algorithm for pump hanger torque which was developed for the HYTRAN pump model is described in the HYTRAN technical description manual.

(a) HSFR Pump Subroutine - Inlet and Torque Analysis - The original HYTRAN pump subroutine included hanger forces due to piston inertia, but not oscillatory forces due to piston pressure. The manufacturer (Abex) of the verification test pump (F-15) had indicated that piston pressure forces were more significant to hanger torque than inertia forces. A more complete calculation of hanger torque was desired to correctly model pump response to changes in load. The improved pump model needed to include hanger torque resulting from piston inertia, piston pressure, and the hanger spring over the entire operating range of controlled hanger (swash) angle, pump shaft speed, and outlet and inlet pressures. Cavitation on the inlet (suction) side and the oscillatory nature of outlet and inlet pressures were important considerations.

It was necessary to compute piston pressure during the complete pump revolution in order to study hanger torque characteristics. The HSFR program basic pump subroutine already included a time domain calculation of piston pressures during the precompression

phase and during the pumping phase when the pump is interacting with a dynamic system load.

The HSFR pump subroutine was expanded to include decompression, calculation of pump inlet flow/pressure dynamics, and calculation of hanger torques due to piston inertia, piston pressure, and the hanger spring. The simulation technique for decompression and inlet flow/pressure calculations is the same time-step calculation used in the precompression and outlet flow calculations of the basic HSFR pump model. Oscillatory inlet pressures are naturally limited to vapor pressure on the negative side of steady state inlet pressure. Accurate calculation of precompression required tracking of cavitation in a piston, if it existed, during the decompression and inlet phases of pump rotation. Calculation of inlet and outlet total oscillatory flow was converted from a parallel technique to a series technique in order to provide continuous tracking of cavitation throughout the full revolution of the pump rotating group.

Calculation of leakage from the pump case into the piston cavity when piston pressure is below nominal case pressure was added, while retaining the original calculation of leakage out of the piston cavity when piston pressure is above case pressure.

(b) Input Data for Return System and Pump Hanger Torque Analysis - Modeling and computation of return system load impedance at the pump inlet is essentially the same as for the pressure side of the system in the basic HSFR main program. The pump inlet is identified as a dummy element (NTYPE = 7, KTYPE = 1). This allows the main program to identify the pump inlet, and to compute and store the return system load impedance at the pump inlet.

The complete HSFR pump model has three subtypes available for use. KTYPE 21 is used when analyzing the pressure side of the system, i.e. no return side model. KTYPE 22 is used for pressure side analysis, but also provides a limited pump inlet analysis sufficient for studying pump hanger torque character-

istics without the need for a return system model. KTYPE 23 is used when analyzing both the pressure and return sides of the system.

Data for the pump is the same for all three pump subtypes. However, for KTYPE's 21 and 22, the system data must contain only the pressure side elements.

New pump input data added for decompression, inlet flow, and torque calculations are

1) hanger offset (HOFF) inches
2) hanger actuator maximum displacement (DISAM) inches
3) actuator lever arm at zero angle (ACTLEVO) inches
4) pumping piston mass (PIMASS) lb-sec^2/inch
5) steady state case pressure (CPRESS) psi
6) case to suction Δp at zero case drain flow (CSPRES) psi
7) diameter of hanger actuator (DIACT) inches

The equation for calculating the actuator lever arm (ACTLEV) at the existing hanger angle is hardmodeled and must be changed to suit the pump being analyzed.

(c) Pump Piston Cylinder Cavitation - Pump inlet flow simulation showed piston cylinder cavitation during decompression at low swash angles, as predicted by Abex. Cavitation was also predicted during inlet port closure just prior to the start of precompression. Transient inlet cavitation also occurred when inlet pressure pulsations were high enough to produce vapor pressure levels, i.e. at a return system resonance condition.

(d) Pump Hanger Torque - The HSFR pump subroutine outputs hanger torque as control pressure (Pc) on the hanger actuator piston. Figure 39 compares the computed and measured actuator control pressure on the F-15 pump. Total actuator control pressure is the result of piston pressure and inertial torque, hanger spring torque, and pump case pressure. Note the increase in pump hanger torque at system resonant pump speeds (2700 and 4050 rpm). Figure 39 shows pump hanger actuator control pressure computed with the 9 ft. test system model. Actuator pressure includes hanger

spring reaction and case pressure. Actuator control pressure is overplotted, as measured in the trombone system which was tuned to produce the same resonant frequencies as the 9 ft. test system. General correlation is quite good, especially at resonant points.

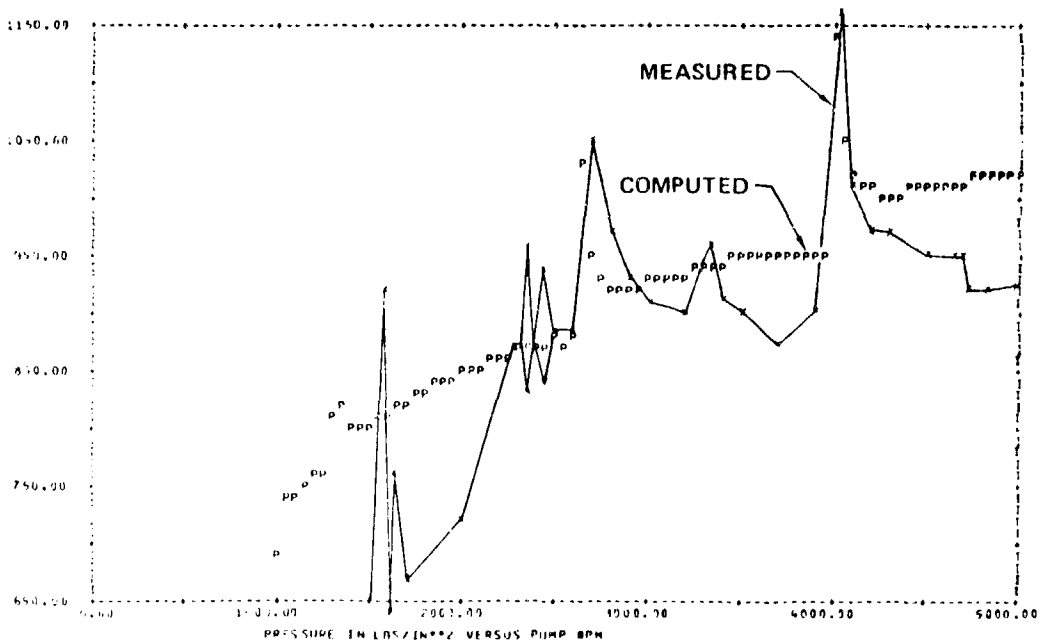

FIGURE 39 HANGER ACTUATOR CONTROL PRESSURE
F-18 PUMP VERIFICATION TEST - SHORT LINE
MIL-H-5606B, 3000 PSI, 110°F, 2.3 GPM

Mechanical resonance of the pump compensator valve was produced by tuning the trombone system to a natural resonance frequency of about 1583 rpm. Peak-to-peak pulsations of 2000 psi were encountered at this condition, and measured compensator valve motion was $\pm$.005 inch.

The high gain compensator valve in the F-15 pump has a relatively low natural frequency. Smaller compensator valves in pumps with normal (slower) response could have a natural frequency in the pump operating speed range. Compensator resonant frequency is another design point which must not coincide with a pump continuous operating speed.

A detailed parametric study of the F-15 pump hanger torque characteristics was conducted using the expanded HSFR program and pump subroutine.

Figure 40 shows average hanger torque at 3600 rpm due to piston pressures as a function of hanger angle, steady state outlet pressure, and oil temperature. Torque due to pumping piston inertial forces are also shown. These torques along with the hanger spring act in the direction of full stroke (maximum hanger angle). The ratio of acceleration to pressure torques agrees with Abex's experience.

The Shuttle (F-14) Abex pump was then modeled in the verification test system to analyze its torque characteristics. Torque characteristics computed by the F-14 pump model are plotted in Figure 41.

Average hanger torque is very sensitive to the pre-compression and decompression pressures, since these pressures act on the hanger at the maximum moment arm via the pistons.

Hanger torque is not significantly affected if the pump inlet flow is computed without dynamic balancing of the inlet flow to the return system load. This allows a hanger torque study to be conducted without having to model the return side of the system.

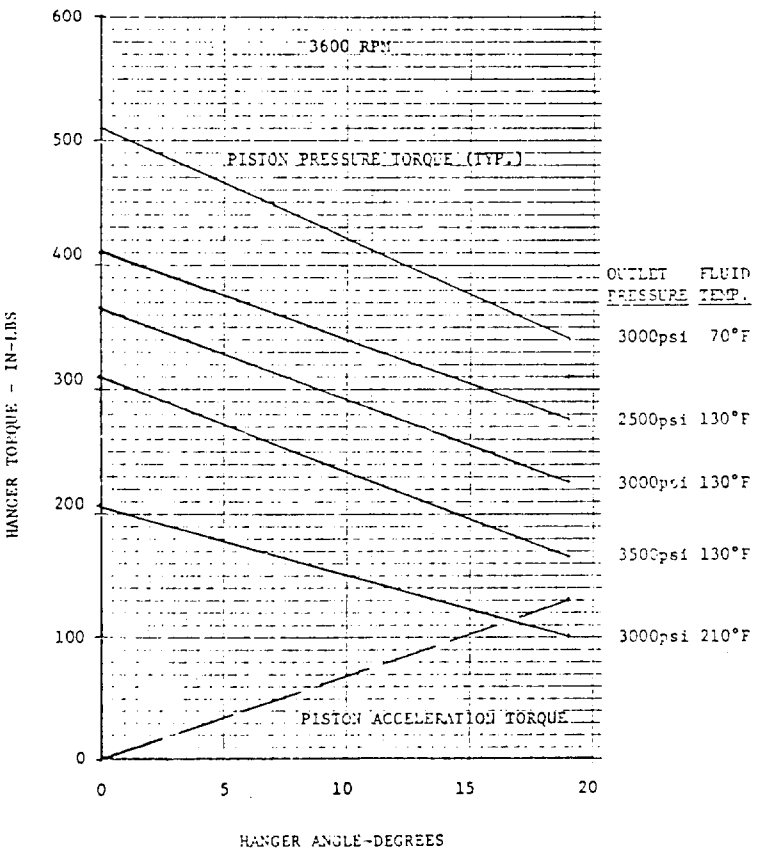

FIGURE 40 F-15 HYDRAULIC PUMP HANGER TORQUE

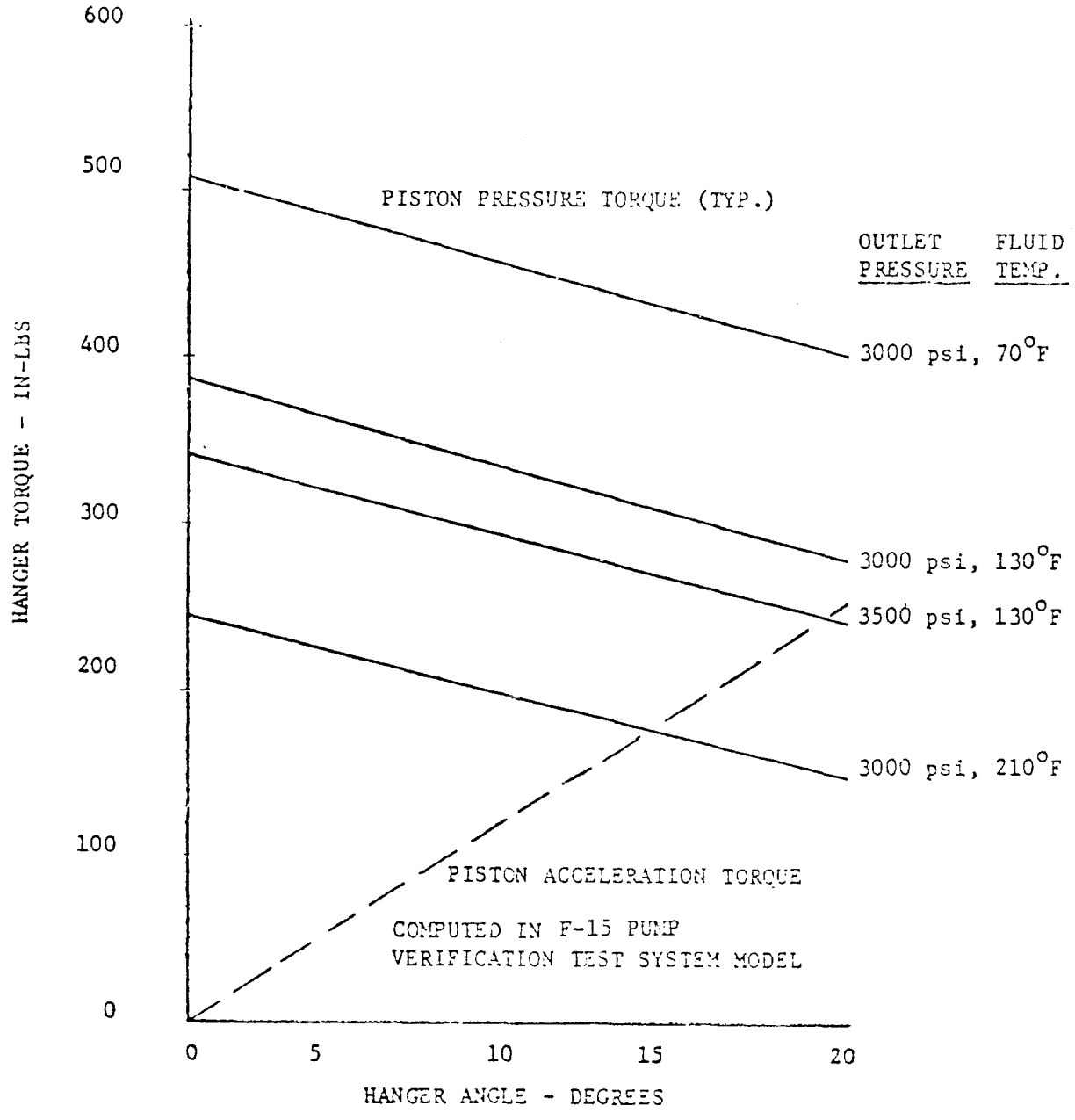

FIGURE 41 F-14 (SHUTTLE) HYDRAULIC PUMP HANGER TORQUE

(e) Effect of Pump Inlet Modeling on Pressure System Pulsations - Figures 42, 43 and 44 show the results of computing oscillatory outlet pressure at the F-15 pump port plate with three different pump inlet models.

The F-15 PC-1 return system is modeled in the same manner as the pressure system, as illustrated in the Volume III user's manual. Figure 42 shows the computed peak oscillatory outlet pressure using a constant pump inlet pressure, i.e., constant pressure at the start of the pre-compression phase.

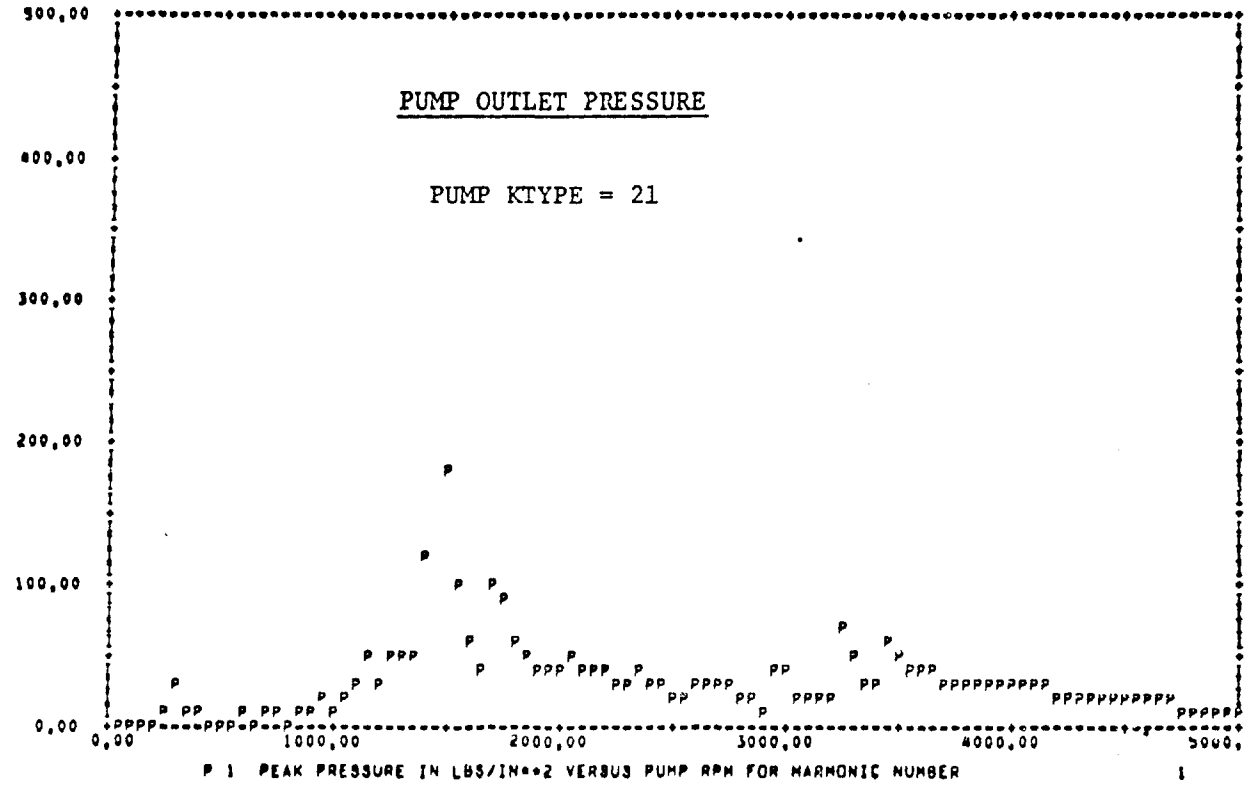

FIGURE 42 F-15 PC-1 PRESSURE SYSTEM FREQUENCY RESPONSE WITH CONSTANT PRESSURE INLET

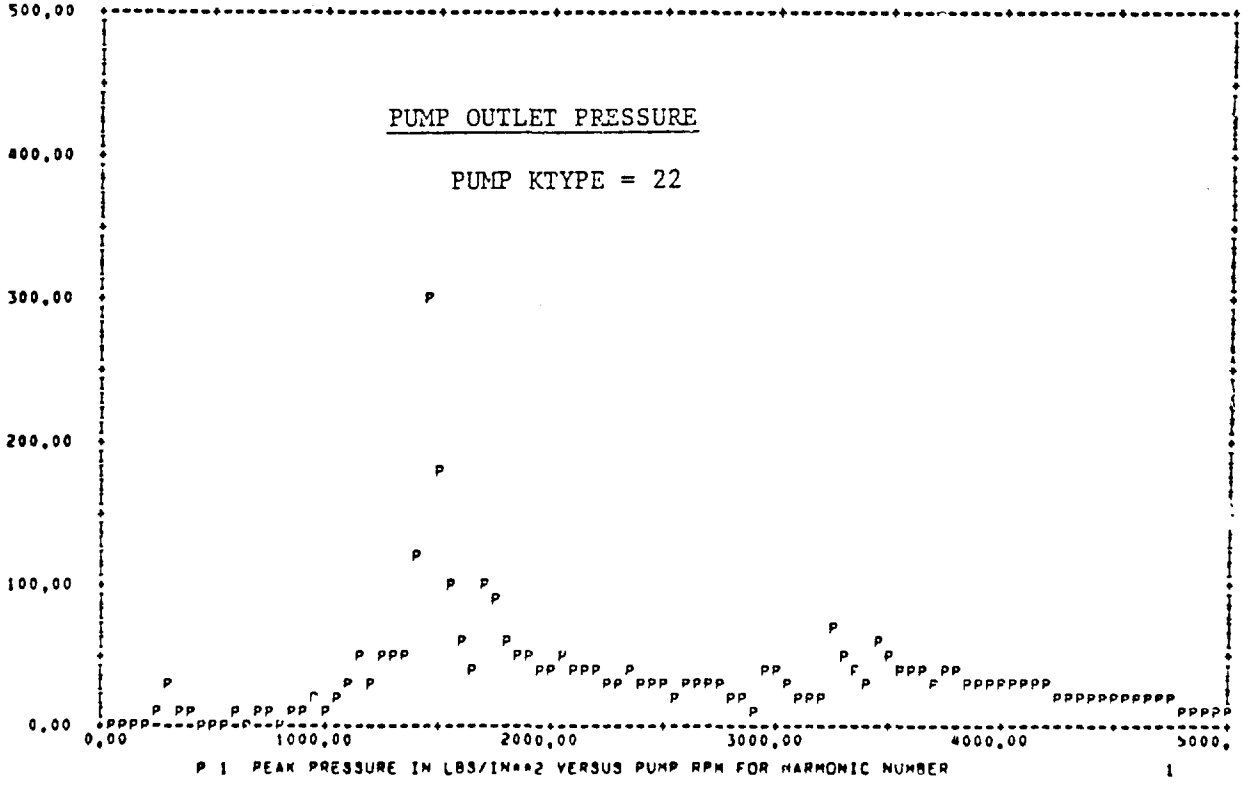

FIGURE 43 F-15 PC-1 PRESSURE SYSTEM FREQUENCY RESPONSE WITH CONSTANT INLET FLOW ANALYSIS

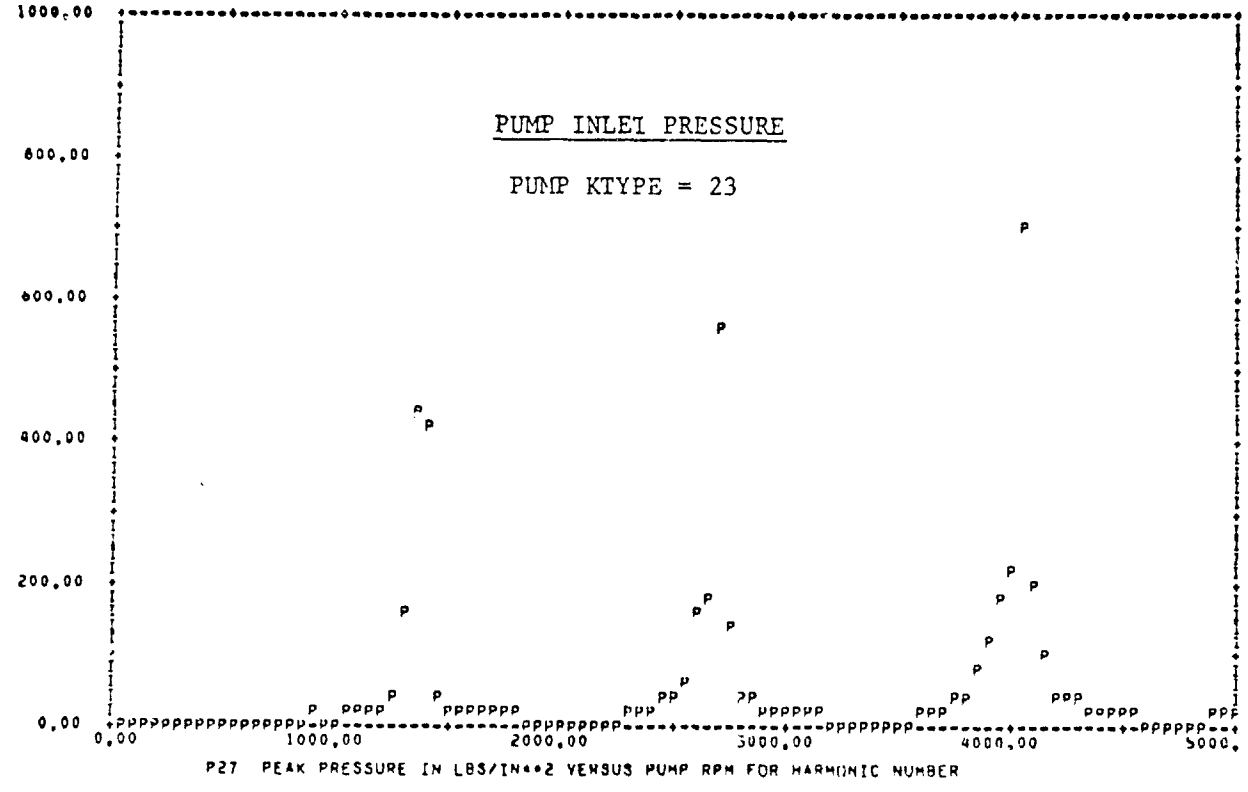

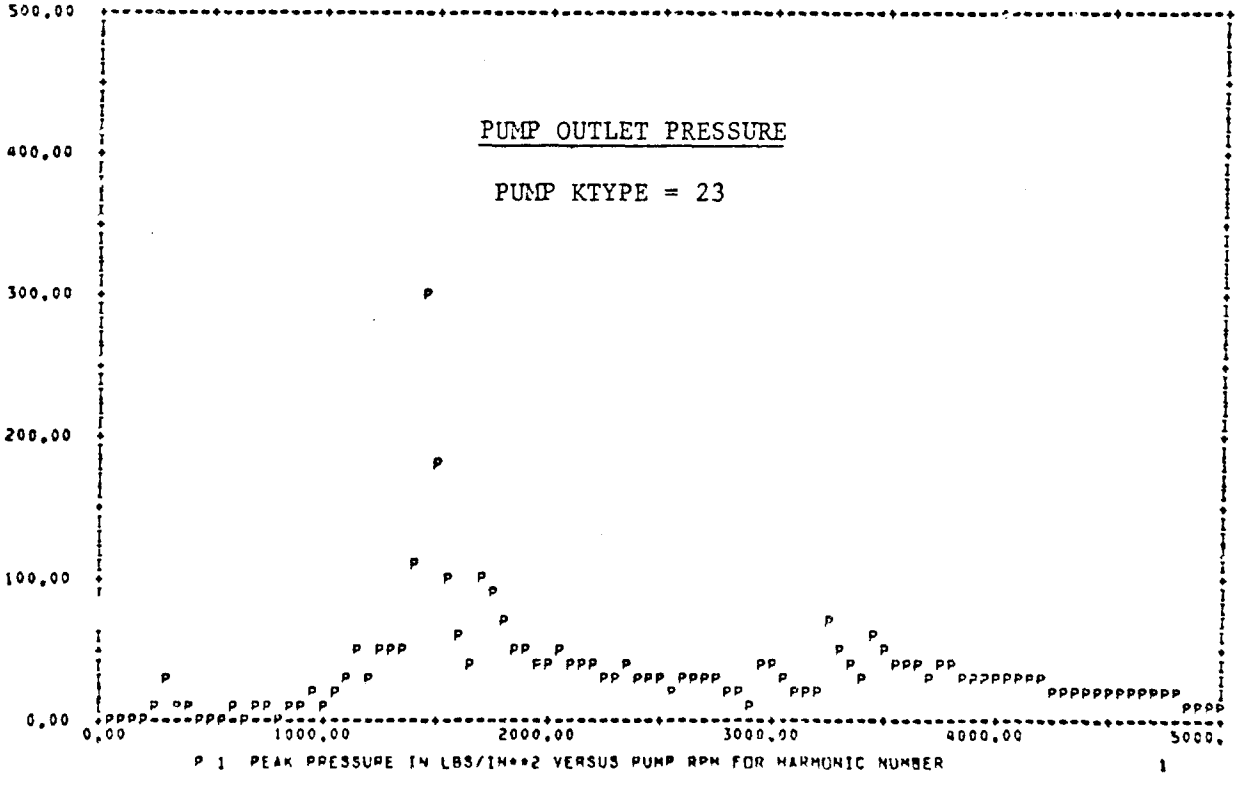

FIGURE 44 F-15 PC-1 PRESSURE SYSTEM FREQUENCY RESPONSE WITH DYNAMICALLY BALANCED INLET/FLOW ANALYSIS

Figure 43 shows the same calculated outlet pressure at the port plate except that a pump inlet flow/pressure analysis is performed based on the inputed constant inlet pressure. This is done by selecting a pump KTYPE = 22, and results in some variation in the initial pressure at the start of precompression.

Figure 44 shows pressure at the pump port plate outlet with a complete dynamic balancing of pump inlet flow and return system load. The inlet analysis is made in the same manner as for the outlet flow, pressure system load. Figure 44 also shows the predicted oscillation pressure at the port plate inlet. Note that the return system has a predicted resonant response at three pump speeds, which are not related to the resonant responses of the pressure system. Verification of inlet system pulsation predictions were not in the scope of the contract. The 400-700 psi peak pulsations predicted in Figure 44 are probably high. However, predicted return system resonant frequencies are probably as accurate as pressure system predicted frequencies.

(f) Pump Precompression: Figure 45 shows typical precompression predicted by the HSFR PUMP subroutine for the F-15 Abex pump. The plotted pressure is the pressure in the piston cylinder at the end of the precompression phase, just before the cylinder cavity communicates with outlet slot in the valve port plate.

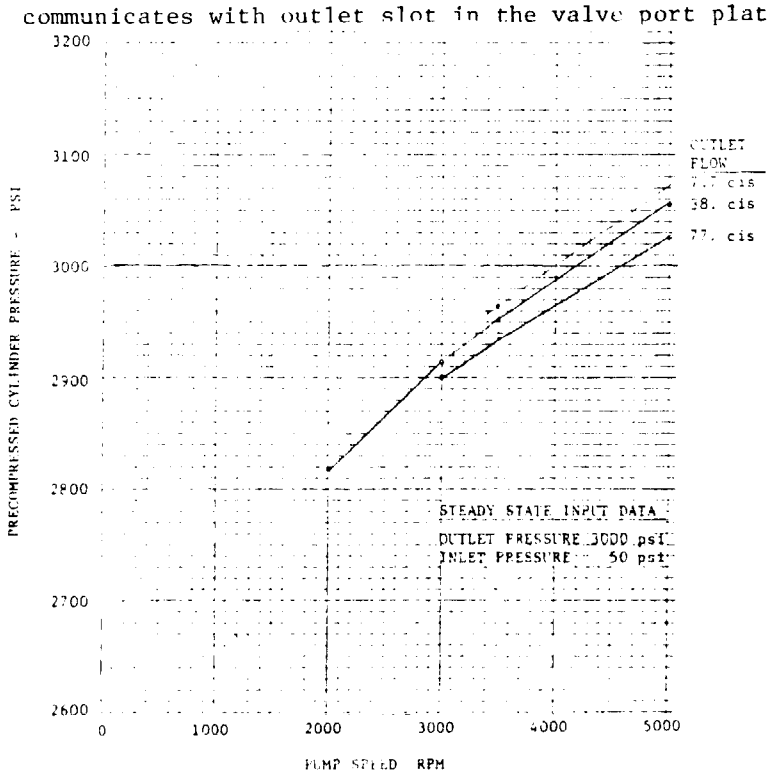

FIGURE 45 COMPUTED PRECOMPRESSION OF F-15 HYDRAULIC PUMP

(3) Miscellaneous HSFR Program Model Developments - Miscellaneous changes and additions made to the HSFR main program and subroutines are listed below.

HSFR Main Program

1) Harmonic of interest selected by input data
2) Acoustic energy analysis capability added
   - Density plots (milliwatts/in^3)
   - Intensity plots (watts)
3) Number of pumping pistons (elements) variable by input data
4) Program run on IBM 360 system
   - changed end of file (EOF) statement
   - changed literal data formats

CDC	IBM
8A10	10A8 (Real *8)
8A10	20A4

5) Pressure/flow phase angle calculation corrected
6) Writing of selected output plots corrected

PUMP Subroutine

1) Added steady state balancing to pump subroutine
   - balances hanger angle (at rated outlet pressure)
   - balances outlet pressure (at maximum hanger angle)
2) Improved sensitivity of pump steady state balancing
3) Modified piston leakage factor for pump inlet flow calculation
   - required to stabilize inlet flow calculation
4) Predefined output plots for studying pump hanger torque, precompression, decompression

WHEQUT Subroutine

1) Revised, made corrections to, and ran Quincke tube subroutine (WHEQUT)

b. HSFR Pump and Basic System Model Verification - Tests were run on two basic test circuit configurations with MIL-H-5606B and MIL-H-83282A fluid. Each of these test series is discussed separately in this section.

(1) Test Set-ups and Circuit Models - Figure 46 is a schematic of the general test circuit used for frequency verification tests. The set-up was essentially the same as used for transient tests. The frequency analysis section of the test circuit is shown in more detail in Figure 47 and 48. Figure 47 shows the detailed dimensions, instrumentation, and configuration of the short, straight, frequency test section (9 ft.) between the pump and load valve. Details of the suction system between the reservoir and pump are also shown. Input data for the short line verification circuit is shown in Figure 49 as an output of the HSFR program.

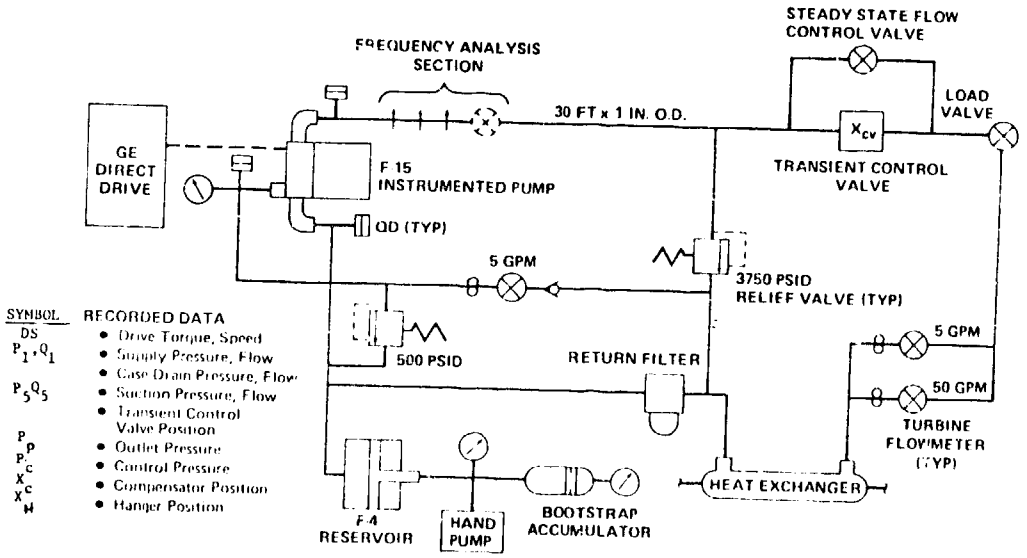

FIGURE 46 HYDRAULIC PUMP VERIFICATION TEST SETUP

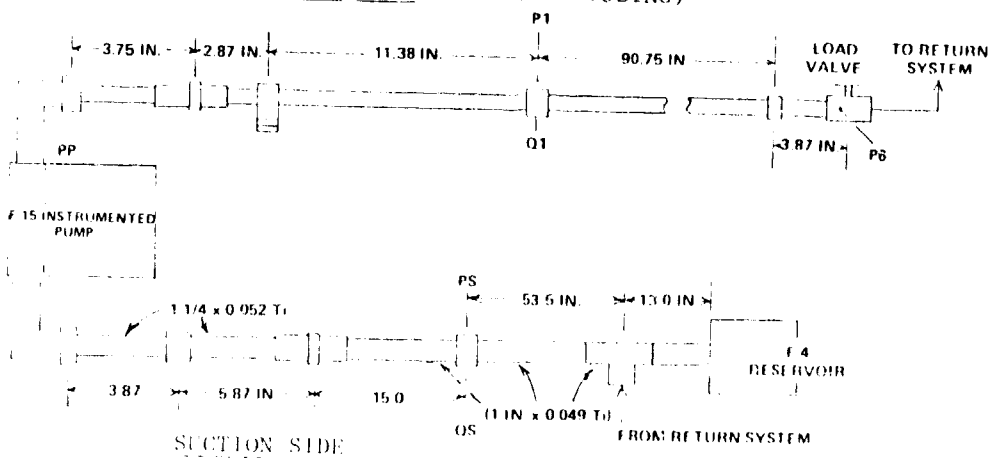

FIGURE 47 9 FT. TEST SYSTEM SCHEMATIC

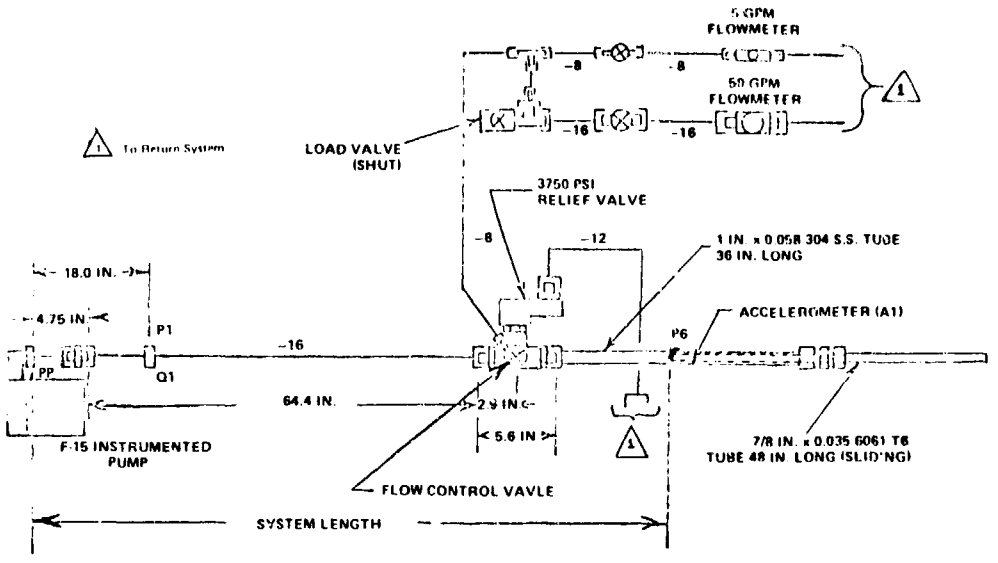

FIGURE 48. SCHEMATIC OF HSFR TROMBONE TEST SYSTEM

Figure 48 shows the details of the trombone frequency analysis test section. The sliding tube permitted the length of the test section and its resonant frequency to be varied with ease. Input data for the trombone verification circuit is shown in Figure 50.

(2) Processing of Frequency Response Data - Digitizing of frequency data through the Biomation waveform analyzer and plotting through the Wang calculator did not produce satisfactory pressure/rpm sweep plots. The basic problems were accurate synchronization of time and rpm signals, and poor resolution due to the long sweep time (one minute). Time did not permit the pursuit of a more accurate method of digitizing frequency response data. Therefore, direct automated overplotting of measured and computed results was not available for frequency response test/model verification.

Overplots were made by manually plotting measured data directly on a reduced computer output plot. Overplots were also made by scaling an analog plot on mylar to the computer plot size, then overlaying the mylar plot on computer plot for shooting a final master. Since manual overplotting is very time consuming, direct comparisons of measured and computed frequency response data is kept to the minimum necessary for basic HSFR program verification. Manual plotting and reproduction distortion introduce some error.

RESPONSE IS CALCULATED FROM 1000.00 TO 3000.00 R.P.M. IN INCREMENTS OF 50.00 R.P.M.
RESPONSE IS PLOTTED FOR THE -FIRST- HARMONIC FREQUENCY
NUMBER OF PUMPING ELEMENTS= 0.

FLUID DATA FOR MIL-H-83282 AT 3000.0 PSIG AND 130.0 DEG F

VISCOSITY = .200E-01 IN**2/SEC
DENSITY = .790E-04 (LB-SEC**2)/IN**4
BULK MODULUS = .223E+06 PSI

ELEMENT NUMBER	N TYPE	K TYPE	PHYSICAL DATA						
1	9	22	.190	.666	1.120	1.172	.698	.570	.160
			.20333	19.50000	3.60000	3.37500	28.75000	26.25000	26.30938	21.750
			50.00000	.06000	.78000	2.07000	.00042	55.00000	190.00000	.690
2	1	-0	6.000	1.200	.100	30000000.000	-0.000	-0.000	-0.000	
3	1	-0	3.500	1.200	.100	30000000.000	-0.000	-0.000	-0.000	
4	1	-0	3.750	1.000	.058	30000000.000	-0.000	-0.000	-0.000	
5	1	-0	2.870	1.000	.058	30000000.000	-0.000	-0.000	-0.000	
6	6	1	-0.000	-0.000	-0.000	-0.000	-0.000	-0.000	-0.000	
7	13	-0	.150	-0.000	-0.000	-0.000	-0.000	-0.000	-0.000	
8	1	-0	11.380	1.000	.058	30000000.000	-0.000	-0.000	-0.000	
9	1	-0	12.000	1.000	.058	30000000.000	-0.000	-0.000	-0.000	
10	1	-0	12.000	1.000	.058	30000000.000	-0.000	-0.000	-0.000	
11	1	-0	12.000	1.000	.058	30000000.000	-0.000	-0.000	-0.000	
12	1	-0	12.000	1.000	.058	30000000.000	-0.000	-0.000	-0.000	
13	1	-0	12.000	1.000	.058	30000000.000	-0.000	-0.000	-0.000	
14	1	-0	12.000	1.000	.058	30000000.000	-0.000	-0.000	-0.000	
15	1	-0	12.000	1.000	.058	30000000.000	-0.000	-0.000	-0.000	
16	1	-0	6.750	1.000	.058	30000000.000	-0.000	-0.000	-0.000	
17	1	-0	3.870	1.000	.058	30000000.000	-0.000	-0.000	-0.000	
18	14	-0	780.000	7.730	-0.000	-0.000	-0.000	-0.000	-0.000	

FIGURE 49 HSFR INPUT DATA FOR SHORT LINE TEST CIRCUIT

HYDRAULIC SYSTEM FREQUENCY RESPONSE PROGRAM
FREQUENCY RESPONSE-F-15 PUMP VERIFICATION TEST-TROMBONE

RESPONSE IS CALCULATED FROM 1000.00 TO 5000.00 R.P.M. IN INCREMENTS OF 50.00 R.P.M.
RESPONSE IS PLOTTED FOR THE -FIRST- HARMONIC FREQUENCY
NUMBER OF PUMPING ELEMENTS= 9.

FLUID DATA FOR MIL-H-83282 AT 3000.0 PSIG AND 210.0 DEG F

VISCOSITY = .744E-02 IN**2/SEC
DENSITY = .770E-04 (LB-SEC**2)/IN**4
BULK MODULUS = .173E+06 PSI

ELEMENT NUMBER	N TYPE	K TYPE	PHYSICAL DATA						
1	9	22	.190	.666	1.120	1.172	.698	.570	.160	
			.20300	19.50000	3.38000	3.37500	28.75000	26.25000	26.80688	21.7500
			50.00000	.06000	.78000	2.07000	.00342	55.00000	150.30000	.6900
2	1	-0	6.000	1.200	.100	30000000.000	-0.000	-0.000	-0.000	
3	1	-0	3.500	1.200	.100	30000000.000	-0.000	-0.000	-0.000	
4	1	-0	16.000	1.000	.058	30000000.000	-0.000	-0.000	-0.000	
5	1	-0	12.000	1.000	.058	30000000.000	-0.000	-0.000	-0.000	
6	1	-0	12.000	1.000	.058	30000000.000	-0.000	-0.000	-0.000	
7	1	-0	12.000	1.000	.058	30000000.000	-0.000	-0.000	-0.000	
8	1	-0	12.000	1.000	.058	30000000.000	-0.000	-0.000	-0.000	
9	1	-0	3.150	1.000	.058	30000000.000	-0.000	-0.000	-0.000	
10	1	-0	2.900	1.000	.100	30000000.000	-0.000	-0.000	-0.000	
11	6	1	-0.000	-0.000	-0.000	-0.000	-0.000	-0.000	-0.000	
12	14	-0	1560.000	1.900	-0.000	-0.000	-0.000	-0.000	-0.000	
13	6	1	-0.000	-0.000	-0.000	-0.000	-0.000	-0.000	-0.000	
14	11	-0	1.000	1.000	.100	30000000.000	-0.000	-0.000	-0.000	
15	1	-0	2.700	1.000	.100	30000000.000	-0.000	-0.000	-0.000	
16	1	-0	12.000	1.000	.058	30000000.000	-0.000	-0.000	-0.000	
17	1	-0	12.000	1.000	.058	30000000.000	-0.000	-0.000	-0.000	
18	1	-0	11.000	1.000	.058	30000000.000	-0.000	-0.000	-0.000	
19	11	-0	.500	1.000	.058	30000000.000	-0.000	-0.000	-0.000	

FIGURE 50 HSFR INPUT DATA FOR TROMBONE TEST CIRCUIT

(3) MIL-H-5606B/9 Ft. System Tests - Figures 51 through 54 show overplots of measured and computed peak pressure pulsations at the inlet of element #9, i.e. P1 in the 9 ft. test circuit. These figures show fundamental frequency pressure pulsations for 0, .5, 2., and 10. gpm steady state flows, respectively. Test conditions were 130°F oil temperature and 3000 psig steady state pump outlet pressure.

Frequency correlation is about 0-2% (0 to 100 rpm) for the 2nd and 3rd resonant speeds. A 2% correlation is good considering possible errors due to temperature shift during the run, circuit length errors, and fluid property and instrumentation errors. Prediction of the first resonant point appears to be about 200 rpm too low. However, this first predicted resonant point is below the natural frequency of the pump compensator valve, as determined during the test series. Measured pressure response below the valve natural frequency (1500 rpm) is washed out, and therefore does not correlate to the computed first resonance, since compensator dynamics are not modeled.

Resonant frequencies of the 9 ft. test circuit are consistent with theory for a line terminated by a fixed orifice, and are only partially dependent on the flow at the load valve.

Measured and predicted resonances correlate well to that computed for the total line length from the pump port plate to the load valve.

$$N = \frac{20}{3} \quad (f_1)$$

where: $f_1 = \frac{c}{2L}$ for a half-wave characteristic

N = pump speed (rpm)

f_1 = fundamental frequency of circuit (cps)

C = acoustic velocity in fluid

= 53,113 in/sec at 130°F

L = circuit length (in)

= 124.1 in.

Harmonic responses (f_2, f_3,...) occur in multiples of the fundamental frequency. Predicted pump speed for the fundamental resonance of the 9 ft. test circuit is 1300 rpm. This is consistent with measured 2nd, and 3rd resonances of 2550 and 3900 rpm.

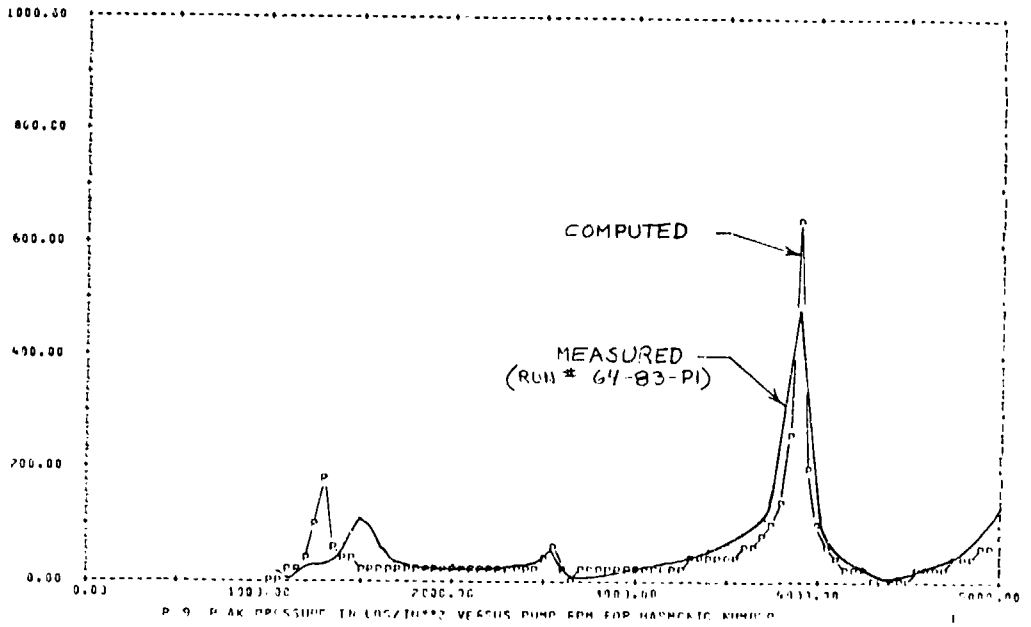

FIGURE 51 COMPUTED VS. MEASURED P1 PRESSURE FREQUENCY RESPONSE
F-15 PUMP VERIFICATION TEST - SHORT LINE
MIL-H-5606B DATA PER NRC OF CANADA
3000 PSI, 130°F 0 GPM

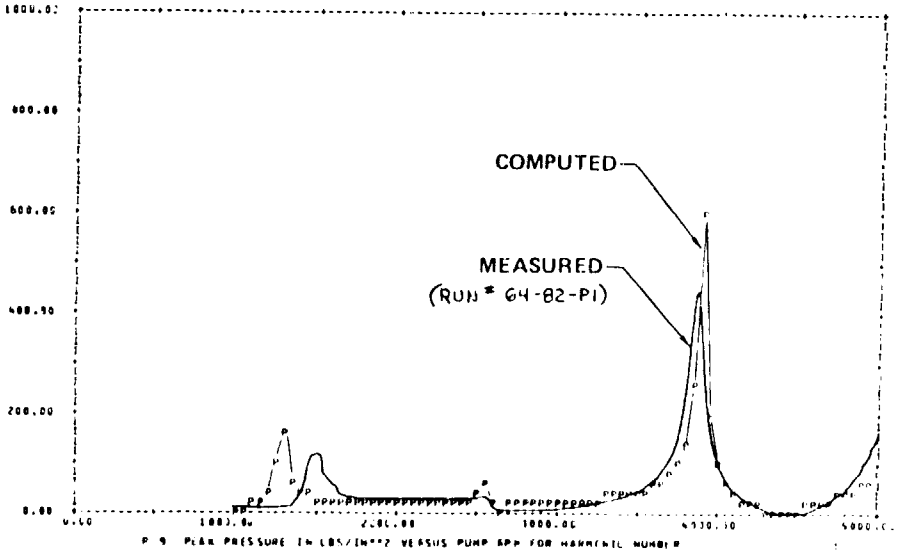

FIGURE 52 COMPUTED VS. MEASURED P1 PRESSURE FREQUENCY RESPONSE
F-15 PUMP VERIFICATION TEST - SPORT LINE
MIL-H-5606B DATA PER NRC OF CANADA
3000 PSI, 130°F, 0.5 GPM

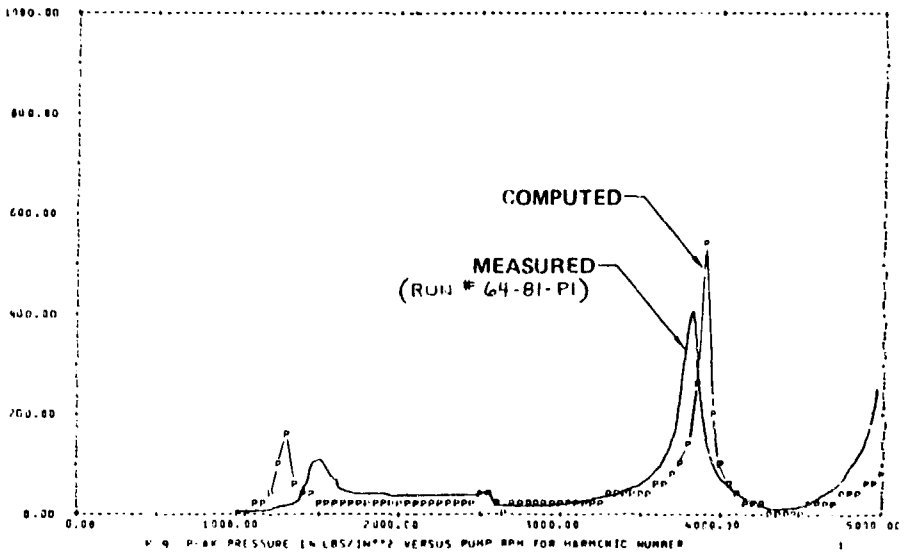

FIGURE 53 COMPUTED VS. MEASURED P1 PRESSURE FREQUENCY RESPONSE
F-15 PUMP VERIFICATION TEST - SHORT LINE
MIL-H-5606B DATA PER NRC OF CANADA
3000 PSI, 130°F, 2 GPM

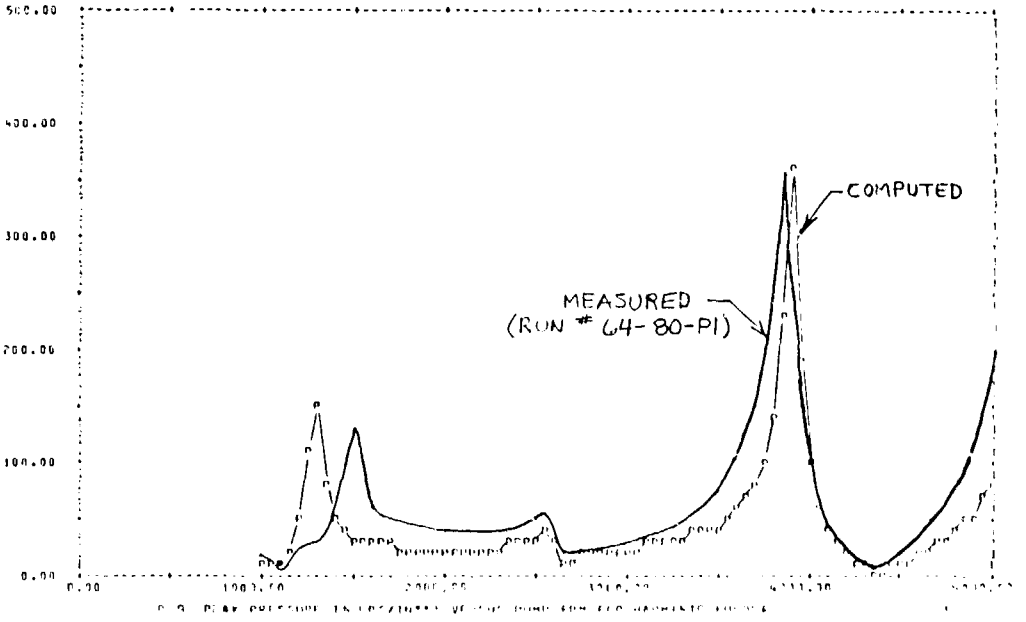

FIGURE 54 COMPUTED VS. MEASURED P1 PRESSURE FREQUENCY RESPONSE
F-15 PUMP VERIFICATION TEST - SHORT LINE
MIL-H-5606B DATA PER NRC OF CANADA
3000 PSI, 130°F, 10 GPM

The computed standing pressure wave at the 3900 rpm resonance point is plotted in Figure 55 for each of the various test flow rates from 0 to 20 gpm. Measured values at "P1" are also plotted. Pressure amplitudes, computed and measured, decrease with increasing flow even though pump studies indicate that precompression/outlet pressure mismatch increases as the hanger angle increases. Decreased termination impedance as the load valve is opened to higher flows reduces the acoustic reflections at the valve such that there is a net reduction in the standing wave amplitude. An increase in pressure amplitude with increasing flow has been observed in a long line simple test circuit and in multi-branch aircraft systems. Note that the standing wave location, i.e. resonant frequency of 3900 rpm, is unaffected by the steady state valve flow rate. The oscillating pressure amplitude at the "P1" instrumentation point location was about 1/2 maximum for the 3rd (3900 rpm) resonance point, and near zero at the 2nd resonance point (2550 rpm).

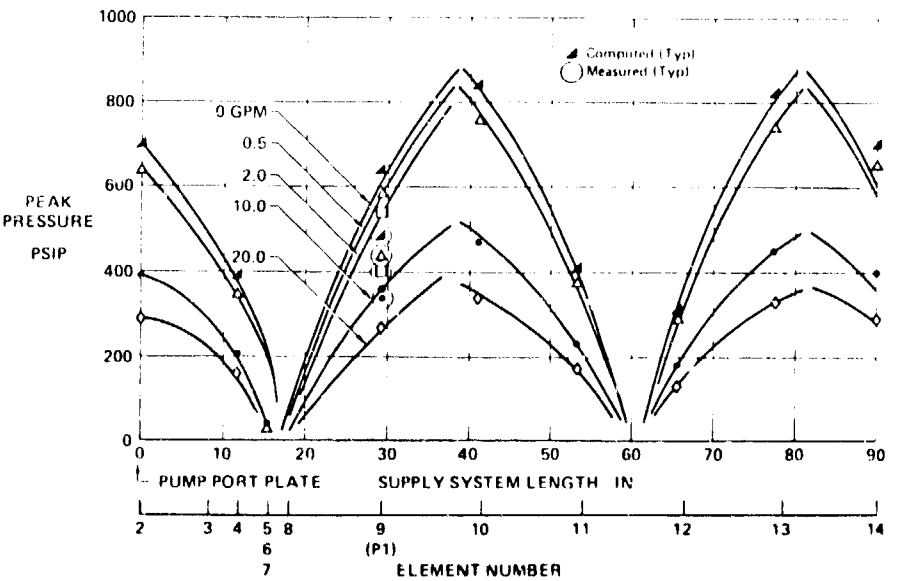

FIGURE 55 FREQUENCY RESPONSE
F-15 PUMP VERIFICATION TEST - SHORT (9 FT.) LINE
STANDING PRESSURE WAVE FOR RESONANT
FREQUENCY AT 3900 RPM

Figure 56 shows the effect of oil temperature on system resonance. The 3rd resonant speed was decreased from 3900 to 3500 rpm for an oil temperature change from 130°F to 210°F. This shift brings the 4th resonant frequency into the range of the plot.

Figure 56 also shows the effect of modeling the pump and pump manifold as a volume instead of a line. The change reduced the accuracy of predicted amplitudes and frequencies. Figure 57 shows a comparison of computed and measured pressure pulsations for the 2nd multiple of the pumping frequency at 0 gpm and 130°F. This is entitled harmonic number 2 on the computer plot, although more conventional terminology would refer to it as the 1st harmonic of the fundamental frequency. Frequency correlation is about the same as for the fundamental frequency, however, amplitude prediction is less accurate. Measured response at 3800 rpm was apparently too sharp to be plotted with a plot increment width of 50 rpm. Second harmonic content (at 1950 rpm) was about 120 psi at the frequency of the third circuit resonance (585 hz). However, much higher pressure (500 psi) was generated when the pump operated at 3900 rpm providing a fundamental pumping frequency of 585 hz, i.e. the third circuit resonance.

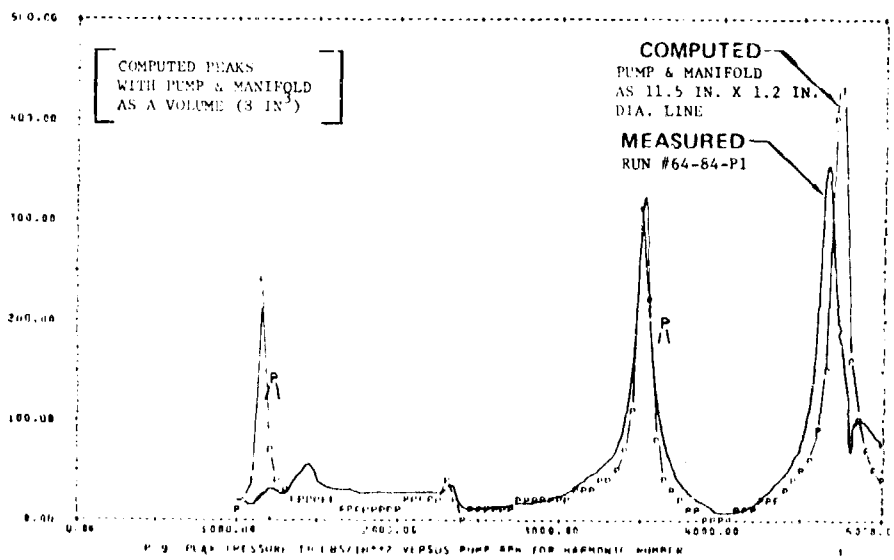

FIGURE 56 COMPUTED VS. MEASURED P1 PRESSURE FREQUENCY RESPONSE
F-15 PUMP VERIFICATION TEST - SHORT LINE
MIL-H-5606B DATA PER NRC OF CANADA
3000 PSI, 210°F, 0.5 GPM

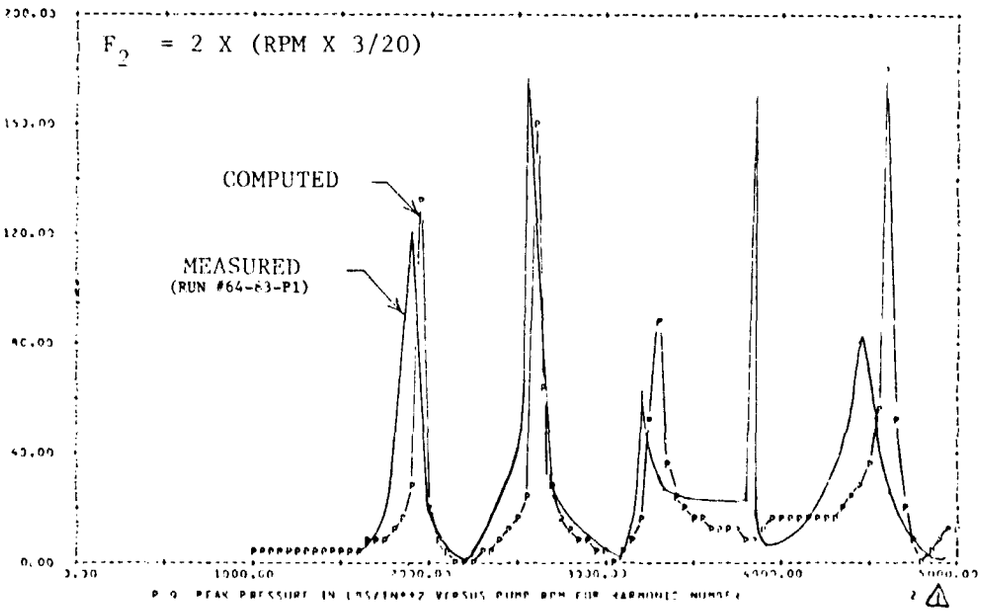

FIGURE 57 COMPUTED VS. MEASURED P1 PRESSURE FREQUENCY RESPONSE
F-15 PUMP VERIFICATION TEST - SHORT LINE
MIL-H-5606B DATA PER NRC OF CANADA
3000 PSI, 130°F, 0 GPM - 2ND HARMONIC

(4) MIL-H-83282A/9 Ft. System Tests - Figure 58 shows an overplot of computed and measured fundamental pressure at the "P1" location for a 2 gpm flow and 130°F oil temperature. Computed response is based on fluid properties derived from Air Force Report AFML-TR-73-81.

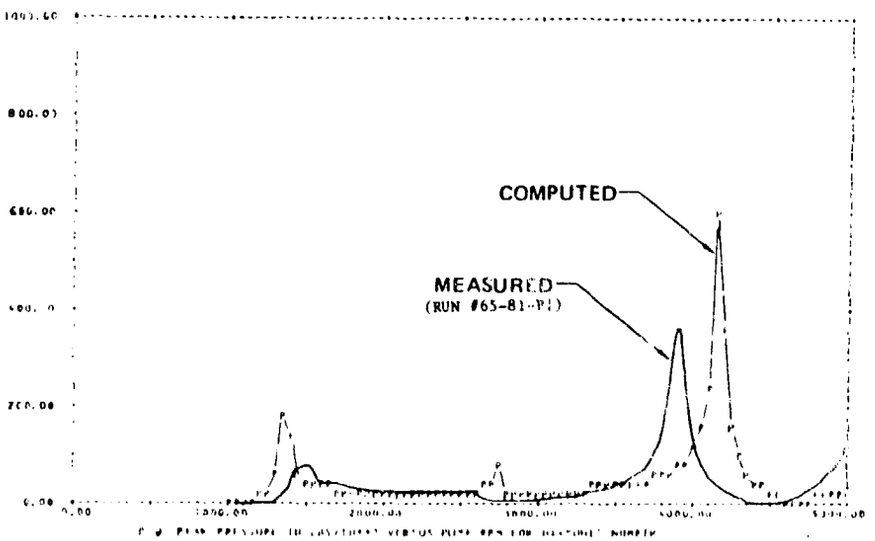

FIGURE 58 COMPUTED VS. MEASURED P1 PRESSURE FREQUENCY RESPONSE
F-15 PUMP VERIFICATION TEST - SHORT LINE
MIL-H-83282 DATA PER AFML-TR-73-81
3000 PSI, 130°F, 2 GPM

Measured resonant frequencies with MIL-H-83282A fluid in the test stand were 200 to 300 rpm lower than those predicted by the HSFR program. Rockwell International reported similar lack of correlation in their HSFR analysis and testing of the shuttle orbiter hydraulic system. MCAIR believes that the error is primarily the result of adiabatic bulk modulus data used in the FLUID subroutine, which was based on the AFML report. The report values were computed from measured isothermal secant bulk data. Figure 59 compares measured results for both oils in the same 9 ft. test system with identical test conditions. This indicates that the bulk modulus for 83282 oil is slightly higher than for MIL-H-5606B oil.

Only two sources of bulk modulus data for the 83282 fluid are known at this time.

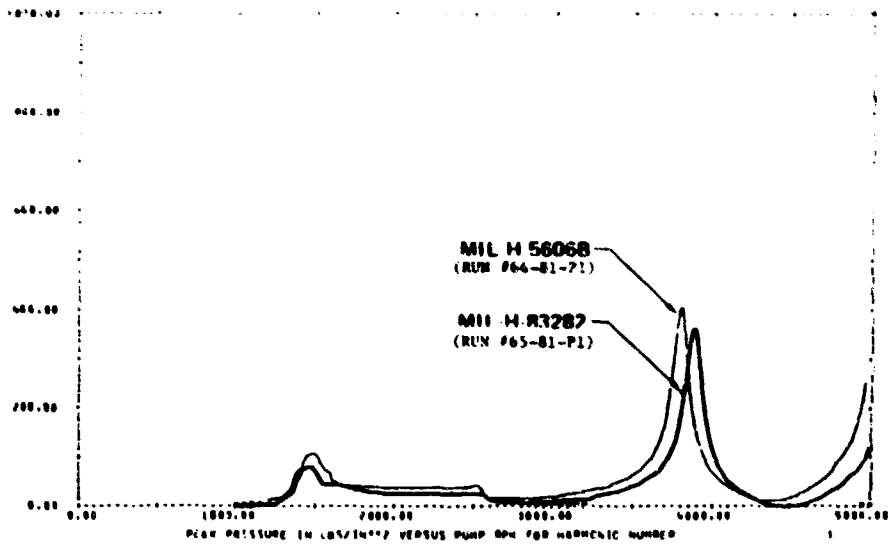

FIGURE 59 COMPARISON BETWEEN MIL-H-5606B AND MIL-H-83282 IN THE SHORT LINE TEST CIRCUIT MEASURED FREQUENCY RESPONSE F-15 PUMP VERIFICATION TEST -SHORT LINE MIL-H-5606B AND MIL-H-83282 3000 PSI, 130°F, 2 GPM

Air Force Materials Laboratory (AFML)

Isothermal secant bulk modulus was measured at 100°F for pressures from 0 - 10,000 psi at Penn State University under an Air Force contract. The AFML used Penn State data from four samples of early formulations of the 83282 fluid to compute adiabatic tangent bulk modulus for various temperatures and pressures. Values computed by the AFML were published in Ref (a).

National Research Council (NRC) of Canada

Adiabatic tangent bulk modulus is determined directly from acoustic velocity measurements. NRC data for MIL-H-83282A (Hanover Chemical Co.) and red oil (sample unknown) are presented in Figure 60. Table 1 compares computed results with the two oils using various data sources for adiabatic tangent bulk modulus. Computed frequency response is compared to the measured response for the resonant speed in the 3600-4200 rpm range. Predicted resonant speed is more accurate with the NRC data for MIL-H-83282A oil, i.e. about 100 rpm high at 130°F. Predicted resonant speed using the red oil bulk data (NRC) for MIL-H-83282A is only 50 rpm higher than the measured value at 130°F.

In May 1976 there were four approved suppliers for MIL-H-83282A fluid; Mobil, Royal, Hanover, Bray. MCAIR verifications tests have been run so far with the Royal fluid. The MCAIR hydraulics lab also has Mobil fluid in stock. Until new data is available on MIL-H-83282A fluid, red oil bulk data (NRC) is recommended for HSFR analysis.

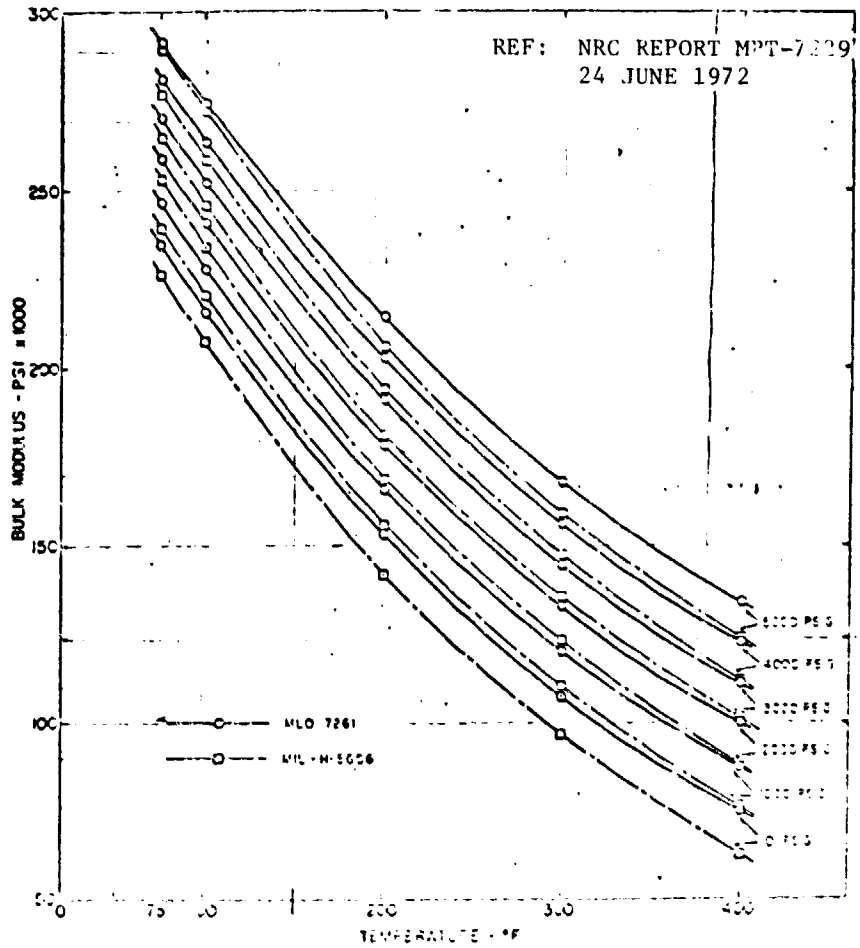

FIGURE 60 ADIABATIC TANGENT BULK MODULUS FOR MLO 7261 AND MIL-H-5606

TABLE 1

COMPARISON OF FREQUENCY RESPONSE PREDICTIONS WITH VARIOUS BULK MODULUS DATA

	Resonant Speed/Amplitude (RPM/PSI)	
MIL-H-5606B	130°F	210°F
TEST	3850 rpm/410 psi	3525 rpm/320 psi
COMPUTED NRC data bulk modulus	3900 /540 (223,000 psi)	3500 /310 (173,000 psi)
MIL-H-83282A		
TEST	3900 /360	3600 /250
COMPUTED AFML data	4150 /600 (250,000 psi)	3850 /480 (195,000 psi)
NRC data	4000 /420 (232,000)	3750 /540 (184,000)
NRC data for MIL-H-5606B	3950 /560 (223,000 psi)	3650 /480 (173,000 psi)

(5) MIL-H-83282A/Trombone System Tests - Figure 61 compares computed and measured peak pressure pulsations in the trombone system at the inlet to element number 5, i.e., P1 in Figure 48. The error in predicted frequency is the same as for MIL-H-83282A fluid in the 9 ft. system. Predicted amplitude is about 90% above the measured value for the 3rd resonant frequency.

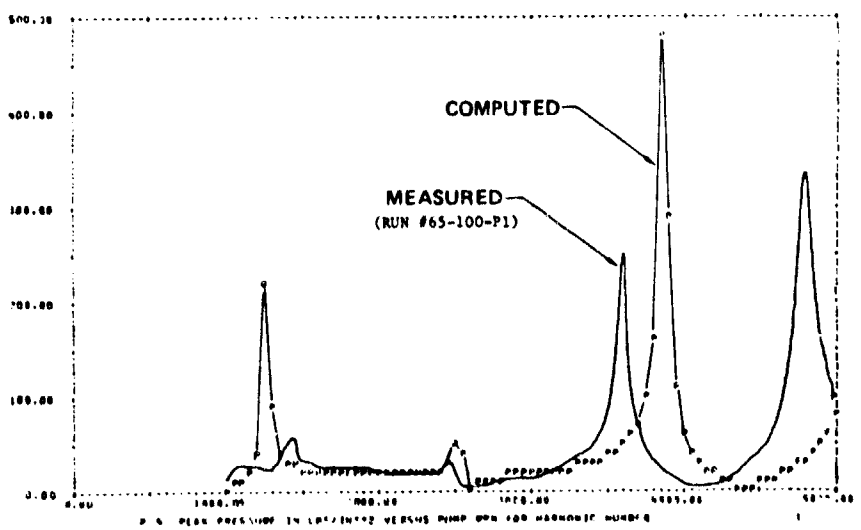

FIGURE 61 COMPUTED VS. MEASURED P1 PRESSURE FREQUENCY RESPONSE
F-15 PUMP VERIFICATION TEST - SHORT LINE
MIL-H-5606B DATA PER NRC OF CANADA
3000 PSI, 210°F, 0.5 GPM

Figure 62 shows computed and measured pressure at the closed end of the test section. Results are consistent with those on the other test system and at the P1 location. Axial acceleration levels at the closed end of the circuit were measured to verify the assumption that dynamic flow is zero at the end of a closed branch. Accelerometer (A1) readings are shown in Figure 63. Axial "g" level was less than 12 g's at the resonant speed of 3550 rpm.

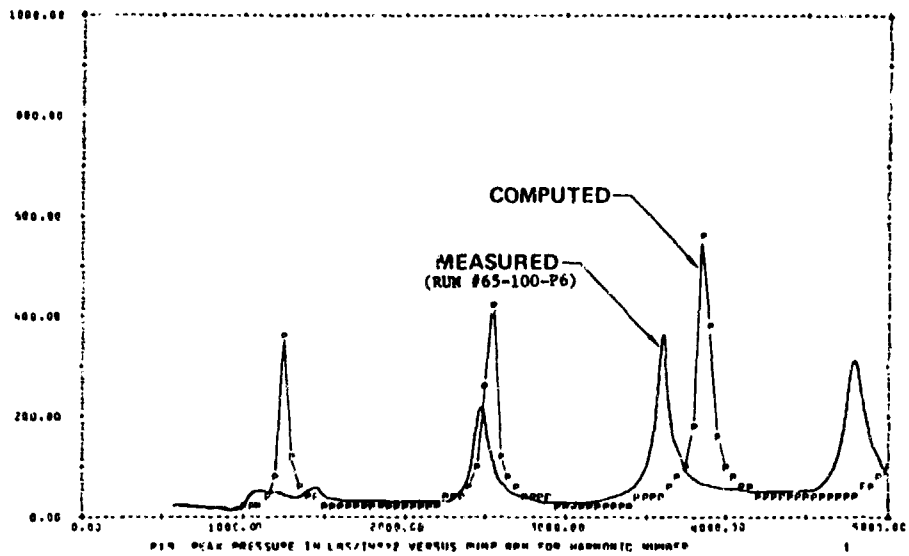

FIGURE 62 COMPUTED VS MEASURED P6 PRESSURE
FREQUENCY RESPONSE
F-15 PUMP VERIFICATION-TROMBONE
MIL-H-83282 DATA PER AFML-TR-73-81
3000 PSI, 210°F, 0.5 GPM
CLOSED END OF TROMBONE

c. CONCLUSIONS

1) System resonant frequency locations predicted by the HSFR program are accurate within about 2% (100 rpm in 5000 rpm) for a simple short line system.

2) Predicted amplitude of oscillating pressure at system resonant frequencies range from 0 to 30% high, i.e. above actual measured pressure pulsations.

3) The accuracy of predicted pressure amplitude at system resonant frequencies decreases for 2nd and higher harmonics of the pumping frequency.

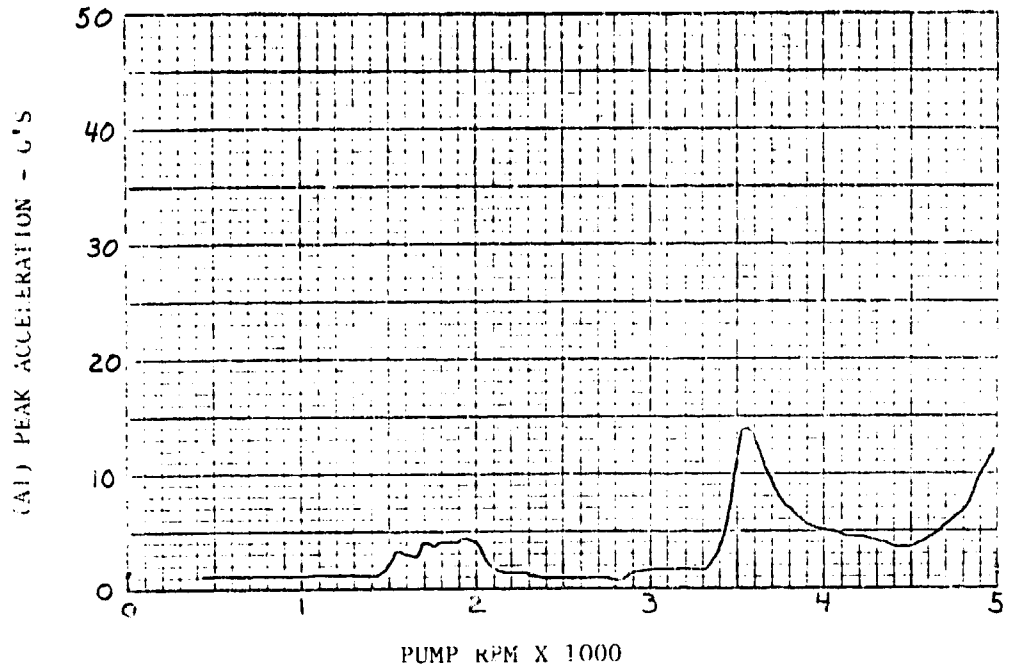

FIGURE 63 F-15 HYDRAULIC PUMP
RUN 79 TROMBONE SYSTEM-MIL-H-83282A
7.7 CIS, 102°F

4) Predicted and measured amplitudes of resonant pressure level decreased with increasing steady state flow from 0 to 10 gpm in the simple short line test circuit. Reduced reflections at the load valve as flow was increased resulted in a net reduction of standing pressure wave amplitude, even though pump predicted pre-compression characteristics degrade with increasing flow for a given shaft speed. An increase in pulsations with higher flow, i.e. the opposite effect, is observed in a single long line test circuit and in full scale iron bird systems comprised of multiple long-line branches. Pump precompression is apparently more significant to pulsation levels than is the change in dynamic load with increasing flow in a long line multibranch system.

5) Resonant frequency locations were unaffected by the pump steady state flow level from 0 to 10 gpm in the short line test system.

6) An 80° increase in oil temperature decreased the system resonant frequency locations by about 400 rpm (pump shaft speed).

7) The internal outlet passages of the F-15 pump port cap and manifold should be modeled as lengths of line (outlet size) rather than as a lumped volume.

8) The use of adaibatic bulk modulus data for MIL-H-5606B hydraulic fluid is recommended when performing HSFR analysis of systems using MIL-H-83282A fluid. The FLUID subroutine is currently programmed in this manner.
9) The HSFR program/PUMP subroutine can be used effectively to study pump hanger torque, port plate valve timing, and piston cylinder cavitation characteristics. Model predictions indicate that the F-15 pump has good overall precompression characteristics throughout the operating range of shaft speed and flow delivery, especially when considering the many variables involved. Predicted decompression results in a slight cavitation condition in the cylinder for all flow rates up to 40 gpm. Such a characteristic is probably good in that acoustic source energy in the return syytem is relatively constant regardless of operating conditions.
10) The HSFR program may be used to study resonance characteristics of a hydraulic suction/return system. However, return system frequency analysis was not part of the contract scope, and is not verified. The accuracy of resonant frequency predictions in the return system should be reasonably good, owing to the use of the same computation method and models as are used for pressure system analysis. The accuracy of predicted amplitude for return system resonance is unknown. Additional pump model development may be required to more accurately represent case to cylinder leakage during the suction phase of the barrel revolution.

2. PULSCO ACOUSTIC FILTER MODEL VERIFICATION

This section covers the development and verification of an HSFR computer program model for a hydraulic system acoustic filter designed and manufactured by the PULSCO Division, American Air Filter Co., Louisville, Kentucky. The test unit is identified as Model ATP-1, P/N 206001-003G, S/N 453. The basic ATP-1 design is sized for and used in a 10 gpm system on the L-1011 commercial transport. Steady state ΔP is about 100 psi at 10 gpm.

Tests were run in the 9 ft. straigh-line test circuit used for verification of the basic HSFR program and F-15 pump. Two test unit locations were used; unit mounted near the pump manifold outlet port, unit mounted 3 1/2 ft. downstream of pump outlet port.

A math model of the PULSCO device was derived as shown in Figure 64. The unit is represented as three lumped volumes and three lines, interconnected as two parallel flow paths. The model is derived by combining the dynamics of three basic HSFR program elements; lumped volumes, lines, and branches. The 2 x 2 matrix equation relates dynamic pressure and flow across the unit. A detailed derivation of the model is contained in the HSFR technical description manual, AFAPL-TR-76-43, Vol. IV.

The math model technique is the same as used for the Quincke tube model (WHEQUT subroutine).

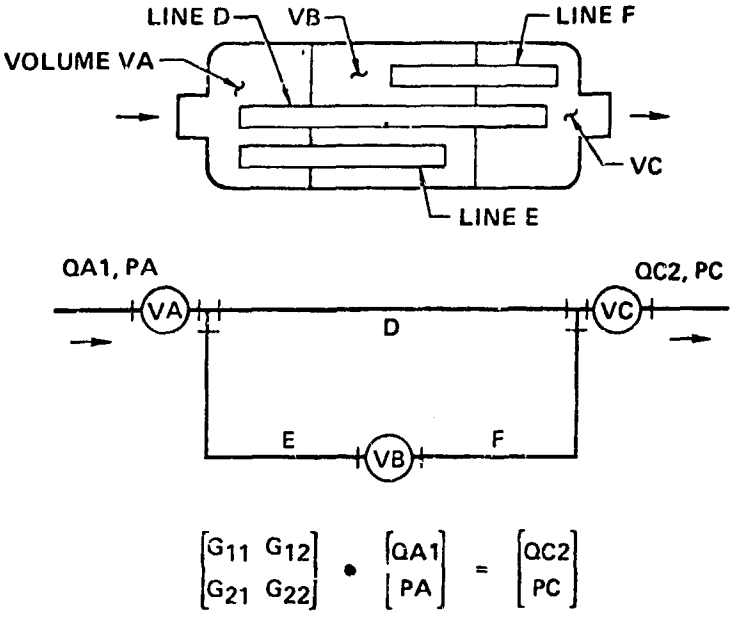

$$\begin{bmatrix} G_{11} & G_{12} \\ G_{21} & G_{22} \end{bmatrix} \bullet \begin{bmatrix} QA1 \\ PA \end{bmatrix} = \begin{bmatrix} QC2 \\ PC \end{bmatrix}$$

FIGURE 64 PULSCO HYDRAULIC ACOUSTIC FILTER COMPUTER MODEL FOR HSFR PROGRAM

Figure 65 is a simplified schematic of the verification test set-up showing the two PULSCO unit locations for which tests were run. Tests were run with MIL-H-83282A fluid. Figure 66 is a listing of input data for the test set-up with the PULSCO unit in the upstream position.

Design cut-off frequency for the ATP-1 is 800 Hz (5333 rpm). Cut-off frequency is defined as the frequency above which attenuation of pressure pulsations is 90% or higher, i.e., the pressure pulsation level transmitted downstream of the unit is less than 10% of the input level. Direct verification of this characteristic would require testing of the PULSCO unit in a circuit with a low termination impedance, i.e., minimum reflecting at the termination.

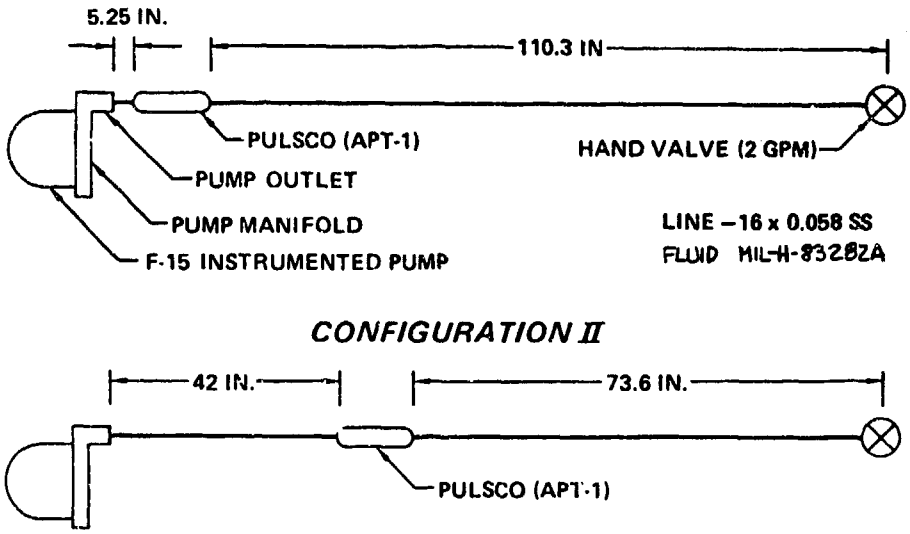

FIGURE 65 PULSCO ACOUSTIC FILTER FREQUENCY VERIFICATION TEST SET-UP

RESPONSE IS CALCULATED FROM 50.00 TO 3000.00 R.P.M. IN INCREMENTS OF 50.00 R.P.M.
RESPONSE IS PLOTTED FOR THE -FIRST- HARMONIC FREQUENCY
NUMBER OF PUMPING ELEMENTS= 9.

FLUID DATA FOR MIL-H-83282 AT 3000.0 PSIG AND 130.0 DEG F

VISCOSITY = .200E-01 IN**2/SEC
DENSITY = .790E-04 (LB-SEC**2)/IN**4
BULK MODULUS = .223E+06 PSI

ELEMENT NUMBER	N TYPE	K TYPE	PHYSICAL DATA							
1	9	21	.190	.066	1.120	1.172	.698	.970	.180	
			.20000	19.50000	3.60000	3.37500	28.75000	26.25000	26.00000	21.75000
			50.00000	.06000	.78000	2.07000	.00042	55.00000	150.00000	.00000
2	1	-0	8.000	1.200	.100	30000000.000	-0.000	-0.000	-0.000	
3	1	-0	3.500	1.200	.100	30000000.000	-0.000	-0.000	-0.000	
4	1	-0	5.890	1.000	.058	30000000.000	-0.000	-0.000	-0.000	
5	2	32	2.222	5.245	2.273	-0.000	-0.000	-0.000	-0.000	
			4.55000	.31000	.10000100000000.00000		-0.00000	-0.00000	-0.00000	-0.00000
			3.45000	.25700	.10000100000000.00000		-0.00000	-0.00000	-0.00000	-0.00000
			3.45000	.25700	.10000100000000.00000		-0.00000	-0.00000	-0.00000	-0.00000
6	1	-0	7.360	1.000	.058	30000000.000	-0.000	-0.000	-0.000	
7	0	1	-0.000	-0.000	-0.000	-0.000	-0.000	-0.000	-0.000	
8	13	-0	.150	-0.000	-0.000	-0.000	-0.000	-0.000	-0.000	
9	1	-0	11.380	1.000	.058	30000000.000	-0.000	-0.000	-0.000	
10	1	-0	12.000	1.000	.058	30000000.000	-0.000	-0.000	-0.000	
11	1	-0	12.000	1.000	.058	30000000.000	-0.000	-0.000	-0.000	
12	1	-0	12.000	1.000	.058	30000000.000	-0.000	-0.000	-0.000	
13	1	-0	12.000	1.000	.058	30000000.000	-0.000	-0.000	-0.000	
14	1	-0	12.000	1.000	.058	30000000.000	-0.000	-0.000	-0.000	
15	1	-0	12.000	1.000	.058	30000000.000	-0.000	-0.000	-0.000	
16	1	-0	12.000	1.000	.058	30000000.000	-0.000	-0.000	-0.000	
17	1	-0	4.395	1.000	.058	30000000.000	-0.000	-0.000	-0.000	
18	1	-0	4.000	1.000	.058	30000000.000	-0.000	-0.000	-0.000	
19	14	-0	780.000	7.700	-0.000	-0.000	-0.000	-0.000	-0.000	

FIGURE 66 HSFR INPUT DATA FOR PULSCO TEST CIRCUIT HYDRAULIC SYSTEM FREQUENCY RESPONSE PROGRAM

The MCAIR verification effort demonstrated the net effect of the PULSCO unit in the basic short line (9 ft) HSFR test circuit. Termination impedance at the load valve is relatively high, and better simulates a real hydraulic system where a downstream pressure filter/manifold results in major reflections of incident pressure pulsations.

a. Test Results and Model Verification - Figure 67 shows the basic response of the basic 9 ft. test circuit, as shown and discussed in Paragraph 1.a. Measured resonances occurred at pump speeds of approximately 1350, 2600, and 3900 rpm. Peak standing wave pressure at the 3900 rpm resonance speed is about 525 psi.

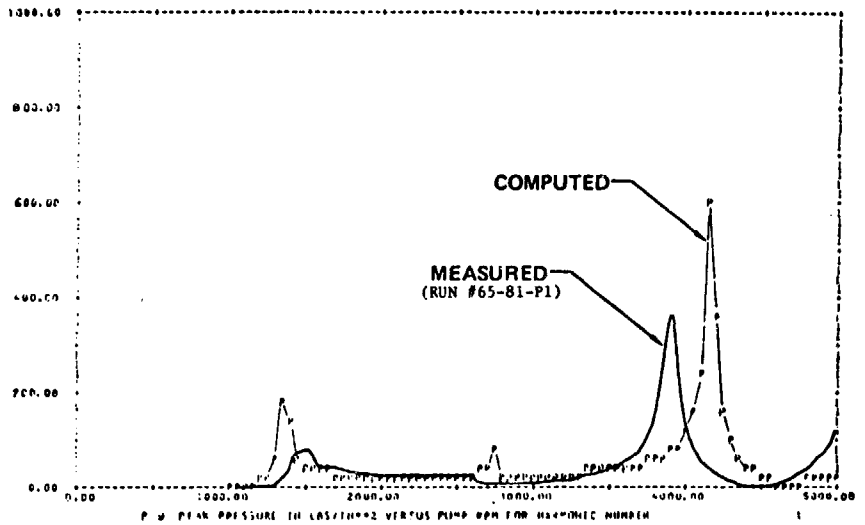

FIGURE 67 COMPUTED VS. MEASURED P1 PRESSURE
FREQUENCY RESPONSE
F-15 PUMP VERIFICATION TEST - SHORT LINE
MIL-H-83282 DATA PER AFML-TR-73-81
3000 PSI, 130°F, 2 GPM

Figure 68 shows an overplot of predicted and measured pressure pulsations (fundamental frequency) at the pump port plate outlet with the PULSCO unit installed close to the pump in the same 9 ft. test circuit. Fluid temperature was 130°F, and steady state flow was 2 gpm. Predicted response is based on adaibatic bulk modulus data for MIL-H-5606B (See Paragraph 1).

By comparing Figures 67 and 68, the PULSCO device obviously alters the acoustics of the test circuit. Resonant frequency location is shifted and maximum pulsation levels are reduced by an order or magnitude (525 psi peak to < 50 psi peak), both upstream and downstream of the test unit.

Reduction in measured pulsation levels occurs for pump speeds from 1000 to 5000 rpm. Figure 69 shows the same comparison of predicted and measured response with the PULSCO unit at the downstream location. The pulsations are reduced significantly from the basic circuit, although not as much at the upstream position (1/4 vs 1/10).

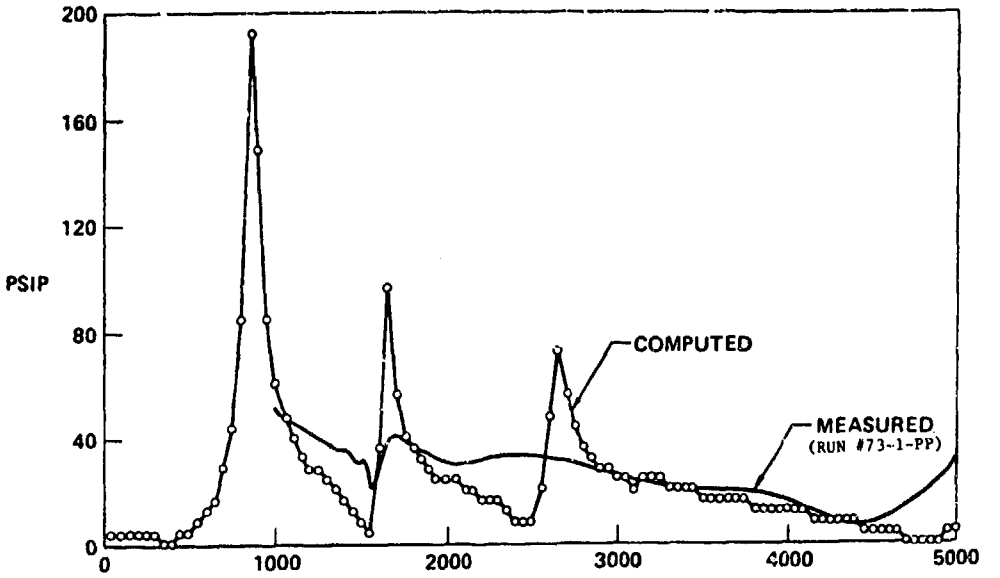

FIGURE 68 PULSCO FREQUENCY VERIFICATION PUMP OUTLET PRESSURE CONFIGURATION I (UPSTREAM LOCATION) 3000 PSI, 130°F, 2 GPM

Figure 68 shows that predicted amplitudes at the pump outlet are good for pump speeds above about 60% of the design cutoff (5333 rpm). By examining computer plots for several locations, low amplitude resonances were predicted at pump speeds of 850, 1650, 2650, 3100, and 4500 rpm. Analog plots of measured data show resonances at 1000, 1600, 2800, and 4400 rpm. Maximum peak pressure in the test circuit over the speed range is 55 psi (1600 rpm). Predicted amplitudes at the lower frequencies are considerably higher than measured values.

Note that resonance points are different than for the basic circuit without the PULSCO unit.

Figure 69 shows that the location of PULSCO unit relative to the pump is significant. It is less effective at the downstream location particularly for speeds below the 60% cutoff value. Resonances are predicted at 750, 2050, 2650, 3100, and 4450 rpm. Resonances were measured at 1300, 2050, 2400, 3200, and 4300 rpm. Measured amplitudes are still < 100 psi above the 60% cutoff speed (3200 rpm). Maximum amplitudes at < 60% of cutoff speed is 150 psi. Amplitude attenuation is evident for pump speeds above 3200 rpm. Pressures downstream of the unit are less than 40 psi, while upstream pressures range up to 150 psi. Predicted maximum amplitudes are 180 psi downstream and 350 psi upstream.

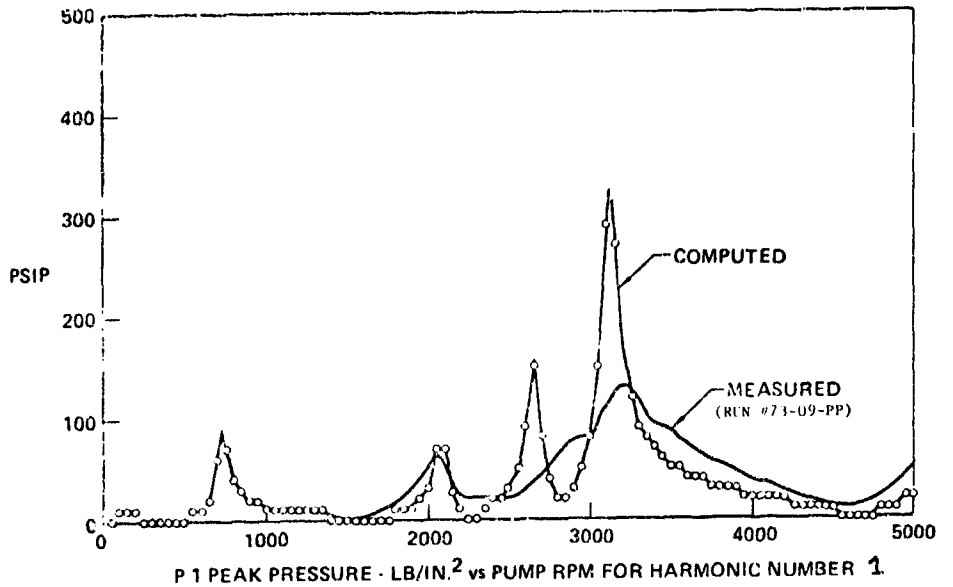

FIGURE 69 PULSCO FREQUENCY VERIFICATION PUMP OUTLET PRESSURE CONFIGURATION II (DOWNSTREAM LOCATION)

Figure 70 compares predicted peak pressure pulsations for the basic 9 ft. test system, a volume element at the pump, and the PULSCO element at the pump. The volume was equivalent to the total volume of the PULSCO unit, 10 in^3. This comparison shows the significant effect of the PULSCO design over a simple volume. Maximum attenuation agrees with the design cutoff frequency (5333 rpm). The apparent natural frequency of the unit is about 2X cutoff (approximately 10,500 rpm). Figure 71 compares predicted circuit response with the PULSCO test unit, two scaled up sizes of the test unit, and a large commercial PULSCO unit (ATP-6) used in the transient model test circuit. All are effective in the using range to 5000 rpm, and unit natural frequency decreases with increasing size.

The effectiveness of the PULSCO unit was also verified in a real system (F-15 iron bird left utility system) under a separate effort. The unit was installed as near the pump as possible. Figures 72 and 73 compare the actual system pressure pulsations before and after installing the PULSCO unit. Results are consistent with the bench test verification results.

b. Conclusions - The HSFR computer program and the model of the PULSCO acoustic filter can provide useful predictions of circuit frequency response when the PULSCO unit is installed in a simple short line system.

Prediction of maximum pulsation amplitudes is good for circuit resonant frequencies above about 60% of the attenuator design cutoff frequency. Predicted amplitudes for circuit resonances below 60% of cutoff are several times measured levels.

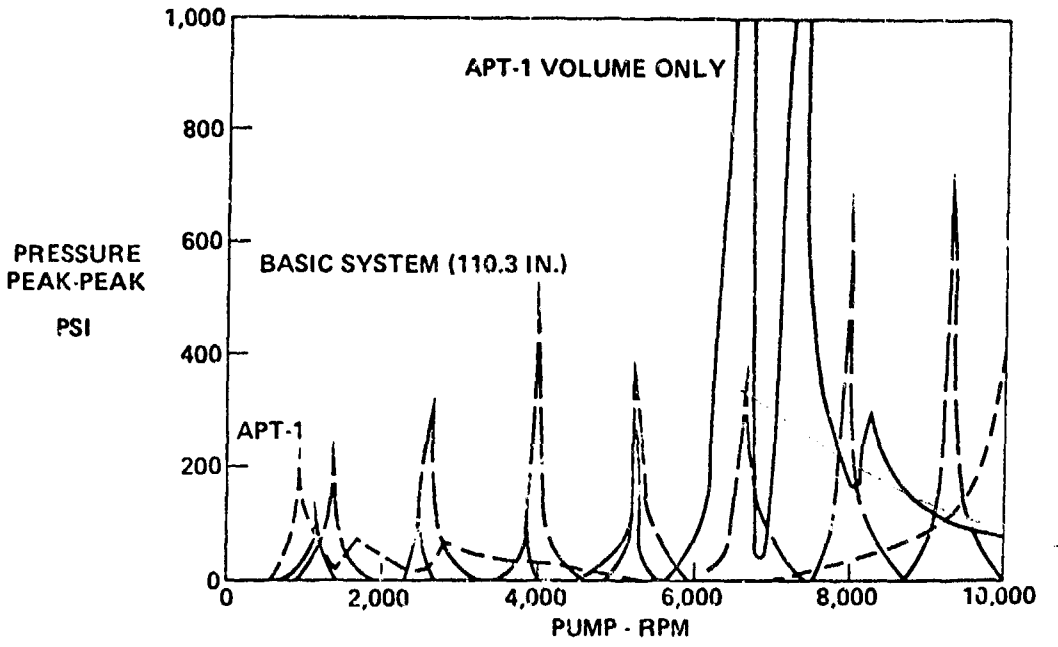

FIGURE 70 PULSCO FREQUENCY VERIFICATION COMPUTED PUMP OUTLET PRESSURE CONFIGURATION I

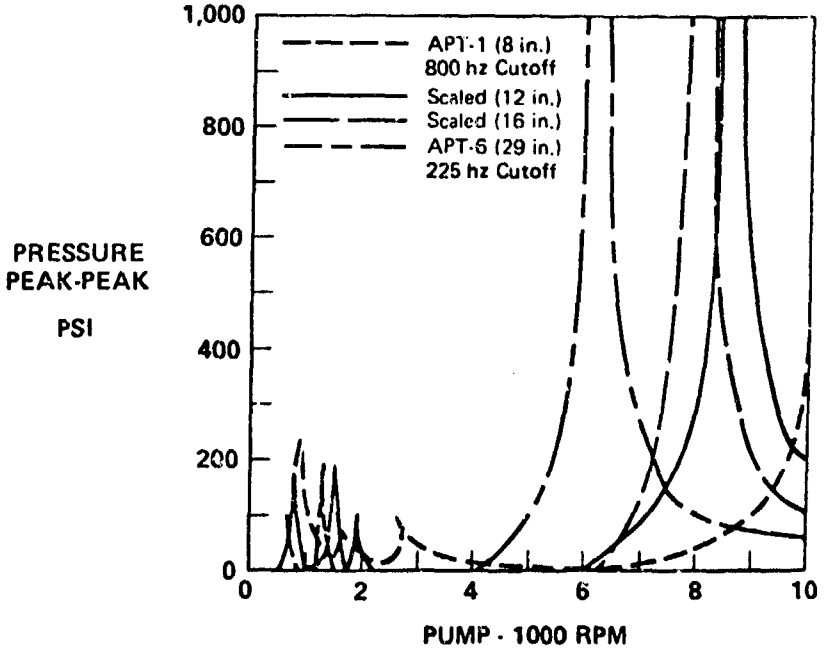

FIGURE 71 PULSCO FREQUENCY VERIFICATION COMPUTED PUMP OUTLET PRESSURE CONFIGURATION I

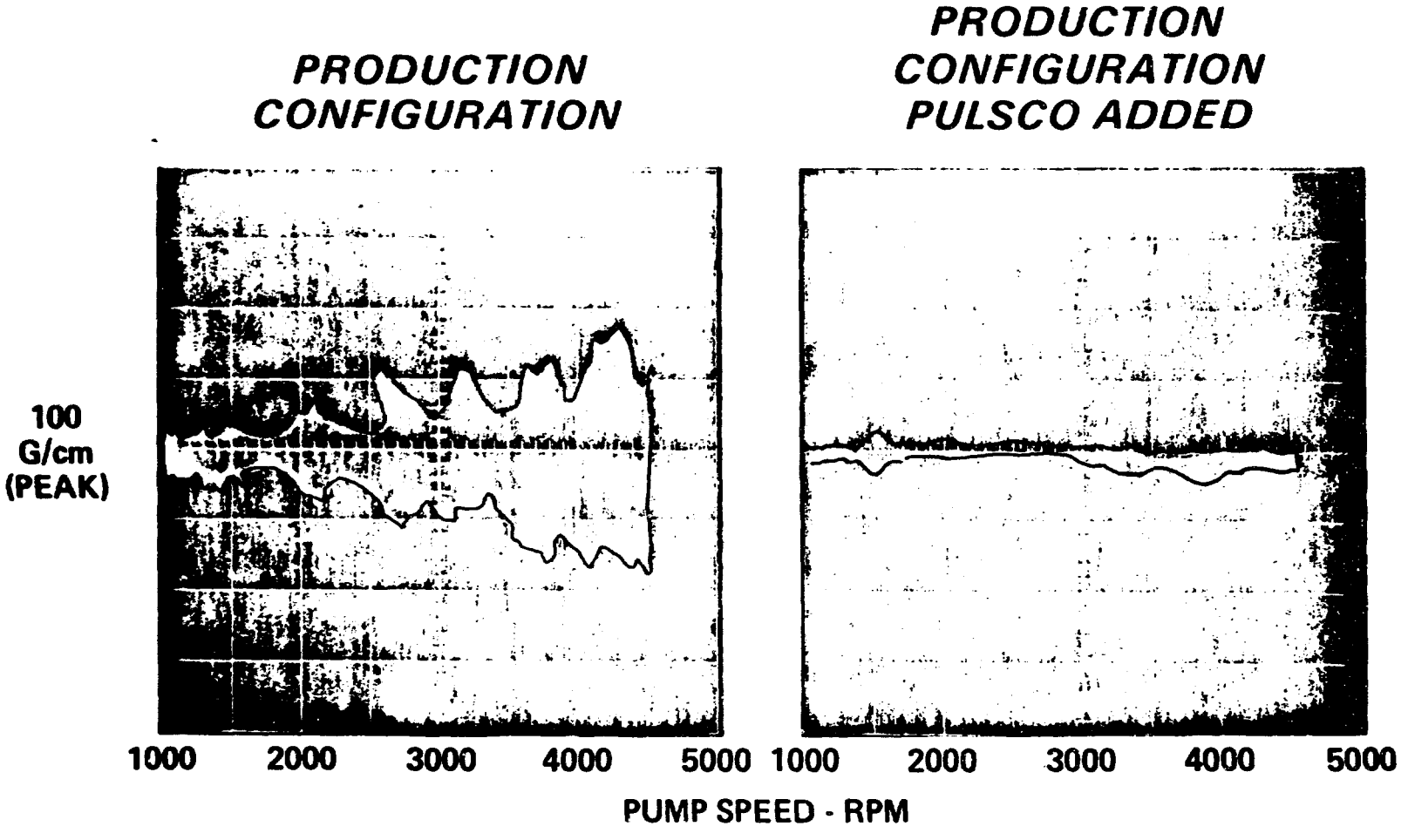

FIGURE 72 F-15 IRON BIRD - LEFT UTILITY SYSTEM
TOTAL LINE ACCELERATION
18.5 IN. LOCATION - RIGHT PUMP OFF

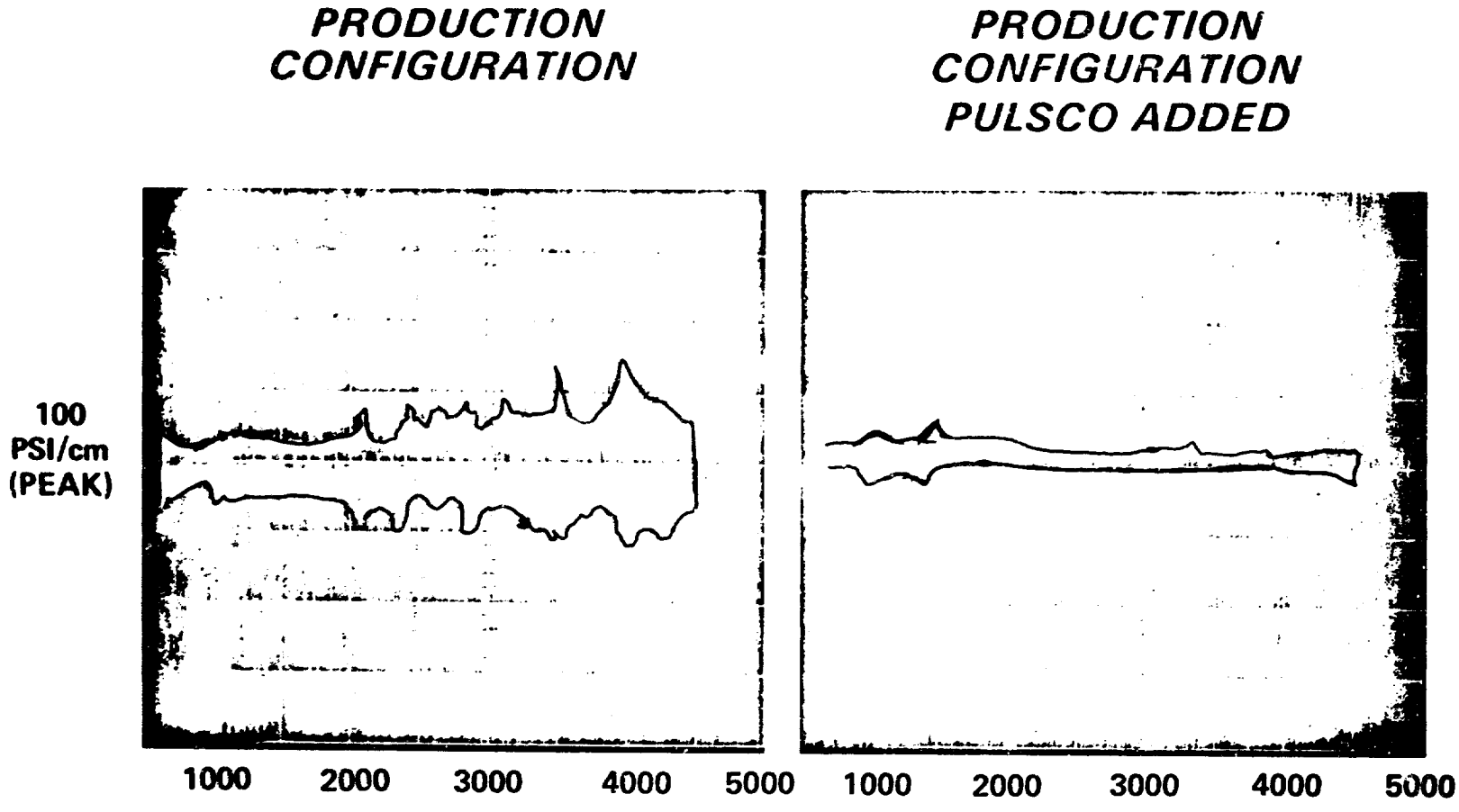

FIGURE 73 F-15 IRON BIRD - LEFT UTILITY SYSTEM
TOTAL PRESSURE PULSATIONS
26.5 IN. LOCATION - RIGHT PUMP OFF

3. F-15 UTILITY FILTER MANIFOLD VERIFICATION

This section covers verification testing of the HSFR filter model. Figure 74 shows the test circuit schematic. A pressure filter in the main supply line is usually the first point in the hydraulic system for major acoustic reflections. Proper simulation of the filter is therefore quite important in predicting the standing pressure wave in the system upstream and downstream of the filter.

The test filter consisted of a production unit as installed in a F-15 utility system manifold (S/N Q103). The manifold inlet check valve was removed. The trombone section was included in the downstream circuit so that the impedance of the circuit downstream of the filter could be varied. Test fluid was MIL-H-83282A hydraulic oil.

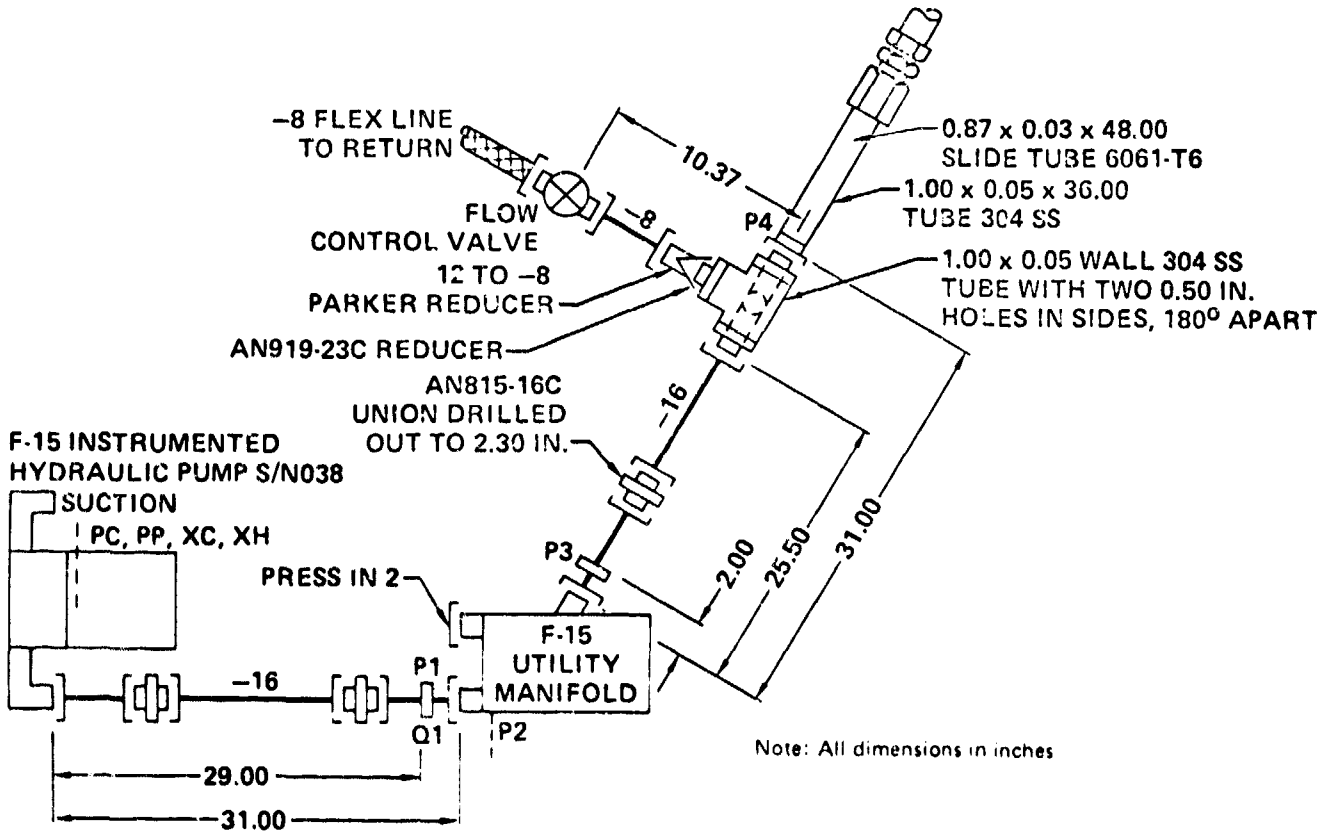

FIGURE 74 F-15 FILTER MANIFOLD HSFR VERIFICATION TEST SETUP

Figure 75 shows the input data used to model the filter test circuit for run 68-09. The filter is represented as a lumped volume. Volume with the filter element installed was measured at 12.82 in^3.

Figures 76, 77, and 78 show typical recorded data for three test conditions. Fundamental and total pulsation pressure response is shown in each figure.

Figures 79 through 82 compare predicted and measured standing wave plots in the test circuit.

Figures 79 and 80 show comparisons for lower frequency resonances at oil temperatures of 100°F and 210°F, respectively. In both cases, the filter was located near to the maximum pressure of the standing wave by adjusting the manifold outlet total length to 75 3/4 inches. Amplitude correlation is good for these low frequency resonances. The standing wave shape is maintained across the filter. Test data indicates some distortion of the wave across the "T". The test and computed data are plotted against axial line lengths as measured to the center of the "T".

RESPONSE IS CALCULATED FROM 50.00 TO 5000.00 R.P.M. IN INCREMENTS OF 50.00 R.P.M.
RESPONSE IS PLOTTED FOR THE -FIRST- HARMONIC FREQUENCY
NUMBER OF PUMPING ELEMENTS= 9.

FLUID DATA FOR MIL-H-83282 AT 3000.0 PSIG AND 210.0 DEG F

VISCOSITY	=	.744E-02	IN**2/SEC
DENSITY	=	.762E-04	LB-SEC**2/IN**4
BULK MODULUS	=	.173E+06	PSI

ELEMENT NUMBER	N TYPE	K TYPE	PHYSICAL DATA							
1	9	21	.190	.666	1.120	1.172	.698	.370	.180	
			.20000	19.50000	9.40000	3.37500	28.75000	24.25000	26.00000	21.75000
			50.00000	.06000	.78000	2.07000	.00042	80.00300	200.00000	.69000
2	1	0	8.000	1.200	.100	30000000.000	0.000	0.000	0.000	
3	1	0	3.500	1.200	.100	30000000.000	0.000	0.000	0.000	
4	1	0	7.500	1.000	.058	30000000.000	0.000	0.000	0.000	
5	1	0	6.000	1.000	.058	30000000.000	0.000	0.000	0.000	
6	1	0	7.000	1.000	.058	30000000.000	0.000	0.000	0.000	
7	1	0	7.500	1.000	.058	30000000.000	0.000	0.000	0.000	
8	1	0	1.000	1.000	.058	30000000.000	0.000	0.000	0.000	
9	1	0	2.000	1.000	.058	30000000.000	0.000	0.000	0.000	
10	1	0	9.000	1.044	.100	30000000.000	0.000	0.000	0.000	
11	3	0	12.420	0.000	0.000	0.000	0.000	0.000	0.000	
12	1	0	5.000	1.044	.100	30000000.000	0.000	0.000	0.000	
13	1	0	2.000	1.000	.058	30000000.000	0.000	0.000	0.000	
14	1	0	4.125	1.000	.058	30000000.000	0.000	0.000	0.000	
15	1	0	6.000	1.000	.058	30000000.000	0.000	0.000	0.000	
16	1	0	6.000	1.000	.058	30000000.000	0.000	0.000	0.000	
17	1	0	3.000	1.000	.058	30000000.000	0.000	0.000	0.000	
18	1	0	1.875	1.000	.058	30000000.000	0.000	0.000	0.000	
19	4	2	0.000	0.000	0.000	0.000	0.000	0.000	0.000	
20	1	0	3.900	1.000	.058	30000000.000	0.000	0.000	0.000	
21	11	0	.100	1.000	.058	30000000.000	0.000	0.000	0.000	
22	1	0	10.375	1.000	.058	30000000.000	0.000	0.000	0.000	
23	14	0	389.610	7.700	0.000	0.000	0.000	0.000	0.000	

FIGURE 75 HSFR INPUT DATA FOR THE F-15
FILTER MANIFOLD TEST CIRCUIT
HYDRAULIC FREQUENCY RESPONSE PROGRAM
F-15 FILTER MANIFOLD VERIFICATION TEST
SHORT TUBE SETUP

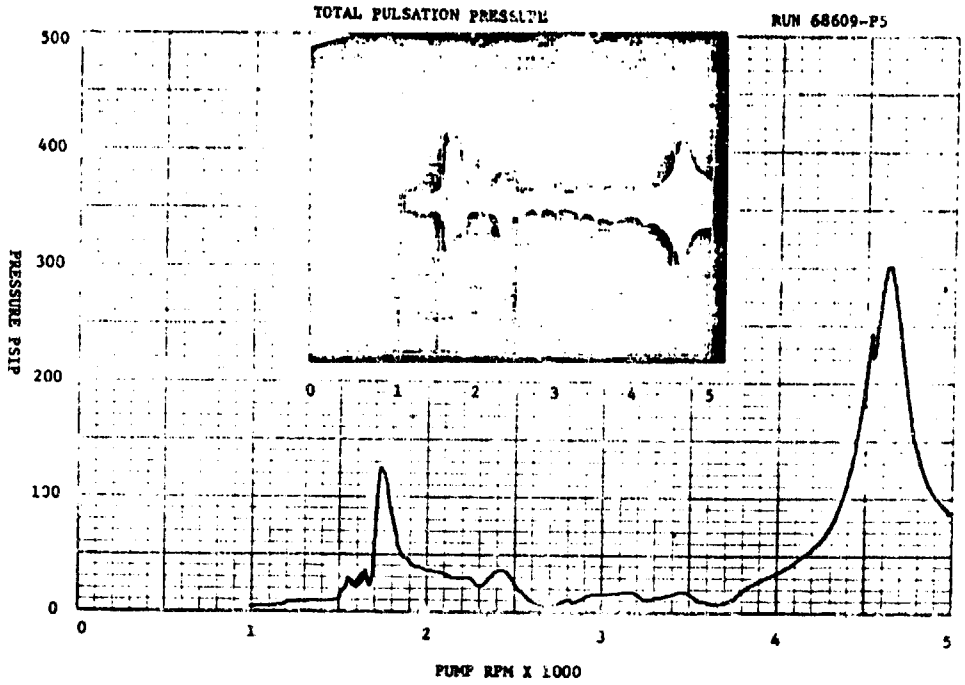

FIGURE 76 F-15 FILTER MANIFOLD VERIFICATION

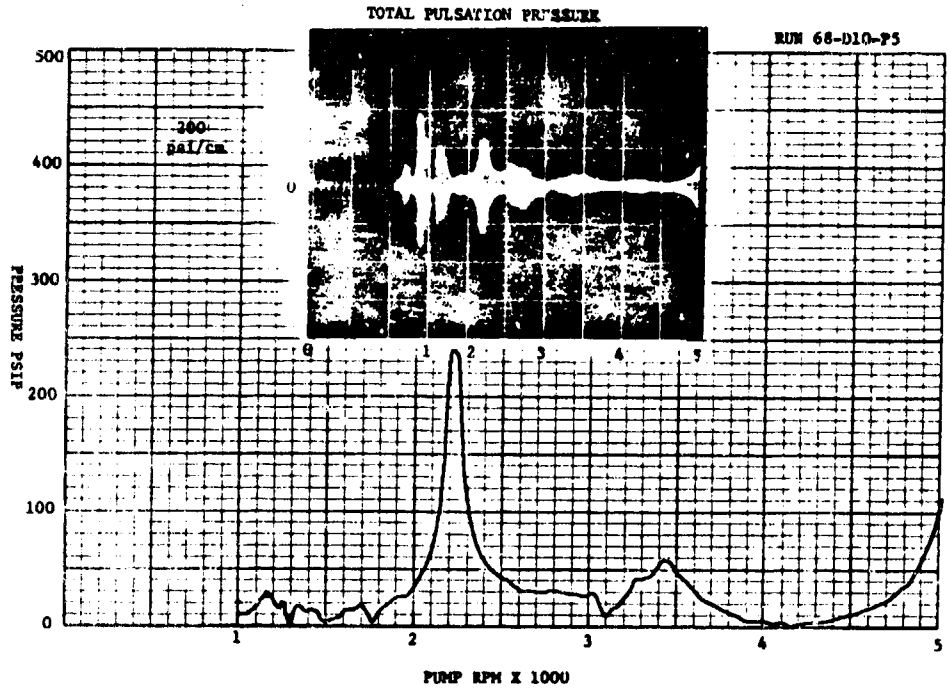

FIGURE 77 F-15 FILTER MANIFOLD VERIFICATION
2 GPM, 100°F FUNDAMENTAL

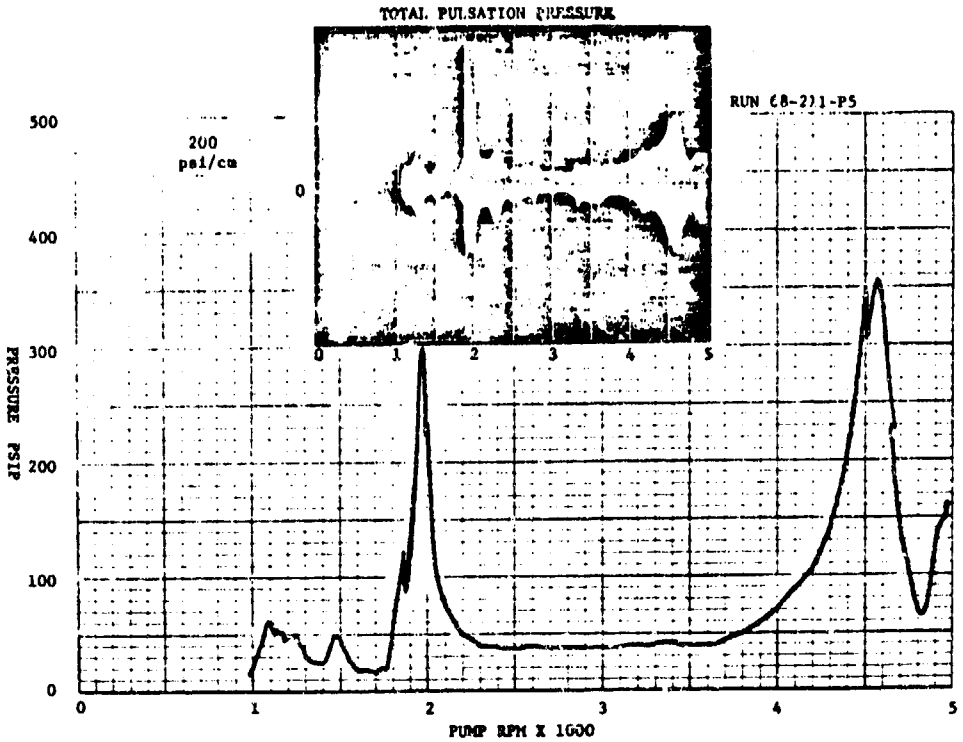

FIGURE 78 F-15 FILTER MANIFOLD VERIFICATION
2 GPM, 210°F FUNDAMENTAL

Figure 81 compares standing waves for a higher resonant frequency of 3500 rpm at 100°F. Predicted amplitudes are several times higher than measured values.

Figure 82 plots the standing wave for a system resonance at a pump speed of 4650 rpm, and an oil temperature of 210°F. For this resonant frequency, the filter is at or near a minimum pressure (maximum flow) point. This was achieved with a manifold outlet to trombone tube length of 31 inches (Figure 74). Predicted resonant frequency was 4800 rpm. Both measured and predicted results show a significant reduction of pulsation amplitude across the filter. However, computed amplitudes are 2 to 3 times higher than measured values.

Resonant frequencies are generally somewhat more in error than that typically predicted for a simple straight line circuit, and may be due to inaccurate representation of internal passages in the filter manifold. The high amplitude error at the higher frequency appears to be associated with pump speed, not temperature.

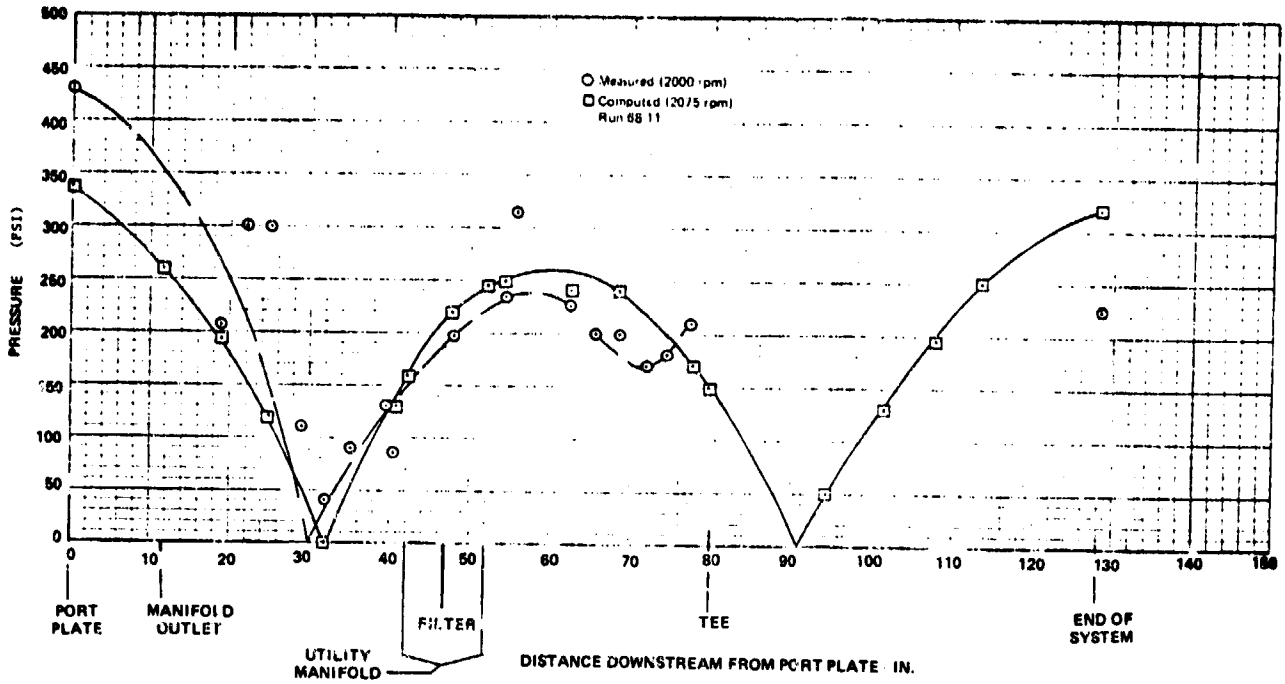

FIGURE 79 F-15 FILTER MANIFOLD VERIFICATION TEST
STANDING PRESSURE WAVE
MIL-H-83282, 100°F, 2 GPM

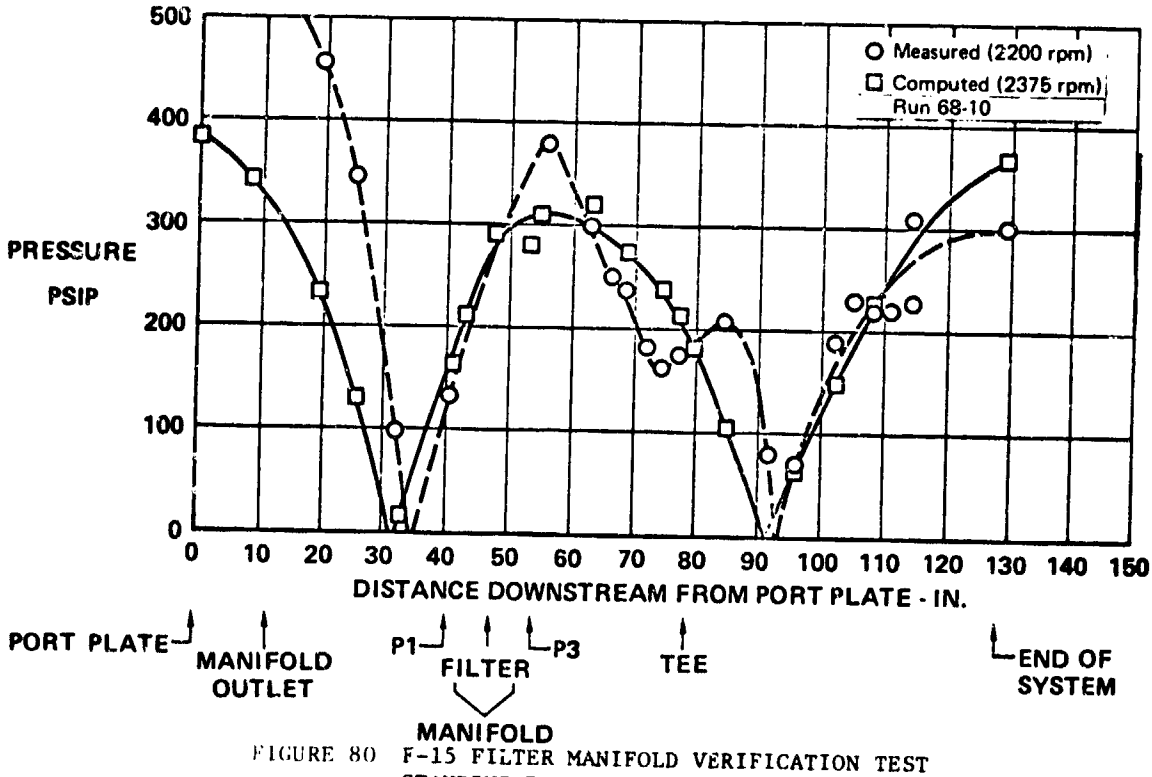

FIGURE 80 F-15 FILTER MANIFOLD VERIFICATION TEST
STANDING PRESSURE WAVE
MIL-H-83282, 210°F 2 GPM

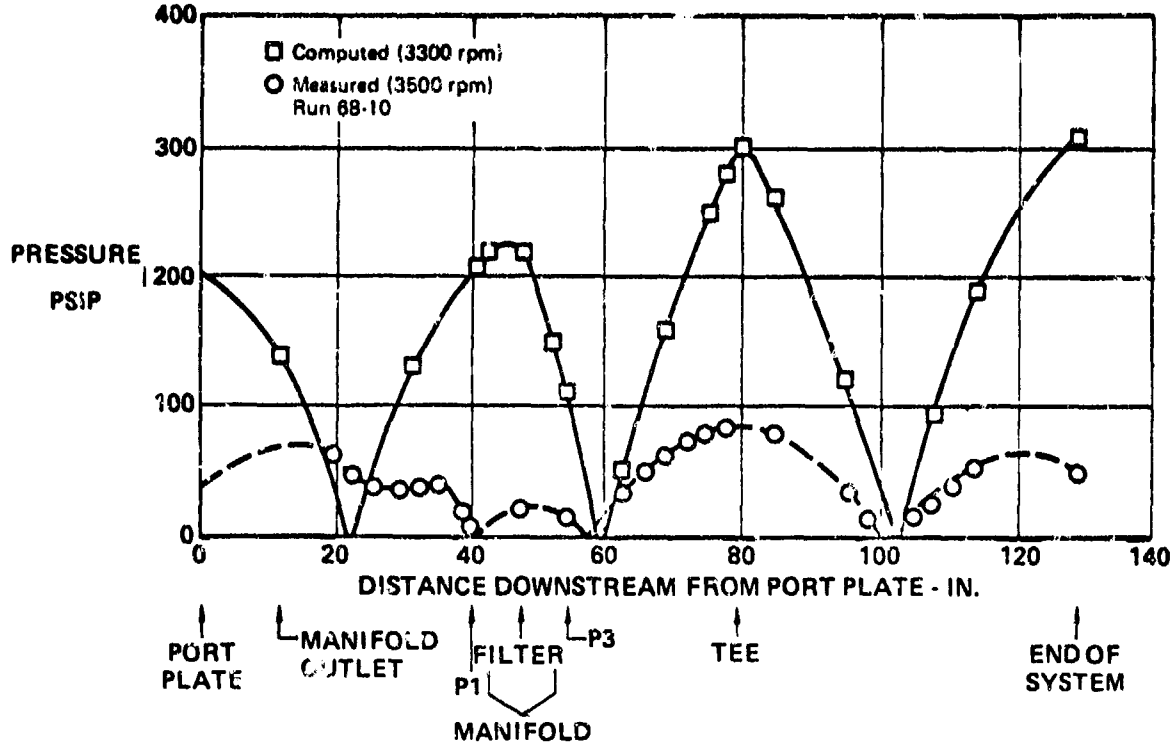

FIGURE 81 F-15 FILTER MANIFOLD VERIFICATION TEST
STANDING PRESSURE WAVE
MIL-H-83282, 100°F, 2 GPM

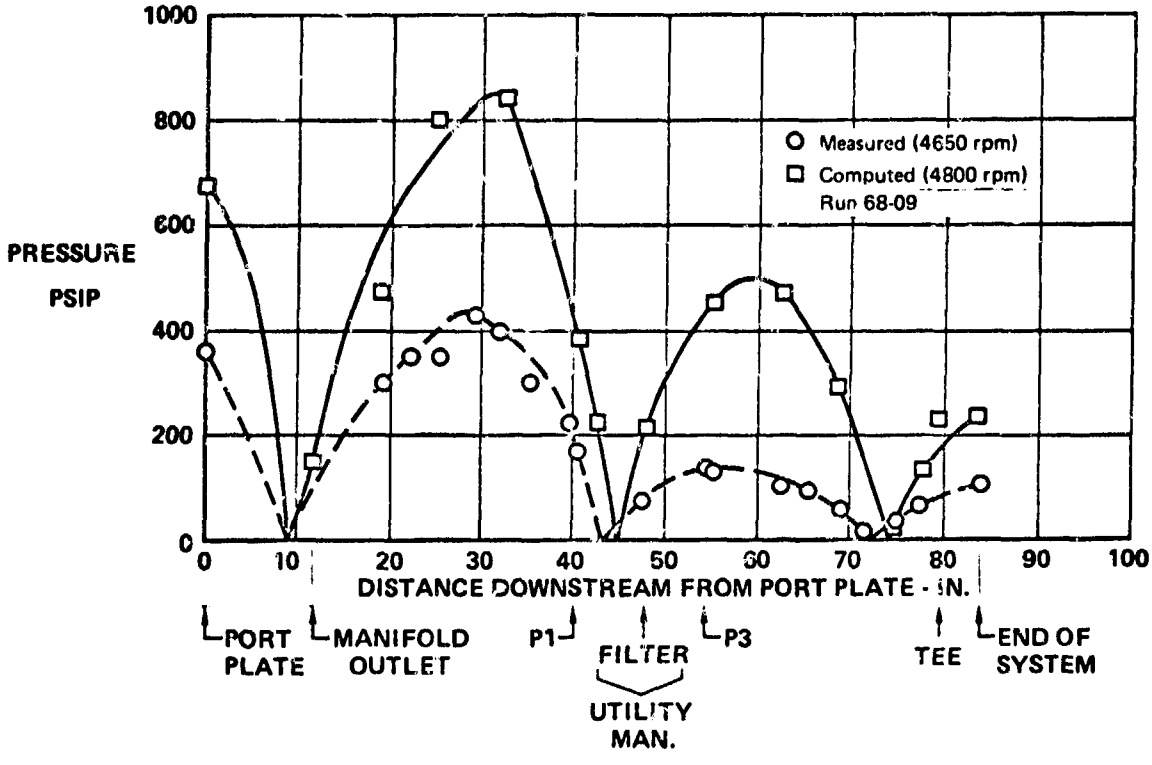

FIGURE 82 F-15 FILTER MANIFOLD VERIFICATION TEST
STANDING PRESSURE WAVE
MIL-H-83282, 210°F, 2 GPM

4. F-4 RESONATOR VERIFICATION TESTS

The lumped volume type resonator used on the F-4 hydraulic pumps was installed and tested in two different positions in the HSFR test circuit. Figure 83 shows the test circuit schematic for each resonator location.

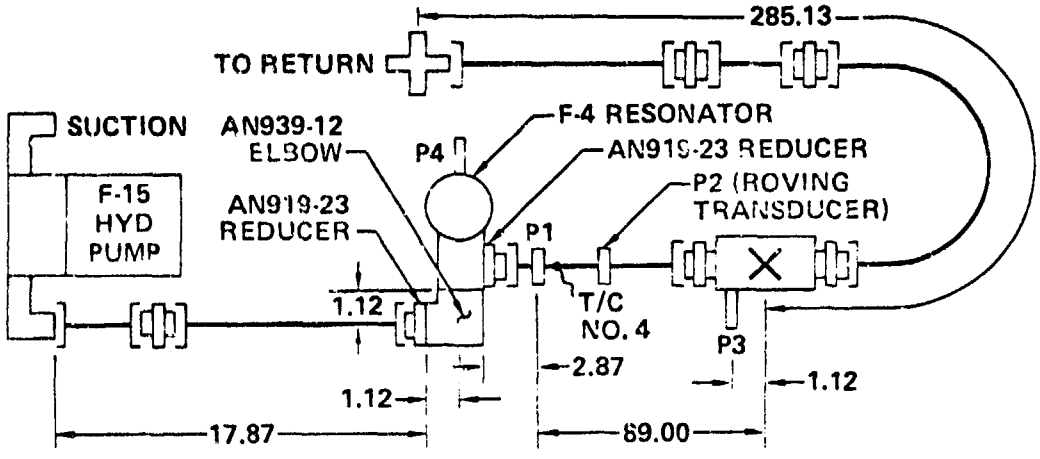

UPSTREAM POSITION

Note: All dimensions in inches

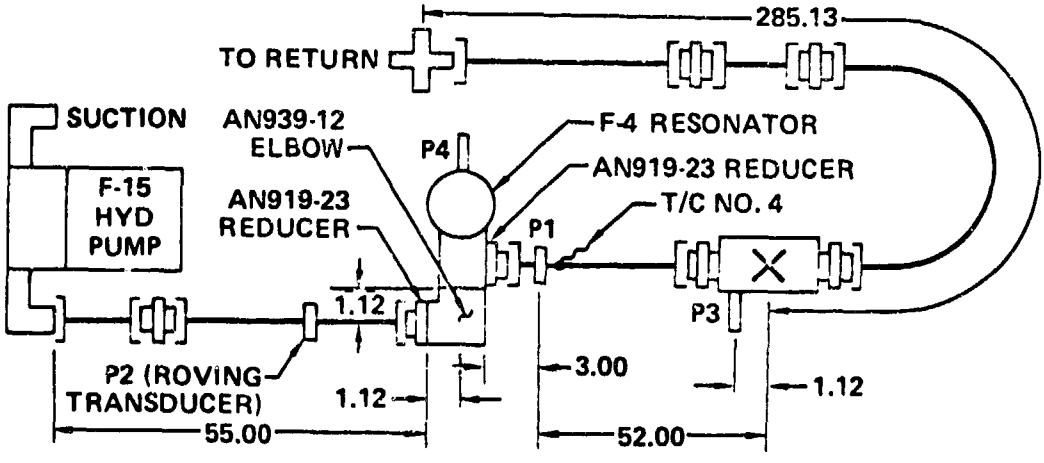

Note: All dimensions in inches DOWNSTREAM POSITION

FIGURE 83 F-4 RESONATOR
HSFR VERIFICATION TEST SETUP

Figure 84 shows the computer input data used for simulating the test circuit with the upstream resonator location. The resonator is simulated as a lumped volume at the end of a short branch line.

Figures 85 and 86 shows typical fundamental frequency response in the test circuits for upstream and downstream resonator locations.

Figures 87 and 88 compare computed and measured standing pressure waves for a circuit resonant condition at each resonator location. Amplitude predictions are not consistent upstream and downstream of the resonator for the downstream installation (Figure 88). Pulsations downstream of the resonator are about the same (200-250 psip) for both locations. However, the downstream location results in significantly higher pulsations between the pump and resonator.

Figures 89 and 90 show standing wave peak pressures in the test circuits for the fundamental frequency. Resonant frequency prediction is good. Amplitude predictions vary from low to high, but the error is considerably less than for filter and hose tests.

RESPONSE IS CALCULATED FROM 50.00 TO 5000.00 R.P.M. IN INCREMENTS OF 50.00 R.P.M.
RESPONSE IS PLOTTED FOR THE -FIRST- HARMONIC FREQUENCY
NUMBER OF PUMPING ELEMENTS= 9.

FLUID DATA FOR MIL-H-83282 AT 3000.0 PSIG AND 130.0 DEG F

VISCOSITY = .200E-01 IN**2/SEC
DENSITY = .783E-04 (LB-SEC**2)/IN**4
BULK MODULUS = .723E+06 PSI

ELEMENT NUMBER	N TYPE	K TYPE	SYSTEM ELEMENT INPUT DATA / PHYSICAL DATA							
1	9	21	.190	.666	1.120	1.172	.698	.970	.180	
			.20003	19.50000	9.40000	9.37500	28.75000	26.25000	26.00000	21.75000
			50.00000	.06000	.78000	2.07000	.00042	80.00000	200.00000	.69000
2	1	0	8.000	1.200	.100	30000000.000	0.000	0.000	0.000	
3	1	0	8.900	1.200	.100	30000000.000	0.000	0.000	0.000	
4	1	0	14.688	1.000	.058	30000000.000	0.000	0.000	0.000	
5	1	0	3.188	1.000	.058	30000000.000	0.000	0.000	0.000	
6	1	0	.491	1.094	.100	30000000.000	0.000	0.000	0.000	
7	1	0	1.266	.878	.100	30000000.000	0.000	0.000	0.000	
8	1	0	1.719	1.119	.100	30000000.000	0.000	0.000	0.000	
9	1	0	1.500	.978	.100	30000000.000	0.000	0.000	0.000	
10	2	0	.250	.291	.100	30000000.000	20.000	0.000	0.000	
11	1	0	2.266	.978	.100	30000000.000	0.000	0.000	0.000	
12	1	0	.891	1.084	.100	30000000.000	0.000	0.000	0.000	
13	1	0	2.000	1.000	.058	30000000.000	0.000	0.000	0.000	
14	1	0	12.000	1.000	.058	30000000.000	0.000	0.000	0.000	
15	1	0	12.000	1.000	.058	30000000.000	0.000	0.000	0.000	
16	1	0	12.000	1.000	.058	30000000.000	0.000	0.000	0.000	
17	1	0	12.000	1.000	.058	30000000.000	0.000	0.000	0.000	
18	1	0	12.000	1.000	.058	30000000.000	0.000	0.000	0.000	
19	1	0	12.000	1.000	.058	30000000.000	0.000	0.000	0.000	
20	1	0	12.000	1.000	.058	30000000.000	0.000	0.000	0.000	
21	1	0	9.479	1.000	.058	30000000.000	0.000	0.000	0.000	
22	1	0	1.125	1.000	.058	30000000.000	0.000	0.000	0.000	
23	14	0	399.610	7.730	0.000	0.000	0.000	0.000	0.000	

FIGURE 84 HSFR INPUT DATA FOR F-4 RESONATOR VERIFICATION HYDRAULIC SYSTEM FREQUENCY RESPONSE PROGRAM

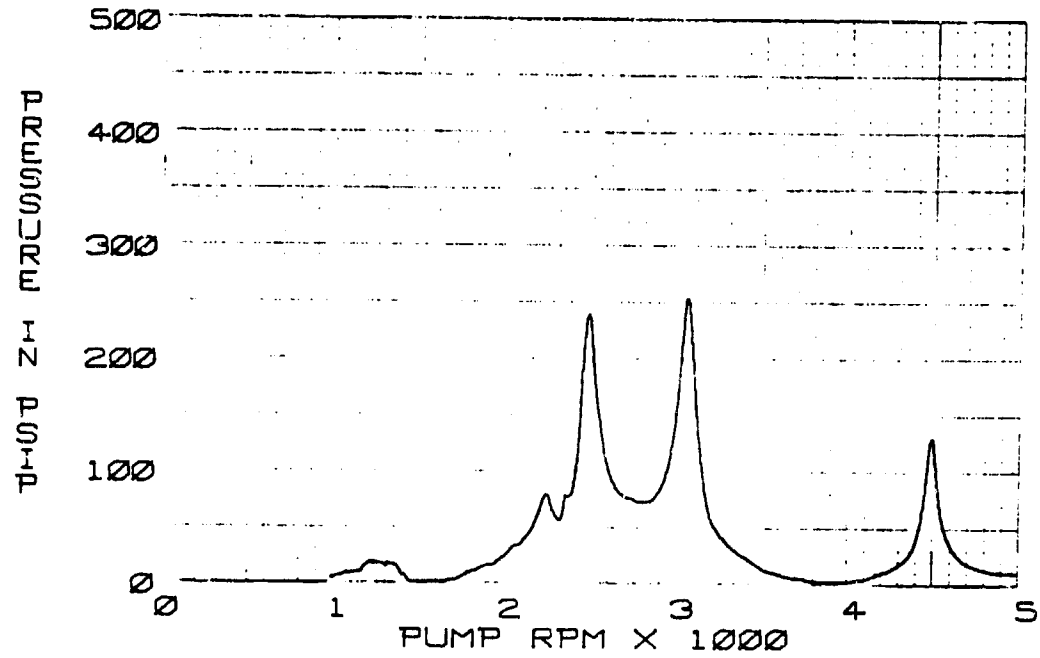

FIGURE 85 F-4 RESONATOR
76-06-P2 FUNDAMENTAL
2 GPM, 130°F
UPSTREAM POSITION

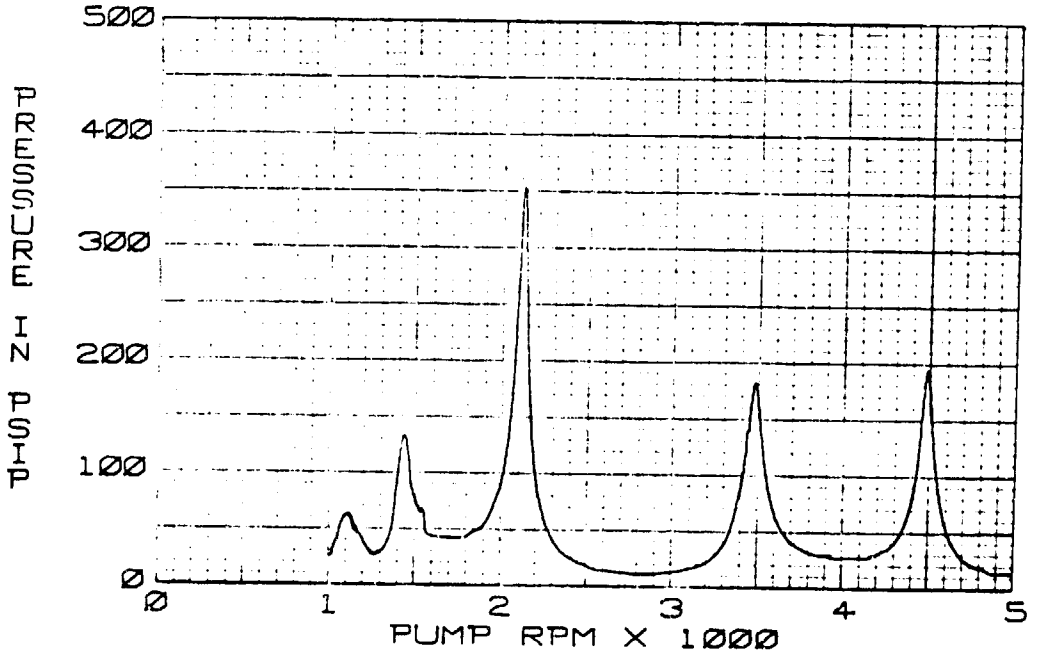

FIGURE 86 F-4 RESONATOR
76-17-P3 FUNDAMENTAL
2 GPM, 130°F
DOWNSTREAM POSITION

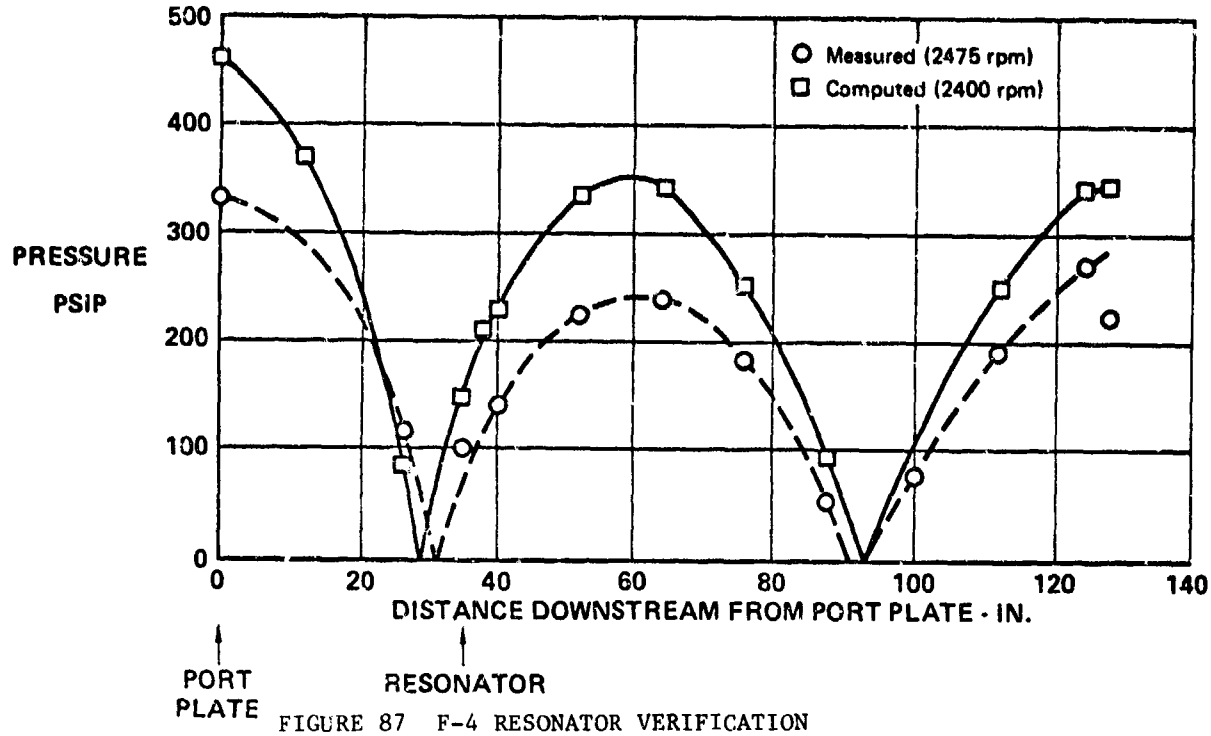

FIGURE 87 F-4 RESONATOR VERIFICATION
STANDING PRESSURE WAVE - FUNDAMENTAL RESPONSE
UPSTREAM POSITION
MIL-H-83282, 130°F

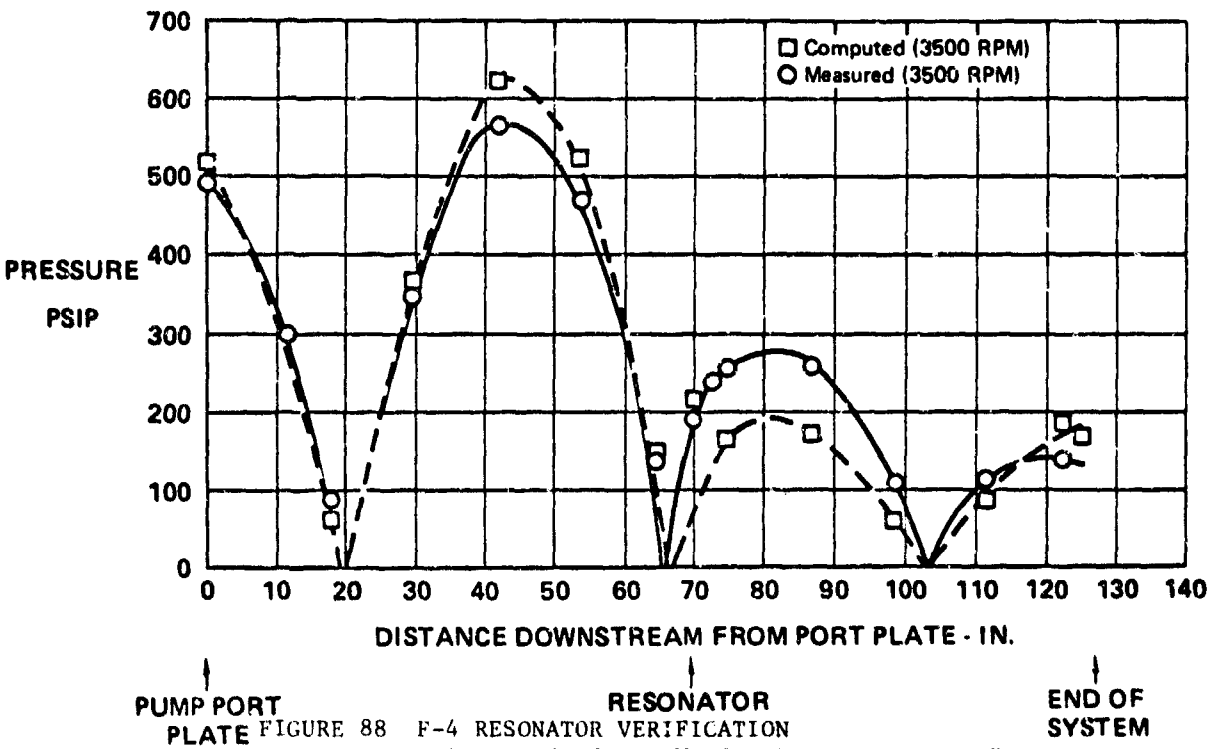

FIGURE 88 F-4 RESONATOR VERIFICATION
STANDING PRESSURE WAVE - FUNDAMENTAL RESPONSE
DOWNSTREAM POSITION
MIL-H-83282, 130°F

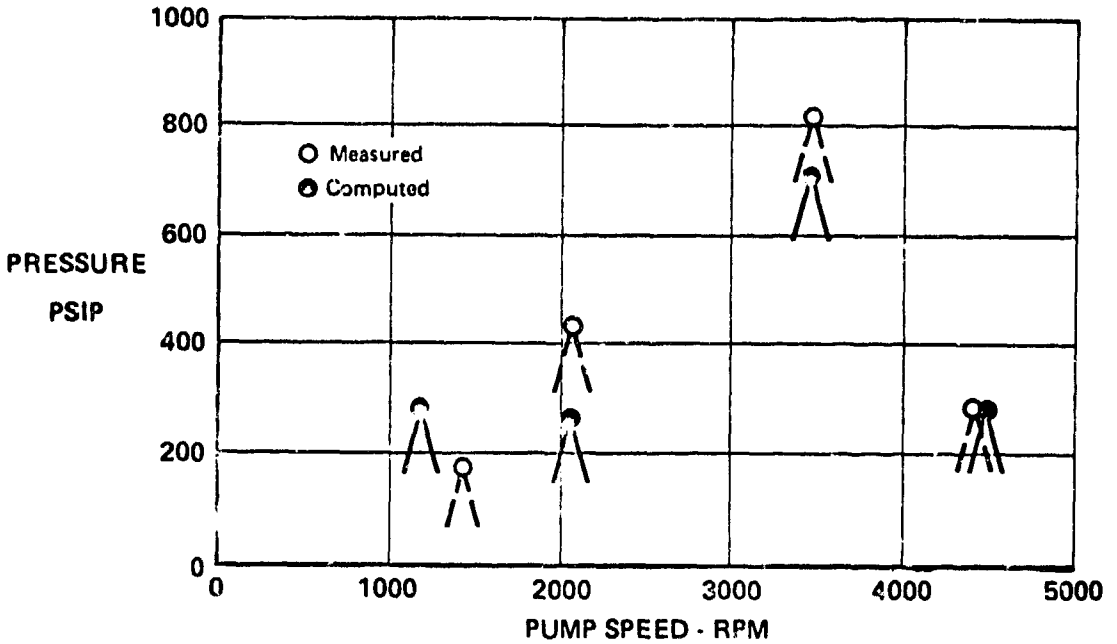

FIGURE 89 F-4 RESONATOR
DOWNSTREAM POSITION
MAXIMUM FUNDAMENTAL PEAK RESPONSE IN TEST CIRCUIT
MIL-H-83282, 130°F

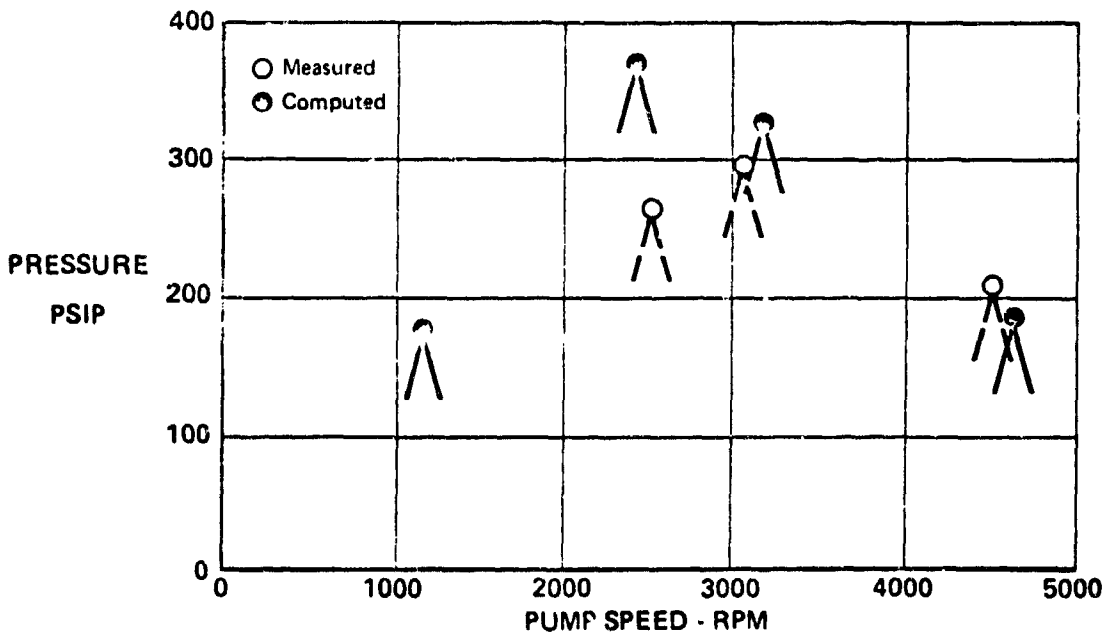

FIGURE 90 F-4 RESONATOR
UPSTREAM POSITION
MAXIMUM FUNDAMENTAL PEAK RESPONSE IN TEST CIRCUIT
MIL-H-83282, 130°F

5. FLEXIBLE HOSE VERIFICATION

Figure 91 shows the test circuit schematics for verification tests of a 1 inch flexible hose at two different locations in the test circuit. The test unit was a Resistoflex steel braided hose, P/N R44597A0204HK, 20 inches in length. Static measurements of equivalent bulk modulus were made on the hose test specimen. These data are plotted in Figure 92 as total volume change vs. pressure. Total effective bulk modulus of the hose and oil is approximatley

$$B_e = \frac{\Delta P \cdot V}{\Delta V} = \frac{3100(124)}{4.69}$$

$$B_e = 81{,}962 \text{ psi.}$$

UPSTREAM LOCATION

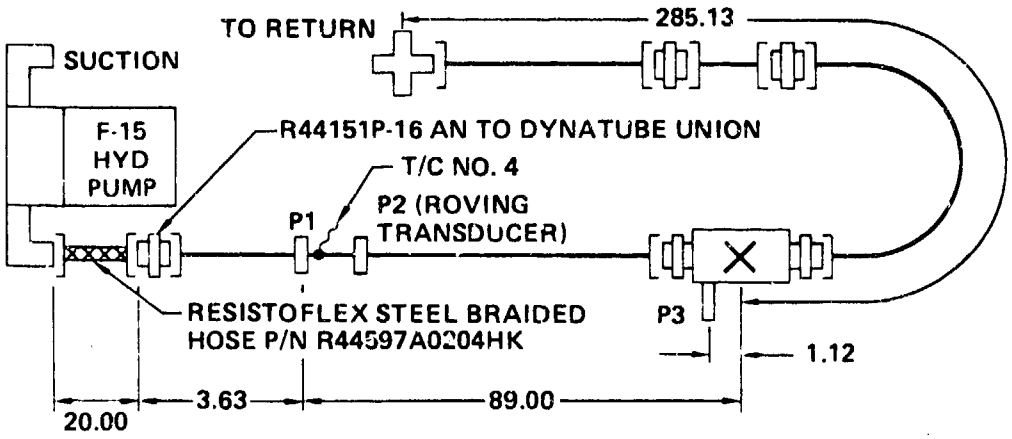

Note: All dimensions in inches

DOWNSTREAM LOCATION

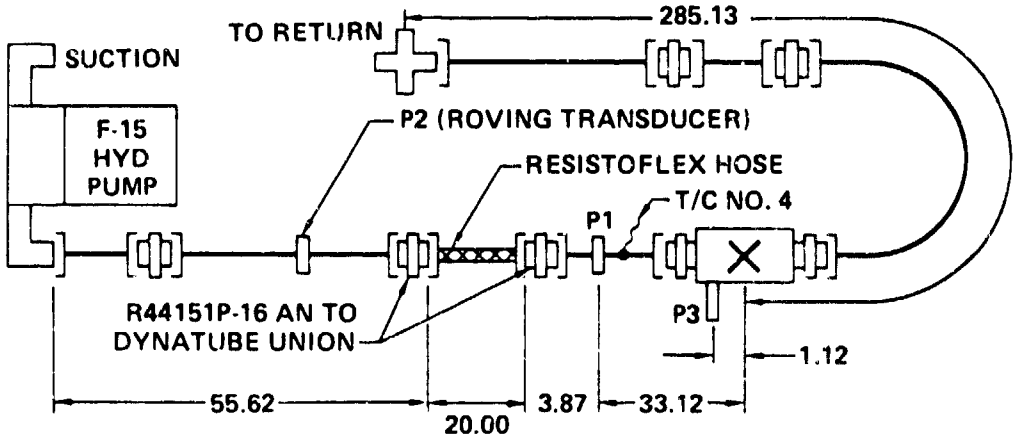

Note: All dimensions in inches

FIGURE 91. USER HOSE VERIFICATION TEST CIRCUITS

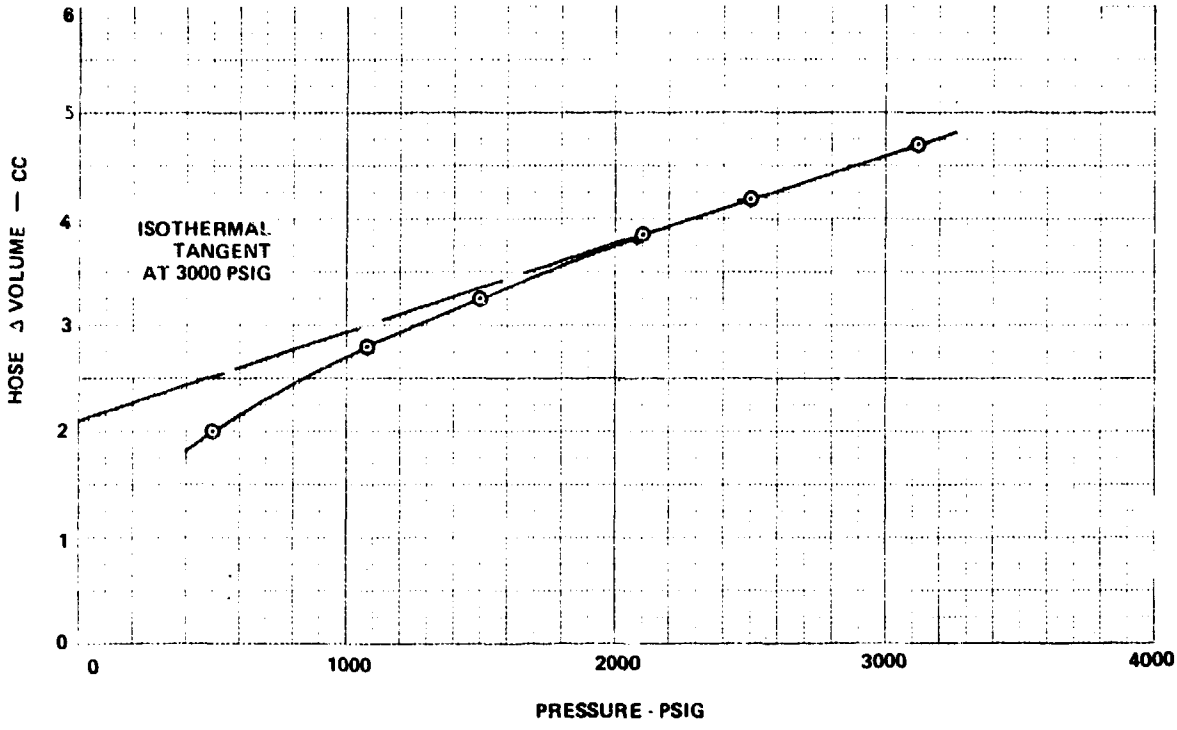

FIGURE 92. BULK MODULUS OF ONE HIGH FLEX HOSE MEASURED WITH MIL-H-83282 FLUID & T = 75°F

Line subroutine models a hose as a line with a local acoustic velocity based simply on the effective hose bulk modulus. The above estimate of effective hose bulk modulus is based on an average volumetric change from 0 to 3100 psi and could be considered as isothermal secant value. The HSFR program typically uses adaibatic bulk modulus for the fluid with modifications to acoustic velocity for line wall material elasticity and mounting. However, the choice of a modulus value for hose simulation is academic considering the difficulty of statically measuring hose modulus, in addition to inherent differences in static and dynamic hose response.

Figure 93 shows the input data used for simulation of the circuit with the upstream hose location. The hose was modeled as a lumped volume at the middle of the hose length in the example data.

Figure 94 shows measured and computed maximum first harmonic peak response in a straight, 1 inch diameter x 128 inches long line circuit. Frequency predictions are quite accurate. However, predicted amplitudes at resonant frequencies are all much lower than measured values.

HYDRAULIC SYSTEM FREQUENCY RESPONSE PROGRAM
FLEXIBLE HOSE VERIFICATION WITH MODELED VOLUME

RESPONSE IS CALCULATED FROM 50.00 TO 5000.00 R.P.M. IN INCREMENTS OF 50.00 R.P.M.
RESPONSE IS PLOTTED FOR THE -FIRST- HARMONIC FREQUENCY
NUMBER OF PUMPING ELEMENTS= 9.

FLUID DATA FOR MIL-H-83282 AT 3000.0 PSIG AND 130.0 DEG F
VISCOSITY - .200E-01 IN**2/SEC
DENSITY - .790E-04 (LB-SEC**2)/IN**4
BULK MODULUS - .223E+06 PSI

ELEMENT NUMBER	N TYPE	K TYPE	PHYSICAL DATA							
1	9	21	.190	.666	1.120	1.172	.698	.570	.180	
			.20000	19.50000	9.40000	3.37500	28.75000	26.25000	26.00000	21.75000
			50.00000	.06000	.78000	2.07000	.00042	80.00000	200.00000	.69000
2	1	0	8.000	1.200	.100	30000000.000	0.000	0.000	0.000	
3	1	0	3.500	1.200	.100	30000000.000	0.000	0.000	0.000	
4	1	0	10.000	1.000	.058	30000000.000	0.000	0.000	0.000	
5	3	0	12.000	0.000	0.000	0.000	0.000	0.000	0.000	
6	1	0	10.000	1.000	.058	30000000.000	0.000	0.000	0.000	
7	1	0	3.630	1.000	.058	30000000.000	0.000	0.000	0.000	
8	1	0	12.000	1.000	.058	30000000.000	0.000	0.000	0.000	
9	1	0	12.000	1.000	.058	30000000.000	0.000	0.000	0.000	
10	1	0	12.000	1.000	.058	30000000.000	0.000	0.000	0.000	
11	1	0	12.000	1.000	.058	30000000.000	0.000	0.000	0.000	
12	1	0	12.000	1.000	.058	30000000.000	0.000	0.000	0.000	
13	1	0	12.000	1.000	.058	30000000.000	0.000	0.000	0.000	
14	1	0	12.000	1.000	.058	30000000.000	0.000	0.000	0.000	
15	1	0	3.975	1.000	.058	30000000.000	0.000	0.000	0.000	
16	1	0	1.125	1.000	.058	30000000.000	0.000	0.000	0.000	
17	14	0	389.510	7.700	0.000	0.000	0.000	0.000	0.000	

3 0 PLOTS FOR INPUT TO ELEMENT NUMBERS 4 5 14

FIGURE 93. HSFR INPUT DATA FOR HOSE VERIFICATION TEST

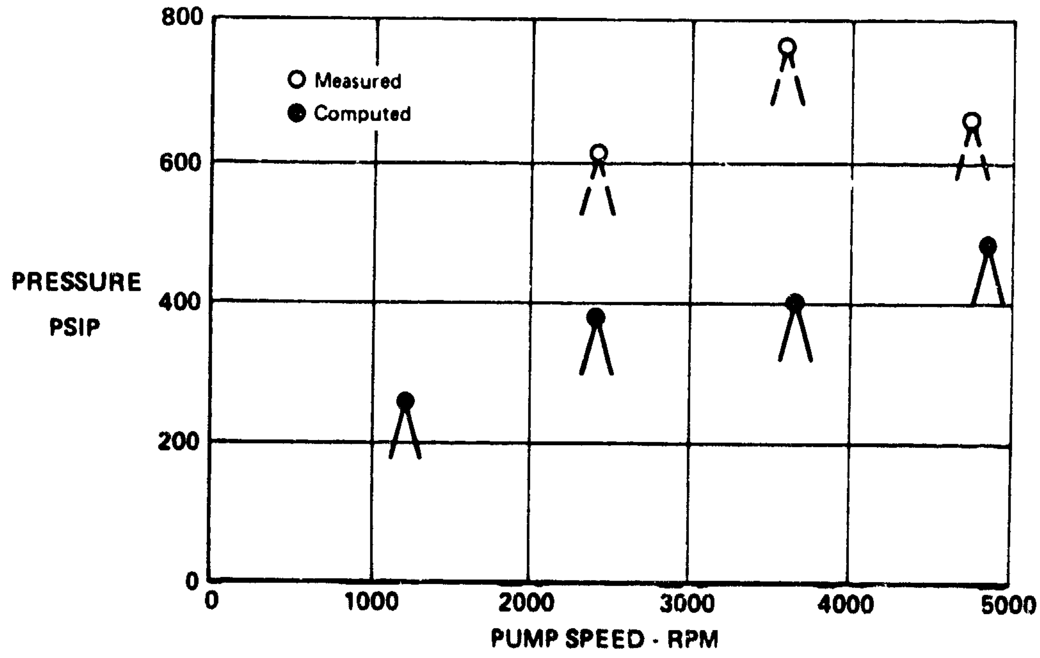

FIGURE 94. MAXIMUM FUNDAMENTAL PEAK RESPONSE IN TEST CIRCUIT
STRAIGHT LINE 1 X .058 X 128 INCHES
MIL-H-83282 130°F 2 GPM

Figures 95 and 96 show typical measurements of fundamental frequency peak pressure response in the test circuit for upstream and downstream hose locations, respectively.

Figure 97 compares peak circuit response with the hose located near the pump outlet. The hose results in a significant reduction of pulsation pressure amplitudes from those of a straight line (600 psip vs 150 psip). The hose circuit has several low level resonances at the lower frequencies which do not appear in the straight line circuit. This indicates that the hose is acting as a reflection point, an effect which is not predicted.

Pressure predicted with the measured hose bulk modulus (81,962 psi) do not reflect the reduced pressures. Lower amplitudes (200 psip) are predicted using a bulk value of 10,000 psi, however significant resonant frequency errors remain, as well as a high amplitude error at the higher frequency. The high predicted amplitudes are similar to the errors in predictions at the higher speeds in the filter verification test.

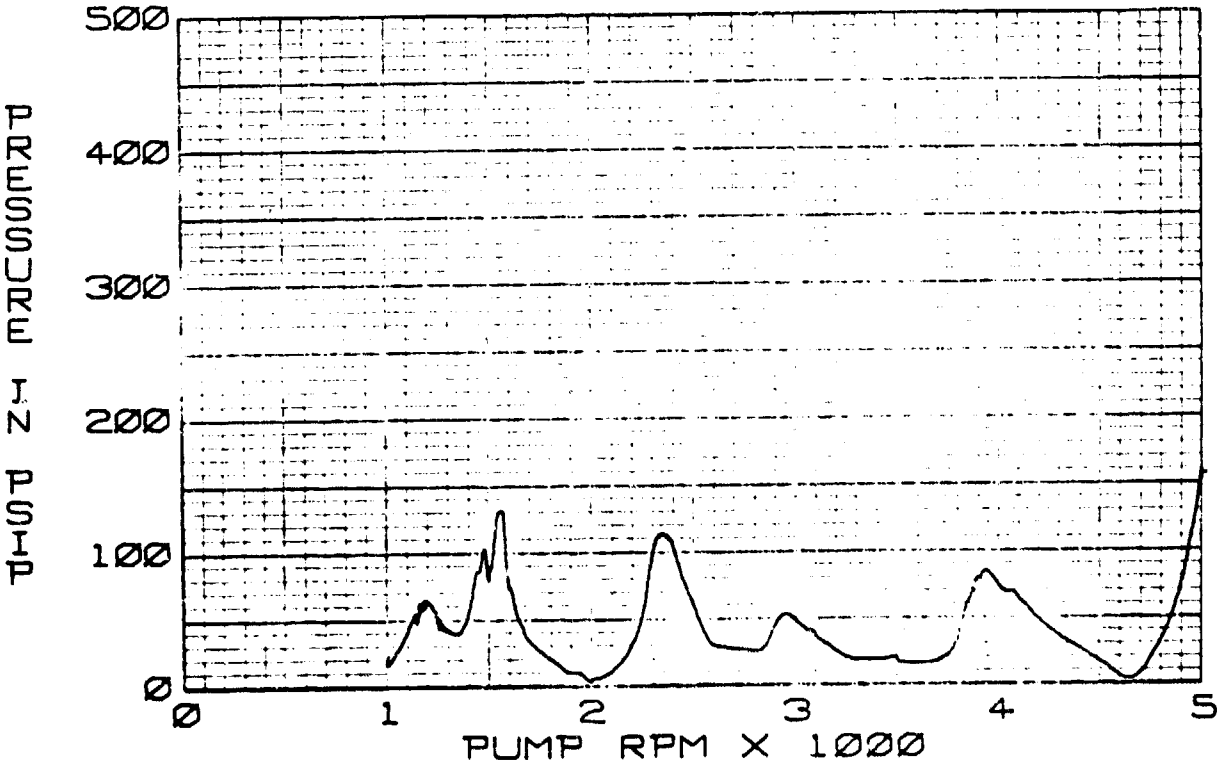

FIGURE 95. STEEL BRAIDED HOSE UPSTREAM LOCATION
74-01-PP FUNDAMENTAL
2 GPM 130°F

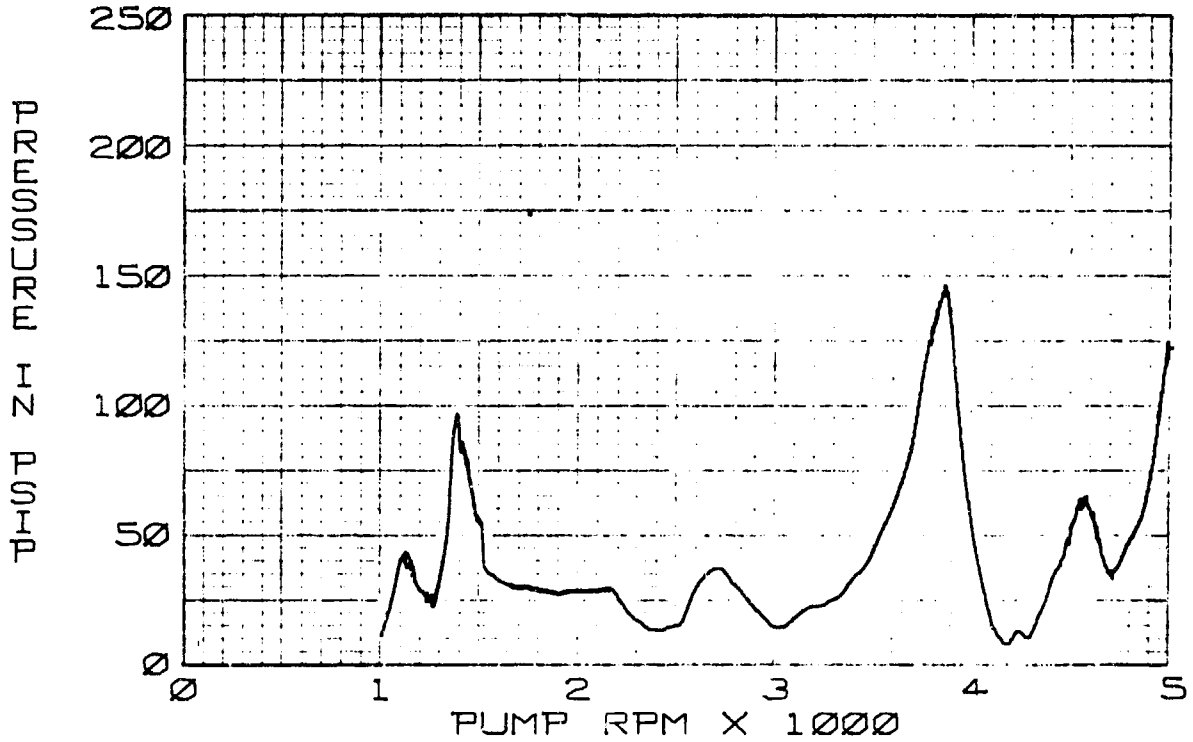

FIGURE 96. STEEL BRAIDED HOSE DOWNSTREAM LOCATION
74-24-P2 FUNDAMENTAL
2 GPM 130°F

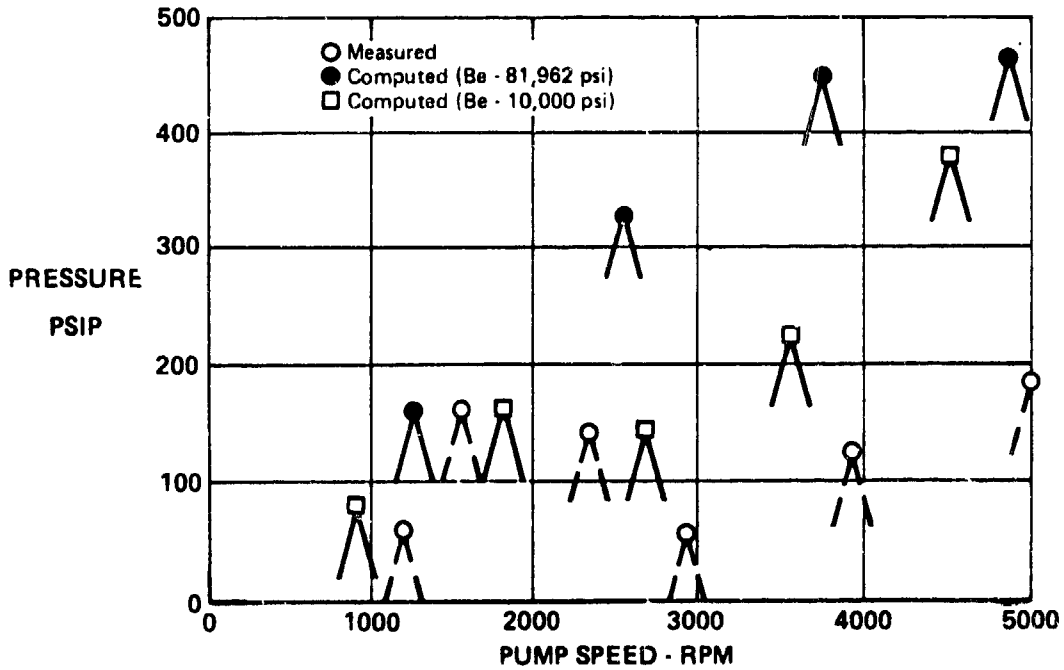

FIGURE 97. MAXIMUM FUNDAMENTAL PEAK RESPONSE IN TEST CIRCUIT
HOSE UPSTREAM LOCATION
MIL-H-83282 130°F 2 GPM

Figure 98 compares peak circuit responses for the hose located in the downstream position. Errors in predicted amplitudes are about the same as for the upstream position. Double resonance points are evident, probably resulting from two lengths in the circuit; pump to hose, hose to valve.

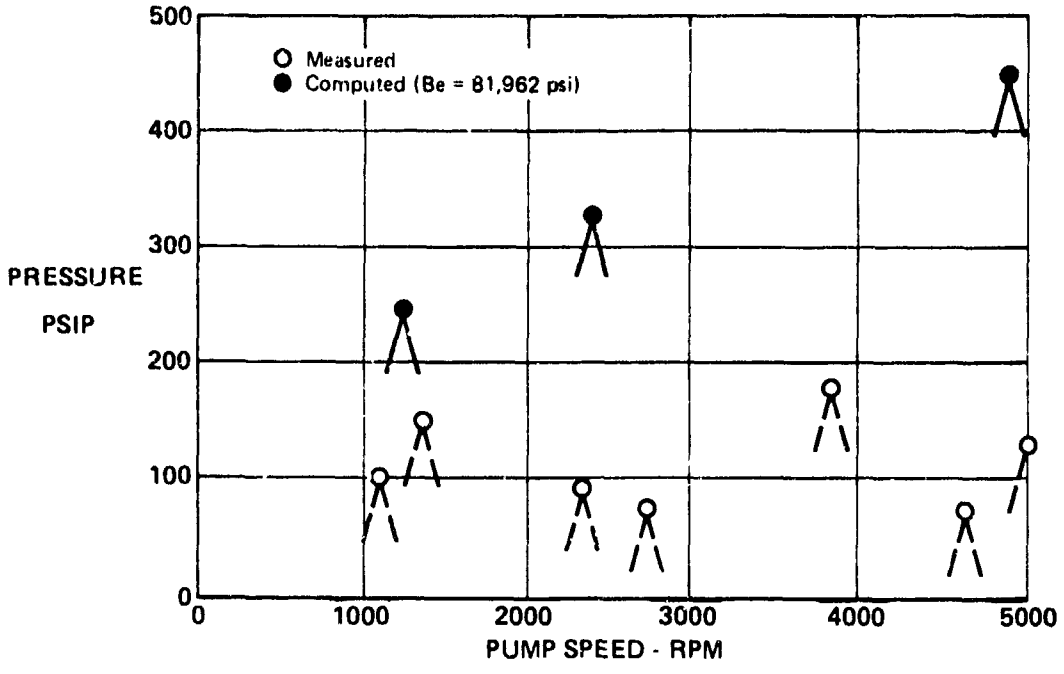

FIGURE 98. MAXIMUM FUNDAMENTAL PEAK RESPONSE IN TEST CIRCUIT HOSE DOWNSTREAM POSITION MIL-H-83282 130°F 2 GPM

Several factors were investigated in an attempt to explain the large errors in predicted amplitudes for the hose circuit at higher speed resonances (2500 to 5000 rpm). Large variations in predicted pulsation amplitude can be effected by varying the hose equivalent bulk modulus. Values of 1000, 10,000, 81,962, and 1,800,000 psi were used. Low values of bulk modulus reduce amplitudes, but produce large errors in predicted resonant frequency by increasing the number of resonant responses, i.e., lowering the natural frequency of the circuit.

The hose was modeled as lumped volumes of 12 in^3 (actual) and 20 in^3 at its center, and 12 in^3 at the downstream end of the hose. Large amplitude errors at the higher speed resonances remained, however resonant frequency predictions were not altered significantly (300 rpm).

The effect of pump pre-compression was examined. Pre-compressed cylinder pressure was varied by changing the estimated leakage during pre-compression in the PUMP subroutine.

Pre-Compressed Pressure	Resonant Speed	Change in Predicted Pulsation Amplitude
1000 to 2000 psi	1175 rpm	± 10%
1600 to 2800 psi	2600 rpm	± 5%
1900 to 3040 psi	3750 rpm	± 10%
2100 to 3120 psi	4800 rpm	± 10%

Resonant frequency prediction was not effected by pre-compression pressure.

6. JET FUEL STARTER (JFS) ACCUMULATOR VERIFICATION

Figure 99 shows the test circuit schematic for each of the two accumulator locations tested. The JFS accumulator was installed on a "T" branch off the main supply line. Gas pre-charge was 1500 psig. Estimated accumulator piston weight is 9.26 lbs (.024 lbs-sec^2/in).

Figure 100 illustrates the input data used for modeling the test circuit with the accumulator in the upstream position. Figure 101 shows a typical fundamental frequency pressure response in this modeled test circuit as a function of pump speed. Figure 102 plots the maximum peak pressure responses measured in the circuit and compares them to the computed values. Resonant frequency predictions are very good. However, amplitude predictions range from very high (1900 rpm), to close (2700 rpm), to low (4150 rpm). Amplitudes are somewhat lower than in the basic straight line circuit (Figure 94) particularly at the lower resonant frequencies.

Amplitudes are approximately the same upstream and downstream of the accumulator "T". Resonant frequency location and separation are shifted from uniform 1200 rpm separation of the straight line configuration.

Figure 103 shows a typical fundamental response measured in the circuit with the accumulator located downstream. Amplitudes are about the same as with the upstream position. However the wide separation in resonant frequencies occurs between the 1st and 2nd response rather than the 2nd and 3rd. Figure 104 plots the maximum peak pressure responses in the circuit (downstream location) and compares them to the computed values. Resonant frequency predictions are accurate as with the other circuit. However, amplitudes predictions are in error by about the same amount.

UPSTREAM LOCATION

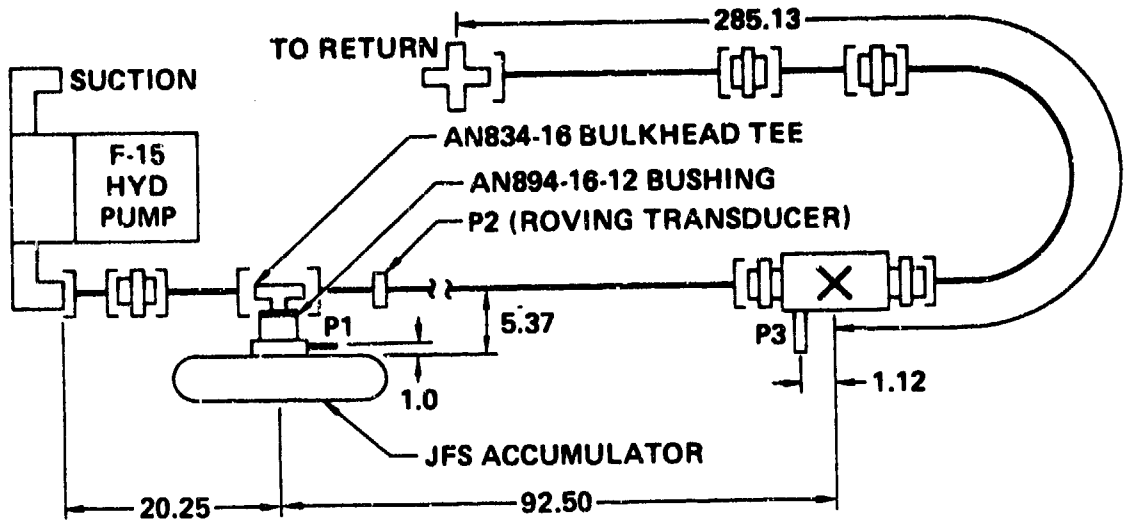

Note: All dimensions in inches

DOWNSTREAM LOCATION

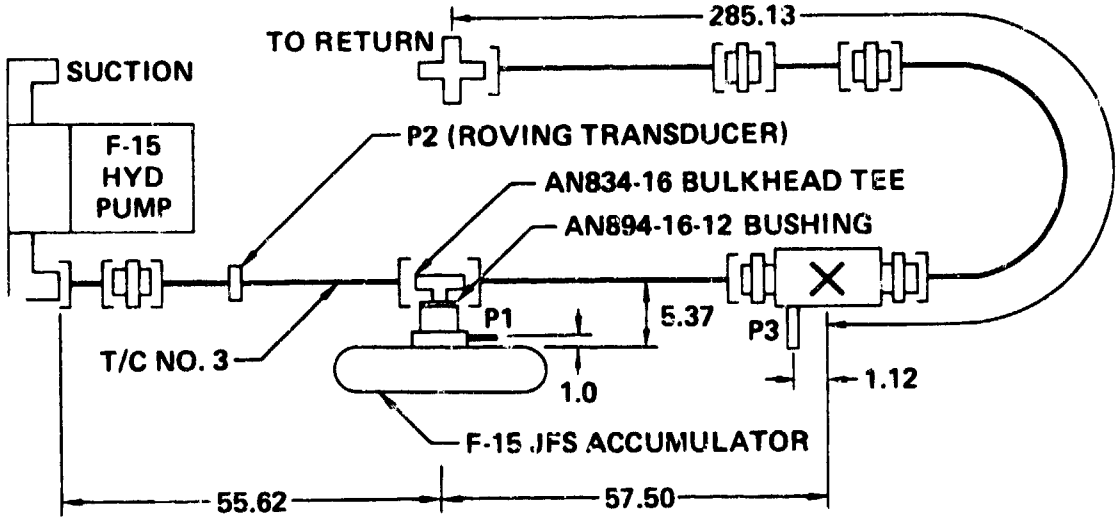

Note: All dimensions in inches

FIGURE 99. JFS ACCUMULATOR TEST CIRCUITS

JFS ACCUMULATOR VERIFICATION -FIRST SYSTEM-

RESPONSE IS CALCULATED FROM 90.00 TO 3000.00 R.P.M. IN INCREMENTS OF 50.00 R.P.M.
RESPONSE IS PLOTTED FOR THE -FIRST- HARMONIC FREQUENCY
NUMBER OF PUMPING ELEMENTS= 9.

FLUID DATA FOR MIL-H-83282 AT 3000.0 PSIG AND 130.0 DEG F

VISCOSITY = .200E-01 IN**2/SEC
DENSITY = .790E-04 LB-SEC**2/IN**4
BULK MODULUS = .225+06 PSI

ELEMENT NUMBER	N TYPE	K TYPE	PHYSICAL DATA							
1	0	22	.190	.666	1.120	1.172	.695	.570	.180	
			.20000	19.50000	9.40000	3.37500	28.75000	26.25000	26.00000	21.75000
			90.00000	.04000	.78000	2.07000	.00042	80.00000	200.00000	.69000
2	1	0	8.000	1.200	.100	30000000.000	0.000	0.000	0.000	
3	1	0	9.500	1.200	.100	30000000.000	0.000	0.000	0.000	
4	1	0	17.125	1.000	.058	30000000.000	0.000	0.000	0.000	
5	1	0	1.203	1.700	.058	30000000.000	0.000	0.000	0.000	
6	1	0	1.922	.950	.100	30000000.000	0.000	0.000	0.000	
7	6	12	0.000	0.000	0.000	0.000	0.000	0.000	0.000	
8	1	0	1.922	.950	.100	30000000.000	0.000	0.000	0.000	
9	1	0	2.453	1.000	.058	30000000.000	0.000	0.000	0.000	
10	1	0	11.125	1.000	.058	30000000.000	0.000	0.000	0.000	
11	1	0	12.000	1.000	.058	30000000.000	0.000	0.000	0.000	
12	1	0	12.000	1.000	.058	30000000.000	0.000	0.000	0.000	
13	1	0	12.000	1.000	.058	30000000.000	0.000	0.000	0.000	
14	1	0	12.000	1.000	.058	30000000.000	0.000	0.000	0.000	
15	1	0	12.000	1.000	.058	30000000.000	0.000	0.000	0.000	
16	1	0	12.000	1.000	.058	30000000.000	0.000	0.000	0.000	
17	1	0	3.875	1.000	.058	30000000.000	0.000	0.000	0.000	
18	1	0	1.125	1.000	.058	30000000.000	0.000	0.000	0.000	
19	14	0	389.610	7.700	0.000	0.000	0.000	0.000	0.000	
20	1	0	2.781	.950	.100	30000000.000	0.000	0.000	0.000	
21	1	0	1.250	.850	.100	30000000.000	0.000	0.000	0.000	
22	15	10	.024	2.500	.188	30000000.000	215.000	70.000	1500.000	
			3000.00000	.10000	0.00000	0.00000	0.00000	0.00000	0.00000	0.00000

FIGURE 100. HSFR INPUT DATA FOR JFS ACCUMULATOR VERIFICATION

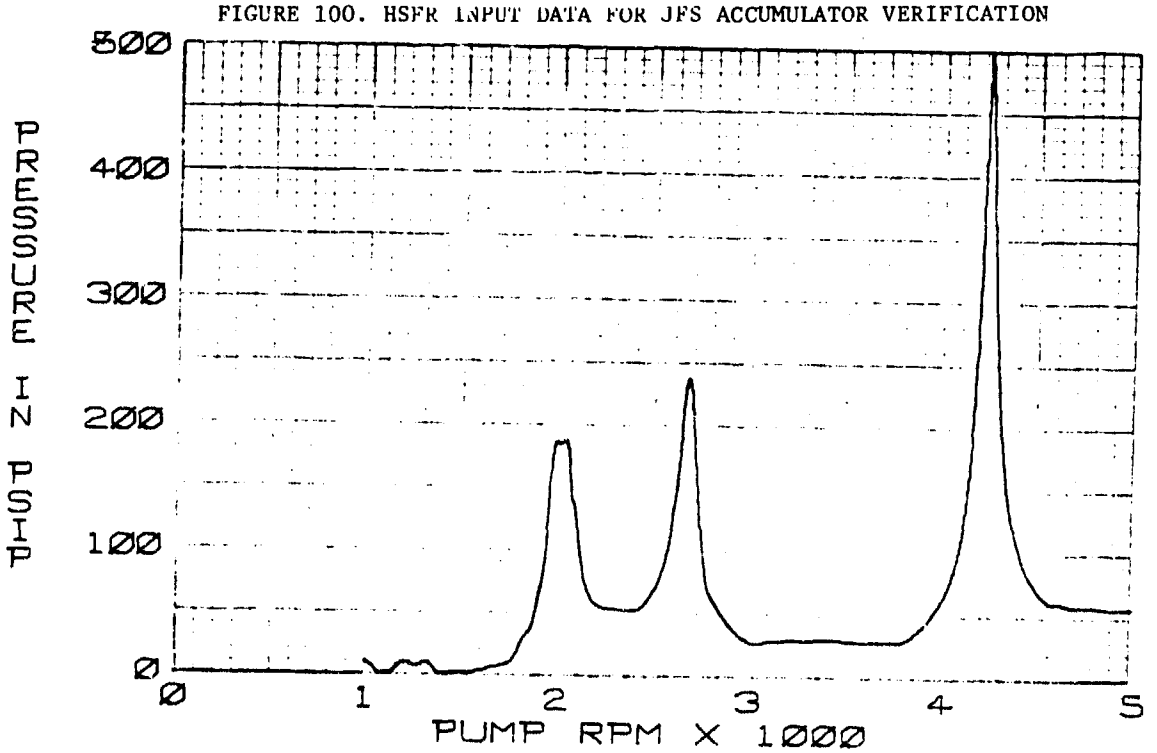

FIGURE 101. F-15 JFS ACCUMULATOR UPSTREAM LOCATION
75-09-P2 FUNDAMENTAL
2 GPM 130°F

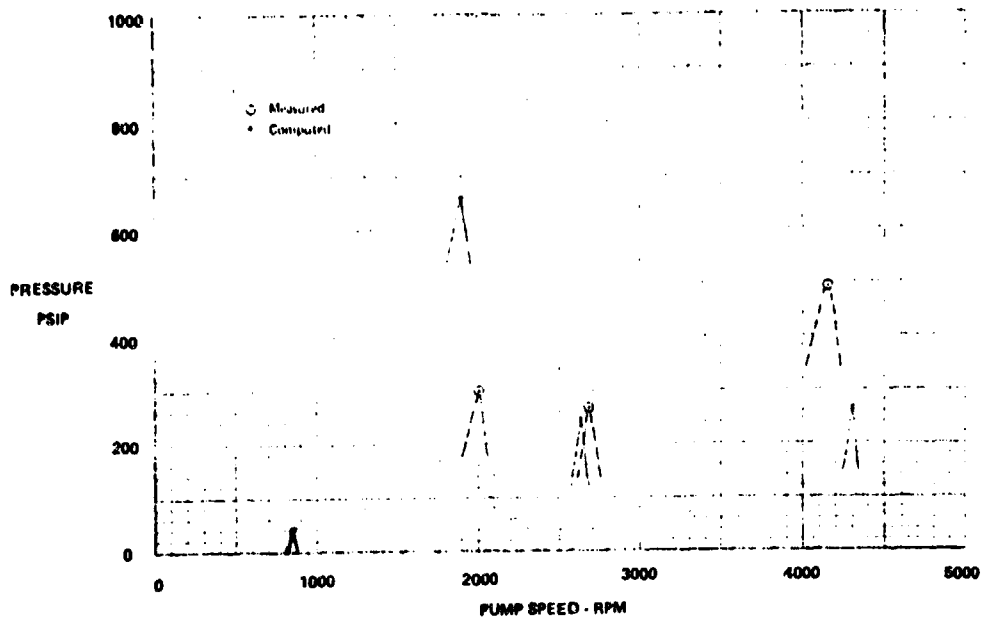

FIGURE 102. MAXIMUM FUNDAMENTAL PEAK RESPONSE IN TEST CIRCUIT F-15 JFS ACCUMULATOR-UPSTREAM POSITION
MIL-H-83282 130°F

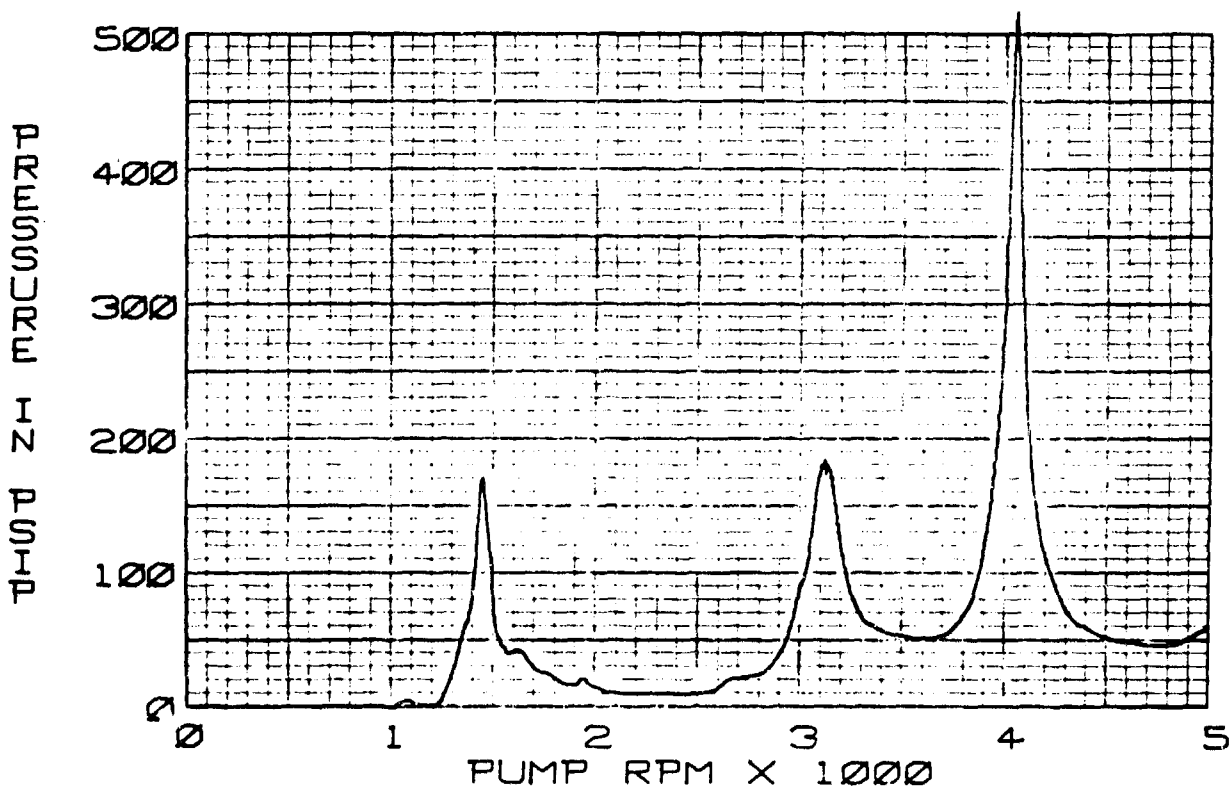

FIGURE 103. F-15 JFS ACCUMULATOR DOWNSTREAM LOCATION
75-19-P2 FUNDAMENTAL
2 GPM 130°F

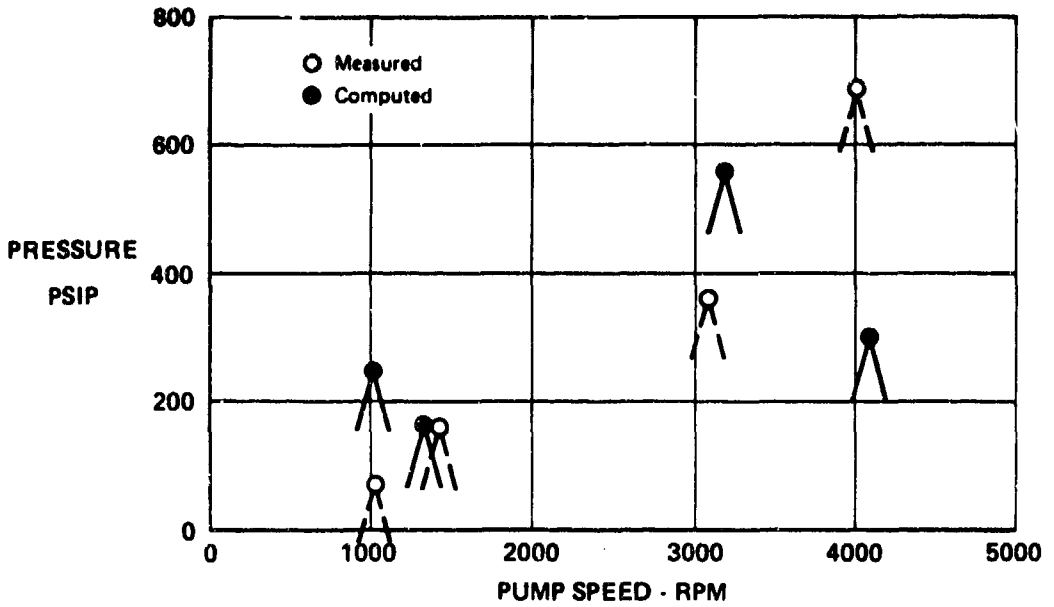

FIGURE 104. MAXIMUM FUNDAMENTAL PEAK RESPONSE IN TEST CIRCUIT F-15 JFS ACCUMULATOR-DOWNSTREAM POSITION MIL-H-83282 130°F

7. HSFR - SUMMARY AND CONCLUSIONS

1) System resonant frequencies predicted by the HSFR program for a simple short line system are accurate within about 2% - 4% (100 rpm from 2500 to 5000 rpm). Resonant frequency locations with the F-4 Helmholz resonator, JFS accumulator, PULSCO attenuator, and F-15 utility filter manifold circuit configurations were also predicted with 2 - 4% accuracy. Predictions of resonant frequencies in the hose circuit were less accurate (10 - 15%) and failed to show all of the resonances in the circuit.

2) Predicted amplitudes of peak pressure pulsations at system resonant frequencies are 30 to 50% lower than values measured in the short straight line system. The accuracy of amplitudes predicted in the filter circuit are about $\pm$ 30% at the lower resonant frequencies (2200 rpm). However, predicted amplitudes in the filter circuit are 200 to 300% high at the higher resonant frequencies (3500, 4650 rpm).

Amplitude predictions are consistently high (0 to 400%) for the hose circuit, with an apparent frequency dependent characteristic similar to the filter circuit. Amplitude predictions were relatively good ($\pm$ 30%) for the F-4 resonator circuit, and poor for the JFS accumulator circuit with no apparent frequency dependence.

3) Predicted and measured amplitudes of resonant pressure level decreased with increasing steady state flow from 0 to 20 gpm in the simple short line test circuit. Reduced reflections at the terminating load valve as flow increases results in a net reduction of the standing pressure wave amplitude, even though predicted pump pre-compression characteristics degrade slightly with increasing flow for a given shaft speed. An

increase in pulsations with higher flow, i.e., the opposite effect, is observed in a single long line test circuit and in full scale iron bird systems comprised of multiple long-line branches. Pump pre-compression may be more significant to pulsation levels than is the change in dynamic load with increasing flow in a long-line multibranch system.

Resonant frequency locations are unaffected by varying pump steady state flow level from 0 to 10 gpm in the short line test system.

4) The HSFR program and the model of the PULSCO acoustic filter provided useful predictions of circuit frequency response when the PULSCO unit is installed in a simple short line system. Prediction of maximum pulsation amplitudes is good for circuit resonant frequencies above about 60% of the attenuator design cutoff frequency, but is several times measured values for circuit resonances below 60% of cutoff levels.

5) The accuracy of predicted pressure amplitude at system resonant frequencies decreases at harmonics of the pumping frequency.

6) An 80°F increase in oil temperature decreased the system resonant frequency locations by about 400 rpm (pump shaft speed).

7) Internal outlet passages of the F-15 pump port cap and manifold should be modeled as lengths of line (outlet size) rather than as a lumped volume.

8) Table 2 compares the overall pressure pulsation characteristics measured in the straight line test circuit with the various components installed.

TABLE 2

COMPARISON OF MEASURED PRESSURE PULSATIONS WITH VARIOUS TEST CIRCUIT CONFIGURATIONS

TEST CIRCUIT CONFIGURATION	NUMBER OF RESONANCES (2000-5000 RPM)	MAX PULSATION IN CIRCUIT (130°F) (2000-5000 RPM)
Short Straight Circuit (1 in OD x 9 ft)	3	770 psip
PULSCO Filter (APT-1)		
o Upstream Location (at pump manifold)	0	40 psip
o Downstream Location	1	150 psip
Hose (1 in. OD x 20 in)		
o Upstream Location	3	180 psip
o Downstream Location	4	160 psip
Filter (F-15 Manifold)	2	300 psip
F-4 Helmholz Resonator		
o Upstream Location	3	300 psip
o Downstream Location	3	670 psip
JFS Accumulator (215 in^3)		
o Upstream Location	3	490 psip
o Downstream Location	2	700 psip

The small (10 gpm) PULSCO acoustic filter was the most effective device in reducing pressure pulsations over the full range of hydraulic pump operating speeds. Pulsations were reduced by an order of magnitude (770 psip to 40 psip). Similar performance was verified with the PULSCO unit installed in the F-15 iron bird utility system. The 20 inch hose produced a significant reduction in amplitudes (770 psip to 180 psip), independent of its location in the circuit. The filter and F-4 resonator were effective to lesser degrees. The large accumulator (JFS) has relatively little effect on circuit pulsation level, particularly at the downstream location. Significant changes in resonant frequencies occurred with different accumulator locations in the circuit. The large piston mass and/or non-flow through installation (tee) reduced its effectiveness.

9) PULSCO and F-4 Helmholz acoustic units are the most effective when installed close to the pump. Locating the F-4 resonator or filter several feet downstream of the pump retains high pulsations upstream of the unit, although significant attenuation of pulsations downstream of the unit are achieved.

10) The HSFR program/PUMP subroutine can be used effectively to study pump hanger torque, port plate valve timing, and piston cylinder cavitation characteristics. Model predictions indicate that the F-15 pump has good overall pre-compression characteristics throughout the operating range of shaft speed and flow delivery. Predicted decompression shows a slight cavitation condition in the cylinder for all flow rates up to 40 gpm.

11) The HSFR program may be used to study resonance characteristics of a hydraulic suction/return system. However, return system frequency analysis was not part of the contract scope, and is not verified. Resonant frequency predictions in the return system should be reasonably good, owing to the use of the same computation method and models as are used for pressure system analysis. The accuracy of predicted pressure amplitude at return system resonances is unknown.

12) The importance of total circuit acoustic analysis cannot be underestimated. While an acoustic attenuator may be sized for a particular frequency, its installation will alter the basic frequency response of the circuit. The net effect of the attenuator or other system change can only be evaluated in the circuit, whether by analysis or test. The complex interrelationship between the pump and system dynamic load cannot be ignored in the acoustic analysis of hydraulic systems.

SECTION V

COMPUTER SIMULATION AND TRANSIENT TEST RESULTS

The transient data obtained in the Dynamics Laboratory from the test bench shown in Figure 105 was used in conjunction with the HYTRAN computer program to verify a mathematical element model. In general for any one element a minimum of six variables were measured and recorded. These variables are the pressures and flows taken from the two instrumentation stations in Figure 105. A portion of this recorded data was used in the HYTRAN computer simulation of the test run to provide boundary conditions. The output from the computer program was the flow and pressure plots at the recorded data points. The plots were compared to the recorded data not input with the simulation and the math model of the element being tested was either corrected or verified from this correlation. To illustrate the verification process the data taken in the laboratory and the computer simulation of the test run is presented below for a line element.

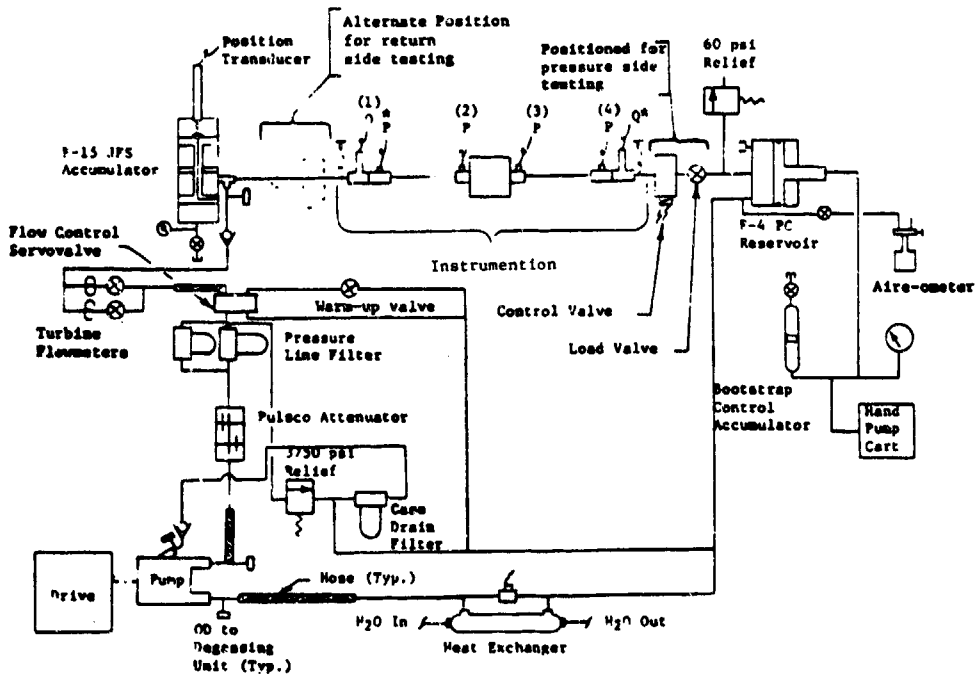

FIGURE 105 STEADY STATE AND TRANSIENT TEST BRANCH HYDRAULIC SCHEMATIC

In the testing of the line element during a turn-off transient (Figure 106), the transient is supplied by a fast valve (1 msec typical closing time) downstream of the line specimen. Steady state values of pressure and flow are being recorded when the valve is closed at time t_1. The response to the valve closure is recorded on magnetic tape for P_1, P_2, P_3, P_4, Q_1, Q_4 and valve position. To analyze the data it is transferred to a computer data file by the methods described in Section III, Paragraph 2. Before data can be processed with the HYTRAN program, the physical description of the test system to be simulated is input. For the line model the two instrumentation sections and the line test specimen is all that is required. The pressure histories at the upstream (P_1) and downstream (P_4) end of the line test setup are used as boundary conditions for the computer simulation of the test run. The HYTRAN computer program calculates the flows and pressures for each time step in the transient analysis using the measured data as the line end boundary conditions as shown in Figure 107.

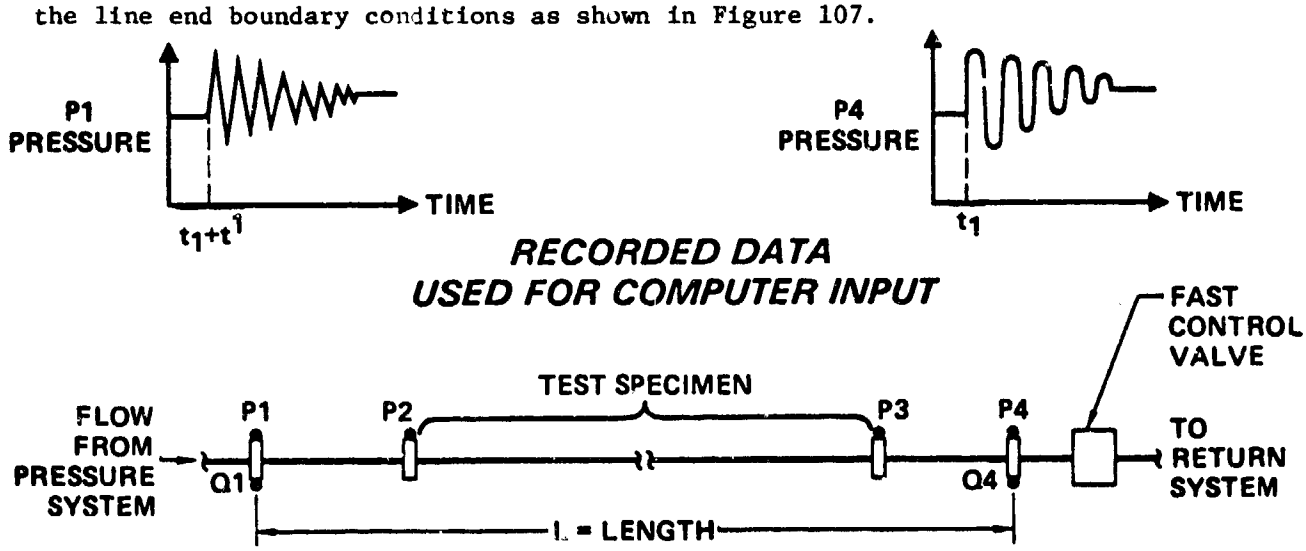

CONDITIONS: STEADY STATE FLOW, Q AT t = 0,
FAST VALVE CLOSED AT $t = t_1$
PRESSURE WAVE REACHES P1 TRANSDUCER
AT $t_1 + t^1$ TIME WHERE:
$t^1 = L/C$
C = VELOCITY OF SOUND IN THE FLUID
Q1, Q4, P1, P2, P3, P4 AND VALVE POSITION ARE RECORDED

FIGURE 106 RECORDING A TURN-OFF TRANSIENT

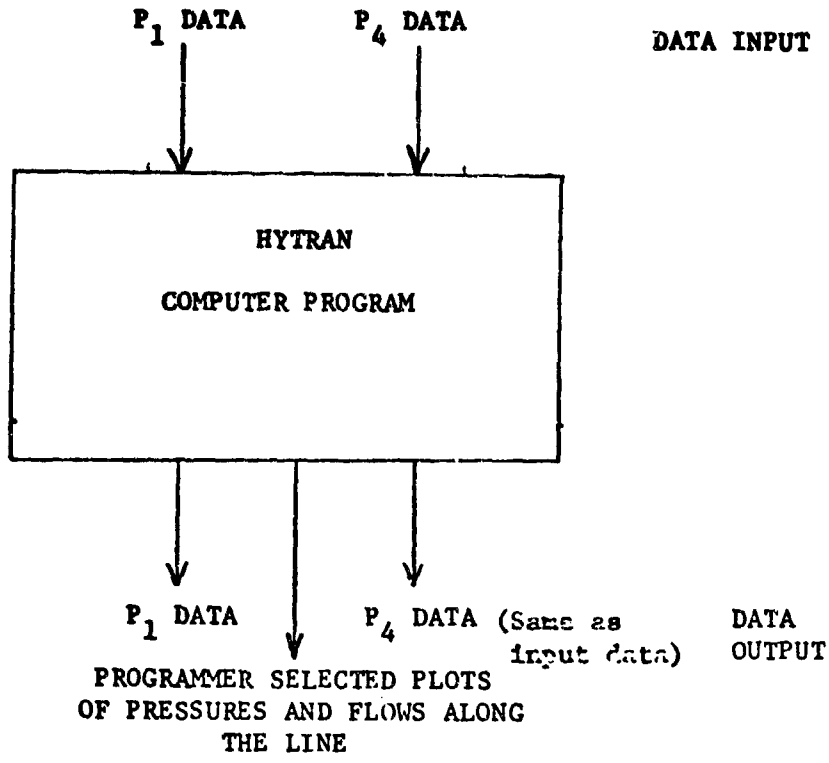

FIGURE 107 INPUT AND OUTPUT OF COMPUTER LINE SIMULATION

The computer simulation which uses a combination of math models and measured data gives plots of flows and pressures in the system. The plotted computer outputs were compared to the recorded data which is not input with the simulation. For the turn off run in Figure 106 this would be Q_1, Q_4, P_2 and P_3. Good computer output/test data correlation verifies the model. Accurate dynamic flow data is necessary to intelligently alter the models, if that is necessary to achieve correlation.

A different boundary condition can be added to the computer simulation of the simple line system by inserting a fast closing valve in the model downstream of the line and using the recorded valve position instead of the line downstream pressure for input data. This technique allows the variables measured in the laboratory to completely define the component of interest.

The majority of the testing was done at 125 and 210°F with flows ranging from 11.55 to 38.5 CIS. The percent of dissolved air in the

hydraulic fluid was less than 1% by volume. Two fluids were used in the transient testing - MIL-H-5606B and MIL-H-83282. Any test conditions that deviated from the above are noted where applicable.

1. LINE MODEL VERIFICATION

An analysis of the test results obtained in the laboratory compared to the HYTRAN computer program line model is presented in this section. The testing for the HYTRAN line model verification was performed on a 1/2" diameter x 30 ft long tube with MIL-H-5606B hydraulic fluid.

The line subroutine uses the classical distributed parameter wave equations to model the lines. The equations are solved using the method of characteristics and finite difference techniques. The steady state and dynamic friction subroutines are called to obtain the friction information for the line. The dynamic friction subroutine uses a decaying function of dQ/dt to calculate the frequency dependent friction.

a. HYTRAN Computer Simulation with Line Test Data - The most accurate test of a computer simulation comes from inputting only the steady-state boundary conditions to the program and letting it predict the resultant transients in the system from a valve opening or closure. To obtain steady state boundary conditions, one has to start at places where flows and pressures are known and easily measured, such as accumulators and reservoirs, to run the simulation. In verifying the line model it would be unwise to include other components into the computer run of the system, since the effects of these other components may not be completely understood, and their math models have not yet been adequately verified. Thus in the line model verification programs only lines and components that have minor effects on the line simulation were used in the computer program. Both turn-off and turn-on transients were compared to the actual computer outputs by over-plotting the measured data on the computed resultant graphs.

For the turn-off transient simulation, a fast closing valve and a line bounded by a constant pressure reservoir was used. The system schematic is shown in Figure 108. This configuration was used for turn-off transient analysis, because the boundary conditions were easily defined after the valve closure. For a turn-on transient,

because of the short return line system (17"), there was very little noticeable effect on the upstream baseline tube; and the steady state boundary conditions were simple to obtain.

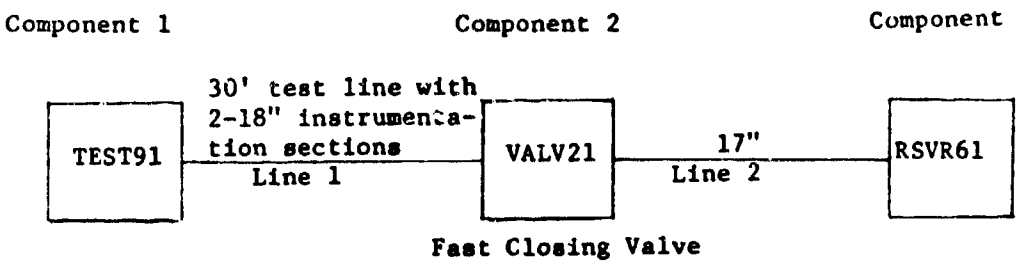

FIGURE 108 COMPUTER PROGRAM SCHEMATIC OF TEST SYSTEM USING P1 DATA INPUT

Three components were used in the program schematic of Figure 108 in the computer simulation. They were, TEST91, VALV21, and RSVR61. TEST91 was a subroutine that used recorded verification test data. For each time step of the transient analysis, a test data value was inserted as the line end point boundary condition. Included in Line 1, were the 30 ft baseline tube, the two 18" instrumentation stations and a 15" line segment, which was immediately upstream of the fast valve. Figure 109 shows the basic test stand arrangement in the laboratory with the appropriate dimensions. VALV21 was a control valve element for which the valve opening or closing characteristics versus time were input. The valve subroutine used tabulated valve strokes to calculate total valve area versus time. Using the data from adjacent lines, it calculated the pressures at its upstream and downstream connections, along with the flow, and returned the data to the lines. Line 2 was a 17" segment of 1/2" diameter tubing going into the reservoir, which was modeled by RSVR61. The 61 reservoir was a constant pressure type used in simulations to provide a steady state boundary condition. Typically the reservoir pressure was set to 50 PSI.

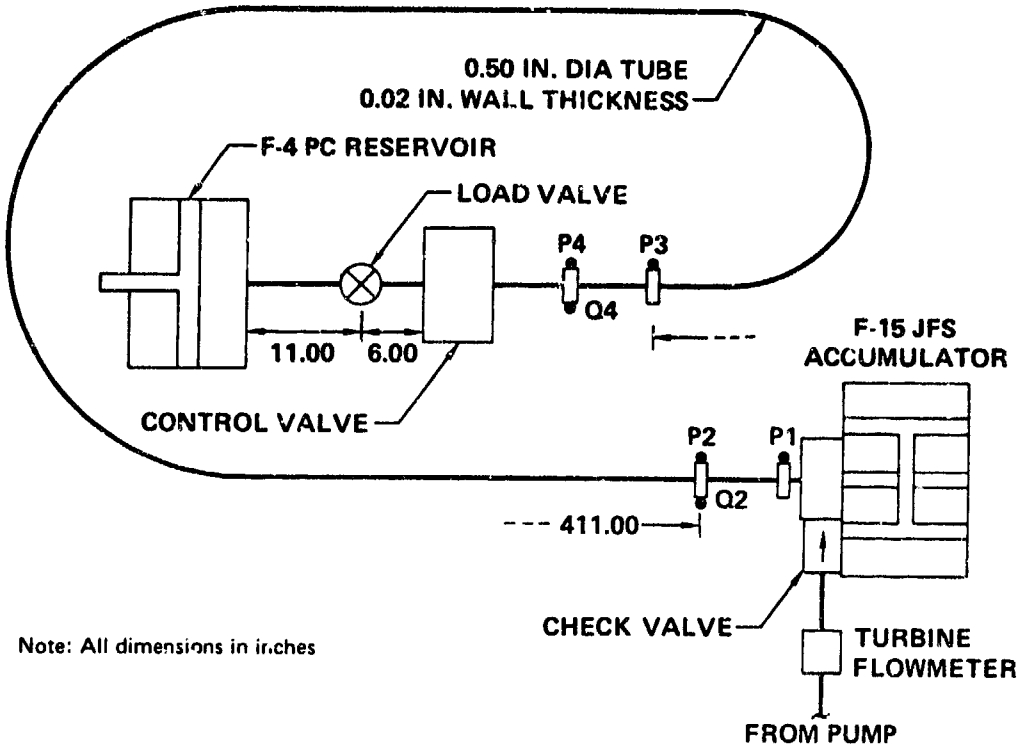

FIGURE 109 TRANSIENT LINE TEST CONFIGURATION

P_1 pressure data was input through TEST91. The valve closing or opening time was manually computed from the test data and then input into the program. The computer program then predicted the flows and pressures at given distances down the lines. For the TEST91 subroutine the data was the actual interior line boundary points. The valve and reservoir subroutines form the boundary conditions of the lines and were solved simultaneously with the associated line characteristic equations.

The HYTRAN program gave plots of pressures at P_1, P_2, P_3 and P_4 and flows at Q_1 and Q_4. The plots of P_2, P_3, P_4, Q_1 and Q_4 were then overplotted with the actual test data for comparison.

The Q_1 and Q_4 data plots were obtained by applying a linearizing equation to the recorded anemometer voltages. The equation was generated by fitting a second degree curve through the calibration plot anemometer voltage vs turbine meter flow. The pressure data was linear, meaning

that transducer voltage is directly proportional to pressure, and no other relationships was developed for plotting the pressure data.

Another set of boundary conditions used in the line model verification involved only the 30 ft tube and the instrumentation sections. The HYTRAN program computer schematic is shown in Figure 110.

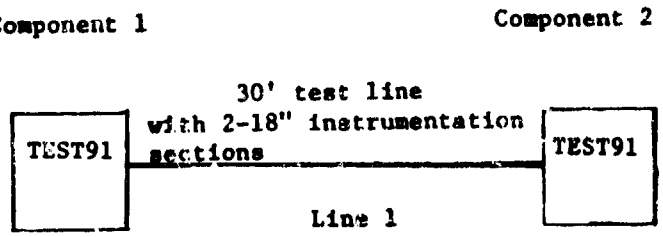

FIGURE 110 HYTRAN SCHEMATIC OF TEST SYSTEM USING P1 AND P4 DATA INPUT

P_1 and P_4 test data was input through the two TEST91 subroutines to provide boundary conditions for the line simulation. Line 1 contained the two 18" instrumentation sections and the 1/2" dia x 30 ft long tube. The HYTRAN program printed plots of P_2, P_3, Q_1 and Q_4 for comparison to the test data.

A HYTRAN computer program output plot of P_1 data that was input with a simulation is shown in Figure 111. The actual P_1 test data (continuous black line) is plotted over the graph of printed P's to demonstrate that comparing computer plotted outputs to test data is entirely acceptable.

The first set of data to be compared to a computer run was for a turn-off transient at 125°F.

With Figure 112 input data and Figure 111 P_1 data, the HYTRAN simulation of the line model was run. Figures 113, 114, and 115 show the computer printed outputs overplotted with laboratory test data. Figure 113 is a plot of the P_4 data over the computer predicted pressure data for the P_4 position. The computer output of P_4 position is not exactly in the same location as the test data. From the test configuration that was simulated, the P_4 transducer is located 396 inches from the P_1 transducer (360 inches for the baseline tube plus 36 inches for the instrumentation sections). The computer printed out the pressure

at 400.98 inches along the line. The reason for this discrepancy is due to the ΔX interval chosen by the program for computation using the method of characteristics. For the 411 inch line in Figure 112 the ΔX was 10.0244 inches. Since pressures and flows are calculated only at each ΔX in the program, the computed values closest to the distances specified by the programmer are output.

The computer output of P_4 agrees favorably with the test data. The asterisks by the P's in Figure 113 indicate pressure values that deviate from the pressure trace. This could be due in part to mechanical vibrations of the tube shown in the P_1 input data (Figure 111) that propagate through the transient calculations in the program.

The data taken in the lab is sampled at a .0002 second interval. This data is not reprocessed in any way for noise content. Consequently all mechanical and noise disturbances do appear in the P_1 data. The method of characteristics used in the computer program for the line model uses every data point as a line end condition. Any small perturbation will be reflected throughout the entire calculation. These changes may be reinforced or subdued depending on flow and pressure conditions existing in the line.

The Q_1 and Q_4 flow plots are shown in Figures 114 and 115.

The hot film anemometers positioned in the flow stream can only measure flow magnitude and not direction. The computer output plots of flow have the actual flow calculated printed out with the letter Q. For flow reversals the magnitude of the flow is printed as an asterisk character. The anemometer data was then directly plotted over the computer plots for comparison.

In Figure 114 the flow reversals of the recorded test data shown by the first, third, fifth, etc. peaks have a definite flow decay, while the even numbered peaks indicate a flatter response. The computer printout does not show this effect.

A possible explanation for the decaying flow reversals in the Q_1 test data comes from the shape of the velocity profile under transient conditions. When a steady state flow in a line is subjected to an abrupt valve closure, the flow first reverses itself along the tube walls. As the reverse flow becomes established the maximum velocity profile drops closer to the tube centerline. Since the hot film probe is in a fixed position close to the tube wall, it can sense this apparent flow decay. The reason this

does not occur for forward flows is because the maximum velocity profile is closer to the centerline of the tube. The line subroutine in HYTRAN does not currrently model this type of behavior. The computer output in Figure 114 indicates this.

The computer plots do not agree in magnitude with the test data except for the initial steady state flows. The actual test data indicates a slower decay rate to the zero flow condition. The computed flows appears to be slightly overdamped.

Figure 115 is the Q_4 computed output data. On the turn-off transient it fails to show the first peak flow near the valve. This is due to the plotting interval chosen for the output plots. Pressure and flow calculations are made in the line simulation of the system transient for every point of the P1 input data, which contains 1000 sampled points. The computer can only plot 101 data points for each graph, thus for 1000 data values every fourth point calculated is plotted.

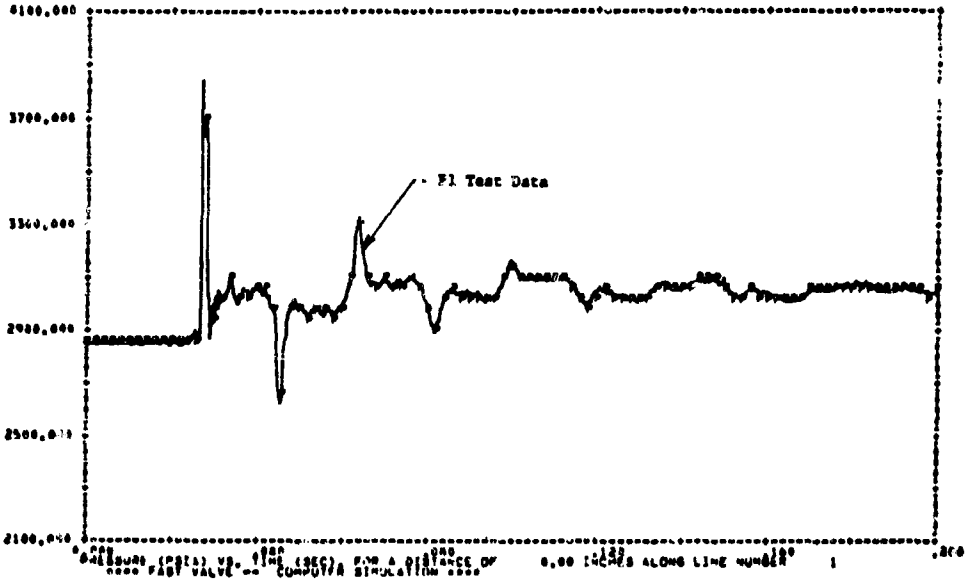

FIGURE 111 P1 TEST DATA FOR A TURN-OFF TRANSIENT

```
THE TRANSIENT RESPONSE IS FROM T=0.0  TO T=  .200 SECONDS AT TIME INTERVALS OF DELT= .00020
        WITH OUTPUT POINTS PLOTTED AT INTERVALS OF  ,  .00200  SECONDS

     FLUID DATA FOR MIL-H-5606E AT  3000.0 PSIG AND 125.0 DEG F
          VISCOSITY     =  .201E-01  IN**2/SEC
          DENSITY       =  .814E-04  (LB-SEC**2)/IN**4
          BULK MODULUS  =  .224E+06  PSI

LINE DATA
LINE NO.   LENGTH      INTERNAL   WALL        MODULUS OF   DELX       CHARACTERISTIC  VELOCITY OF
                       DIA        THICKNESS   ELASTICITY              IMPEDANCE       SOUND
  1        411.0000    .4440      .0200       .300E+08     10.0200    20.1911         40010.0209
  2         17.0000    .4440      .0200       .300E+08     17.0000    20.1911         40010.0209
 COMPS.   1 INTEGER DATA   1  91   0  -1   1  -0  -0  -0  -0  -0  -0  -0  -0  -0  -0  -0
 COMPS.   2 INTEGER DATA   2  21   3   1  -2  -0  -0  -0  -0  -0  -0  -0  -0   4  -0  -0
REAL DATA CARD #   1    .2200E-01  .6500E+00 -0.        -0.        -0.        -0.        -0.        -0.
REAL DATA CARD #   2   0.          .1700E+01  .1030E-01  .2000E+00 -0.        -0.        -0.        -0.
REAL DATA CARD #   3    .3270E+06  .3270E+06  0.         0.        -0.        -0.        -0.        -0.
 COMPS.   3 INTEGER DATA   3  41   1   2  -0  -0  -0  -0  -0  -0  -0  -0  -0  -0  -0  -0
REAL DATA CARD #   1    .5000E+02 -0.        -0.        -0.        -0.        -0.        -0.        -0.
```

FIGURE 112 INPUT DATA FOR A TURN-OFF TRANSIENT LINE SIMULATION

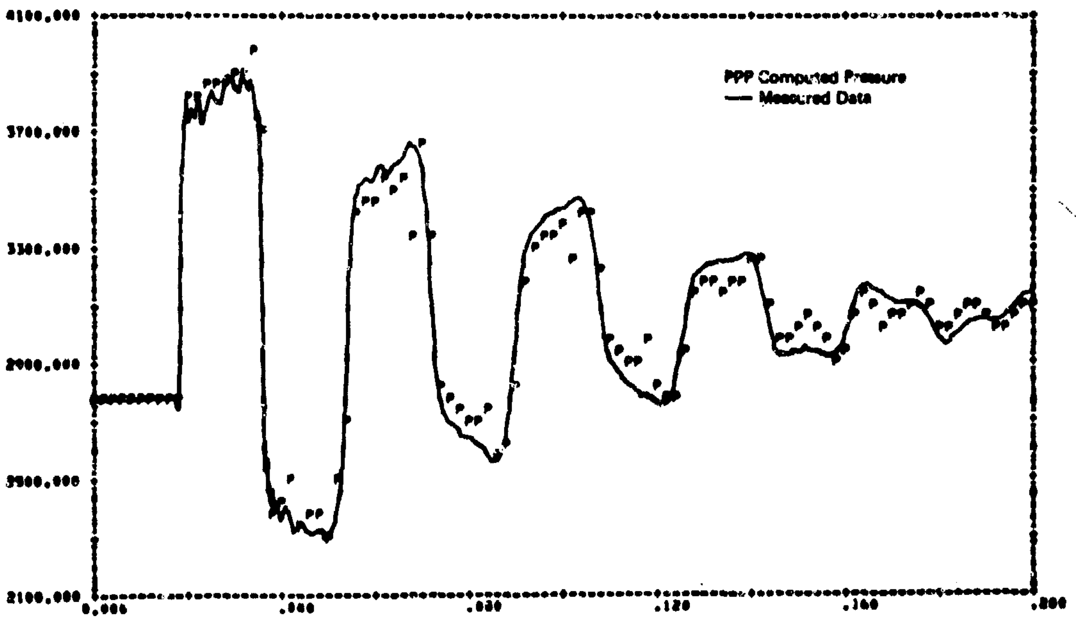

FIGURE 113 COMPUTED VS. MEASURED P4 PRESSURE FOR A TURN-OFF TRANSIENT

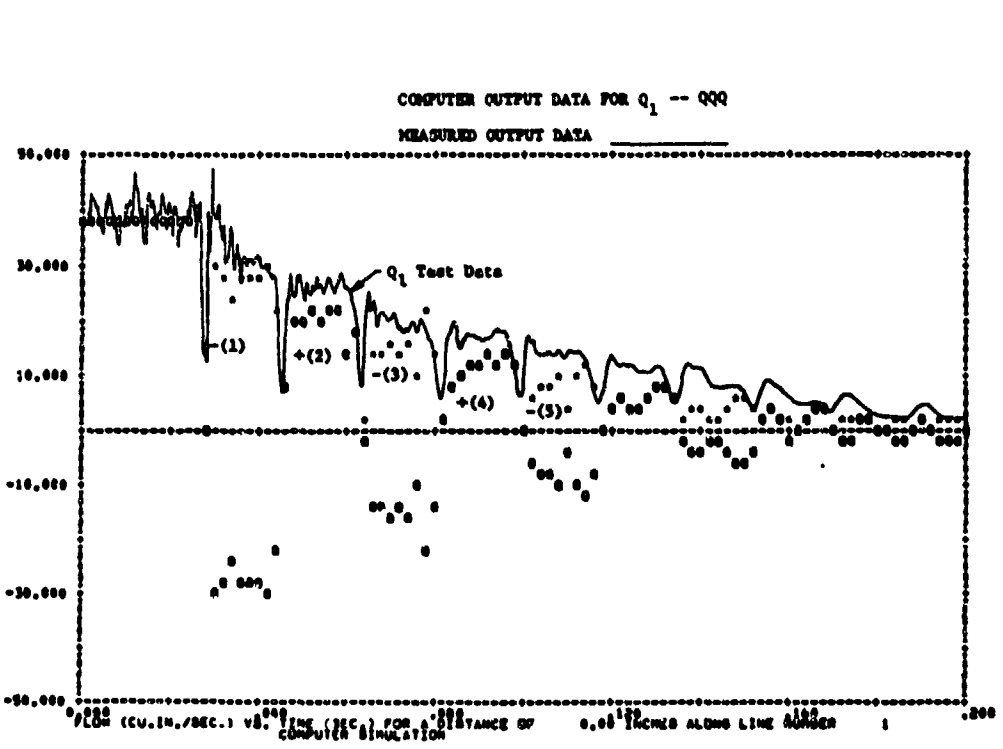

FIGURE 114 COMPUTED VS. MEASURED Q1 FLOW FOR A TURN-OFF TRANSIENT

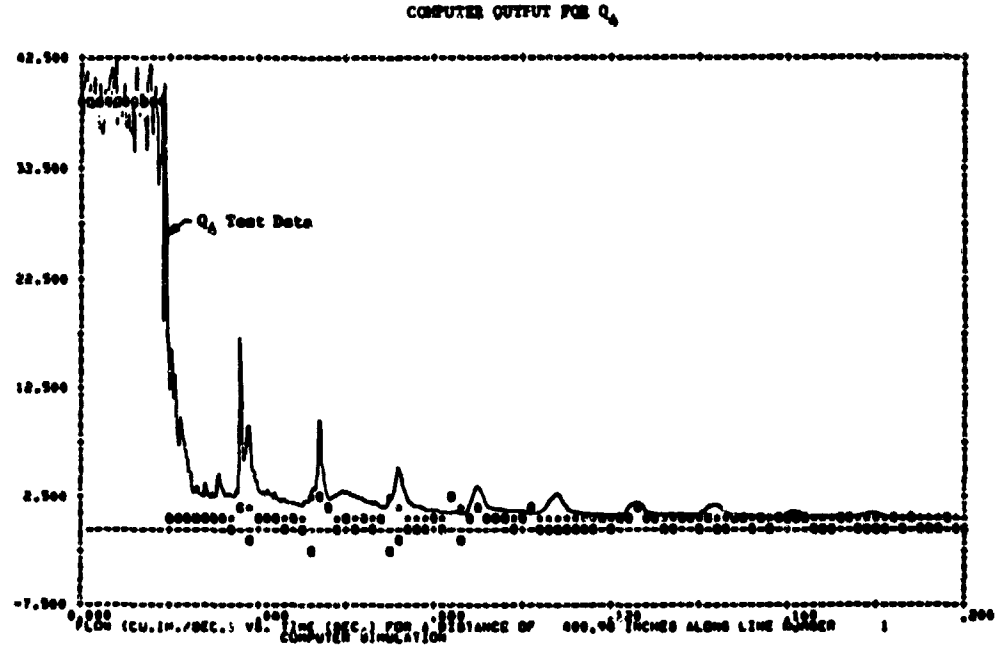

FIGURE 115 COMPUTED VS. MEASURED Q4 FLOW FOR A TURN-OFF TRANSIENT

A turn-on transient at 125°F was simulated with the computer program. The data input for the computer run is in Figure 116 with the computer input information given in Figure 117. The output pressures and flows are shown in Figures 118, 119 and 120. The P_4 pressure data trace in Figure 118 indicates good correlation with the computer output plots, although the first peak pressure points for the P_4 test data are higher by about 150 PSI for the maximum value. The flow test data in Figures 119 and 120 show a gradual increase to the first maximum value from the zero flow condition. The computer prediction in both Figures 119 and 120 jump to a flow level immediately on opening the valve. The gradual increase in the test data could be attributed to the time it takes the fluid to develop a good velocity profile.

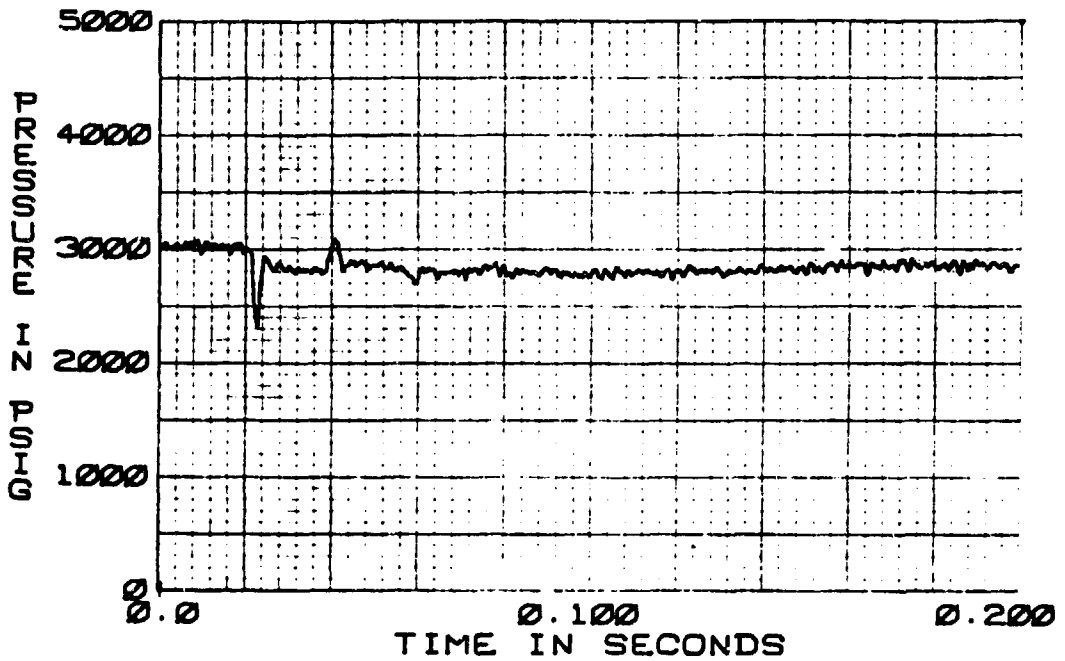

FIGURE 116 .5 IN DATA 30 FT. TUBE P1 TURN ON TRANSIENT
38.5 C15, 125 DEG F

```
THE TRANSIENT RESPONSE IS FROM T=0.0  TO T=   .200 SECONDS AT TIME INTERVALS OF DELT= .00020
        WITH OUTPUT POINTS PLOTTED AT INTERVALS OF   ,   .00200  SECONDS

FLUID DATA FOR MIL-H-5606B AT  3000.0 PSIG AND 125.0 DEG F
        VISCOSITY    =  .201E-01  LBF-SEC**2/IN**4
        DENSITY      =  .814E-04  LB-SEC**2)/IN**4
        BULK MODULUS =  .232E+06  PSI

LINE DATA LINE NO.   LENGTH        INTERNAL DIA      WALL THICKNESS    MODULUS OF ELASTICITY   DELX          CHARACTERISTIC IMPEDANCE   VELOCITY OF SOUND
     1          411.0000          .4440             .0280             .300E+08                10.0244       26.1911                    49010.4249
     2           17.0000          .4440             .0280             .300E+08                17.0000       26.1911                    49010.4249
  COMP#,  1 INTEGER DATA     1   91   0   -1   1   -0   -0   -0   -0   -0   -0   -0   -0   -0   -0   -0   -0
  COMP#,  2 INTEGER DATA     2   21   3    1  -2   -0   -0   -0   -0   -0   -0   -0   -0    4   -0   -0
 REAL DATA CARD #   1     .2200E-01  .6500E+00 -0.          -0.          -0.          -0.          -0.          -0.
 REAL DATA CARD #   2  0.            .1200E-01  .1300E-01   .2000E+00 -0.          -0.          -0.          -0.
 REAL DATA CARD #   3  0.            0.         .3270E+00   .3270E+00 -0.          -0.          -0.          -0.
  COMP#,  3 INTEGER DATA     3   61   1    2   -0   -0   -0   -0   -0   -0   -0   -0   -0   -0   -0   -0
 REAL DATA CARD #   1     .5000E+02 -0.          -0.          -0.          -0.          -0.          -0.          -0.
```

FIGURE 117 INPUT DATA FOR A TURN-ON TRANSIENT LINE SIMULATION

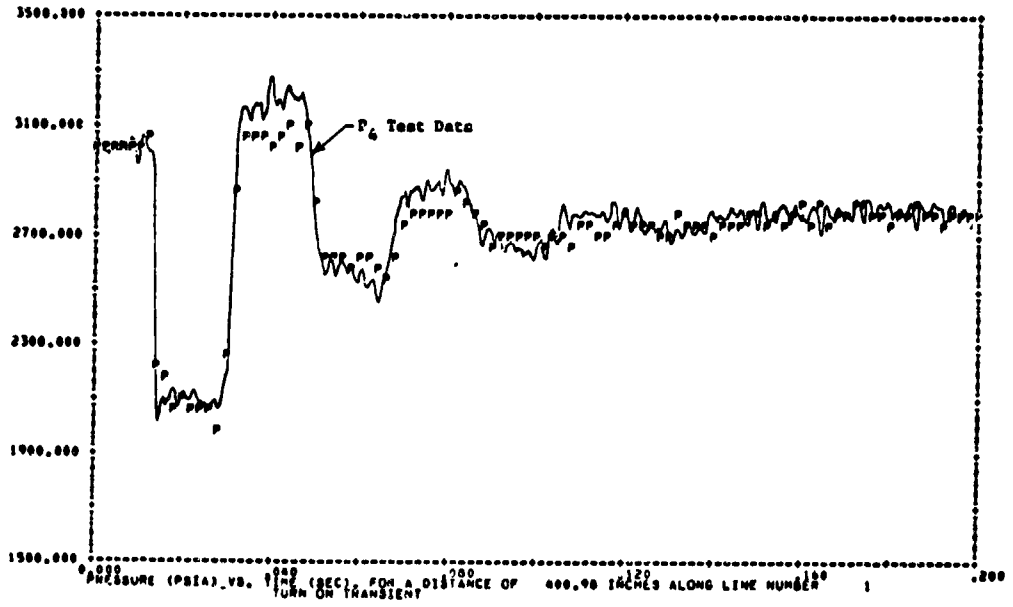

FIGURE 118 COMPUTED VS. MEASURED P4 PRESSURE FOR A TURN-ON TRANSIENT

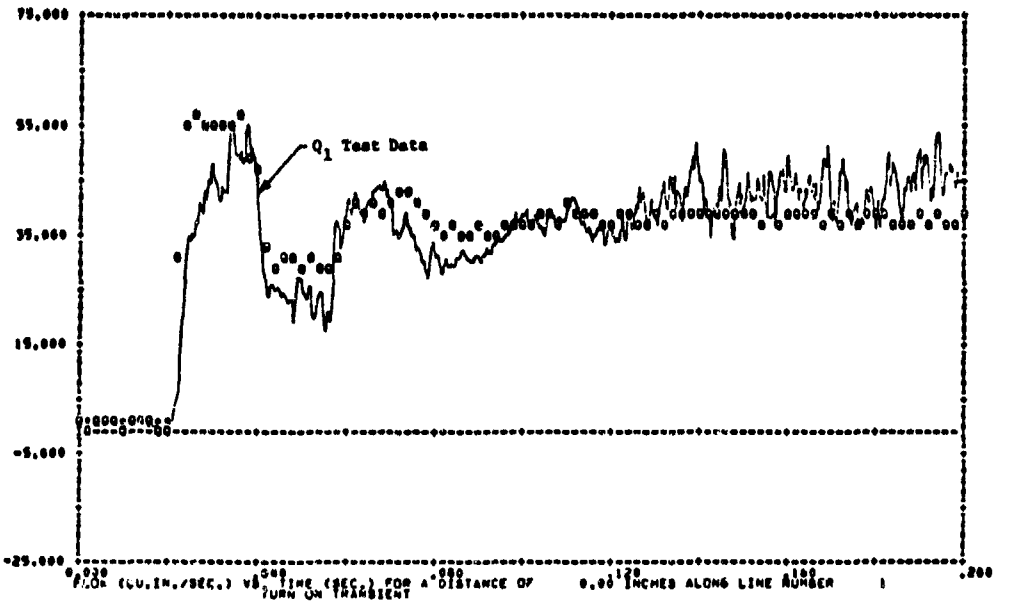

FIGURE 119 COMPUTED VS. MEASURED P4 PRESSURE FOR A TURN-ON TRANSIENT

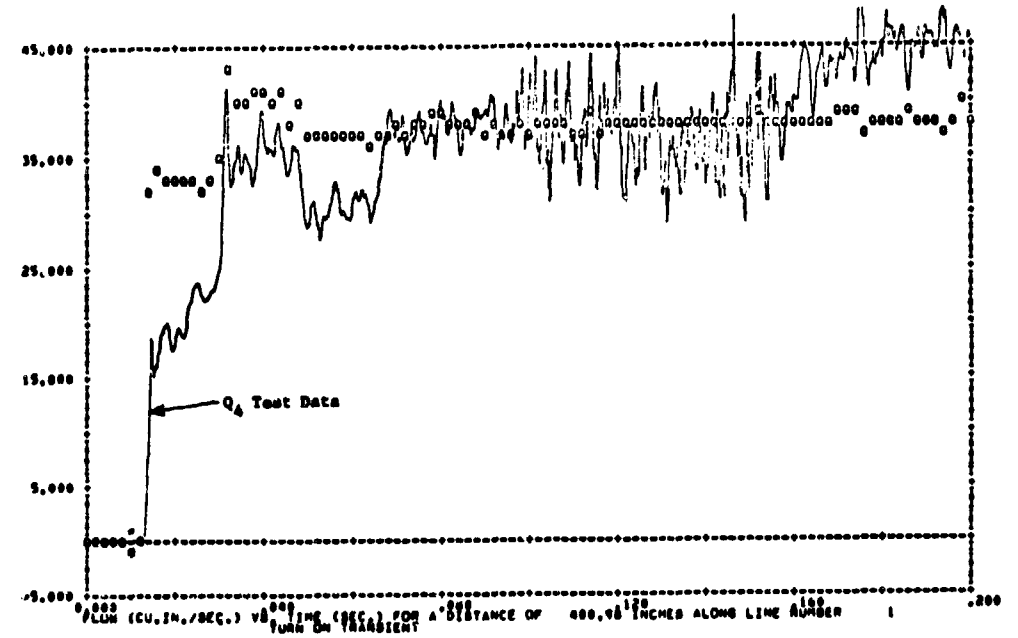

FIGURE 120 COMPUTED VS. MEASURED Q4 FLOW FOR A TURN-ON TRANSIENT

The steady state flow at the end of the data run rises to about 45 CIS. This is more exaggerated in Figure 119 than 120 because of the plotting scales. The increase did not show up in the computer plots because the P_1 input data did not contain enough pressure information to account for the increased flow in the system. These results bring out some of the problems with the hot film anemometers in the laboratory. Because of their positioning in the system they are not capable of measuring a mean flow, only a local velocity limited to a specific region close to the tube wall. The rise in steady state flow after .16 seconds in Figure 120 indicates an area of turbulence around the probe tip. This eventually settles to 38.5 CIS steady state flow after the flow profile has been allowed to develop. The HYTRAN line model does not account for any delay that can occur in the establishment of turbulent flow.

b. Effect on Dynamic Friction on Transients - Using the P_1 data in Figure 111 the system in Figure 109 was simulated by the HYTRAN computer program. The important difference in this simulation was that the effect of dynamic friction was omitted from the simulation. The DFRICD subroutine is used by the line model to calculate pressure loss due to dynamic friction caused by fluid acceleration. The computer results of the simulation are shown in Figures 121 and 122. Figure 121 is an overplot of P_4 data on the computer predicted results. This plot shows the importance of modeling frequency dependent or dynamic friction effects in the computer program. The predicted pressure peaks are less attenuated than the data resulting in a much squarer waveform. Also the pressure amplitudes take longer to dissipate with only the static line friction in the model. The frequency dependent effects are clearly indicated by this plot. Figure 122 is the flow plot for this simulation.

c. High Temperature Line Model Verification - The HYTRAN computer simulation of a turn-off transient at 210°F used Figure 123 test data and Figure 124 input data. Figures 125, 126 and 127 show the computer printed outputs overplotted with laboratory test data. Figure 125 is a plot of the P_4 data over the computer predicted pressure data for the P_4 position.

The computer output of P_4 agrees favorably with the test data. On the data curve, the initial pressure peaks contain mechanical vibrations which damp out as the run progresses in time.

The Q_1 and Q_4 flow plots are shown in Figures 126 and 127.

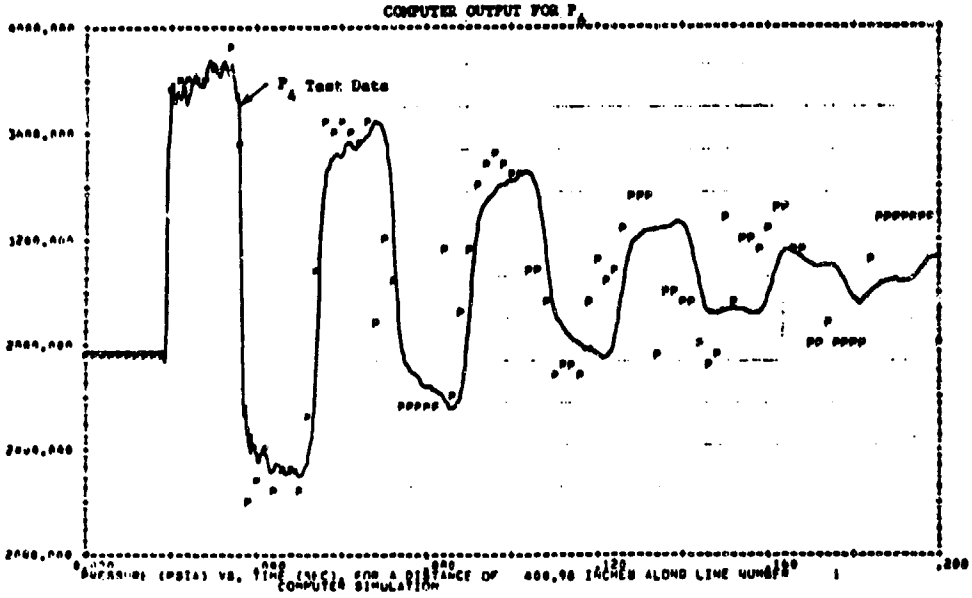

FIGURE 121 LINE SIMULATION WITHOUT DYNAMIC FRICTION - P4 PRESSURE

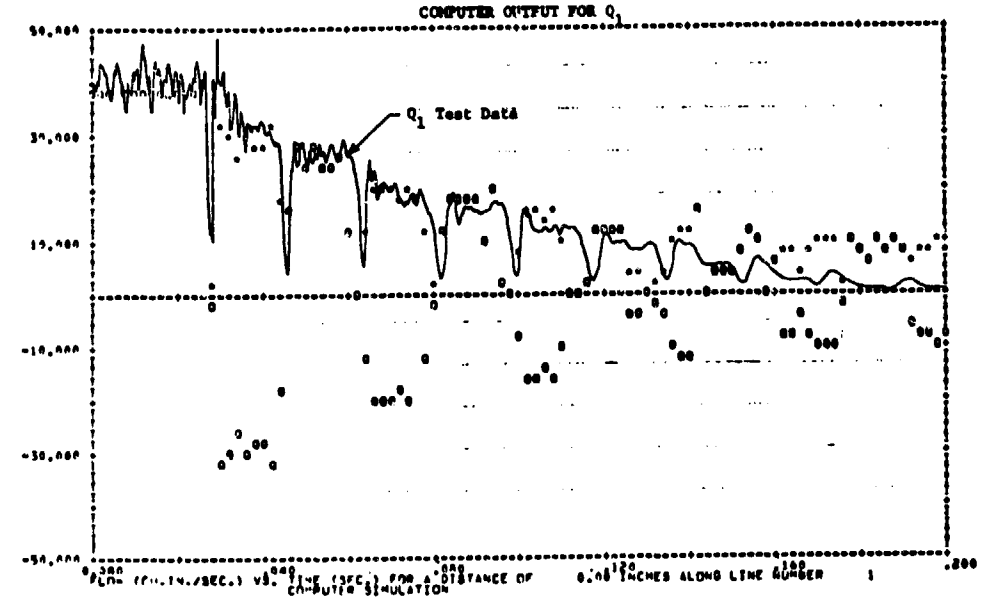

FIGURE 122 LINE SIMULATION WITHOUT DYNAMIC FRICTION - Q1 FLOW

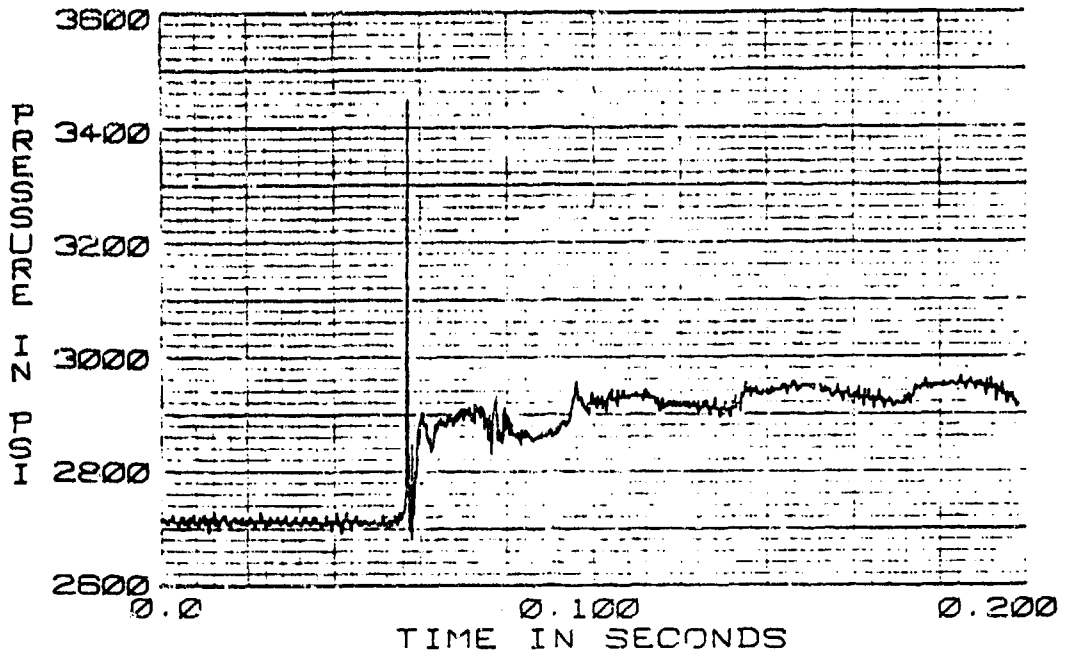

FIGURE 123 .5 DIA. X 30 FT TUBE
10C05 - P1 TURN-OFF TRANSIENT
38.5 C15 210 DEG F

**** RUN NO. 10C05-P1 TURN-OFF TRANSIENT ****

THE TRANSIENT RESPONSE IS FROM T=0.0 TO T= .200 SECONDS AT TIME INTERVALS OF DELT= .00020
WITH OUTPUT POINTS PLOTTED AT INTERVALS OF , .00200 SECONDS

FLUID DATA FOR MIL-H-5606H AT 3000.0 PSIG AND 210.0 DEG F

VISCOSITY = .4026E-02 IN**2/SEC
DENSITY = .7508E-04 (LB-SEC**2)/IN**4
BULK MODULUS = .173E+06 PSI

LINE DATA LINE NO.	LENGTH	INTERNAL DIA	WALL THICKNESS	MODULUS OF ELASTICITY	DELX	CHARACTERISTIC IMPEDANCE	VELOCITY OF SOUND
1	600.0000	.4000	.0200	.30OE+08	8.9796	22.6711	40805.1720
2	17.0000	.4000	.0200	.30OE+08	17.0000	22.6711	40805.1720

COMPR. 1 INTEGER DATA 1 81 0 -1 1 -0 -0 -0 -0 -0 -0 -0 -0 -0 -0 -0 -0

COMPR. 2 INTEGER DATA 2 21 5 1 -2 -0 -0 -0 -0 -0 -0 -0 -0 4 -0 -0

REAL DATA CARD # 1	.2200E-01	.6500E+00 -0.	-0.	-0.	-0.	-0.	-0.
REAL DATA CARD # 2	0.	.6720E-01	.6770E-01	.2000E+00 -0.	-0.	-0.	-0.
REAL DATA CARD # 3	.3320E+00	.332UE+00	0.	0.	-0.	-0.	-0.

COMPR. 3 INTEGER DATA 3 81 1 2 -0 -0 -0 -0 -0 -0 -0 -0 -0 -0 -0 -0

REAL DATA CARD # 1 .5000E+02 -0. -0. -0. -0. -0. -0.

FIGURE 124 10C05 TURN-OFF TRANSIENT COMPUTER INPUT DATA

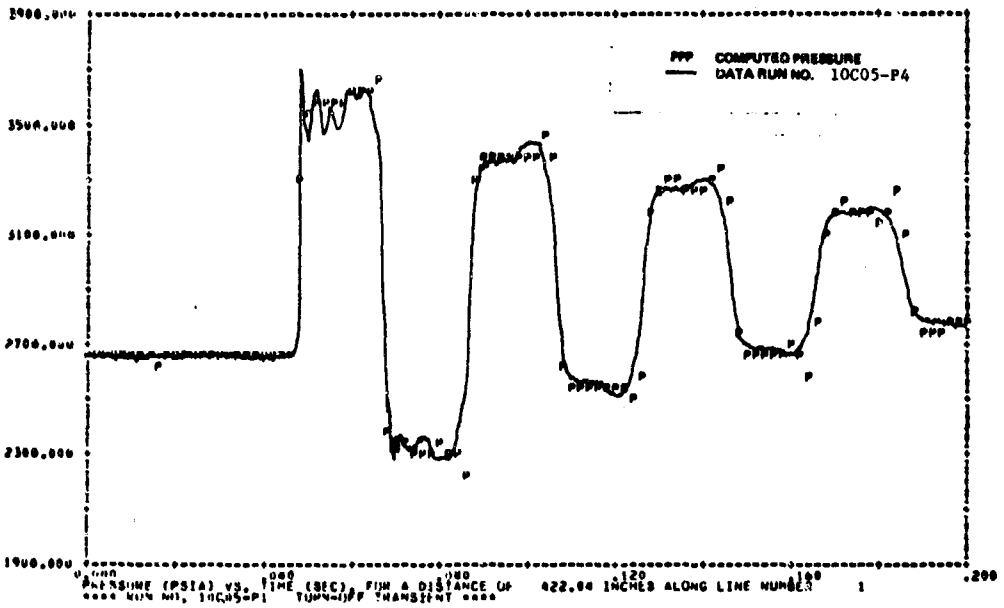

FIGURE 125 10C05 - P4 TURN-OFF TRANSIENT

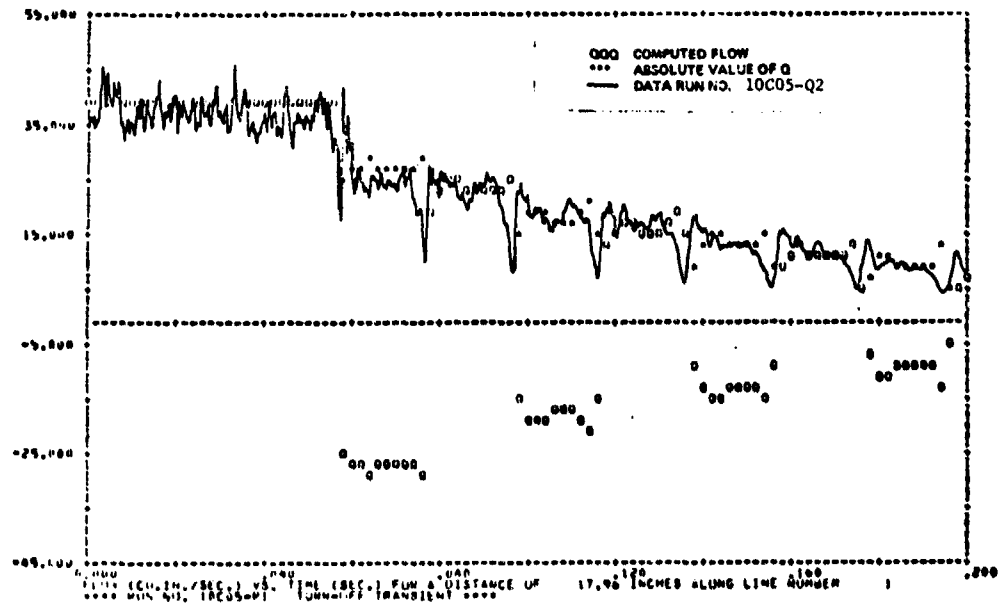

FIGURE 126 10C05 - Q2 TURN-OFF TRANSIENT

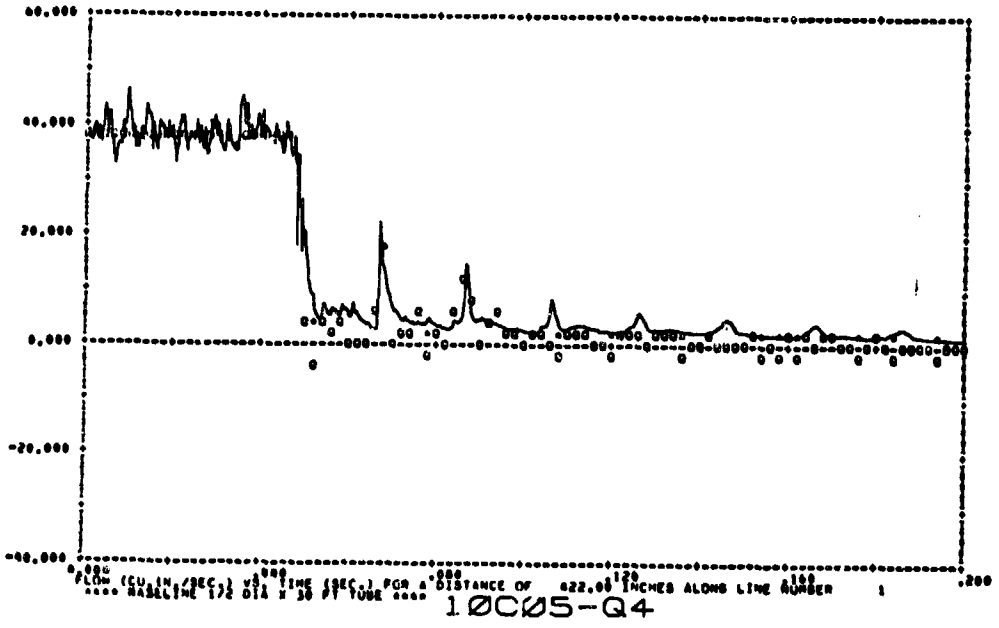

FIGURE 127 10C05 - Q4 TURN-OFF TRANSIENT

A turn-on transient at 210°F was simulated with the computer program. The data input for the computer run is shown in Figure 128. The output pressures and flows are shown in Figures 129 and 130. The P_4 pressure data trace indicates good correlation with the computer output plots, although the initial pressure dip for the P_4 test data is not present in the computed plot. The flow test data for Figure 130 shows a gradual increase to the first maximum value from the zero flow condition. The computer prediction in both figures jump to a flow level immediately on opening the valve. The gradual increase in the test data could be attributed to the time it takes the fluid to develop a good velocity profile.

c. Conclusions - The HYTRAN line model calculations of flows and pressure compare well with the test data measured in the lab. Some discrepancies exist between the data and the mathematically predicted results as already noted. The results indicate that the line model is reasonably good.

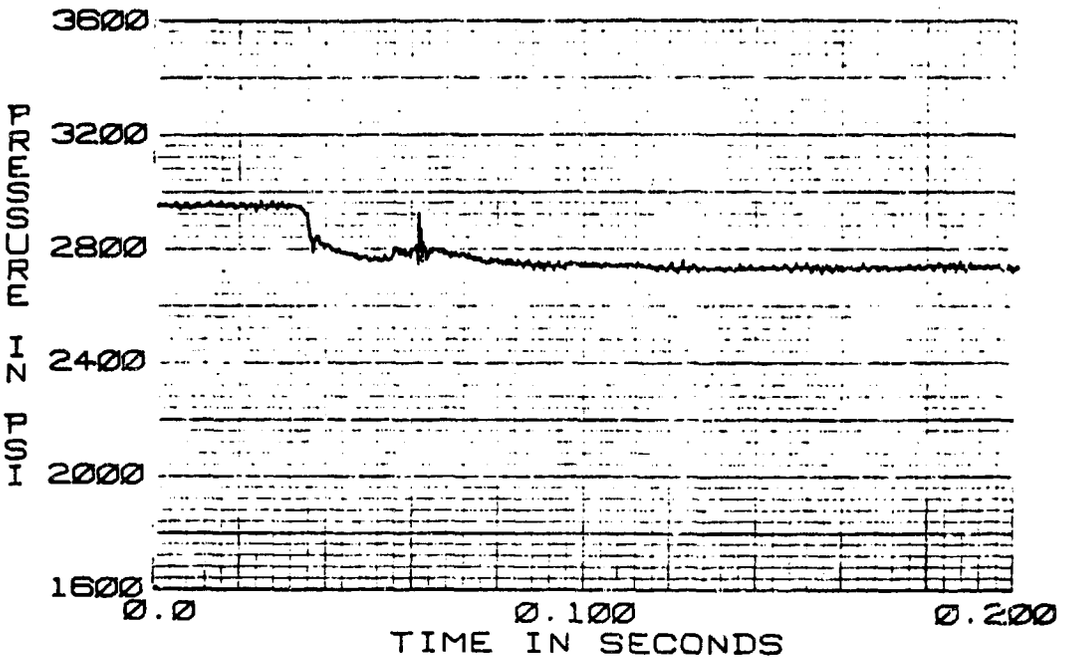

FIGURE 128 .5 DIA. X 30 FT. TUBE
10C05 + P1 TURN-ON TRANSIENT
38.5 C15 210 DEG F

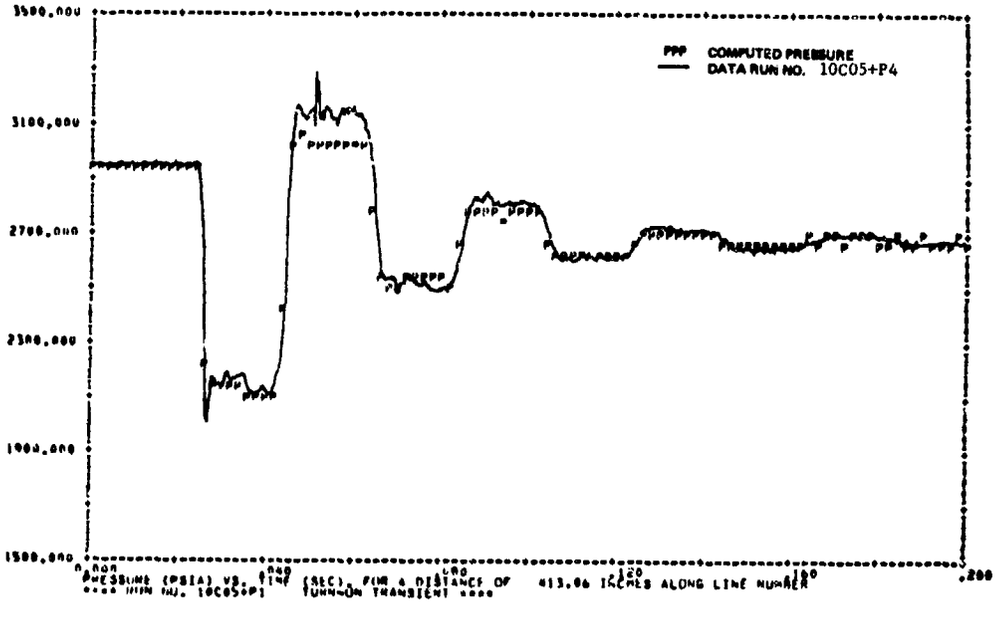

FIGURE 129 10C05 + P4 TURN-ON TRANSIENT

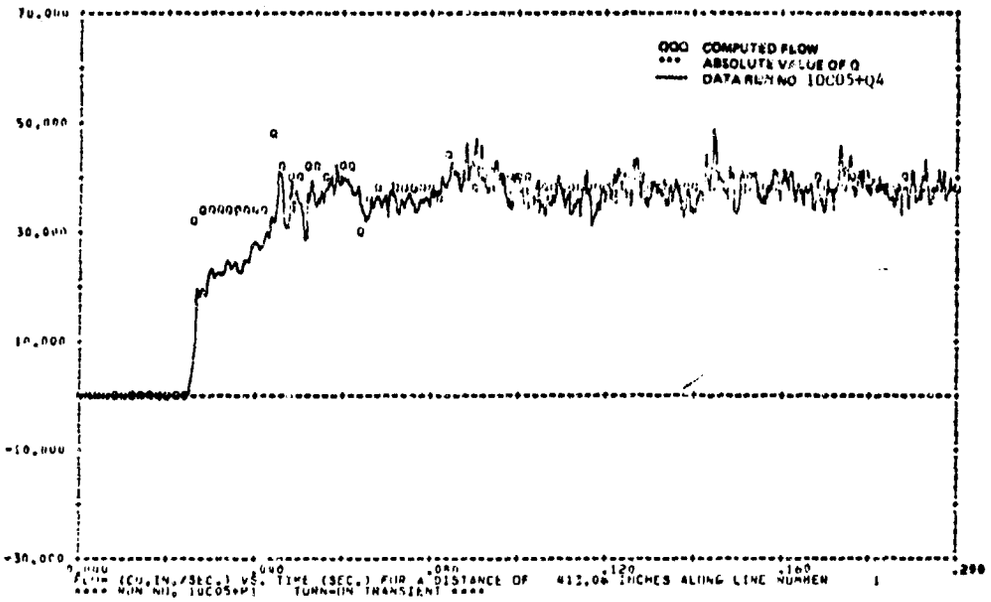

FIGURE 130 10C05 + Q4 TURN-ON TRANSIENT

2 HYTRAN CAVITATION MODEL VERIFICATION

In this section the test results obtained for cavitation effects in a system return long line are compared to the HYTRAN computer program line model. The testing on the line was performed on a 1/2 inch tube with MIL-H-5606B. In the HYTRAN program the pressures at the component ports are calculated. If this pressure is less than the oil vapor pressure, cavitation conditions exist at the line end points.

The return line test series was run on the system configuration shown in Figure 131.

The following parameters were recorded in the laboratory for the test runs: P_1, P_2, Q_2, P_3, Q_3, P_4 and valve position. P_1, P_4, P_5 and Q_3 were recorded directly onto cassette tape.

The test runs are listed in Table 3.

a. Computer Simulation with Return Line Test Data - A return line turn-off transient at 125°F and 38.5 CIS was simulated with the HYTRAN computer program. The input boundary conditions were the 10-07-P5 pressure taken immediately downstream of the JFS accumulator in Figure 132 and the 10-07-P4 pressure next to the F-4 reservoir in Figure 133. The system input data

is shown in Figure 134. The dynamic friction at the line end points were set to zero whenever the pressure fell to the fluid vapor pressure in the DFRICD subroutine. The computed results in Figures 135, 136, 137, 138 and 139 show good correlation to the data. The predicted pressures are slightly higher than the data and the phasing between the measured data and computed results is better but after the third pressure peak they drift apart as shown in Figures 135 and 136. All pressures and flows do settle to the proper steady state values.

The flow plots in Figures 138 and 139 shown the deceleration of the fluid after the turn-off command at 890 milliseconds. The flow is then reflected and gradually dampens out.

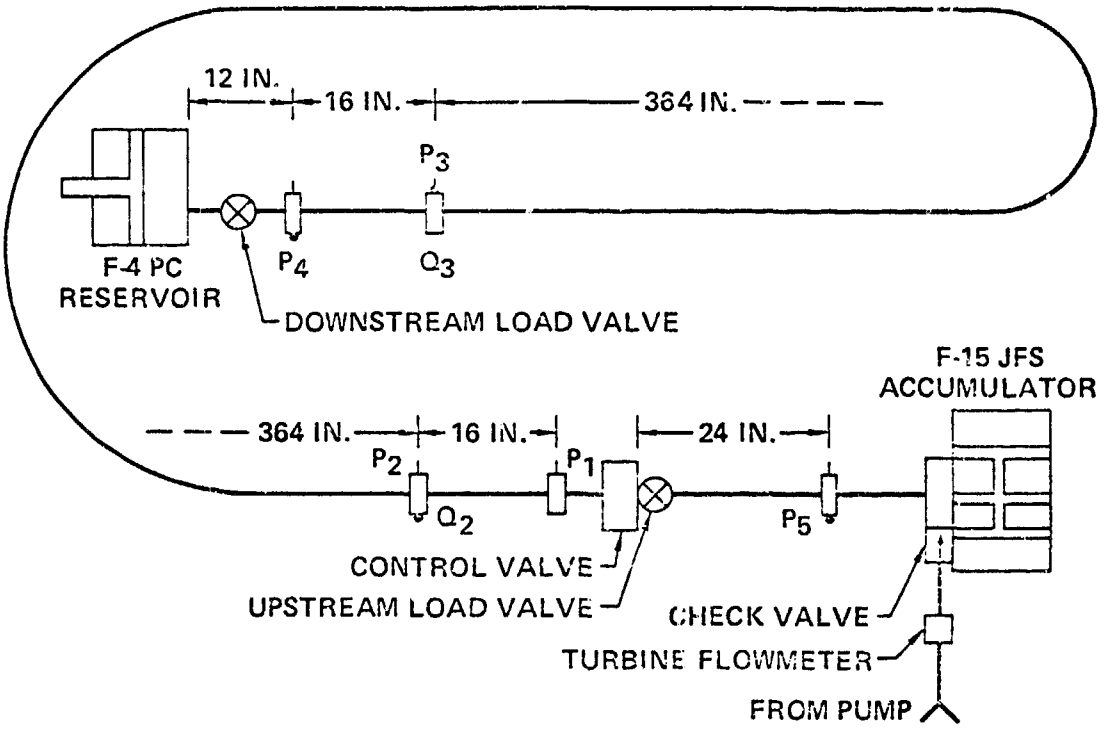

FIGURE 131 RETURN SIDE TRANSIENT TEST CONFIGURATION
.5 IN. DIA. X 30 FT. LONG LINE

TABLE 3

TEST CONDITIONS FOR 1/2" DIA X 30 FT LINE

Test Specimen	Run #	Flow Condition	Flow Rate (CIS)	Temp (°F)
1/2" dia x 30 ft line	10-07-XX*	Turn-Off	38.5	125
"	10-07+XX	Turn-On	38.5	125
"	10-08-XX	Turn-Off	11.55	125
"	10-08+XX	Turn-On	11.55	125
"	10-09-XX	Turn-Off	38.5	210
"	10-09+XX	Turn-On	38.5	210
"	10-10-XX	Turn-Off	11.55	210
"	10-10+XX	Turn-On	11.55	210

*XX - Denotes measured data parameter

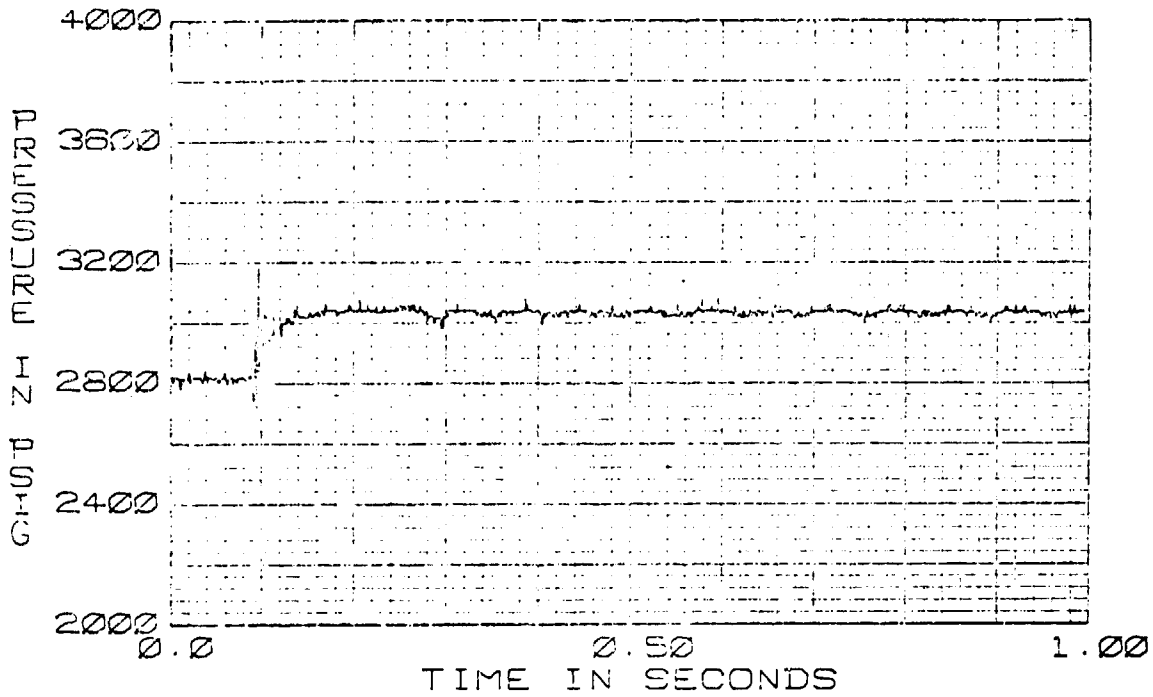

FIGURE 132 .5 IN. DIA. X 30 FT. TUBE
10-07-P5 TURN-OFF TRANSIENT
38.5 C15 125 DEG F

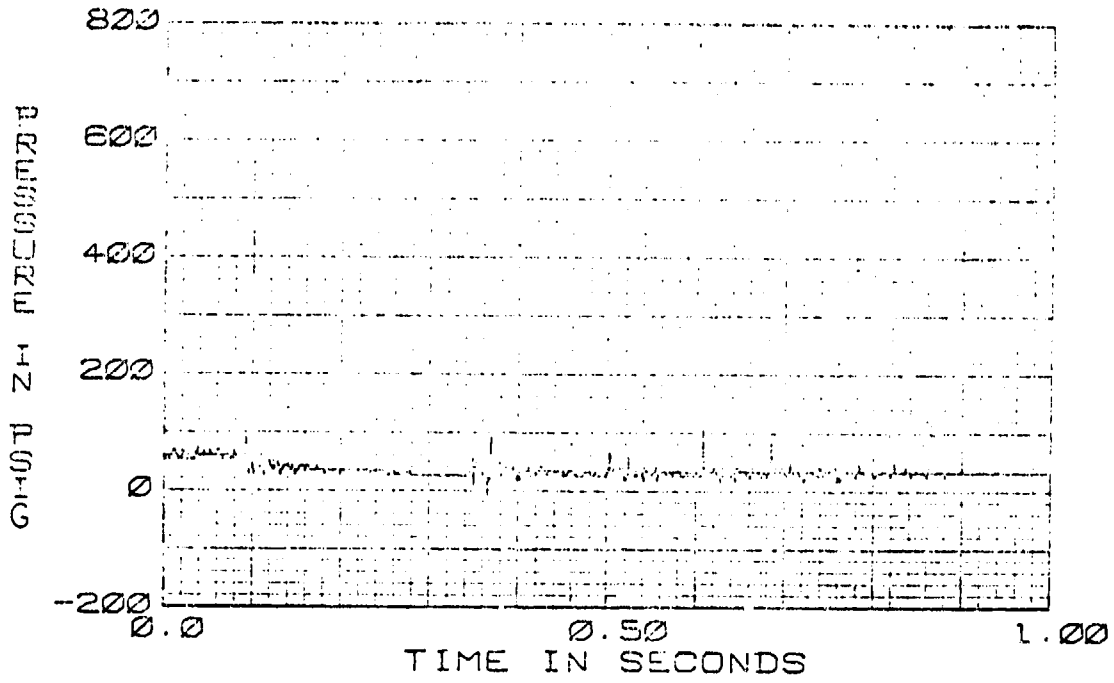

FIGURE 133 .5 IN. DIA. X 30 FT TUBE
10-07-P4 TURN-OFF TRANSIENT
38.5 C15 125 DEG F

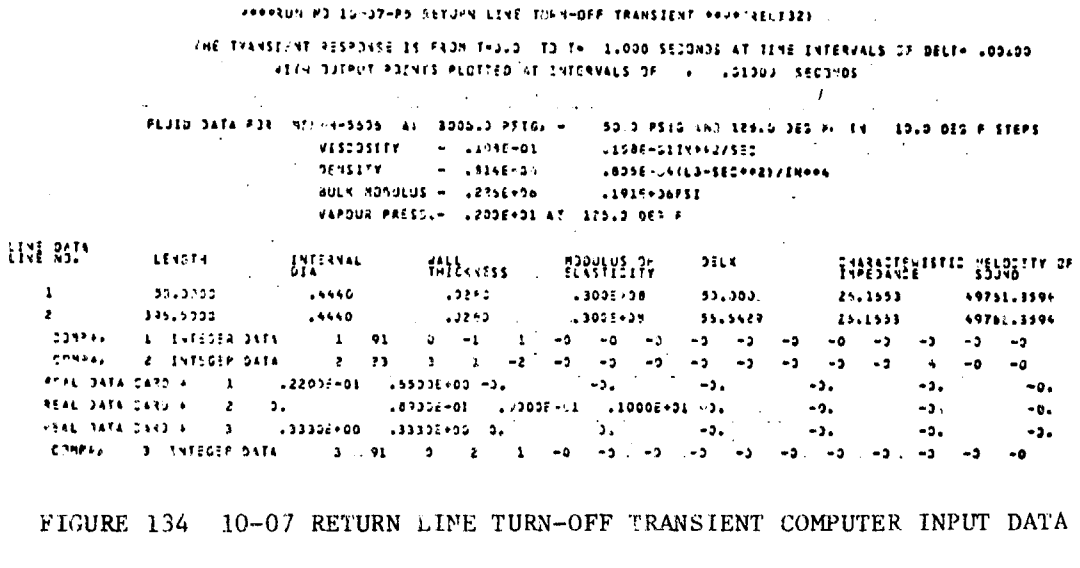

FIGURE 134 10-07 RETURN LINE TURN-OFF TRANSIENT COMPUTER INPUT DATA

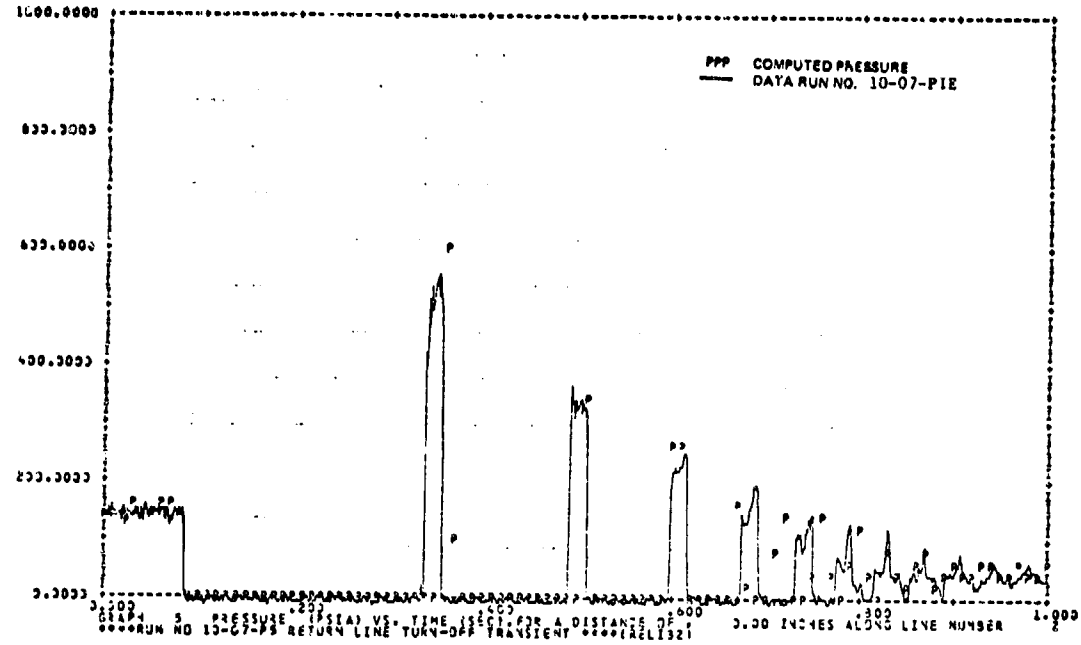

FIGURE 135 10-07-P1E TURN-OFF TRANSIENT

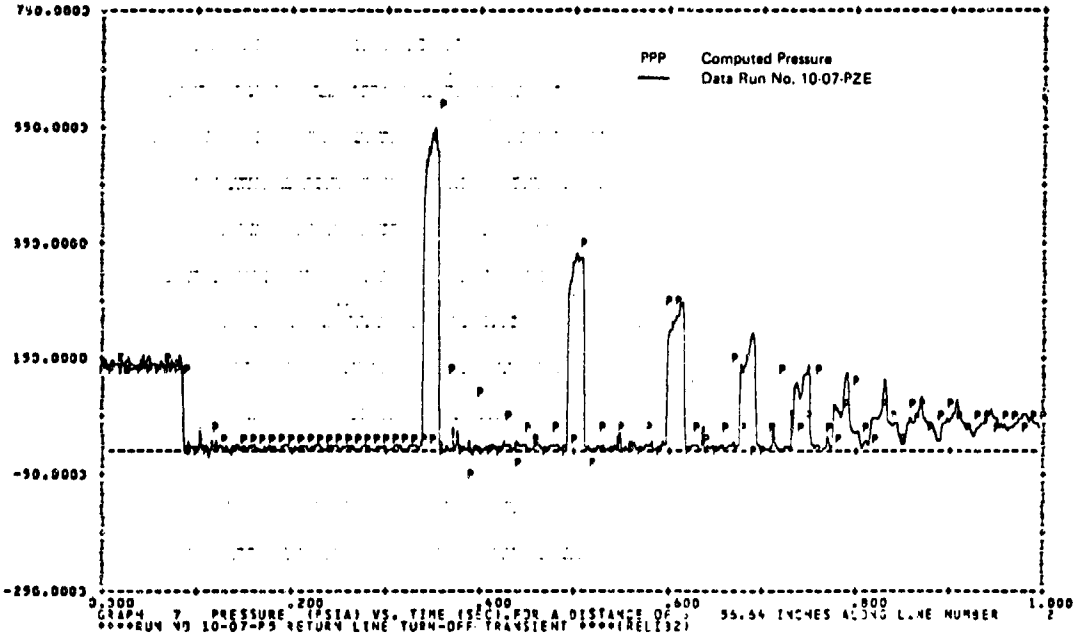

FIGURE 136 10-07-PZE TURN-OFF TRANSIENT

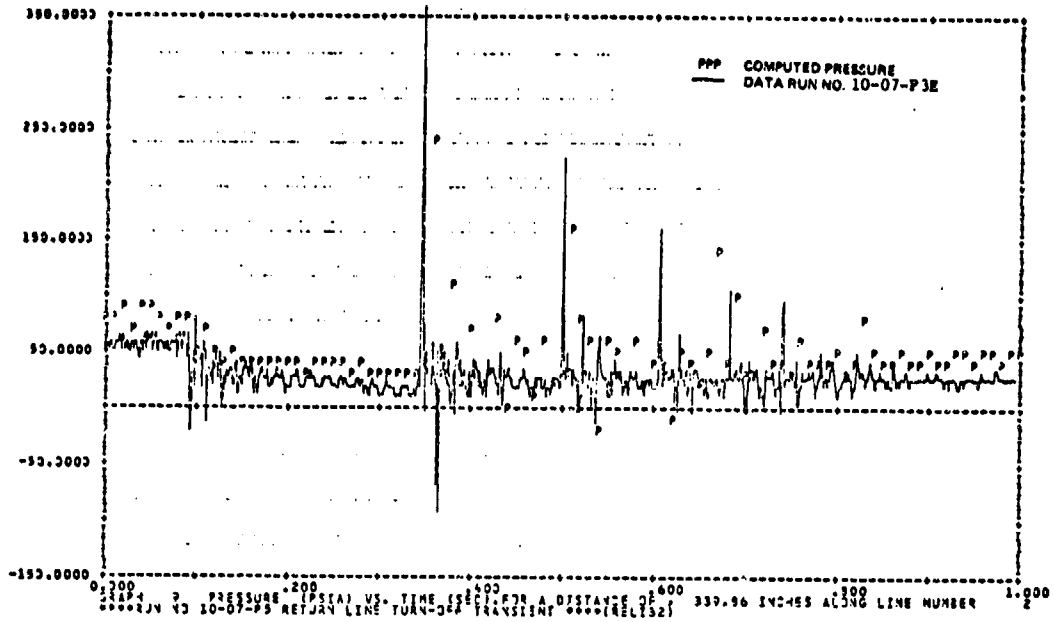

FIGURE 137 10-07-P3E TURN-OFF TRANSIENT

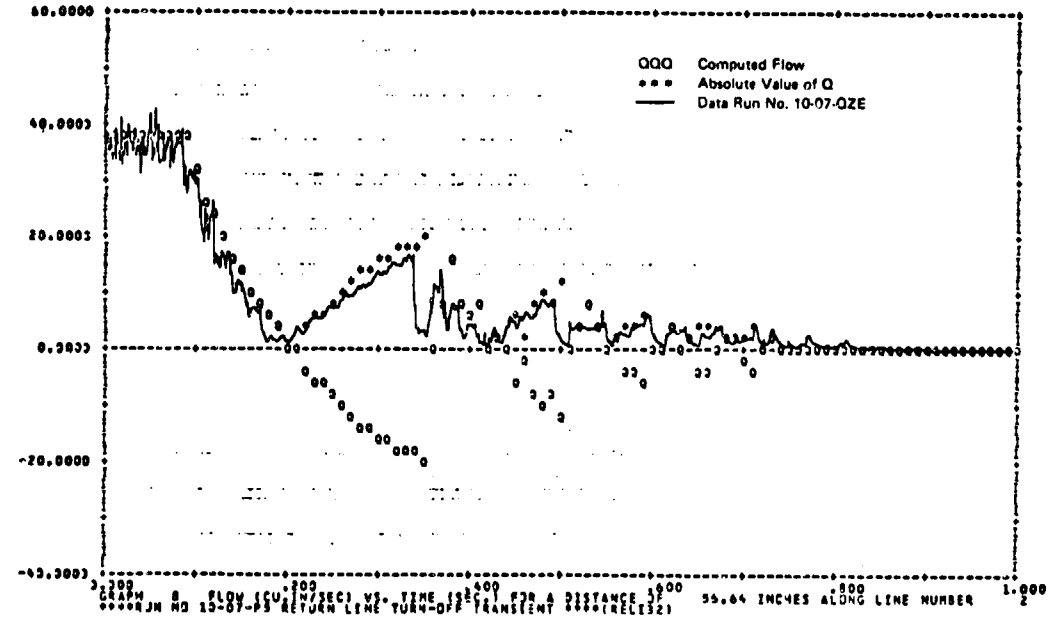

FIGURE 138 10-07-QZE TURN-OFF TRANSIENT

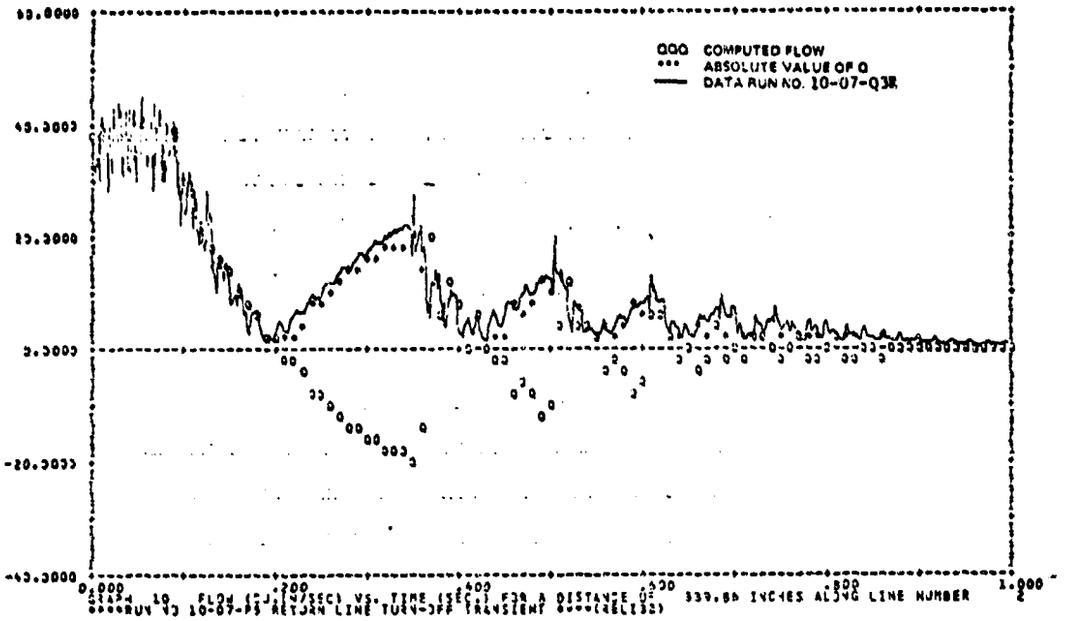

FIGURE 139 10-07-Q3E TURN-OFF TRANSIENT

A turn-on transient at 125°F was simulated with the computer program at 38.5 CIS flow. The data input for the computer run is shown in Figures 140 and 141 with the computer input information given in Figure 142. One output pressure is shown in Figure 143.

The first pressure peak in Figure 143 correlates with the computed output pressure. Subsequent computed pressures do not match the data. However, the calculated data does settle down to the proper steady state value. This run was made with the fluid vapor pressure at 2.0 psi and the dynamic friction term set to zero whenever the line end points were equal to or less than the fluid vapor pressure. The computer predicted results show a much shorter reflection time for the second pressure peak. The actual pressure data cavitates more in the 100 to 250 millisecond period.

The flow plot in 144 indicates why the computed results do not correlate. After the initial turn-on at 80 millisecond the flow in the line makes a sharp dip. This physically is due to the filling of the return line from the high pressure. The computed data shows a small dip at 110 milliseconds which is enough to completely fill the dowstream line in the simulation but not in the actual data run.

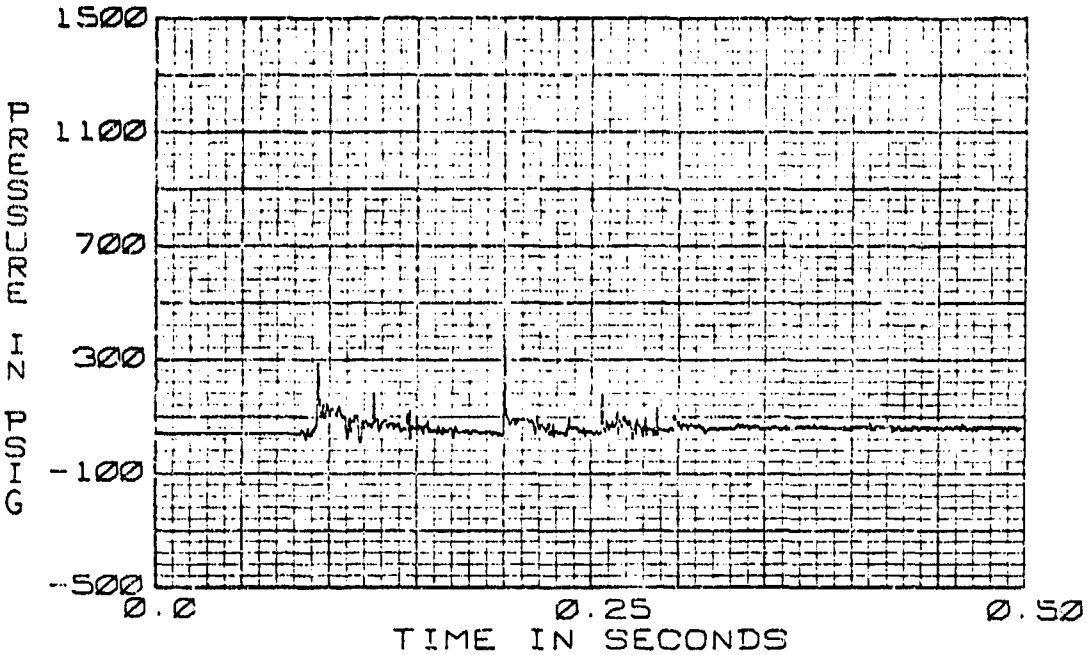

FIGURE 140 0.5 IN. DIA. X 30 FT. TUBE
10-07+P4 TURN-ON TRANSIENT
38.5 C15 125 DEG F

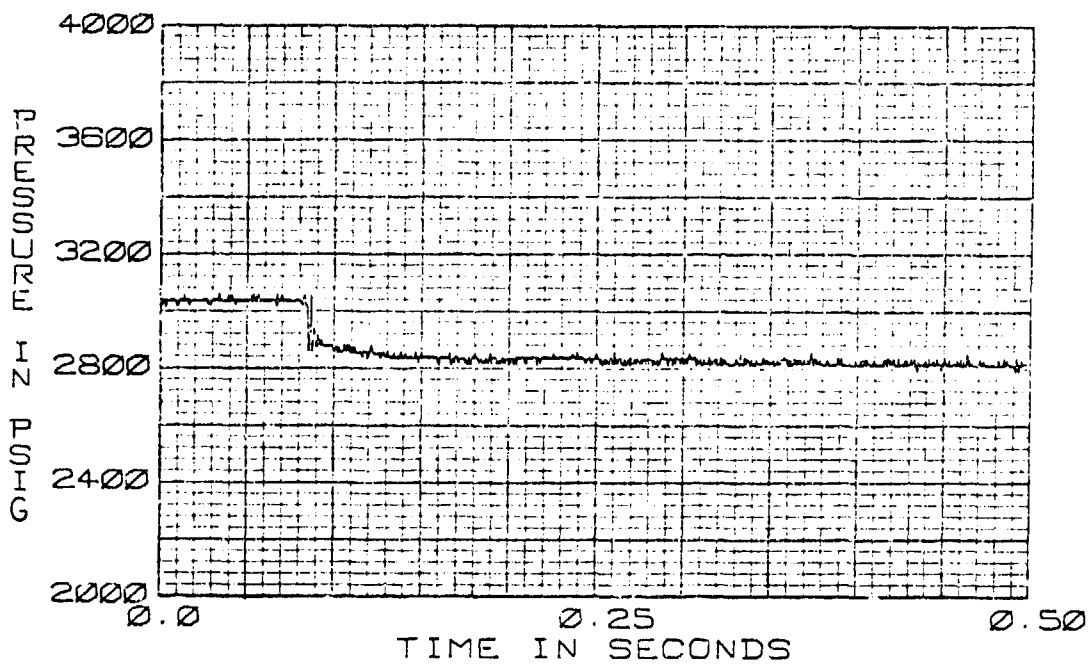

FIGURE 141 0.5 IN. DIA. X 30 FT. TUBE
10-07+P5 TURN-ON TRANSIENT
38.5 C15 125 DEC. F

```
**** RUN NO 10-07+P1 RETURN LINE TURN-ON TRANSIENT **** (REL133)

THE TRANSIENT RESPONSE IS FROM T=0.0  TO T=  .500 SECONDS AT TIME INTERVALS OF DELT= .00050
        WITH OUTPUT POINTS PLOTTED AT INTERVALS OF  ,  .00500  SECOND*

   FLUID DATA FOR  MIL-H-5606  AT  3000.0 PSIG, -    50.0 PSIG AND 125.0 DEG F  IN   10.0 DEG F STEPS
                    VISCOSITY   =  .108E 01        .158E-01LB**2/SEC
                    DENSITY     =  .814E-04        .805E-04(LB-SEC**2)/IN**4
                    BULK MODULUS =  .286E+06       .191E+06PSI
                    VAPOUR PRESS.=  .280E-01 AT  125.0 DEG F
  PICK-UP TAKEN AT LINE 10,VEL OF SOUND IN LINE   1  IS    3.SPER CENT IN ERROR

LINE DATA
LINE NO.    LENGTH      INTERNAL DIA   WALL THICKNESS   MODULUS OF ELASTICITY   DELX      CHARACTERISTIC IMPEDANCE   VELOCITY OF SOUND
    1       24.0000        .4440          .0280            .303E+08          24.0000        26.1653                48038.8888
    2      196.5000        .4440          .0280            .300E+08          26.4333        26.1653                49761.3594
 COMP.,  1 INTEGER DATA    1  91   0  -1   1  -0  -0  -0  -0  -0  -0  -0  -0  -0  -0  -0  -0
 COMP.,  2 INTEGER DATA    2  23   3   1  -2  -0  -0  -0  -0  -0  -0  -0  -0   4  -0  -0
 REAL DATA CARD .  1    .2280E-01  .6500E+00 -0.          -0.          -0.          -0.          -0.          -0.
 REAL DATA CARD .  2    0.         .4000E-01  .0600E-01   .5000E+00 -0.          -0.          -0.          -0.
 REAL DATA CARD .  3    0.         0.         .3370E+00   .3370E+00 -0.          -0.          -0.          -0.
 COMP.,  3 INTEGER DATA    3  91   0   2   1  -0  -0  -0  -0  -0  -0  -0  -0  -0  -0  -0
```

FIGURE 142 10-07 TURN-ON TRANSIENT COMPUTER INPUT DATA

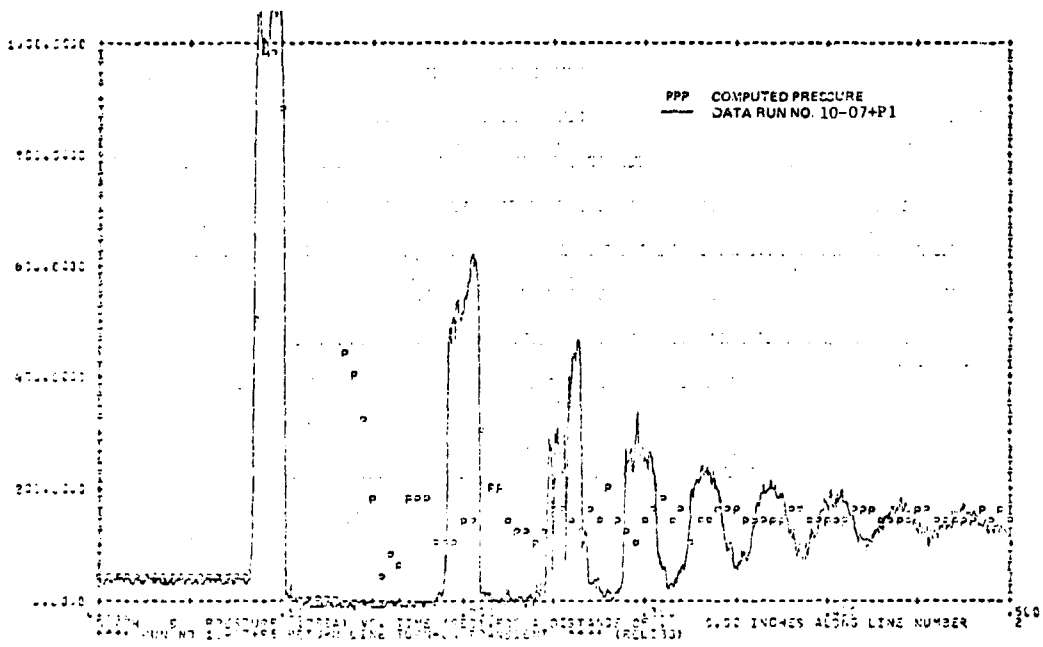

FIGURE 143 10-07+P1 TURN-ON TRANSIENT

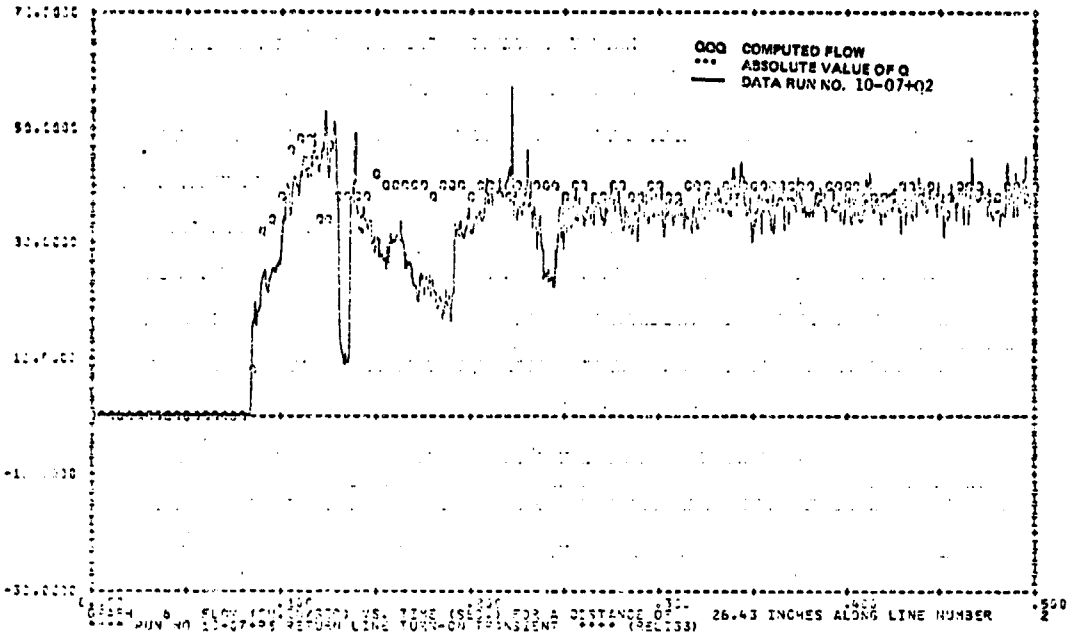

FIGURE 144 10-07+02 TURN-ON TRANSIENT

While the flow is increasing in the turn-on transient it remains laminar well past the normal transition Reynolds number. Similarly for turn-off transients the flow remains turbulent for a longer time period. The FRIC subroutine in HYTRAN does not account for this phenomena. Once the transition flow is reached the appropriate turbulent or laminar factor is included in the computation. Thus the computer program is predicting higher losses than actually existed in the line. Figures 145, 146 and 147 show data from a run made with the turbulent friction factor set to zero. They show much better correlation to the actual data. Since the friction term was incorrect, the pressure does not settle to the proper steady state value.

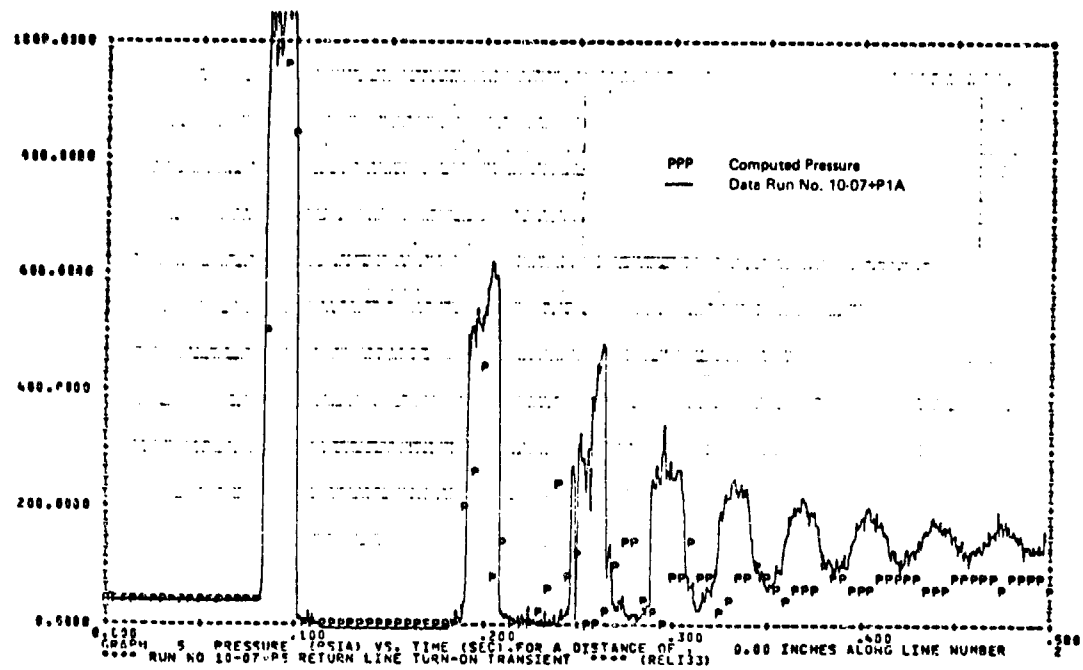

FIGURE 145 10-07-P1A TURN-ON TRANSIENT

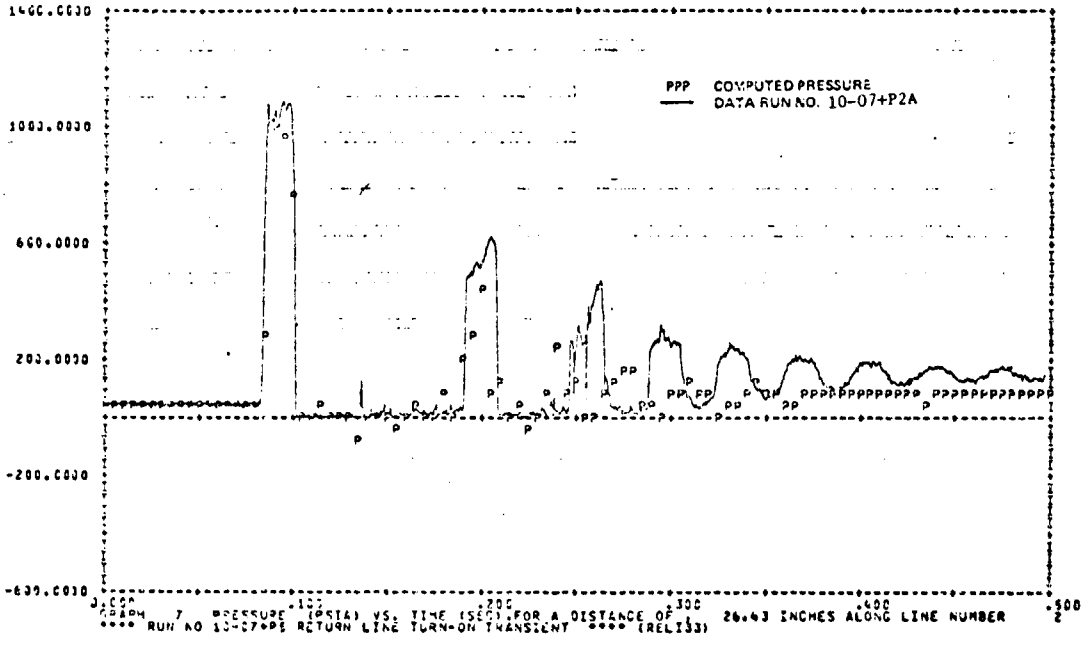

FIGURE 146 10-07+P2A TURN-ON TRANSIENT

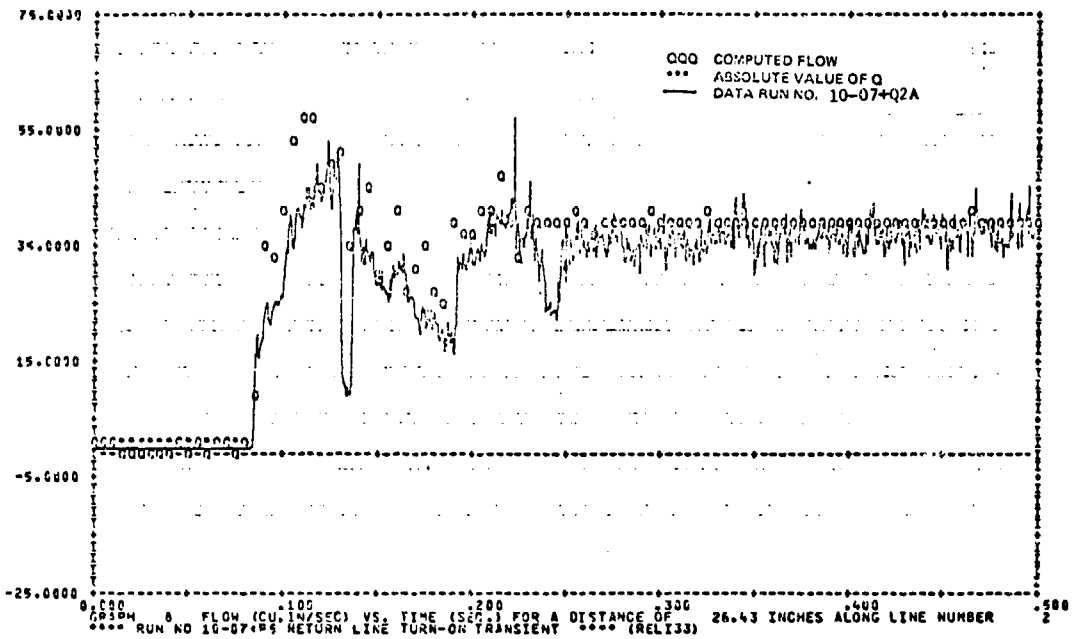

FIGURE 147 10-07+Q2A TURN-ON TRANSIENT

b. Conclusions - The HYTRAN line model calculations of flows and pressures under cavitation conditions did not compare well with the test data measured in the lab. For turn-off transients reasonable correlation was obtained when the line dynamic friction was set to zero. DFRICD was zeroed whenever the pressure at either end point was equal to or less than the fluid vapor pressure.

The computer output results for the turn-on transients also did not compare well with the data. The majority of the error may be attributed to the use of the turbulent friction term when the Reynolds number reaches the transition number, while in reality the line flow is still laminar.

3. PUMP MODEL VERIFICATION

The transient test results are compared to the HYTRAN computer pump subroutine - PUMP51.

The transient test series were run on the system configuration shown in Figure 148.

A brief summary of the test conditions for the F-15 instrumented pump is shown in Table 4.

TABLE 4

TRANSIENT PUMP TESTING

Test Series No.	Fluid Type	Special Conditions
63	MIL-H-5606B	Check Valves in Pump Manifold MIL-H-5606B Oil
64	MIL-H-5606B	No check valves in Pump Manifold MIL-H-5606B Oil
65	MIL-H-83282	No check valves in Pump Manifold MIL-H-83282 Oil Corrected Hanger Position

Data recorded for each test condition were:

- o System supply line pressure (P1)
- o Suction pressure (PS)
- o Case drain pressure (PCD or P2)
- o Line pressure near control valve (P5)
- o Transient control valve position (XCV)
- o Pump control (actuator) pressure (PC)
- o Pump Outlet Pressure (PP)
- o Hanger Position (XH)
- o Compensator Spool position (XC)
- o Drive torque (DT)
- o Drive speed (DS)

The system reservoir pressure was kept at 50 psig by an independent bootstrap accumulator source as shown in Figure 148.

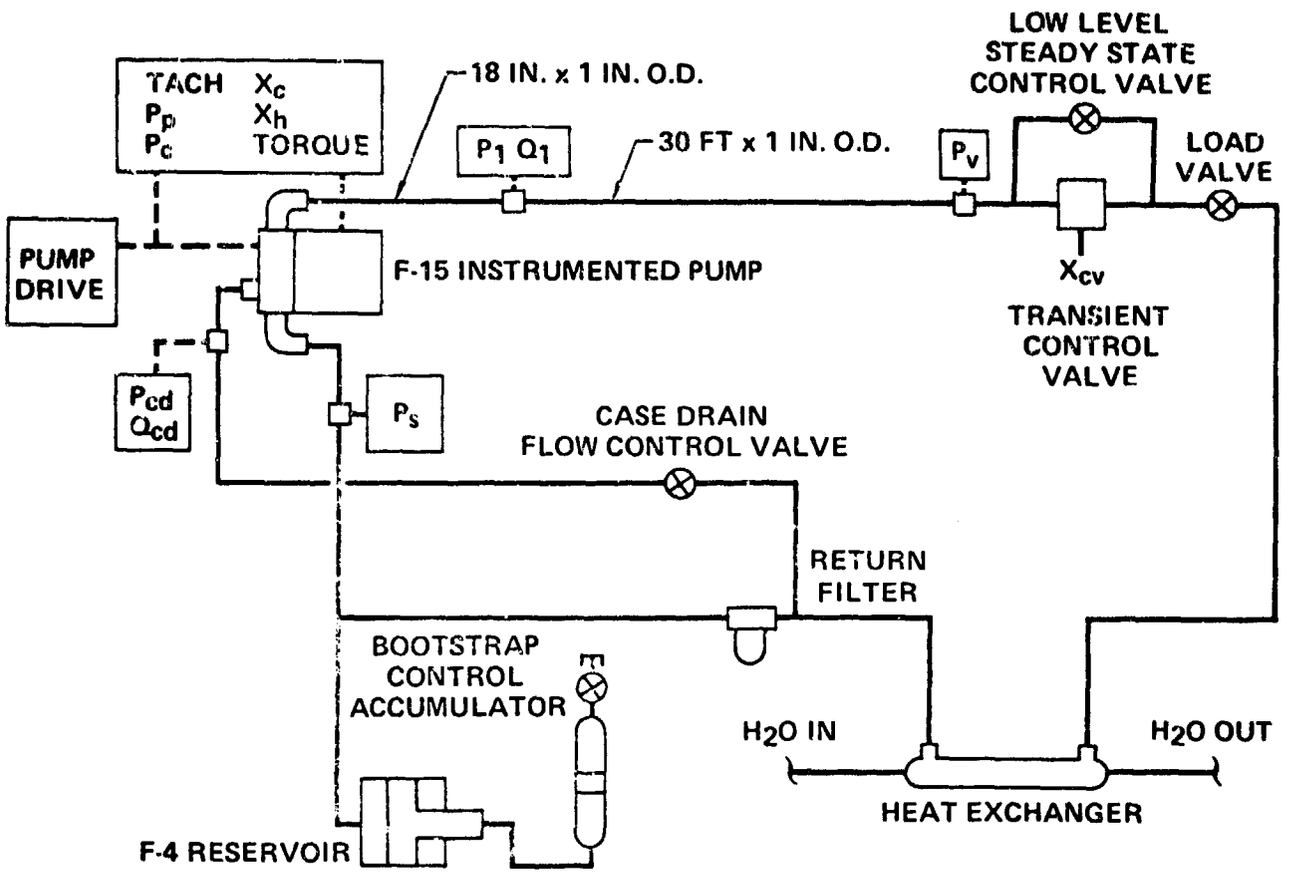

FIGURE 148. TRANSIENT PUMP TEST SETUP

a. Test Series 63 - Transient Tests with Check Valves in Pump Manifold - The first transient test series with the F-15 instrumented pump was performed with check valves in the pump manifold at the pump outlet and case drain lines. These check valves were designed to keep the lines to the pump from draining when the pump is removed from the manifold. Their presence also affects the pump internal dynamic operating characteristics. MIL-H-5606B hydraulic oil was used in the test fixture.

All the 63 series tests are shown in Table 5 which contains the run numbers for each test.

TABLE 5

Hytran Pump Model Verification Test -63 Series

Steady State Flow Levels (CIS) Lo	Hi	Control Valve Operating Time (SEC) On	Off	Case Pressure At SS Leakage Condition (1.5-3.8 CIS)	Pump Speed (RPM)	Temperature Pump Inlet (Deg F)	Run Number Turn On (63-XX+XX) Turn Off(63-XX-XX)
I. Load Level Effects							
2.0 -	19.25	.002	.002	100 PSIG	4000	130	63-01
2.0 -	38.5	.002	.002	100 PSIG	4000	130	63A02
2.0 -	77.0	.002	.002	100 PSIG	4000	130	63-03
II. Loading Rate Effects							
2.0 -	77.0	.010	.010	100 PSIG	4000	130	63-11
2.0 -	77.0	.020	.020	100 PSIG	4000	130	63-12
III. Speed Effects							
2.0 -	57.75	.002	.002	100 PSIG	1600	130	63-20
2.0 -	57.75	.002	.002	100 PSIG	2500	130	63-21
2.0 -	57.75	.002	.002	100 PSIG	3000	130	63-22
2.0 -	57.75	.002	.002	100 PSIG	3700	130	63-23
2.0 -	57.75	.002	.002	100 PSIG	5000	130	63-24
IV. Case Pressure Level Effects							
2.0 -	77.0	.002	.002	220 PSIG	4000	130	63-40
V. High Flow - Small Load Changes							
77.0 -	115.5	.002	.002	100 PSIG	4000	130	63-50
115.5 -	154	.002	.002	100 PSIG	4000	130	63-51

In run number 63-03-P1 Figure 149 the pressure transducer is located approximately 18" from the pump manifold outlet pressure port. The initial pressure spike at about .028 seconds shows the arrival of the transient pressure wave caused by the control valve closure and the subsequent pump response. Run number 63-03-P5 in Figure 150 which is the pressure trace close to the control valve shows the initial waterhammer wave occurring at .018 sec and the subsequent pump response superimposed on this wave at .037 sec. It should be noted that this spike is not related to the waterhammer phenomena but is simply the pressure response characteristic of the pump being hit by the original waterhammer wave.

The high frequency content of the pressure traces results from the pump rpm. The typical operating speed was 4000 rpm or a frequency of 600 hz for a nine piston pump.

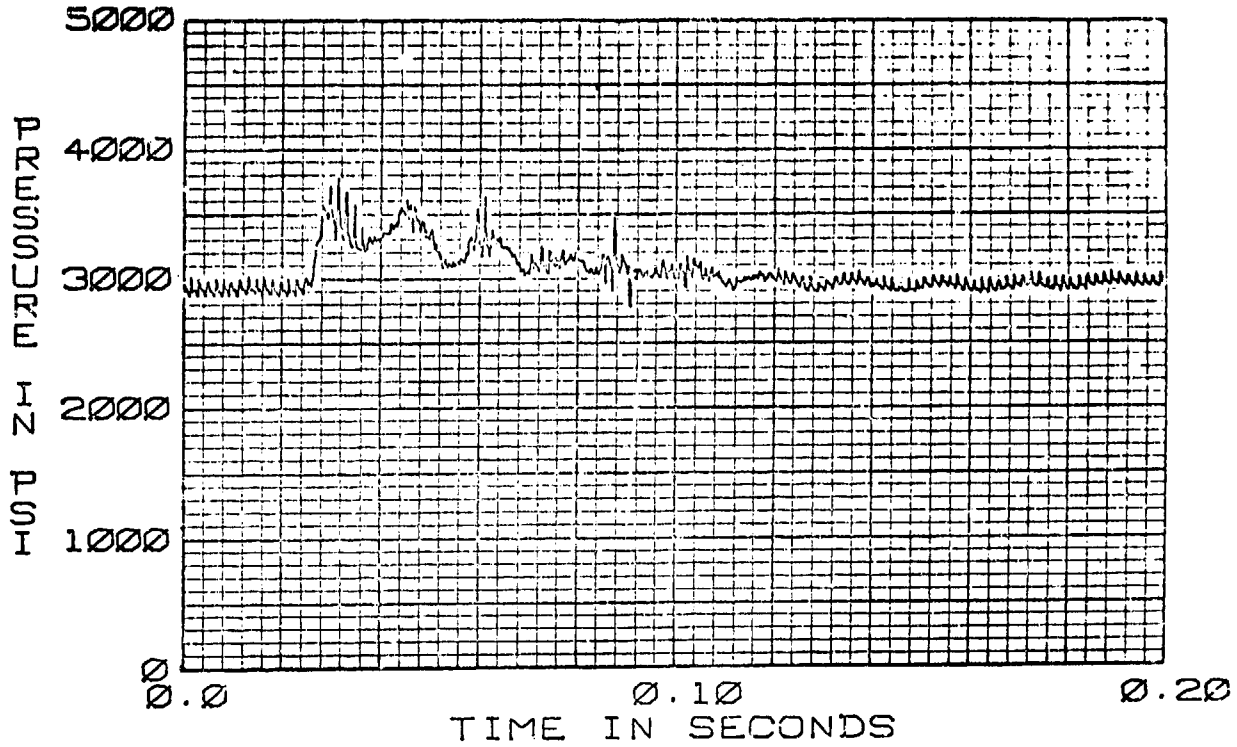

FIGURE 149. F-15 HYDRAULIC PUMP
63-03-P1 TURN-OFF TRANSIENT
77 CIS 130 DEG F

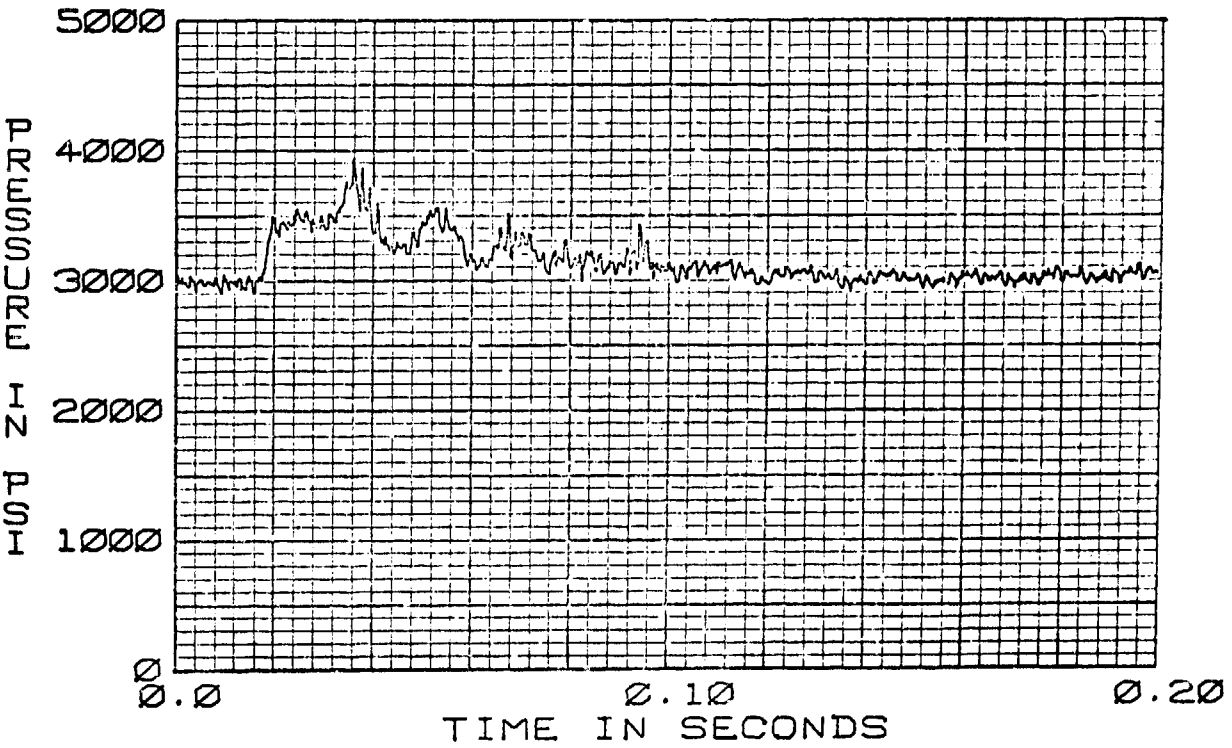

FIGURE 150. F-15 HYDRAULIC PUMP
63-03-P5 TURN-OFF TRANSIENT
77 CIS 130°F

b. Test Series 64 - Transient Tests without Check Valves in Pump Manifold - To observe the dynamic pump characteristics it was necessary to remove the check valves in the pump outlet and case drain lines. Many of the tests made in the 63 series were run again. Table 6 is a listing of the HYTRAN pump model verification tests on the F-15 instrumented pump. MIL-H-5606B hydraulic fluid was used in the test system.

A comparison of runs with and without the check valves in the manifold show the effects that the valves have on the pump dynamics. In Figure 149 the check valve in the output pressure line keeps the pressure from falling below 3000 psi. The internal pump pressure in Figure 151 drops below 2000 psi and follows the actuator control pressure (63-03-PC Figure 52) response. Both inlet and case pressures in Figures 153 and 154 exhibit large peak to peak pressure values, the 63-03-PCD run appears to show a transducer resonance problem around 40 milliseconds.

TABLE 6

Hytran Pump Model Verification Test -64 Series

Steady State Flow Levels (CIS) Lo	Hi	Control Valve Operating Time (SEC) On	Off	Case Pressure At SS Leakage Condition (1.5-3.8 CIS)	Pump Speed (RPM)	Temperature Pump Inlet (Deg F)	Run Number Turn On (64-XX+XX) Turn Off(64-XX+XX)
I. Load Level Effects							
2	- 19.25	.002	.002	100 PSIG	4000	130	64-01
2	- 38.5	.002	.002	100 PSIG	4000	130	64-02
2	- 77.0	.002	.002	100 PSIG	4000	130	64-03
II. Temperature Effects							
2	- 77.0	.002	.002	100 PSIG	4000	210	64-30
III. Case Pressure Level Effects							
2	- 77.0	.002	.002	120 PSIG	4000	130	64-40
IV. Suction Transient Cavitation							
2	- 154	.002	.002	100 PSIG	4000	130	64-60 (P_{RESV}=50 PSIG)
2	- 154	.002	.002	100 PSIG	4000	130	64-61 (P_{RESV}=25 PSIG)
2	- 154	.002	.002	100 PSIG	4000	130	64-62 (P_{RESV}=10 PSIG)

With the check valves removed in Figures 155 and 156 64-03-P1 and -PP fall below the steady state pressure of 3000 psi during the transient. PP is the internal pump pressure used to control the actuator position, and P1 is the pump outlet pressure about 18" from the pump manifold. In 64-03-PP the initial waterhammer wave hits the inlet of the pump temporarily stopping the outlet flow. The pump responds to this condition by increasing the outlet pressure to about 3500 psi at 32 milliseconds into the run. Much of the energy of this pressure wave is absorbed by the pump and converted to actuator and subsequent hanger motion. It is interesting to note that the pump outlet pressure wave does follow the compensator spool position as shown in Figure 157. The measured spool position closely tracks the pressure for all the test runs that were made. This fact was used in the model to compute the pump outlet pressure knowing a valve position.

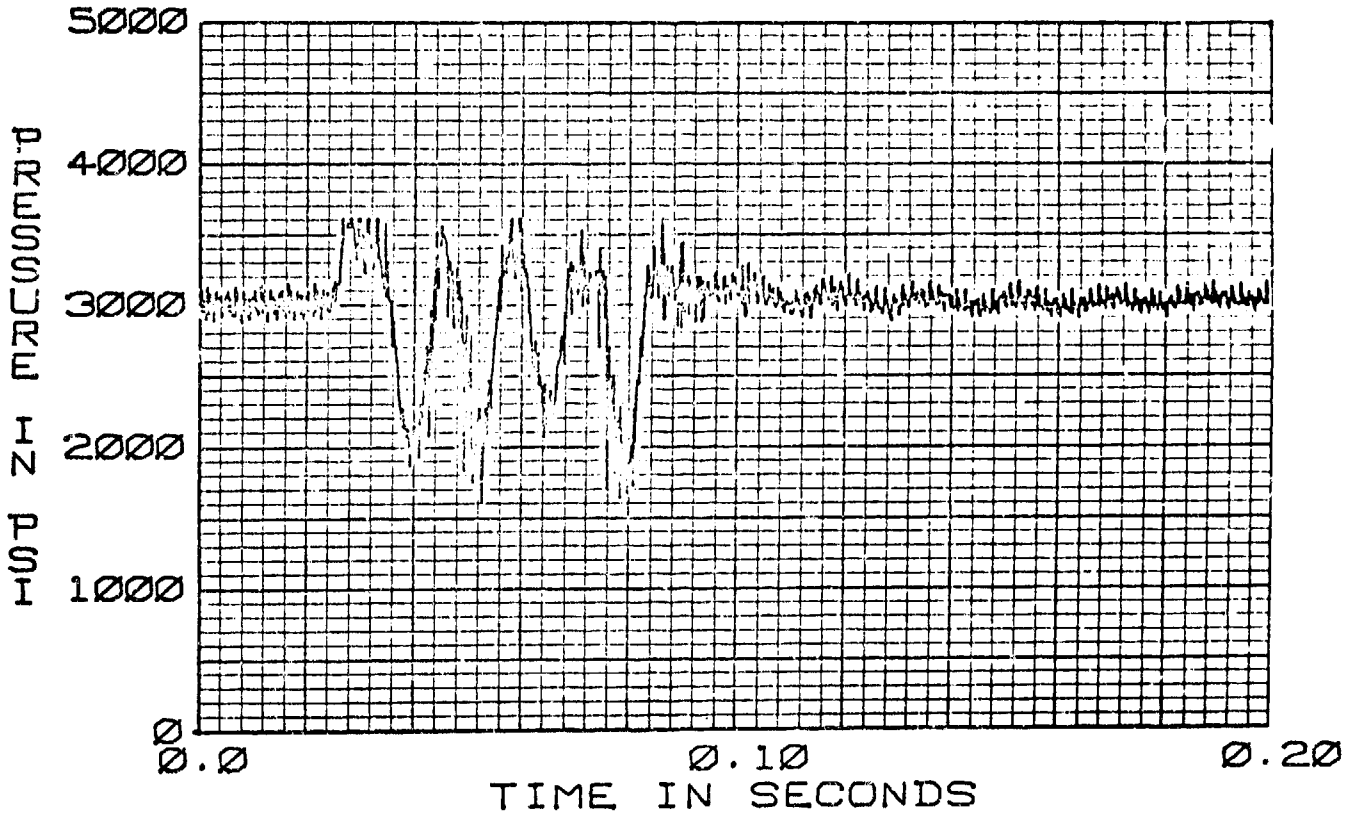

FIGURE 151. F-15 HYDRAULIC PUMP
63-03-PP TURN-OFF TRANSIENT
77 CIS 130°F

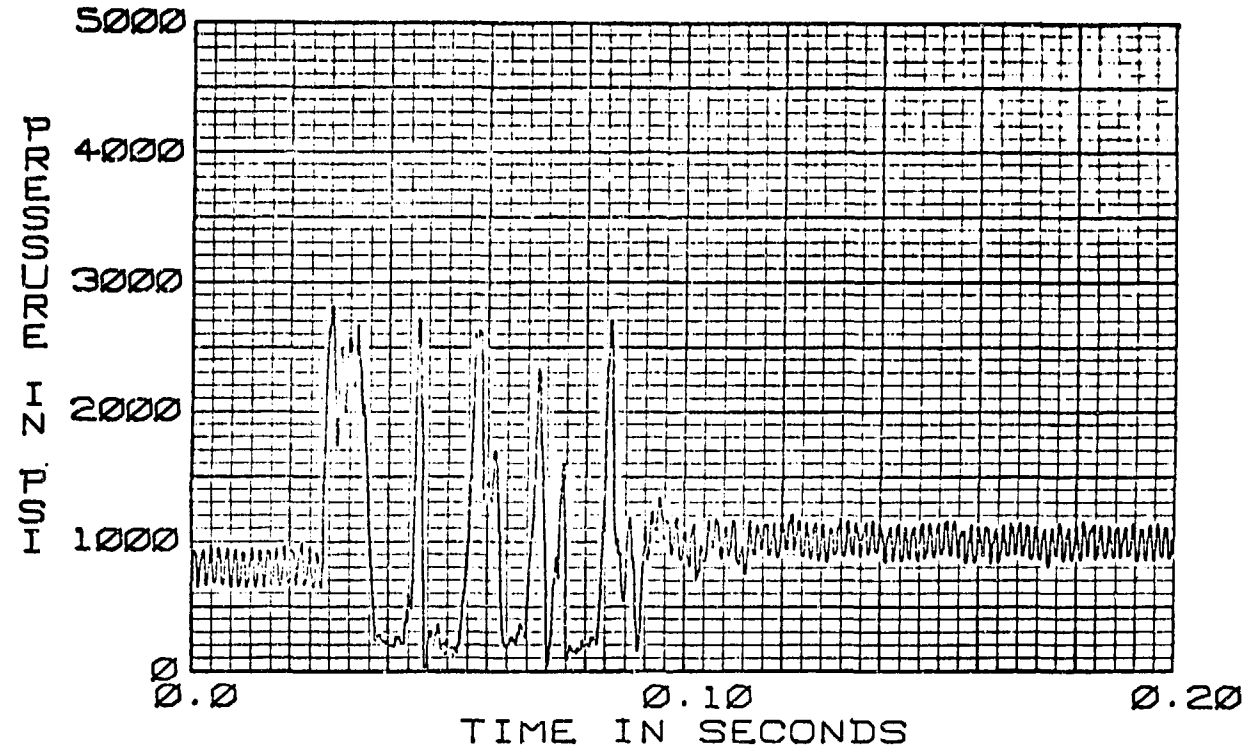

FIGURE 152. F-15 HYDRAULIC PUMP
63-03-PC TURN-OFF TRANSIENT
77 CIS 130°F

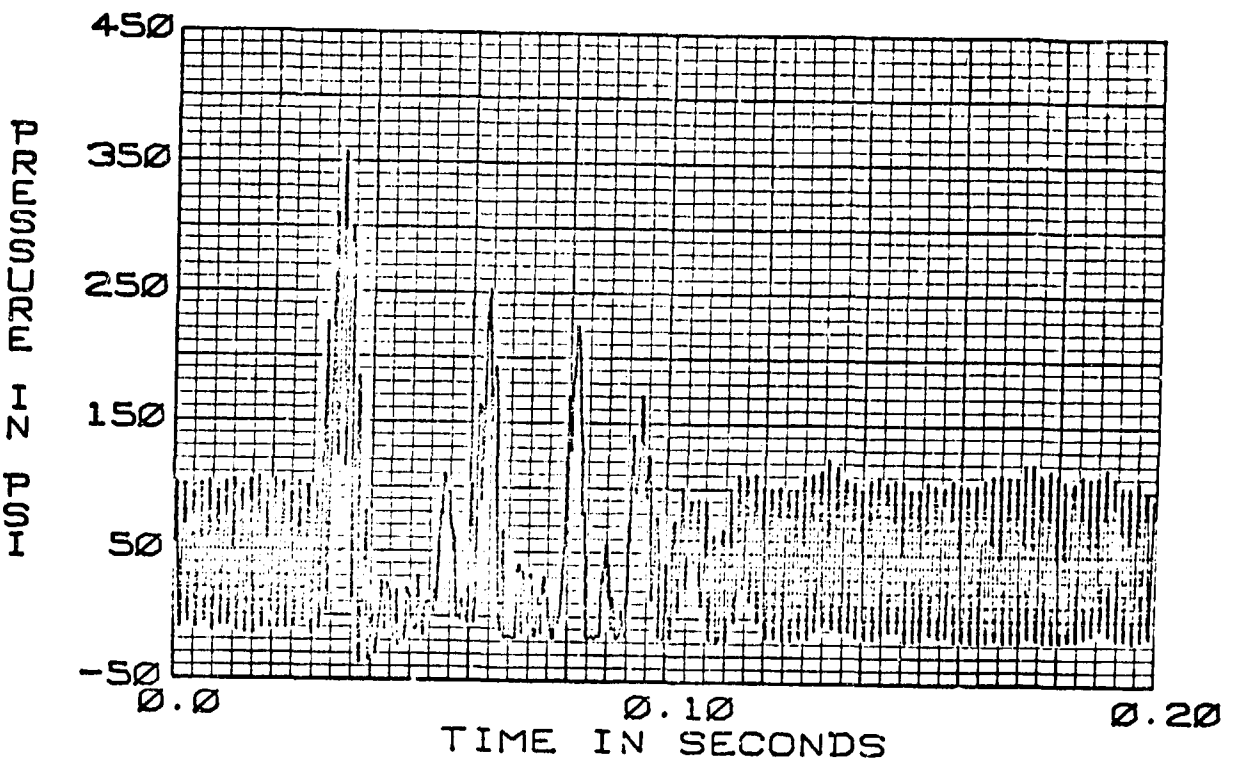

FIGURE 153 F-15 HYDRAULIC PUMP
63-03-PS TURN-OFF TRANSIENT
77 CIS 130°F

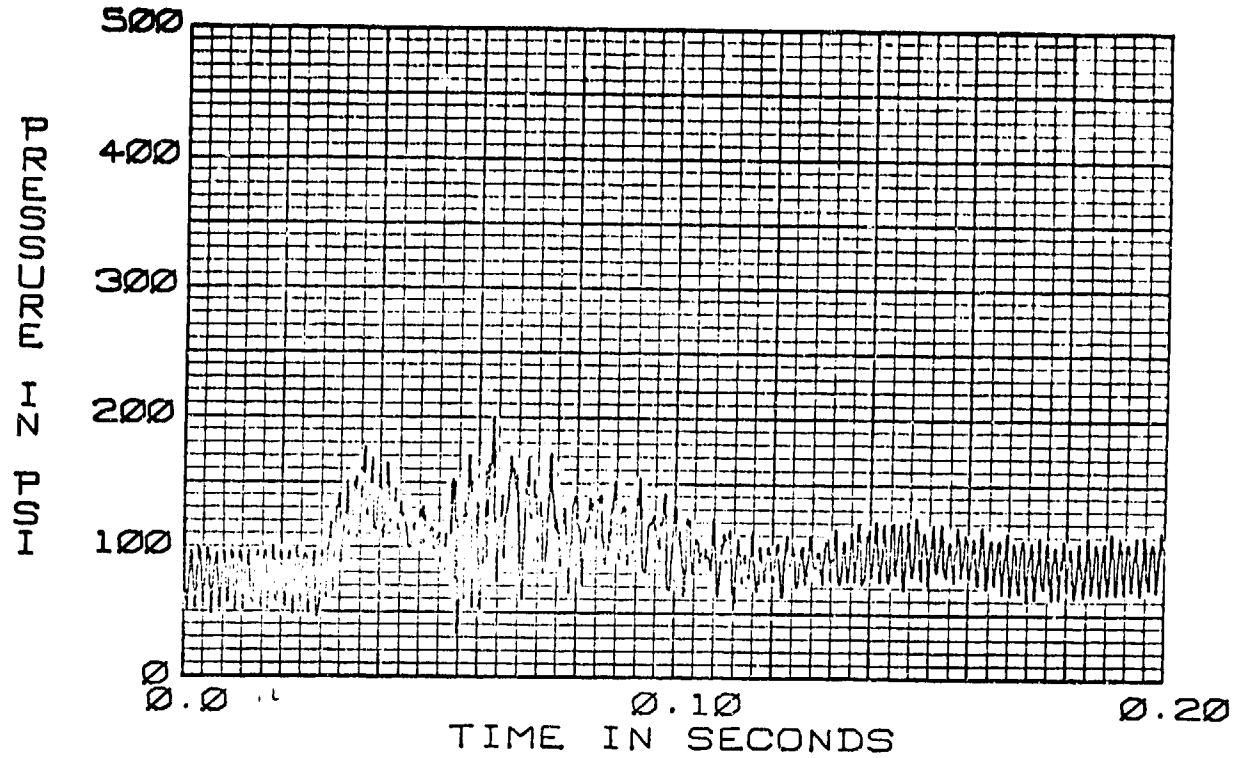

FIGURE 154. F-15 HYDRAULIC PUMP
63-03-PCD TURN-OFF TRANSIENT
77 CIS 130°F

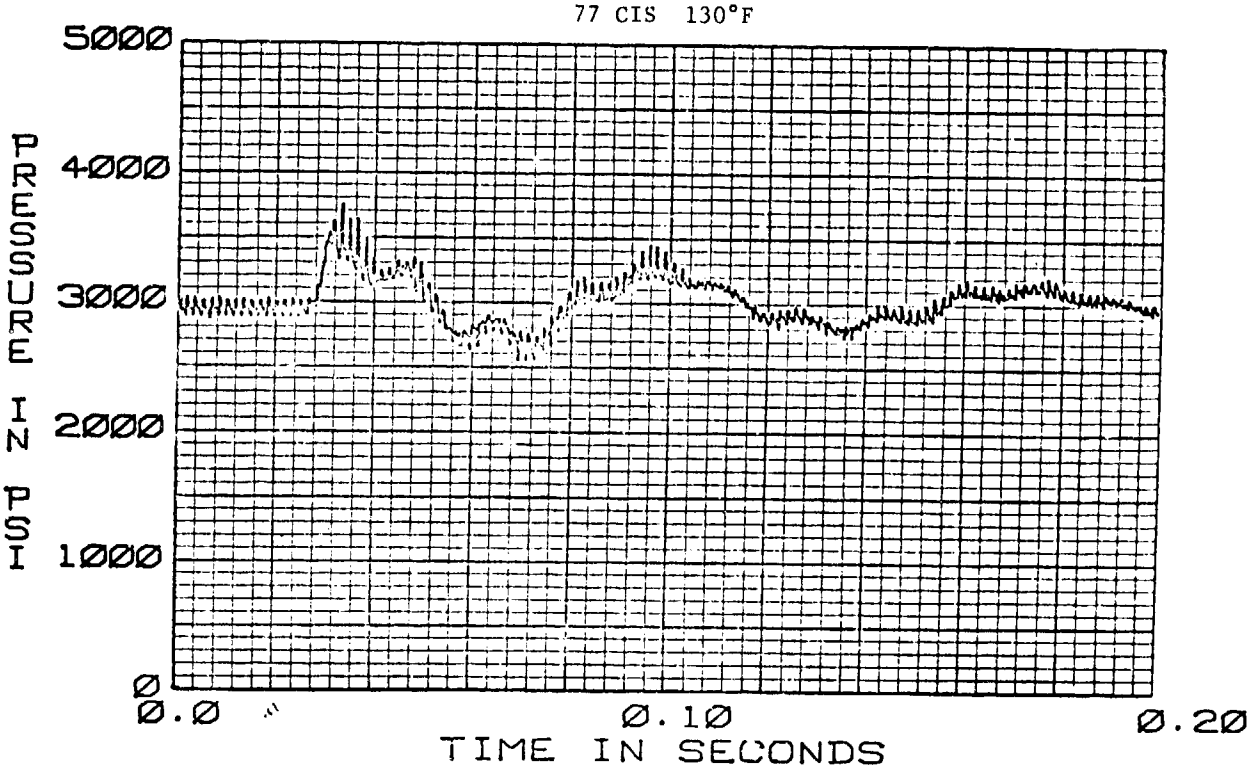

FIGURE 155. F-15 HYDRAULIC PUMP
64-03-P1 TURN-OFF TRANSIENT
77 CIS 130°F

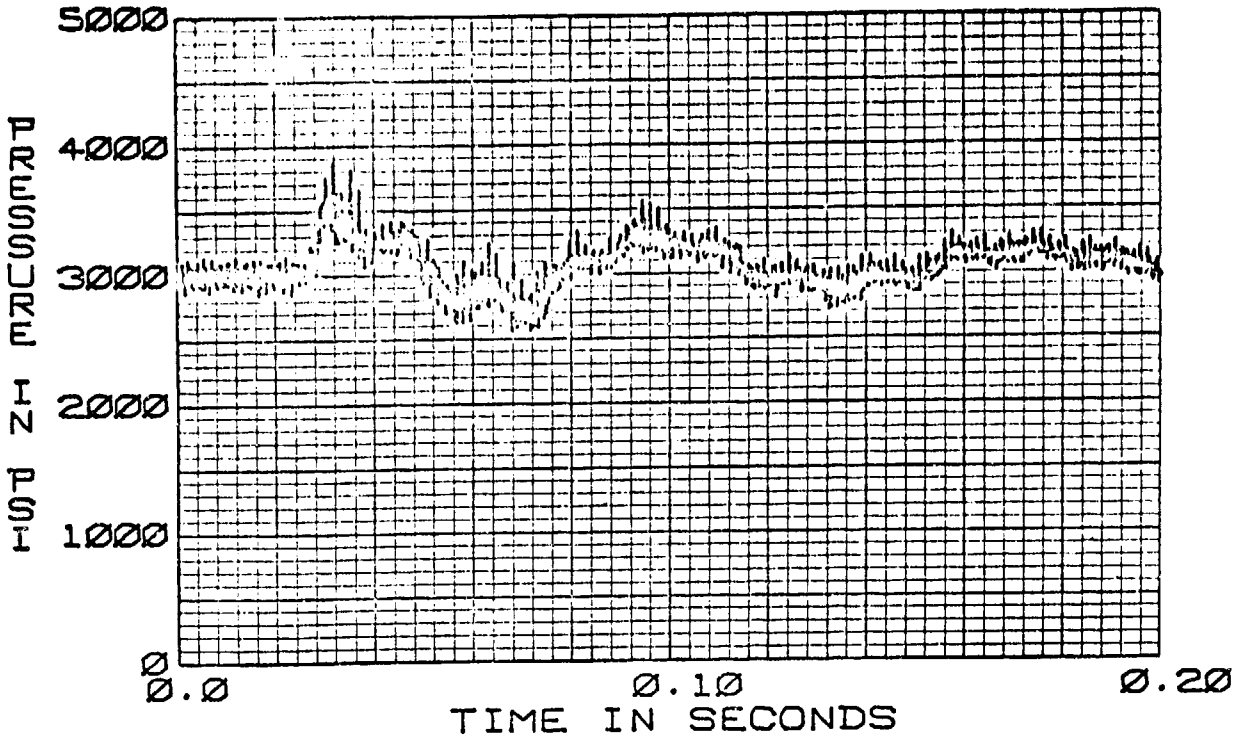

FIGURE 156. F-15 HYDRAULIC PUMP
64-03-PP TURN-OFF TRANSIENT
77 CIS 130°F

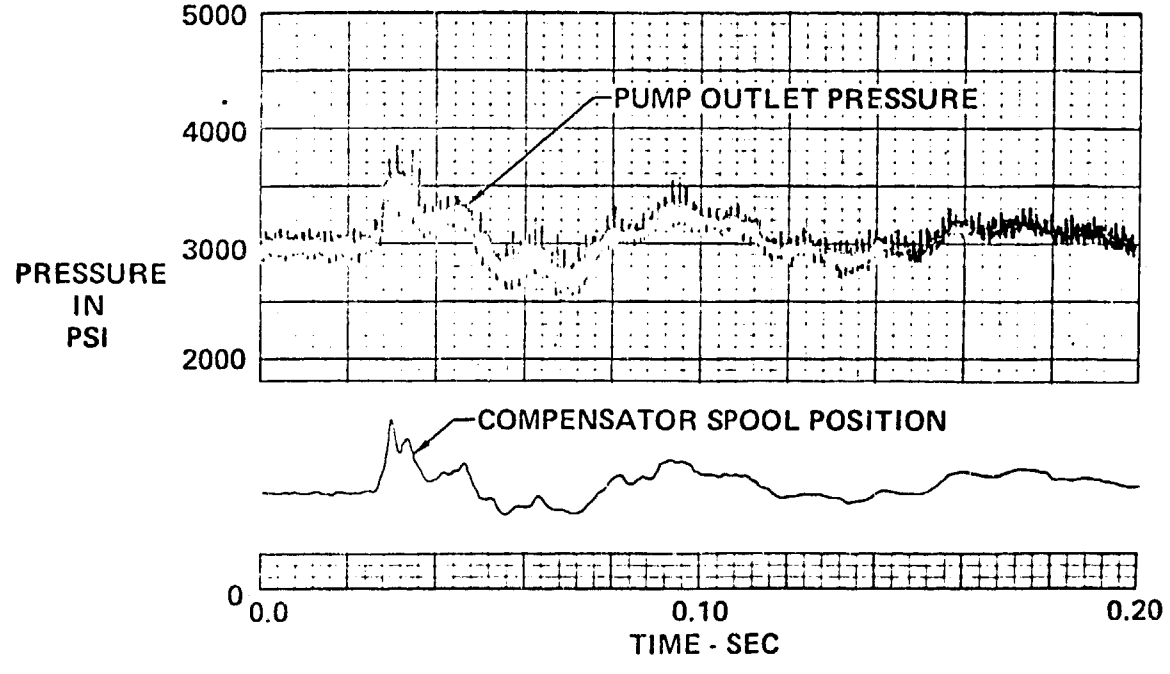

FIGURE 157. COMPENSATOR SPOOL POSITION COMPARED TO PUMP OUTLET PRESSURE
F-15 INSTRUMENTED PUMP TURN-OFF TRANSIENT WITHOUT CHECK VALVES IN MANIFOLD
FLOW - 77 CIS TEMP - 130°F

One notes the same type of phase similarity between the pump input pressure 64-03-PS, Figure 158, and the actuator control pressure 64-03-PC, Figure 159. The inlet pressure transducer trace (Figure 158) does show a 100 psi peak-to-peak pressure like 63-03-PC in Figure 159. The case pressure 64-03-PCD, in Figure 160, has only about a 20 psi peak to peak pressure. At 50 milliseconds in 64-03-PCD there is a pump response that may be related to some pressure inbalance inside the pump This spike is not due to transducer resonance mainly because of its low frequency content.

c. Test Series 65 - Pump Transient Tests without Check Valves in the Manifold - The development fixture oil was replaced with MIL-H-83282, and the pump steady state and transient tests were rerun to determine the effect, if any, on pump performance. A list of the transient tests are shown in Table 7.

The other results of the transient tests with MIL-H-83282 appear to be identical to those obtained with MIL-H-5606B in the 64 series.

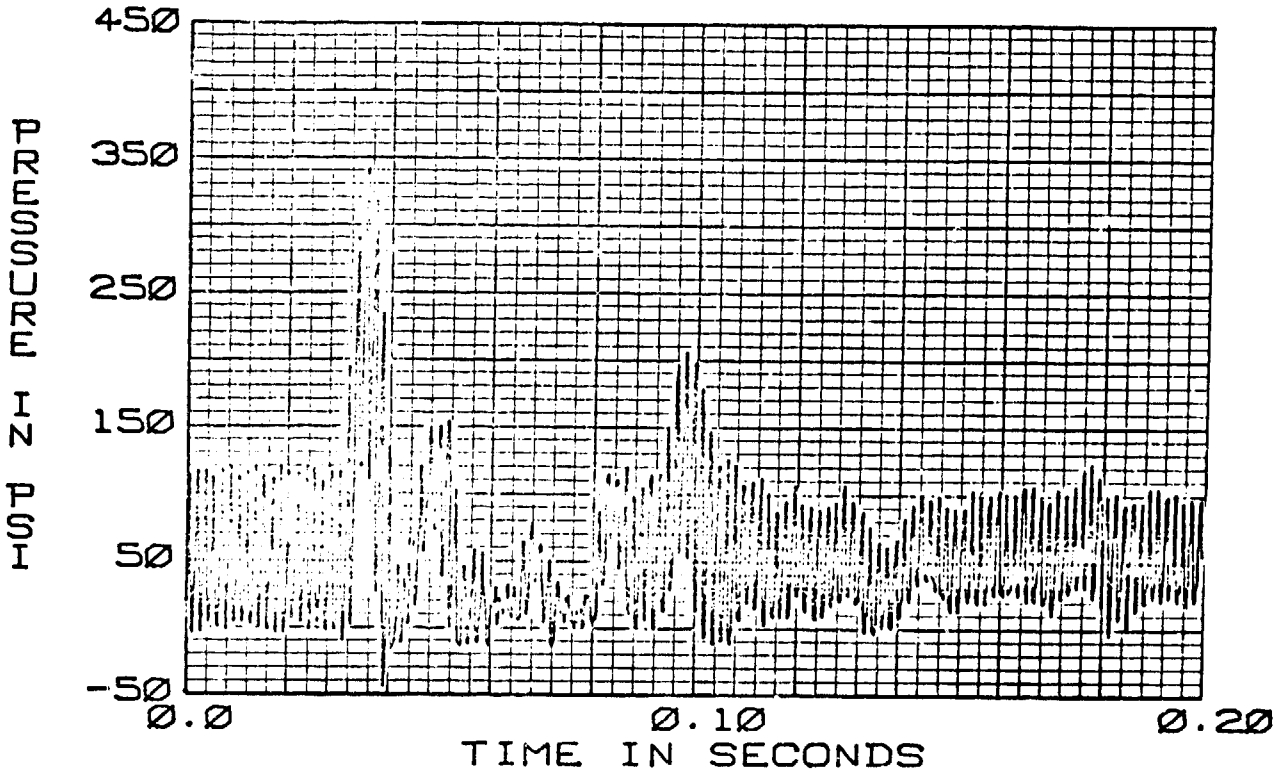

FIGURE 158. F-15 HYDRAULIC PUMP
64-03-PS TURN-OFF TRANSIENT
77 CIS 130°F

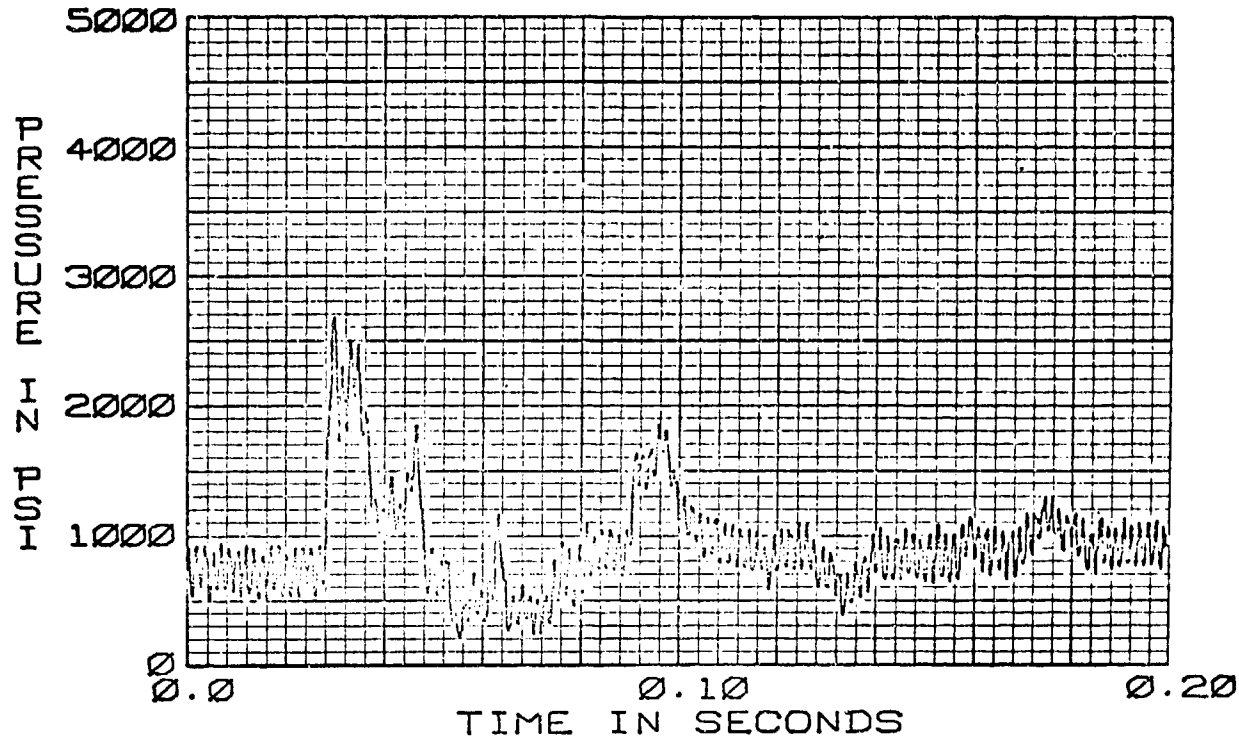

FIGURE 159. F-15 HYDRAULIC PUMP
64-03-PC TURN-OFF TRANSIENT
77 CIS 130°F

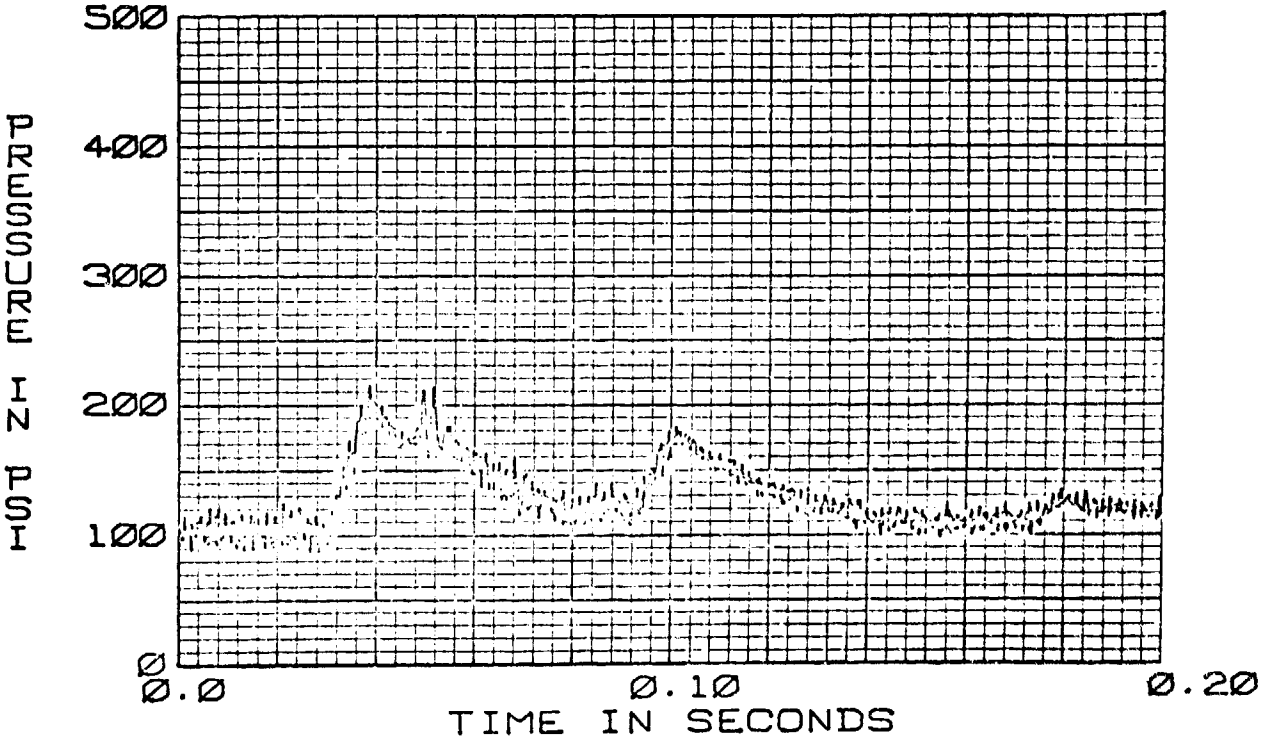

FIGURE 160. F-15 HYDRAULIC PUMP
64-03-PCD TURN-OFF TRANSIENT
77 CIS 130°F

TABLE 7

Hytran Pump Model Verification Test - 65 Series

Steady State Flow Levels (CIS) Lo	Hi	Control Valve Operating Time (SEC) On	Off	Case Pressure At SS Leakage Condition (1.5-3.8 CIS)	Pump Speed (RPM)	Temperature Pump Inlet (DEG F)	Run Number Turn-On (65-XX+XX) Turn-Off(65-XX+XX)
I. Load Level Effects							
2 -	19.25	.002	.002	57 PSIG	4000	130	65-01
2 -	38.5	.002	.002	58 PSIG	4000	130	65-02
2 -	77.0	.002	.002	90 PSIG	4000	130	65-03
2 -	77.0	.002	.002	58 PSIG	4000	130	65A03
2 -	154.0	.002	.002	49 PSIG	4000	130	65-04
II. Speed Effects							
2 -	57.75	.002	.002	49 PSIG	3000	130	65-22
2 -	57.75	.002	.002	49 PSIG	5000	130	65-24
III. Temperature Effects							
2 -	77.0	.002	.002	53 PSIG	4000	210	65-30
IV. Suction Transient Cavitation							
2 -	154.0	.002	.002	29 PSIG	4000	130	65-61 (P_{RESV}=25 PSIG)

d. Verification of the HYTRAN Pump Model - For pump verification it was necessary to establish adequate boundary conditions. The inlet pressure, and case drain pressure were chosen. The suction pressure transducer was located about 24 inches from the pump inlet, and the case transducer was 13 inches from the pump case drain port. Figure 161 shows the HYTRAN program schematic used in the pump verification runs.

Looking at the PS and PCD traces for any of the 63, 64 or 65 series runs, one notes the superposition of the pumps ripple frequency on the pressure wave. At 4000 rpm the frequency of the nine piston pump is

$$4000 \frac{\text{REV}}{\text{MIN}} * 9 \frac{\text{CYCLES}}{\text{REV}} * \frac{1 \text{ MIN}}{60 \text{ SEC}} = 600 \frac{\text{CYCLES}}{\text{SEC}}$$

This ripple frequency superimposed on the pressure trace made the boundary conditions very noisy. The noise manifested itself in the pump math model and produced erroneous results. Typically at 4000 rpm the pump input pressure would vary over a one hundred psi range in 1.6 milliseconds. The data was sampled at a .2 millisecond time step, thus the calculation internal was .2 milliseconds. So in 8 Δts the input pressure could vary by as much as 100 psi. In a complicated model where many factors are interdependent this rapid change produced bad correlation. It became necessary to modify the data to remove the pump noise. This was

accomplished by using a 100 Hz filter on the pressure signals when they were played back from the analog tape into the waveform analyzer. F65-03-PS in Figure 162 is a filtered suction pressure trace for a turn-off transient at 77 CIS and 130°F. The unfiltered pressure trace is shown in Figure 163. The unfiltered run had 100 psi peak to peak pulsations. After filtering they were reduced to 5 psi peak to peak. The basic pump pulsation frequency still remains, but a 5 psi change over 1.6 milliseconds provides a better boundary condition than a 100 psi change.

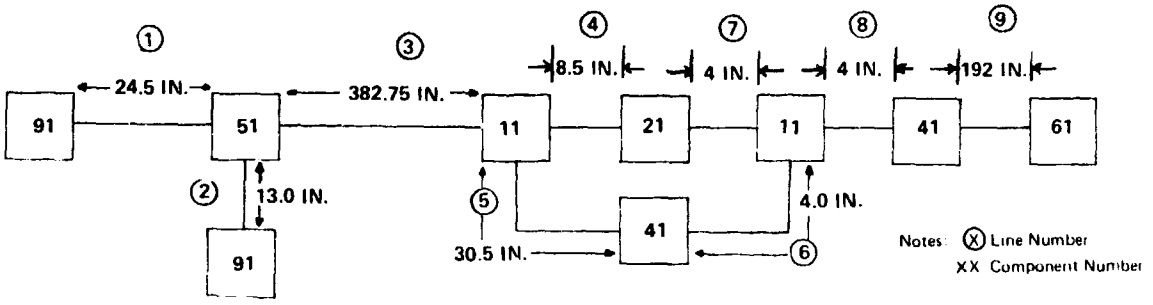

FIGURE 161. HYTRAN SCHEMATIC DIAGRAM FOR PUMP VERIFICATION

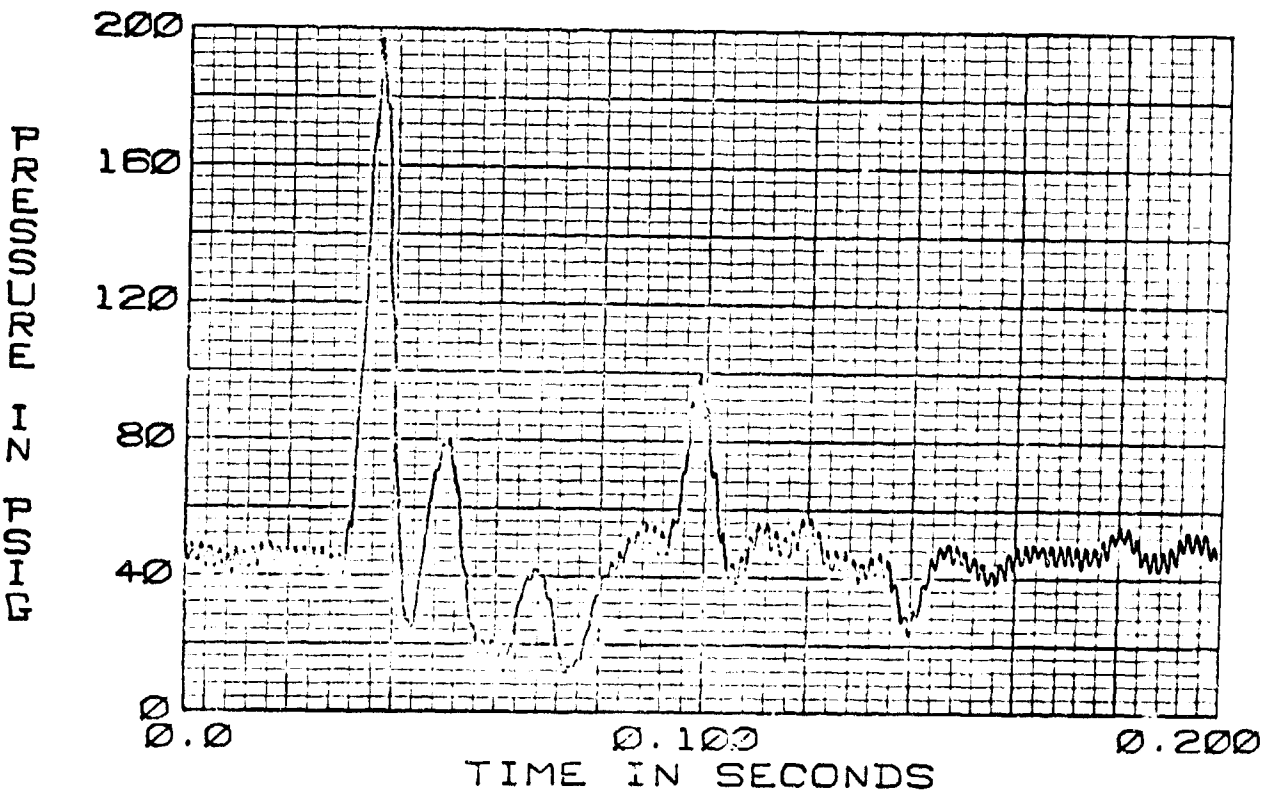

FIGURE 162. F-15 HYDRAULIC PUMP
F65-03-PS TURN-OFF TRANSIENT
77 CIS 130°F

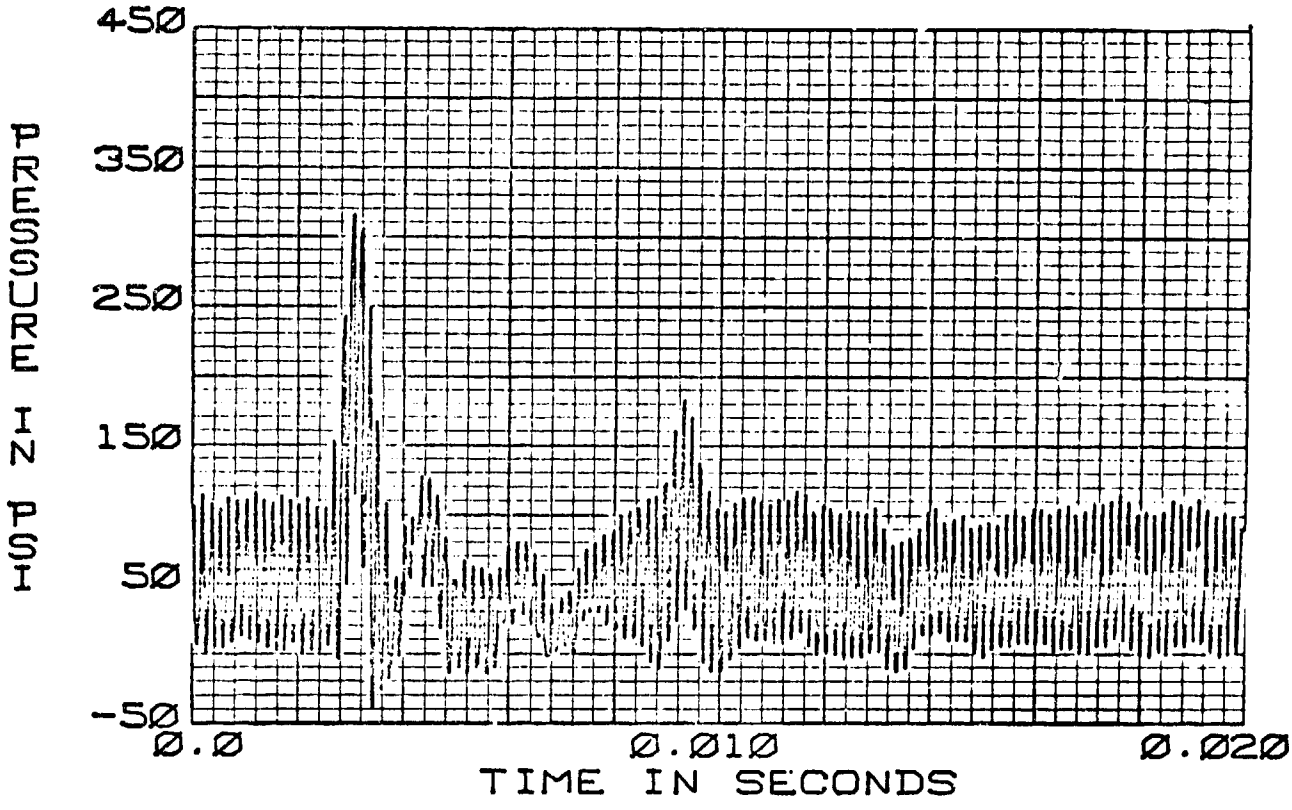

FIGURE 163. F-15 HYDRAULIC PUMP
65-03-PS TURN-OFF TRANSIENT
77 CIS 130°F

The main reason for filtering the data is because the internal pump flow and leakages are treated as though the pump has a continuous output rather than a summation of nine individual pumping pistons thus requiring a reasonably continuous input. A model which includes the dynamics of each piston would by necessity, be considerably more complex and consume much more computer time than the current pump model.

Another analytical consideration was linearizing any leakage paths and assuming them constant for a constant output pressure. The alternative would be to go into very detailed calculations with the leakage dependent on piston load, hanger angle, rpm and almost anything else one cares to add. Unfortunately, this too would probably be inaccurate so instead a simple leakage model was chosen. A steady state verification test with MIL-H-83282 showed that the case drain pressure versus case drain flow was linear from maximum to zero case flow. This translates to a linear leakage path from case to inlet at any flow or pressure conditions. These results help to verify the simple leakage model.

In developing the model significant attention has been paid to the compensator valve dynamics. The forces on the valve are a combination of the outlet pressure force pushing against the case pressure and spring forces, with damping and flow forces acting in either direction.

The compensator valve position is assumed to be directly proportional to the differential pressure between outlet and case. The compensator position is used to determine the pressures and flows connected with the valve.

During the initial verification effort the computer results indicated that the actuator pressures were out of phase with the measured data. To correct the phasing the effects of valve damping and hanger inertia were included in the computation. This provided enough lag to obtain the proper alignment.

The internal case pressure was found to be about 50 to 100 psi higher than the measured case pressure 13 inches downstream of the pump manifold case outlet. This discrepancy was significant at the lower case drain flow rates. The measured case pressure (Figure 164) showed a rise, a small dip then another rise to the maximum pressure. The hanger position 65-03-XH in Figure 10 also exhibited this same characteristic. The computed results for internal case pressure missed the first dip altogether and overshot the second one.

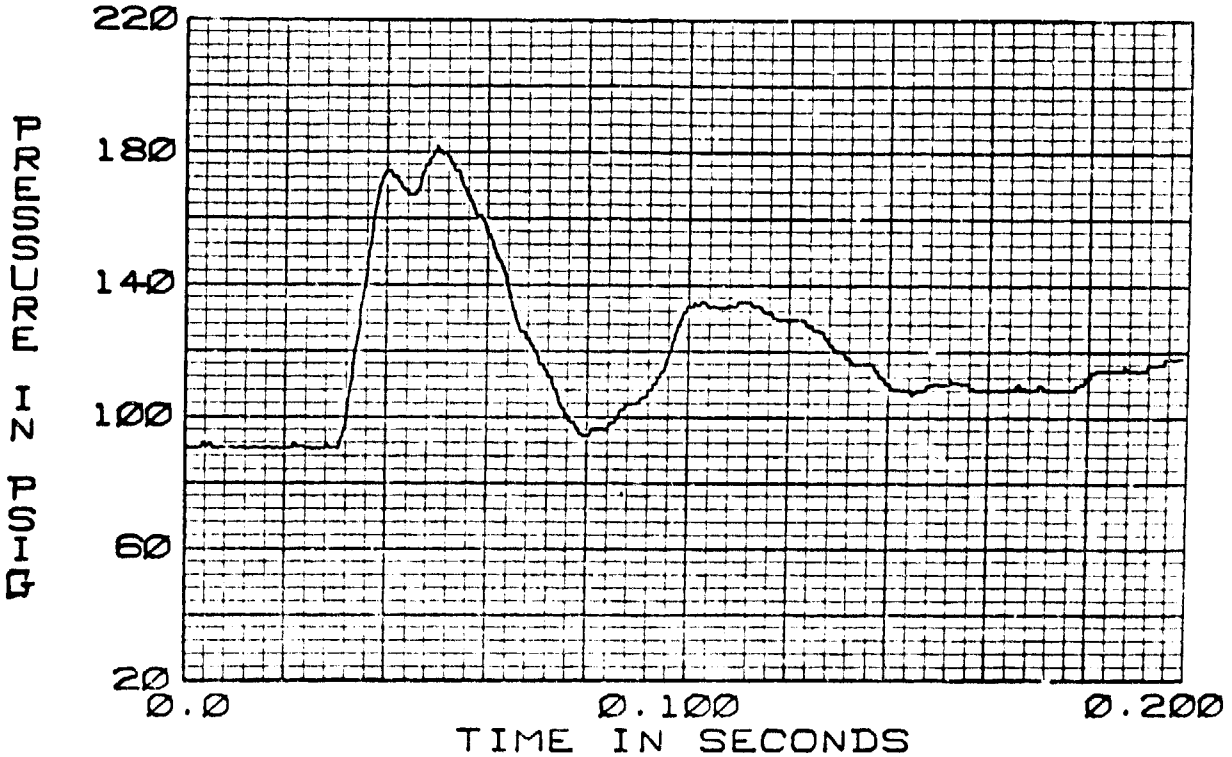

FIGURE 164. F-15 HYDRAULIC PUMP
F65-03-PCD TURN-OFF TRANSIENT
77CIS 130°F

Not having an internal case drain pressure transducer hampered the investigation on whether this was an accurate result. This hanger position is affected by case pressure but other factors as piston and actuator spring forces have a much greater contribution.

Our initial assumption was the internal case pressure characteristics should not deviate much from the measured line pressure. Studying the F-15 pump and manifold schematics a quick disconnect fitting in the pump case drain line was found to have a significant orifice. A spring loaded poppet closes off the case drain lines when the pump is removed from the manifold to prevent oil spillage. With the pump mounted the flow out the case drain line is impaired by three slots in the quick disconnect fitting. This opening had an area of about .04 in^2. The addition of this orifice in the case drain computation significantly improved the computer simulation.

The computer simulation could now reasonably predict the initial response characteristics of the pump. Problems still existed however in the subsequent pump reaction to the initial transient. The general trend was that the pump model was extremely underdamped. Different values of hanger damping were tried without much success. The hanger damping term accounts for velocity dependent friction factors in the pump. These factors include the effects of hanger motion on the changes in precompression and decompression when the hanger is in motion, plus many other terms that cannot be accurately measured. Values below 15 psi/in/sec for hanger damping did not improve the pump damping characteristics. Initial transient pressures would undershoot and the subsequent response was extremely underdamped. Values above 30 psi/in/sec had exactly the opposite effect. A reasonable value of hanger damping appears to be 25 psi/in/sec.

The pump case volume was increased from 250 to 500 cubic inches to see how the damping characteristics changed. The results of the run show that the case pressure did not have the pressure dip on the initial transient. The hanger oscillated at about 25 cycles/second after the initial response and did not dampen as quickly as the data shown in Figure 10 in Section III.

The valve dynamics are an important part of the computer simulation. An initial value of .001" was used as the overlap for the value spool. The test results indicated a much larger deadband area, on checking with the pump manufacturer it was found that .016" was a more nominal value for the compensator valve overlap rather than the value obtained originally. The

effects of different valve overlap can be seen in the computer printouts of the pump actuator or control pressure in Figures 165, 166 and 167. In Figure 165 the measure actuator pressure vs time is overplotted on the computer results at .012" valve overlap. At 7.5 milliseconds the pressures show a rise to 1500 psi. Other spikes occur at 13 and 19 milliseconds and show little sign of decay. With a .016" valve overlap in Figure 166 the spike at 7.5 milliseconds is about 100 psi less and the pressure wave at 19 milliseconds is gone. The run at .020" overlap in Figure 167 show that the pressure at 7.5 milliseconds drops to 1300 psi. At this larger valve overlap the measured pressure trace is out of phase with the predicted results.

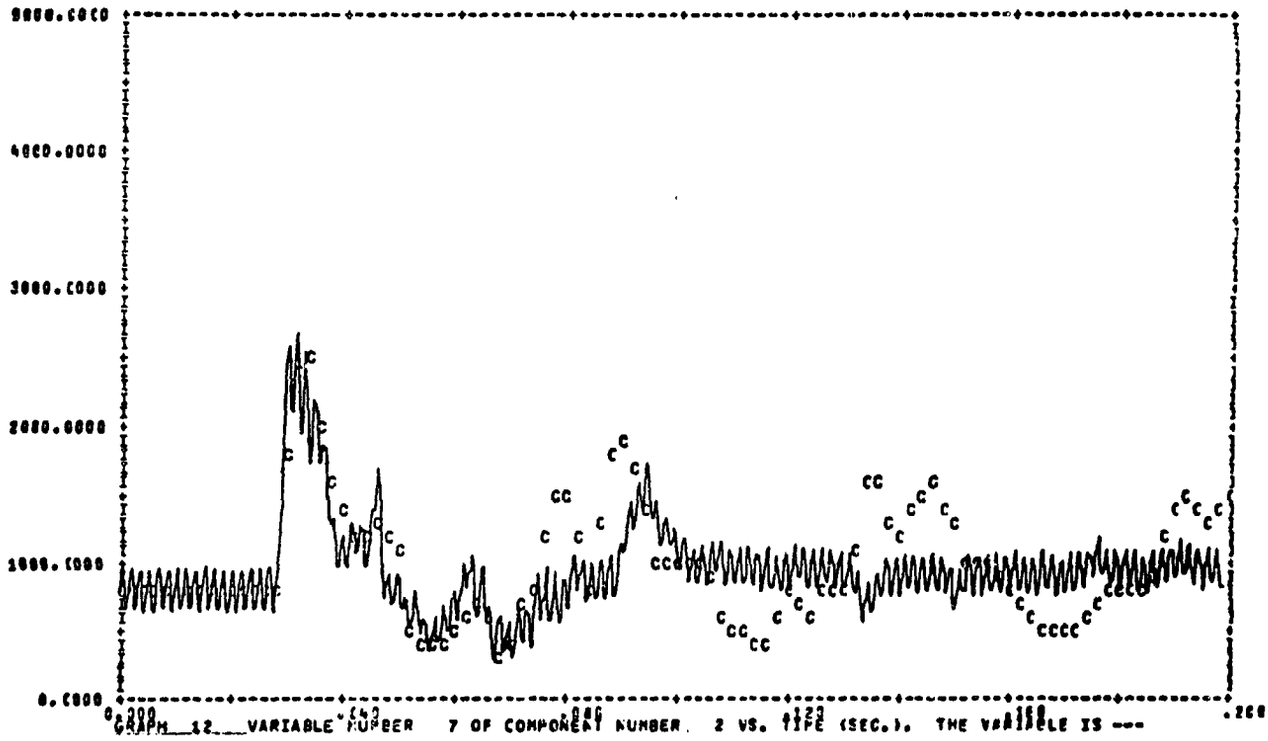

FIGURE 165. .012" VALVE OVERLAP

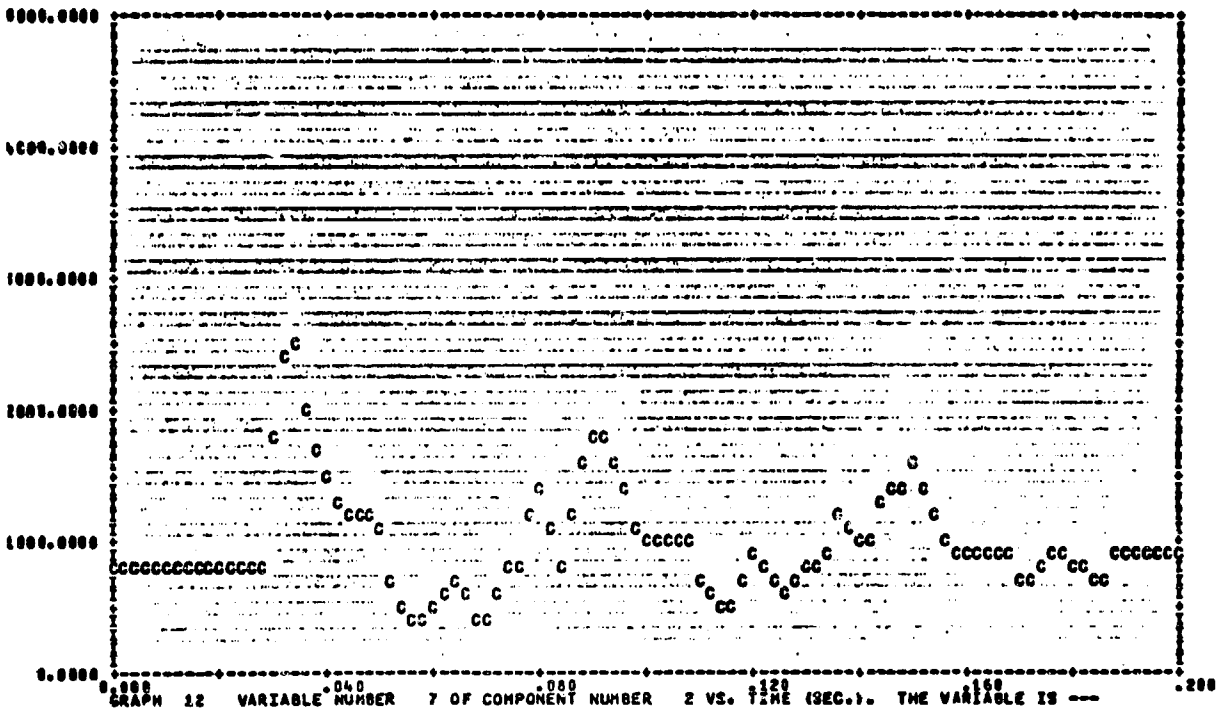

FIGURE 166. 016" VALVE OVERLAP

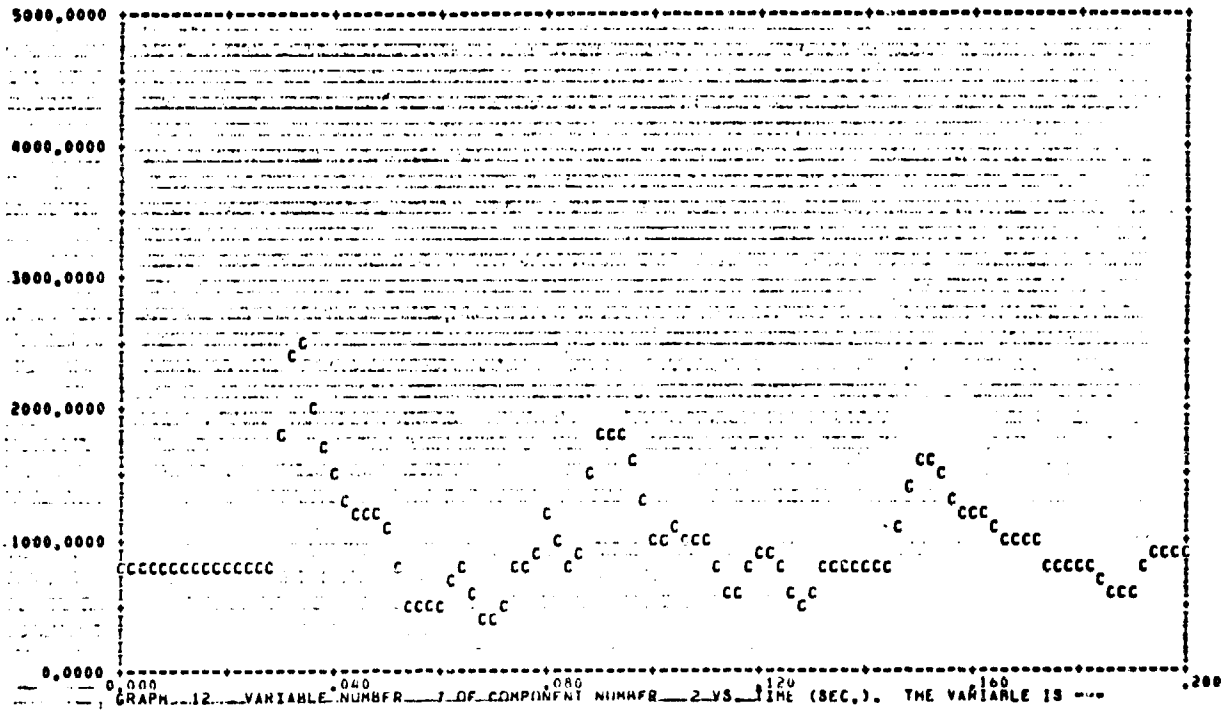

FIGURE 167. .020 VALVE OVERLAP

A pump turn-off transient simulation was run with MIL-H-83282 at a temperature of 130°F and a steady state flow of 77 CIS. The data in Figures 162 and 164 were input with the configuration data in Figure 168 for the HYTRAN program. The results of the simulation are shown in Figures 169, 170, 171, 172, 173, and 174. All the overplotted pressure data has been changed to absolute pressure to match the computer output. Figures 169, 170 show that the first 40 milliseconds of the simulation give good correlation with the actual data. At 50 milliseconds in Figure 169 the computed pressure drops to 2550 psi compared to the measured 2800 psi.

```
****DATA RUN NO. 65-03-PS AND -PC  F-15 PUMP****(FIPM78A)

THE TRANSIENT RESPONSE IS FROM T=0.0  TO T=  .200 SECONDS AT TIME INTERVALS OF DELT= .00020
WITH OUTPUT POINTS PLOTTED AT INTERVALS OF  ,  .00200  SECONDS

FLUID DATA FOR MIL-H-83282 AT  3000.0 PSIG, -   50.0 PSIG AND 130.0 DEG F IN   10.0 DEG F STEPS
VISCOSITY     =  .203E-01        .153E-01IN**2/SEC
DENSITY       =  .79JE-04        .791E-04(LB-SEC**2)/IN***4
BULK MODULUS =  .223E+06         .187E+06PSI
VAPOUR PRESS.=  .200E+01 AT  130.0 DEG F
FIX-UP TAKEN AT LINE 13,VEL OF SOUND IN LINE  4 IS  15.4PER CENT IN ERROR
FIX-UP TAKEN AT LINE 18,VEL OF SOUND IN LINE  5 IS  60.1PER CENT IN ERROR
FIX-UP TAKEN AT LINE 18,VEL OF SOUND IN LINE  7 IS  58.6PER CENT IN ERROR
FIX-UP TAKEN AT LINE 19,VEL OF SOUND IN LINE  8 IS  59.8PER CENT IN ERROR

LINE DATA
LINE NO.      LENGTH      INTERNAL DIA    WALL THICKNESS   MODULUS OF ELASTICITY      DELX      CHARACTERISTIC IMPEDANCE   VELOCITY OF SOUND
    1        24.5000        .9020            .0490            .300E+08            12.2500          5.1559                49789.5131
    2        13.0000        .3130            .0260            .300E+08            13.0000         50.2549                50944.4460
    3       392.7500        .9840            .0590            .300E+08            10.0724          5.4696                50255.3193
    4         8.5000        .3940            .0580            .300E+08             8.5000          5.4696                42533.0333
    5        30.5000        .4440            .0280            .300E+08            10.1667         25.5997                50162.9453
    6         4.0000        .4440            .0280            .300E+08             4.0000         25.5997                20000.0000
    7         4.1250        .9020            .0490            .300E+08             4.1250          6.1559                23625.0000
    8         4.0000        .9020            .0490            .300E+08             4.0000          6.1559                20000.0000
    9       192.0000        .9020            .0490            .300E+08            10.1053          6.1559                49789.5131
 COMP#,  1 INTEGER DATA    1  91   0  -1   1  -0  -0  -0  -0  -0  -0  -0  -0  -0  -0  -0  -0
 COMP#,  2 INTEGER DATA    2  51   4   1  -3  -2  -0  -0  -0  -0  -0  -0  -0  -0  -0  -0  -0
REAL DATA CARD #  1  .297DE+04  .2000E+04  .1500E+00  .2500E+00   0.   .1500E-01  .6500E+00  .6500E+00
REAL DATA CARD #  2  .3070E+00  .4300E+03  .7000E+02  .1300E+03  .4700E+03  .2150E+03  .3500E-01  .2500E+02
REAL DATA CARD #  3  .3000E+01  .7500E+00  .3000E+00  .2000E-02  .1000E-02  .3000E-02  .2000E-01  .2500E+03
REAL DATA CARD #  4  .5000E+01  .4300E+04  .3600E-01  .5000E-01   0.   .3500E-02  .1000E+01  .8000E+01
 COMP#,  3 INTEGER DATA    3  91   0   2   1  -0  -0  -0  -0  -0  -0  -0  -0  -0  -0  -0  -0
 COMP#,  4 INTEGER DATA    4  11   0   3  -4  -5  -0  -0  -0  -0  -0  -0  -0  -0  -0  -0  -0
 COMP#,  5 INTEGER DATA    5  21   3   4  -7  -0  -0  -0  -0  -0  -0  -0  -0   4  -0  -0
REAL DATA CARD #  1  .2200E-01  .6500E+00  -0.  -0.  -0.  -0.  -0.  -0.  -0.  -0.
REAL DATA CARD #  2   0.   .2000E-01  .2500E-01  .2000E+00  -0.  -0.  -0.  -0.  -0.
REAL DATA CARD #  3  .6160E+00  .6160E+00   0.   0.  -0.  -0.  -0.  -0.  -0.  -0.
 COMP#,  6 INTEGER DATA    6  41   1   5  -5  -0  -0  -0  -0  -0  -0  -0  -0  -0  -0  -0
REAL DATA CARD #  1  .2100E-01  .6500E+00  -0.  -0.  -0.  -0.  -0.  -0.  -0.  -0.
 COMP#,  7 INTEGER DATA    7  11   3   6   7  -8  -0  -0  -0  -0  -0  -0  -0  -0  -0  -0
 COMP#,  8 INTEGER DATA    8  41   1   8  -9  -0  -0  -0  -0  -0  -0  -0  -0  -0  -0  -0
REAL DATA CARD #  1  .5400E+00  .6500E+00  -0.  -0.  -0.  -0.  -0.  -0.  -0.  -0.
 COMP#,  9 INTEGER DATA    9  61   1   9  -0  -0  -0  -0  -0  -0  -0  -0  -0  -0  -0  -0
REAL DATA CARD #  1  .5000E+02  -0.  -0.  -0.  -0.  -0.  -0.  -0.  -0.  -0.
```

FIGURE 168. HYTRAN INPUT DATA FOR PUMP TURN-OFF TRANSIENT

The predicted pressure does rise at 65 milliseconds like the data but overshoot in the calculated pressure at 50 milliseconds prevented any correlation. The relative phasing between the measured and computed data completely falls apart after 120 milliseconds into the simulation as seen in Figure 169. The actuator pressure data F65-03-PC (F denotes that the data was played back through a 100 Hz filter) in Figure 171 matches the predicted results up to 65 milliseconds. The maximum computed pressure at 40 milliseconds is 2500 psi compared to the actual 2250 psi. The resulting simulation shows high pressure responses while the test data dampens out quickly. The mechanism by which the pump compensator is able to dampen is not thoroughly understood and thus it is not included in the computer model.

The filtered pump outlet pressure (Figure 172) gives a clearer picture of the results shown in Figure 169 for P1. The pump pressure keeps dropping after 40 milliseconds instead of leveling off as shown by the data.

The initial response of the predicted hanger position in Figure 173 adequately simulates this pump parameter. At 40 milliseconds the measured data shows a leveling off then a rapid dip. The computed values exhibit a similar behavior but not as pronounced. Again one notes that the hanger dampens quickly to its zero flow position while the predicted results oscillate at about 25 Hz with minor damping. The valve position plot in Figure 174 shows the computed value at 40 milliseconds to be below the actual data. The predicted valve position after that time does not reverse as the measured results indicate.

A simulation of a pump turn-on transient was run at 130°F. The data in Figures 175 and 176 were the input boundary conditions. The input configuration data is shown in Figure 177. The output data for the computer simulation is shown in Figures 178, 179, 180, 181, 182 and 183.

The results for the turn-on transient are similar to the turn-off in that the simulation deviates from the measured data around 40 milliseconds. The computed response of the pump after the initial transient is underdamped when compared to the data. The resonant frequency is not as high a frequency as for the computed turn-off transient. The actuator control pressure (Figure 180) has a 100 psi overshoot at 120 milliseconds which is smaller than the

values in Figure 171. The hanger position (Figure 182) also shows a quicker damping than the turn-off transient (Figure 173). The computed hanger position does show a little dip at 39 milliseconds like the data. However, the predicted value never reaches the actual maximum at 50 milliseconds.

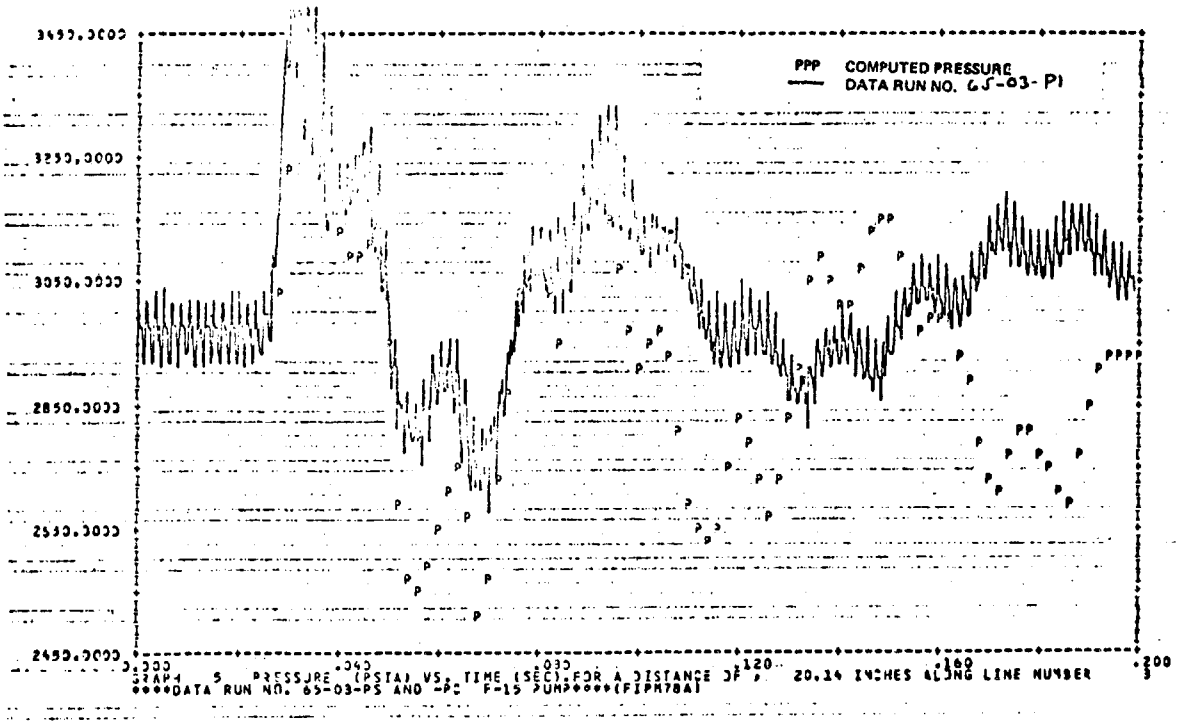

FIGURE 169. 65-03-P1 TURN-OFF TRANSIENT

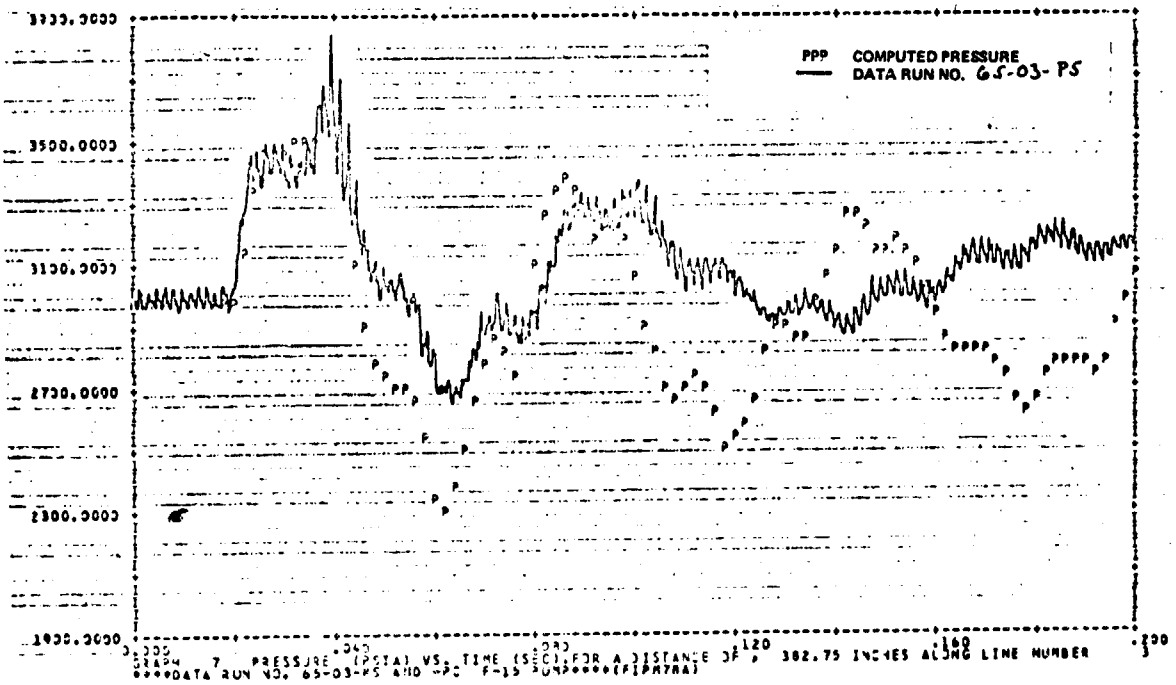

FIGURE 170. 65-03-P5 TURN-OFF TRANSIENT

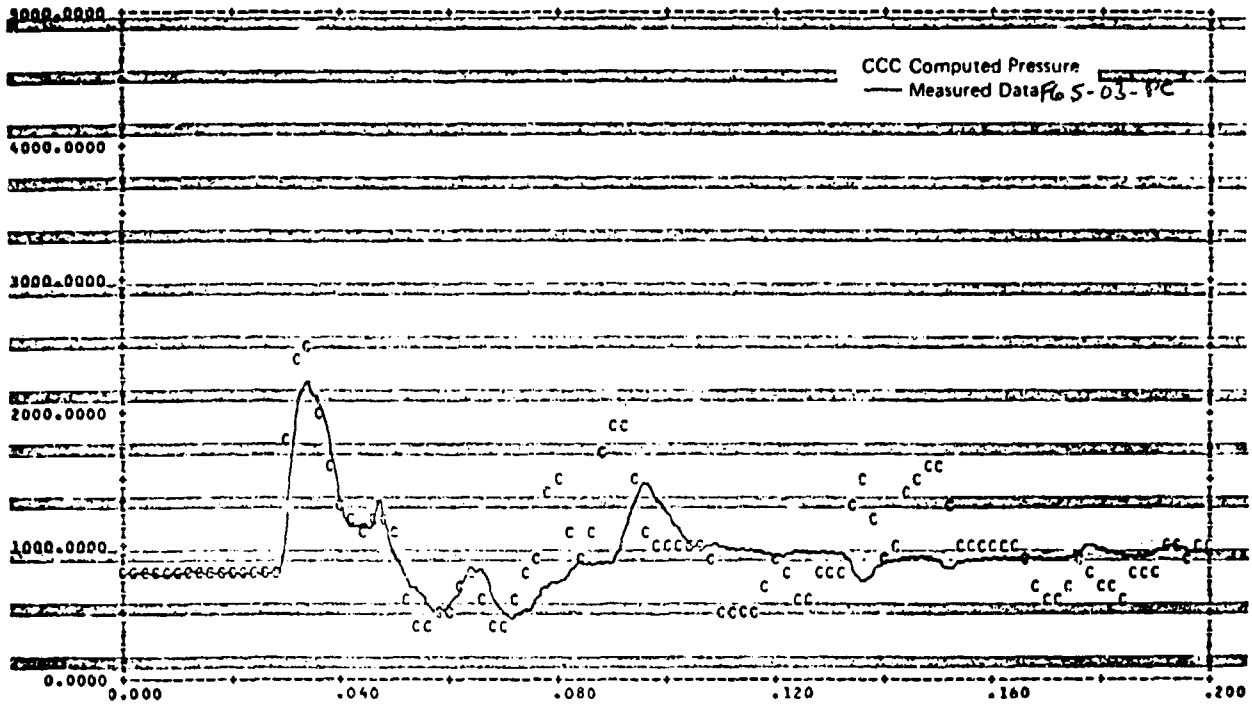

ACTUATOR PRESSURE (PSIA) vs TIME (SEC)

FIGURE 171. F65-03-PC TURN-OFF TRANSIENT

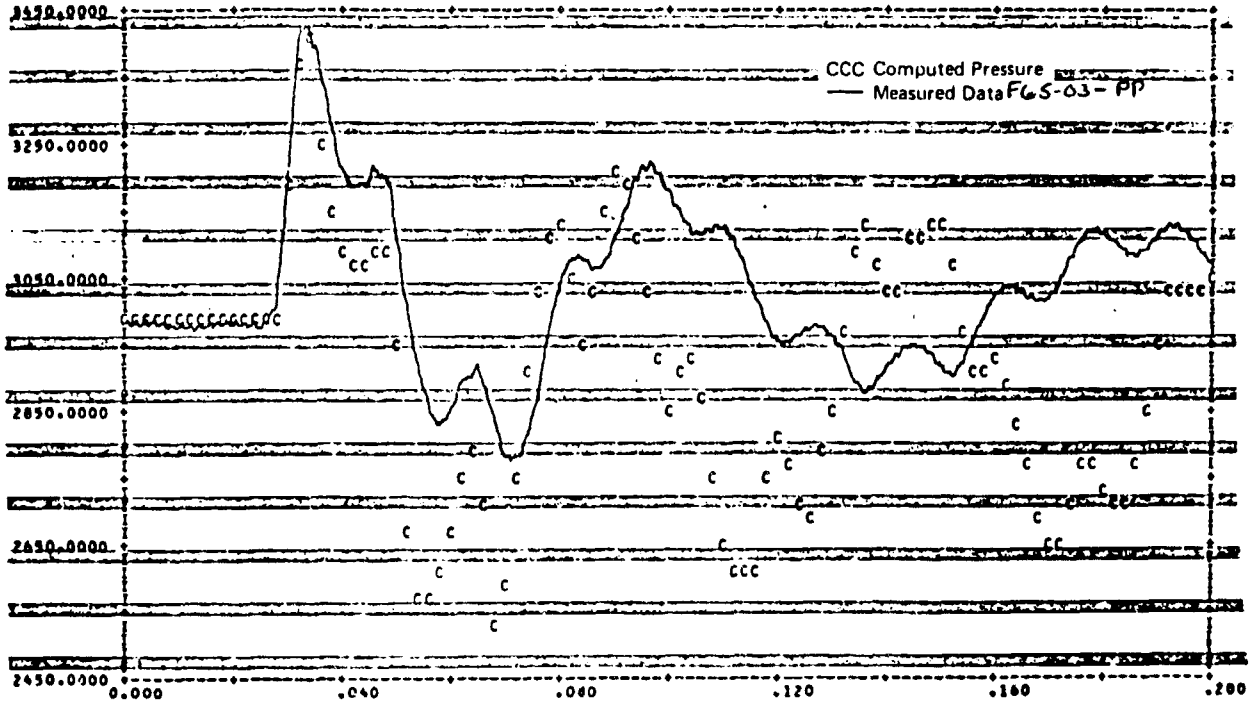

PUMP OUTLET PRESSURE (PSIA) vs TIME (SEC)

FIGURE 172. F65-03-PP TURN-OFF TRANSIENT

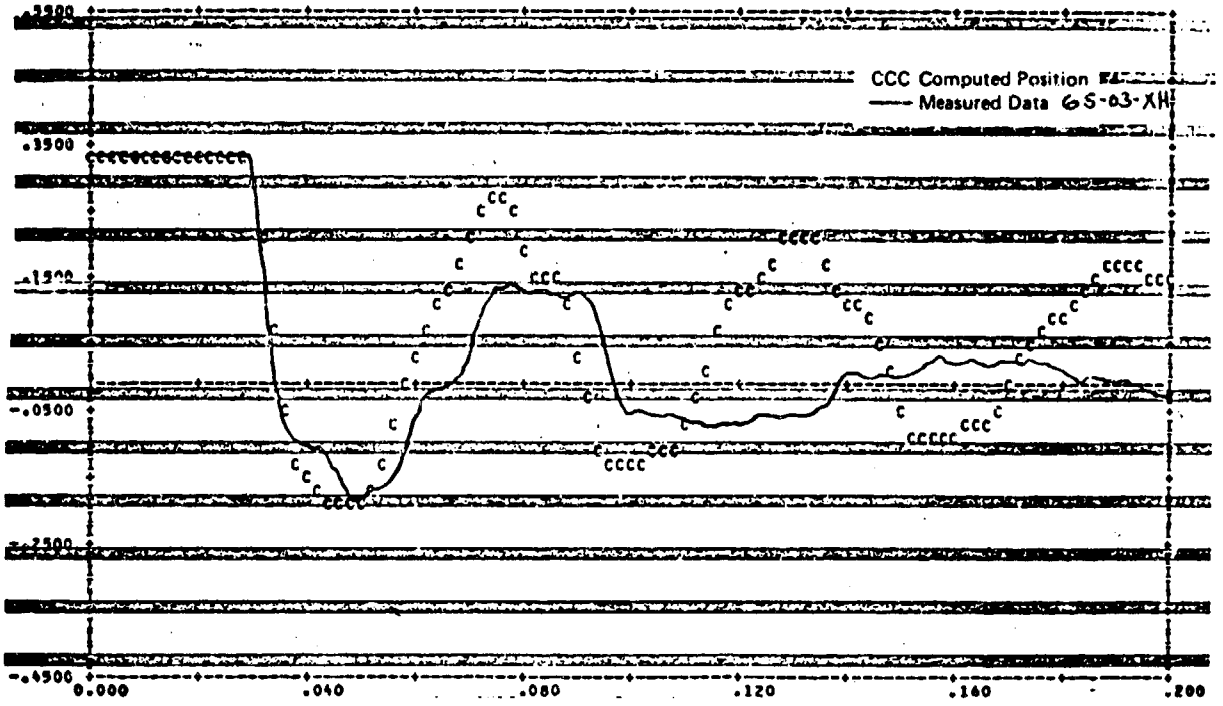

HANGAR POSITION (IN.) vs TIME (SEC)

FIGURE 173. 65-03-XH

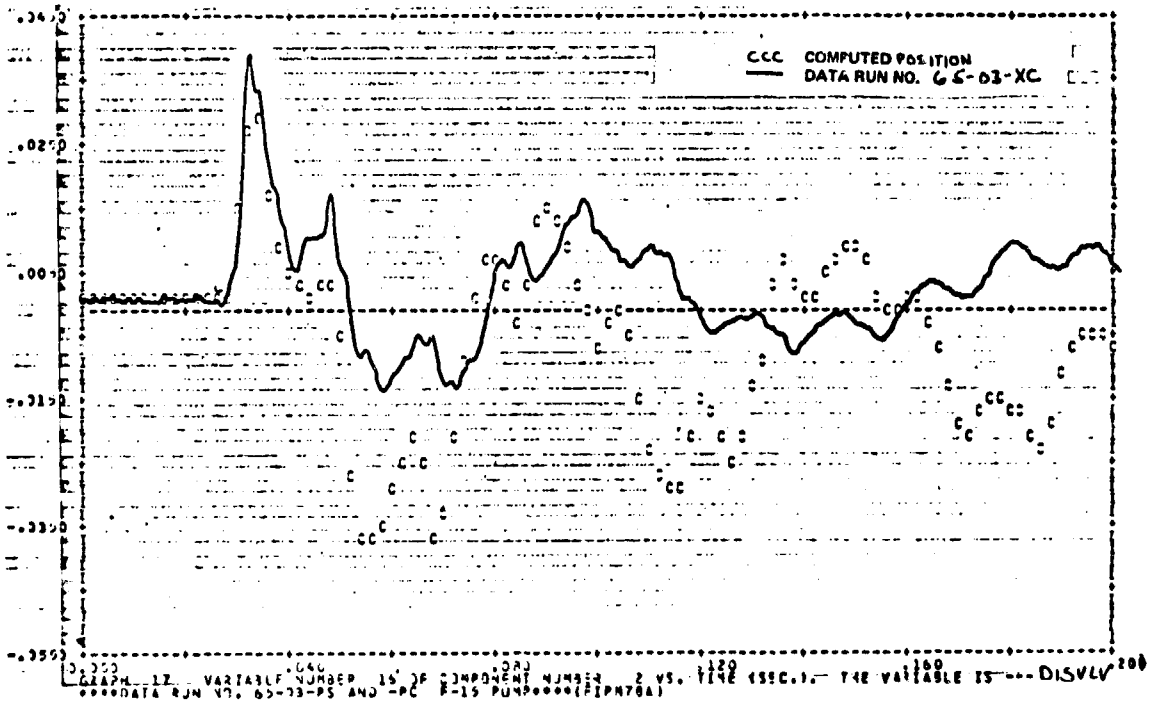

FIGURE 174. 65-03-XC TURN-OFF TRANSIENT

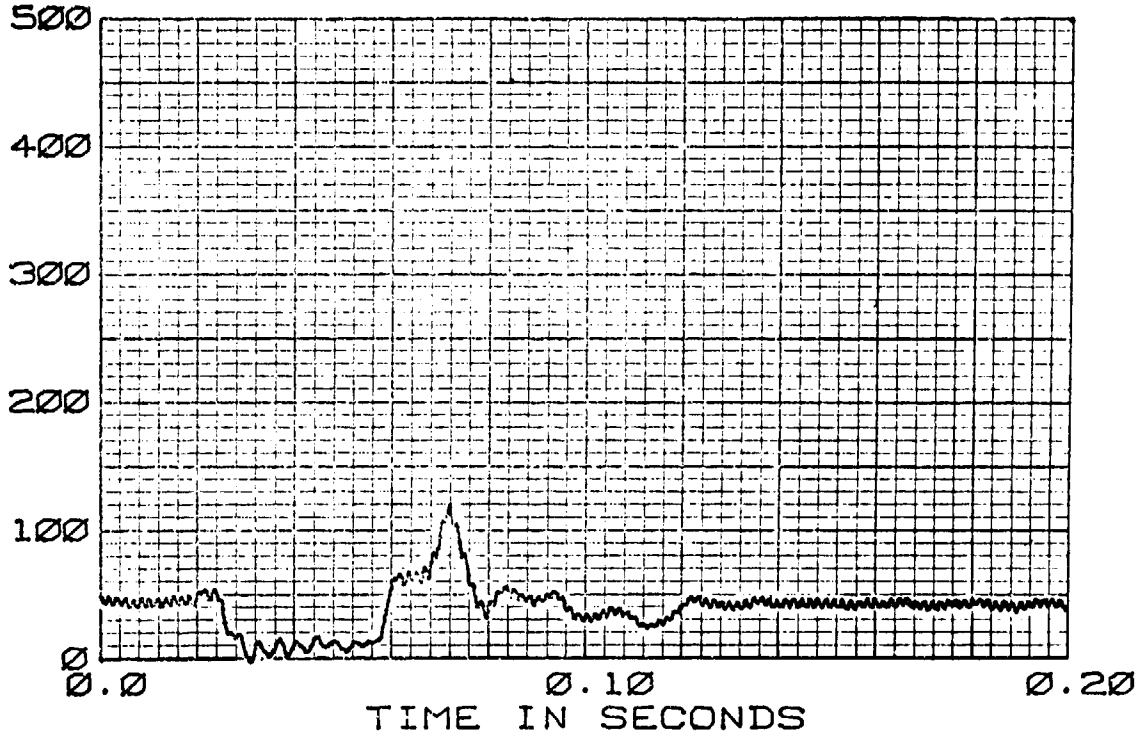

FIGURE 175. F-15 HYDRAULIC PUMP
65-03+PS TURN-ON TRANSIENT
77 CIS 130°F

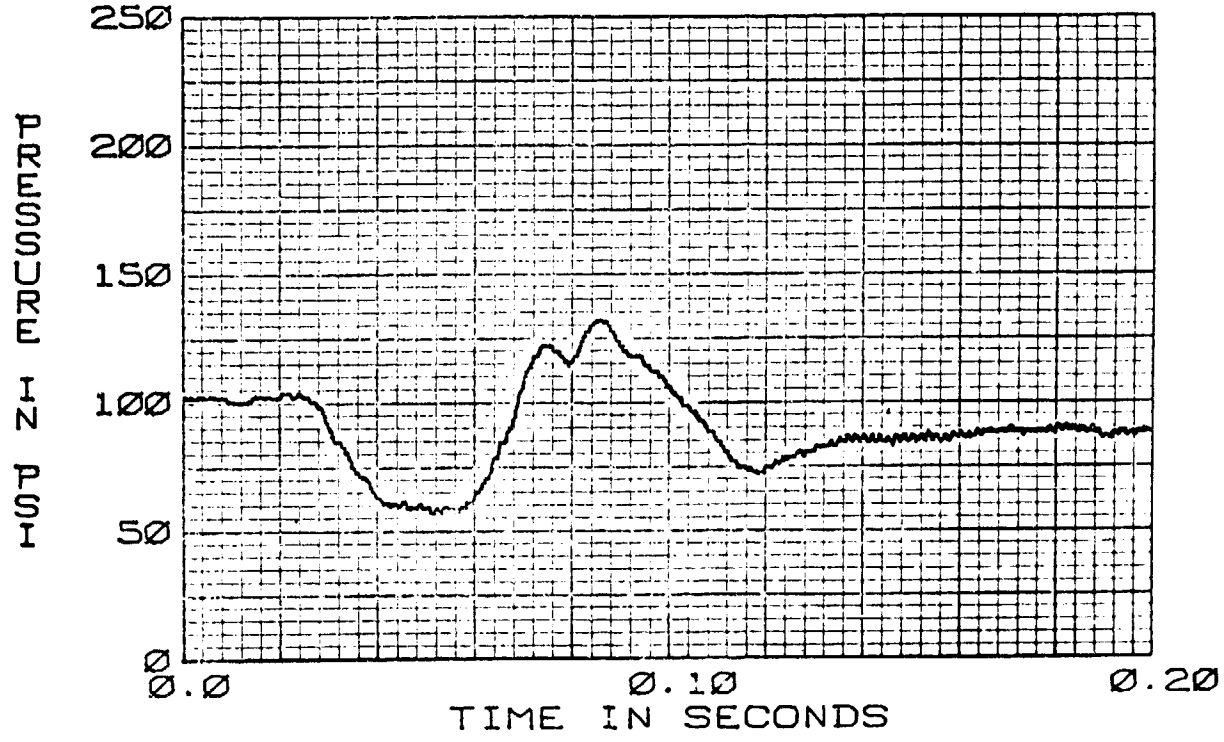

FIGURE 176. F-15 HYDRAULIC PUMP
65-03+PCD TURN-ON TRANSIENT
77 CIS 130°F

```
****DATA RUN NO. 65-03+PS AND +PC  F-15 PUMP****(FTPM17)

THE TRANSIENT RESPONSE IS FROM T=0.0  TO T=  .200 SECONDS AT TIME INTERVALS OF DELT= .00020
WITH OUTPUT POINTS PLOTTED AT INTERVALS OF  ,  .00200 SECONDS

FLUID DATA FOR  MIL-H-83282 AT  3000.0 PSIG, -  50.0 PSIG AND 130.0 DEG F  IN  10.0 DEG F STEPS
                VISCOSITY   - .200E-01      .153E-01IN**2/SEC
                DENSITY     - .790E-04      .781E-04(LB-SEC**2)/IN**4
                BULK MODULUS - .223E+06     .187E+06PSI
                VAPOUR PRESS.- .200E+01 AT  130.0 DEG F
 FIX-UP TAKEN AT LINE 18,VEL OF SOUND IN LINE   4 IS   15.4PER CENT IN ERROR
 FIX-UP TAKEN AT LINE 18,VEL OF SOUND IN LINE   6 IS   60.1PER CENT IN ERROR
 FIX-UP TAKEN AT LINE 18,VEL OF SOUND IN LINE   7 IS   58.6PER CENT IN ERROR
 FIX-UP TAKEN AT LINE 18,VEL OF SOUND IN LINE   8 IS   59.8PER CENT IN ERROR

LINE DATA
LINE NO.    LENGTH      INTERNAL DIA   WALL THICKNESS   MODULUS OF ELASTICITY   DELX       CHARACTERISTIC IMPEDANCE   VELOCITY OF SOUND
   1        13.0000       .9020          .0490            .300E+08            13.0000        6.1559                  49785.6131
   2        13.0000       .3190          .0280            .300E+08            13.0000       50.2548                  50844.4460
   3       382.7500       .8840          .0580            .300E+08            10.0724        6.4696                  50255.3193
   4         8.5000       .8840          .0580            .300E+08             8.5000        6.4696                  62500.0000
   5        30.5000       .4440          .0280            .300E+08            10.1667       25.5947                  50162.9463
   6         4.0000       .4440          .0280            .300E+08             4.0000       25.5987                  20000.0000
   7         4.1250       .9020          .0490            .300E+08             4.1250        6.1559                  20625.0000
   8         4.0000       .9020          .0490            .300E+08             4.0000        6.1559                  20000.0000
   9       192.0000       .9020          .0490            .300E+08            10.1053        6.1559                  49785.6131
 COMP#,  1 INTEGER DATA    1  91   0  -1   1  -0  -0  -0  -0  -0  -0  -0  -0  -0  -0  -0
 COMP#,  2 INTEGER DATA    2  51   4   1  -3  -2  -0  -0  -0  -0  -0  -0  -0  -0  -0  -0
REAL DATA CARD #  1  .2870E+04  .2000E+04  .1500E+00  .2500E+00  0.  .1600E-01  .6500E+00  .6500E+00
REAL DATA CARD #  2  .3070E+00  .4000E+03  .7000E+02  .1300E+03  .4700E+03  .2150E+03  .3500E-01  .2500E+02
REAL DATA CARD #  3  .3000E+01  .7500E+00 -.3000E+00  .2000E-02  .1000E-02  .3000E-02  .2000E-01  .2300E+03
REAL DATA CARD #  4  .5000E+01  .4000E+04  .3600E-01  .5000E-01  0.  .3500E-02  .1000E+01  .8000E+01
 COMP#,  3 INTEGER DATA    3  91   0   2   1  -0  -0  -0  -0  -0  -0  -0  -0  -0  -0  -0
 COMP#,  4 INTEGER DATA    4  11   0   3  -4  -5  -0  -0  -0  -0  -0  -0  -0  -0  -0  -0
 COMP#,  5 INTEGER DATA    5  21   3   4  -7  -0  -0  -0  -0  -0  -0  -0  -0   4  -0  -0
REAL DATA CARD #  1  .2200E-01  .6500E+00 -0.  -0.  -0.  -0.  -0.  -0.  -0.
REAL DATA CARD #  2  0.  .1500E-01  .2000E-01  .2000E+00 -0.  -0.  -0.  -0.  -0.
REAL DATA CARD #  3  0.  0.  .6160E+00  .6160E+00 -0.  -0.  -0.  -0.  -0.
 COMP#,  6 INTEGER DATA    6  41   1   5  -6  -0  -0  -0  -0  -0  -0  -0  -0  -0  -0  -0
REAL DATA CARD #  1  .2100E-01  .6500E+00 -0.  -0.  -0.  -0.  -0.  -0.  -0.
 COMP#,  7 INTEGER DATA    7  11   0   6   7  -8  -0  -0  -0  -0  -0  -0  -0  -0  -0  -0
 COMP#,  8 INTEGER DATA    8  41   1   8  -9  -0  -0  -0  -0  -0  -0  -0  -0  -0  -0  -0
REAL DATA CARD #  1  .5400E+00  .6500E+00 -0.  -0.  -0.  -0.  -0.  -0.  -0.
 COMP#,  9 INTEGER DATA    9  61   1   9  -0  -0  -0  -0  -0  -0  -0  -0  -0  -0  -0  -0
REAL DATA CARD #  1  .4000E+02 -0.  -0.  -0.  -0.  -0.  -0.  -0.
```

FIGURE 177. HYTRAN INPUT DATA FOR PUMP TURN-ON TRANSIENT

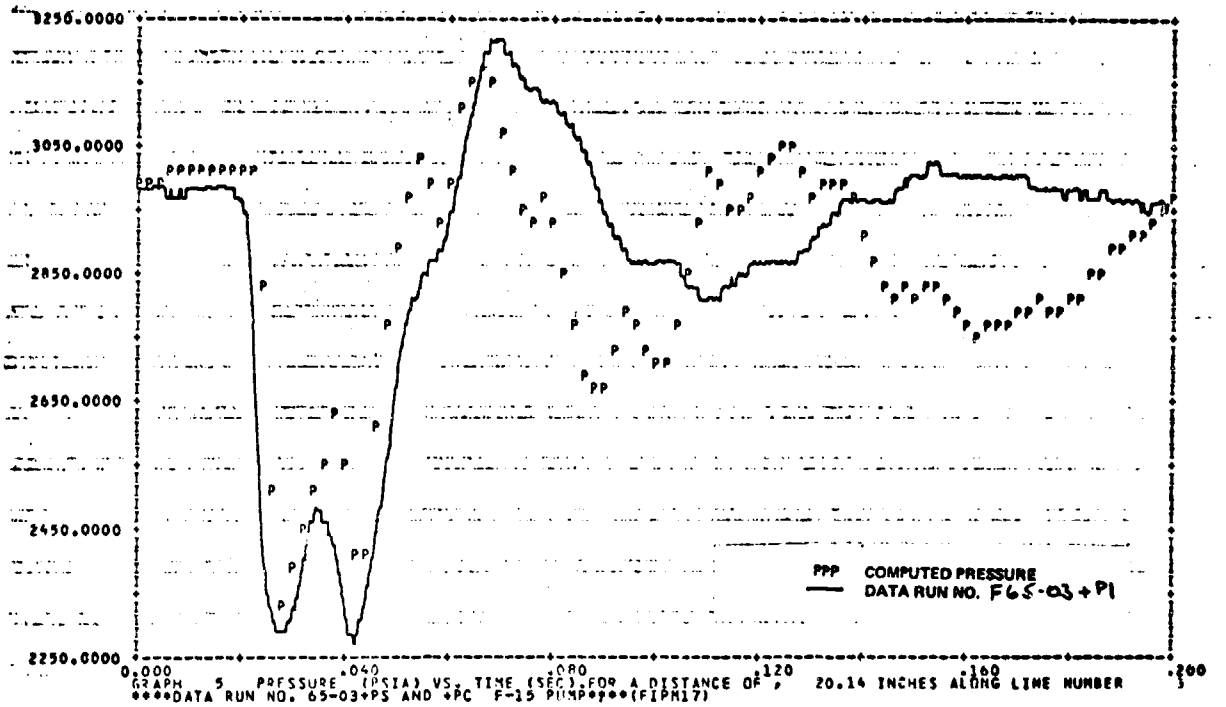

FIGURE 178. F65-03+P1 TURN-ON TRANSIENT

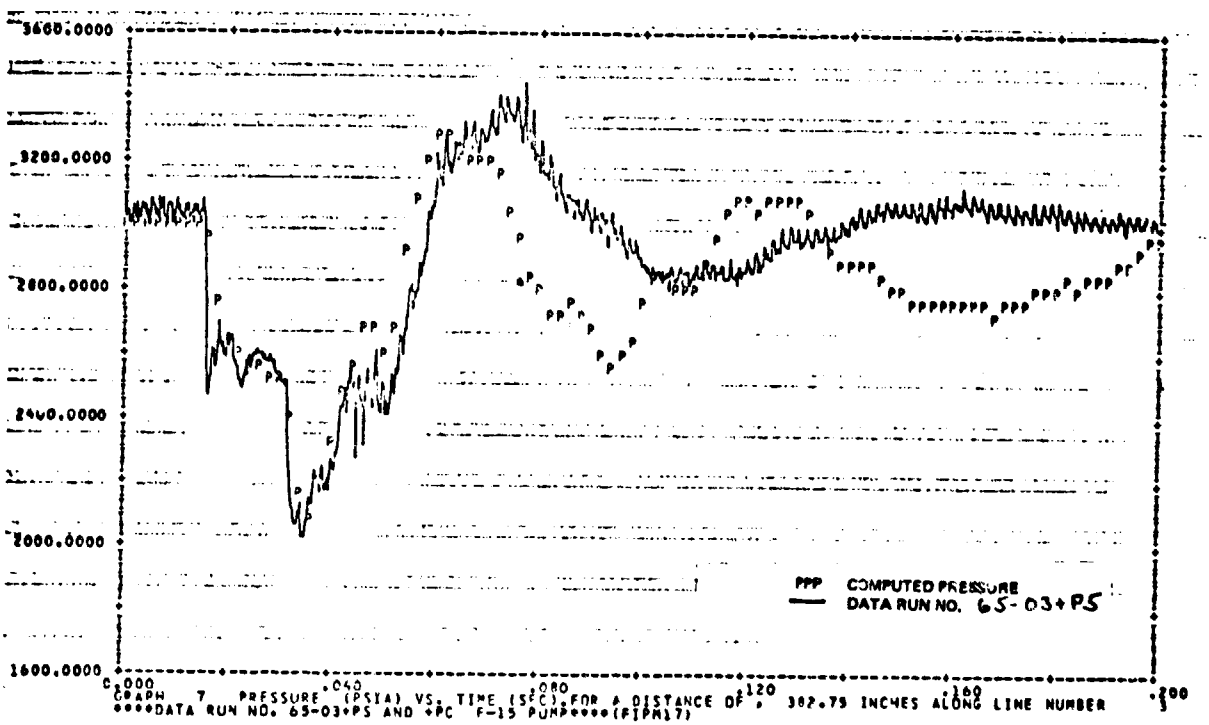

FIGURE 179. 65-03+P5 TURN-ON TRANSIENT

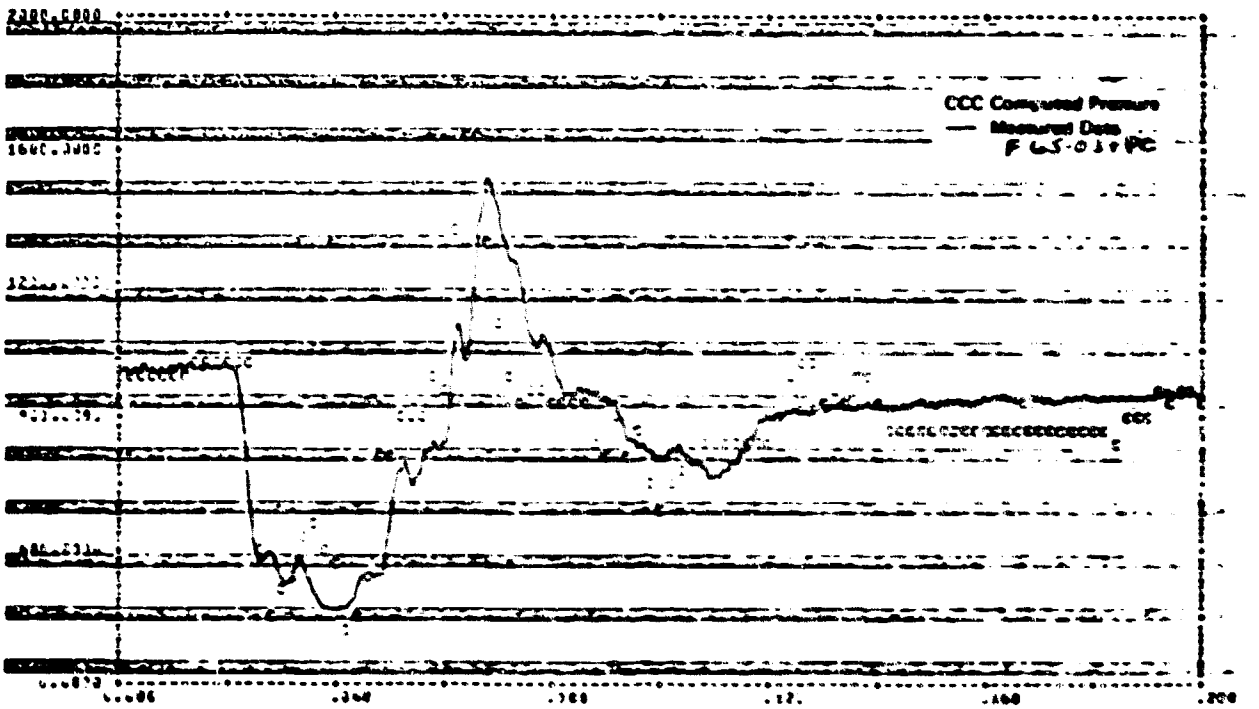

ACTUATOR PRESSURE (PSIA) vs TIME (SEC)

FIGURE 180. F65-03+PC TURN-ON TRANSIENT

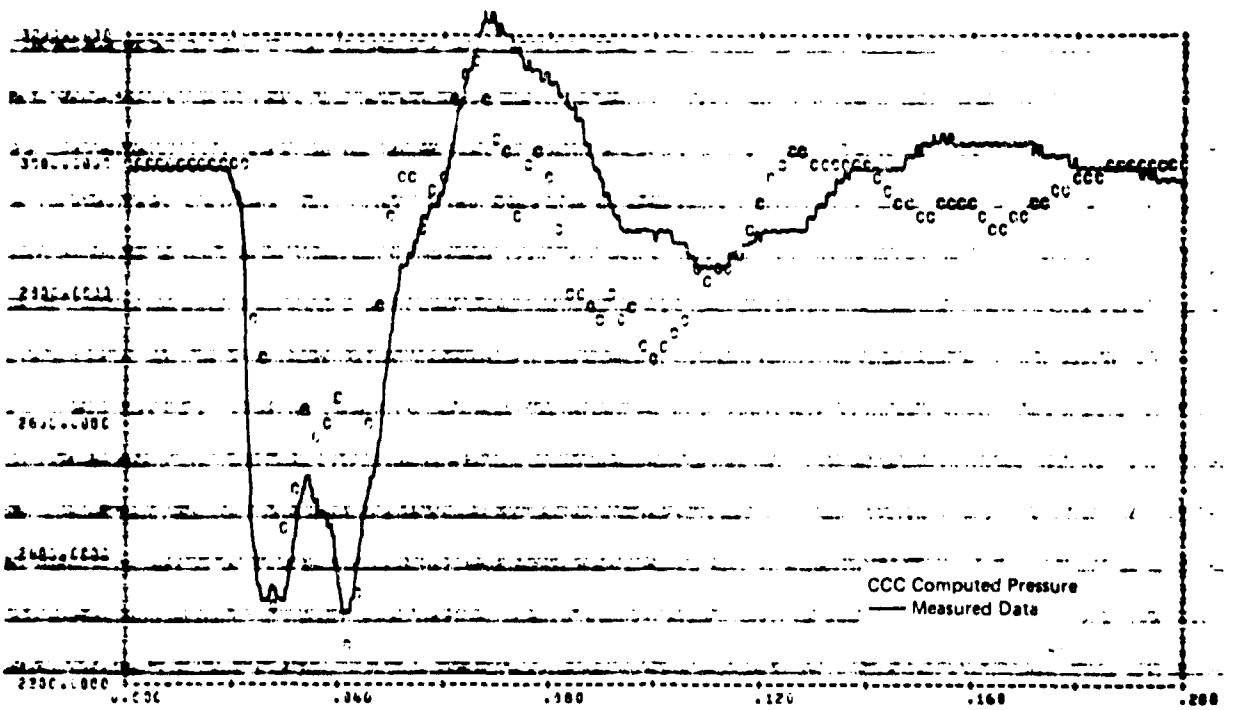

PUMP OUTLET PRESSURE (PSIA) vs TIME (SEC)

FIGURE 181. F65-03+PP TURN-ON TRANSIENT

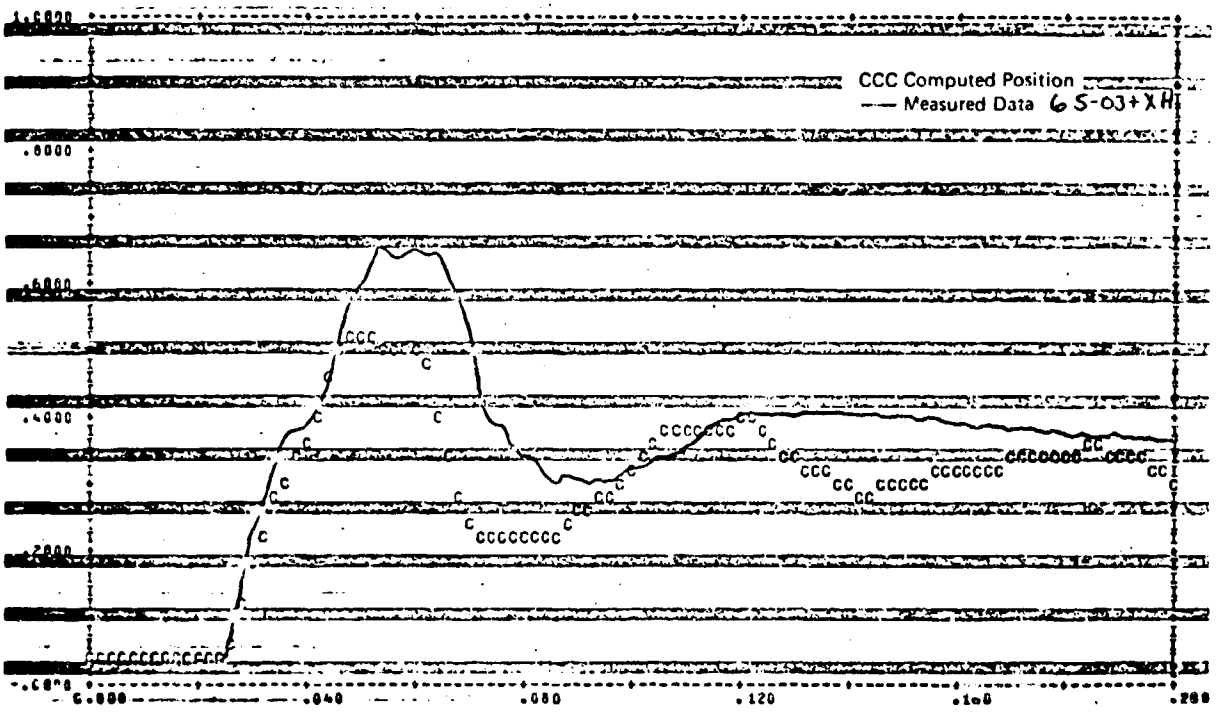

HANGAR POSITION (IN.) vs TIME (SEC)

FIGURE 182. 65-03+XH TURN-ON TRANSIENT

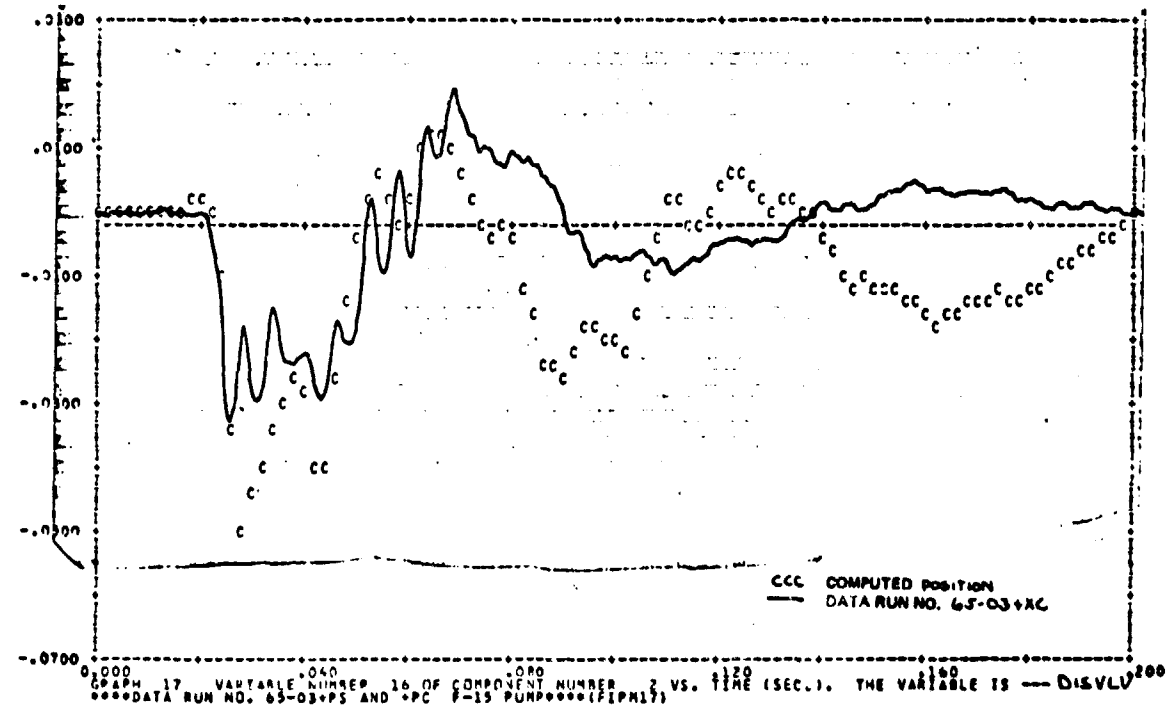

FIGURE 183. 65-03+XC TURN-ON TRANSIENT

e. Conclusions - Extensive testing has been completed on the F-15 instrumented pump. Test conditions were established to try and reproduce many of the operating conditions the pump would encounter during its normal life. Actual pump operating time was approximately 150 hrs during the test period. Obviously much more data was recorded that could possibly be verified with the pump model. The extensive nature of the contract does not allow for a more thorough analysis of the pump model at this time. A disapportionate number of manhours in relation to other component models has already been spent on pump verification. This was because of the importance of the pump in its relation to the remainder of the system. Further detailed analysis will not take place under this current phase of the contract.

For the initial pump response, the PUMP51 subroutine adequately predicts the measured data values. Since the initial transient is usually the most severe, the results do reflect actual operating characteristics. However, subsequent pump/system interaction is not accurately computed. The calculations do reflect the PUMP51 subroutine stability. If time where available for a more detailed study of the test data, the pump subroutine could probably be improved.

The errors in the subroutine may be attributable to a number of factors. Lack of cavitation effects caused by improper filling of the pistons; the effect of hanger angle and pump RPM; the forces on the hanger contributed by the pistons due to bulk modulus effects at different pressures and temperatures; friction effects on the actuator and valve; are some of the factors not included in the pump model. Other sources of error exist in the model itself. Not adequately defining the flow forces on the valve, assuming linear leakage characteristics, the treatment of hanger inertia could all introduce small errors into the simulation.

The data taken in the lab does contain much of the information needed to produce a better pump model. However, it would be desireable to further modify the F-15 instrumented pump by adding a case drain pressure transducer, the lack of which has thwarted our verification efforts. A few tests would then need to be rerun.

4. FILTER MODEL VERIFICATION

In this section the test results obtained in the laboratory on a hydraulic oil filter are compared to the HYTRAN computer program filter model (FILT81). The oil filter used in the testing is shown in Figure 184. The filter specifications are in Figure 185. All testing on the filter was performed on a 1/2 inch system with MIL-H-5606B hydraulic fluid. The filter subroutine (FILT81) is a model of an inline, non-bypass filter with a standard cleanable element and no moving parts.

The filter test series was run on two different system configurations. Table 8 contains a listing of all the test runs.

To study the pressure effects of a filter in a hydraulic system, it was necessary to locate the filter close to the fast valve. This is an area of high pressure transients when the valve opens or closes. The system configuration is shown in Figure 186. The long length of tubing in the system was used to increase the reflection time of the pressure and flow transients.

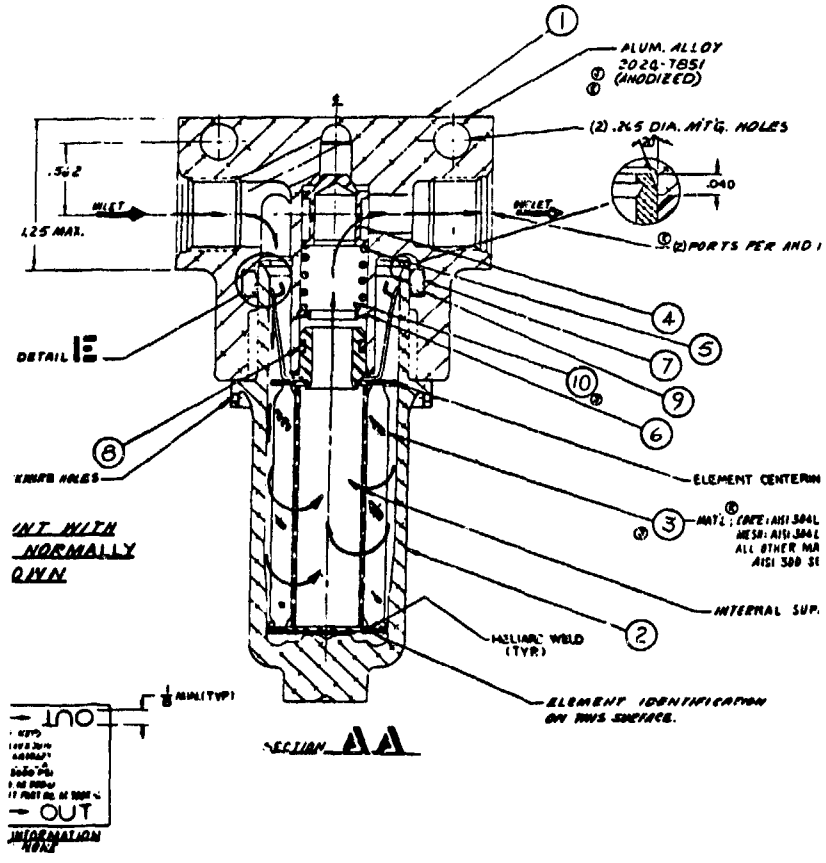

FIGURE 184. AC-900-61 OIL FILTER

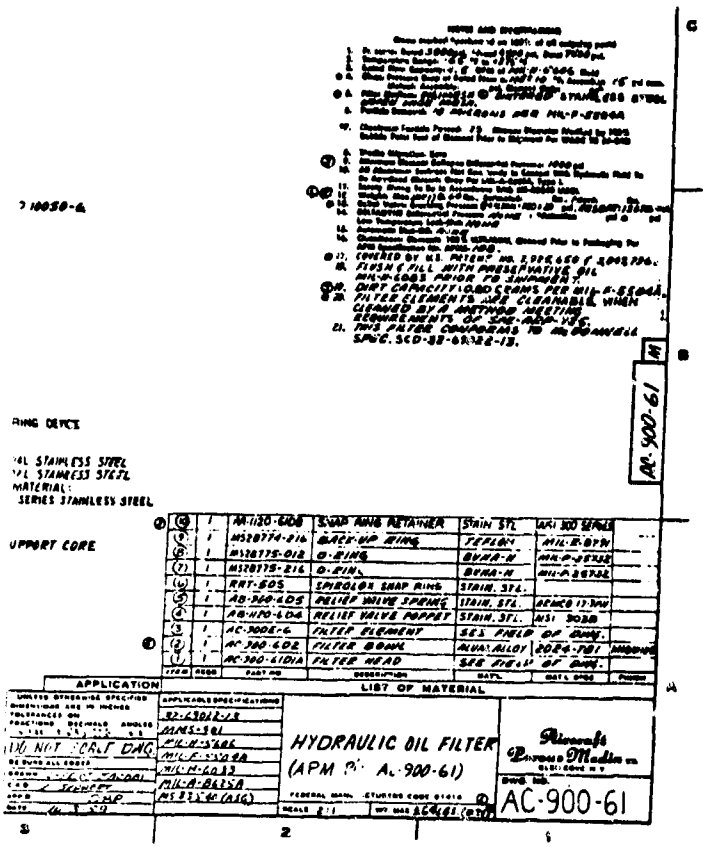

FIGURE 185. FILTER SPECIFICATIONS

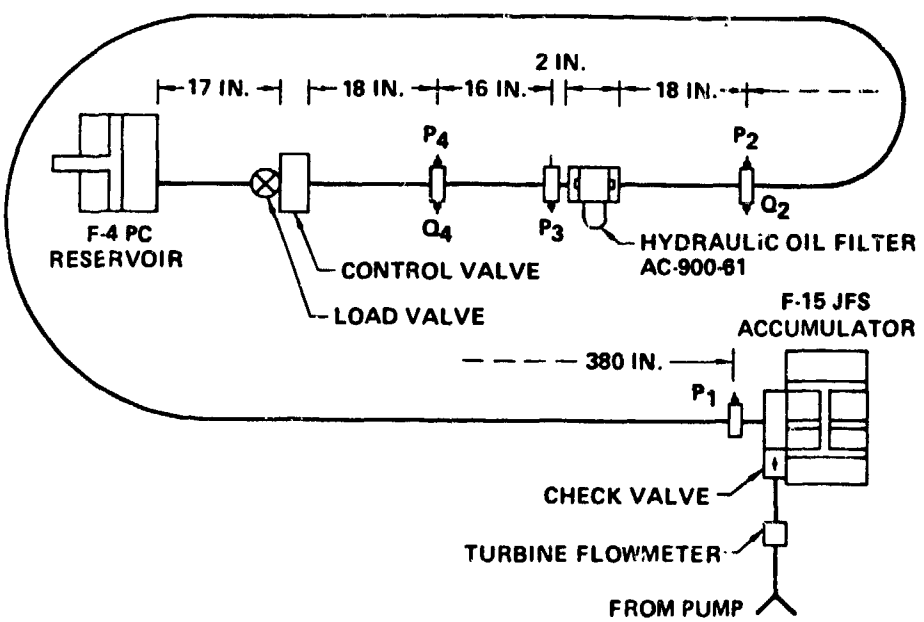

FIGURE 186. DOWNSTREAM TRANSIENT TEST CONFIGURATION FOR AC-900-61 OIL FILTER

Table 8. TEST CONDITIONS FOR FILTER AC-900-61

TEST ELEMENT	RUN #	FLOW CONDITION	FLOW RATE (CIS)	TEMP DEG F
		Filter at upstream position		
Filter Without Element	50B01-xx	Turn-Off	38.5	125
"	50B01+xx	Turn-On	38.5	125
"	50B02-xx	Turn-Off	11.55	125
"	50B02+xx	Turn-On	11.55	125
Filter With Element	51C01-xx	Turn-Off	38.5	125
"	51C01+xx	Turn-On	38.5	125
"	51B02-xx	Turn-Off	11.55	125
"	51B02+xx	Turn-On	11.55	125
		Filter at Downstream Position		
Filter Without Element	50A01-xx	Turn-Off	38.5	125
"	50A01+xx	Turn-On	38.5	125
"	50A02-xx	Turn-Off	11.55	125
"	50A02+xx	Turn-On	11.55	125
Filter with Element	51A01-xx	Turn-Off	38.5	125
"	51A01+xx	Turn-On	38.5	125
"	51A02-xx	Turn-Off	11.55	125
"	51A02+xx	Turn-On	11.55	125

The following parameters were recorded in the laboratory for the test runs. P_1, P_2, Q_2, P_3, P_4, Q_4 and valve position. P_1, P_2, P_4 and Q_4 were recorded on analog tape and played back later.

The filter was then placed near the upstream end of the system to observe the flow effects since the flow amplitudes are greater near the accumulator. The system configuration is shown in Figure 187. The following parameters were recorded for the test runs: P_1, P_2, Q_2, P_3, Q_3, P_4 and valve position. P_1, P_3, P_4 and Q_3 were recorded directly on cassette tape.

a. Computer Simulation With Filter Test Data - A turn-on transient at 125°F and 11.55 CIS flow was simulated with the HYTRAN program. The input data used is shown in Figure 188. The system input data is in Figure 189.

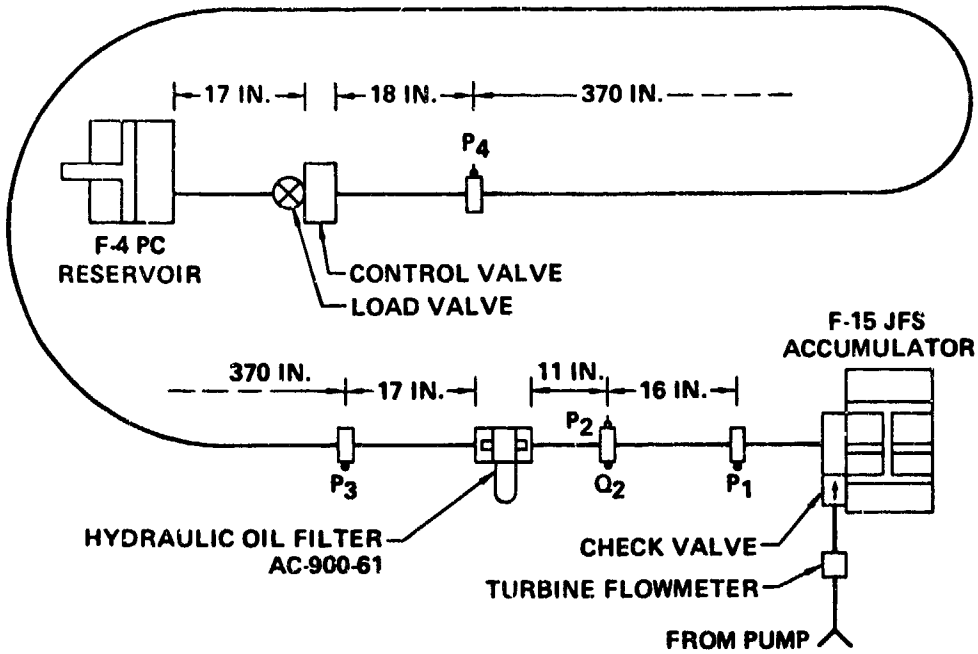

FIGURE 187. UPSTREAM TRANSIENT TEST CONFIGURATION FOR AC-900-61 OIL FILTER

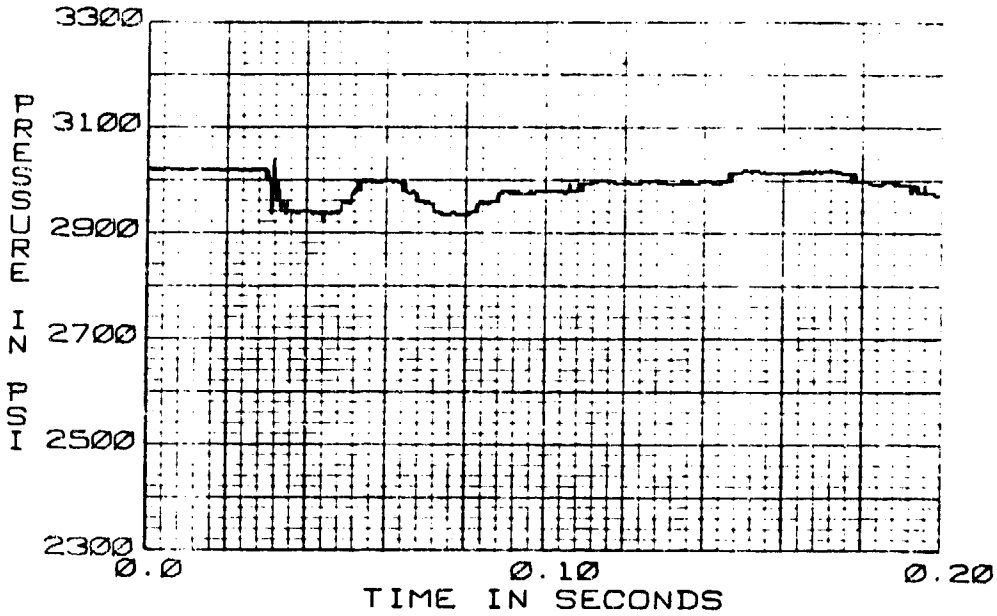

FIGURE 188. AC-900-61D1 FILTER HOUSING (NO ELEMENT) 50B02+P1 TURN-ON TRANSIENT 11.55 CIS 125°F

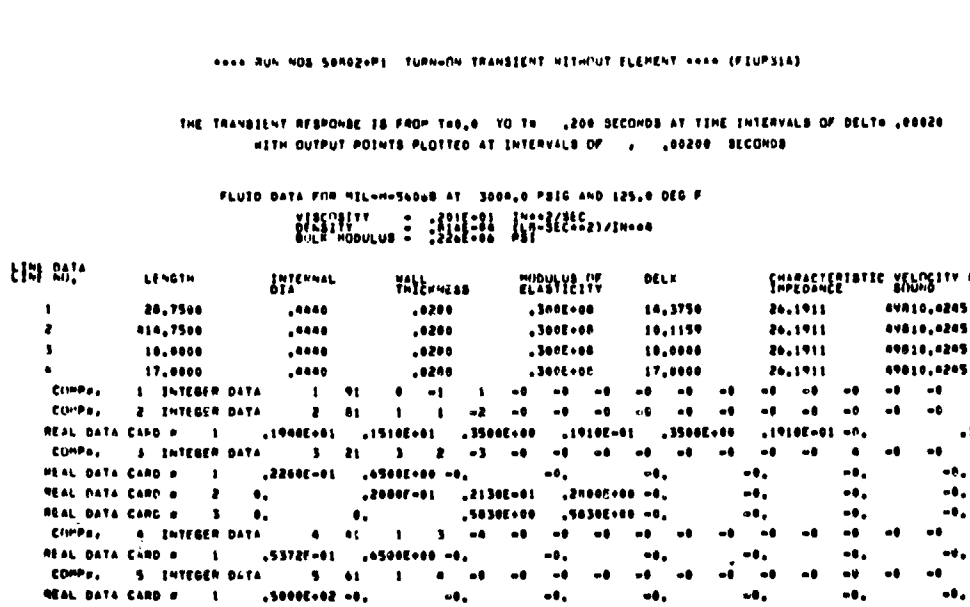

FIGURE 189. RUN 50B02 HYTRAN INPUT DATA FOR FILTER MODEL VERIFICATION

For this low flow condition, a restrictor was inserted 10" downstream of the control valve. This was done to simulate the annular volumes in the control valve which totaled about 4 cubic inches. At this low flow condition, the valve passages require a short time to completely fill on a turn-on transient. This charging effect can be seen on the data taken in the lab. Therefore, it was necessary for the computer simulation to completely define the volumes in the control valve as an extra line length to obtain accurate results.

The filter was located in the maximum flow region of the system to study the flow effects on the component (see Figure 187). An interesting result of the test, however, shows what a good frequency filter the hydraulic filter is. The data in Figure 190 was taken 11 inches upstream of the filter. High frequency pressure signals between 500 and 1000 Hz are superimposed on the pressure trace. Figure 191 is the pressure data 17 inches downstream of the filter. The high frequency content of the P2 trace has been filtered out as the pressure signal passed through the filter component.

The computer output data shows good correlation to the actual pressure values in Figures 190, 191, and 192. In Figure 192, the data signal contains a sharp downward spike on the first pressure dip. This is due to the filling of annular passages in the control valve.

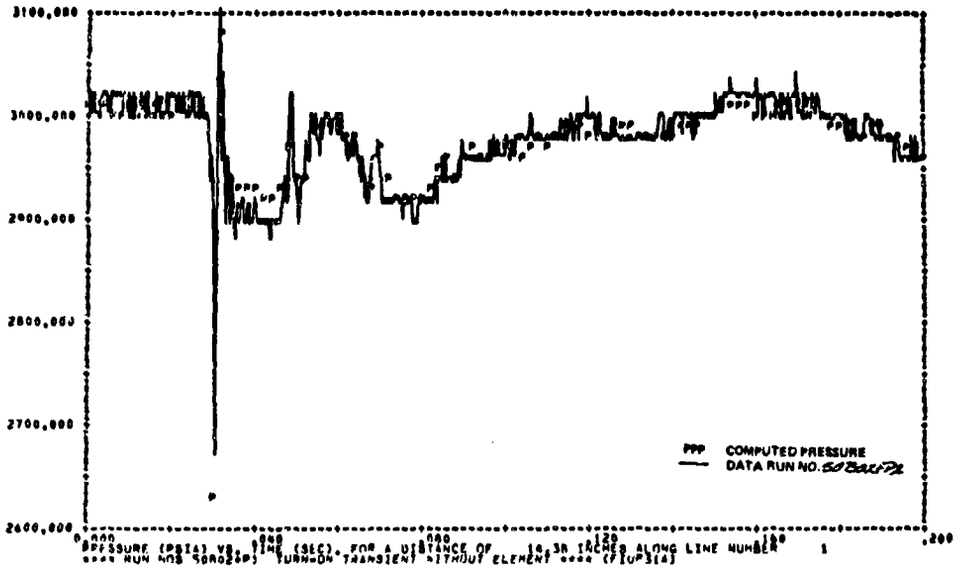

FIGURE 190. 50B02+P2 TURN-ON TRANSIENT

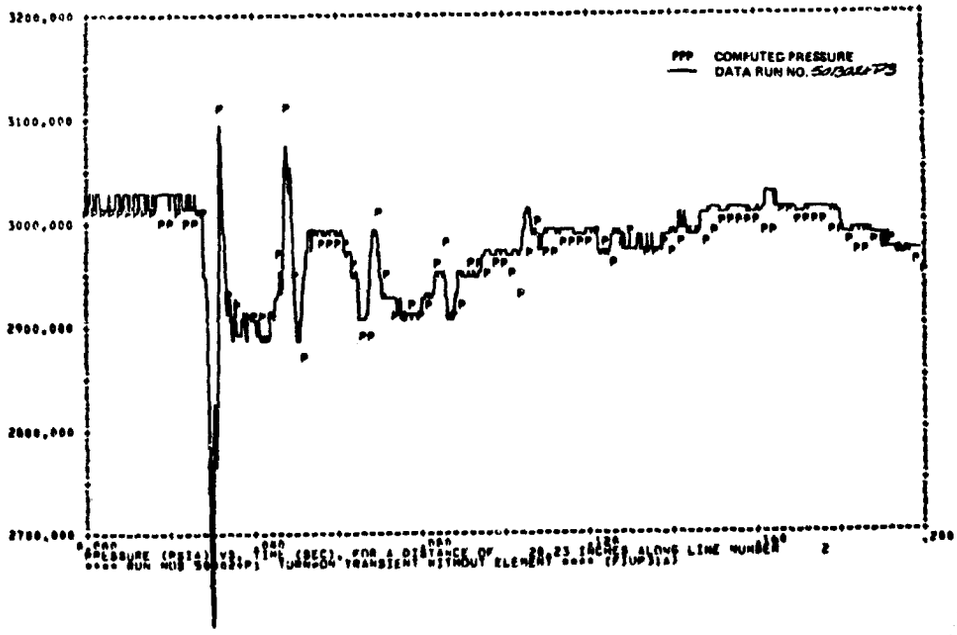

FIGURE 191. 50B02+P3 TURN-ON TRANSIENT

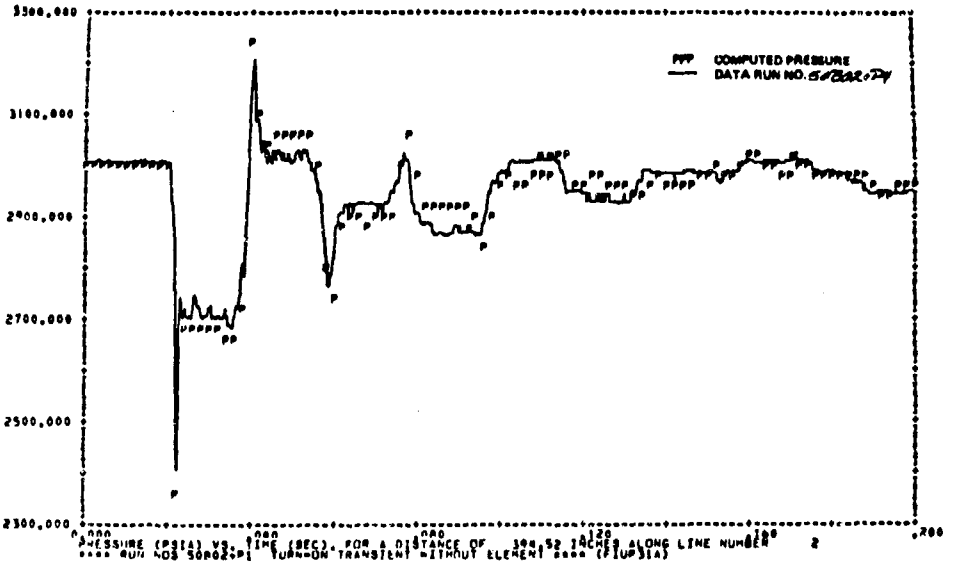

FIGURE 192. 50B02+P4 TURN-ON TRANSIENT

The flow plot of Figure 193 again illustrates the difference in the computed and measured flowrates. The computed flow is an average flow value across the entire velocity profile in the line. The measured flowrate of the hot film anenometers is a localized segmented flow out of a small region of the velocity profile. The data run in Figure 193 shows how the flow on turn-on is less than the computed predicted results. As the velocity profile developes in the line and the localized flow approaches the average flow, the computed values show a better correlation to the data.

A turn-off transient at 125°F and 11.55 CIS flow was simulated with the HYTRAN program using the measured data of Figure 194 and computer input data in Figures 195. This run contained a hydraulic oil filter with a filter element.

Figure 196 is an overplot of the computed pressure data 20 inches downstream of the filter with the pressure data measured 17 inches downstream of the filter. Again, the program indicates reasonable correlation to the data run. On the actual data plot note, the precursor downward pressure spike prior to the first pressure peak due to the mechanical stress signal arriving via the walls of the tube before the pressure signal.

Figures 197 and 198 are the flow plots for this simulation. The actual steady state flow measured appears to be about 2 CIS lower than that predicted by the program.

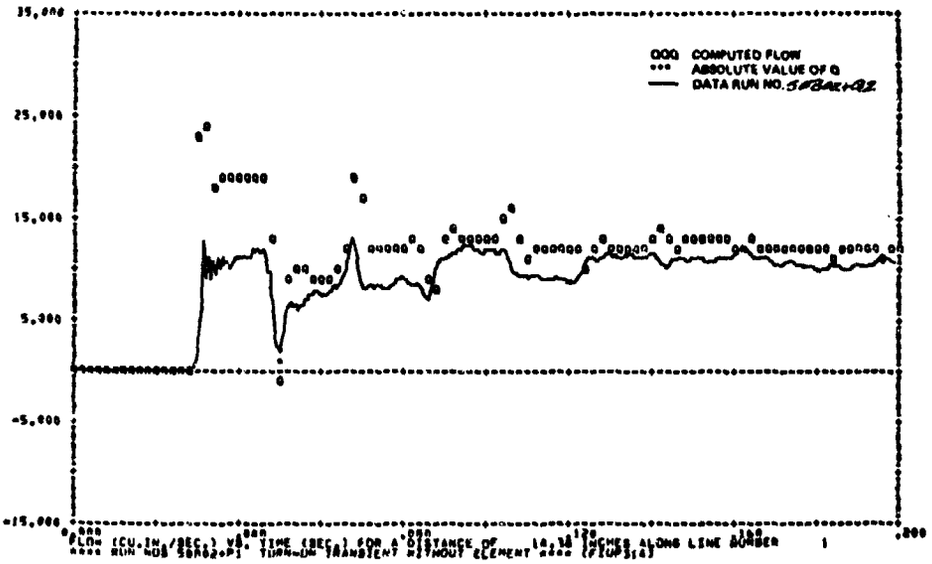

FIGURE 193. 50B02+Q2 TURN-ON TRANSIENT

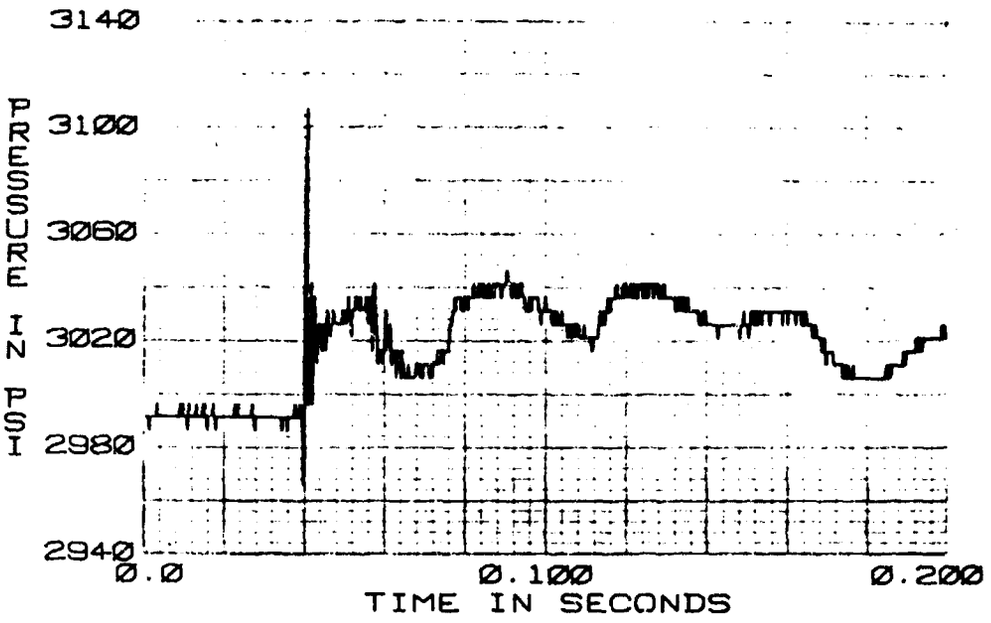

FIGURE 194. AC-900-61D1 FILTER WITH ELEMENT 51B02-P1 TURN-OFF TRANSIENT
11.55 CIS 125°F

```
**** RUN 51B02-P1  TURN-OFF TRANSIENT WITH ELEMENT **** (FIUP17)

THE TRANSIENT RESPONSE IS FROM T=0.0  TO T=  .200 SECONDS AT TIME INTERVALS OF DELT= .00020
        WITH OUTPUT POINTS PLOTTED AT INTERVALS OF  .00200  SECONDS


FLUID DATA FOR  OIL=N=5606  AT  3000.0 PSIG, =   90.0 PSIG AND 125.0 DEG F  IN   10.0 DEG F STEPS
                VISCOSITY    =  .201E-01        .158E-01LN**2/SEC
                DENSITY      =  .814E-04        .805E-04(LM-SEC**2)/IN**4
                BULK MODULUS =  .226E+06        .191E+06PSI
                VAPOUR PRESS.=  .200E+01 AT  125.0 DEG F

LINE DATA
LINE NO.    LENGTH          INTERNAL DIA    WALL THICKNESS   MODULUS OF ELASTICITY   DELX          CHARACTERISTIC IMPEDANCE   VELOCITY OF SOUND
   1        20.7500          .0440           .0240            .300E+08               10.3750       20.1911                    49810.0245
   2        814.7500         .0440           .0240            .300E+08               10.1159       20.1911                    49810.0245
   3        17.0000          .0440           .0240            .300E+08               17.0000       20.1911                    49810.0245
  COMPR,  1  INTEGER DATA      1  91   0  -1   1  -0  -0  -0  -0  -0  -0  -0  -0  -0  -0  -0  -0  -0
  COMPR,  2  INTEGER DATA      2  81   1   1  -2  -0  -0  -0  -0  -0  -0  -0  -0  -0  -0  -0  -0  -0
 REAL DATA CARD #    1     .1890E+01  .1894E+01  .3500E+08  .1910E-01  .3500E+08  .1910E-01 -0.          .1020E+01
  COMPR,  3  INTEGER DATA      3  21   3   2  -3  -0  -0  -0  -0  -0  -0  -0  -0  -0  -0  -0  -0  -0
 REAL DATA CARD #    1     .2200E+01  .6500E+00 -0.        -0.        -0.        -0.        -0.        -0.
 REAL DATA CARD #    2     0.         .3200E+01  .3250E+01  .2000E+00 -0.        -0.        -0.        -0.
 REAL DATA CARD #    3     .1010E+00  .1010E+00  0.        0.        -0.        -0.        -0.        -0.
  COMPR,  4  INTEGER DATA      4  81   1   3  -0  -0  -0  -0  -0  -0  -0  -0  -0  -0  -0  -0  -0  -0
 REAL DATA CARD #    1     .5000E+02 -0.        -0.        -0.        -0.        -0.        -0.        -0.
```

FIGURE 195. RUN 51B02 HYTRAN INPUT DATA FOR FILTER MODEL VERIFICATION

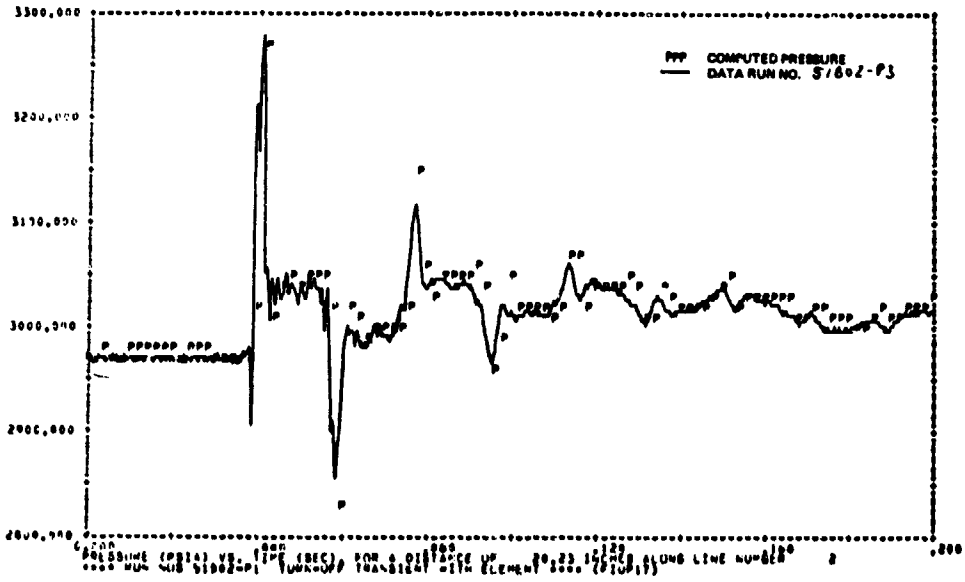

FIGURE 196. 51B02-P3 TURN-OFF TRANSIENT

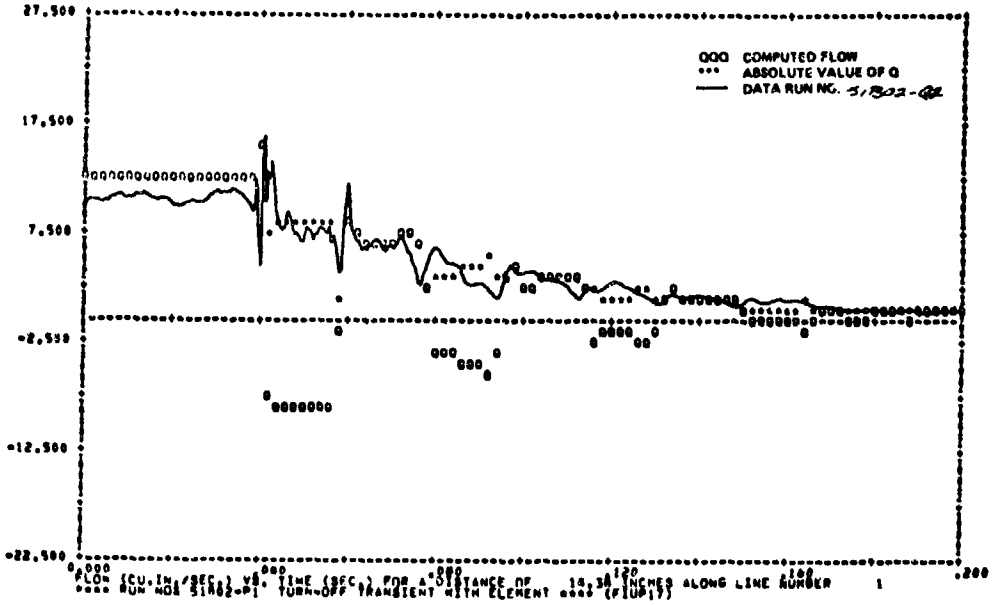

FIGURE 197. 51B02-Q2 TURN-OFF TRANSIENT

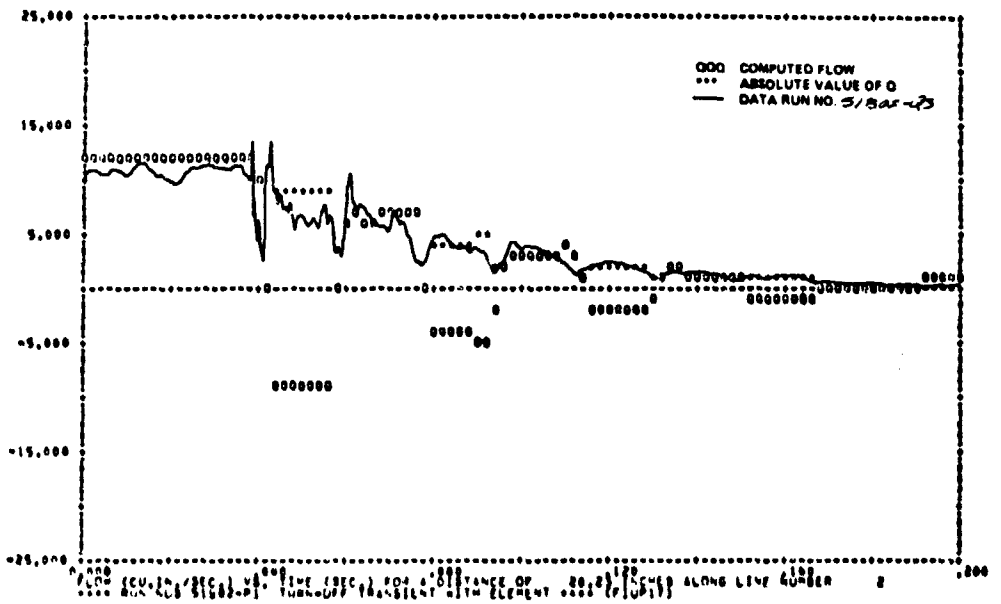

FIGURE 198. 51B02-Q3 TURN-OFF TRANSIENT

Figure 199 is the input boundary pressure for the data of Figure 200. The filter is located in the downstream location in Figure 186. Overplots of the computer runs were made in Figures 201, 202, 203 and 204. For the recorded data in Figure 203, note the dip prior to the first pressure peak. This precursor is due to the arrival of the mechanical line vibration before the pressure wave. The plots shown in Figures 201 and 202 are the pressure traces up and downstream of the filter component. There is a slight time delay in the pressure signal as it passes through the filter bowl. Also note some amplitude damping for this turn-off transient on the upstream pressure trace (Figure 201). Both pressure and flow (Figure 204) computer printouts show good correlation to the measured data.

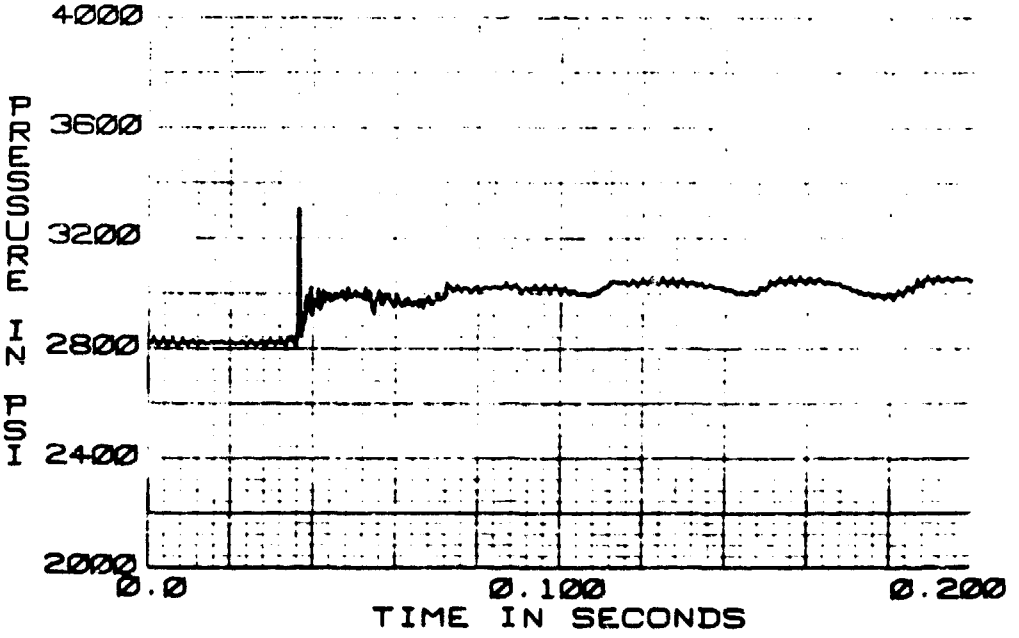

FIGURE 199. AC-900-61D1 FILTER HOUSING (NO ELEMENT) 50A01-P1 TURN-OFF TRANSIENT 38.5 CIS 125°F

```
**** RUN NO 50A01-P1 TURN-OFF TRANSIENT WITHOUT ELEMENT **** (FIDN27)

THE TRANSIENT RESPONSE IS FROM T=0.0  TO T=   .200 SECONDS AT TIME INTERVALS OF DELT= .0002
     WITH OUTPUT POINTS PLOTTED AT INTERVALS OF   ,   .00200  SECONDS

FLUID DATA FOR MIL-H-5606B AT  3000.0 PSIG AND 125.0 DEG F
          VISCOSITY     =  .2015-01  IN**2/SEC
          DENSITY       =  .8146-04  (LB-SEC**2)/IN**4
          BULK MODULUS  =  .226E+06  PSI
```

LINE DATA LINE NO.	LENGTH	INTERNAL DIA	WALL THICKNESS	MODULUS OF ELASTICITY	DELX	CHARACTERISTIC IMPEDANCE	VELOCITY OF SOUND
1	405.5333	.4440	.0280	.300E+08	10.1375	26.1911	49810.4245
2	32.6200	.4440	.0280	.300E+08	10.8733	26.1911	49810.4245
3	17.0300	.4440	.0280	.300E+08	17.0000	26.1911	49810.4245

```
 COMP4,   1  INTEGER DATA    1  91   0  -1   1  -0  -0  -0  -0  -0  -0  -0  -0  -0  -0  -0
 COMP4,   2  INTEGER DATA    2  81   1   1  -2  -0  -0  -0  -0  -0  -0  -0  -0  -0  -0  -0
REAL DATA CARD 4    1   .1940E+01   .1510E+01   .3500E+00   .1910E-01   .3500E+00   .1910E-01 -0.         .1000E-03
 COMP4,   3  INTEGER DATA    3  21   3   2  -3  -0  -0  -0  -0  -0  -0  -0  -0   4  -0  -0
REAL DATA CARD 4    1   .2200E-01   .6500E+00 -0.        -0.         -0.         -0.         -0.         -0.
REAL DATA CARD 4    2   0.          .2700E-01   .2750E-01   .2000E+00 -0.         -0.         -0.         -0.
REAL DATA CARD 4    3   .3360E+00   .3360E+00  0.          0.         -0.         -0.         -0.         -0.
 COMP4,   4  INTEGER DATA    4  61   1   3  -0  -0  -0  -0  -0  -0  -0  -0  -0  -0  -0  -0
REAL DATA CARD 4    1   .5000E+02 -0.         -0.         -0.         -0.         -0.         -0.         -0.
```

FIGURE 200. RUN 50A01 HYTRAN INPUT DATA FOR FILTER MODEL VERIFICATION

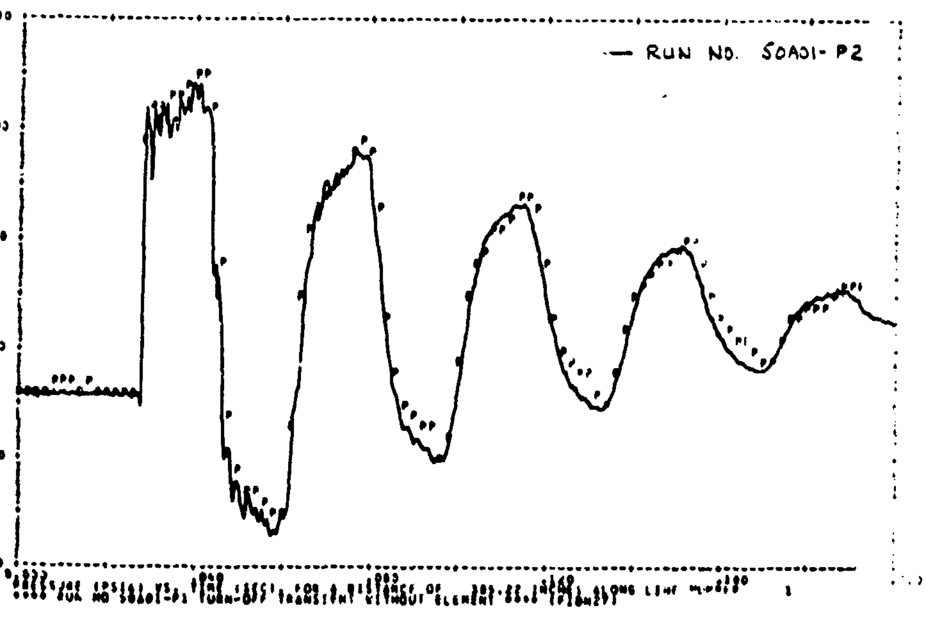

FIGURE 201. 50A01-P2 TURN-OFF TRANSIENT

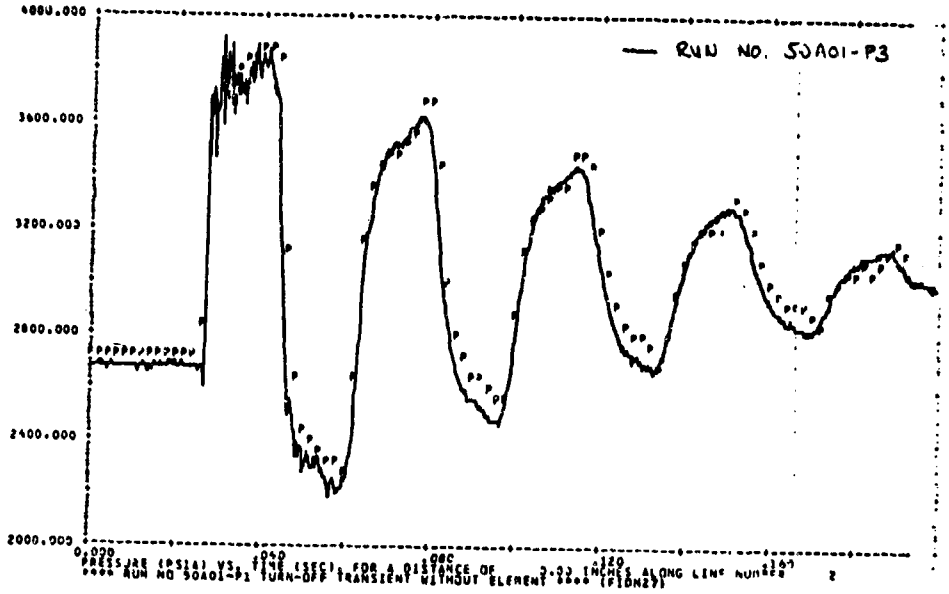

FIGURE 202. 50A01-P3 TURN-OFF TRANSIENT

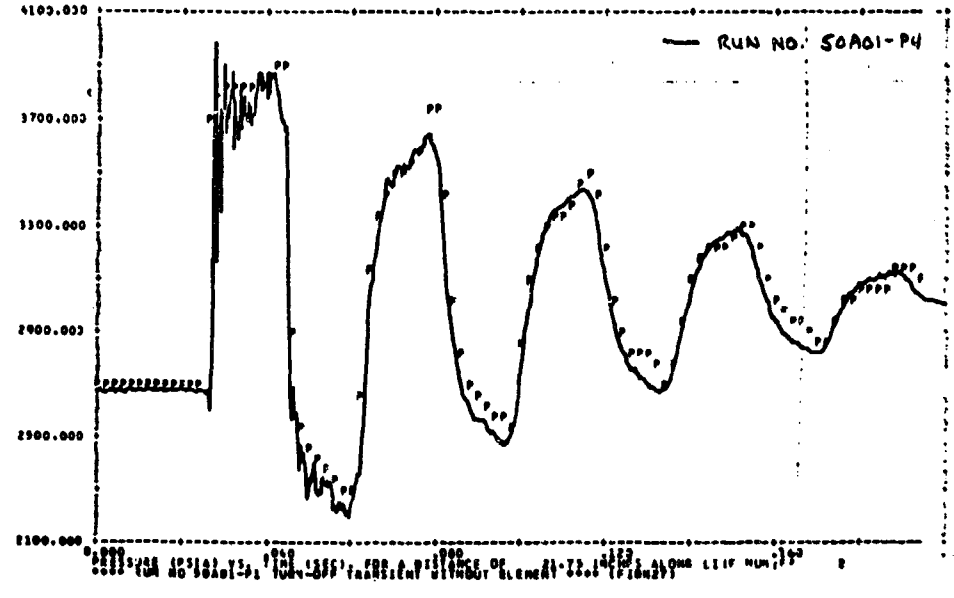

FIGURE 203. 50A01-P4 TURN-OFF TRANSIENT

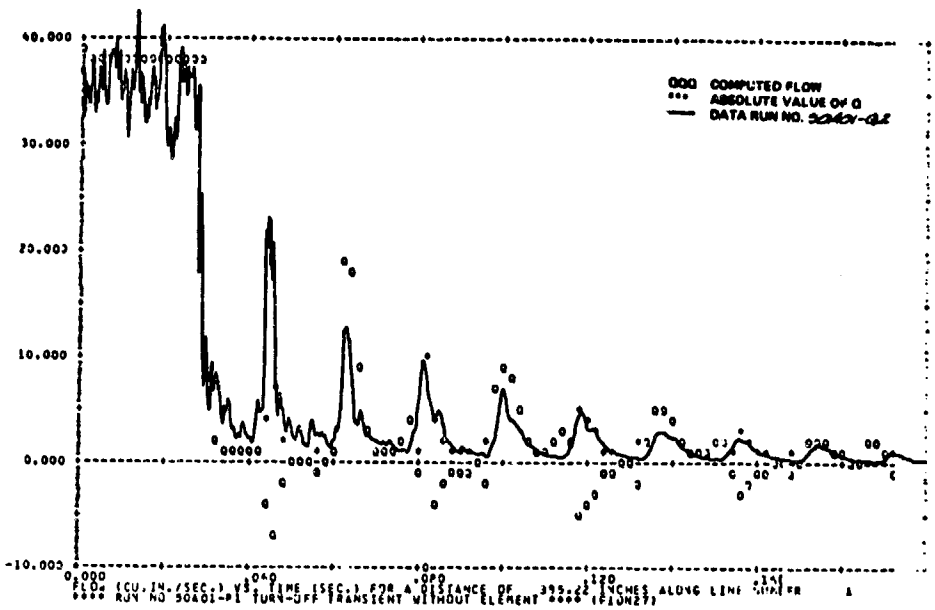

FIGURE 204. 50A01-Q2 TURN-OFF TRANSIENT

The next computer simulation used 51A01-P1 data in Figure 205 taken in the lab at 125°F and 38.5 CIS for a turn-off transient. Input with the P1 data was the input system configuration and test conditions shown in Figure 206.

The plots in Figure 207 and 208 are up and downstream pressures on either side of the oil filter. All the overplots of pressure in Figures 207, 208 and 209 show good correlation with the computer predicted results. From the pressure plots the actual plotting is off by a character making the simulation appear to be in error in the predicted damping frequency.

The computed flow values in Figure 210 match well the anemometer test measurements. The computer program predicted correctly the first flow reversal magnitude and also some of the subsequent flow magnitudes.

b. Observations - The filter component was located near the fast closing control valve in Figure 186 to study the filter's volumetric effects on the system during turn-on and turn-off transients. An interesting result obtained from the lab data showed the filter with an element, attenuated the pressure wave less than a filter without an element for turn-off transients. This can be graphically shown by overlaying Figures 201 and 207 (without element).

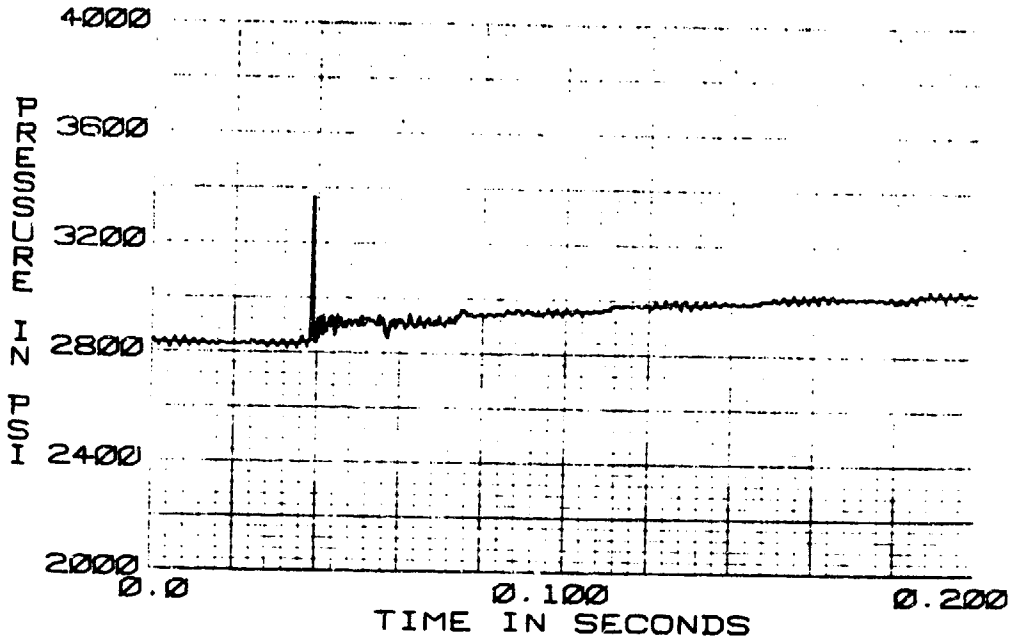

FIGURE 205. AC-900-61D1 FILTER WITH ELEMENT 51A01-P1 TURN-OFF TRANSIENT 38.5 CIS 125°F

**** FOR THIS 51A01-P1 TURN-OFF TRANSIENT WITH ELEMENT **** (P1IN.19)

THE TRANSIENT RESPONSE IS FROM T=0.0 TO T= .200 SECONDS AT TIME INTERVALS OF DELT= .00020
WITH OUTPUT POINTS PLOTTED AT INTERVALS OF . .00200 SECONDS

FLUID DATA FOR MIL-H-5606 AT 3000.0 PSIG, 50.0 PSIG AND 125.0 DEG F IN 10.0 DEG F STEPS

VISCOSITY	= .201E-01	.154E-01IN**2/SEC
DENSITY	= .81QE-04	.805E-04(LB-SEC**2)/IN**4
BULK MODULUS	= .226E+06	.191E+06PSI
VAPOUR PRESS.	= .200E+01 AT	125.0 DEG F

LINE NO.	DATA	LENGTH	INTERNAL DIA	WALL THICKNESS	MODULUS OF ELASTICITY	DELX	CHARACTERISTIC IMPEDANCE	VELOCITY OF SOUND
1		15.5400	.0400	.0240	.30E+08	10.1375	26.1911	49810.4265
2		34.6200	.0400	.0240	.30E+08	11.5400	26.1911	49810.4265
3		17.2800	.0400	.0240	.30E+08	17.0800	26.1911	49810.4265
COMPO.	1	INTEGER DATA	1 91 0 -1 1 -0 -0 -0 -0 -0 -0 -0 -0 -0 -0 -0 -0 -0					
COMPO.	2	INTEGER DATA	2 81 1 1 -2 -0 -0 -0 -0 -0 -0 -0 -0 -0 -0 -0 -0 -0					
REAL DATA CARD #	1		.1000E+01 .1000E+01 .3500E+00 .1910E+01 .3500E+00 .1910E+01 -0.					.1020E+01
COMPO.	3	INTEGER DATA	3 21 3 2 -3 -0 -0 -0 -0 -0 -0 -0 -0 0 -0 -0					
REAL DATA CARD #	1		.2200E+01 .4500E+00 -0. -0. -0. -0. -0.					-0.
REAL DATA CARD #	2		0. .2020E+01 .2978E+01 .2000E+00 -0. -0. -0.					-0.
REAL DATA CARD #	3		.3370E+00 .3370E+00 0. 0. -0. -0. -0.					-0.
COMPO.	4	INTEGER DATA	4 41 1 3 -0 -0 -0 -0 -0 -0 -0 -0 -0 -0 -0 -0 -0					
REAL DATA CARD #	1		.5000E+02 -0. -0. -0. -0. -0. -0.					-0.

FIGURE 206. RUN 51A01 HYTRAN INPUT DATA FOR FILTER MODEL VERIFICATION

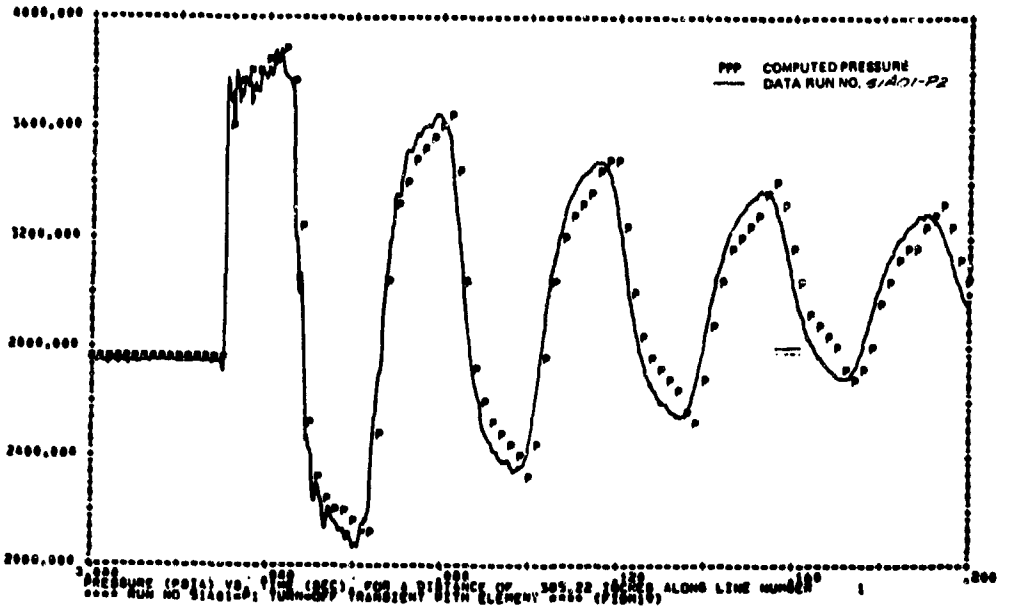

FIGURE 207. 51A01-P2 TURN-OFF TRANSIENT

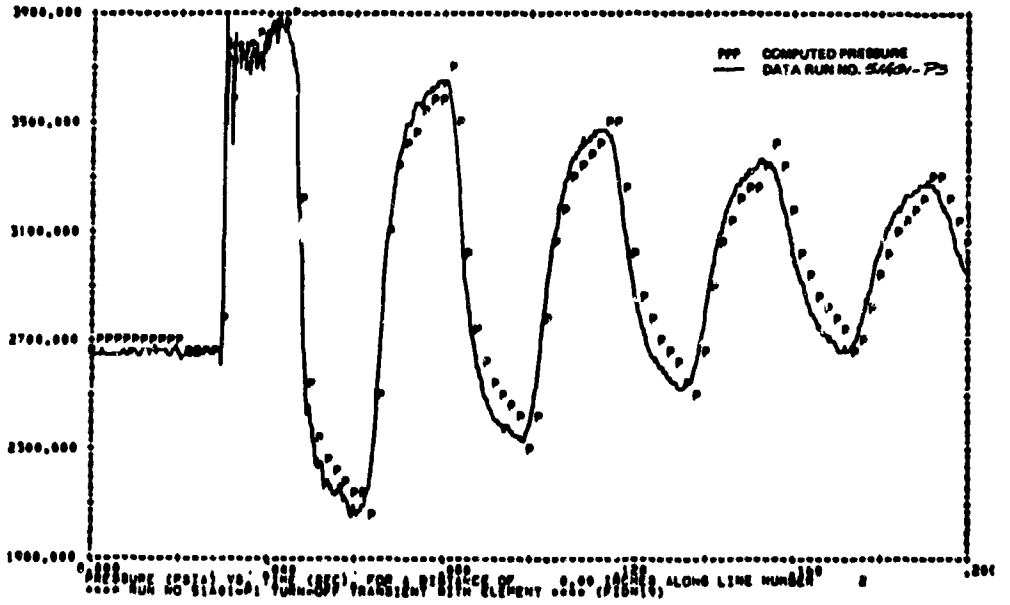

FIGURE 208. 51A01-P3 TURN-OFF TRANSIENT

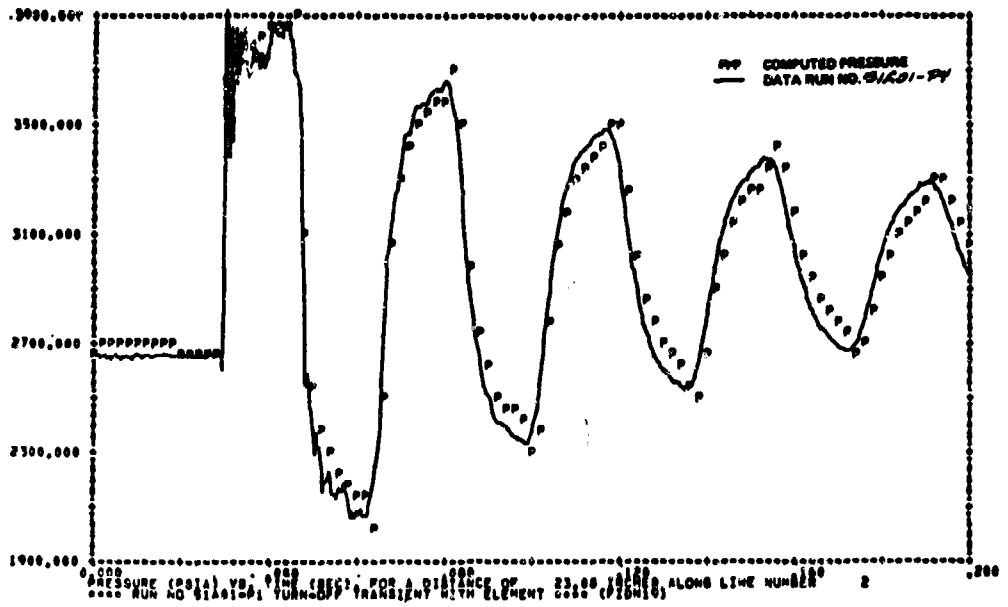

FIGURE 209. 51A01-P4 TURN-OFF TRANSIENT

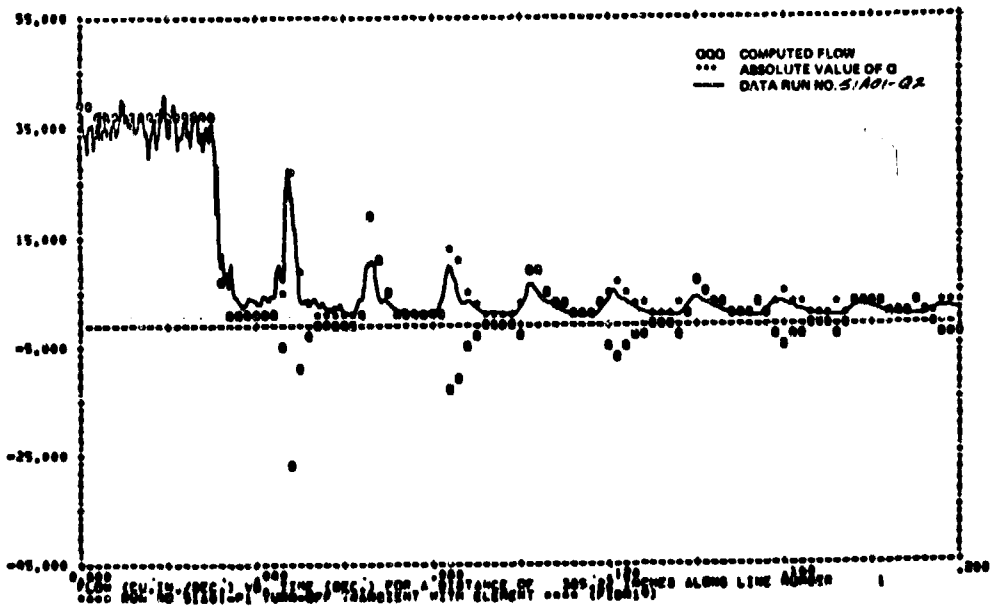

FIGURE 210. 51A01-Q2 TURN-OFF TRANSIENT

These pressures were recorded 18" upstream of the filter. The third and fourth pressure dips are at about 2500 and 2700 PSI respectively. While the corresponding dips in Figure 205, a filter with an element, are about 2400 and 2600 PSI. The remaining pressure data taken at the P3 and P4 transducer positions for both runs also indicate the same results.

In Figure 210, the first flow reversal has a magnitude of 27 CIS which is 4 CIS larger than the corresponding flow in Figure 204. Subsequent flow reversals also indicate similar results. The flow data confirms what the pressure data has shown. The flow rates in the filter with an element are slightly higher than those in a filter without an element resulting in less pressure attenuation.

At first glance, it would appear that the data is mislabeled, but the low flow rate runs (51A02, 51A02) also indicate this phenomena, and the HYTRAN computer program also predicts the same results.

The reasons why an empty filter housing would attenuate a pressure signal more than a filter with an element in this system configuration is not clearly understood. Perhaps the charging time constant of a filter with an element changes significantly as the element is removed resulting in the attenuation difference.

c. Using Filter Model With Head Exchanger Test Data - An attempt was made to use the filter subroutine (FILT81) as the model for a heat exchanger with the test data measured in the lab on a F-4 utility heat exchanger. Table 9 contains a summary of the tests that were performed. The system configuration is shown in Figure 211.

TABLE 9

TEST CONDITIONS FOR F-4 UTILITY HEAT EXCHANGER

Run No.	Transient Condition	Flow (GPM)	Temeprature (°F)
62-08-XX	Turn-Off	3	125
62-08+XX	Turn-On	3	125
62-10-XX	Turn-Off	3	210

A run was made using the test conditions and the 62-08+P4 and 62-08+P5 data as the boundary conditions. The results of the turn-on simulation is shown in Figure 212, 213, 214 and 215. The simulation indicates that the filter model was insensitive to the return line transients. Figure 212 is the position immediately downstream of the fast control valve shown in Figure 211.

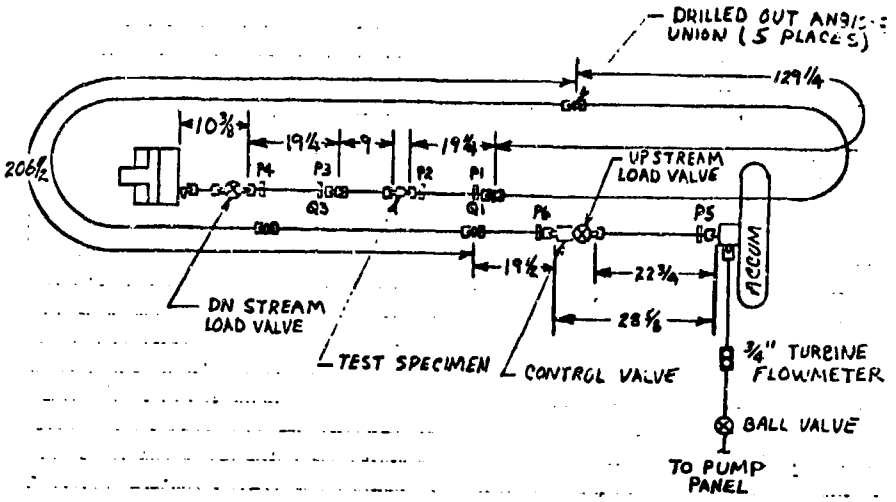

FIGURE 211. HEAT EXCHANGER TEST CONFIGURATION

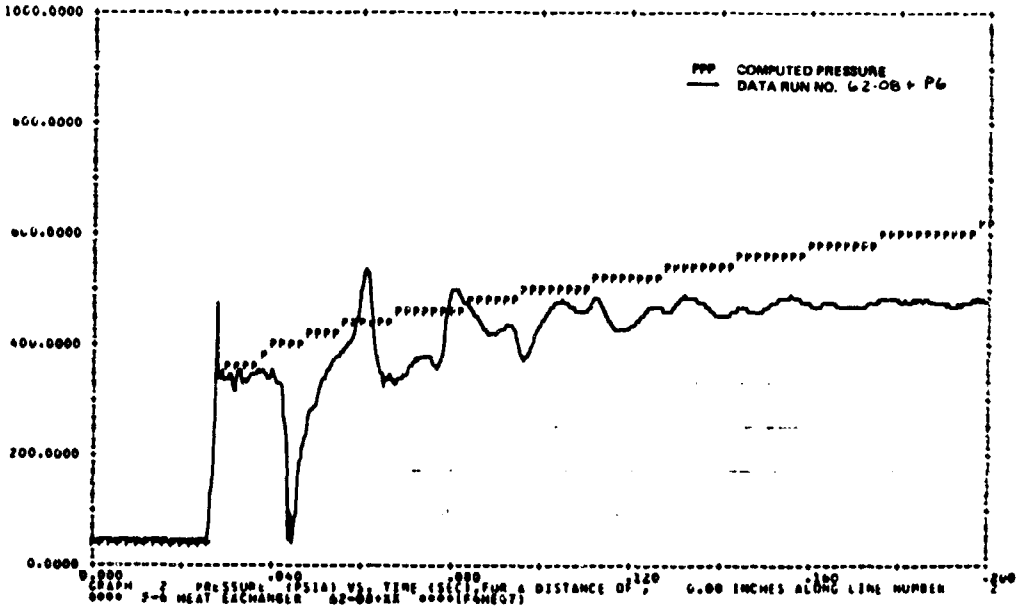

FIGURE 212. 62-08+P6 TURN-ON TRANSIENT

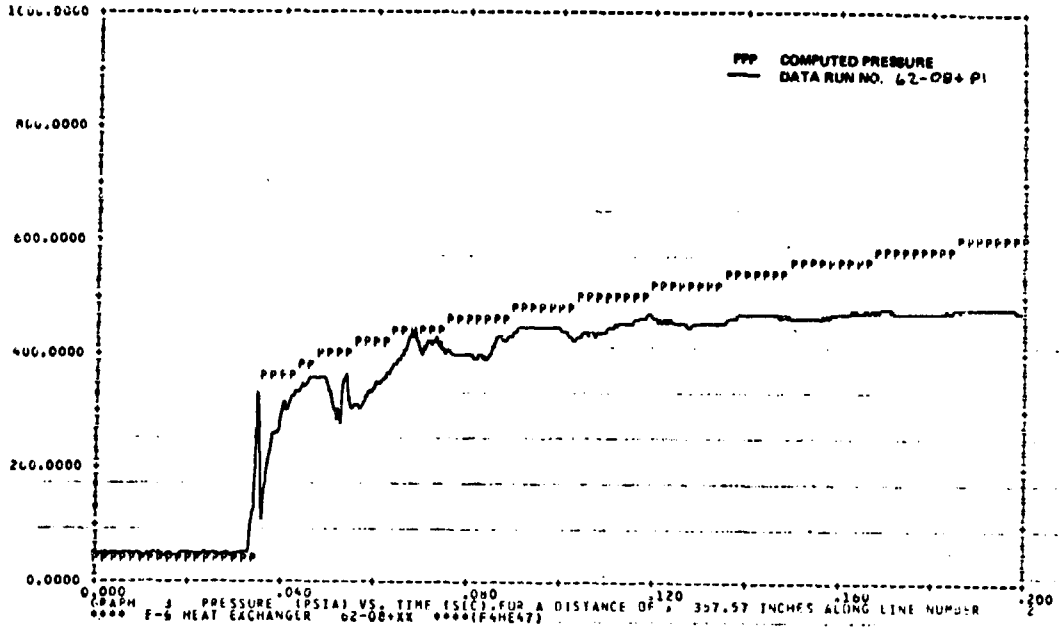

FIGURE 213. 62-08+P1 TURN-ON TRANSIENT

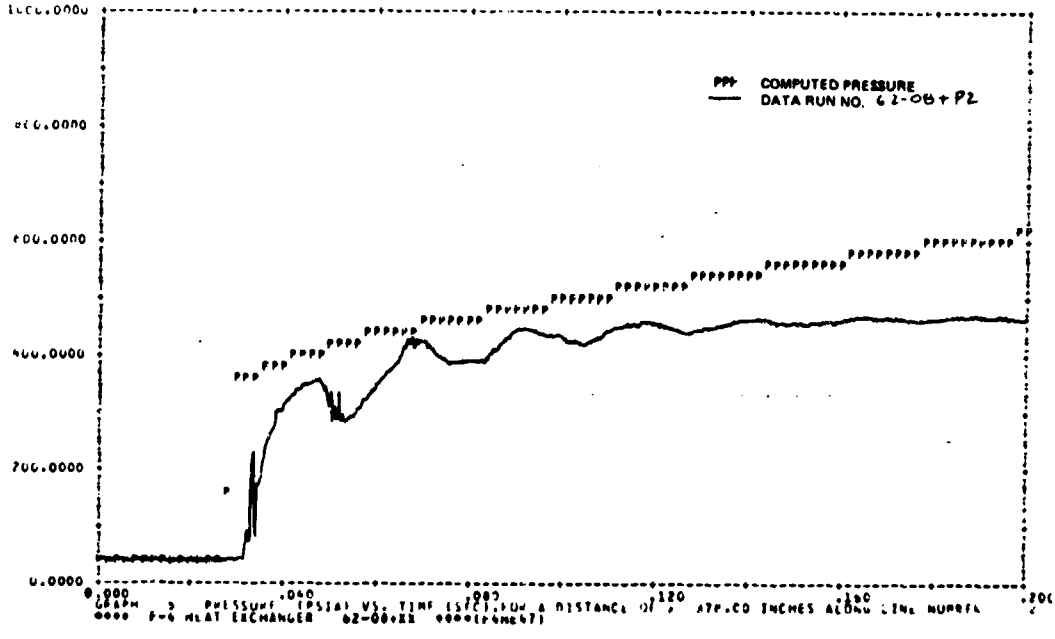

FIGURE 214. 62-08+P2 TURN-ON TRANSIENT

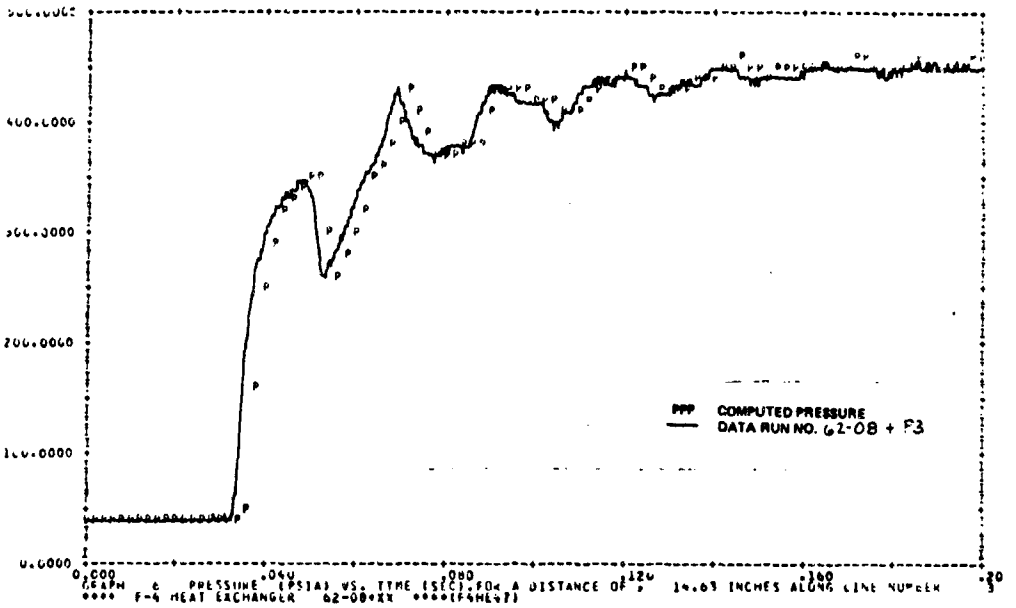

FIGURE 215. 62-08+P3 TURN-ON TRANSIENT

The sharp dip in return pressure to 50 psi at 43 milliseconds is not simulated by the computer program. Also at 200 milliseconds the calculated pressure is about 100 psi above the data. The computed data in Figure 215 matches the P4 input data characteristics, but the pressure wave is sharply attenuated by the volume of the model and does not pass through to the upstream side as shown by the computed output in Figure 214.

From the simulations made using the test data, the filter model is not adequate in simulating a heat exchanger in a return line. Further work on the model would be required for adequate verification.

d. Conclusions - The HYTRAN filter model calculations of flows and pressures compare reasonably well with the test data measured in the lab. Because of the small filter used, there was very little difference between the filter with and without an element. The basic difference between the filter and the line was that the filter supplied more attenuation to the pressure signal and slowed down the wave speed slightly.

Return side test data showed that the filter model was not adequate for use as a heat exchanger.

5. CHECK VALVE MODEL VERIFICATION

The test results obtained in the laboratory on a MCAIR miniature check valve are compared to the HYTRAN computer program check valve model (CVAL31). The check valve used in the testing is shown in Figure 216. The testing was performed on a 1/2 inch system with MIL-H-5606B hydraulic fluid.

The subroutine CVAL31 models a simple undamped check valve. The check valve is assumed to have a variable orifice characteristic between the fully open and fully closed positions. Reverse flow can take place transiently until the valve closes.

The model used to calculate the steady state pressure drop assumes a straight line flow pressure drop characteristic between the cracking pressure and the fully open position. In the transient analysis, the flow through the valve is calculated using the normal valve equations, with the valve orifice area being proportional to the valve displacement. The check valve test series was run on the system configuration shown in Figure 217.

The following parameters were recorded in the laboratory for the test runs: P_1, P_2, Q_2, P_3, P_4 and valve position. P_1, P_2, P_3, and P_4 were recorded directly onto cassette tape.

The test conditions are shown in Table 10.

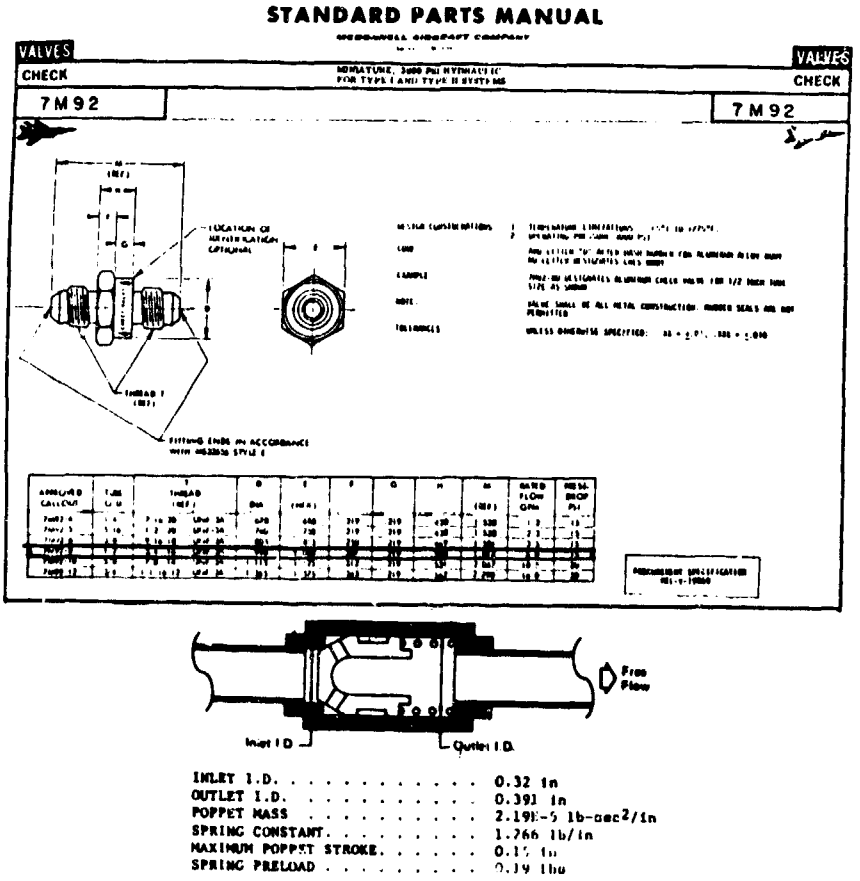

FIGURE 216. MCAIR MINIATURE CHECK VALVE

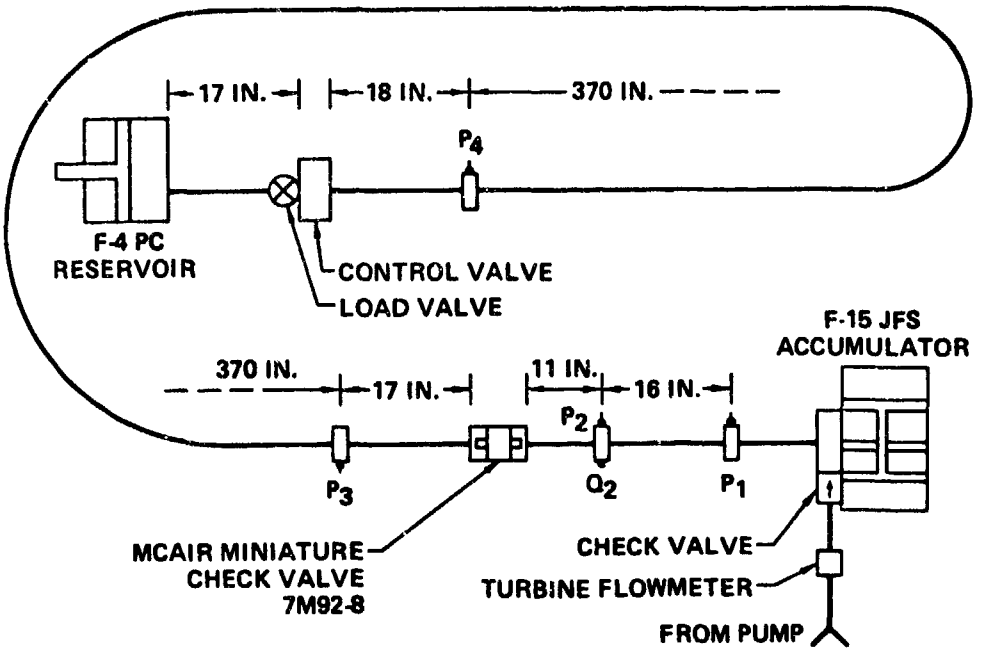

FIGURE 217. TRANSIENT TEST CONFIGURATION MCAIR MINIATURE CHECK VALVE 7M92-8

TABLE 10. TEST CONDITIONS FOR MCAIR MINIATURE CHECK VALVE 7M92-8

TEST SPECIMEN	RUN #	FLOW CONDITION	FLOW RATE (CIS)	TEMP (DEG F)
MCAIR Miniature Check Valve 7M92-8	55-01-XX*	Turn-Off	38.5	125
	55-01+XX	Turn-On	38.5	125
	55-02-XX	Turn-Off	11.55	125
	55-02+XX	Turn-On	11.55	125
	55-05-XX	Turn-Off	38.5	210
	55-05+XX	Turn-On	38.5	210
	55-06-XX	Turn-Off	38.5	210
	55-06+XX	Turn-On	38.5	210

* - XX denotes measured data parameters.

a. Computer Verification of Check Valve Model with Test Data - The first data run of the MCAIR miniature check valve to be compared to a computer run was for a turn-off transient at 125°F and 38.5 CIS. The valve closing time was determined from the P_3 data and the acoustic velocity in the tube. The data from Figure 218 was input into the computer program with the system schematic information in Figure 219. The oscillations in the P_1 pressure occur when the check valve poppet is seated on a turn-off transient. The resultant pressure wave generated by the valve closure oscillates in the 22-inch line between the accumulator and the check valve.

Figure 220 is a plot of the P_3 data over the computer predicted pressure at the P_3 position 20 inches downstream of the check valve. The computer results show good correlation on the first three pressure peaks in Figure 220. From the fourth peak on, the computed pressures are not damped enough to conform to the actual plotted data run. Figure 221, 396 inches upstream from the check valve, also indicates the same results. The average steady state pressure in the computer simulation is about the same as the actual test results.

The first initial pressure rise corresponds to the closing of the check valve with a small local flow existing in the downstream end of the 417 inch line. As the pressure drops off the flow proceeds towards the check valve.

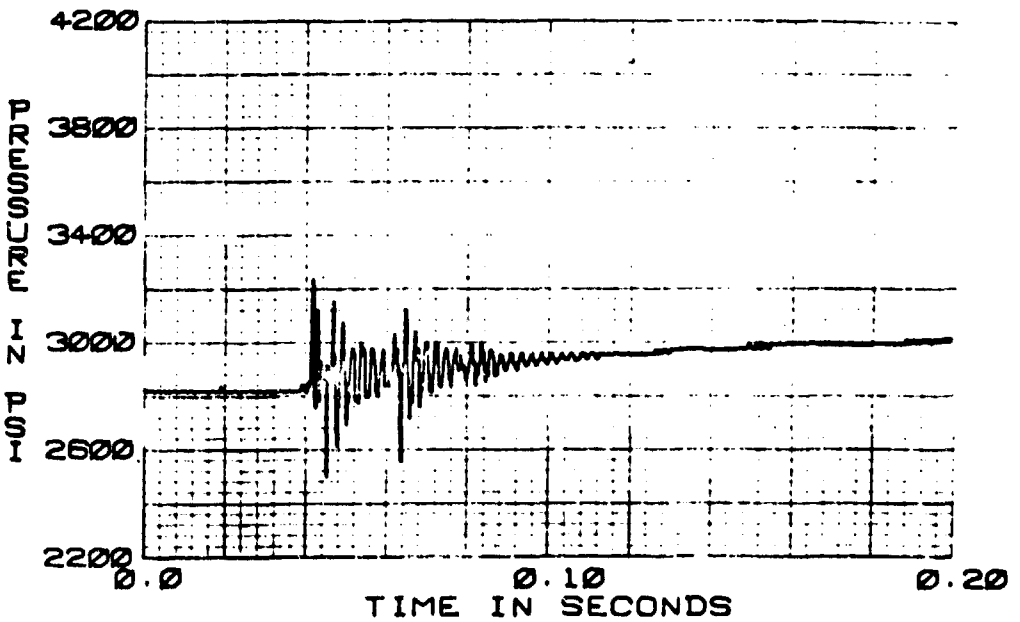

FIGURE 218. 7M92-8 CHECK VALVE 55-01-P1 TURN-OFF TRANSIENT 38.5 CIS 125°F

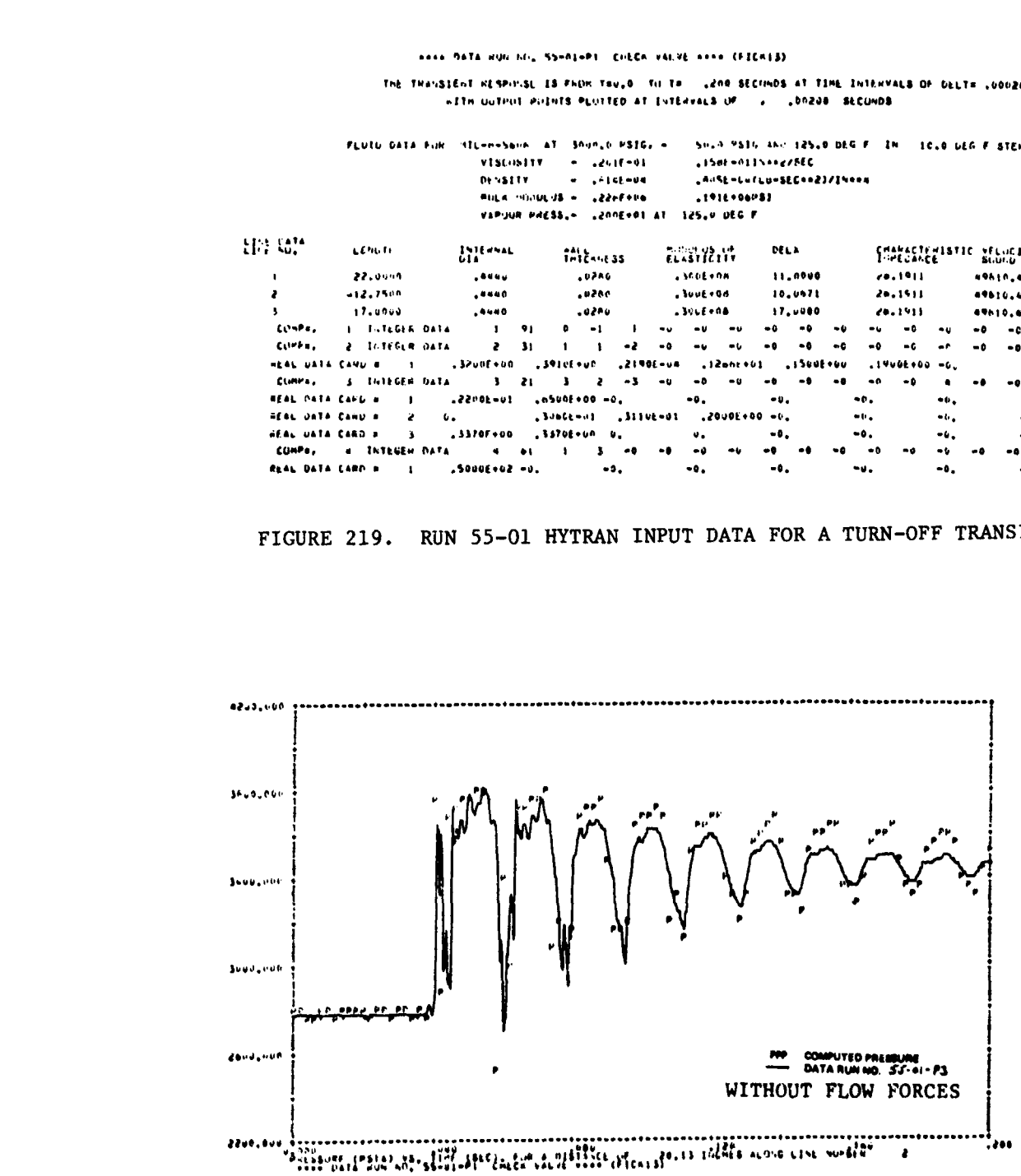

```
**** DATA RUN NO. 55-01-P1  CHECK VALVE **** (FICR13)

THE TRANSIENT RESPONSE IS FROM TAU,0  TO TF  .200 SECONDS AT TIME INTERVALS OF DELTF= .00020
 WITH OUTPUT POINTS PLOTTED AT INTERVALS OF  ,  .00200  SECONDS

 FLUID DATA FOR  MIL-H-5606  AT  3000.0 PSIG, =    90.0 PSIG AND 125.0 DEG F  IN   10.0 DEG F STEPS
                 VISCOSITY    =  .261E-01          .150E-01LB**SEC/SQ**2/IN****
                 DENSITY      =  .41CE-04          .40?E-04LB*LB-SEC**2/IN****
                 BULK MODULUS =  .22?E+06          .191E+06PSI
                 VAPOUR PRESS.=  .200E+01 AT  125.0 DEG F

LINE DATA CARD NO.   LENGTH        INTERNAL DIA      WALL THICKNESS     MODULUS OF ELASTICITY     DELA          CHARACTERISTIC IMPEDANCE   VELOCITY OF SOUND
        1            22.0000         .4440             .0280             .300E+08                11.0000       ?8.1911                    49810.6245
        2            12.7500         .4440             .0280             .300E+08                10.0471       ?8.1911                    49810.6245
        3            17.0000         .4440             .0280             .30LE+08                17.0000       ?8.1911                    49810.6245
 COMPR,  1  INTEGER DATA     1  91   0  -1   1  -0  -0  -0  -0  -0  -0  -0  -0  -0  -0  -0  -0  -0
 COMPR,  2  INTEGER DATA     2  31   1   1  -2  -0  -0  -0  -0  -0  -0  -0  -0  -0  -0  -0  -0  -0
REAL DATA CARD #   1    .320QE+00  .391CE+00  .2190E-08  .12ORE+01  .1500E+00  .19?0E+00 -0.          -0.
 COMPR,  3  INTEGER DATA     3  21   3   2  -3  -0  -0  -0  -0  -0  -0  -0  -0  -0  -0  -0  -0  -0
REAL DATA CARD #   1    .2200E-01  .0500E+00 -0.          -0.          -0.          -0.          -0.          -0.
REAL DATA CARD #   2    0.         .3?0CE-01  .311?E-01  .20?0E+00 -0.          -0.          -0.          -0.
REAL DATA CARD #   3    .3370F+00  .3370E+00  0.          0.          -0.          -0.          -0.          -0.
 COMPR,  4  INTEGER DATA     4  01   1   3  -0  -0  -0  -0  -0  -0  -0  -0  -0  -0  -0  -0  -0  -0
REAL DATA CARD #   1    .5000E+02 -0.          -0.          -0.          -0.          -0.          -0.          -0.
```

FIGURE 219. RUN 55-01 HYTRAN INPUT DATA FOR A TURN-OFF TRANSIENT

FIGURE 220. 55-01-P3 TURN-OFF TRANSIENT WITHOUT FLOW FORCES

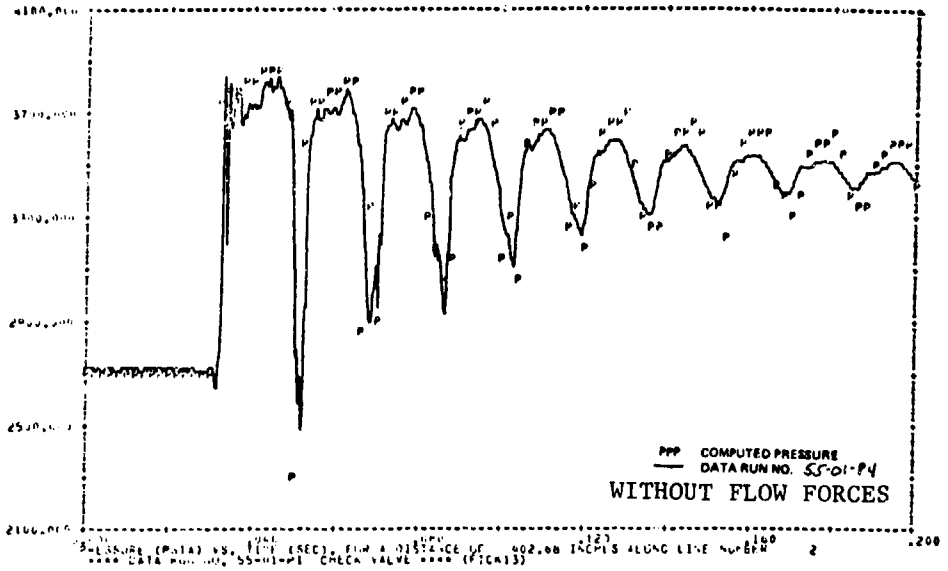

FIGURE 221. 55-01-P4 TURN-OFF TRANSIENT

Because the check valve poppet is closed, the pressure remains at a level higher than the source pressure. The rectified effect results because pressure and flow oscillations in the 22 inch line are not able to completely override the forces on the poppet which keep the valve closed.

The check valve model does not account for displacement flow due to poppet motion, variations in orifice characteristics with poppet position, or secondary pressure drops due to other flow restrictions. Perhaps the most significant effect not modeled in the CVAL31 subroutine is the flow forces on the poppet. These were not included initially because they are not well defined theoretically and really depend on the actual valve geometry.

The majority of the error in Figure 220 can thus be attributed to flow force effects on the poppet. They are the most predominant forces present in the check valve in this test configuration during the turn-off transient.

An attempt was made to simulate some of the axial flow forces in the check valve by equating it with the net change of momentum as shown in the following expression:

$$F_A = 2 * C_d * \Delta P * W * l$$

where

C_d = discharge coefficient for valve shot width (.65 assumed)

ΔP = pressure drop across the poppet

W = peripheral width of the orifice

l = axial length of the orifice

The area of the opening was approximated by the following algorithm:

$$wl = A = K\ Xp\ /(1 + Xp)$$

where

A = orifice opening

K = constant determined from max poppet opening and check valve inlet area

Xp = poppet position

The net axial force was

$$F_A = 2 * C_d * \Delta P * K\ * Xp\ (1 + X_p)$$

The computer simulation using P1 input data was again run with the axial flow force included in the check valve model. The P_3 data is overplotted with the computer run in Figures 222 and 223. The simulation shows better correlation with the data but not a significant improvement.

The computer output flow plots are shown in Figures 224 and 225. The data runs for these two plots are plotted over the computer runs. Figure 224 shows the flow oscillating in the 22 inch line between the accumulator and check valve. This corresponds to the P1 pressure trade in Figure 218. Figure 225 is the flow 20 inches upstream of the check valve.

The HYTRAN computer simulation of a turn-on transient at 125°F and 38.5 CIS was run using the input data of Figure 226 and system data from Figure 227. The computer output graphs of pressure overplotted with the test data are shown in Figures 228, 229, and 230.

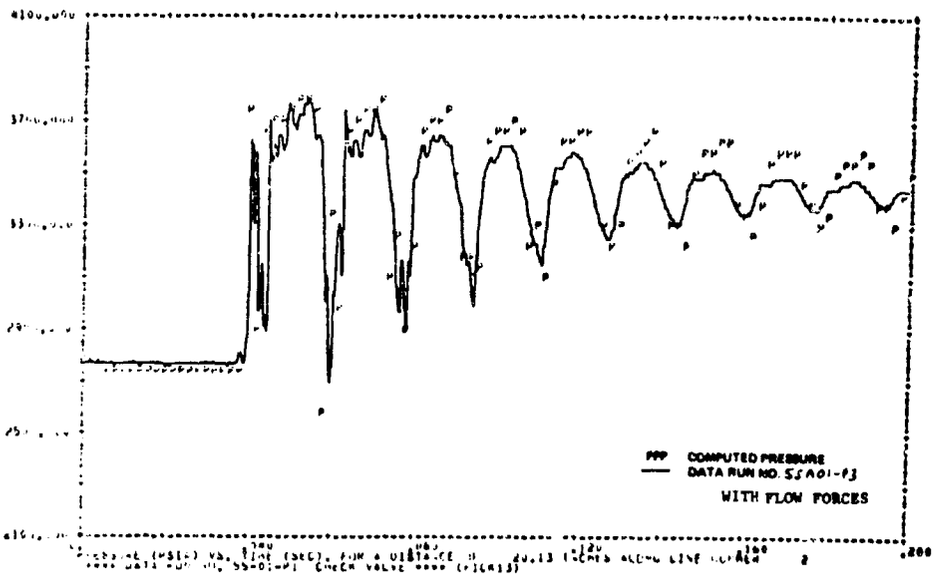

FIGURE 222. 55A01-P3 TURN-OFF TRANSIENT

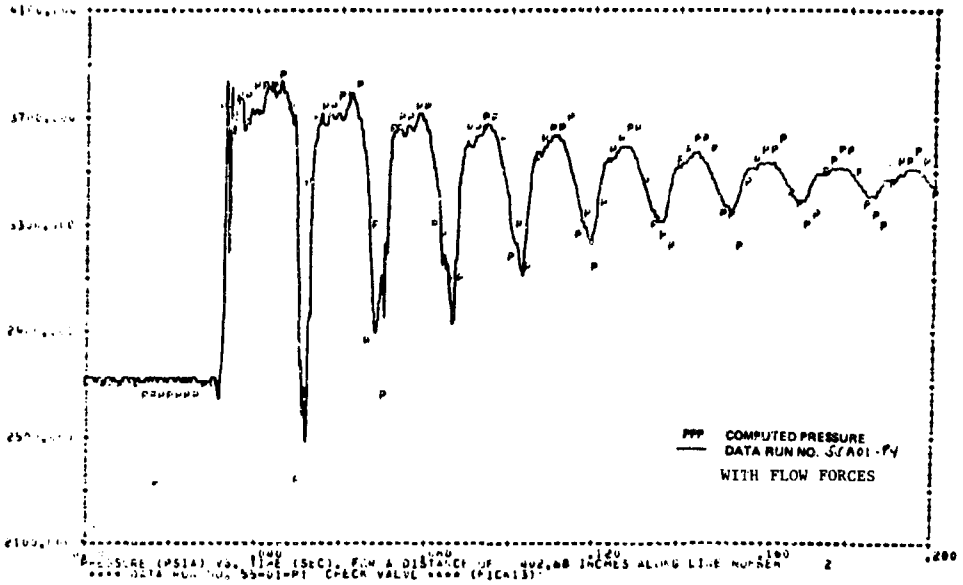

FIGURE 223. 55A01-P4 TURN-OFF TRANSIENT

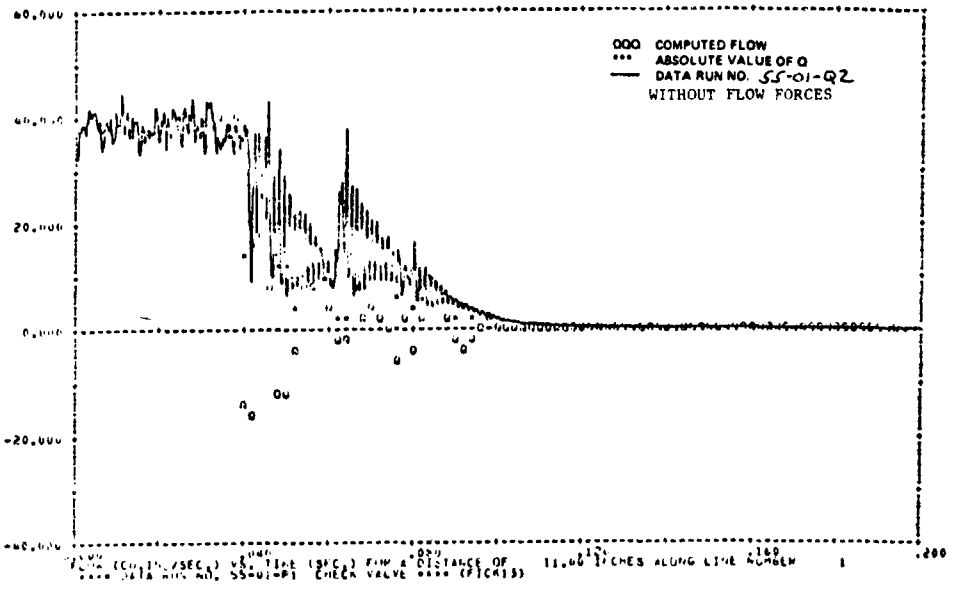

FIGURE 224. 55-01-Q2 TURN-OFF TRANSIENT

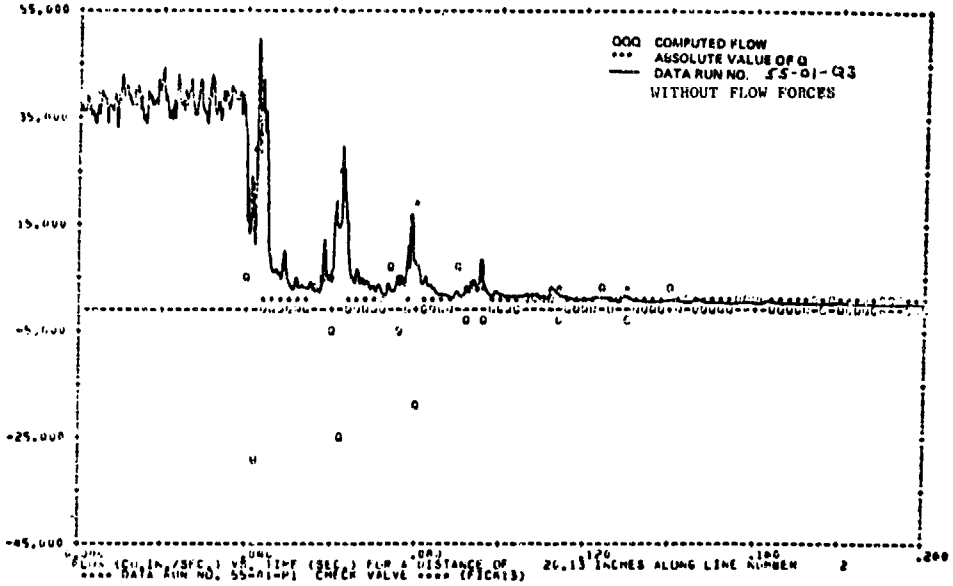

FIGURE 225. 55-01-Q3 TURN-OFF TRANSIENT

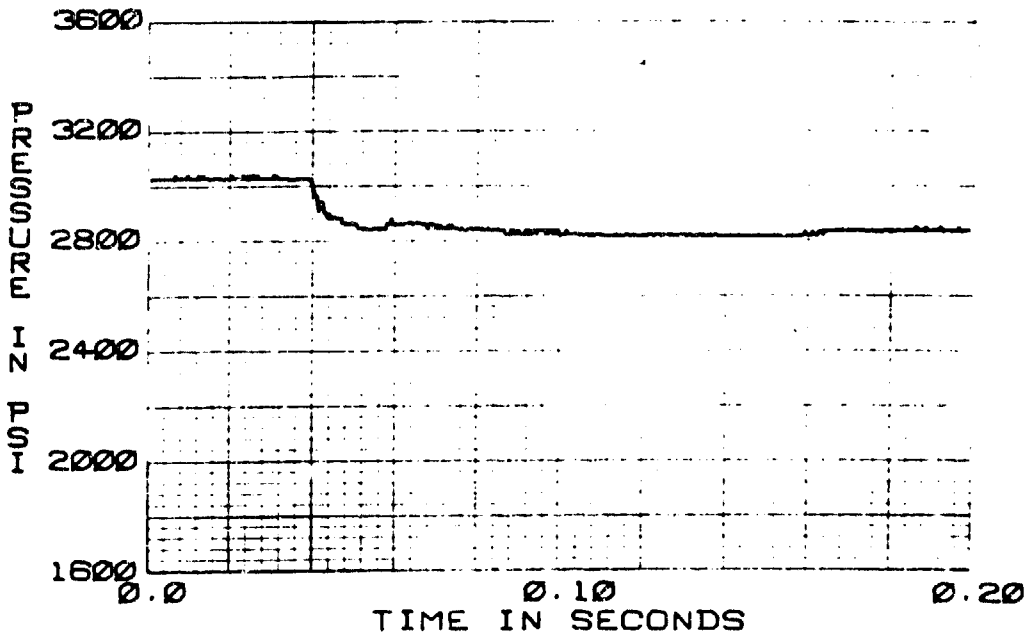

FIGURE 226. 7M92-8 CHECK VALVE 55-01+P1 TURN-ON TRANSIENT
38.5 CIS 125°F

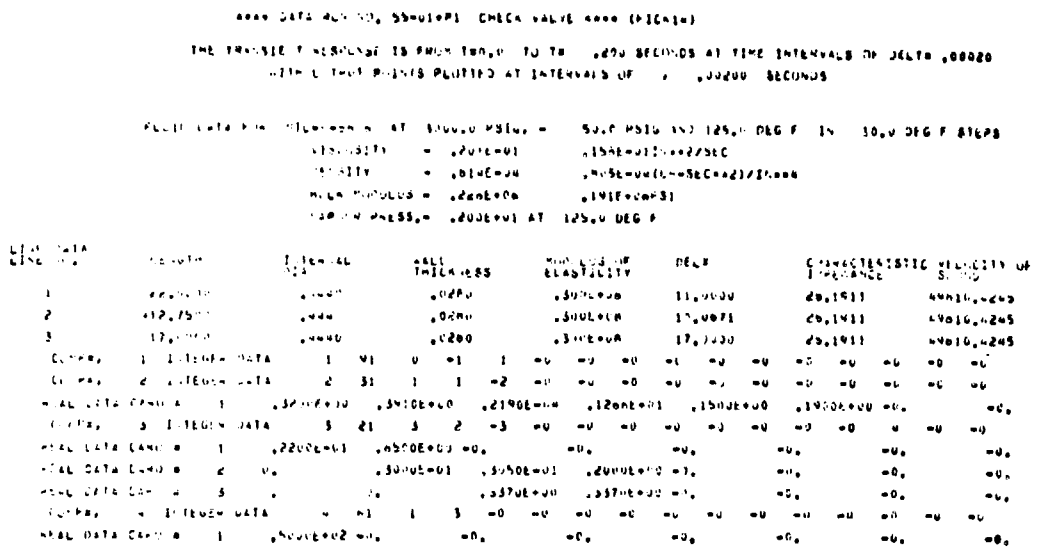

FIGURE 227. RUN 55-01 HYTRAN INPUT DATA FOR A TURN-ON TRANSIENT WITHOUT FLOW FORCES

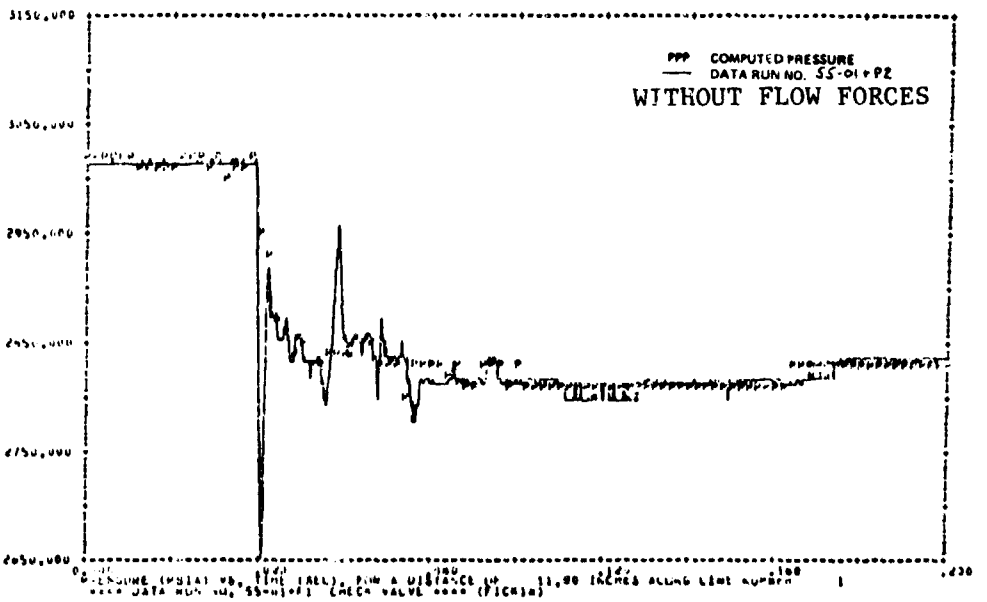

FIGURE 228. 55-01+P2 TURN-ON TRANSIENT

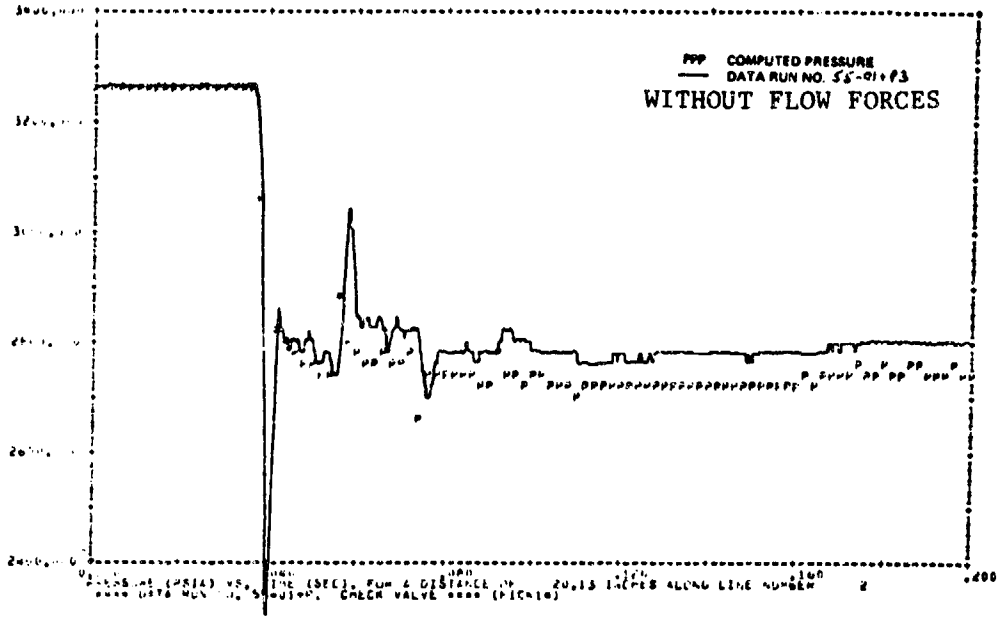

FIGURE 229. 55-01+P3 TURN-ON TRANSIENT

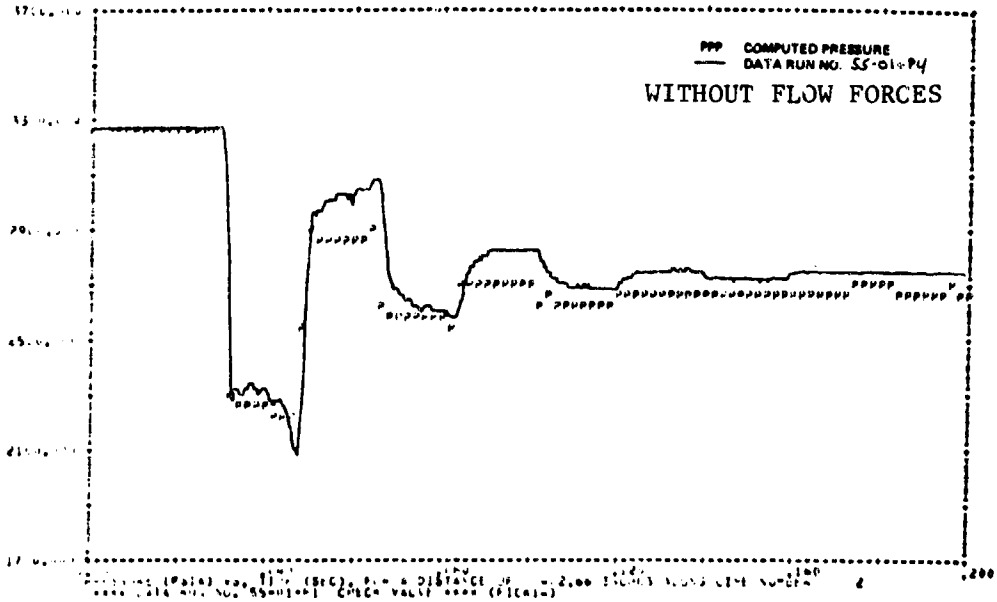

FIGURE 230. 55-01+P4 TURN-ON TRANSIENT

The initial steady state pressure of the test data in Figure 228 is about 3020 psi while the initial steady state pressure on the P3 data in Figure 229 is 3260 psi. This apparent discrepancy in steady state pressure can be explained by noting the P2 and P3 pressure transducer locations and the initial system condition. The P2 pressure transducer is located 11 inches upstream of the check valve while P3 is 17 inches downstream of the same valve and the control valve is closed. When the control valve was originally closed, the pressure was elevated above source pressure in the line between the check valve and the control valve. This high pressure still remains locked between these valves, thus the pressure differential.

The HYTRAN steady state program initializes the pressures in the line upstream of the check valve to the first P1 data value and pressure downstream of the check valve is set to the initial P3 data value.

The computer calculated flow plots are shown in Figures 231 and 232 plotted over the data runs. The data runs were played back from analog tape. The timing of the valve closure is different on these runs due to the decreased sensitivity of the taped recording. Therefore, the data runs slightly underlap the computer results in Figures 231 and 232.

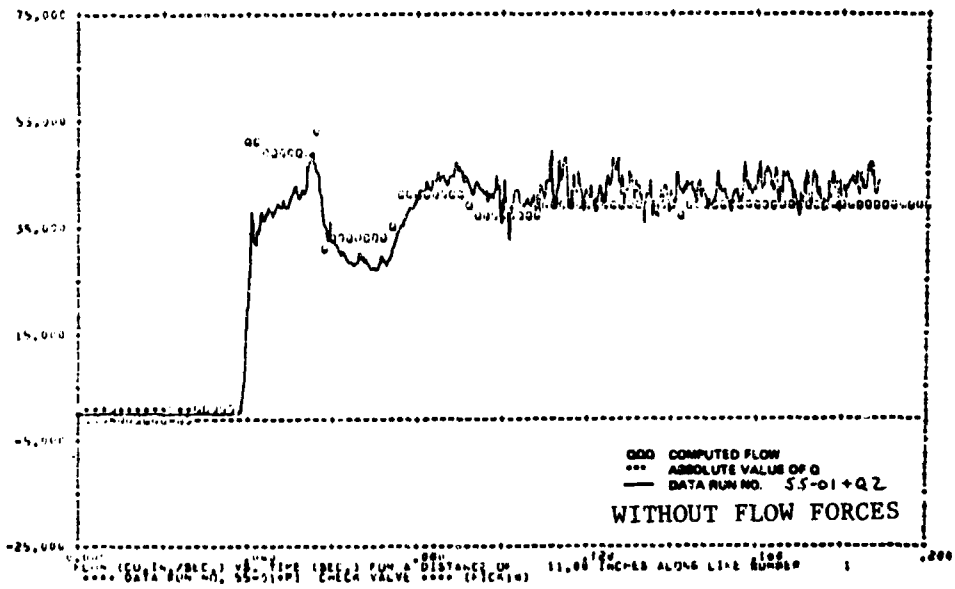

FIGURE 231. 55-01+Q2 TURN-ON TRANSIENT

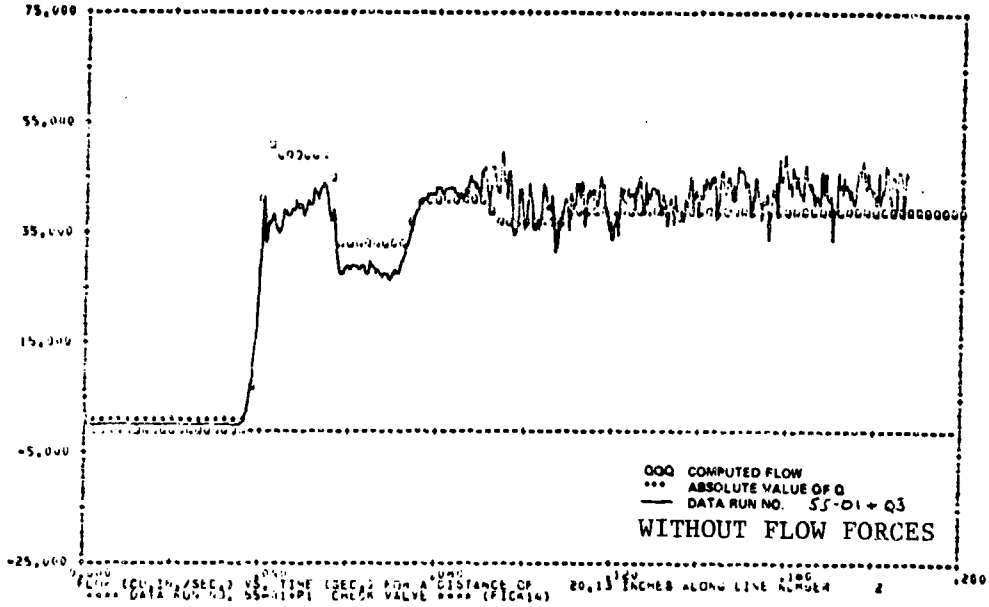

FIGURE 232. 55-01+Q3 TURN-ON TRANSIENT

b. Verification of the Check Valve Model with Return Side Test Data

The MCAIR miniature check valve was tested in the return line configuration shown in Figure 233. The list of test runs is in Table 11.

The computer output for a turn-off transient is shown in Figures 234, 235, and 236. In Figure 235, the predicted steady state values are about 20 psi toohigh. At 130 milliseconds the computed pressure drops to 20 psi. The actual drop in pressure occurs at 140 milliseconds.

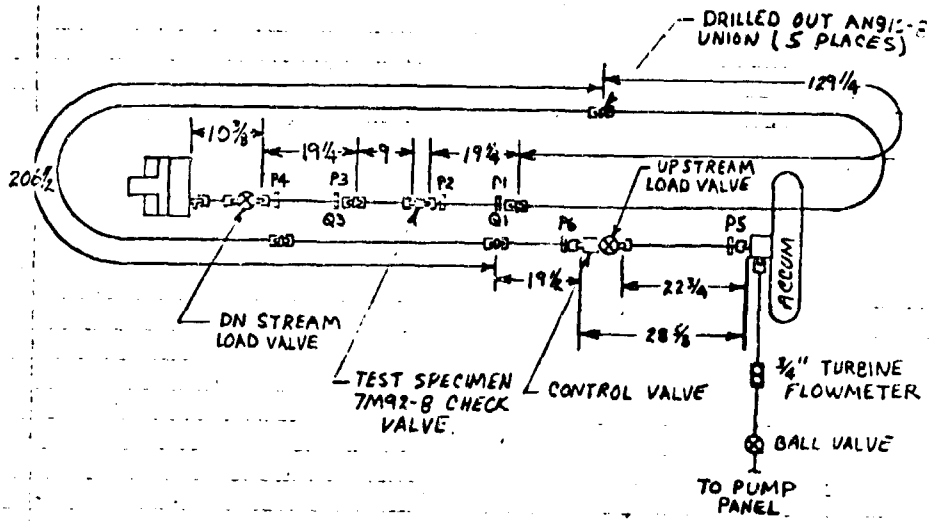

FIGURE 233. RETURN SIDE TEST CONFIGURATION

TABLE 11

CHECK VALVE - RETURN TEST SERIES

Run No.	Transient Condition	Steady State Flow (CIS)	Temperature (°F)
55-07-XX	Turn-Off	38.5	125
55-07+XX	Turn-On	38.5	125
55-08-XX	Turn-Off	11.55	125
55-08+XX	Turn-On	11.55	125
55-09-XX	Turn-Off	38.5	210
55-09+XX	Turn-On	38.5	210
55-10-XX	Turn-Off	11.55	210
55-10+XX	Turn-On	11.55	210

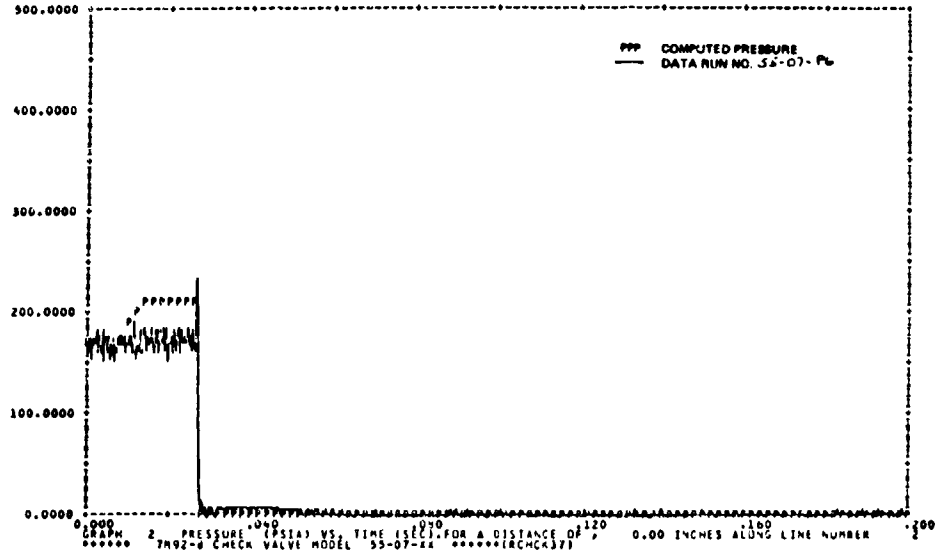

FIGURE 234. 55-07-P6 TURN-OFF TRANSIENT

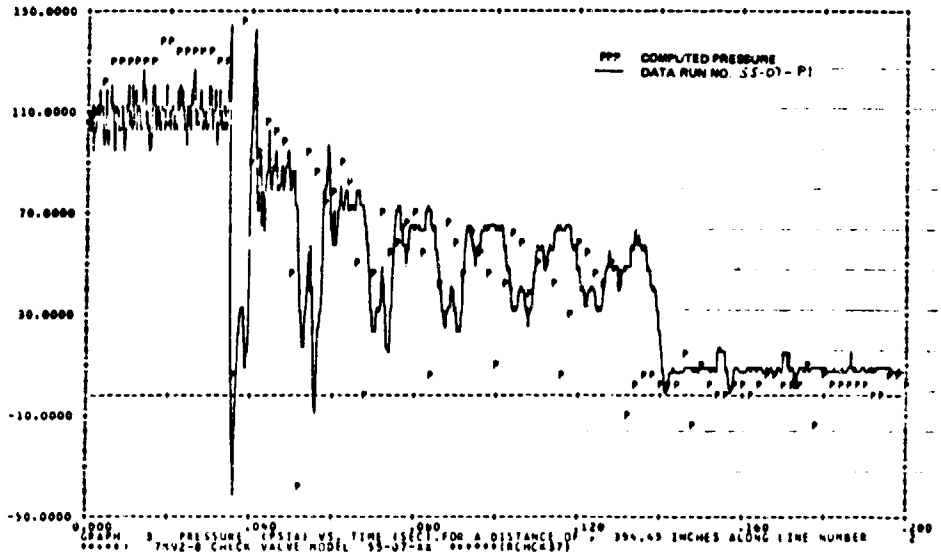

FIGURE 235. 55-07-P1 TURN-OFF TRANSIENT

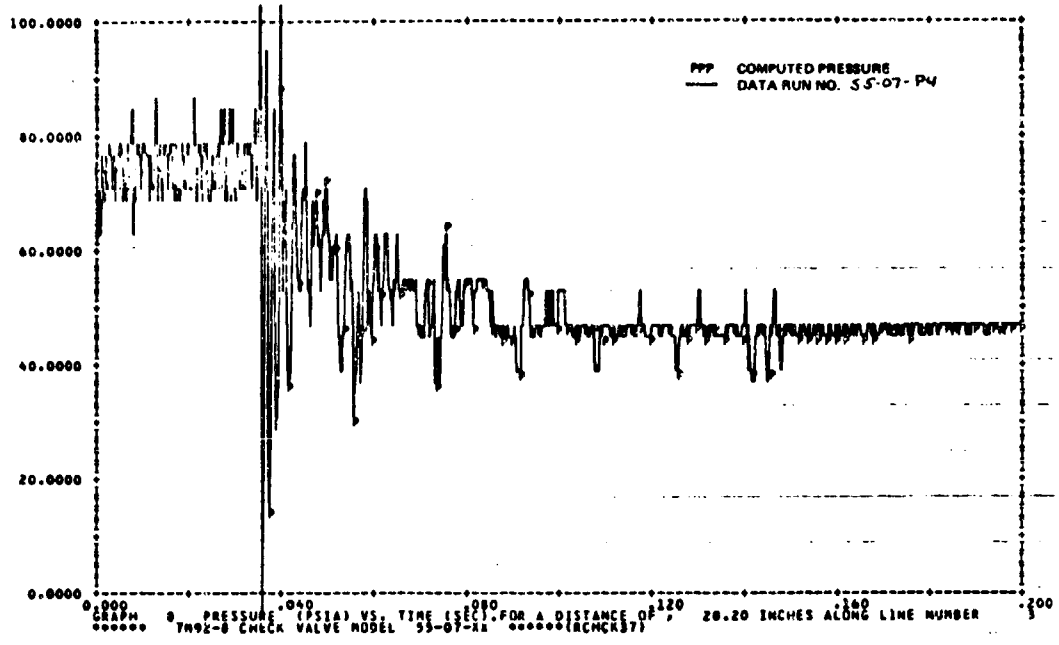

FIGURE 236. 55-07-P4 TURN-OFF TRANSIENT

3. Conclusions - The HYTRAN check valve model compares favorably to the test data measured in the lab. Discrepancies exist between the data and the mathematically predicted results as already noted in this section. The majority of the model error can be attributed to the absence of adequate flow force effects on the poppet in the calculation. The actual forces are not well defined theoretically and really depend upon the actual valve geometry.

Attempts to include axial flow forces in the calculations contributed some improvement for the 125°F and 210°F, 11.55 and 38.5 CIS turn-off transient calculations.

Since the CVAL31 subroutine was written for a general check valve it appears that this model is completely adequate for what it was designed to accomplish.

6. RESTRICTOR MODEL VERIFICATION

In this section the test results obtained in the laboratory on a Lee Jet and a Lee Visco Jet are compared to the HYTRAN computer program restrictor model (REST41). The restrictors used in the testing are shown in Figure 237. The Lee Jet contains a calibrated orifice and two matched filters. The orifice was measured to be approximately 0.00945" in diameter. The Lee Jet was installed in a 1/4" AN union for testing.

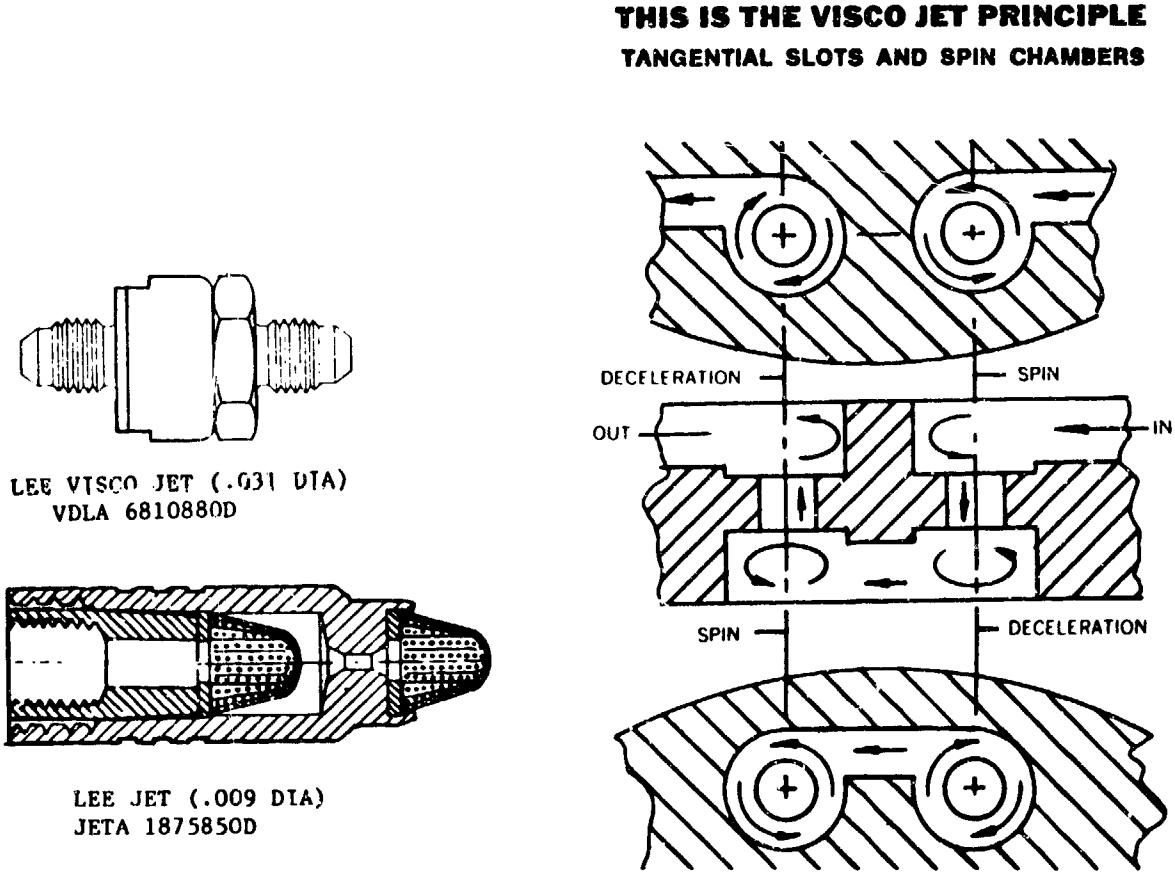

FIGURE 237 LEE JET AND LEE VISCO JET

The Lee Visco Jet consists basically of slotted discs mounted one upon the other to form an extremely complex fluid passage. A reasonable degree of viscosity compensation without the use of any moving parts results from this arrangement. The .031" diameter miniature insert stacked disc type Visco Jet has the same pressure drop rating as the .009" dia Lee Jet.

The Lee and Visco Jets were compared to determine if there was any appreciable attenuation effects due to the presence of the stacked discs over the ordinary orifice. The testing was performed on a 1/2 inch system with MIL-H-5606B hydraulic fluid.

The subroutine REST41 models a fixed, two way, orifice restrictor with two connections. The coefficient of discharge is assumed the same for flow in either direction. It is assumed that the restrictor does not have any ancillary parts and that the oil volume is sufficiently small so integration is not required.

The restrictor test series was run on the system configuration shown in Figure 238. The system pressure line was teed into about 45" upstream of the control valve. The test section consisted of a 15 1/2" length tube, two 19 1/4" instrumented sections containing the four pressure transducers, the test specimen and a shut-off valve which was closed for the testing. The other end of the valve was connected to the return line for bleeding of this short bypass section.

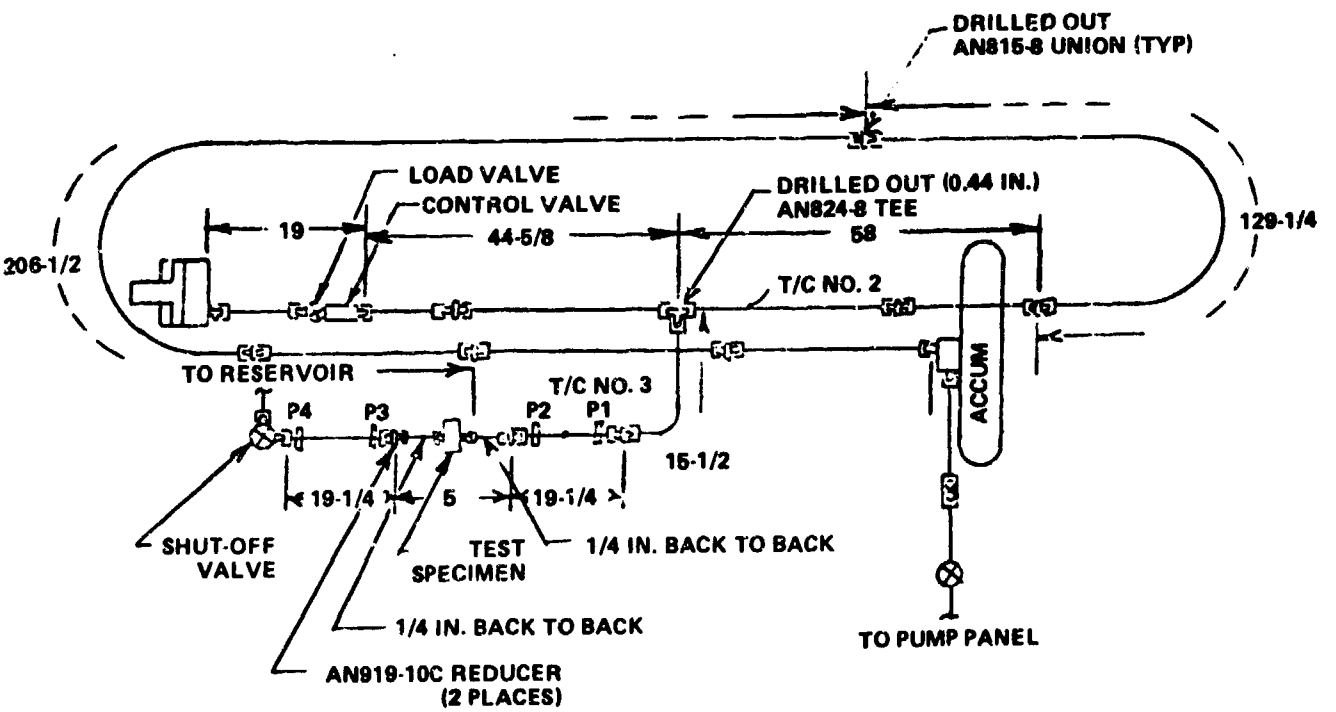

FIGURE 238 TRANSIENT TEST CONFIGURATION FOR LEE JET AND VISCO JET

The following parameters were recorded in the laboratory for the test runs: P_1, P_2, P_3 and P_4. The anemometers were not used because they could not accurately measure the low flow rates in this short section.

The test conditions are shown in Table 12.

TABLE 12 TEST CONDITIONS FOR LEE JET AND LEE VISCO JET

Test Specimen	Run #	Flow Condition	Flow Rate (CIS)	Temp (DEG F)
Lee Jet (.009 dia) JETA 1875850D	60-01-XX*	Turn-Off	38.5	125
"	60-01+XX	Turn-On	38.5	125
"	60-05-XX	Turn-Off	38.5	215
"	60-05+XX	Turn-On	38.5	215
Lee Visco Jet (.031 Dia) VDLA 6810880D	59-01-XX	Turn-Off	38.5	130
"	59-01+XX	Turn-On	38.5	125
"	59-05-XX	Turn-Off	38.5	215
"	59-05+XX	Turn-On	38.5	220

* - XX denotes measured data parameters

a. Computer Simulation with Restrictor Test Data

A turn-off transient at 125°F and 38.5 CIS was simulated with the HYTRAN computer program using the input data of Figure 239 and the system data shown in Figure 240. The output pressure plots are shown in Figures 241 and 242.

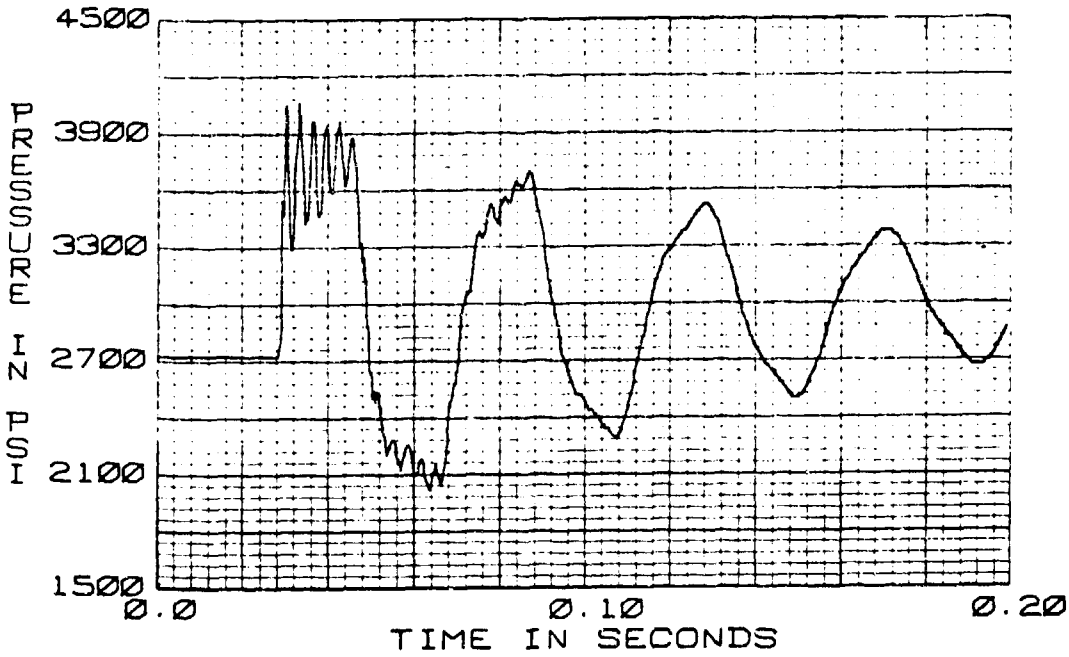

FIGURE 239 LEE JET .009 IN. DIA.
60-01-P1 TURN-OFF TRANSIENT
38.5 CIS 125°F

**** DATA RUN NO, 60-01-P1 LEE JET **** (FILJ5R)

THE TRANSIENT RESPONSE IS FROM T=0.0 TO T= .200 SECONDS AT TIME INTERVALS OF DELT= .00020
WITH OUTPUT POINTS PLOTTED AT INTERVALS OF . .00200 SECONDS

FLUID DATA FOR MIL-H-5606 AT 3000.0 PSIG, = 50.0 PSIG AND 125.0 DEG F IN 10.0 DEG F STEPS

VISCOSITY	= .4511E-01	.1566E-01LB-SEC/IN**2/SEC
DENSITY	= .8114E-04	.8058E-04(LB-SEC**2)/IN**4
BULK MODULUS	= .2206E+06	.1911E+06PSI
VAPOUR PRESS,	= .2006E+01 AT	125.0 DEG F

LINE DATA NO.	LENGTH	INTERNAL DIA	PIPE THICKNESS	MODULUS OF ELASTICITY	DELX	CHARACTERISTIC IMPEDANCE	VELOCITY OF SOUND
1	19.2500	.0000	.0280	.3011E+08	19.2500	20.1911	49810.4245
2	21.2500	.0000	.0280	.3011E+08	19.8250	20.1911	49810.4245

COMPR. 1 INTEGER DATA 1 91 0 -1 1 -0 -0 -0 -0 -0 -0 -0 -0 -0 -0 -0

COMPR. 2 INTEGER DATA 2 -1 1 1 -2 -0 -0 -0 -0 -0 -0 -0 -0 -0 -0 -0

REAL DATA CARD # 1 .9650E-02 .9000E+00 -0. -0. -0. -0. -0. -0.

COMPR. 3 INTEGER DATA 3 11 0 2 -0 -0 -0 -0 -0 -0 -0 -0 -0 -0 -0 -0

FIGURE 240 RUN 60-01 HYTRAN INPUT DATA FOR LEE JET

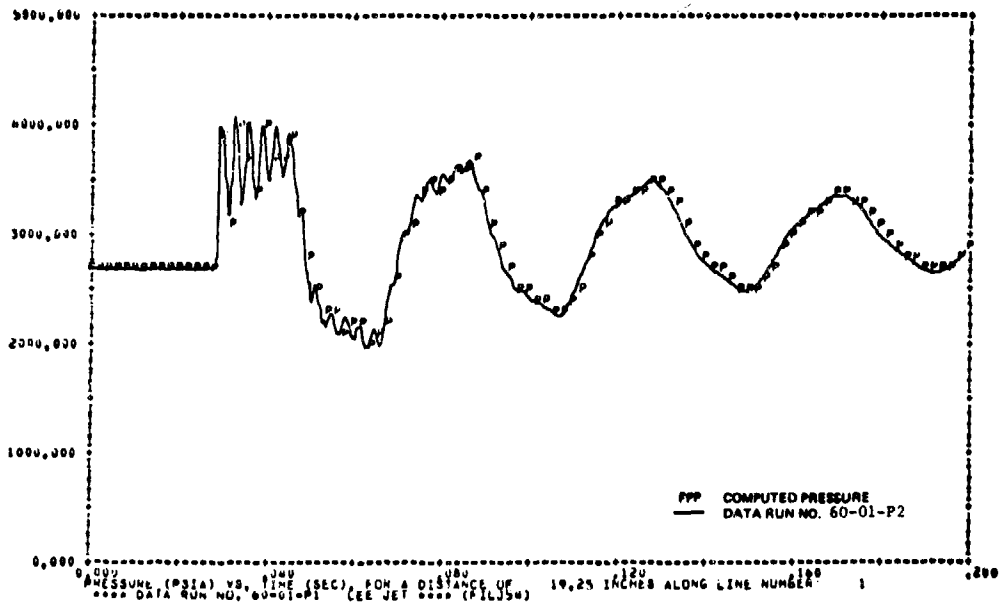

FIGURE 241 60-01-P2 TURN-OFF TRANSIENT

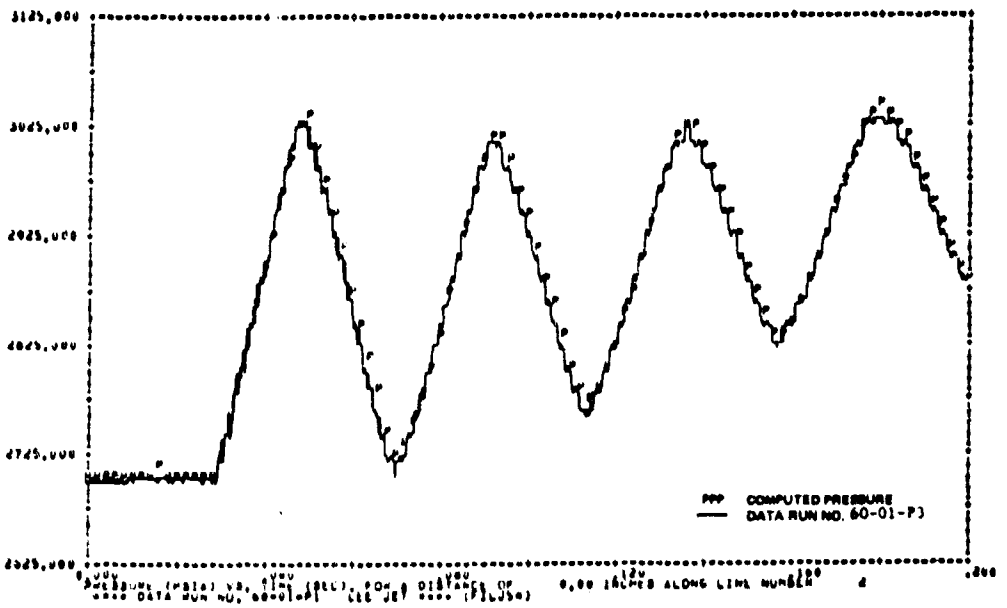

FIGURE 242 60-01-P3 TURN-OFF TRANSIENT

The computer results show excellent correlation to the laboratory test data for both up and downstream of the Lee Jet restrictor in the dead ended line. The oscillating pressure shown on the 239 input data curve occurs in the line from the point where the system is teed off to the test specimen. This resonance was simulated by the computer program as indicated in Figure 241. The maximum pressure obtained in the line upstream of the Lee Jet was 4000 psi. This was a 1300 psi jump from the steady state level. Downstream of the Lee Jet the maximum pressure reached was about 3025 psi as shown in Figure 242. This was only about a 320 psi rise above the initial steady state pressure.

No flow measurements were made in this dead ended system because of the extremely low flow rates involved. However, the computer program did compute the flows in the line as shown in Figure 243. The flow is upstream of the restrictor.

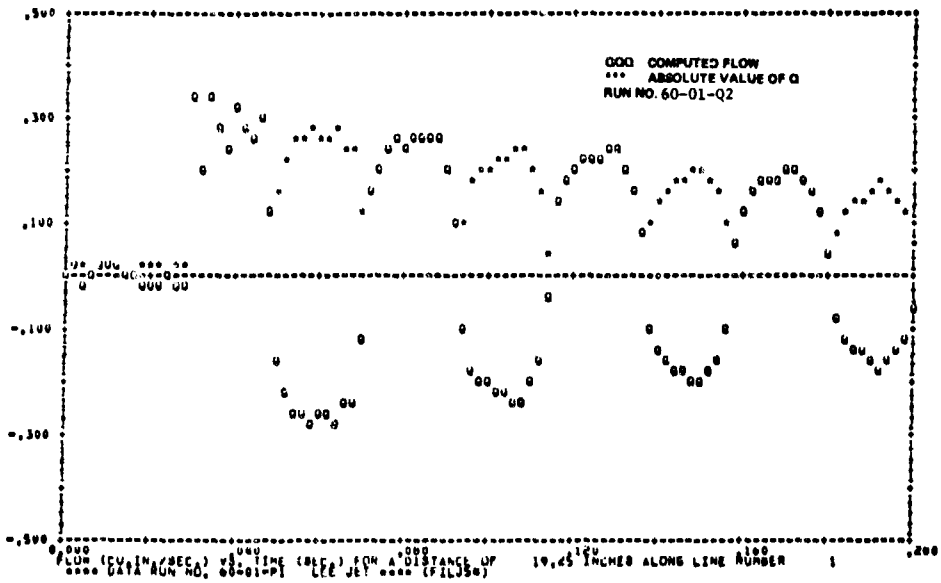

FIGURE 243 60-01-02 TURN-OFF TRANSIENT

A turn-off transient at 130°F and 38.5 CIS was simulated on the HYTRAN computer program using the input data for the Lee Visco Jet in Figure 244.

The computer output pressure and flow plots are shown in Figures 245 and 246. The computer pressure plots show good correlation with the lab data.

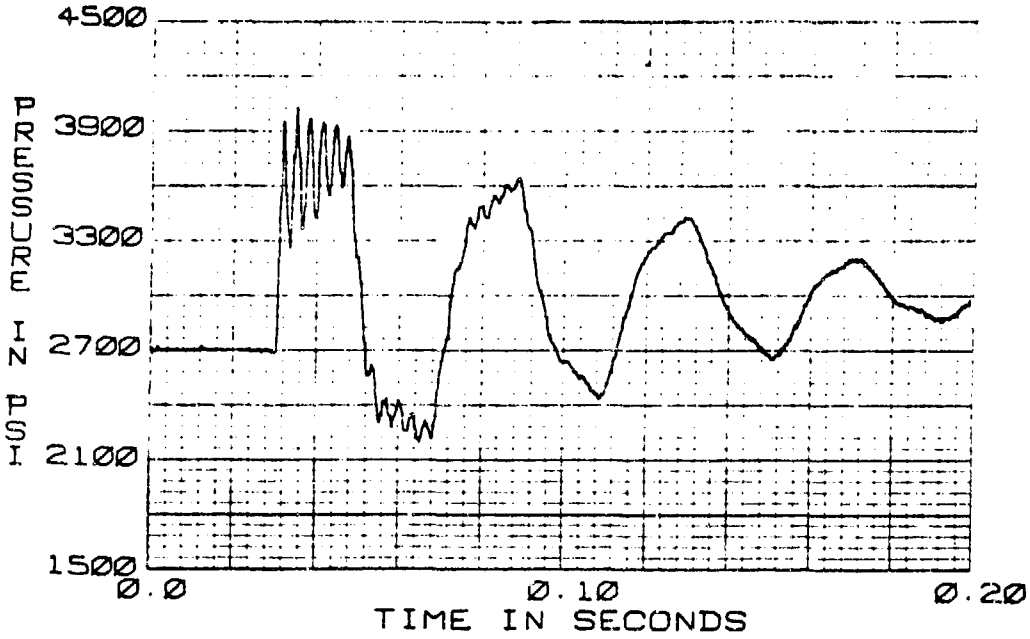

FIGURE 244 LEE VISCO JET .031 IN. DIA.
59-01-P1 TURN-OFF TRANSIENT
38.5 CIS 130°F

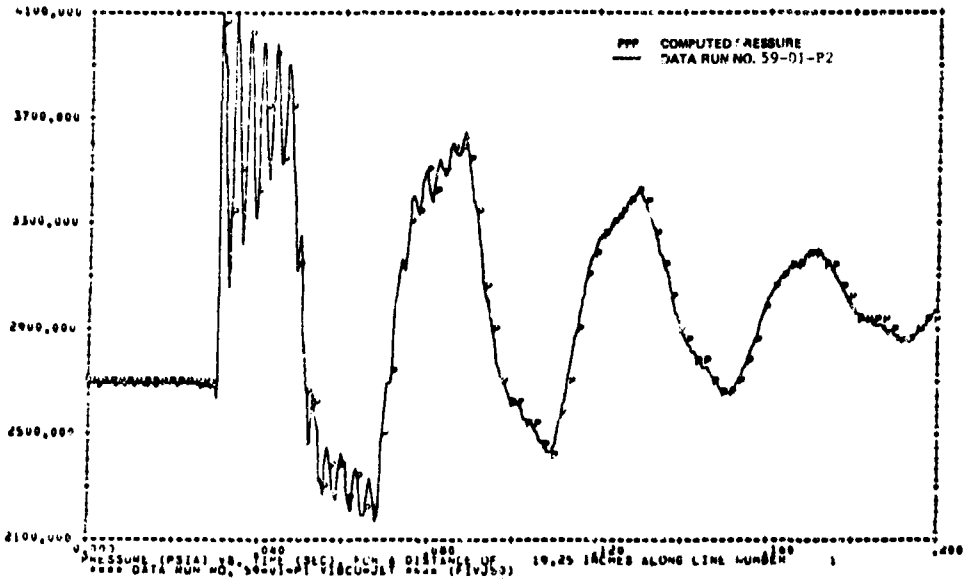

FIGURE 245 59-01-P2 TURN-OFF TRANSIENT

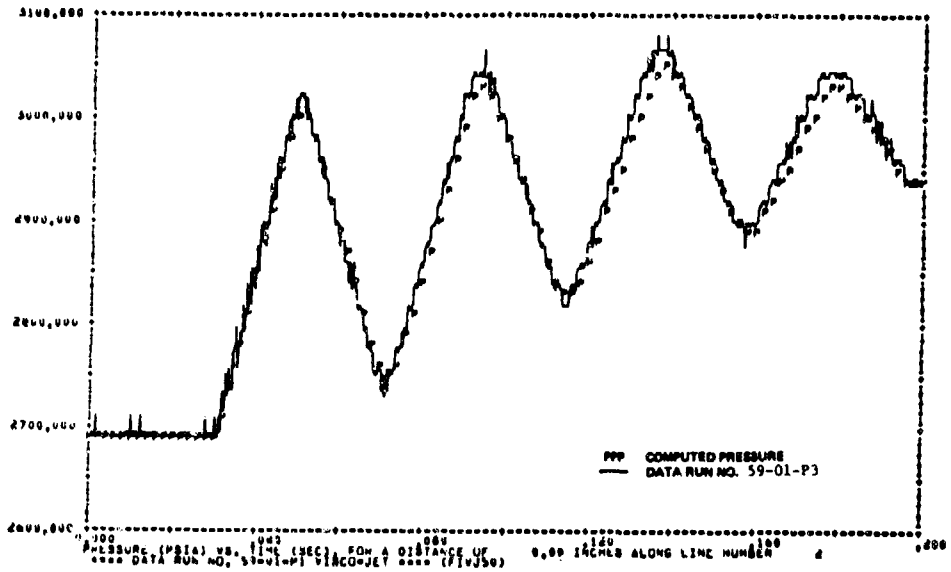

FIGURE 246 59-01-P3 TURN-OFF TRANSIENT

There was also no appreciable attenuation effects through the Visco Jet as was initially suspected. This can be seen in Figure 246 which was downstream of the Visco Jet. The Visco Jet appears to behave the same way transiently as the simple Lee Jet with the orifice.

A turn-on transient at 125°F and 38.5 CIS was simulated with the computer program using the data input from Figure 247 and the computer input information given in Figure 248. The output pressures and flows are shown in Figures 249, 250 and 251. The pressure data indicates good correlation with the computer output plots. The maximum pressure reached upstream of the Visco Jet was about 3200 psi as shown in Figure 249.

b. Observations - To show the relative phase relationship between the input and output pressures of a Lee Jet, P2 and P3 were plotted versus time in Figure 252. The data run plotted was a turn-off transient at 125°F and 38.5 CIS. The plot shows that over a 180° cycle of P2 the P3 pressure just rises, while during the next 180° of P2, where P2 falls then rises, the P3 pressure just falls.

Plot of P2 over P3 for a turn-on transient follow exactly the same relationships as well as P2 and P3 plots for the Lee Visco jet.

c. Conclusions - The HYTRAN restrictor model (subroutine REST41) calculations of pressures compare reasonably well with the test data measured in the lab. The results indicate that the restrictor model is relatively good.

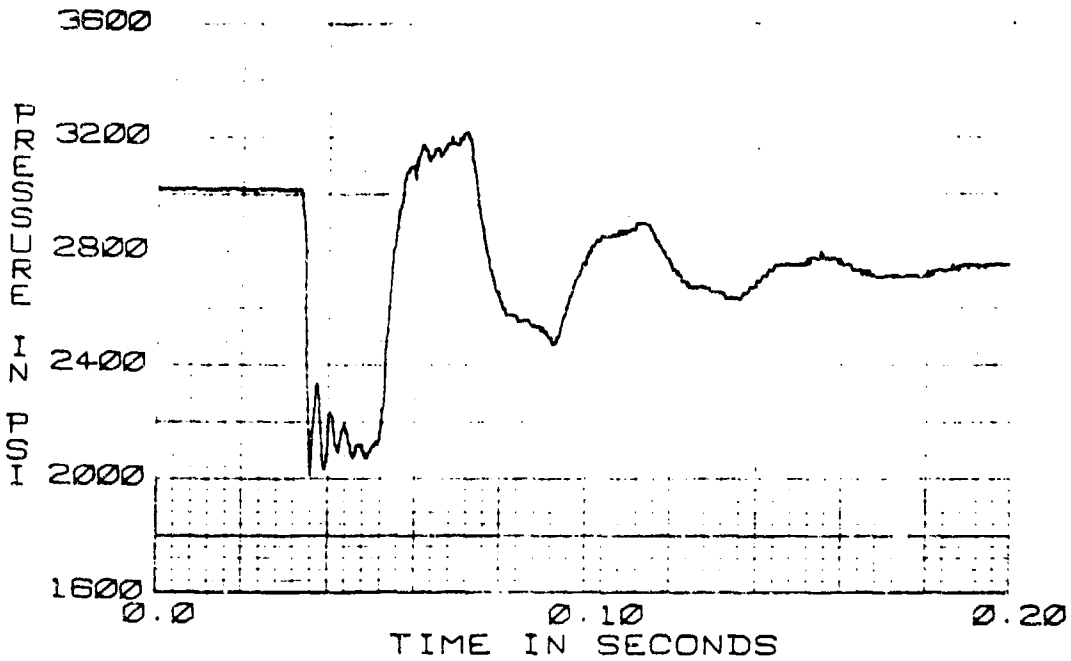

FIGURE 247 LEE VISCO JET .031 IN DIA.
59-01-P1 TURN-ON TRANSIENT
38.5 CIS 125°F

**** DATA RUN 00, 59-01-P1 VISCO-JET **** (FIVJ51)

THE TRANSIENT RESPONSE IS FROM 0.0 TO T= .200 SECONDS AT TIME INTERVALS OF DELT= .00020
WITH OUTPUT POINTS PLOTTED AT INTERVALS OF .00200 SECONDS

FLUID DATA FOR MIL-H-5606 AT 3000.0 PSIG, & 50.0 PSIG AND 125.0 DEG F IN 10.0 DEG F STEPS

VISCOSITY = .201E-01 .158E-01LBF-SEC/IN**2
DENSITY = .814E-04 .805E-04(LB-SEC**2)/IN**4
BULK MODULUS = .226E+06 .191E+06PSI
VAPOUR PRESS.= .20UE+01 AT 125.0 DEG F

LINE DATA LINE NO.	LENGTH	INTERNAL DIA	WALL THICKNESS	MODULUS OF ELASTICITY	DELR	CHARACTERISTIC IMPEDANCE	VELOCITY OF SOUND
1	14.2500	.0440	.0209	.30UE+08	14.2500	28.1911	49818.0265
2	41.2500	.0440	.0280	.3)[illegible]E+08	14.0250	28.1911	49819.0265

COMPR. 1 INTEGER DATA 1 01 0 -1 1 -0 -0 -0 -0 -0 -0 -0 -0 -0 -0 -0 -0
COMPR. 2 INTEGER DATA 2 01 1 1 -2 -0 -0 -0 -0 -0 -0 -0 -0 -0 -0 -0 -0
REAL DATA CARD # 1 .9450E-02 .9080E+00 -0. -0. -0. -0. -0. -0. -0.
COMPR. 3 INTEGER DATA 3 11 0 2 -0 -0 -0 -0 -0 -0 -0 -0 -0 -0 -0 -0

FIGURE 248 RUN 59-01 HYTRAN INPUT DATA FOR LEE VISCO JET

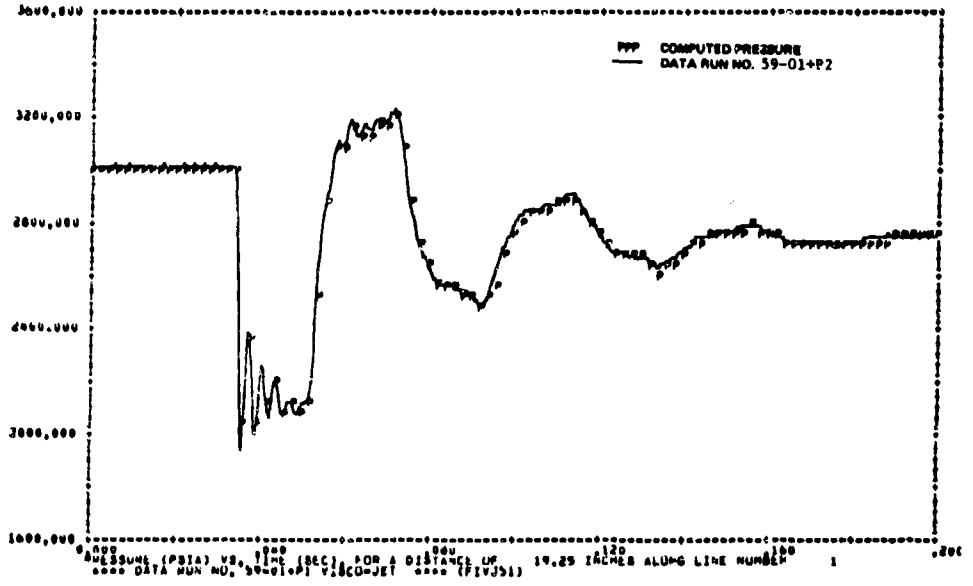

FIGURE 249 59-01+P2 TURN-ON TRANSIENT

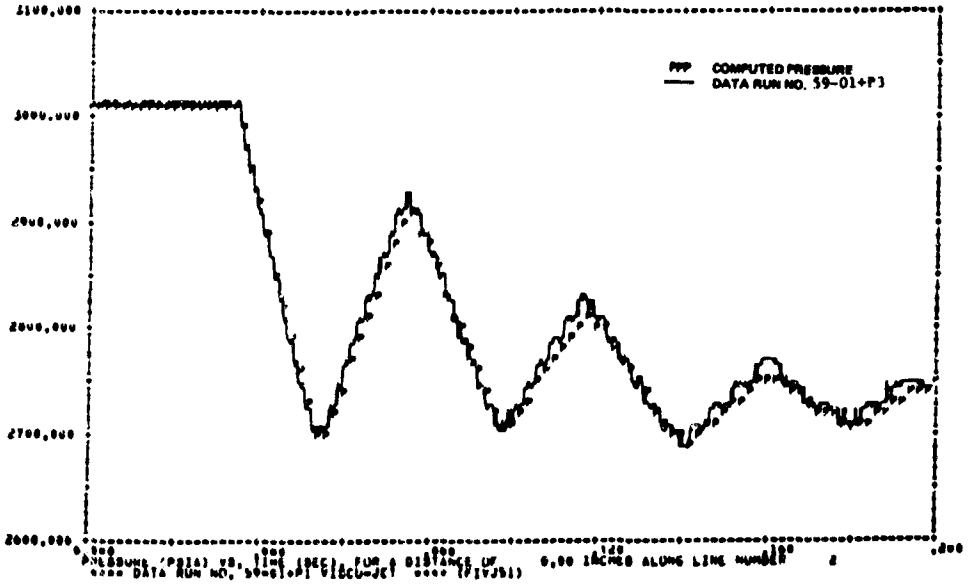

FIGURE 250 59-01+P3 TURN-ON TRANSIENT

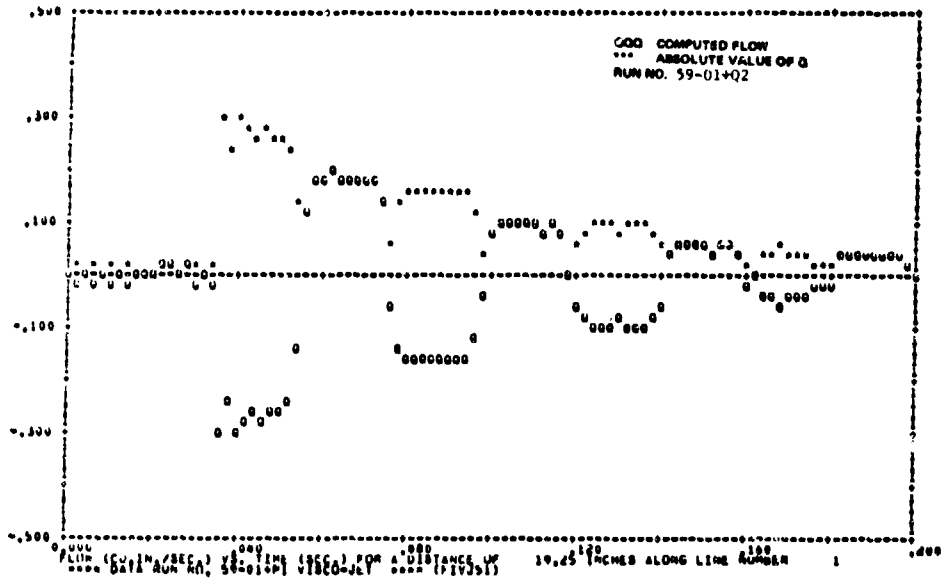

FIGURE 251 59-01+Q2 TURN-ON TRANSIENT

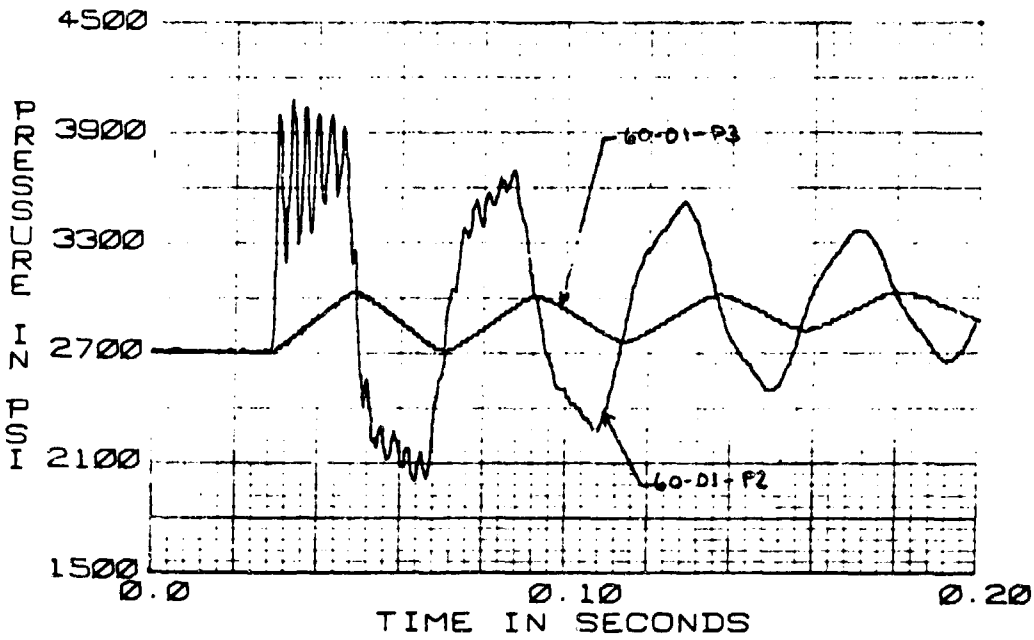

FIGURE 252 COMPARISON BETWEEN P2 AND P3 FOR A LEE JET .009 IN DIA. TURN-OFF TRANSIENT

7. ONE-WAY RESTRICTOR MODEL VERIFICATION

This section test results obtained in the laboratory on an F-15 system type restrictor (CONAIR PN 286-5590-105) are compared to the HYTRAN computer program one-way restrictor subroutine CVAL33. The testing was performed on a 1/2 inch system with MIL-H-5606B hydraulic fluid.

The restrictor's configuration and dimensions are shown in Figure 253.

The CVAL33 subroutine models a simple undamped one-way restrictor. The check valve portion of the restrictor is assumed to have a variable orifice characteristic between the fully open and fully closed positions. Some reverse flow can take place transiently through the orifice when the valve closes.

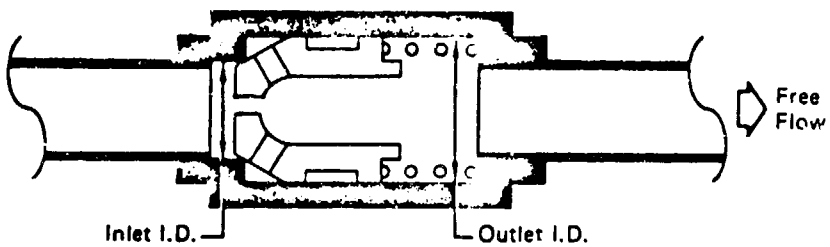

FIGURE 253 TYPE 33 ONE-WAY RESTRICTOR

The model used to calculate the steady state pressure drop assumes a straight line flow pressure drop characteristic between the cracking pressure and the fully open position. In the transient analysis the flow through the valve is computed using a parallel orifice arrangement. The flow through the valve area is proportional to the valve displacement and the flow through the orifice is proportional to the orifice diameter and discharge coefficient.

The restrictor test series was run on the system configuration shown in Figure 254.

The following parameters were recorded in the laboratory for the test runs: P_1, P_2, Q_2, P_3, P_4, Q_3 and valve position. P_1, P_3, P_4 and Q_3 were recorded directly onto cassette tape.

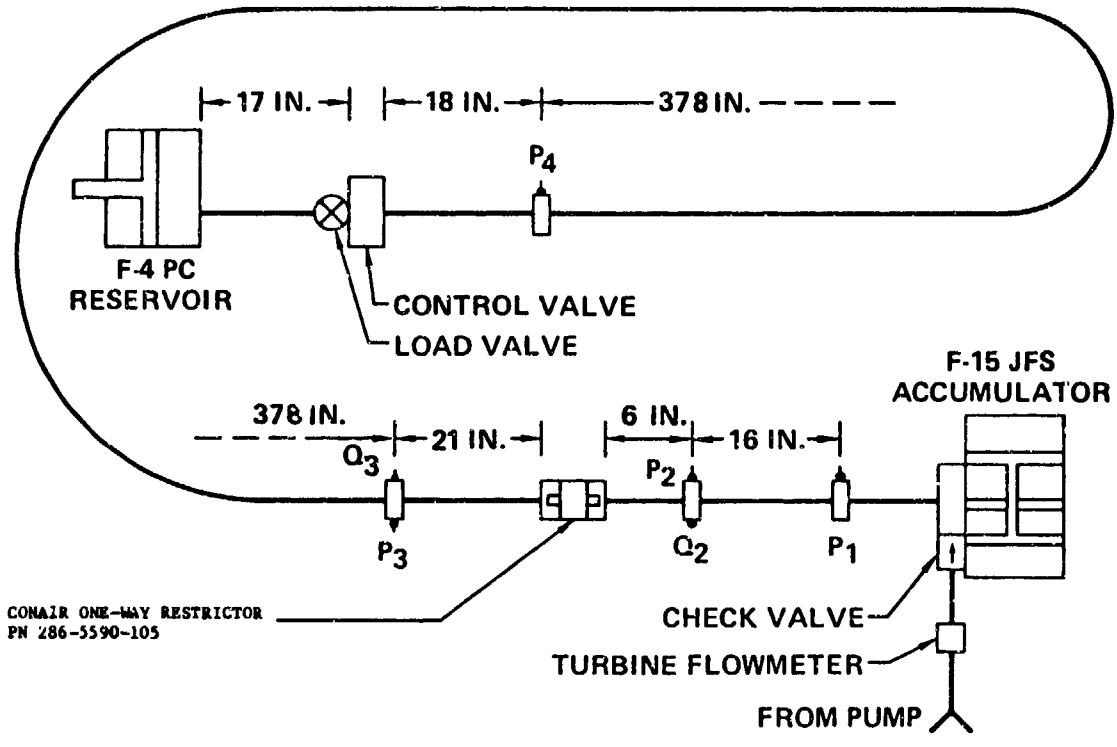

FIGURE 254 TRANSIENT TEST CONFIGURATION FOR ONE-WAY RESTRICTOR

a. Computer Simulation with One-Way Restrictor Test Data

The first data run of the CONAIR one-way restrictor to be compared to a computer run was for a turn-off transient at 130°F and 38.5 CIS. The valve closing time was determined from the P_4 pressure data and the acoustic velocity in the tube. The data from Figure 255 was input into the computer program with the input data shown in Figure 256. The results are shown over plotted with data in Figure 257, 258, 259 and 260.

The one-way restrictor is installed so that the flow is in the restricted direction, thus in Figures 257 and 258 the pressure drop across the restrictor is over 300 PSI.

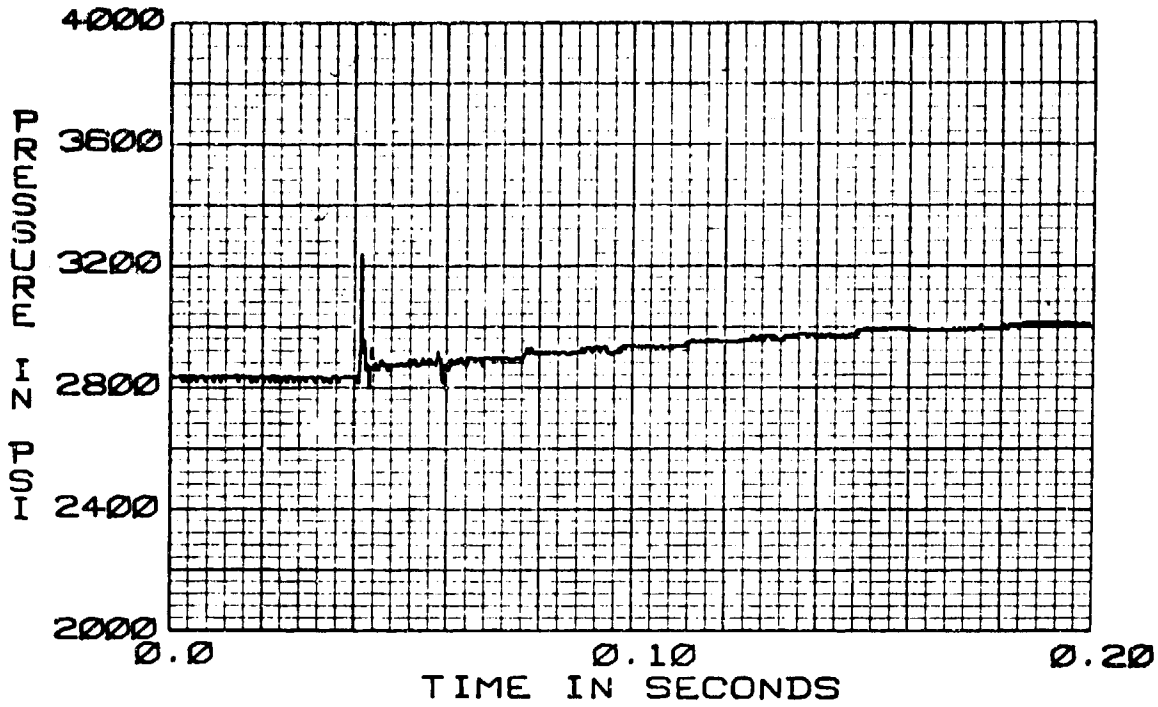

FIGURE 255 CONAIR 5590-105 F-15 RESTRICTOR
56-01-P1 TURN-OFF TRANSIENT
38.5 CIS 130°F

**** DATA RUN NO. 56-01-P1 RESTRICTOR **** (FIRS42)

THE TRANSIENT RESPONSE IS FROM T=0.0 TO T= .200 SECONDS AT TIME INTERVALS OF DELT= .00020
WITH OUTPUT POINTS PLOTTED AT INTERVALS OF , .00200 SECONDS

FLUID DATA FOR MIL-H-5606 AT 3000.0 PSIG, - 50.0 PSIG AND 130.0 DEG F IN 10.0 DEG F STEPS

VISCOSITY	= .186E-01	.148E-01LN**2/SEC
DENSITY	= .813E-04	.803E-04(LB-SEC**2)/IN**4
BULK MODULUS	= .223E+06	.187E+06PSI
VAPOUR PRESS.	= .200E+01 AT 130.0 DEG F	

LINE DATA LINE NO.	LENGTH	INTERNAL DIA	WALL THICKNESS	MODULUS OF ELASTICITY	DELX	CHARACTERISTIC IMPEDANCE	VELOCITY OF SOUND
1	21.6250	.4440	.0280	.300E+08	10.8125	25.9624	49460.3746
2	416.6250	.4440	.0280	.300E+08	9.9196	25.9624	49460.3746
3	17.0000	.4440	.0280	.300E+08	17.0000	25.9624	49460.3746

COMP#, 1 INTEGER DATA 1 91 0 -1 1 -0 -0 -0 -0 -0 -0 -0 -0 -0 -0 -0

COMP#, 2 INTEGER DATA 2 33 1 -2 1 1 -0 -0 -0 -0 -0 -0 -0 -0 -0 -0

REAL DATA CARD # 1 .3950E+00 .7870E+00 .9060E-04 .2024E+01 .1470E+00 .9149E+00 .1435E+00 .8900E+00

COMP#, 3 INTEGER DATA 3 21 3 2 -3 -0 -0 -0 -0 -0 -0 -0 -0 4 -0 -0

REAL DATA CARD # 1 .2200E-01 .8500E+00 -0. -0. -0. -0. -0. -0.

REAL DATA CARD # 2 0. .3120E-01 .3320E-01 .2000E+00 -0. -0. -0. -0.

REAL DATA CARD # 3 .3320E+00 .3320E+00 0. 0. -0. -0. -0. -0.

COMP#, 4 INTEGER DATA 4 61 1 3 -0 -0 -0 -0 -0 -0 -0. -0 -0 -0 -0 -0

REAL DATA CARD # 1 .9000E+02 -0. -0. -0. -0. -0. -0. -0.

FIGURE 256 RUN 56-01 HYTRAN INPUT DATA FOR A TURN-OFF TRANSIENT

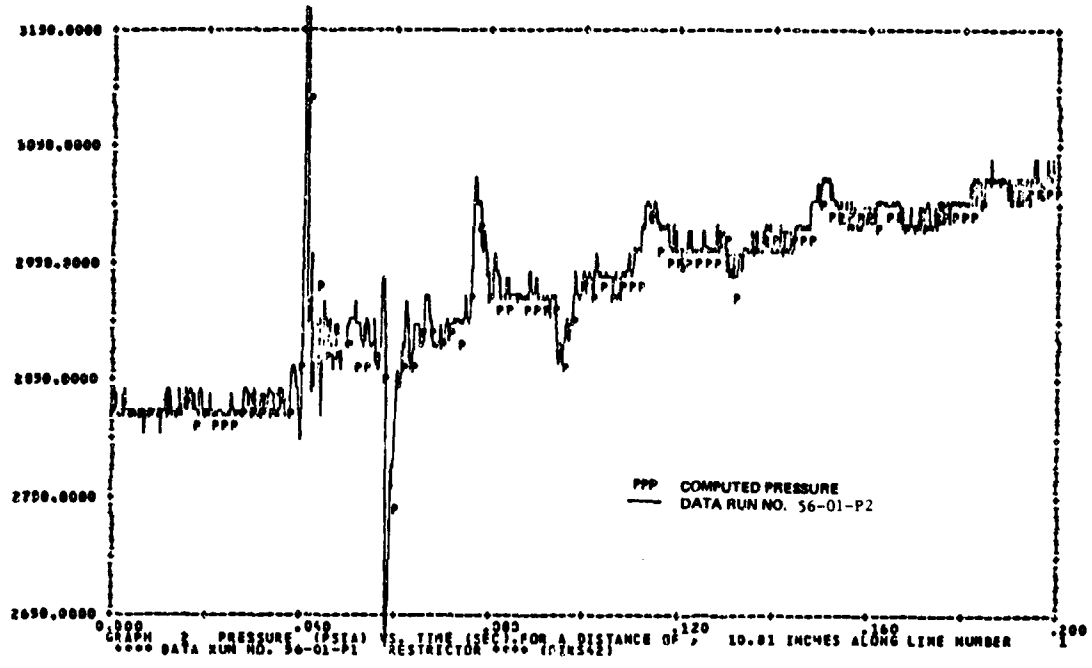

FIGURE 257 56-01-P2 TURN-OFF TRANSIENT

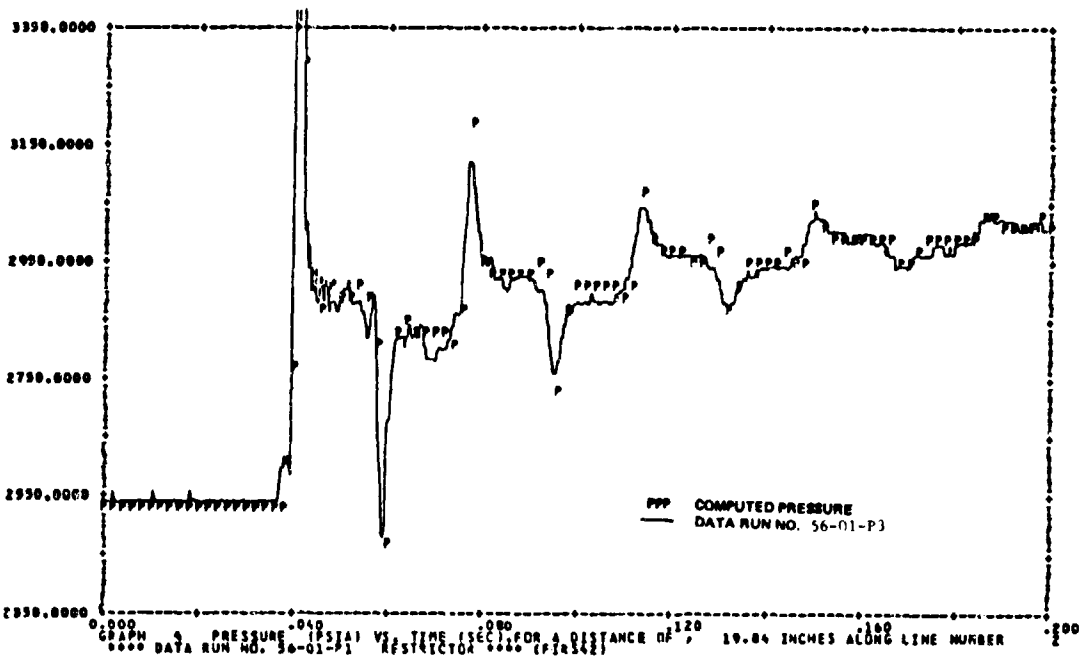

FIGURE 258 56-01-P3 TURN-OFF TRANSIENT

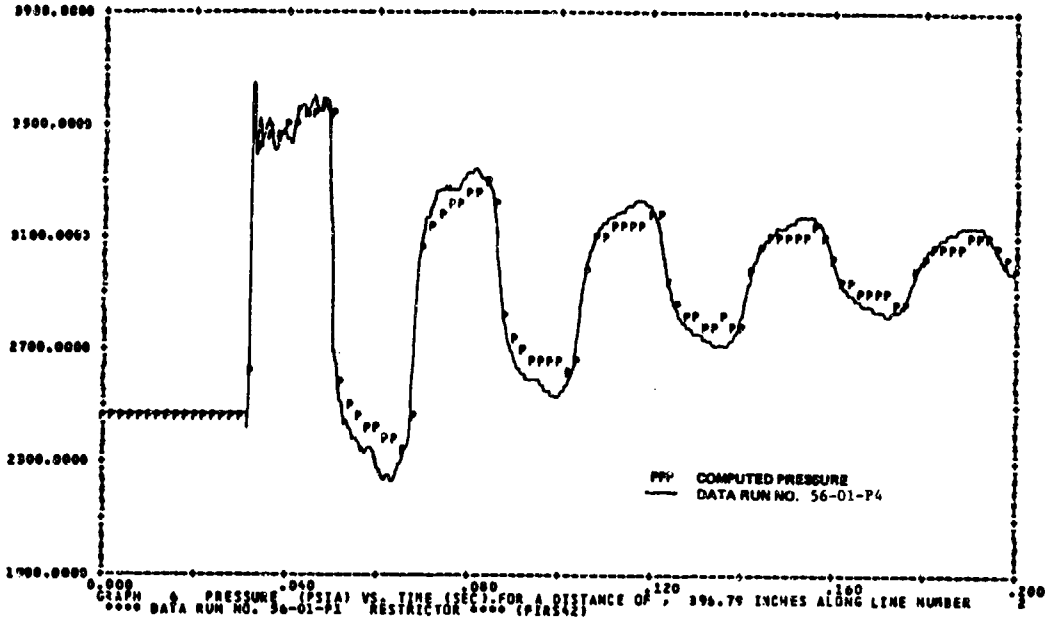

FIGURE 259 56-01-P4 TURN-OFF TRANSIENT

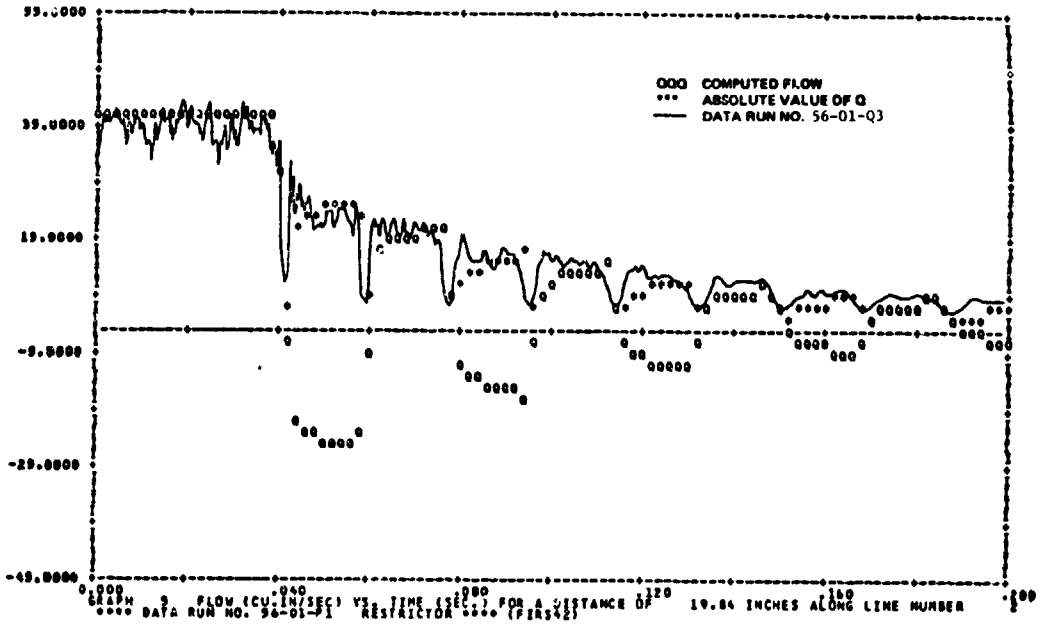

FIGURE 260 56-01-03 TURN-OFF TRANSIENT

Figure 259 is a plot of the P4 data over the computer predicted pressure at the P4 position 18 inches upstream of the control valve. The computer results indicate good correlation with the test data. Figures 257 and 258 on either side of the restrictor also show favorable comparisons. The computed maximum value for the first peak pressure is not plotted in Figures 257 and 258. For this HYTRAN program output only one point is plotted for every ten that are calculated. The test data indicates a max value because all the sampled data points are plotted. For Figure 258 the computed max value was 3550 PSI. The measured value was 3660 PSI.

The restrictor model does not account for displacement flow due to poppet motion, variations in orifice characteristics with poppet position, or secondary pressure drops due to other flow restrictions. Axial flow forces however are included in the one-way restrictor model. The net axial force is computed as:

$$F_A = 2*C_d*\Delta P*ARFAC \quad (1)$$

where

C_d = discharge coefficient for valve slot width (.65 assumed)

ΔP = pressure drop across the poppet

ARFAC = area subjected to flow forces

The computer output flow plot is shown in Figure 260 with the data run plotted over it.

The HYTRAN computer simulation of a turn-on transient at 125°F and 38.5 CIS was run using the input data of Figure 261 and system data from Figure 262. The computer output graphs of pressure overplotted with the test data are shown in Figures 263, 264 and 265.

The computer results correlate well with the test data for both up and downstream of the one-way restrictor. The P2 test data is considerably noisier than the other pressure data because it was played back from an analog tape unit.

The computer calculated flow plot is shown in Figure 266 plotted over the data run. The test data for the initial flow peak does not reach the predicted results. This discrepancy exists because the anemometer does not measure the bulk or average flow in the tube but only local velocity.

c. Conclusions - The HYTRAN one-way restrictor model (subroutine CVAL33) calculations of pressures and flows compare reasonably well with the test data measured in the lab. A few discrepancies exist between the data and mathematically predicted results as already noted. The results indicate that the model is adequate for the conditions tested.

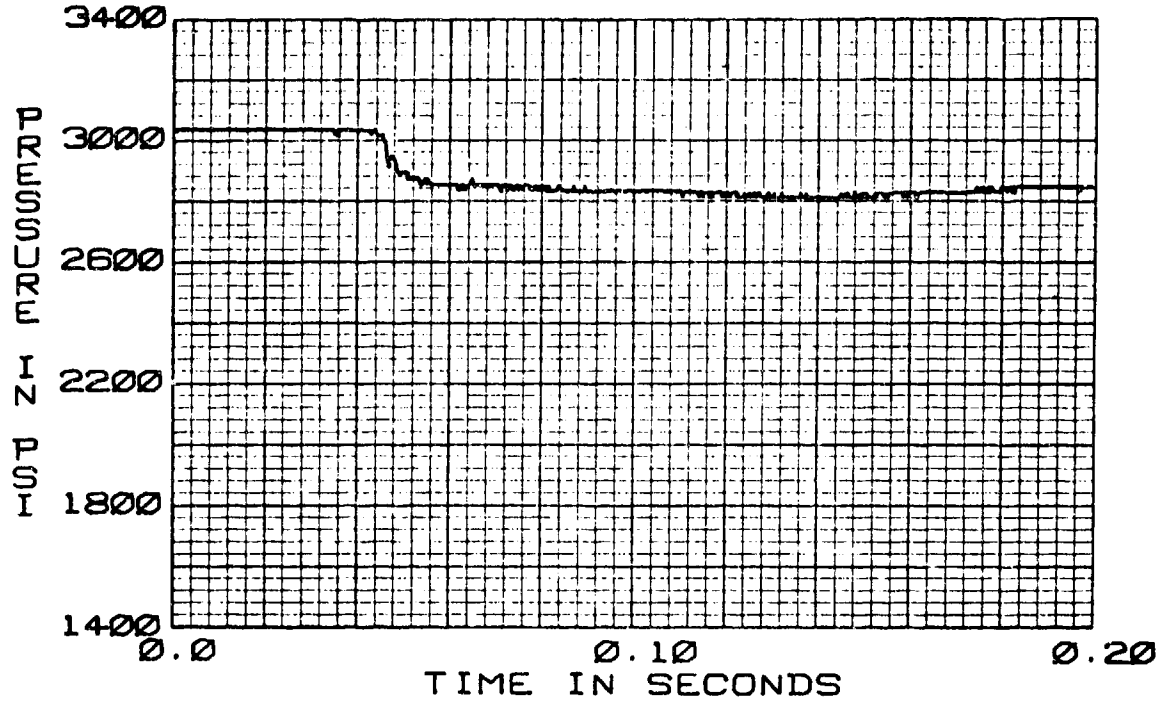

FIGURE 261 CONAIR 5590-105 F-15 RESTRICTOR
56-01+P1 TURN-ON TRANSIENT
38.5 CIS 125°F

```
**** DATA RUN NO. 56-01+P1   RESTRICTOR **** (FIRS43)

THE TRANSIENT RESPONSE IS FROM T=0.0  TO T=  .200 SECONDS AT TIME INTERVALS OF DELT= .00020

WITH OUTPUT POINTS PLOTTED AT INTERVALS OF  =  .00200  SECONDS

FLUID DATA FOR  MIL-H-5606  AT  3000.0 PSIG, -   90.0 PSIG AND 125.0 DEG F  IN  10.0 DEG F STEPS
                VISCOSITY   = .198E-01      .158E-01IN**2/SEC
                DENSITY     = .814E-04      .805E-04LB-SEC**2/IN**4
                BULK MODULUS = .226E+06     .191E+06PSI
                VAPOUR PRESS.= .200E+01 AT  125.0 DEG F

LINE DATA
LINE NO.    LENGTH      INTERNAL DIA    WALL THICKNESS   MODULUS OF ELASTICITY   DELR        CHARACTERISTIC IMPEDANCE   VELOCITY OF SOUND
   1        21.6250       .4440           .0280            .300E+08            10.8125        26.1653                49761.3594
   2       416.6250       .4440           .0280            .300E+08            10.1616        26.1653                49761.3594
   3        17.0000       .4440           .0280            .300E+08            17.0000        26.1653                49761.3594
 COMP#,  1 INTEGER DATA     1  91   0  -1   1  -0  -0  -0  -0  -0  -0  -0  -0  -0  -0  -0
 COMP#,  2 INTEGER DATA     2  33   1  -2   1   1  -0  -0  -0  -0  -0  -0  -0  -0  -0  -0
REAL DATA CARD #   1    .3950E+00  .7270E+00  .9060E-04  .2024E+01  .1470E+00  .9149E+00  .1939E+00  .8900E+00
 COMP#,  3 INTEGER DATA     3  21   3   2  -3  -0  -0  -0  -0  -0  -0  -0  -0   4  -0  -0
REAL DATA CARD #   1    .2200E-01  .6500E+00 -0.        -0.        -0.        -0.        -0.        -0.
REAL DATA CARD #   2    0.         .3700E-01  .3900E-01  .2000E+00 -0.        -0.        -0.        -0.
REAL DATA CARD #   3    0.         0.         .8320E+00  .8320E+00 -0.        -0.        -0.        -0.
 COMP#,  4 INTEGER DATA     4  61   1   3  -0  -0  -0  -0  -0  -0  -0  -0  -0  -0  -0  -0
REAL DATA CARD #   1    .9000E+02 -0.        -0.        -0.        -0.        -0.        -0.        -0.
```

FIGURE 262 RUN 56-01 HYTRAN INPUT DATA FOR A TURN-ON TRANSIENT

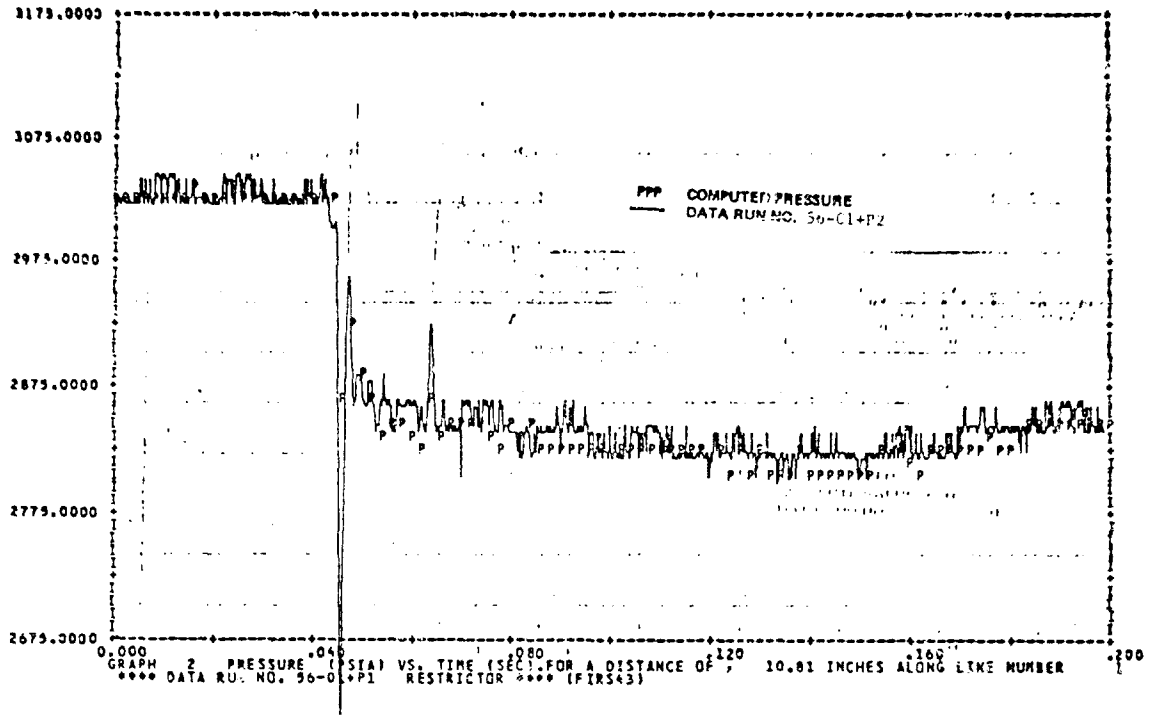

FIGURE 263 56-01+P2 TURN-ON TRANSIENT

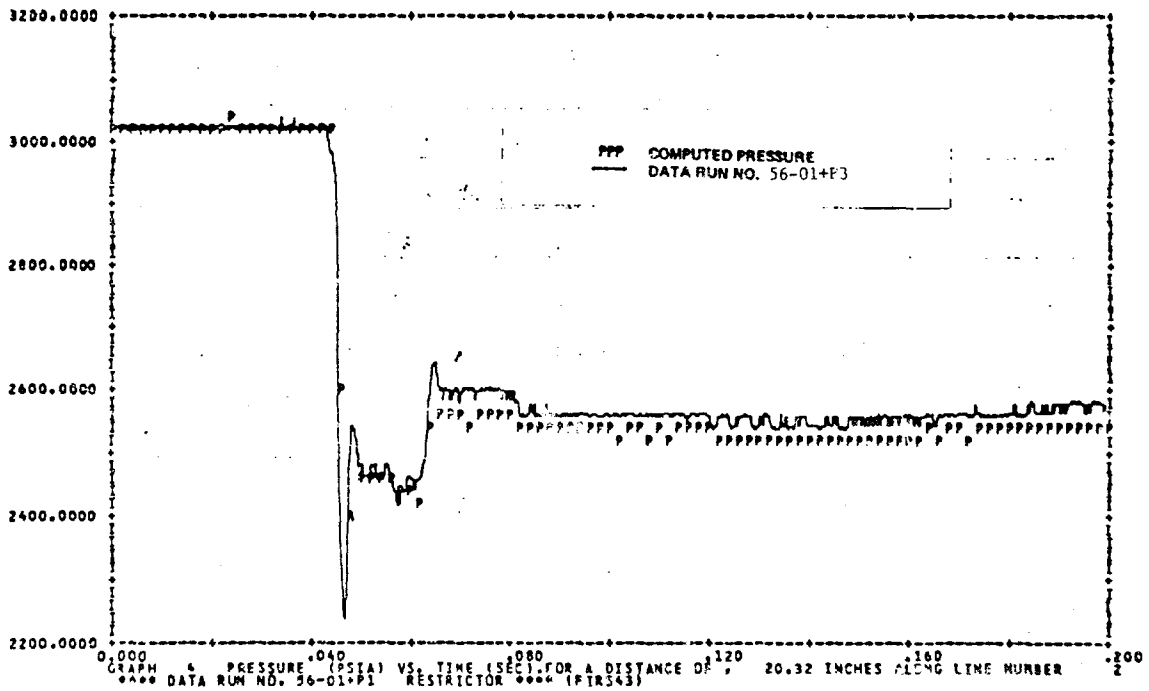

FIGURE 264 56-01+P3 TURN-ON TRANSIENT

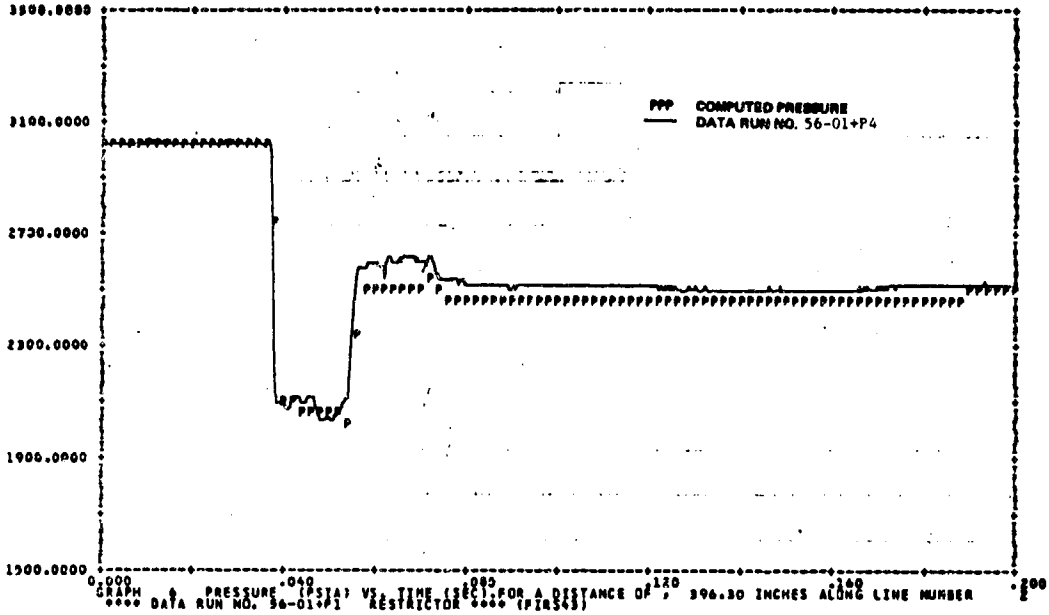

FIGURE 265 56-01+P4 TURN-ON TRANSIENT

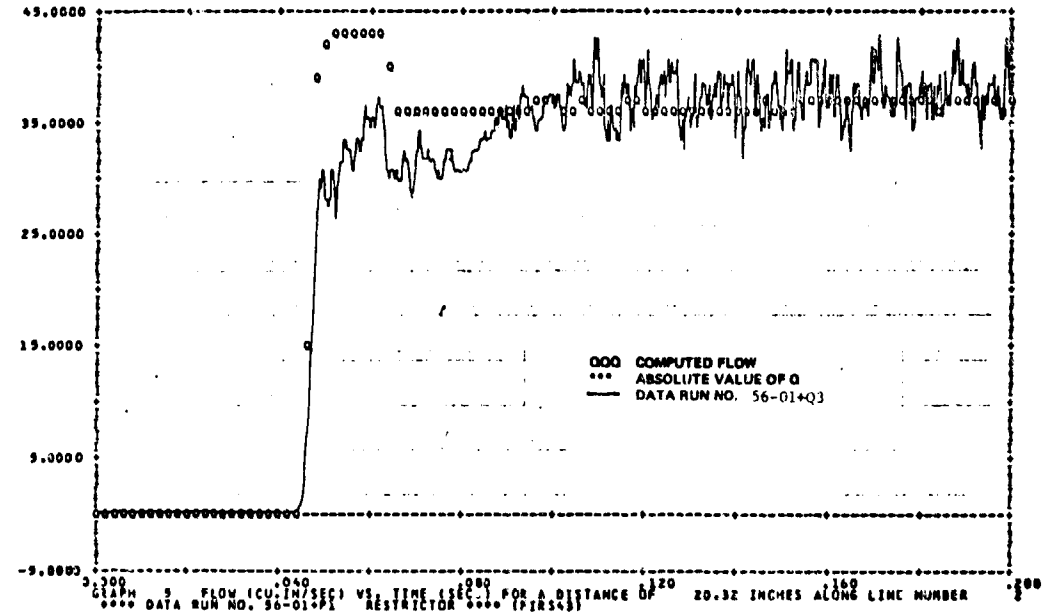

FIGURE 266 56-01+Q3 TURN-ON TRANSIENT

8. HOSE MODEL VERIFICATION

The test results obtained in the laboratory on a 1/4" and 5/8" flexible hose are compared to the HYTRAN computer program hose model in the line subroutine. The testing was performed on a 1/2 inch system with MIL-H-5606B hydraulic fluid.

The hose model is incorporated as part of the line subroutine in the HYTRAN program. The line subroutine uses the classical distributed parameter wave equations to model the lines and hoses. The equations are solved using the method of characteristics and finite difference techniques.

In the line subroutine, an effective bulk modulus is computed for the hose combining both hose and fluid characteristics. The effective bulk modulus is calculated from the following equation:

$$\frac{1}{BULK_e} = \frac{1}{BULK_{hose}} + \frac{1}{BULK_{oil}} \qquad (1)$$

The velocity of sound in the hose is then computed using $BULK_e$. The $BULK_e$ and velocity of sound calculation are the basic differences between the line and hose models in the line subroutine.

The hose test series was run on the system configuration shown in Figure 267.

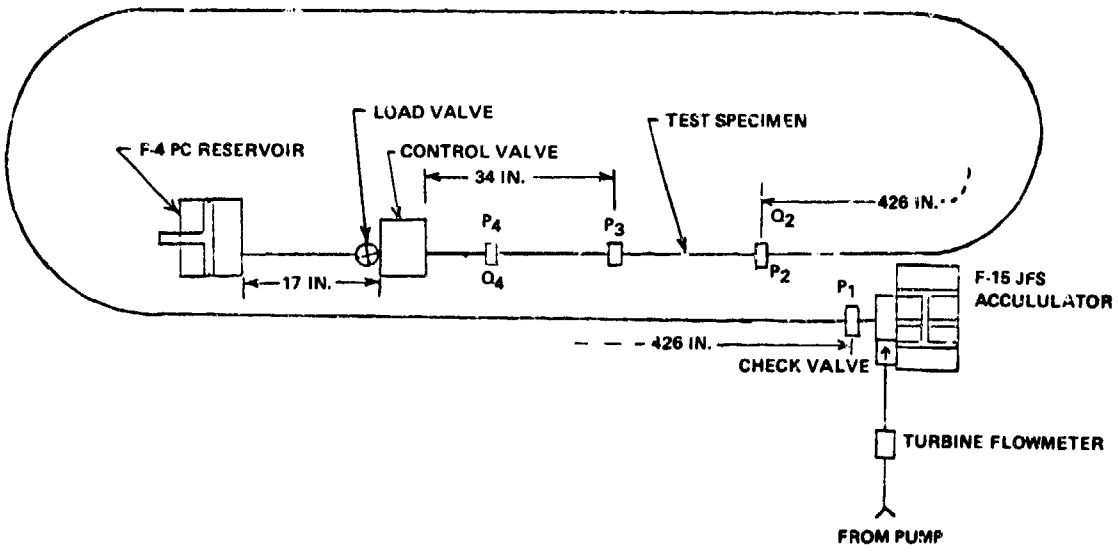

FIGURE 267 TRANSIENT TEST CONFIGURATION FOR 1/4 IN. AND 5/8 IN. FLEXIBLE HOSES

The following parameters were recorded in the laboratory for the test runs: P_1, P_2, Q_2, P_3, P_4, Q_4 and valve position. P_1, P_3, P_4 and Q_4 were recorded directly onto cassette tape.

The test conditions are shown in Table 13.

TABLE 13 TEST CONDITIONS FOR 1/4 IN. AND 5/8 IN. STEEL BRAIDED TEFLON HOSES

Test Specimen	Run #	Flow Condition	Flow Rate (CIS)	Temp (Deg F)
1/4" Dia x 22" LG, steel braided Teflon hose P/N 730900-4-0240	57-01-XX*	Turn-Off	38.5	130
	57-01+XX	Turn-On	38.5	130
	57-02-XX	Turn-Off	11.55	130
	57-02+XX	Turn-On	11.55	125
	57-05-XX	Turn-Off	38.5	210
	57-05+XX	Turn-On	38.5	210
	57-06-XX	Turn-Off	11.55	210
	57-06+XX	Turn-On	11.55	210
5/8" dia x 24" Lg Steel Braided Teflon Hose P/N 730900-10-0240	58-01-XX	Turn-Off	38.5	125
	58-01+XX	Turn-On	38.5	125
	58-02-XX	Turn-Off	11.55	125
	58-02+XX	Turn-On	11.55	125
	58-05-XX	Turn-Off	38.5	210
	58-05+XX	Turn-On	38.5	210
	58-06-XX	Turn-Off	11.55	210
	58-06+XX	Turn-On	11.55	210

* - XX denotes measured data parameters

a. Computer Simulation with Hose Test Data - A turn-off transient in a 1/2" system with a 1/4" dia x 19" long steel braided teflon hose was simulated using the data of Figure 268 and the input data in Figure 269. The HYTRAN program conditions were set at 38.5 CIS and 130°F. The computer output pressures and flows are shown in Figures 270, 271, 272 and 273.

The data in Figure 270 was recorded approximately 19" upstream of the 1/4" hose. The computer results indicate good amplitude correlation with the data. However the predicted frequency of the decaying pressure waveform is slightly less than the data frequency. In Figure 270 at 0.2 sec the computer results are in error by about 6 milliseconds. The computer predicted data in Figure 271 immediately downstream of the 19" long hose and Figure 272, 17" downstream of the hose indicate the same results.

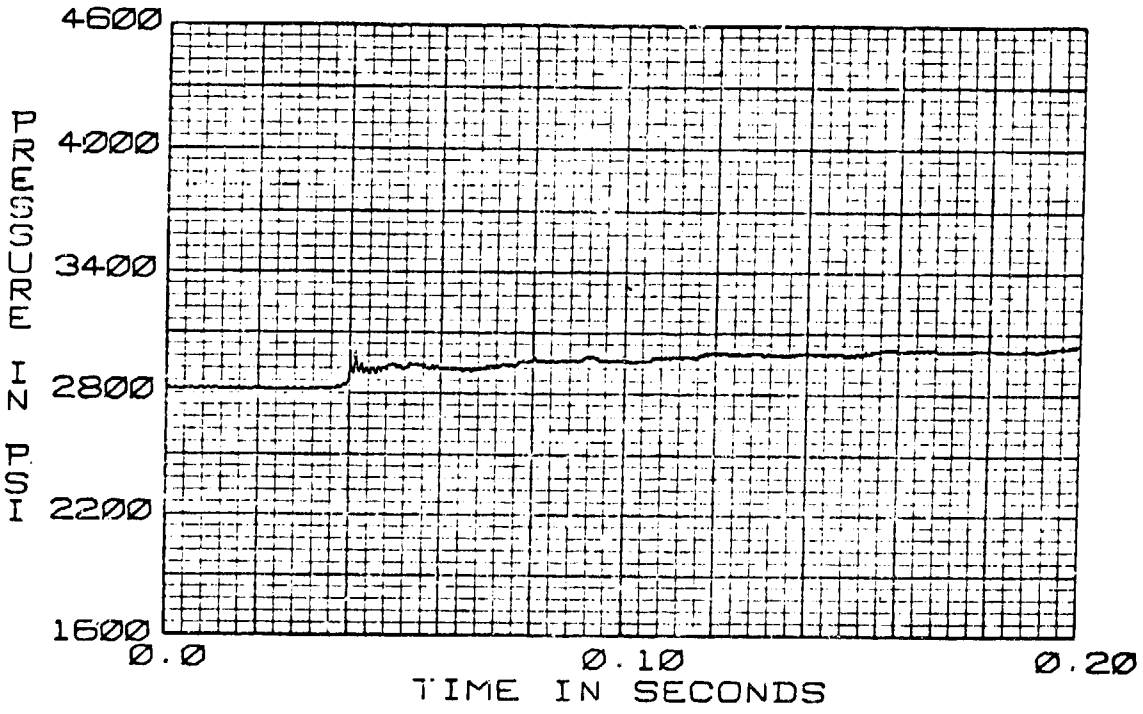

FICURE 268 .25 IN. STEEL BRAIDED HOSE
57-01-P1 TURN-OFF TRANSIENT
38.5 CIS 130°F

**** DATA RUN NO. 57-01-P1 1/4 INCH HOSE **** (FI4H648)

THE TRANSIENT RESPONSE IS FROM T=0.0 TO T= .280 SECONDS AT TIME INTERVALS OF DELT= .00020
WITH OUTPUT POINTS PLOTTED AT INTERVALS OF , .00200 SECONDS

FLUID DATA FOR MIL-H-5606 AT 3000.0 PSIG, 90.0 PSIG AND 130.0 DEG F IN 10.0 DEG F STEPS

VISCOSITY	.106E-01	.148E-01LB**2/SEC
DENSITY	.813E-04	.803E-04(LB-SEC**2)/IN**4
BULK MODULUS	.223E+06	.167E+06PSI
VAPOUR PRESS.	.200E+01 AT	140.0 DEG F

LINE DATA LINE NO.	LENGTH	INTERNAL DIA	WALL THICKNESS	MODULUS OF ELASTICITY	DELX	CHARACTERISTIC IMPEDANCE	VELOCITY OF SOUND
1	428.1298	.4440	.0280	.300E+08	9.9964	25.9624	49460.3746
2	19.0000	.1956	.1510	.760E+07	6.3333	72.6922	28771.8316
3	36.1253	.4440	.0280	.300E+08	12.0417	25.9624	49460.3746
4	17.3000	.4440	.0280	.300E+08	17.0000	25.9624	49460.3746

COMP., 1 INTEGER DATA 1 91 8 -1 1 -0 -0 -0 -0 -0 -0 -0 -0 -0 -2 -0

COMP., 2 INTEGER DATA 2 21 3 1 -4 -0 -0 -0 -0 -0 -0 -0 -0 4 -0 -0

REAL DATA CARD + 1 .2200E-01 .6900E+00 -0. -0. -0. -0. -0. -0.

REAL DATA CARD + 2 0. .2860E-01 .2900E-01 .2000E+00 -0. -0. -0. -0. -0.

REAL DATA CARD + 3 .3038E+00 .3038E+00 0. 0. -0. -0. -0. -0.

COMP., 3 INTEGER DATA 3 61 1 4 -0 -0 -0 -0 -0 -0 -0 -0 -0 -0 -0 -0

REAL DATA CARD + 1 .5000E+02 -0. -0. -0. -0. -0. -0. -0.

FIGURE 269 RUN 57-01 HYTRAN INPUT DATA FOR TURN-OFF TRANSIENT

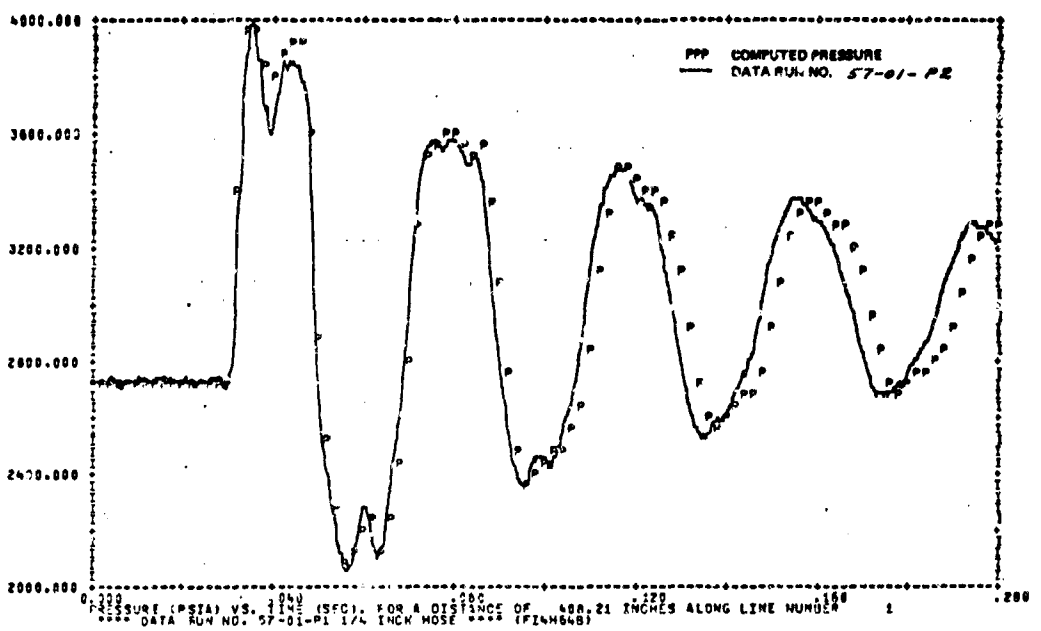

FIGURE 270 57-01-P2 TURN-OFF TRANSIENT

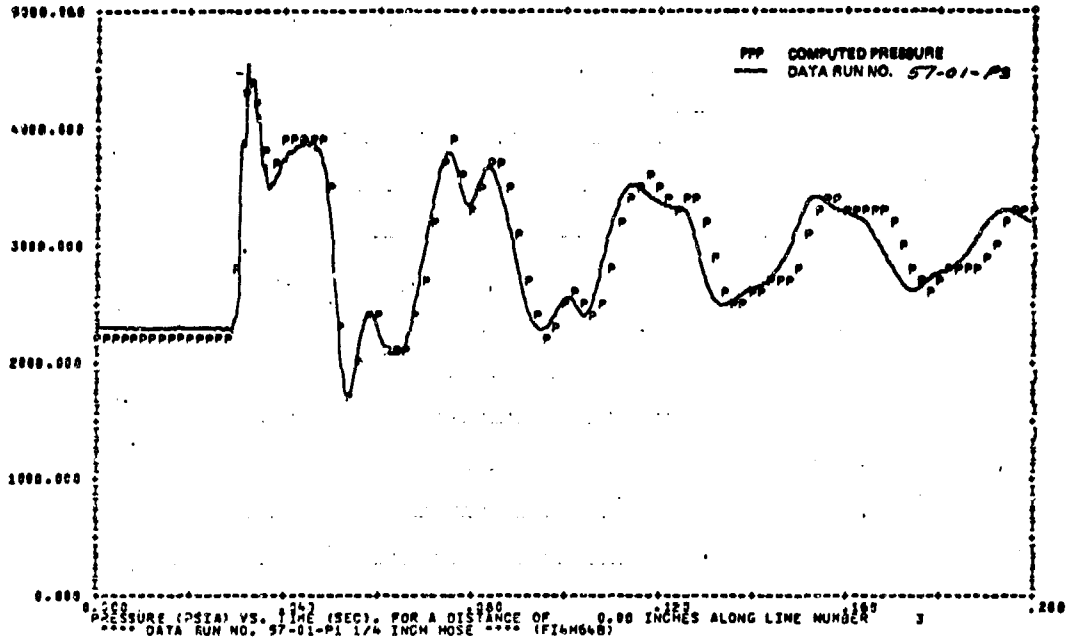

FIGURE 271 57-01-P3 TURN-OFF TRANSIENT

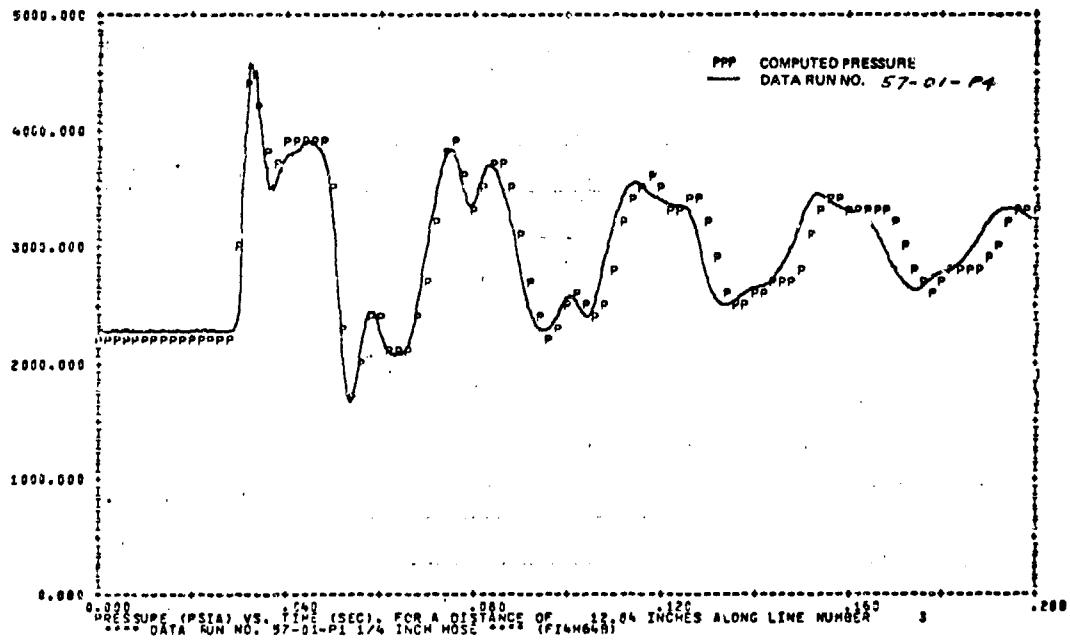

FIGURE 272 57-01-P4 TURN-OFF TRANSIENT

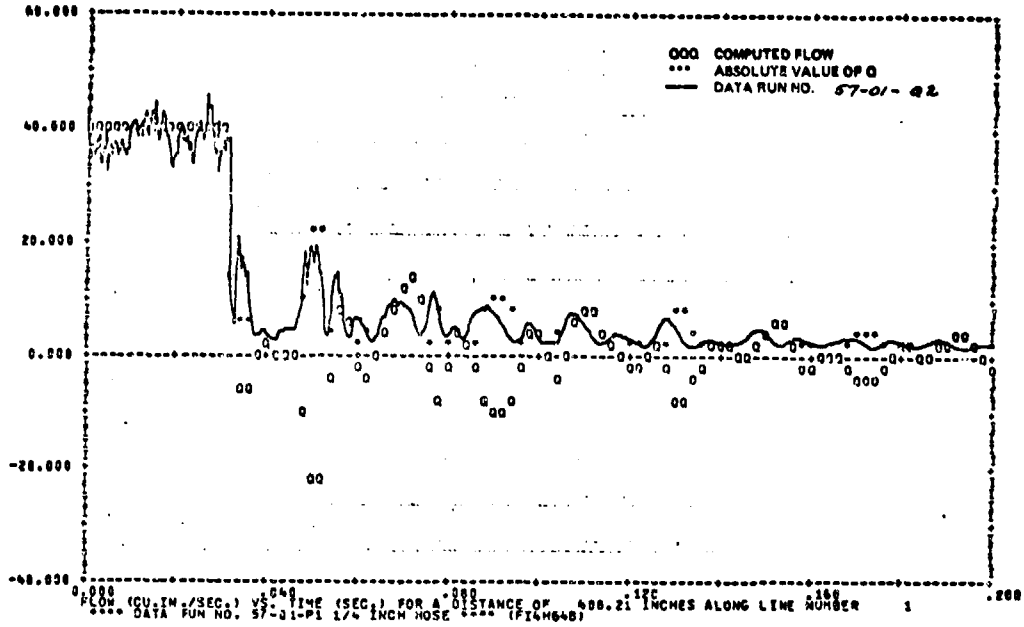

FIGURE 273 57-01-Q2 TURN-OFF TRANSIENT

The source of this discrepancy in frequency may be attributable to the lack of appropriate turbulent damping characteristics in the dynamic friction subroutine DFRICD. Since little is known about the effects of dynamic friction under turbulent flow conditions, DFRICD uses the same equations to calculate turbulent as well as laminar flow pressure drops under dynamic conditions. A computer run was made to determine the effect of leaving the turbulent pressure drop update out of the simulation. Figure 274 shows a minor increase in the amplitude of the decaying waveform and a slight increase in the computer predicted frequency. Figures 275 and 276 indicate the same results. A better update for dynamic losses under turbulent conditions would improve the hose simulation.

Another source of the frequency error in Figure 268 could come from the characteristic solutions of different line sizes in a long length of tubing. Unfortunately test data is not available to conform or dispute this.

A turn-on transient was simulated with the HYTRAN program using the test data from Figure 277 and the input data of Figure 278. The output pressures and flows are shown in Figures 279, 280 and 281.

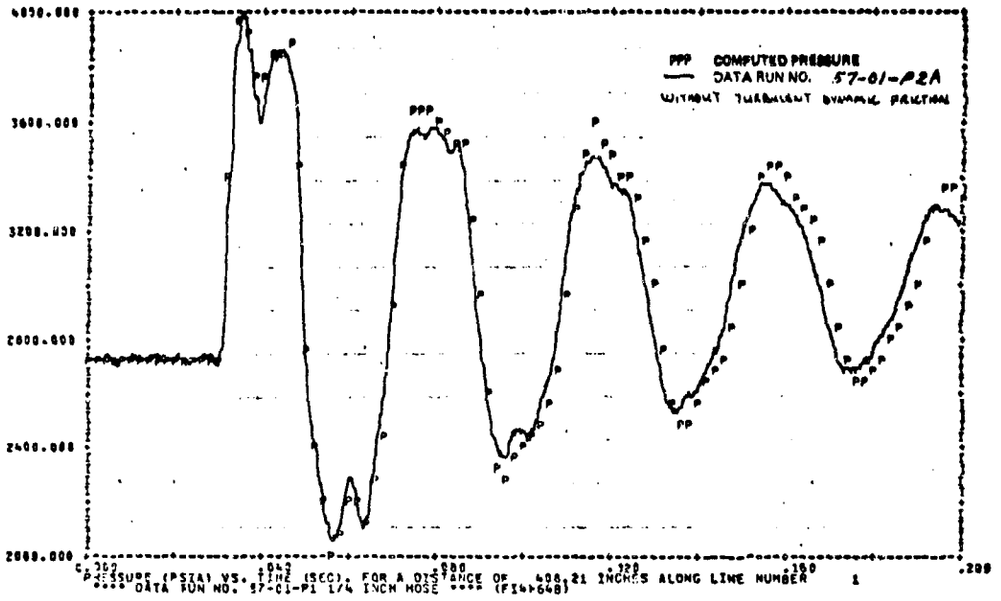

FIGURE 274 57-01-P2A TURN-OFF TRANSIENT

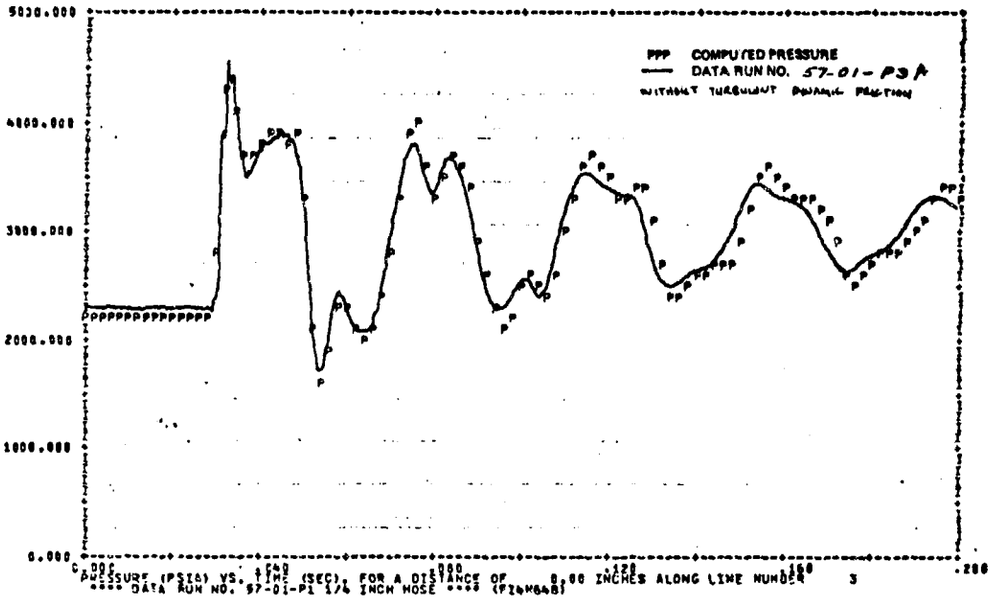

FIGURE 275 57-01-P3A TURN-OFF TRANSIENT

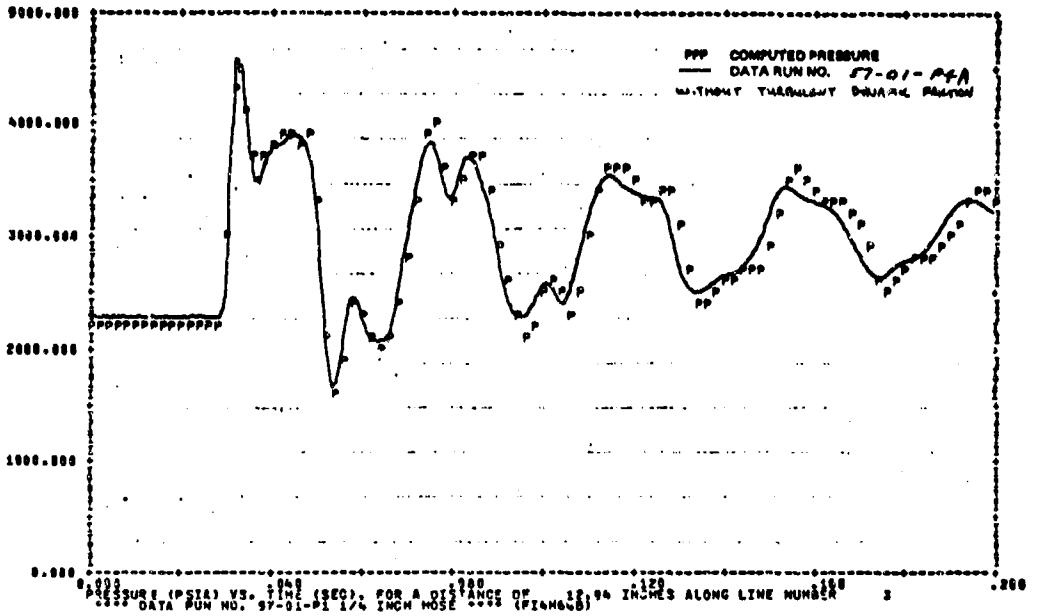

FIGURE 276 57-01-P4A TURN-OFF TRANSIENT

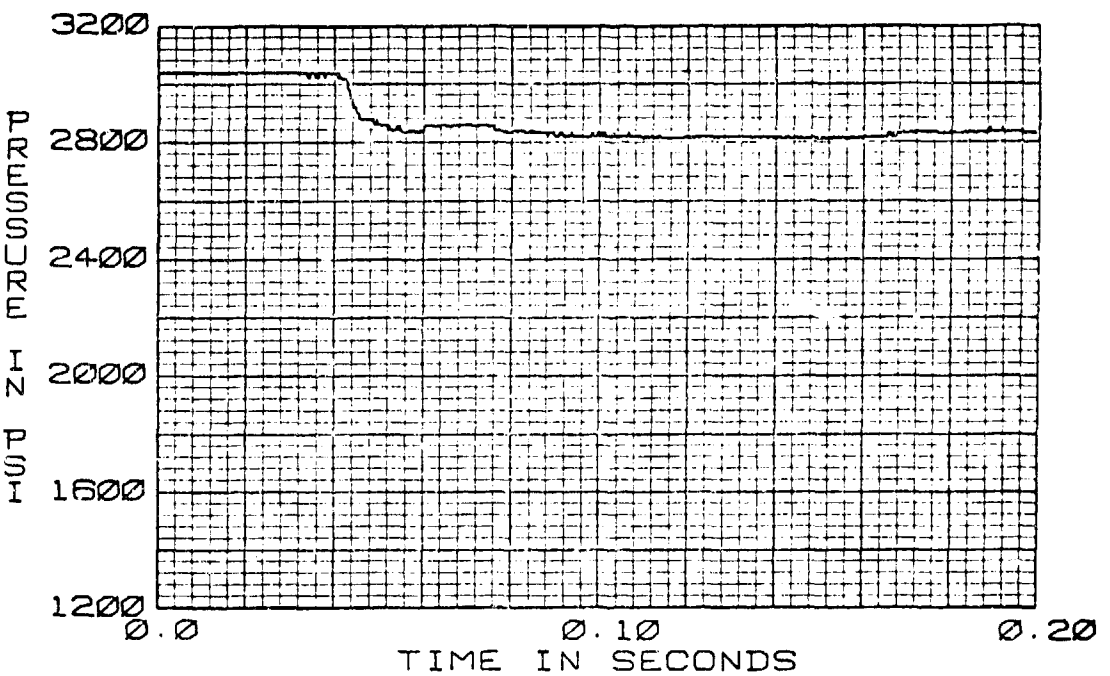

FIGURE 277 .25 IN. STEEL BRAIDED HOSE
57-01+P1 TURN-ON TRANSIENT
38.5 CIS 130°F

```
**** DATA RUN NO. 57-01+P1 1/4 INCH HOSE **** (FI4M65)

THE TRANSIENT RESPONSE IS FROM T=0.0 TO T=  .200 SECONDS AT TIME INTERVALS OF DELT= .00020

 WITH OUTPUT POINTS PLOTTED AT INTERVALS OF  ,  .00200  SECONDS

FLUID DATA FOR  MIL-H-5606  AT  3000.0 PSIG, -    90.0 PSIG AND 130.4 DEG F  IN   10.0 DEG F STEPS
                VISCOSITY   =  .166E-01        .148E-01IN**2/SEC
                DENSITY     =  .81JE-04        .803E-04(LB-SEC**2)/IN**4
                BULK MODULUS =  .223E+06       .187E+06PSI
                VAPOUR PRESS.=  .2CCE+J1 AT  130.0 DEG F

LINE DATA
LINE NO.    LENGTH      INTERNAL DIA    WALL THICKNESS    MODULUS OF ELASTICITY    DELX      CHARACTERISTIC IMPEDANCE    VELOCITY OF SOUND
    1       428.1250        .4440           .0280             .300E+08            9.9984          25.9624                 49460.3748
    2        19.3000        .1930           .1510             .769E+05            6.3333          74.3710                 26771.0316
    3        35.1250        .4440           .0280             .300E+08           12.0417          25.9624                 49460.3748
    4        17.0000        .4440           .0280             .300E+08           17.0000          25.9624                 49460.3748
 COMP+,  1  INTEGER DATA      1   91    8   -1    1   -0   -0   -0   -0   -0   -0   -0   -0   -0   -0   -0   -0
 COMP+,  2  INTEGER DATA      2   21    3    3   -4   -0   -0   -0   -0   -0   -0   -0   -0    4   -0   -0
REAL DATA CARD +    1    .2290E-01   .6500E+00 -0.          -0.          -0.          -0.          -0.          -0.
REAL DATA CARD +    2    0.          .3180E-01   .3280E-01   .2000E+00 -0.          -0.          -0.          -0.
REAL DATA CARD +    3    0.          0.          .3370E+00   .3370E+00 -0.          -0.          -0.          -0.
 COMP+,  3  INTEGER DATA      3   61    1    4   -0   -0   -0   -0   -0   -0   -0   -0   -0   -0   -0   -0
REAL DATA CARD +    1    .5000E+02 -0.          -0.          -0.          -0.          -0.          -0.          -0.
```

FIGURE 278 RUN 57-01 HYTRAN INPUT DATA FOR A TURN-ON TRANSIENT

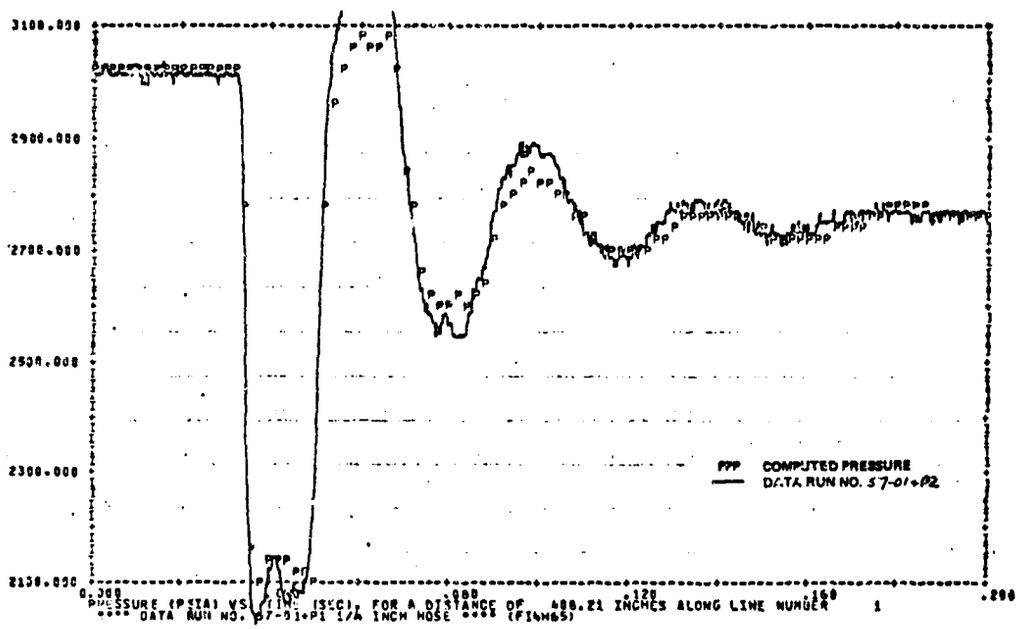

FIGURE 279 57-01+P2 TURN-ON TRANSIENT

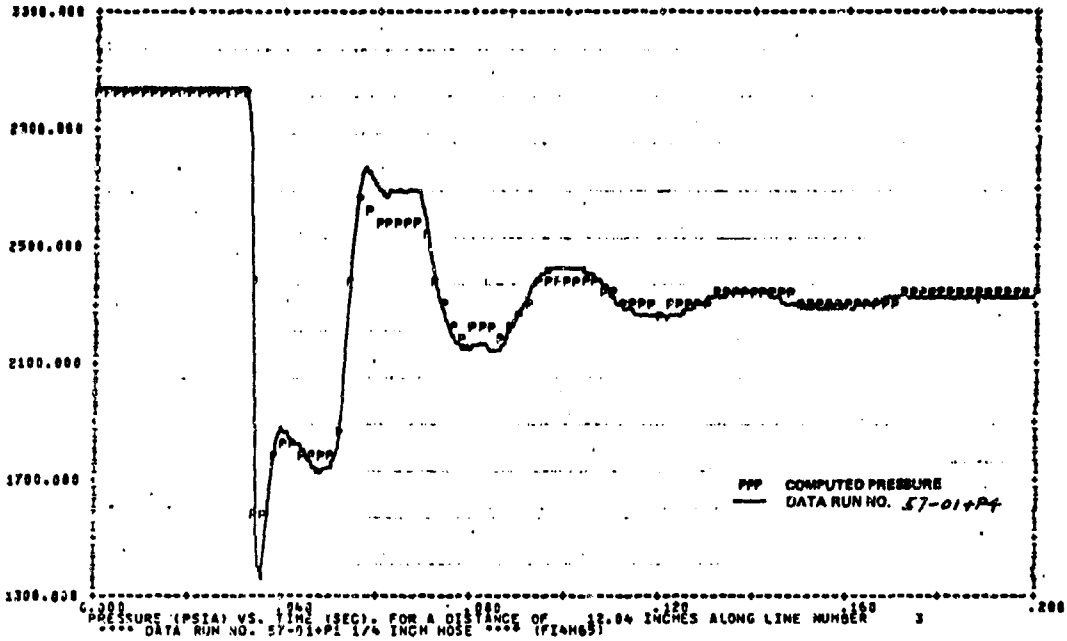

FIGURE 280 57-01+P4 TURN-ON TRANSIENT

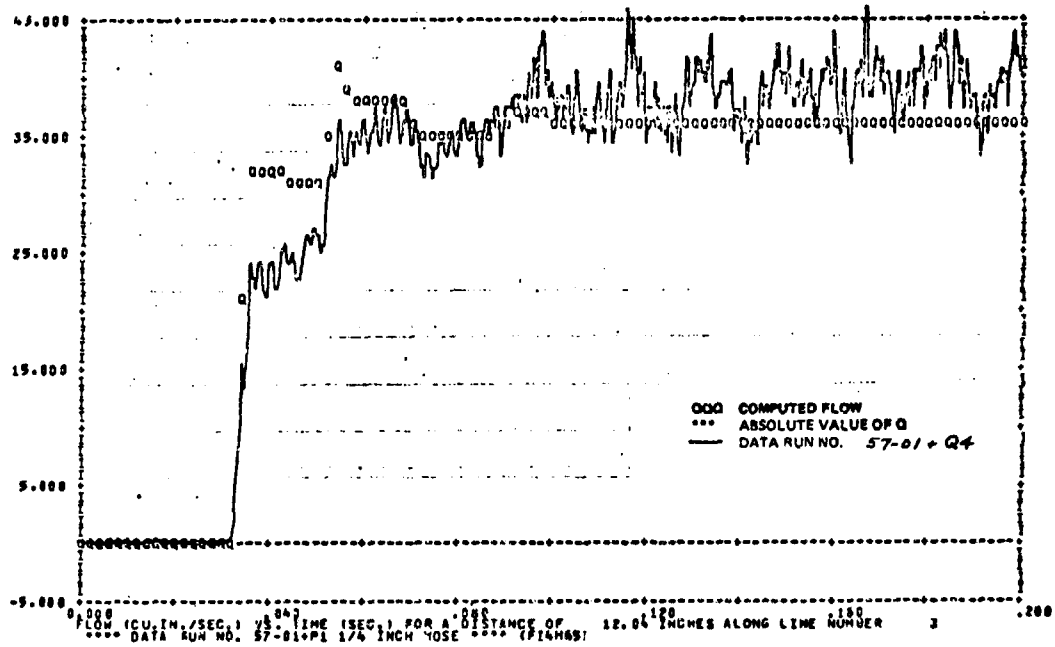

FIGURE 281 57-01+Q4 TURN-ON TRANSIENT

Figure 279 shows a small frequency error between the computed frequency and test results. The first predicted pressure peak at .06 seconds is about 100 psi below the actual value. Likewise for Figure 280 the computed reflected pressure wave amplitude for the turn-on transient is less than the test data. Under predicting the amplitude of the reflected pressure wave also occurred for the 1/2" x 30' line simulation. This may be due to poor dynamic pressure loss predictions for the turbulent flow region in the HYTRAN program.

A 5/8" steel braided Teflon hose was next used in the computer simulation at 38.5 CIS flow and 125°F with the input data of Figure 282 and Figure 283. The results are shown in Figures 284, 285, 286, 287 and 288.

In Figure 284 the computer predicted output has a slightly higher frequency than the test results.

This discrepancy between the predicted and actual damping frequency can be due in part to the lack of an adequate turbulent pressure loss term in the DFRICD subroutine.

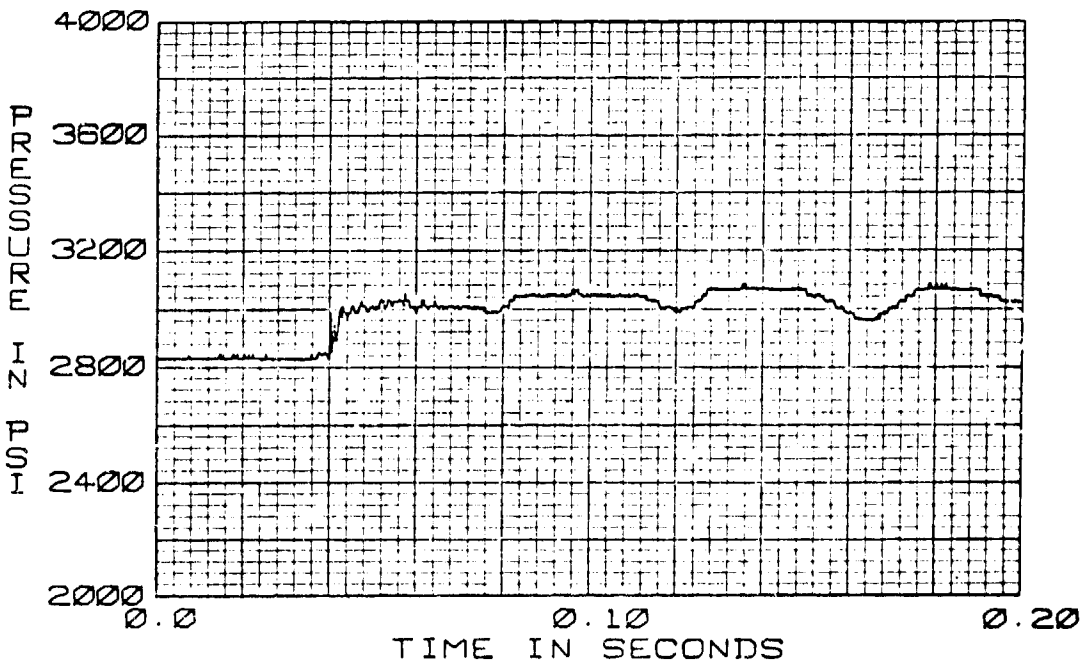

FIGURE 282 5/8 IN. STEEL BRAIDED HOSE
58-01-P1 TURN-OFF TRANSIENT
38.5 CIS 125°F

```
**** DATA RUN NO. 58-01-P1 5/8 INCH HOSE ****(FISH72)

THE TRANSIENT RESPONSE IS FROM T=0.0  TO T=   .200 SECONDS AT TIME INTERVALS OF DELT= .00020
          WITH OUTPUT POINTS PLOTTED AT INTERVALS OF   ,   .00200  SECONDS

FLUID DATA FOR  MIL-H-5606  AT  3000.0 PSIG, -    50.0 PSIG AND 125.0 DEG F  IN   10.0 DEG F STEPS
                    VISCOSITY    -  .198E-01       .158E-01IN**2/SEC
                    DENSITY      -  .814E-04       .805E-04(LB-SEC**2)/IN**4
                    BULK MODULUS -  .226E+06       .191E+06PSI
                    VAPOUR PRESS.-  .200E+01 AT  125.0 DEG F

LINE DATA
LINE NO.      LENGTH        INTERNAL DIA     WALL THICKNESS    MODULUS OF ELASTICITY    DELX      CHARACTERISTIC IMPEDANCE    VELOCITY OF SOUND
    1        429.9000          .4440            .0280              .300E+08            9.9884          26.1653                49761.3594
    2         19.8000          .5403            .0330              .261E+08            9.9000          13.7112                38571.3333
    3         37.5000          .4440            .0280              .300E+08           12.5000          26.1653                49761.3594
    4         17.0000          .4440            .0280              .300E+08           17.0000          26.1653                49761.3594
 COMP+,  1 INTEGER DATA      1  91   0  -1   1  -0  -0  -0  -0  -0  -0  -0  -0  -0  -0  -0
 COMP+,  2 INTEGER DATA      2  21   3   3  -4  -0  -0  -0  -0  -0  -0  -0   4  -3  -0
REAL DATA CARD +   1    .2280E-01   .6930E+00 -0.        -0.        -0.        -0.        -0.        -0.
REAL DATA CARD +   2    0.          .3020E-01   .3120E-01   .2000E+00 -0.        -0.        -0.        -0.
REAL DATA CARD +   3    .3370E+00   .3370E+00  0.          0.        -0.        -0.        -0.        -0.
 COMP+,  3 INTEGER DATA      3  61   1   4  -0  -0  -0  -0  -0  -0  -0  -0  -0  -0  -0  -0
REAL DATA CARD +   1    .5080E+02 -0.        -0.        -0.        -0.        -0.        -0.        -0.
```

FIGURE 283 RUN 58-01 HYTRAN INPUT DATA FOR A TURN-OFF TRANSIENT

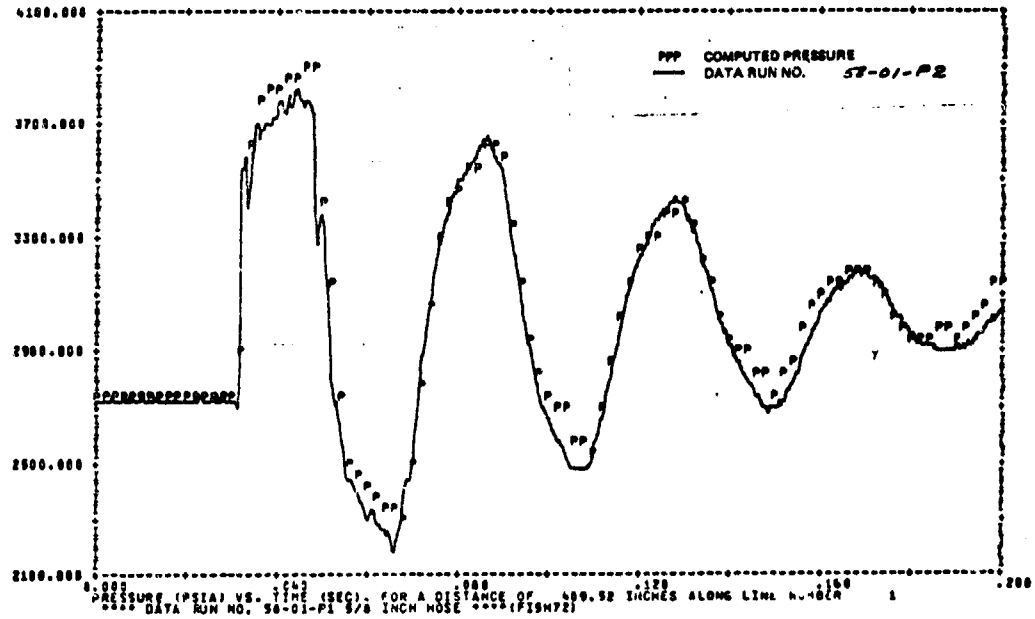

FIGURE 284 58-01-P2 TURN-OFF TRANSIENT

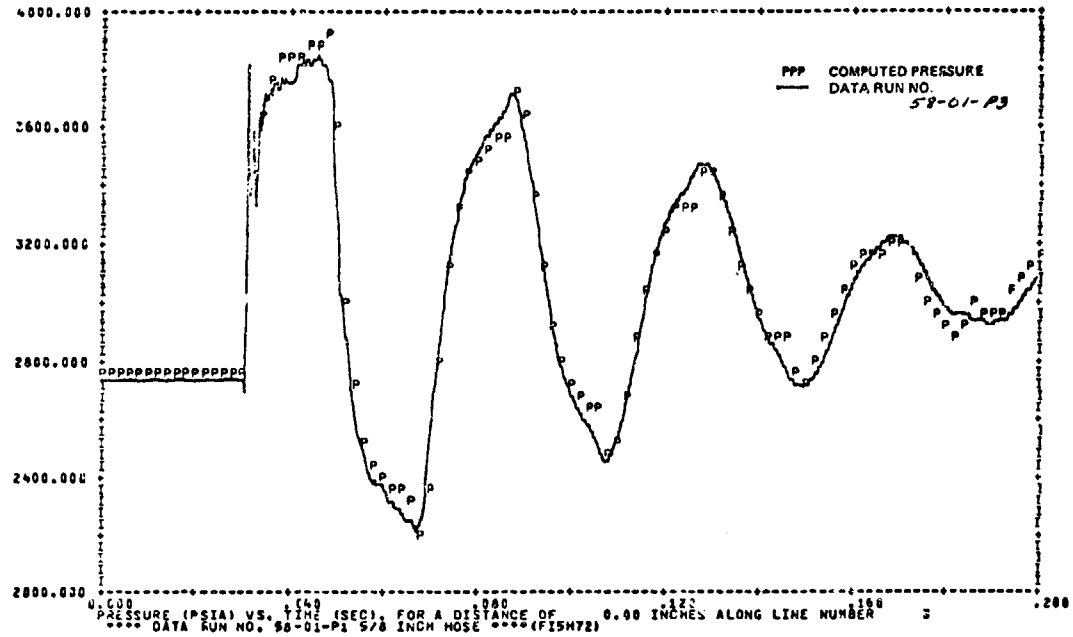

FIGURE 285 58-01-P3 TURN-OFF TRANSIENT

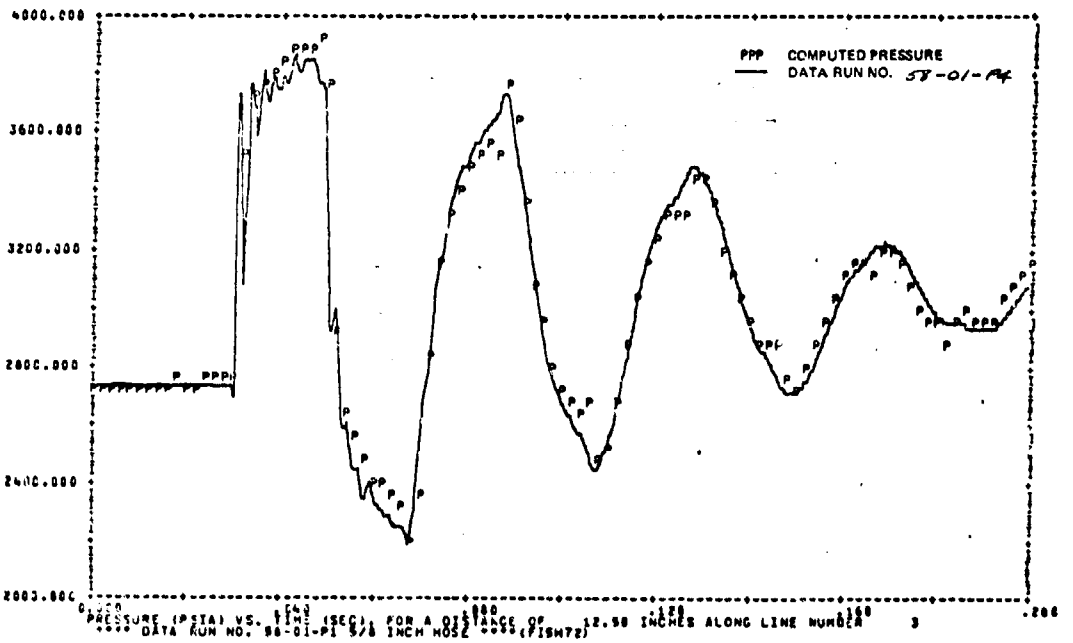

FIGURE 286 58-01-P4 TURN-OFF TRANSIENT

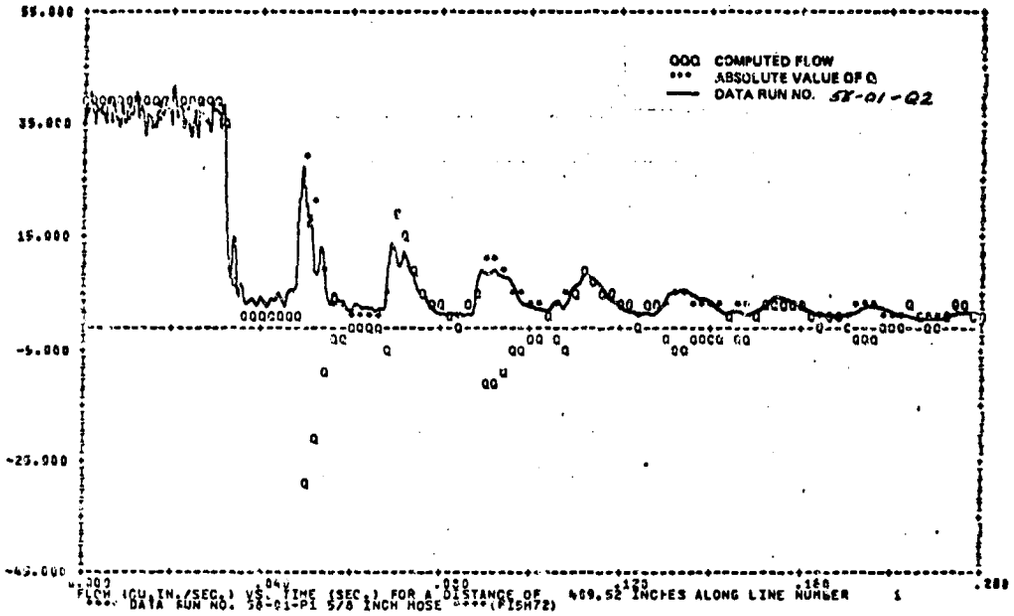

FIGURE 287 58-01-Q2 TURN-OFF TRANSIENT

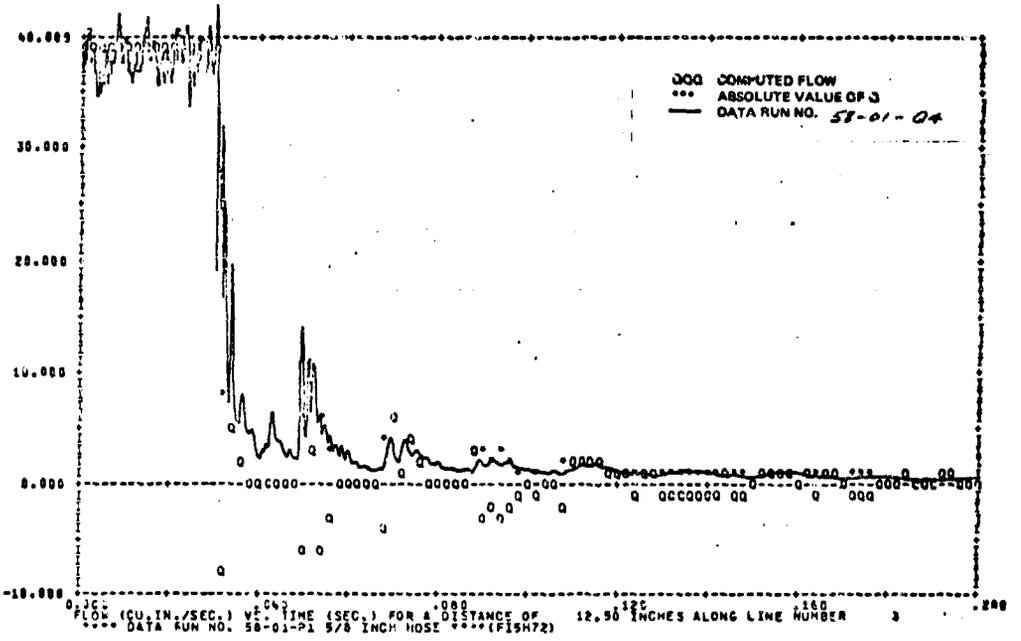

FIGURE 288 58-01-Q4 TURN-OFF TRANSIENT

A turn-on transient with a 5/8" hose was simulated to observe whether it would indicate the same under prediction on the calculation of the reflected pressure wave as in run #57-01 with the 1/4" hose. After inputting the data of Figure 289 and Figure 290 into the HYTRAN program, the results were as expected. Figures 291, 292 and 293 all show that between .06 and .08 seconds the computed pressure values are less than the test data. The pressure plots also show that the frequency of the predicted values is actually faster than the measured results. This follows the same pattern as the turn-off transient for the 5/8" hose.

The anemometer flow data is shown plotted over the computer results in Figure 294.

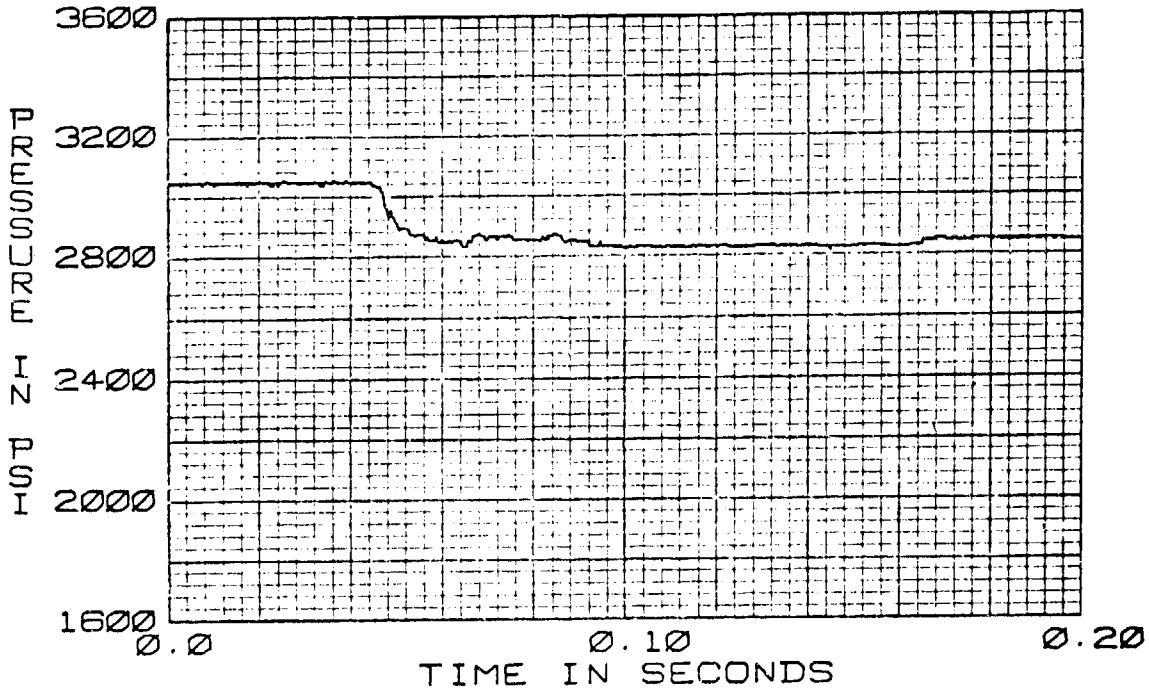

FIGURE 289 5/8 IN. STEEL BRAIDED HOSE
58-01+P1 TURN-ON TRANSIENT
38.5 CIS 125°F

```
**** DATA RUN NO. 58-01+P1 5/8 INCH HOSE ****(FISH73)

THE TRANSIENT RESPONSE IS FROM T=0.0  TO T=  .200 SECONDS AT TIME INTERVALS OF DELT= .00020
        WITH OUTPUT POINTS PLOTTED AT INTERVALS OF  ,  .00200  SECONDS

FLUID DATA FOR  KIL-H-5606  AT  3000.0 PSIG, =   50.0 PSIG AND 125.0 DEG F  IN   10.0 DEG F STEPS
                VISCOSITY    =  .198E-01        .158E-01IN**2/SEC
                DENSITY      =  .814E-04        .805E-04(LB-SEC**2)/IN**4
                BULK MODULUS =  .22oE+06        .191E+06PSI
                VAPOUR PRESS,=  .200E+01 AT  125.0 DEG F

LINE DATA
LINE NO.    LENGTH      INTERNAL DIA    WALL THICKNESS    MODULUS OF ELASTICITY    DELX      CHARACTERISTIC IMPEDANCE    VELOCITY OF SOUND
   1        429.5000        .4400           .0280             .300E+08           9.9886          26.1653              49761.3594
   2         19.0000        .5600           .5030             .281E+06           9.5000          13.7112              38571.3333
   3         37.5000        .4440           .0280             .300E+08          12.5000          26.1653              49761.3594
   4         17.0000        .4440           .0280             .300E+08          17.0000          26.1653              49761.3594
  COMP#,  1  INTEGER DATA     1  91   0  -1   1  =0  -0  =0  =0  -0  =0  =0  -0  -0  =0  -0  =0
  COMP#,  2  INTEGER DATA     2  21   3   3  -4  -0  -0  =0  =0  -0  =0  =0  -0  -0   4  -0  =0
 REAL DATA CARD #   1   .2200E-01  .6560E+00 -0.      -0.      -0.      -0.      -0.      -0.
 REAL DATA CARD #   2   0.         .3620E-01  .3720E-01  .2000E+06 -0.      -0.      -0.      -0.
 REAL DATA CARD #   3   0.         0.         .3370E+00  .3370E+00 -0.      -0.      -0.      -0.
  COMP#,  3  INTEGER DATA     3  61   1   4  -0  -0  -0  -0  -0  -0  -0  -0  -0  -0  -0  -0
 REAL DATA CARD #   1   .5000E+02 -0.      -0.      -0.      -0.      -0.      -0.      -0.
```

FIGURE 290 58-01 HYTRAN INPUT DATA FOR A TURN-ON TRANSIENT

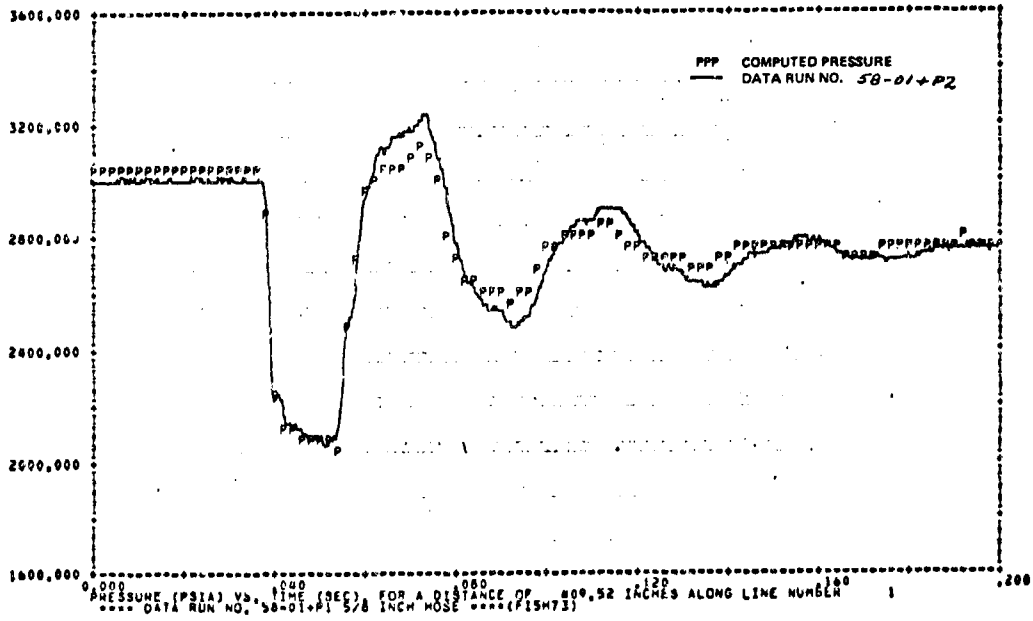

FIGURE 291 58-01+P2 TURN-ON TRANSIENT

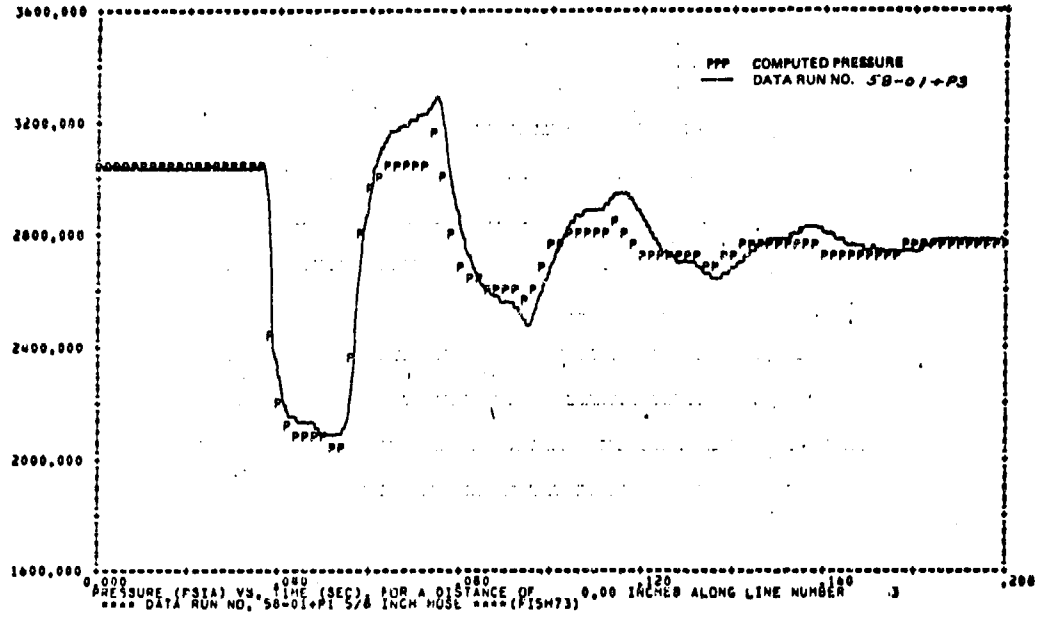

FIGURE 292 58-01+P3 TURN-ON TRANSIENT

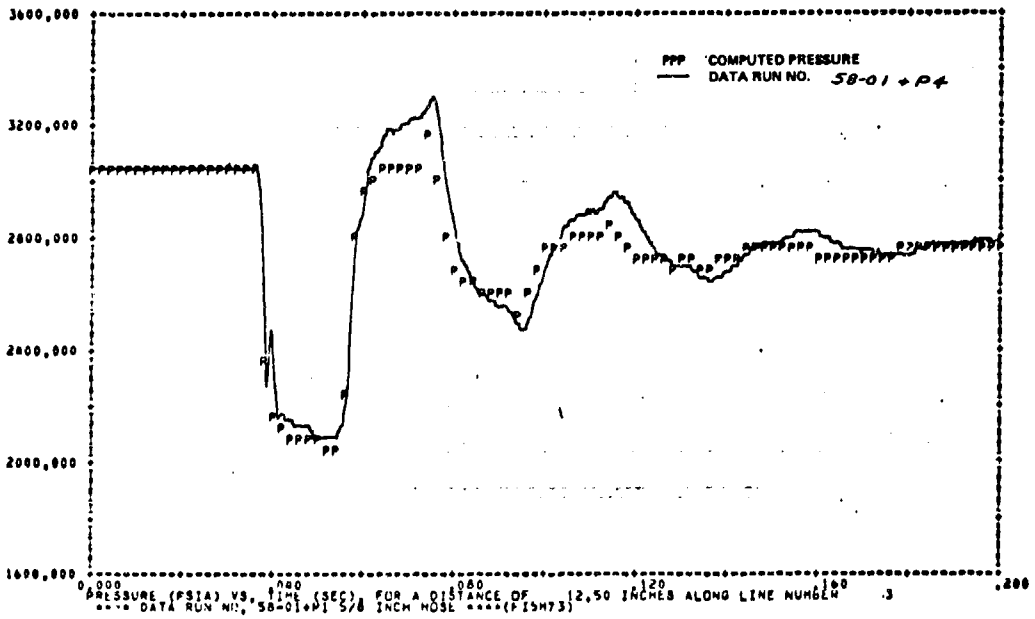

FIGURE 293 58-01+P4 TURN-ON TRANSIENT

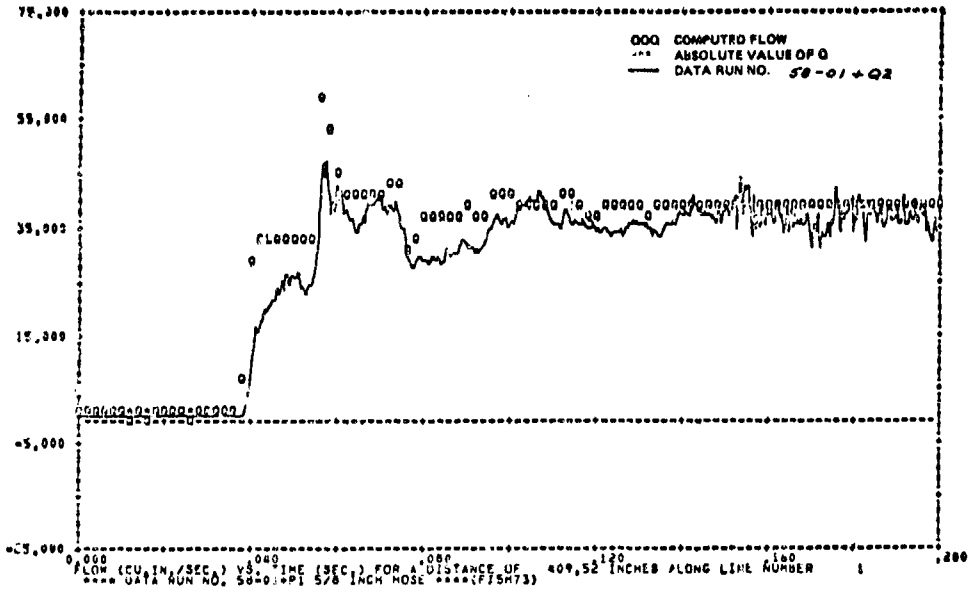

FIGURE 294 58-01+Q2 TURN-ON TRANSIENT

b. Conclusions - The hose model calculations of flows and pressures did not compare well with the test data. For the 1/4" hose the computer results predicted a lower frequency than was actually measured. However, the amplitudes on the computed pressures match well with the test results. The 5/8" hose computer results showed a higher frequency than the test data. The amplitude correlation with the computed pressures was good. In turn-on transients for both hoses the HYTRAN program consistently under predicted the maximum pressure amplitude of the test data.

9. TWO STAGE RELIEF VALVE MODEL VERIFICATION

The test results obtained on a two stage high response relief valve are compared to the HYTRAN computer program valve model - subroutine CVAL34. The test on the relief valve was performed on a one inch system with MIL-H-83282.

Subroutine CVAL34 models a two stage relief valve of the type shown in Figure 295. This is a high response device used to limit pressure surges and prevent system overpressures due to pump failure.

The relief valve is assumed to have a variable orifice characteristic between the fully open and fully closed positions. The effects of flow forces on the poppet are not included since these are not very well defined theoretically and depend on the actual valve geometry.

In the steady state section the relief valve is assumed to be closed with no pilot flow. In the transient analysis the flow through the valve is computed with the normal valve equations. The poppet position is predicted from the previous time step and is used to compute the valve orifice area.

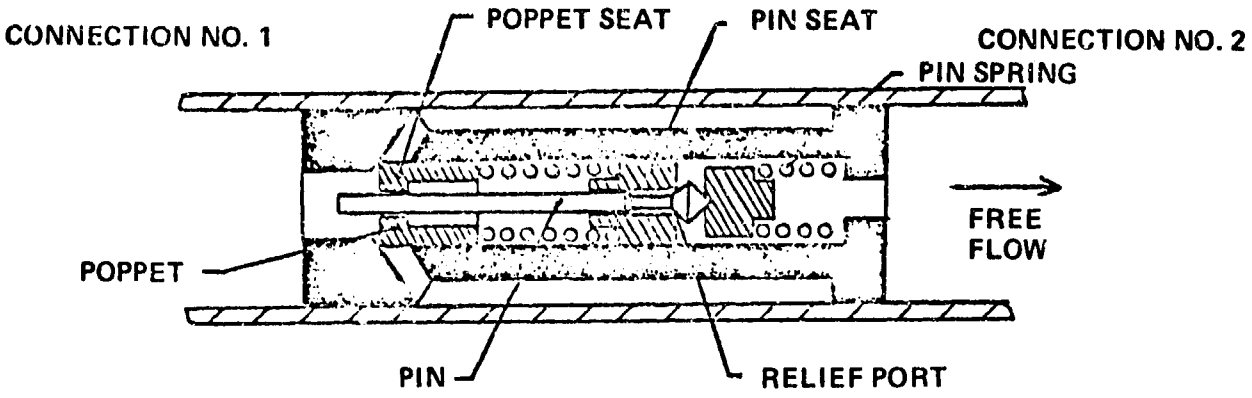

FIGURE 295 TYPE NO. 34 TWO STAGE RELIEF VALVE

The two stage relief valve test series was run on the system configuration shown in Figure 296.

The following parameters were recorded for the test runs: P1, P2, P3, P4, P5, Q5, P6, P7 and XV - the valve position.

The test runs are listed in Table 14. Typically a baseline run was made without the relief valve in the system, then a run was made with the relief valve. Only turn-off transients were investigated.

TABLE 14

TWO STAGE RELIEF VALVE TEST RUNS

Run Number	Test Condition	Steady State Flow (CIS)	Temperature (°F)
72-05-XX	Turn-off	100	132
72-06-XX	"	150	131
72-07-XX	"	100	207
72-08-XX	"	150	211
72-09-XX	"	100	131
72-10-XX	"	150	132
72-11-XX	"	100	210
72-12-XX	"	150	212

XX-Denotes run parameter

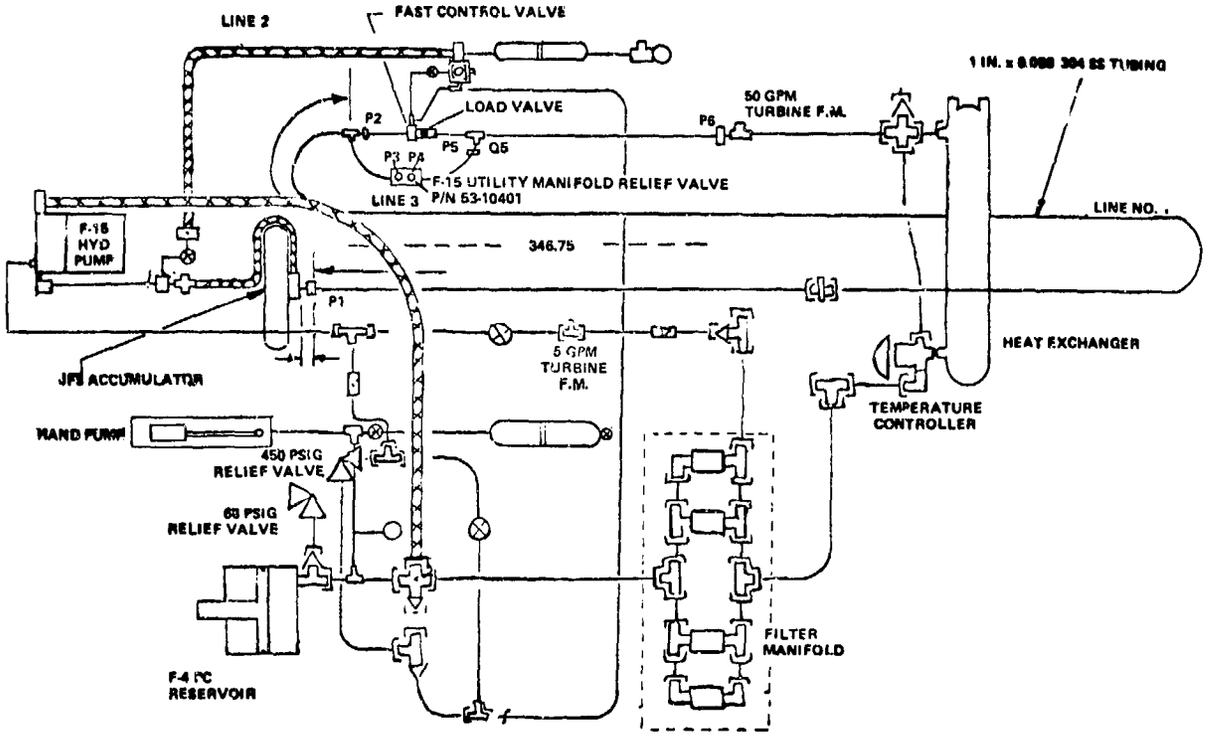

FIGURE 296 TWO STAGE RELIEF VALVE TEST BENCH SCHEMATIC

The first four test runs on the valve (72-01-XX thru 72-04-XX) were made without the accumulator shown in Figure 296 in the system. The upstream boundary condition at the P1 transducer was found to be too noisy for use in the computer program. The insertion of the accumulator downstream of the pump did provide a better boundary condition.

a. Computer Simulation Without the Test Data - Test results indicated that the control valve used to generate the transients was bouncing on closure. An attempt was made to simulate the exact valve characteristics. But the strain gage device on the spring used to close the valve was not capable of determining an actual poppet position. Therefore adequate simulation of the two stage relief valve was not possible.

A computer simulation was made without the test data. The boundary conditions chosen were similar to the actual test data. This baseline run was made without the two-stage relief valve in place. Figure 297 is the printout of the pressure zero inches along line number two. (See Figure 296). The initial peak pressure reaches 375 psi and does not dampen appreciably in the simulation. The flow at this same point is in Figure 298. The pressure 20 inches along line number three in Figure 299 also reaches 3750 psi.

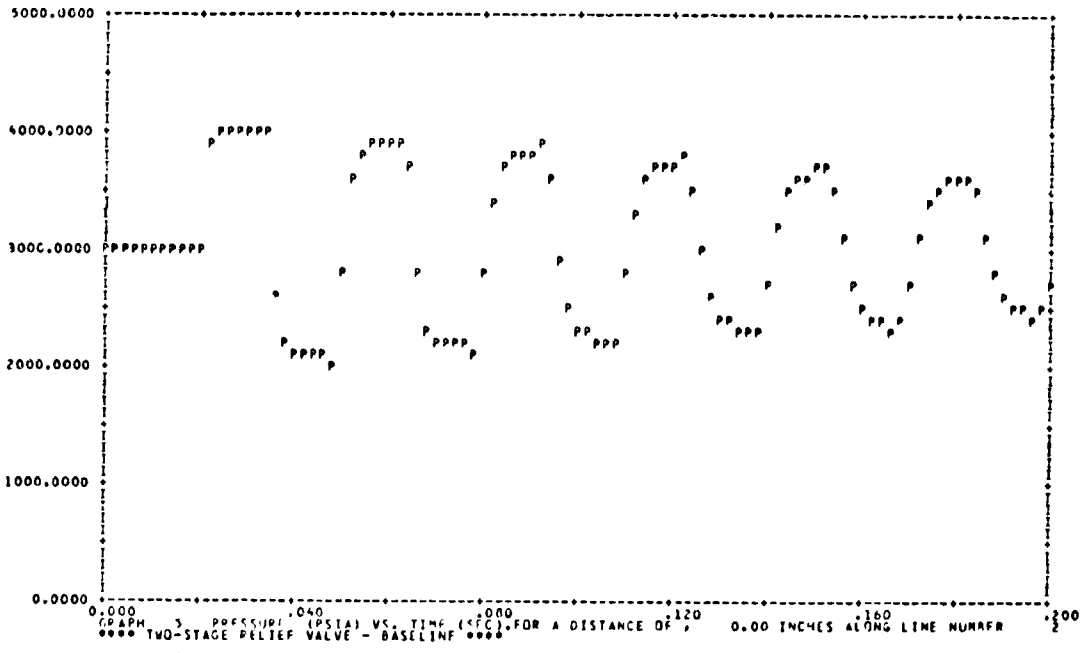

FIGURE 297 PRESSURE 0,0 INCHES ALONG LINE 2

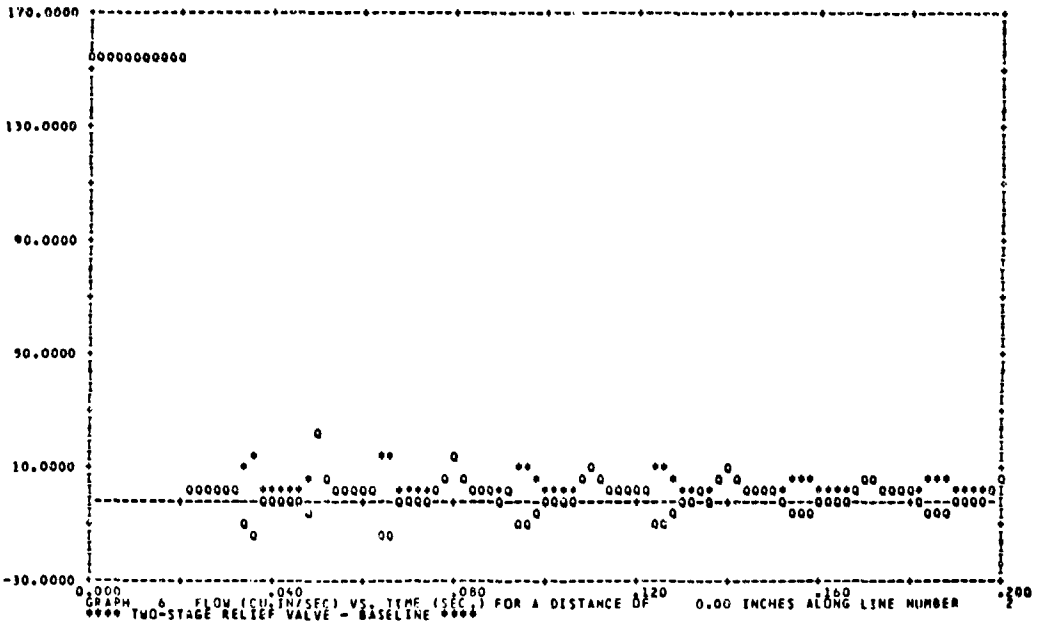

FIGURE 298 FLOW 0,0 INCHES ALONG LINE 2

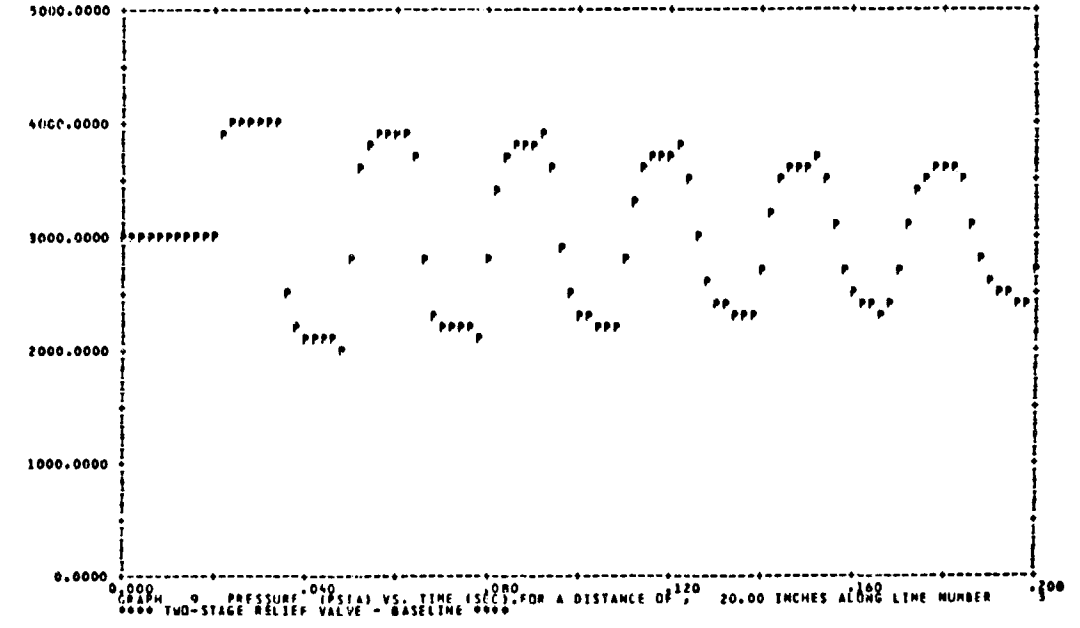

FIGURE 299 PRESSURE 20,0 INCHES ALONG LINE 3

Next a computer run was made at 100 CIS with the two-stage relief valve in the system. In Figure 300 zero inches along line 3 the peak pressure reaches the relief valves cracking pressure of 3750 psi at 22 msec into the simulation. The relief valve opens and the pressure drops to 3200 psi in less than 2 msec. The flow in line 3 quickly increases as the two stage relief valve opens and then gradually closes until fully closed at 130 msec as shown in Figure 301. Figures 302 and 303 are plots of the poppet position and internal cavity pressure for the valve. The cavity pressure is typically system pressure until the valve relieves then it falls to system return pressure. The pressures and flows immediately downstream of the relief valve are shown in Figures 304 and 305.

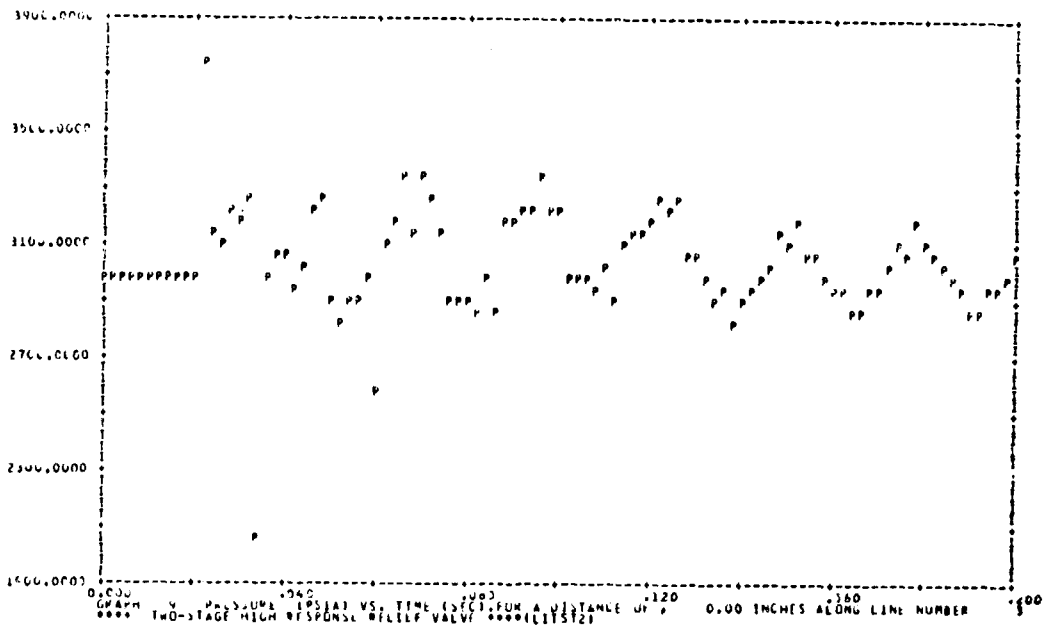

FIGURE 300 PRESSURE 0,0 INCHES ALONG LINE 3

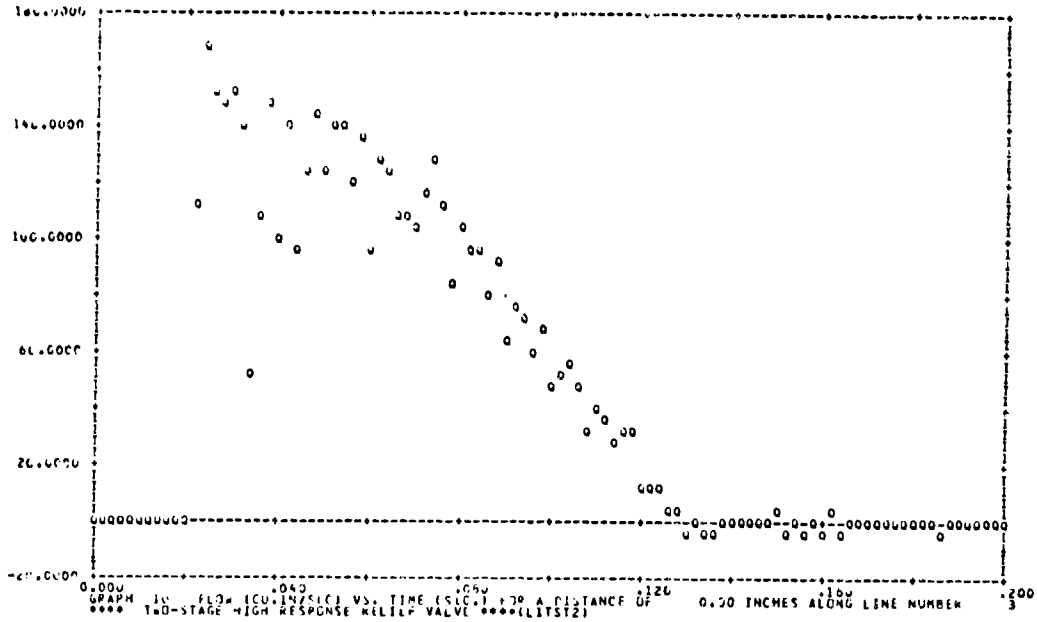

FIGURE 301 FLOW 0,0 INCHES ALONG LINE 3

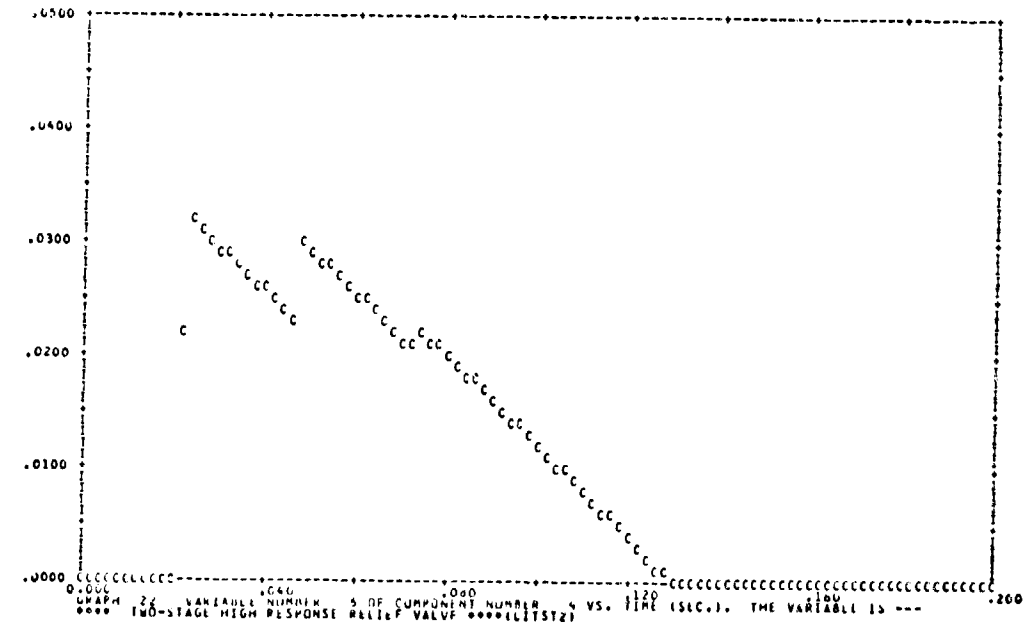

FIGURE 302 POPPET POSITION

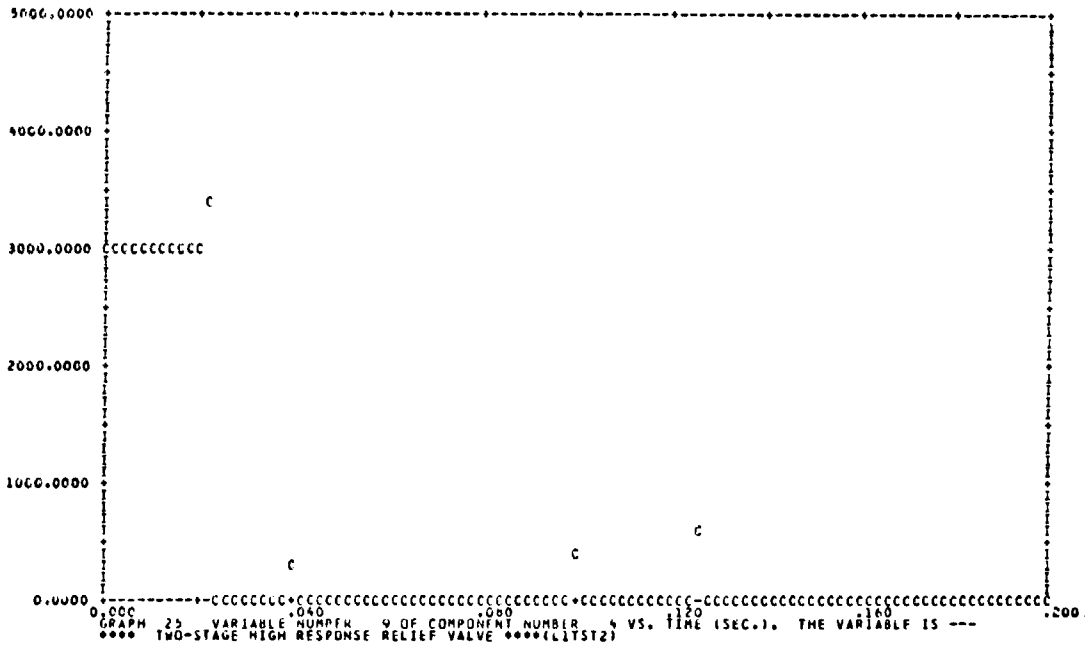

FIGURE 303 CAVITY PRESSURE - PCAV

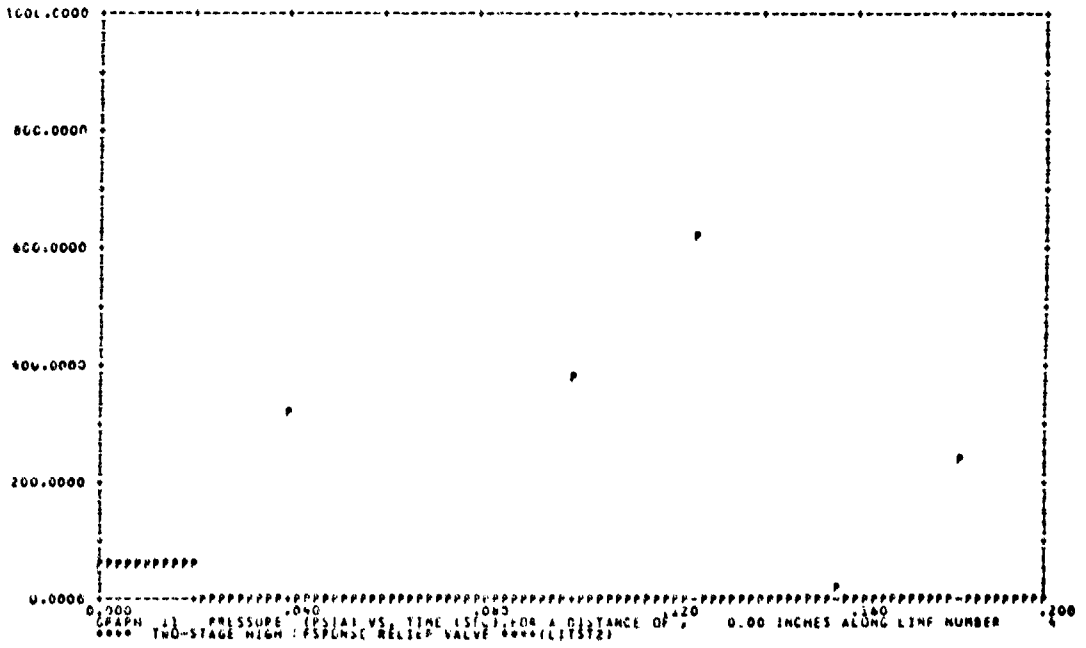

FIGURE 304 PRESSURE 0,0 INCHES ALONG LINE 4

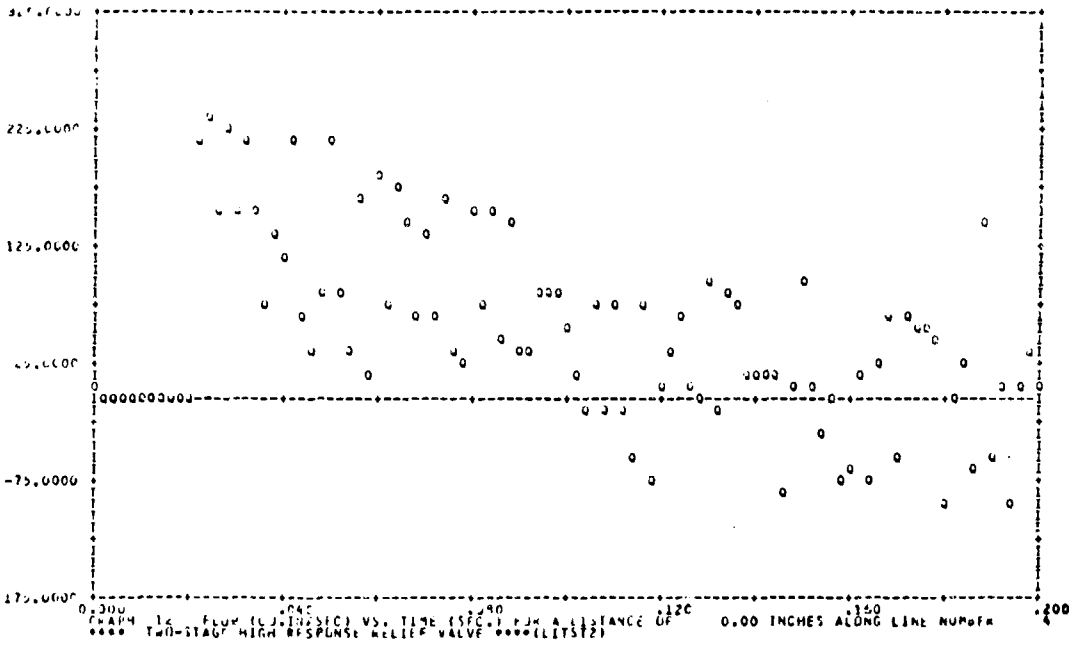

FIGURE 305 FLOW 0,0 INCHES ALONG LINE 4

b. Observations - The effects of the valve in the system can readily be seen by comparing a valve run with its baseline counterpart. The main effects are observed at the 150 CIS flow rate. Figure 297 shows that pressure in the dead ended line reaches about 4000 psi a short time after the fast control valve is closed. With the two stage high response relief valve in the system Figure 300 shows an initial pressure spike only reaching the valve relief pressure of 3750 psi. Comparable results can be observed for the remainder of the test runs.

c. Conclusions - The malfunctioning control valve did not provide the necessary sharp turn-off transients in the test system, and prevented the computer program verification of the two stage relief valve model. The computer runs made without the test data indicate that the relief valve model reasonably simulated the actual valve's operating characteristics.

10. HYTRAN PROGRAM VERIFICATION FOR PRESSURE EFFECTS

In this section the pressure effects on test results are compared to the HYTRAN computer program simulation runs. The testing was performed on a 1/2 inch system with MIL-H-83282 hydraulic fluid. The pump operating speed was 4000 RPM.

The pressure effects test series was run on the system configuration shown in Figure 306. The following parameters were recorded for the test runs: P_1, P_2, Q_2, P_3, P_4, P_5, Q_5, P_6, P_7 and control valve position XV.

The data recorded in this test series is designated 71.

Table 15 contains an itemized list of the pressure effects tests. Test conditions were established to study the changes to the system response at pump operating pressures ranging from 1500 to 3750 psig. The pump outlet pressure was varied by adjusting the preload pressure of the compensator spring. The effects of different flow rates and temperatures at these outlet pressures were also monitored.

a. Test Results and Computer Program Verification - The first simulation was made at a pump outlet pressure of 3000 psig. The pump provided a steady state flow of 100 CIS before the control valve was turned off. The data in Figures 307 and 308 were input with the system configuration data in Figure 309 at a temperature of 134°F. The results of the simulation are shown in Figures 310, 311, 312 and 313. The P6 transducer was located about 2 inches from the entrance of the F-4 reservoir. Figure 314 shows that the pressure transducer oscillated at a high frequency during the transient. A cavity exists between the pressure transducer diaphram and the tube outer wall. The transducer location at a peak pressure or mechanical standing wave location coupled with the small volume could account for this resonant condition as shown in Figure 314.

The computer results show excellent correlation with the measured data at this pressure condition. In Figure 310 the program accurately predicts the measured peak pressure at 28 milliseconds. There is about a 4% difference in phasing between the predicted results and the lab data at 0.2 seconds. This slight error may be attributable to many factors,

relating to the data and the HYTRAN program. The data errors may result from an inaccurate temperature reading or valve closing time. The main source of program errors come from the dynamic friction algorithm and the lack of adequate bulk modulus data for the hydraulic fluid. Despite all of these factors, the predicted pressure valves and the signal phasing are within 5% of the measured data.

TABLE 15 PRESSURE EFFECTS TESTING

RUN NUMBER	STEADY STATE FLOW (CIS)	STEADY STATE PRESSURE (PSIG)	RESERVOIR PRESSURE (PSIG)	TEMP (°F)	TRANSIENT
71-01-XX*	100	3000	55	134	Turn-Off
71-01+XX	100	3000	54.5	130	Turn-On
71-02-XX	10	3000	55	130	Turn-Off
71-02+XX	10	3000	54.5	128	Turn-On
71-03-XX	100	3000	55	207	Turn-Off
71-03+XX	100	3000	54	208	Turn-On
71-04-XX	10	3000	55	208	Turn-Off
71-04+XX	10	3000	56	206	Turn-On
71-05-XX	100	2500	55	134	Turn-Off
71-05+XX	100	2500	55	130	Turn-On
71-06-XX	10	2500	55	130	Turn-Off
71-06+XX	10	2500	55	130	Turn-On
71-07-XX	100	2500	55.5	211	Turn-Off
71-07+XX	100	2500	55	205	Turn-On
71-08-XX	10	2500	55	210	Turn-Off
71-08+XX	10	2500	56	207	Turn-On
71-09-XX	38.5	3000	55.5	208	Turn-Off
71-09+XX	38.5	3000	53.5	211	Turn-On
71-10-XX	38.5	3000	55	131	Turn-Off
71-10+XX	38.5	3000	54.5	129	Turn-On
71-11-XX	97.5	2000	56	135	Turn-Off
71-11+XX	97.5	2000	53.5	132	Turn-On
71-12-XX	10	2000	55.5	132	Turn-Off
71-12+XX	10	2000	55	130	Turn-On
71-13-XX	100	2000	54	208	Turn-Off
71-13+XX	100	2000	53	207	Turn-On
71-14-XX	10	2000	55.5	210	Turn-Off
71-14+XX	10	2000	54.5	208	Turn-On
71-15-XX	85	1500	54.5	133	Turn-Off
71-15+XX	85	1500	54.5	131	Turn-On
71-16-XX	10	1500	55	134	Turn-Off
71-16+XX	10	1500	54.5	131	Turn-On
71-17-XX	85	1500	55	215	Turn-Off
71-17+XX	85	1500	54.5	209	Turn-On
71-18-XX	10	1500	55.5	209	Turn-Off
71-18+XX	10	1500	56	209	Turn-On
71-19-XX	100	3500	56	134	Turn-Off
71-19+XX	100	3500	55	134	Turn-On
71-20-XX	10	3500	55.5	133	Turn-Off
71-20+XX	10	3500	54.5	130	Turn-On
71-21-XX	100	3500	55	210	Turn-Off
71-21+XX	100	3500	56	209	Turn-On
71-22-XX	10	3500	56	209	Turn-Off
71-22+XX	10	3500	54.5	208	Turn-On
71-23-XX	100	3750	54.5	134	Turn-Off
71-23+XX	100	3750	54.5	130	Turn-On
71-24-XX	10	3750	54.5	130	Turn-Off
71-24+XX	10	3750	54.5	130	Turn-On
71-25-XX	100	3750	55	211	Turn-Off
71-25+XX	100	3750	54	208	Turn-On
71-26-XX	10	3750	55.5	208	Turn-Off
71-26+XX	10	3750	55	207	Turn-On
71-27-XX	57	3000	65	135	Turn-Off
71-27+XX	57	3000	60	130	Turn-On

* - XX denotes measured data parameters

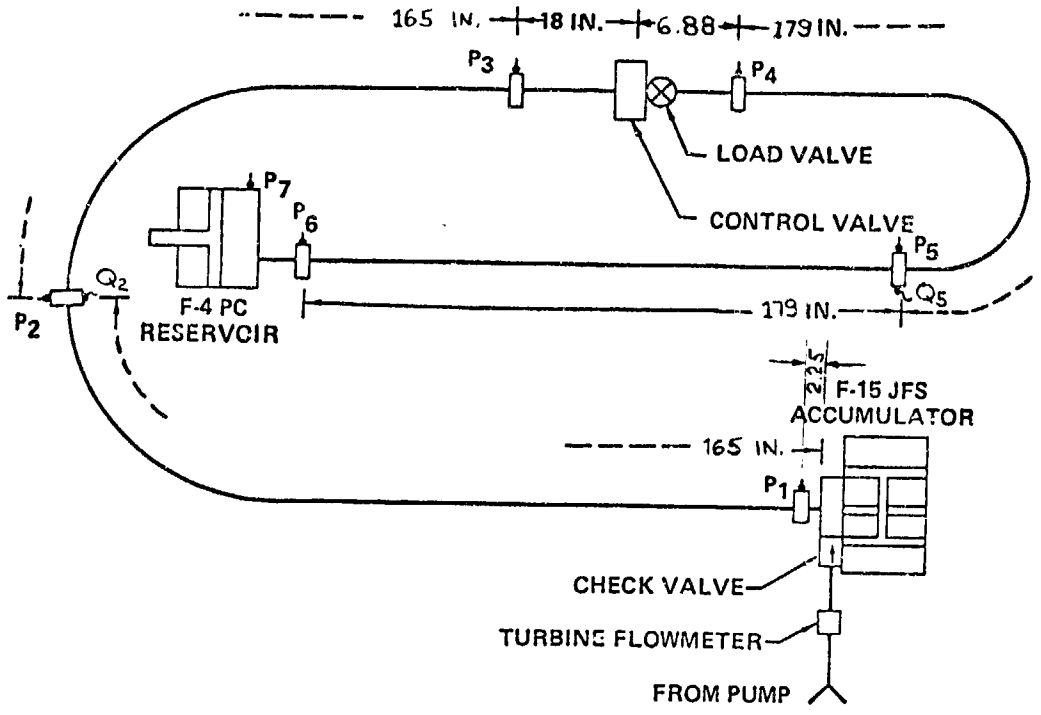

FIGURE 306 PRESSURE EFFECTS TESTING SYSTEM SCHEMATIC

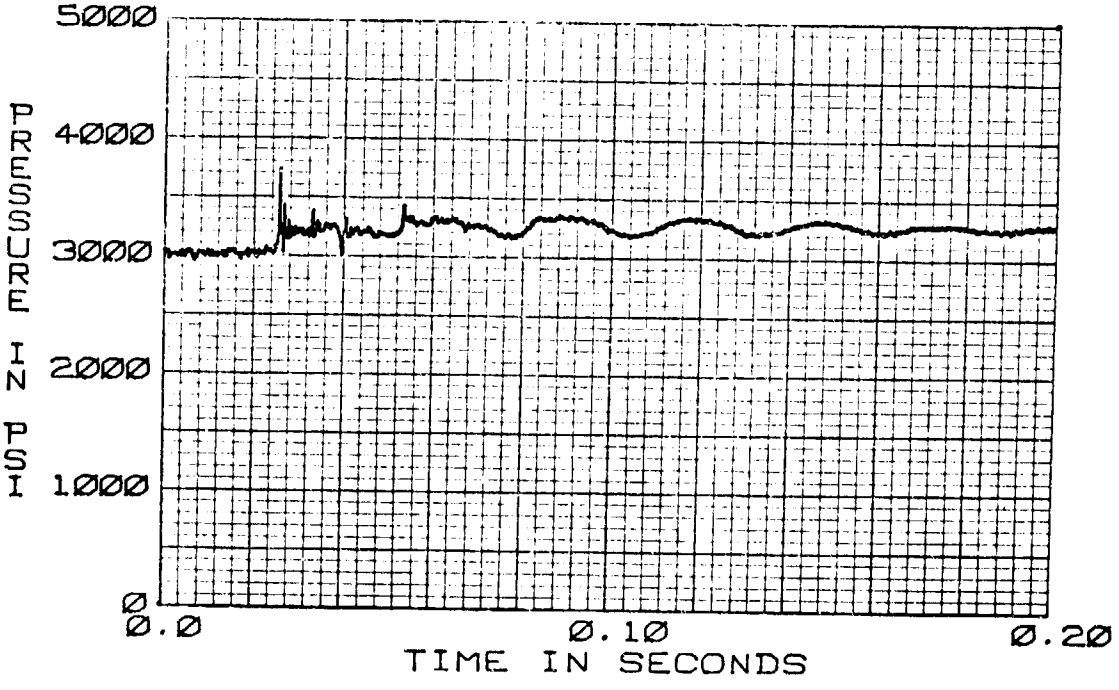

FIGURE 307 PRESSURE EFFECTS
71-01-P1 TURN-OFF TRANSIENT
100 CIS 130°F

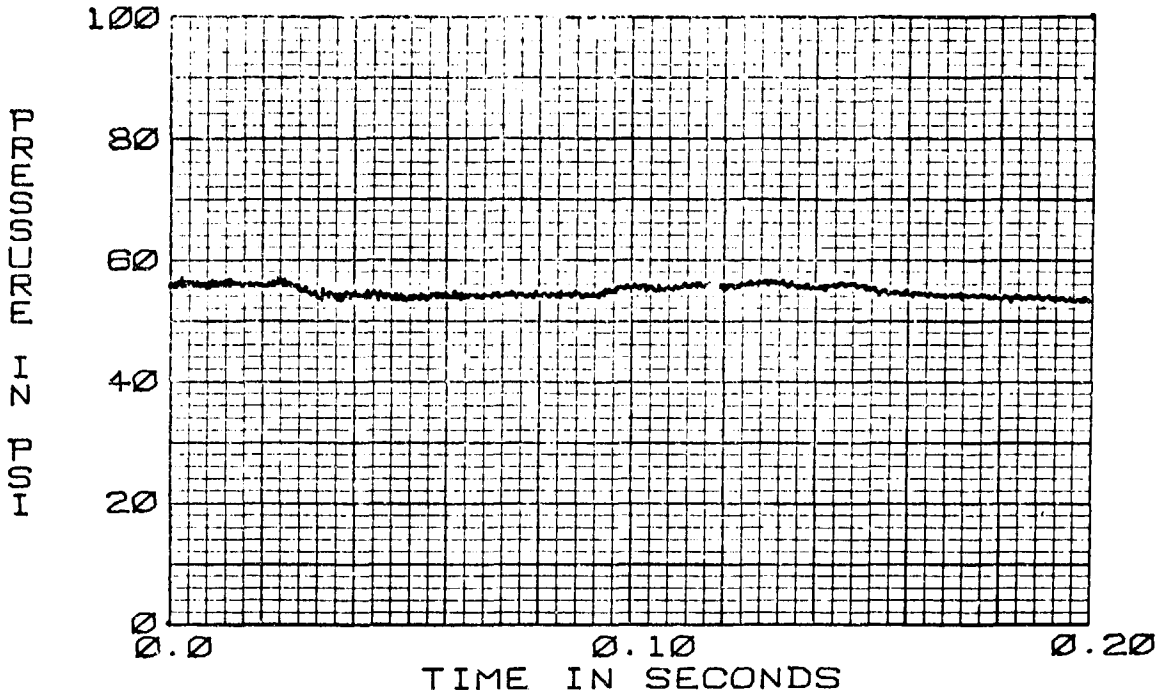

FIGURE 308 PRESSURE EFFECTS
71-01-P1 TURN-OFF TRANSIENT
100 CIS 130°F

*** PRESSURE EFFECTS RUN NO. 71-01-P1***(PRES38)

THE TRANSIENT RESPONSE IS FROM T=0.0 TO T= .200 SECONDS AT TIME INTERVALS OF DELT= .00020
WITH OUTPUT POINTS PLOTTED AT INTERVALS OF , .00200 SECONDS

FLUID DATA FOR MIL-H-83282 AT 3000.0 PSIG, - 50.0 PSIG AND 134.0 DEG F IN 10.0 DEG F STEPS

VISCOSITY	- .188E-01	.145E-01IN**2/SEC
DENSITY	- .789E-04	.780E-04(LB-SEC**2)/IN**4
BULK MODULUS	- .220E+06	.184E+06PSI
VAPOUR PRESS.	- .200E+01 AT 134.0 DEG F	

LINE DATA LINE NO.	LENGTH	INTERNAL DIA	WALL THICKNESS	MODULUS OF ELASTICITY	DELX	CHARACTERISTIC IMPEDANCE	VELOCITY OF SOUND
1	346.3000	.4440	.0280	.300E+08	10.1853	25.4337	49929.1145
2	364.0000	.4440	.0280	.300E+08	10.1867	25.4337	49929.1145

COMP*, 1 INTEGER DATA 1 91 0 -1 1 -0 -0 -0 -0 -0 -0 -0 -0 -0 -0 -0

COMP*, 2 INTEGER DATA 2 23 3 1 -2 -0 -0 -0 -0 -0 -0 -0 -0 4 -0 -0

REAL DATA CARD # 1 .2200E-01 .6500E+00 -0. -0. -0. -0. -0. -0.

REAL DATA CARD # 2 0. .1900E-01 .2000E-01 .2000E+00 -0. -0. -0. -0.

REAL DATA CARD # 3 .9370E+00 .9370E+00 0. 0. -0. -0. -0. -0.

COMP*, 3 INTEGER DATA 3 91 0 2 1 -0 -0 -0 -0 -0 -0 -0 -0 -0 -0 -0

FIGURE 309 RUN 71-01 HYTRAN INPUT DATA FOR A TURN-OFF TRANSIENT

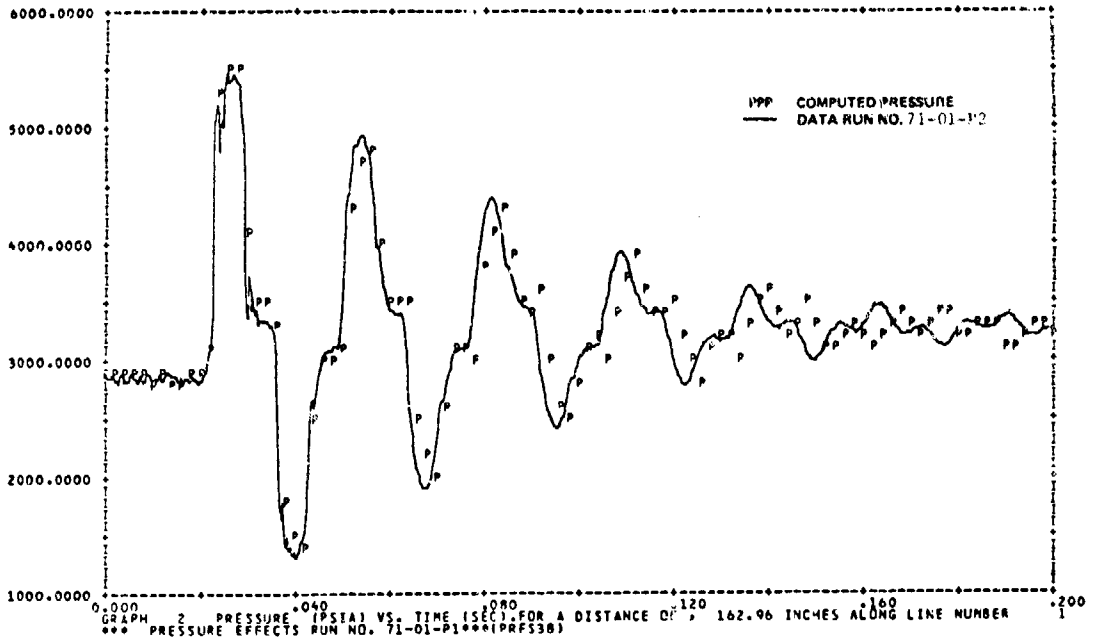

FIGURE 310 71-01-P2 TURN-OFF TRANSIENT

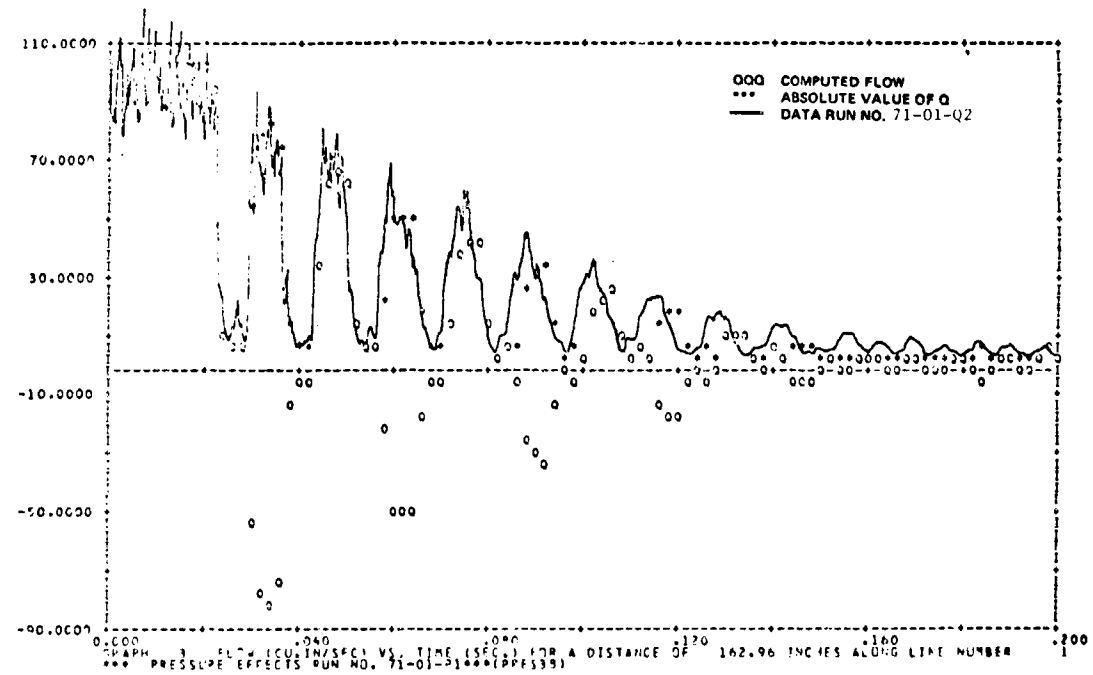

FIGURE 311 71-01-Q2 TURN-OFF TRANSIENT

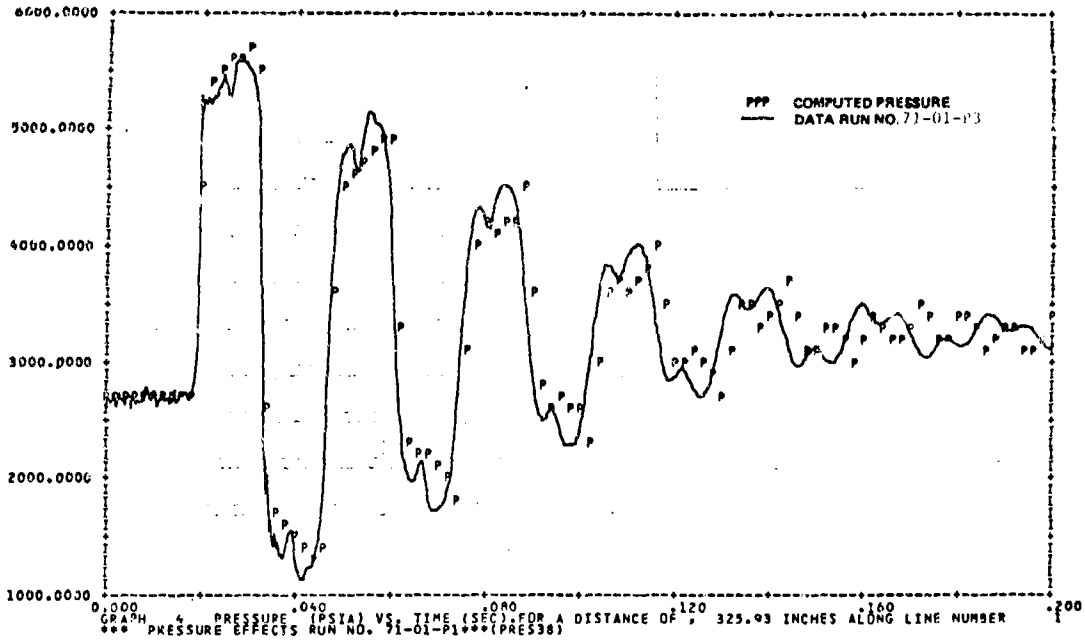

FIGURE 312 71-01-P3 TURN-OFF TRANSIENT

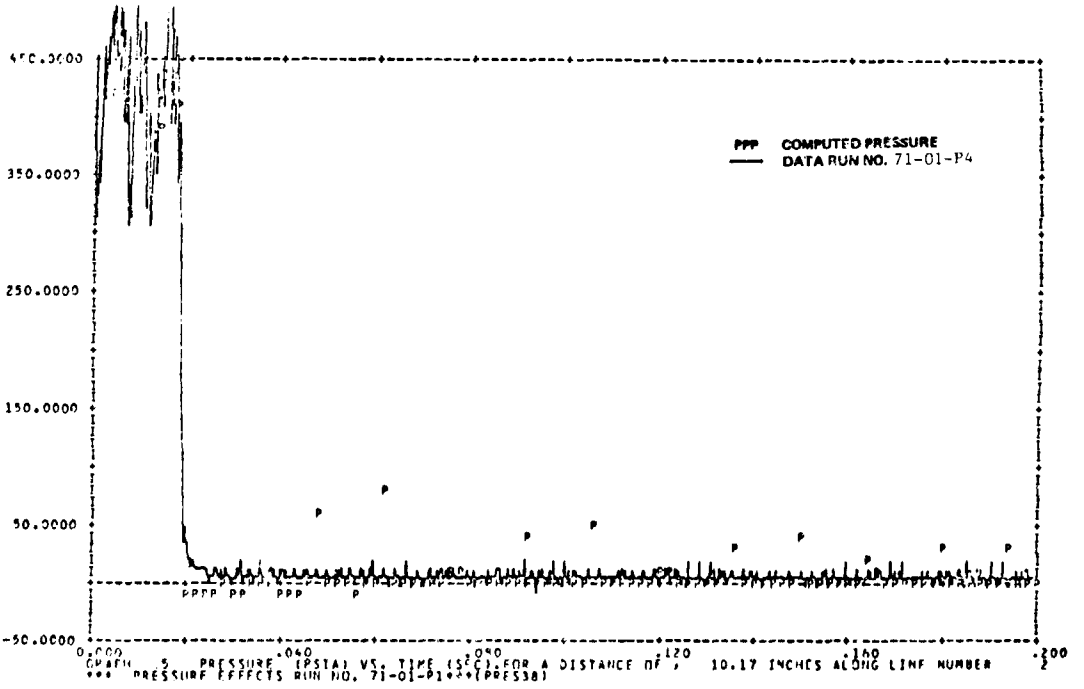

FIGURE 313 71-01-P4 TURN-OFF TRANSIENT

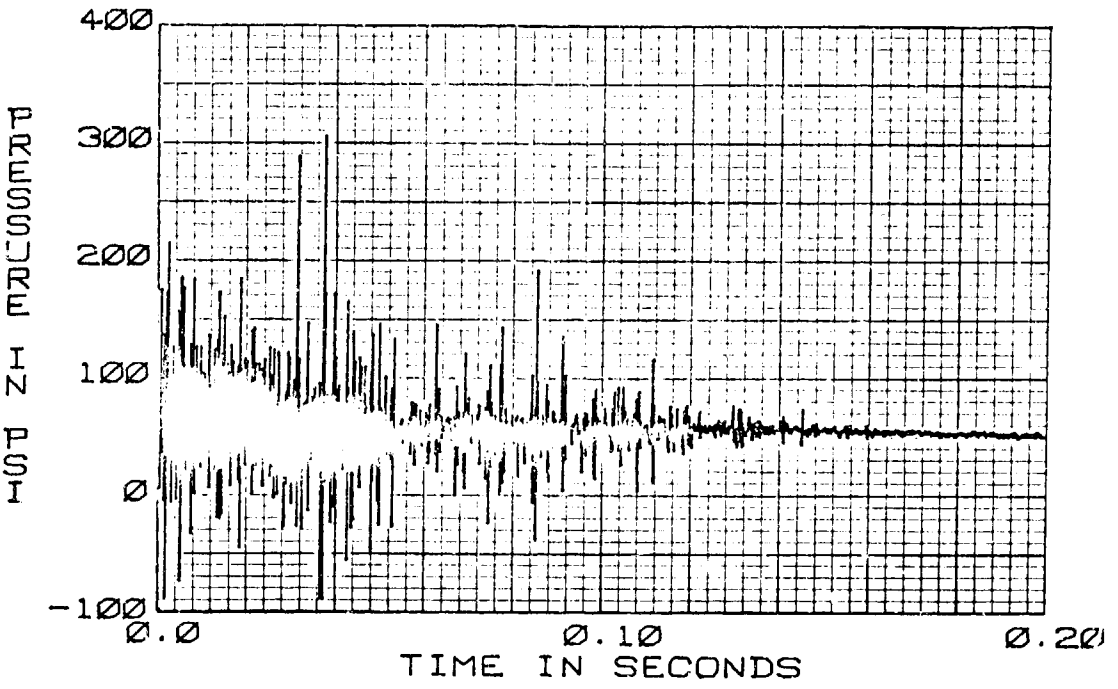

FIGURE 314 PRESSURE EFFECTS
71-01-P6 TURN-OFF TRANSIENT
100 CIS 130°F

A turn-on transient was also made with the input data in Figures 315, 316 and 317. The steady state flow was 100 CIS and the temperature 130°F. The computer output in Figure 318, 319, 320 and 321 show good correlation with the test data. In Figure 320 the predicted pressure dip at 20 millisecond closely follows the data. However the computed pressures from about 30 to 80 milliseconds fall 150 to 200 psi below the actual values. This is typical of all the HYTRAN simulations of turn-on transients. It indicates that the damping terms provided by the dynamic friction function are perhaps too conservative.

The test data in Figures 322 and 323 were input with the data in Figure 324 for a turn-off transient simulation at a system pressure of 1500 psig, a temperature of 133°F and a 85 CIS steady state flow rate. The results in Figures 325, 326, 327 and 328 show good correlation with the measured data.

```
***  PRESSURE EFFECTS RUN NO. 71-01+P1***(PRES39)

THE TRANSIENT RESPONSE IS FROM T=0.0  TO T=   .200 SECONDS AT TIME INTERVALS OF DELT= .00025
          WITH OUTPUT POINTS PLOTTED AT INTERVALS OF  ,  .00200  SECONDS

FLUID DATA FOR  MIL-H-83282 AT  3000.0 PSIG, -    50.0 PSIG AND 130.0 DEG F  IN   10.0 DEG F STEPS
                VISCOSITY     -  .200E-01        .153E-01IN**2/SEC
                DENSITY       -  .790E-04        .781F-04(LB-SEC**2)/IN**4
                BULK MODULUS  -  .223E+06        .187E+06PSI
                VAPOUR PRESS.-  .200E+01 AT  130.0 DEG F
```

LINE DATA LINE NO.	LENGTH	INTERNAL DIA	WALL THICKNESS	MODULUS OF ELASTICITY	DELX	CHARACTERISTIC IMPEDANCE	VELOCITY OF SOUND
1	366.3000	.4440	.0280	.300E+08	10.1833	25.5997	50162.9463
2	366.0000	.4440	.0280	.300E+08	10.1667	25.5997	50162.9463

```
 COMP#,   1  INTEGER DATA      1   91    0   -1    1  -0   -0   -0   -0   -0   -0   -0   -0   -0   -0   -0
 COMP#,   2  INTEGER DATA      2   23    3    1   -2  -0   -0   -0   -0   -0   -0   -0   -0    4   -0   -0
REAL DATA CARD #    1     .2200E-01   .6500E+00 -0.          -0.          -0.          -0.          -0.
REAL DATA CARD #    2   0.           .1400E-01   .1640E-01   .2000E+00 -0.          -0.          -0.
REAL DATA CARD #    3   0.         0.           .9370E+00   .9370E+00 -0.          -0.          -0.
 COMP#,   3  INTEGER DATA      3   91    0    2    1  -0   -0   -0   -0   -0   -0   -0   -0   -0   -0   -0
```

FIGURE 315 RUN 71-01 HYTRAN INPUT DATA FOR A TURN-ON TRANSIENT

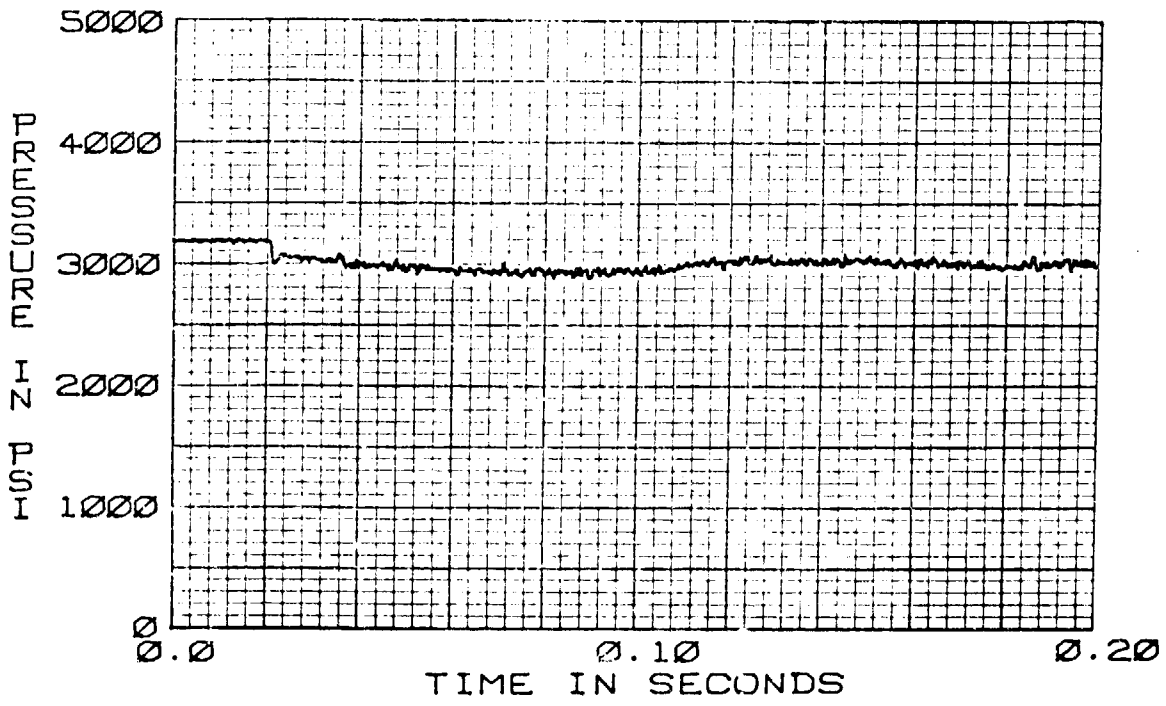

FIGURE 316 PRESSURE EFFECTS
71-01+P1 TURN-ON TRANSIENT
100 CIS 130°F

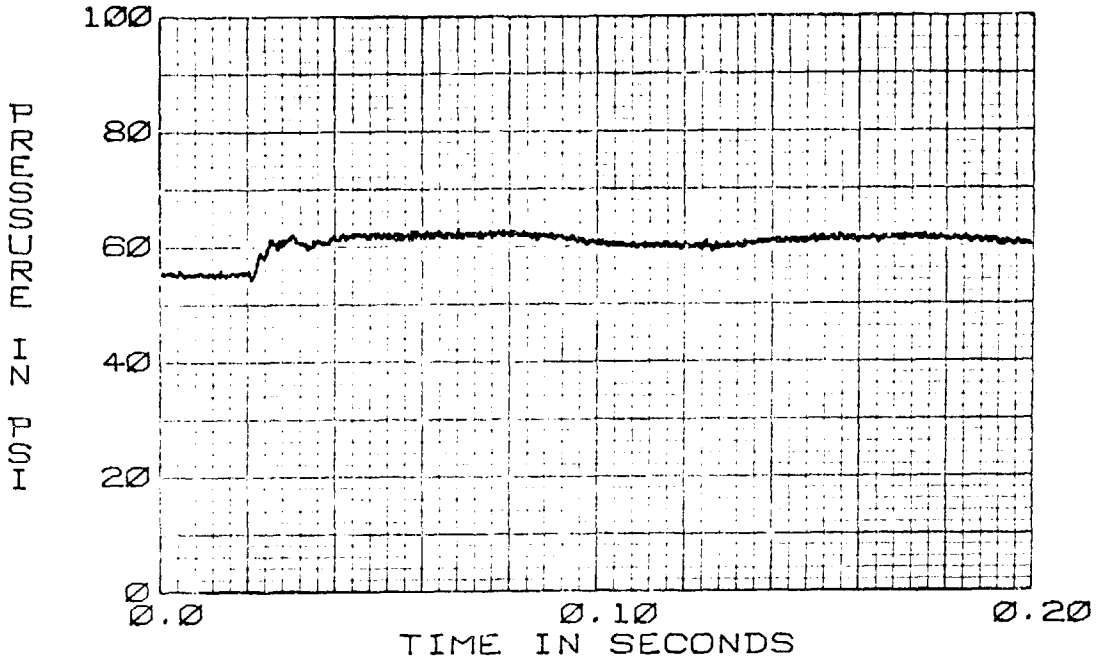

FIGURE 317 PRESSURE EFFECTS
71-01+P7 TURN-ON TRANSIENT
100 CIS 130°F

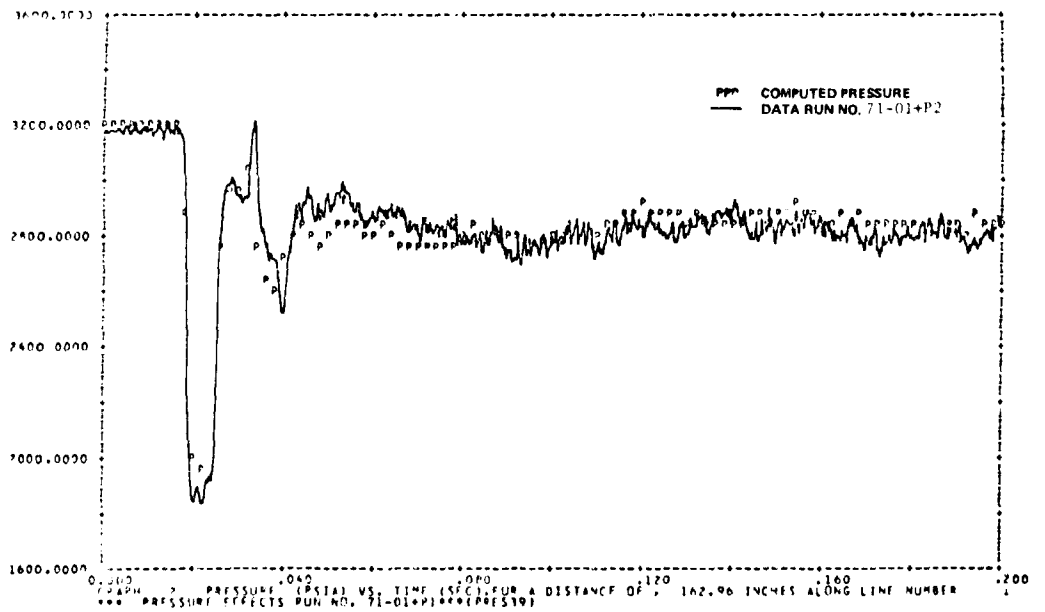

FIGURE 318 71-01+P2 TURN-ON TRANSIENT

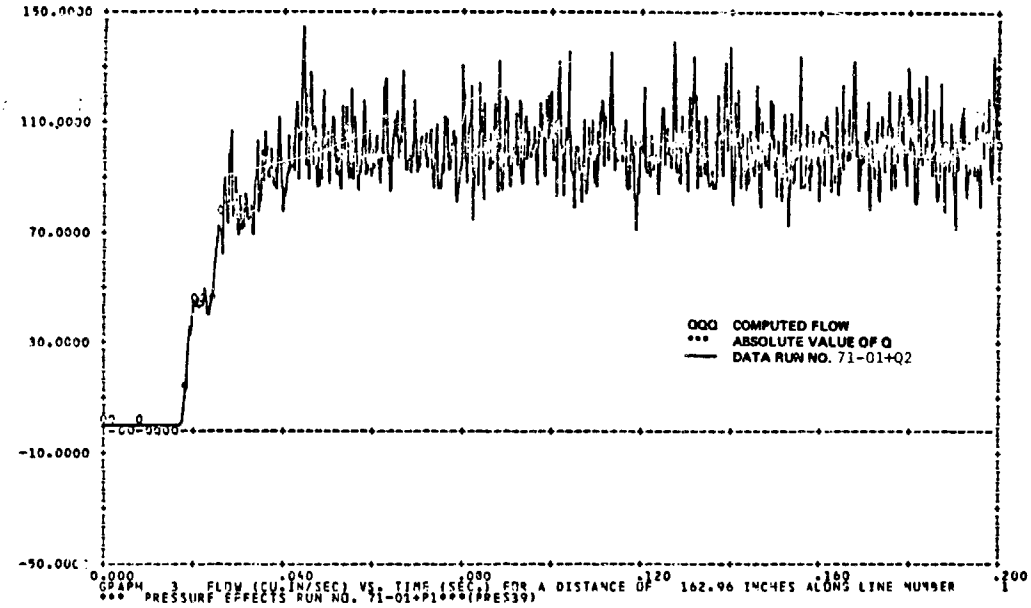

FIGURE 319 71-01+Q2 TURN-ON TRANSIENT

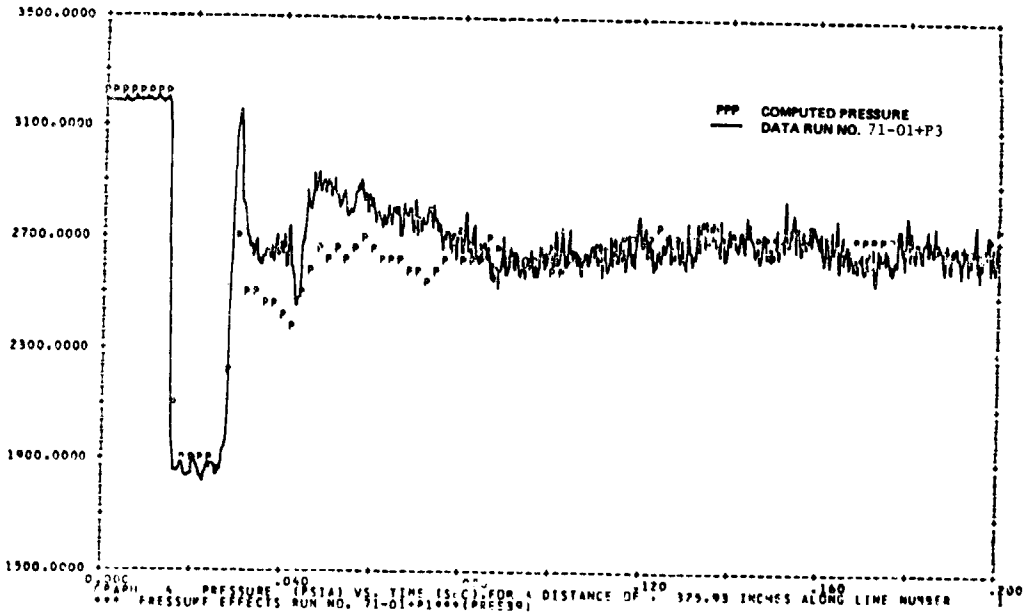

FIGURE 320 71-01+P3 TURN-ON TRANSIENT

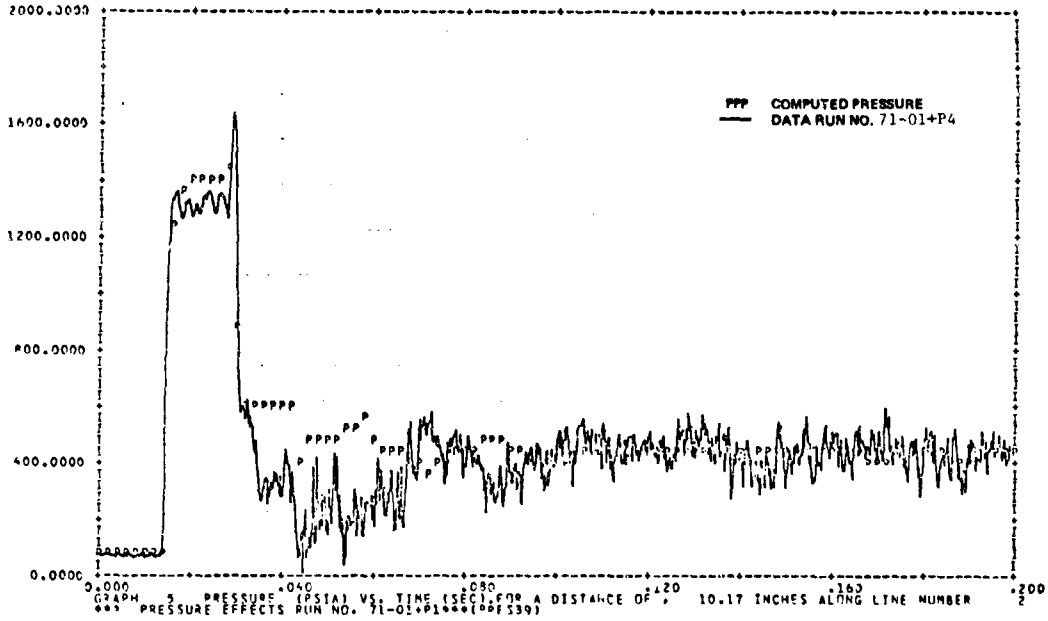

FIGURE 321 71-01+P4 TURN-ON TRANSIENT

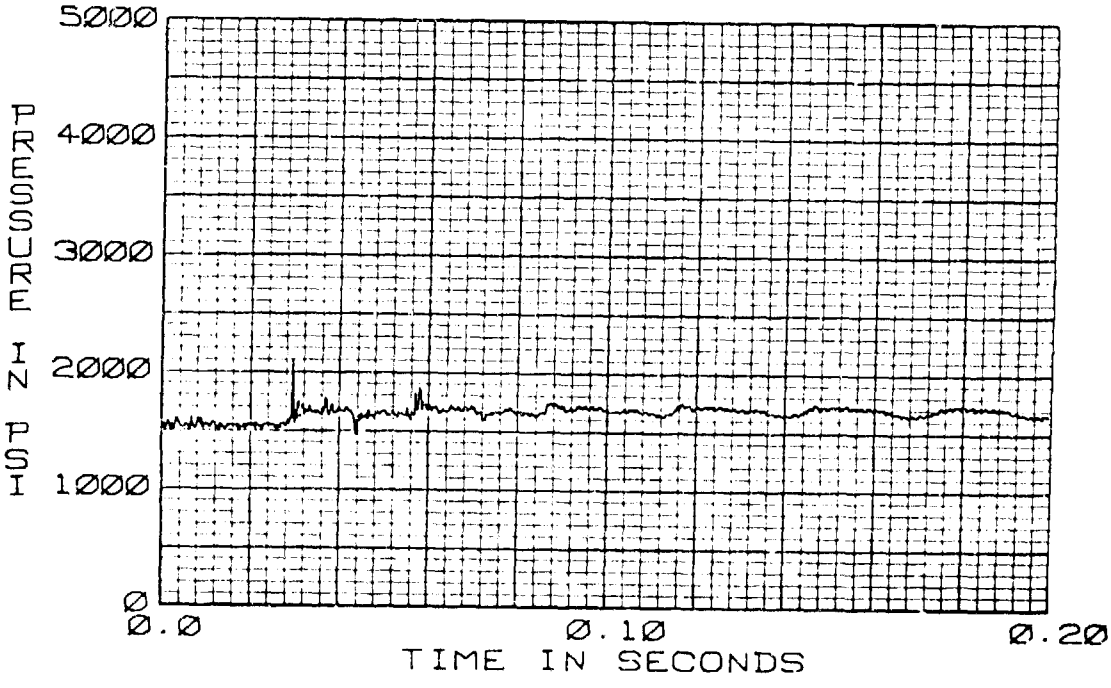

FIGURE 322 PRESSURE EFFECTS
71-15-P1 TURN-OFF TRANSIENT
85 CIS 130°F

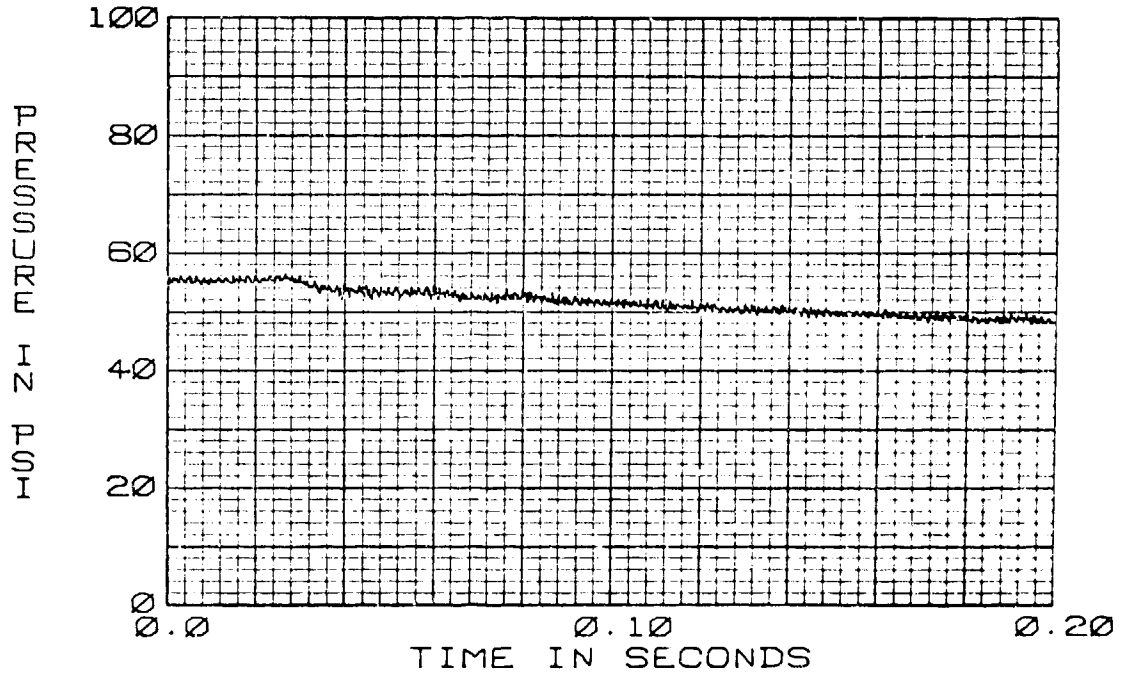

FIGURE 323 PRESSURE EFFECTS
71-15-P7 TURN-OFF TRANSIENT
85 CIS 130°F

**** PRESSURE EFFECTS RUN NO.71-15-P1 ****(PRES40)

THE TRANSIENT RESPONSE IS FROM T=0.0 TO T= .200 SECONDS AT TIME INTERVALS OF DELT= .00020
WITH OUTPUT POINTS PLOTTED AT INTERVALS OF , .00200 SECONDS

FLUID DATA FOR MIL-H-83282 AT 1500.0 PSIG, - 50.0 PSIG AND 133.0 DEG F IN 10.0 DEG F STEPS

VISCOSITY	= .167E-01	.147E-01LBF*SEC/IN**2
DENSITY	= .784E-04	.780E-04(LB-SEC**2)/IN**4
BULK MODULUS	= .202E+06	.185E+06PSI
VAPOUR PRESS.	= .200E+01 AT 133.0 DEG F	

LINE DATA

LINE NO.	LENGTH	INTERNAL DIA	WALL THICKNESS	MODULUS OF ELASTICITY	DELX	CHARACTERISTIC IMPEDANCE	VELOCITY OF SOUND
1	348.3000	.4440	.0280	.300E+08	9.8943	24.4459	48294.9412
2	300.0000	.4440	.0280	.300E+08	9.8919	24.4459	48294.9412

COMP#, 1 INTEGER DATA 1 91 0 -1 1 -0 -0 -0 -0 -0 -0 -0 -0 -0 -0 -0

COMP#, 2 INTEGER DATA 2 23 3 1 -2 -0 -0 -0 -0 -0 -0 -0 4 -0 -0

REAL DATA CARD # 1 .2200E-01 .6500E+00 -0. -0. -0. -0. -0. -0. -0.

REAL DATA CARD # 2 0. .2080E-01 .2080E-01 .2000E+00 -0. -0. -0. -0. -0.

REAL DATA CARD # 3 .1094E+01 .1094E+01 0. 0. -0. -0. -0. -0. -0.

COMP#, 3 INTEGER DATA 3 91 0 2 1 -0 -0 -0 -0 -0 -0 -0 -0 -0 -0

FIGURE 324 RUN 71-15 HYTRAN INPUT DATA FOR A TURN-OFF TRANSIENT

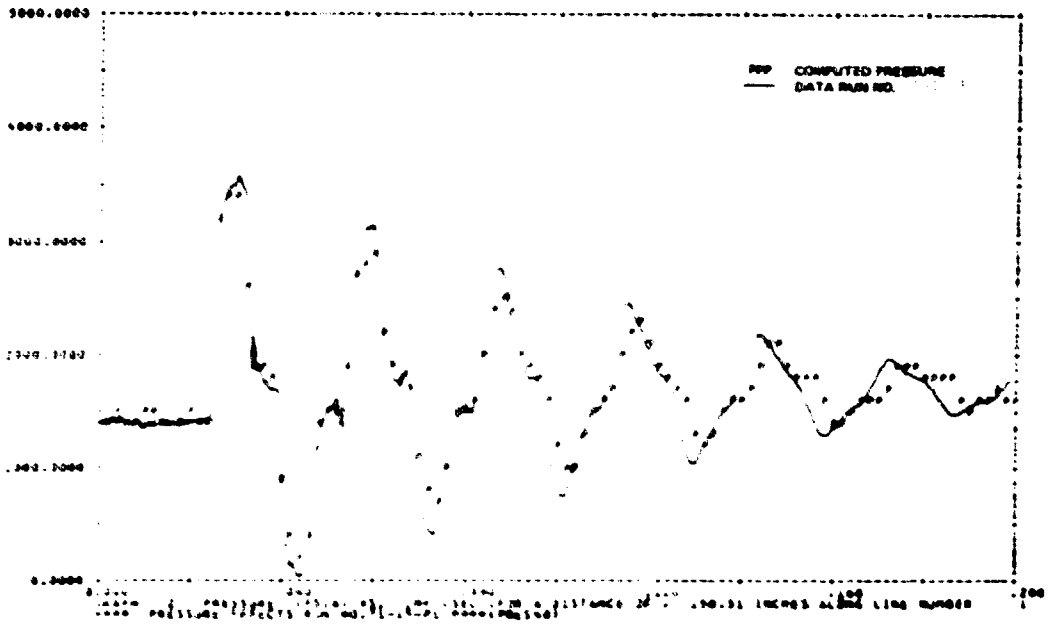

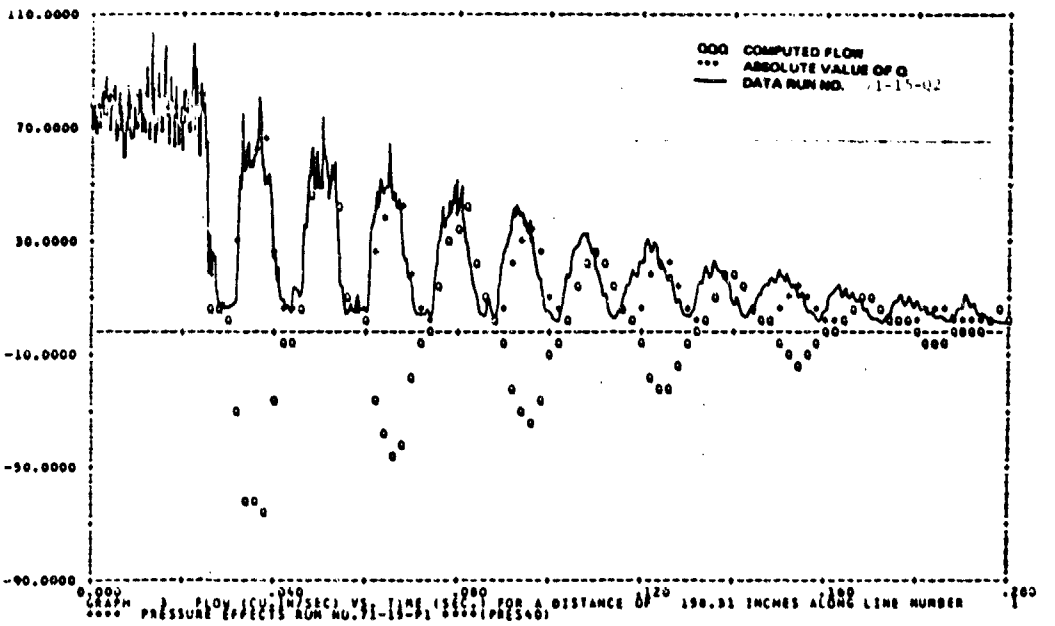

FIGURE 326 71-15-Q2 TURN-OFF TRANSIENT

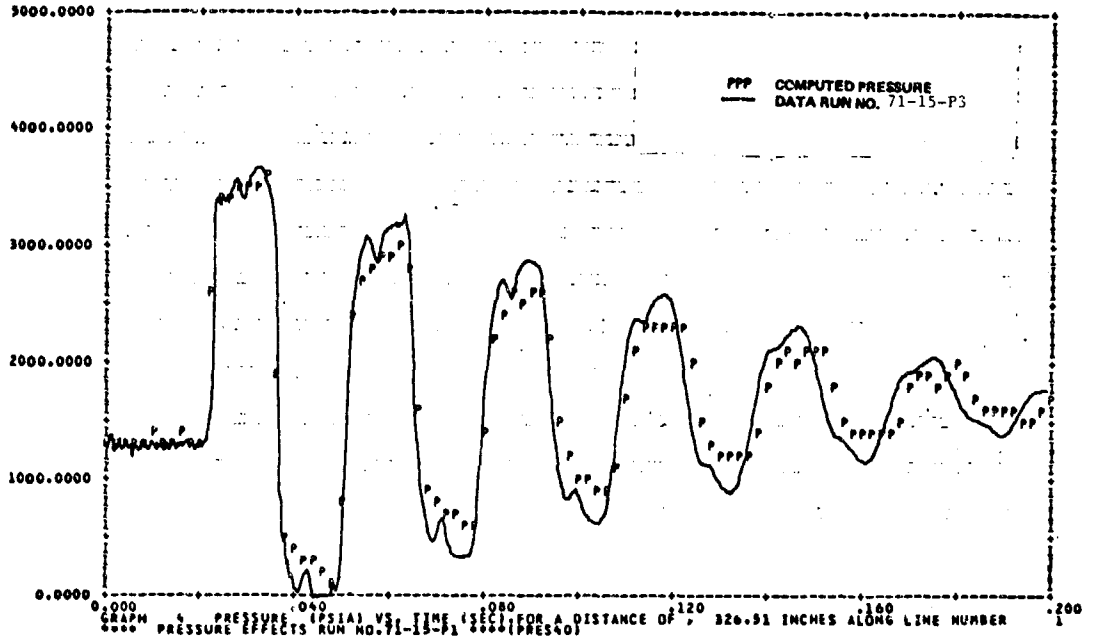

FIGURE 327 71-15-P3 TURN-OFF TRANSIENT

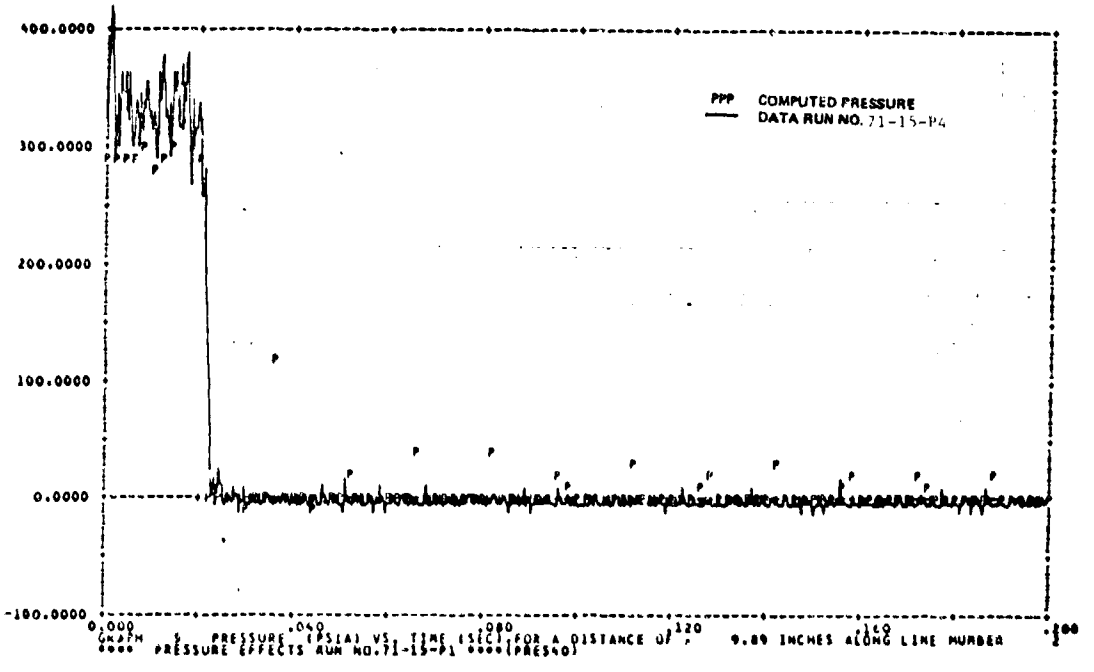

FIGURE 328 71-15-P4 TURN-OFF TRANSIENT

The turn-on transient run with the input data in Figures 329, 330 and 331 also shows that even at this lower system pressure the HYTRAN program is still able to accurately predict the system transients. The results are shown in Figures 332, 333, 334 and 335. In Figure 333 the measured flow does not rise as quickly as the computed data. This discrepancy exists because the hot film anemometers used in measuring the flow records local velocity changes in the line's velocity profile, where as the computer program calculates average line velocities.

A computer simulation at 3750 psig and at 211°F and 100 CIS was tried. The input data is shown in Figures 336, 337 and 338. The results in 339, 340, and 341 again show good correlation to the actual data.

Likewise for a turn-on simulation the predicted data in Figures 342, 343, 344 and 345 give good correlation. The input data is in Figures 346, 347 and 348.

b. Conclusions - The HYTRAN calculations of flows and pressures compare reasonably well with the test data measured in the Lab. The verification results indicate that the mathematical theory used in the HYTRAN program is applicable to systems with pressure ranges from 1500 to 3750 PSIG.

```
****  PRESSURE EFFECTS RUN NO.71-15+P1 ****(PRESS1)

THE TRANSIENT RESPONSE IS FROM T=0.0  TO T=  .200 SECONDS AT TIME INTERVALS OF DELT= .00020
          WITH OUTPUT POINTS PLOTTED AT INTERVALS OF  ,  .00200  SECONDS


FLUID DATA FOR  MIL-H-83282 AT  1500.0 PSIG, -    50.0 PSIG AND 131.0 DEG F  IN   10.0 DEG F STEPS
                VISCOSITY    -  .172E-01        .151E-01IN**2/SEC
                DENSITY      -  .785E-04        .781E-04(LB-SEC**2)/IN**4
                BULK MODULUS -  .204E+06        .186E+06PSI
                VAPOUR PRESS.-  .200E+01 AT  131.0 DEG F

LINE DATA
LINE NO.    LENGTH          INTERNAL DIA      WALL THICKNESS    MODULUS OF ELASTICITY    DELX          CHARACTERISTIC IMPEDANCE    VELOCITY OF SOUND
   1        346.3400          .4440             .0280             .300E+08              9.8943          24.5318                  48380.6164
   2        366.0000          .4440             .0280             .300E+08              9.8919          24.5318                  48380.6164
 COMP#,  1  INTEGER DATA      1   91    0   -1    1   -0   -0   -0   -0   -0   -0   -0   -0   -0   -0   -0
 COMP#,  2  INTEGER DATA      2   23    3    1   -2   -0   -0   -0   -0   -0   -0   -0   -0    4   -0   -0
REAL DATA CARD #   1    .2200E-01   .6500E+00 -0.          -0.          -0.          -0.          -0.          -0.
REAL DATA CARD #   2    0.          .1700E-01   .1900E-01    .2000E+00 -0.          -0.          -0.          -0.
REAL DATA CARD #   3    0.          0.          .1094E+01    .1094E+01 -0.          -0.          -0.          -0.
 COMP#,  3  INTEGER DATA      3   91    0    2    1   -0   -0   -0   -0   -0   -0   -0   -0   -0   -0   -0
```

FIGURE 329 RUN 71-15 HYTRAN INPUT DATA FOR A TURN-ON TRANSIENT

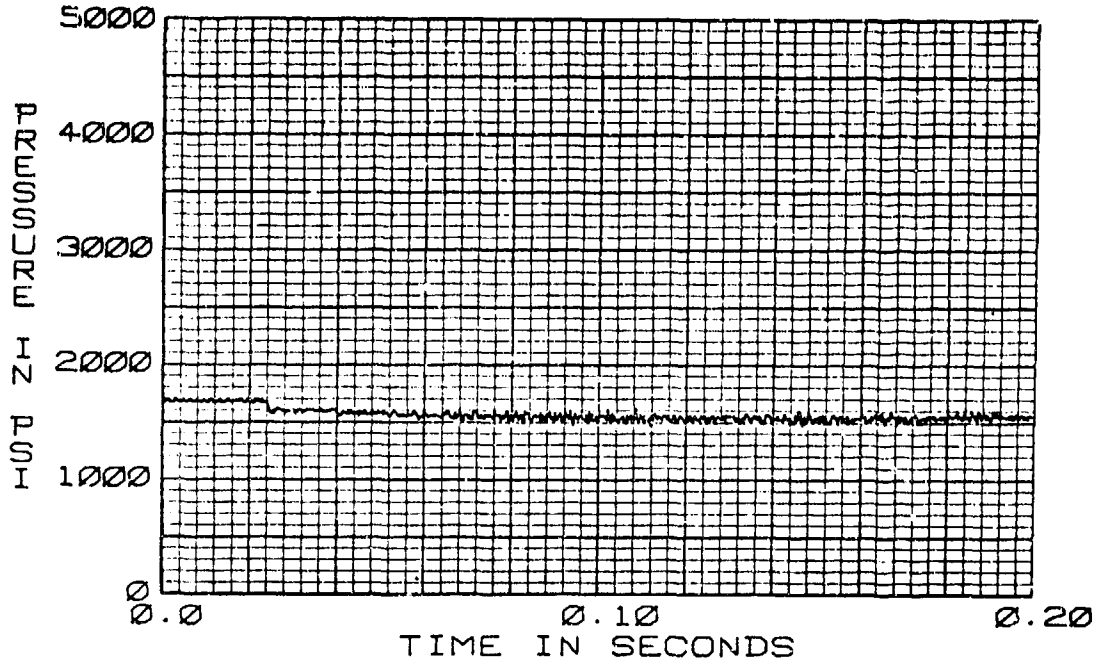

FIGURE 330 PRESSURE EFFECTS
71-15+P1 TURN-ON TRANSIENT
85 CIS 130°F

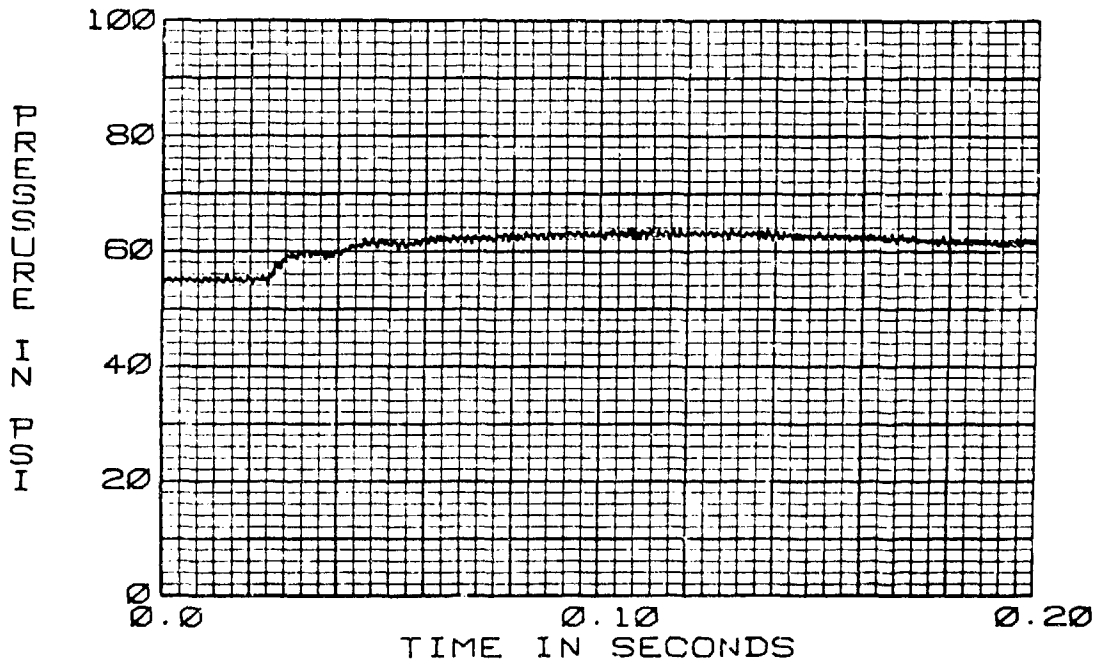

FIGURE 331 PRESSURE EFFECTS
71-15+P7 TURN-ON TRANSIENT
85 CIS 130°F

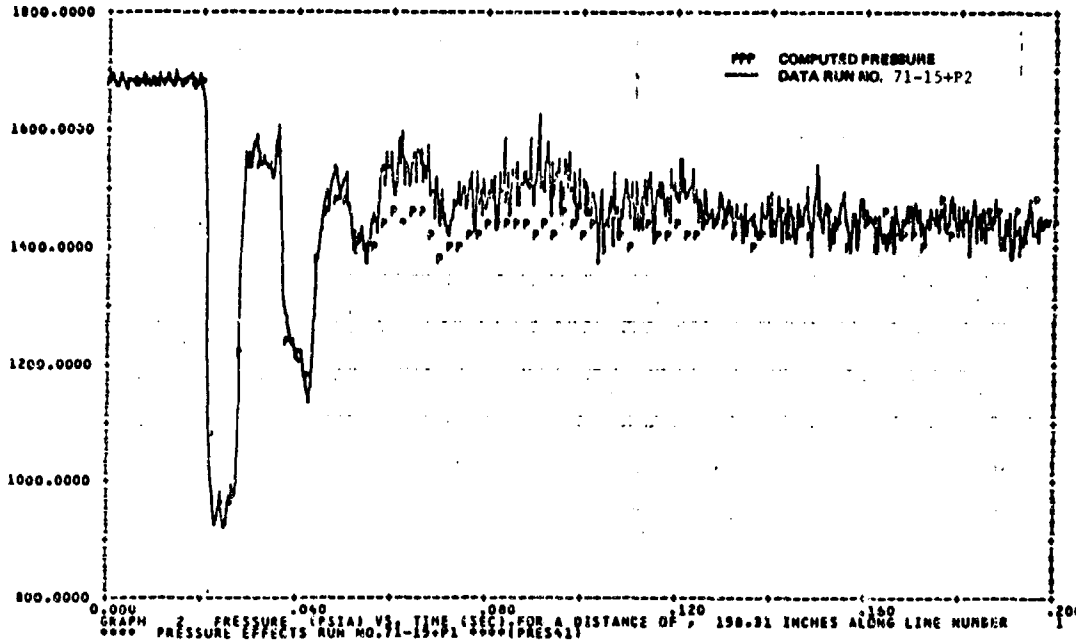

FIGURE 332 71-15+P2 TURN-ON TRANSIENT

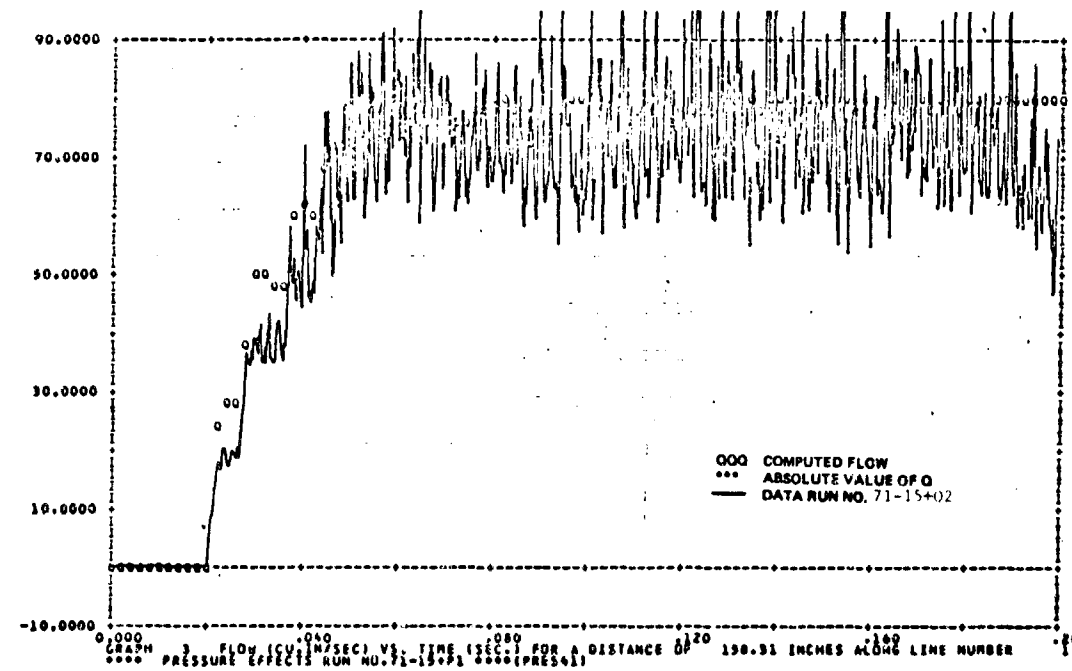

FIGURE 333 71-15+Q2 TURN-ON TRANSIENT

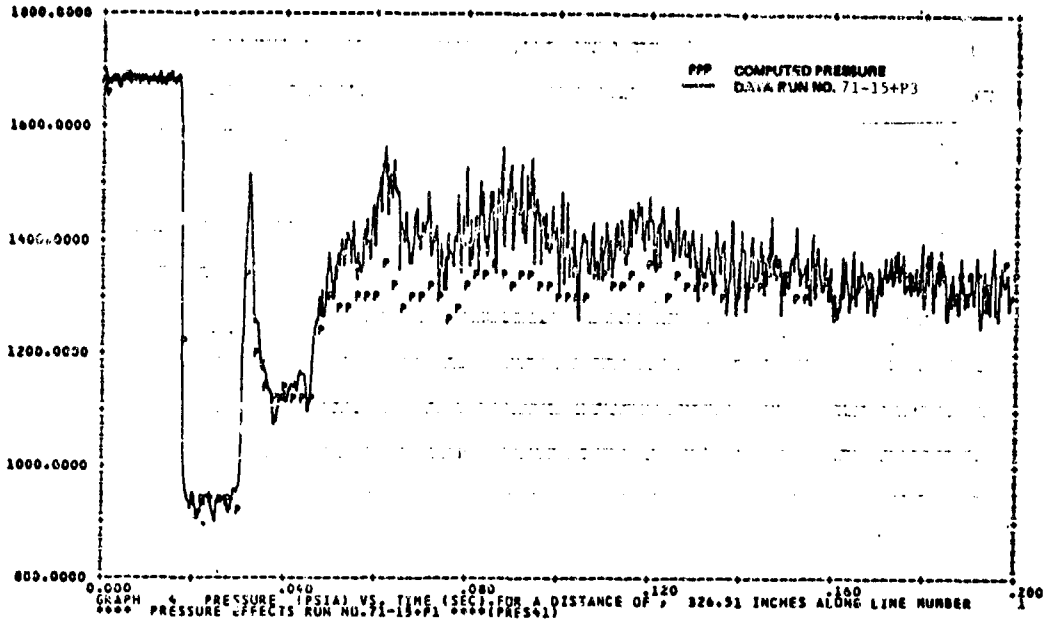

FIGURE 334 71-15+P3 TURN-ON TRANSIENT

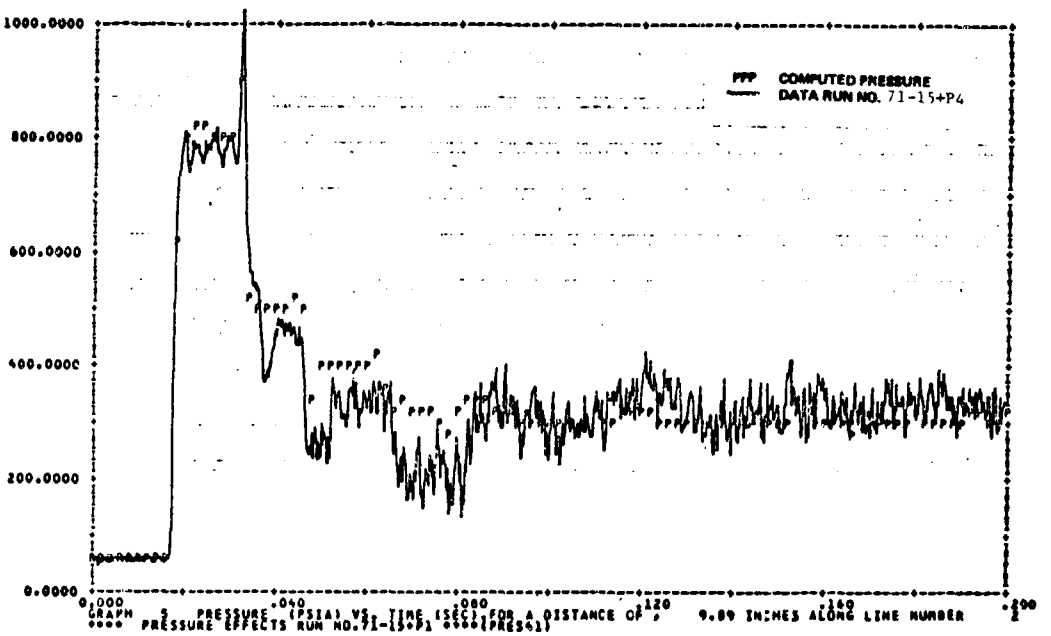

FIGURE 335 71-15+P4 TURN-ON TRANSIENT

```
**** PRESSURE EFFECTS RUN NO.71-25-P1 ****(PRES42)

THE TRANSIENT RESPONSE IS FROM T=0.0 TO T=  .200 SECONDS AT TIME INTERVALS OF DELT= .00020
        WITH OUTPUT POINTS PLOTTED AT INTERVALS OF  ,  .00200  SECONDS

FLUID DATA FOR  MIL-H-83282 AT  3750.0 PSIG, -    50.0 PSIG AND 211.0 DEG F  IN   10.0 DEG F STEPS
                VISCOSITY   -  .777E-02        .600E-02IN**2/SEC
                DENSITY     -  .764E-04        .793E-04(LB-SEC**2)/IN**4
                BULK MODULUS -  .182E+06       .137E+06PSI
                VAPOUR PRESS.-  .200E+01 AT  211.0 DEG F
```

LINE DATA LINE NO.	LENGTH	INTERNAL DIA	WALL THICKNESS	MODULUS OF ELASTICITY	DELX	CHARACTERISTIC IMPEDANCE	VELOCITY OF SOUND
1	348.3000	.4440	.0280	.300E+08	9.3595	22.9711	46571.9114
2	366.0000	.4440	.0280	.300E+08	9.3846	22.9711	46571.9114

COMPS, 1 INTEGER DATA	1	91	0	-1	1	-0	-0	-0	-0	-0	-0	-0	-0	-0	-0	-0		
COMPS, 2 INTEGER DATA	2	23	3	1	-2	-0	-0	-0	-0	-0	-0	-0	-0	4	-0	-0		
REAL DATA CARD # 1	.2200E-01	.6500E+00	-0.			-0.		-0.		-0.		-0.		-0.				
REAL DATA CARD # 2	0.	.1500E-01	.1600E-01	.2000E+00	-0.		-0.		-0.		-0.							
REAL DATA CARD # 3	.7620E+00	.7620E+00	0.	0.		-0.		-0.		-0.								
COMPS, 3 INTEGER DATA	3	91	0	2	1	-0	-0	-0	-0	-0	-0	-0	-0	-0	-0	-0		

FIGURE 336 RUN 71-25 HYTRAN INPUT DATA FOR A TURN-OFF TRANSIENT

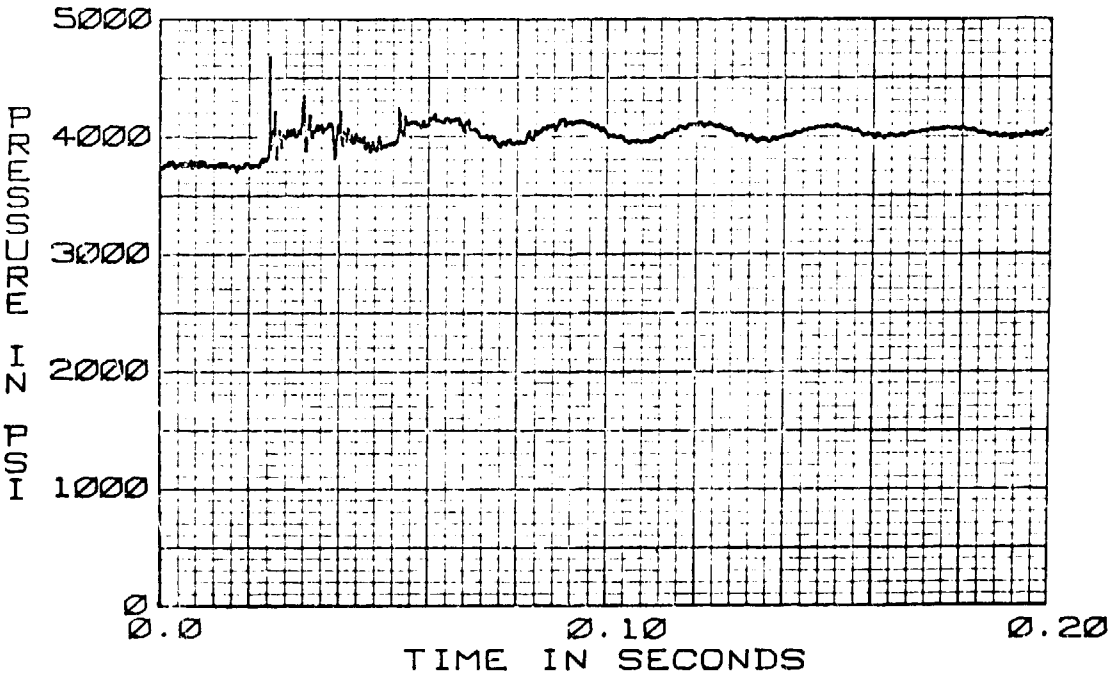

FIGURE 337 PRESSURE EFFECTS
71-25-P1 TURN-OFF TRANSIENT
100 CIS 210°F

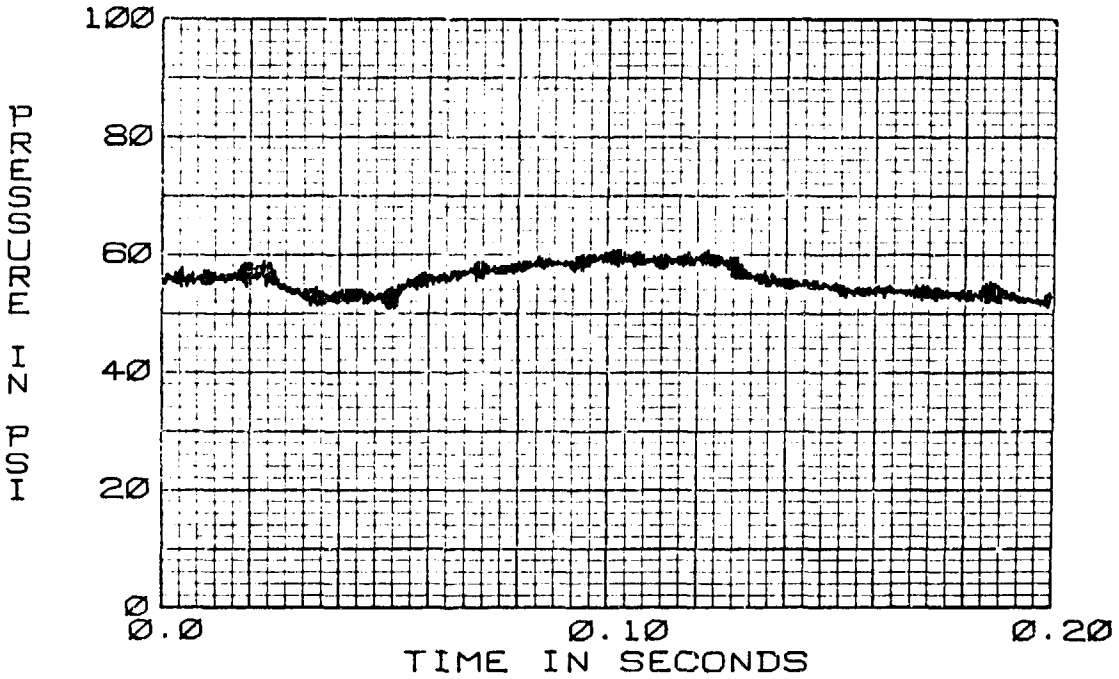

FIGURE 338 PRESSURE EFFECTS
71-25-P7 TURN-OFF TRANSIENT
100 CIS 210°F

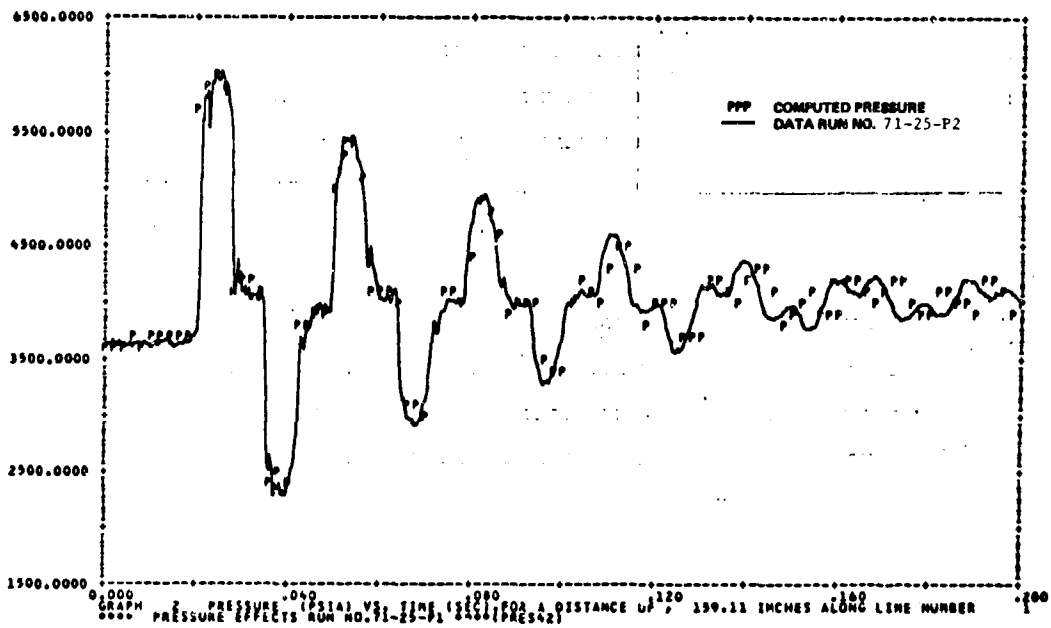

FIGURE 339 71-25-P2 TURN-OFF TRANSIENT

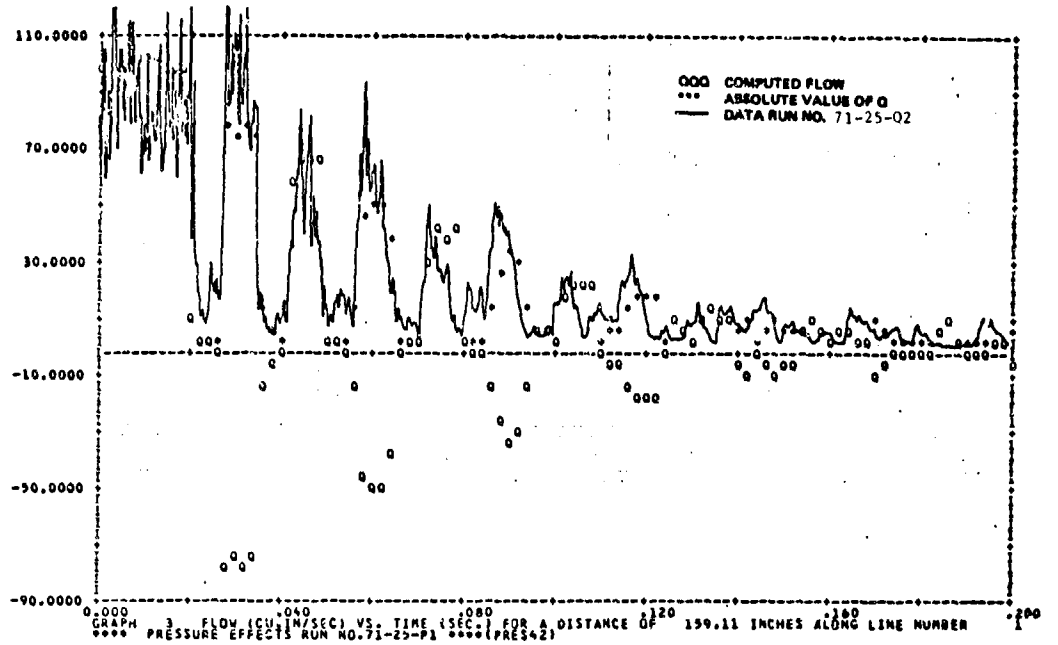

FIGURE 340 71-25-Q2 TURN-OFF TRANSIENT

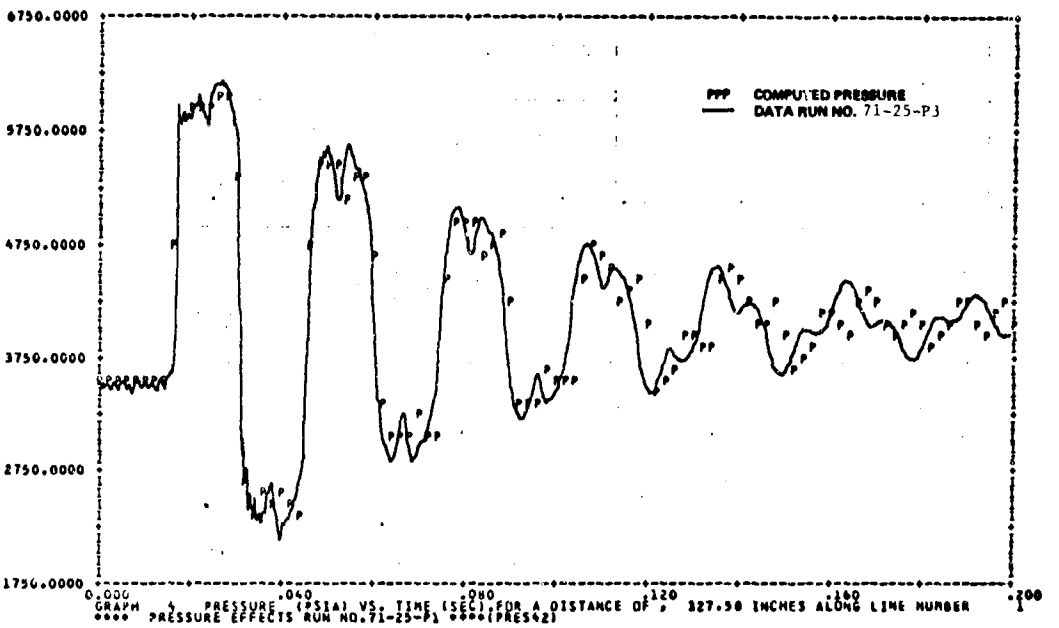

FIGURE 341 71-25-P3 TURN-OFF TRANSIENT

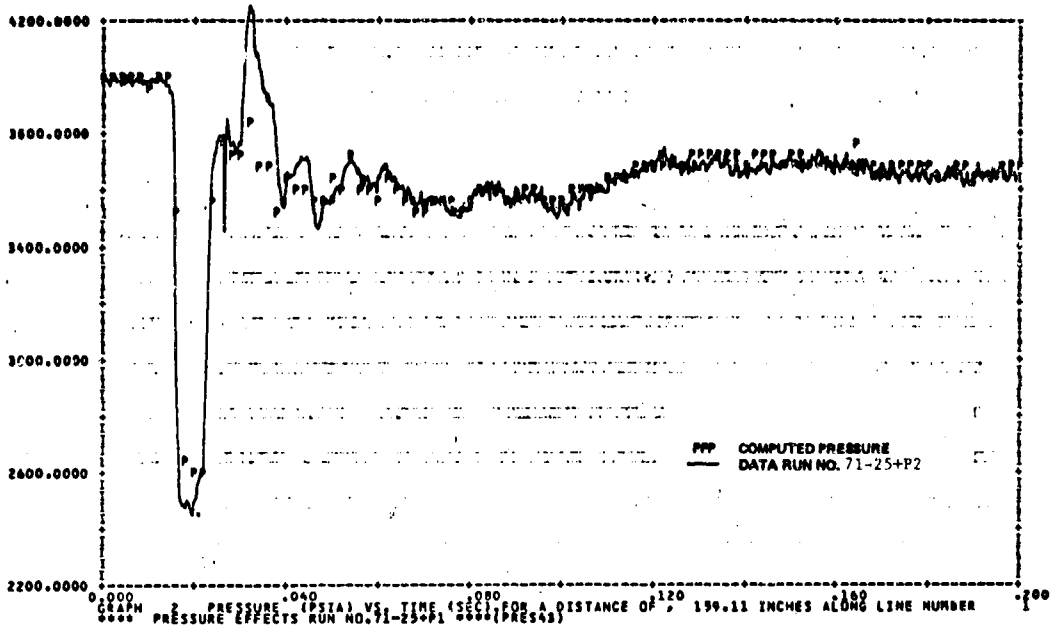

FIGURE 342 71-25+P2 TURN-ON TRANSIENT

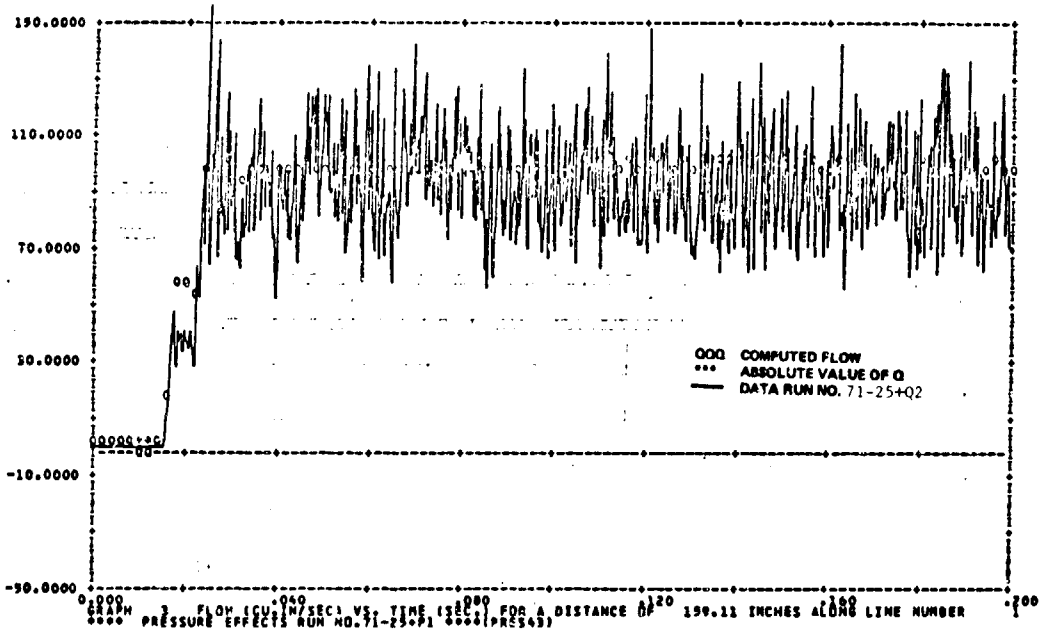

FIGURE 343 71-25+Q2 TURN-ON TRANSIENT

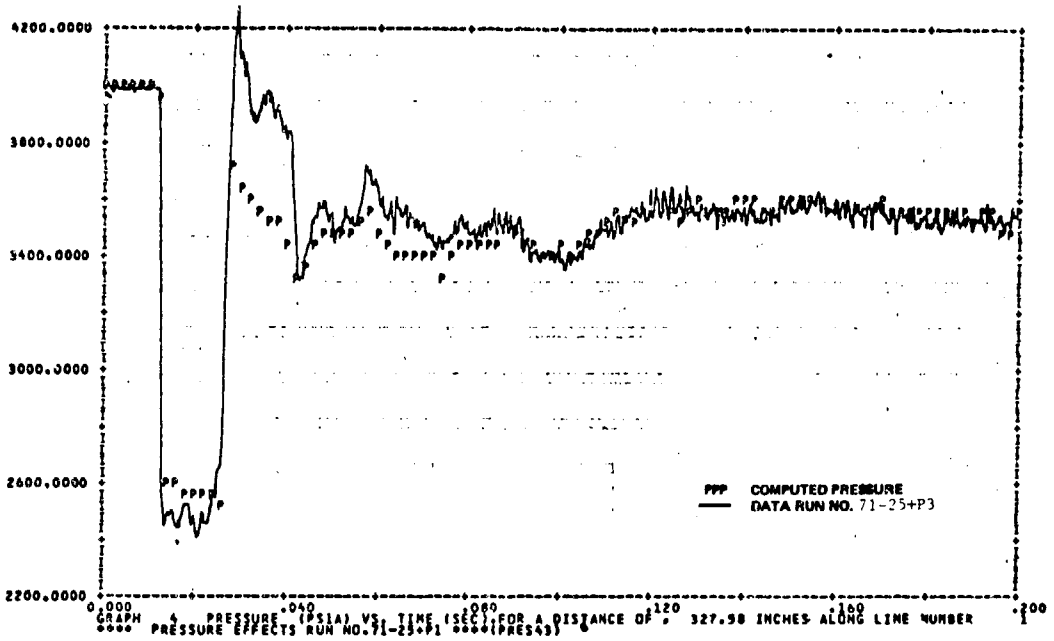

FIGURE 344 71-25+P3 TURN-ON TRANSIENT

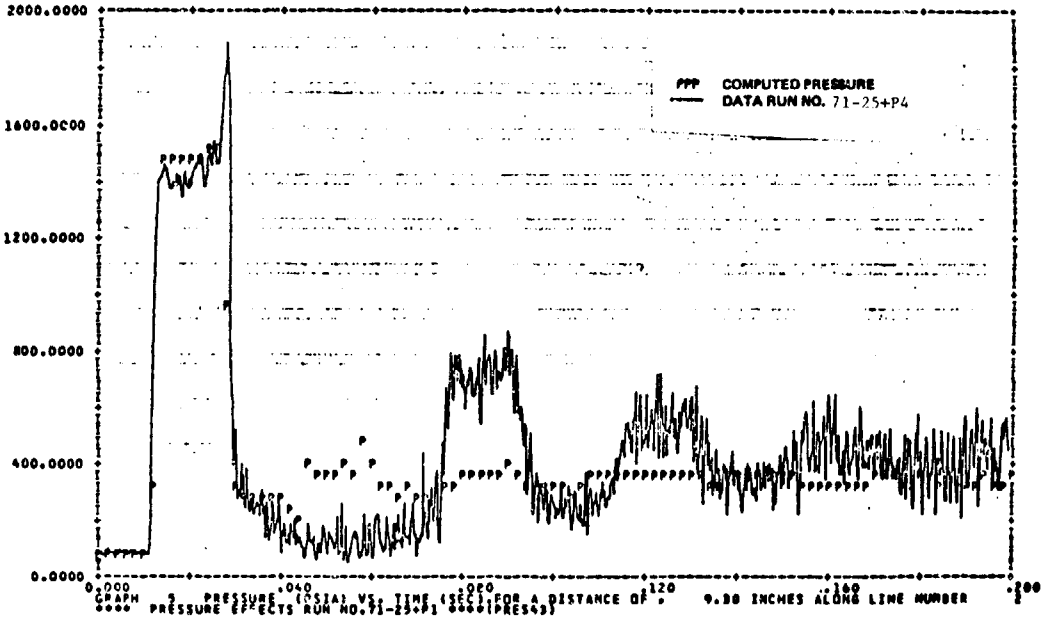

FIGURE 345 71-25+P4 TURN-ON TRANSIENT

```
****  PRESSURE EFFECTS RUN NO.71-25+P1 ****(PRES43)

THE TRANSIENT RESPONSE IS FROM T=0.0  TO T=  .200 SECONDS AT TIME INTERVALS OF DELT= .00020
        WITH OUTPUT POINTS PLOTTED AT INTERVALS OF  ,  .00200  SECONDS

FLUID DATA FOR  MIL-H-83282 AT  3750.0 PSIG, -    50.0 PSIG AND 208.0 DEG F  IN   10.0 DEG F STEPS
                VISCOSITY    -  .709E-02      .616E-02IN**2/SEC
                DENSITY      -  .765E-04      .754E-04(LB-SEC**2)/IN**4
                BULK MODULUS -  .183E+06      .139E+06PSI
                VAPOUR PRESS.-  .200E+01 AT  208.0 DEG F

LINE DATA
LINE NO.    LENGTH      INTERNAL DIA    WALL THICKNESS    MODULUS OF ELASTICITY    DELX      CHARACTERISTIC IMPEDANCE    VELOCITY OF SOUND
    1       346.3000        .4440           .0280              .300E+08          9.3595          23.0686                  46704.3714
    2       366.0000        .4440           .0280              .300E+08          9.3646          23.0686                  46704.3714
 COMP#,  1  INTEGER DATA     1  91   0  -1   1  -0  -0  -0  -0  -0  -0  -0  -0  -0  -0  -0  -0
 COMP#,  2  INTEGER DATA     2  23   3   1  -2  -0  -0  -0  -0  -0  -0  -0  -0   4  -0  -0
REAL DATA CARD #  1    .2200E-01   .6500E+06 -0.        -0.        -0.        -0.        -0.        -0.
REAL DATA CARD #  2    0.          .1160E-01   .1340E-01   .2000E+00 -0.        -0.        -0.        -0.
REAL DATA CARD #  3    0.          0.          .7620E+00   .7620E+00 -0.        -0.        -0.        -0.
 COMP#,  3  INTEGER DATA     3  91   0   2   1  -0  -0  -0  -0  -0  -0  -0  -0  -0  -0  -0
```

FIGURE 346 RUN 71-25 HYTRAN INPUT DATA FOR A TURN ON TRANSIENT

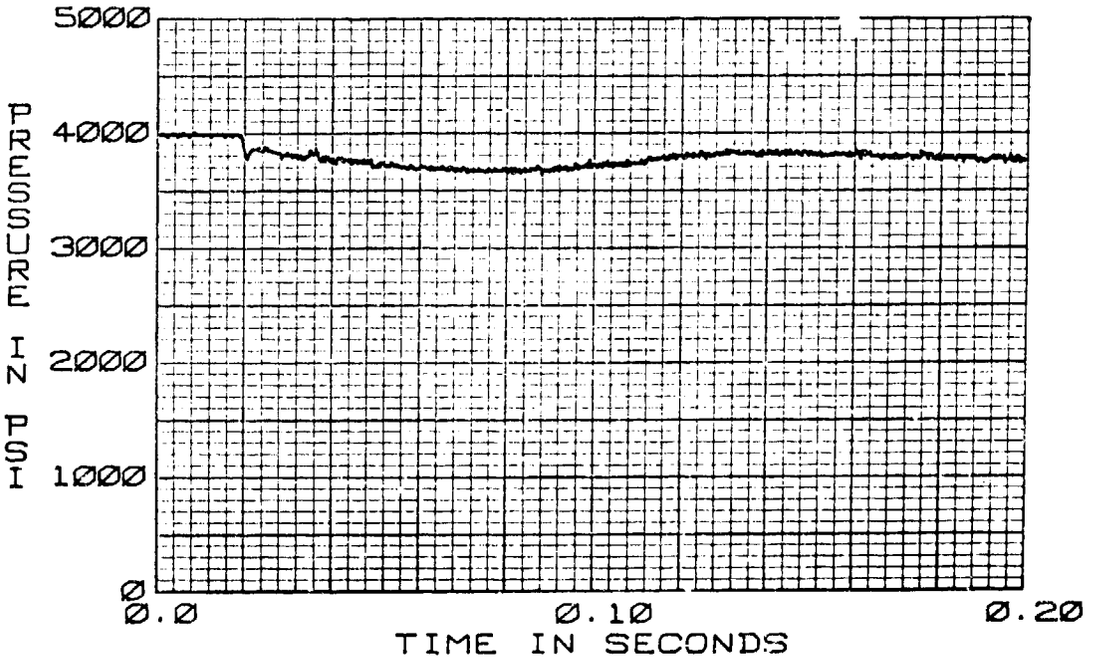

FIGURE 347 PRESSURE EFFECTS
71-25+P1 TURN-ON TRANSIENT
100 CIS 210°F

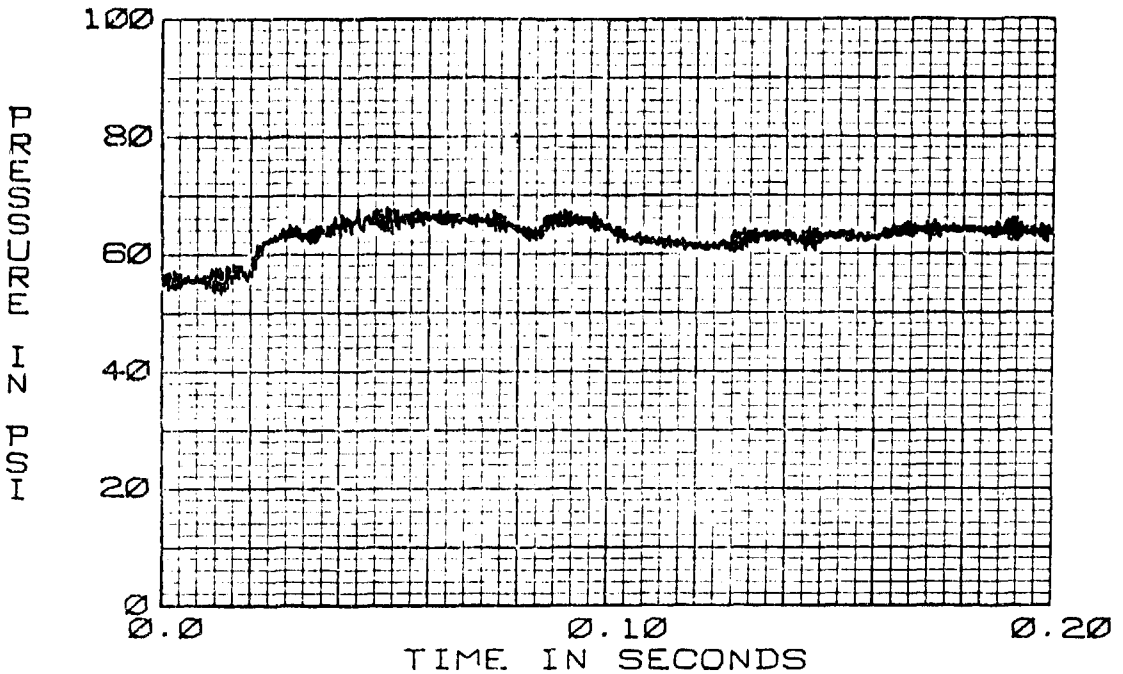

FIGURE 348 PRESSURE EFFECTS
71-25+P7 TURN-ON TRANSIENT
100 CIS 210°F

11. HYTRAN PROGRAM VERIFICATION FOR AIR EFFECTS AND RESERVOIR MODEL

In this section the test results on return line transients are presented. The effects of different system air content levels were monitored at various valve closure rates and system operating temperatures. The testing was performed on a 1/2" line system with MIL-H-83282 hydraulic fluid.

The air effects/reservoir testing is a continuation of the investigation of the cavitation effects in return line systems. The computer simulation of the turn-on and turn-off transients using the HYTRAN line cavitation model gave reasonable correlation to the test data.

The air effects/reservoir testing was run on the system configuration shown in Figure 349.

The following parameters were recorded for the test runs: P1, P2, P3, Q3, P4, Q4, P5, P6, and XCV-the valve position. The P4 pressure transducer is located 3.5 inches upstream of the F-4 PC reservoir and the P5 transducer measures the pressure inside. The difference between P4 and P5 represent the entry and exit losses from the one inch line to the large volume of the reservoir.

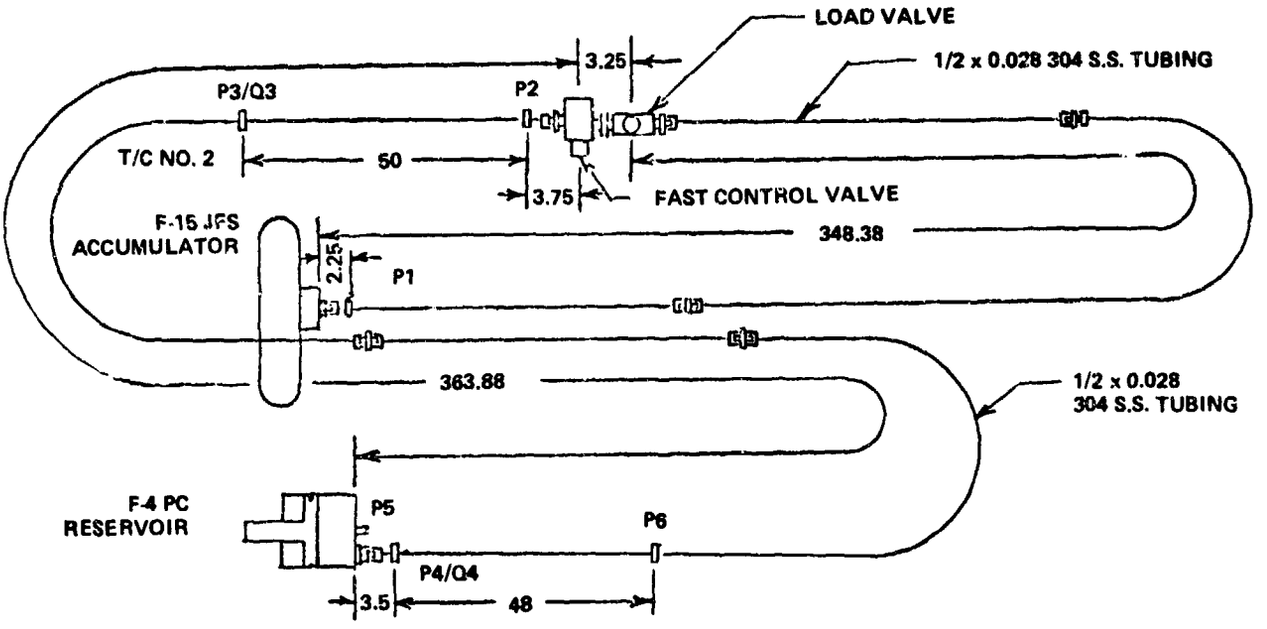

FIGURE 349. AIR EFFECTS TEST SETUP

The test runs are listed in Table 16. All the runs were made at 57 CIS and the reservoir pressure was kept close to 65 psig. The control valve operating times were varied from 2 to 16 milliseconds. Nitrogen gas was introduced while the system was running through a quick disconnect fitting downstream of the pump outlet. After the nitrogen was dissolved into the systems fluid the air content was measured with a mercury filled aire-ometer. Transient tests were run at 0.4, 12, 25, 30, 38 and 48 percent dissolved air by volume.

a. Cavitation Effects Testing at Different Air Contents - The first test series was run at 0.4% system air content. Run numbers 70-01-XX and 70-A1-XX were turn-off transients with valve closure rates of 4 and 16 milliseconds respectively. The plotted data is found in Figures 350, 351, 352, 353, 354, 355 and 356. All the pressures are plotted as gage pressures.

In Figure 350 valve closure time was 4 milliseconds. The initial transient spike at .33 seconds goes to 1000 psig. With the slower valve closing time, Figure 356 shows that 940 psig is the maximum pressure. The frequency of the decaying pressure is the same in both plots.

Figure 352 shows the flow decelerating rapidly after valve closure to zero flow at .24 seconds. The flow reverses and accelerates until the cavity collapses causing the pressure wave at .34 seconds. The pressure rises to 950 psig and the flow drops to almost zero. The flow eventually stops and the line pressure settles at about 62 psig, the reservoir pressure.

The P4 transducer was located 3.5 inches from the entrance to the reservoir. In Figure 353 the pressure spikes reach 460 psig. The flow trace in Figure 354 shows exactly when these pressure spikes occurred. This can also be seen in the internal reservoir pressure in Figure 355.

TABLE 16. AIR EFFECTS/RESERVOIR TESTING

Run Number	Flow Rate (CIS)	Reservoir Pressure (PSIG)	Control Valve Operat. Time (msec)	System Air Content (%)	Temp. (°F)	Transient
70-01-XX	57	64.5	4	0.4	137	Turn-Off
70-01+XX	"	60.0	2	"	128	Turn-On
70-A1-XX	"	64.0	16	"	136	Turn-Off
70-02-XX	"	65.0	4	"	213	Turn-Off
70-02+XX	"	57.0	2	"	208	Turn-On
70-A2-XX	"	65.0	12	0.4	212	Turn-Off
70-05-XX	"	66.0	4	12	136	Turn-Off
70-05+XX	"	60.0	2	"	132	Turn-On
70A05-XX	"	65.0	16	"	133	Turn-Off
70A06-XX	"	65.0	12	"	210	Turn-Off
70-06-XX	"	65.5	4	"	209	Turn-Off
70-06+XX	"	58.5	2	12	207	Turn-On
70-11-XX	"	66.0	4	25	132	Turn-Off
70-11+XX	"	60.0	2	"	130	Turn-On
70A11-XX	"	65.0	16	"	136	Turn-Off
70A12-XX	"	65.0	12	"	212	Turn-Off
70-12-XX	"	65.5	4	"	212	Turn-Off
70-12+XX	"	58.0	2	25	207	Turn-On
70-13-XX	"	65.0	4	30	137	Turn-Off
70-13+XX	"	60.0	2	"	130	Turn-On
70A13-XX	"	64.5	16	"	133	Turn-Off
70A14-XX	"	65.0	12	"	212	Turn-Off
70-14-XX	"	64.0	4	"	212	Turn-Off
70-14+XX	"	59.0	2	30	208	Turn-On
70-15-XX	"	65.0	4	38	135	Turn-Off
70-15+XX	"	60.0	2	"	125	Turn-On
70A15-XX	"	64.5	16	"	130	Turn-Off
70A16-XX	"	66.5	12	"	213	Turn-Off
70-16-XX	"	63.5	4	"	210	Turn-Off
70-16+XX	"	57.0	2	38	207	Turn-On
70-17-XX	"	65.0	4	48	132	Turn-Off
70-17+XX	"	60.0	2	"	126	Turn-On
70A17-XX	"	63.5	16	"	135	Turn-Off
70A18-XX	"	65.0	12	"	212	Turn-Off
70-18-XX	"	65.0	4	"	210	Turn-Off
70-18+XX	57	60.0	2	48	207	Turn-On

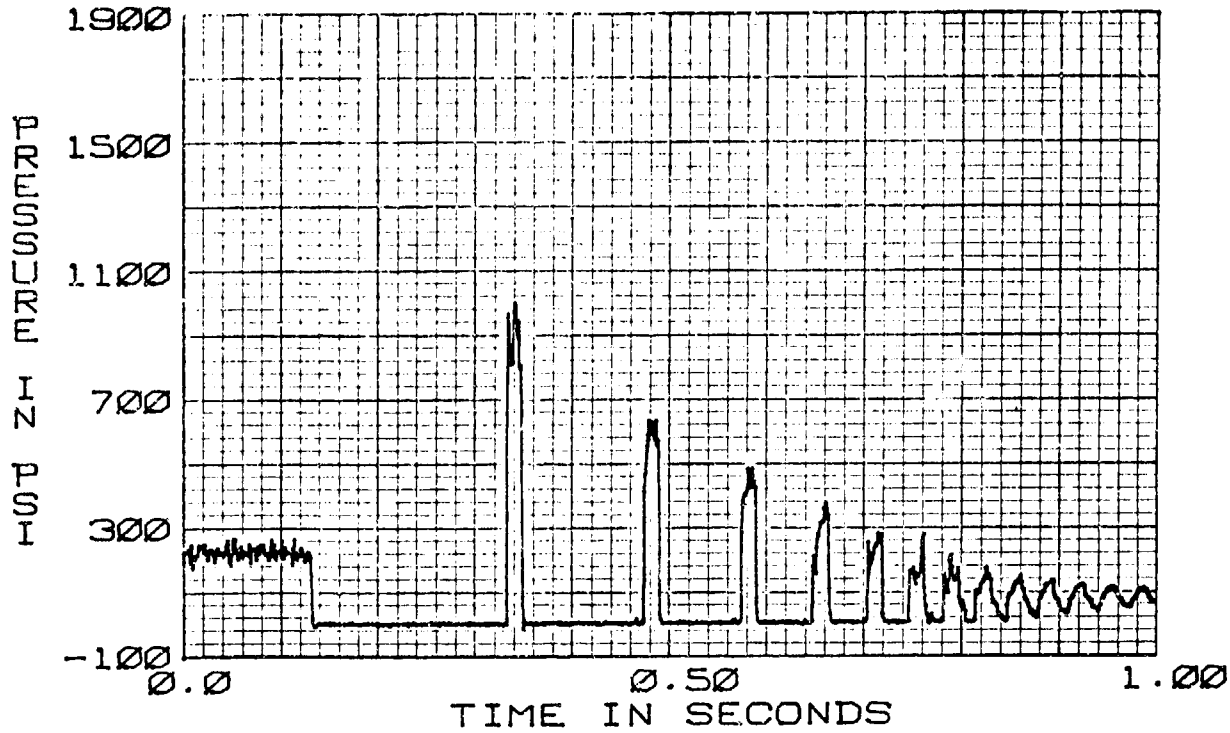

FIGURE 350. CAVITATION EFFECTS
70-01-P2 TURN-OFF TRANSIENT
57 CIS 130°F

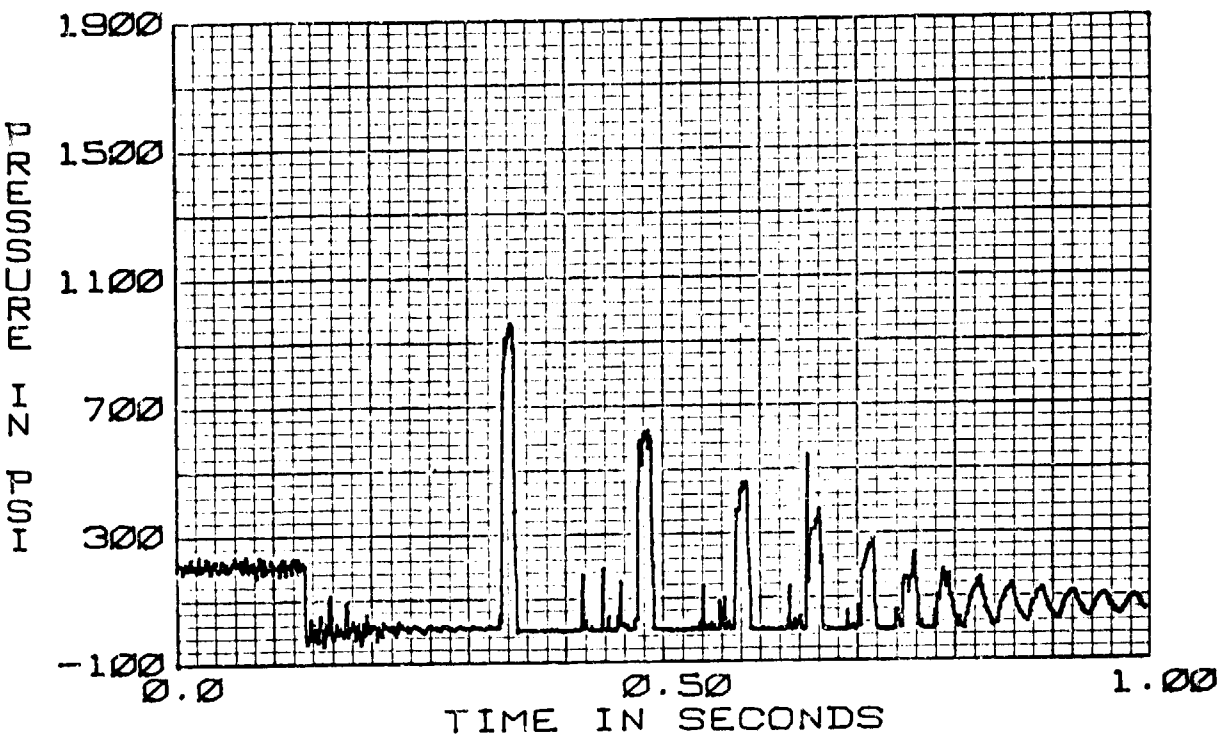

FIGURE 351. CAVITATION EFFECTS
70-01-P3 TURN-OFF TRANSIENT
57 CIS 130°F

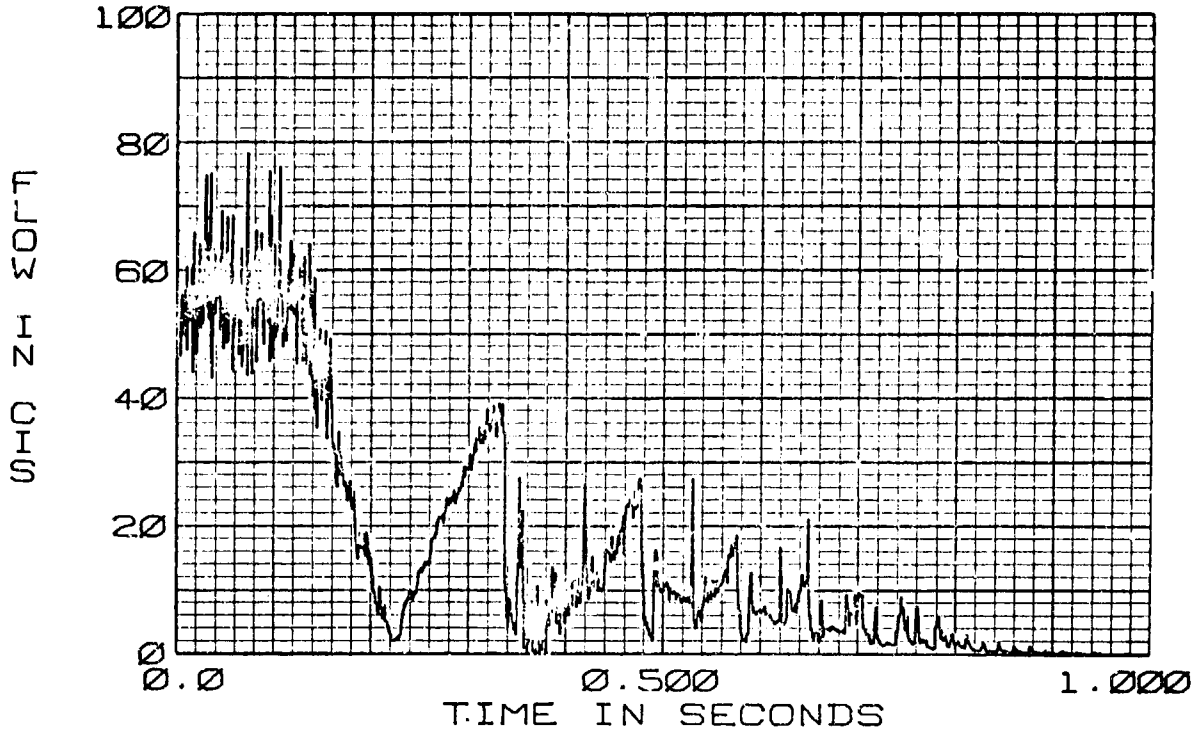

FIGURE 352. CAVITATION EFFECTS
70-01-Q3 TURN-OFF TRANSIENT
57 CIS 130°F

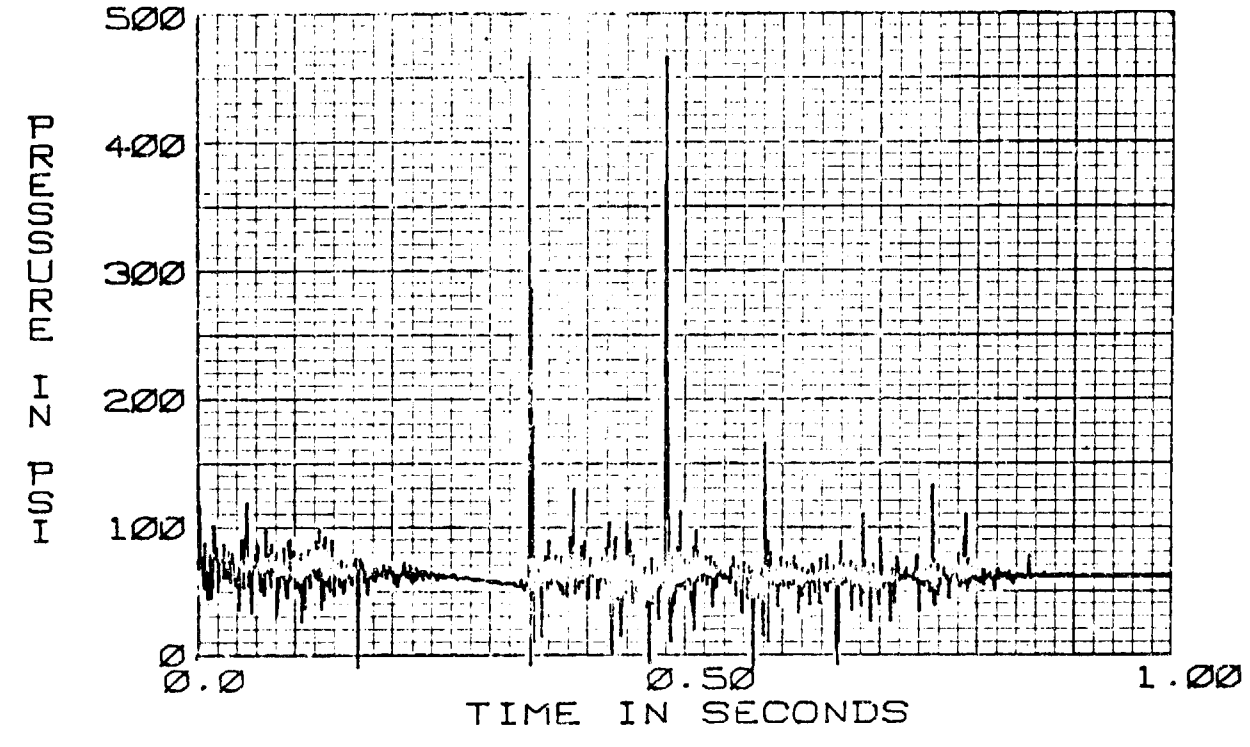

FIGURE 353. CAVITATION EFFECTS
70-01-P4 TURN-OFF TRANSIENT
57 CIS 130°F

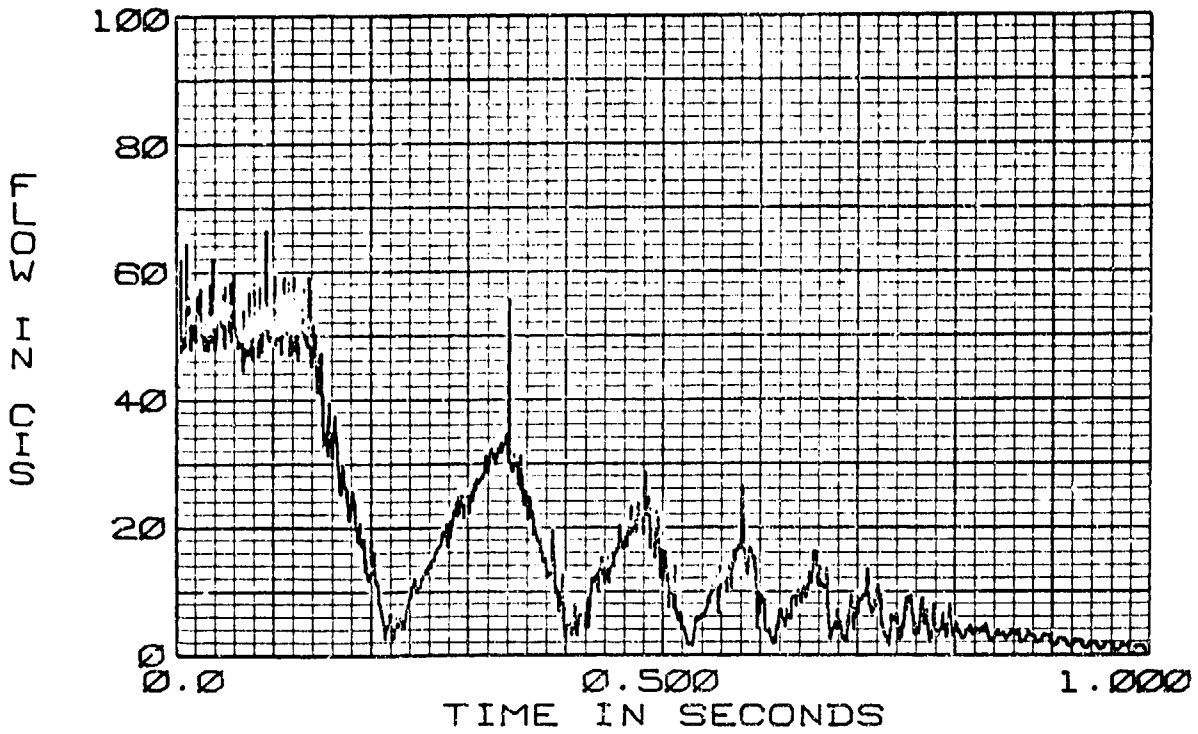

FIGURE 354. CAVITATION EFFECTS
70-01-Q4 TURN-OFF TRANSIENT
57 CIS 130°F

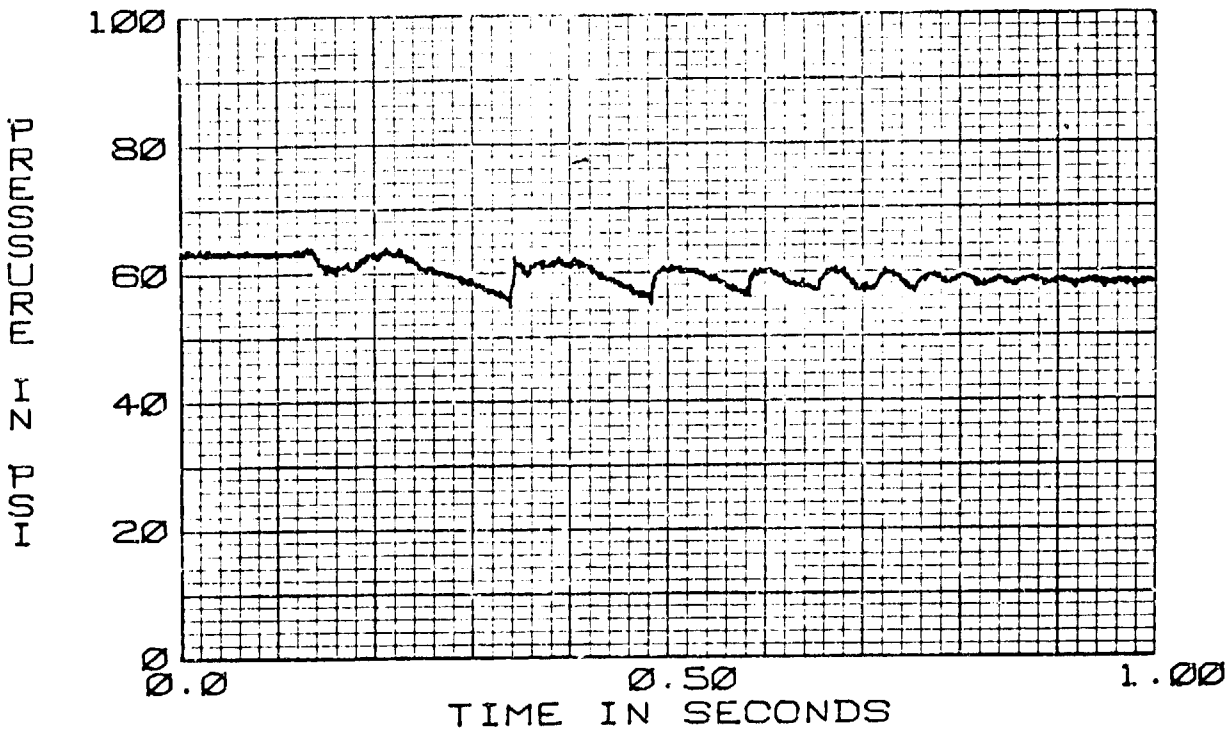

FIGURE 355. CAVITATION EFFECTS
70-01-P5 TURN-OFF TRANSIENT
57 CIS 130°F

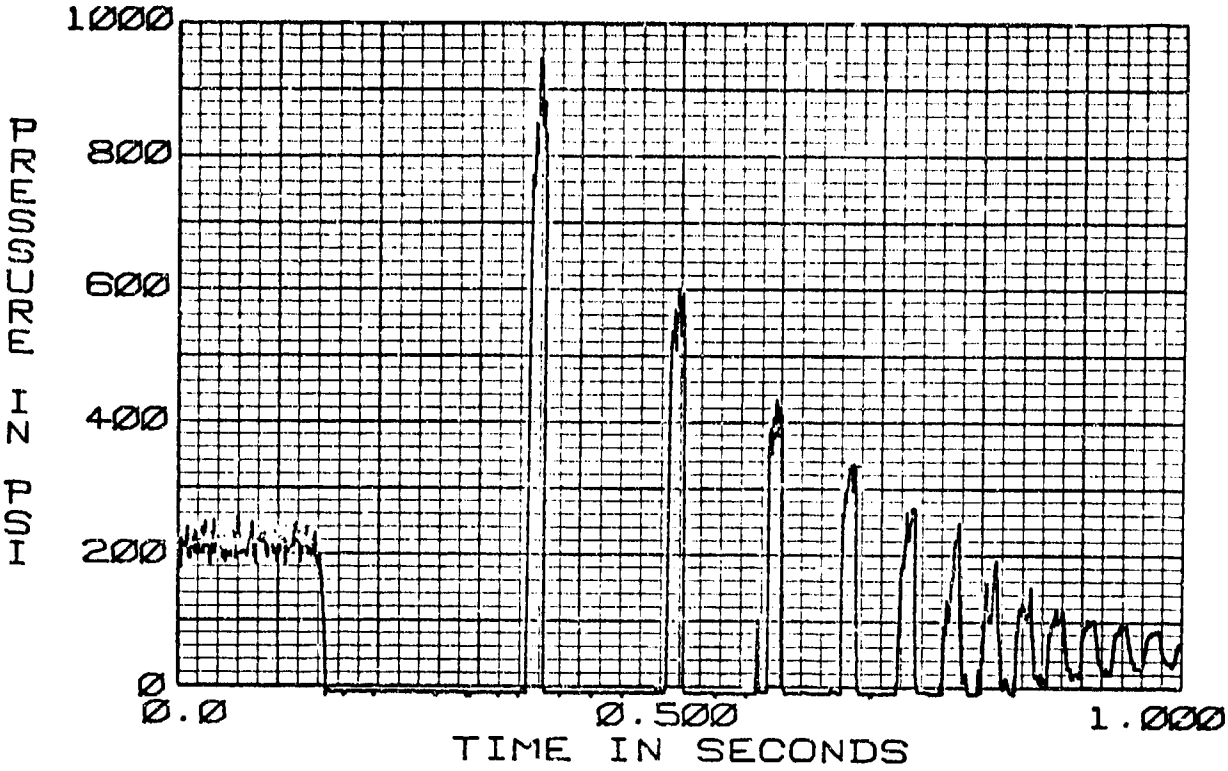

FIGURE 356. CAVITATION EFFECTS
70-A1-P2 TURN-OFF TRANSIENT
57 CIS 130°F

A turn-on transient run was made at 0.4% air content. The results are shown in Figures 357, 358, 359, 360, 361 and 362.

Turn-on and turn-off transients were next run with 12% air content in the test fixture. Results from this testing is found in Figures 363, 364, 365, 366, 367 and 368. Figures 363 and 368 show the effects of different valve closure rates on the peak pressure spike in the return line system. The peak pressure for the 4 millisecond valve closure in Figure 363 was 900 psig at .34 seconds. The corresponding peak pressure in Figure 368 with a 16 millisecond valve closing time was 850 psig. Again the pressure decaying frequency was the same for the two traces. The 12% air content turn-off transient runs indicate a more damped pressure and flow decay. In Figure 363 there are a total of 10 pressure peaks, while Figure 350 has 13. The initial pressure peaks reach 900 psig, but the second peak in Figure 363 is about 100 psig below the same spike in Figure 350. The flow in Figure 365 settles to zero a little faster than shown in Figure 352. The turn-on transient data for the 12% air content runs are not noticeably different than the ones at .4% air content.

Run numbers 70-11- and 70-11+ were made with 25% air content dissolved in the test system. The higher air content runs are significantly different from the 0.4% and 12% runs. In Figure 369 turn-off transient the air coming out of solution has a significant damping effect on the return transient pressure spikes.

The turn-on transient run in Figure 370 also exhibits a more damped response than Figure 357.

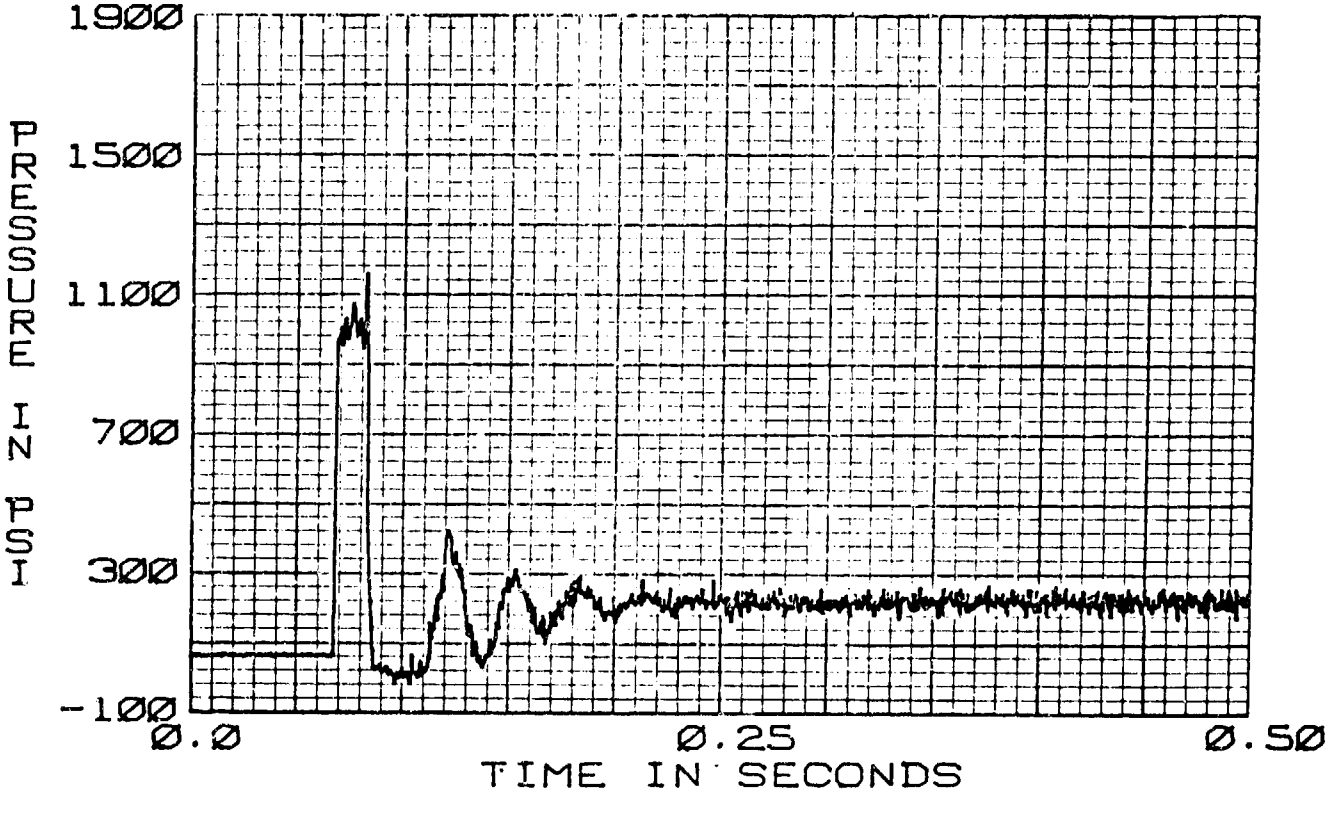

FIGURE 357. CAVITATION EFFECTS
70-01+P2 TURN-ON TRANSIENT
57 CIS 130°F

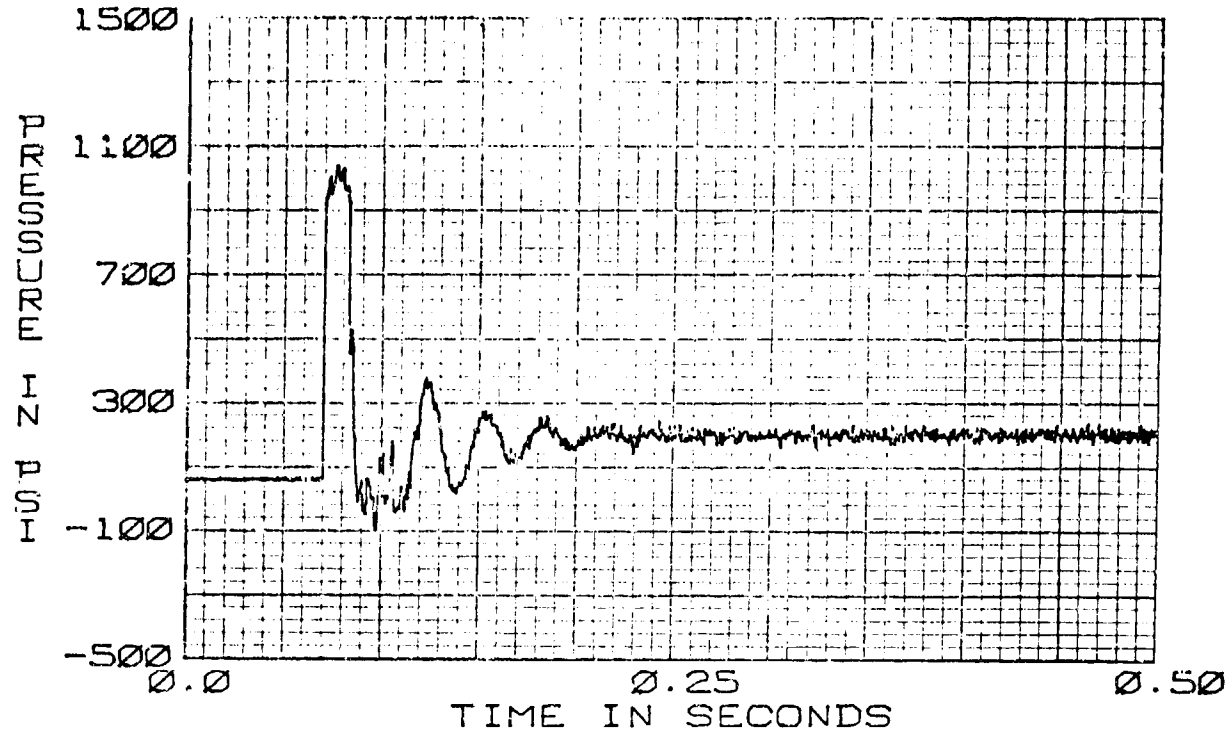

FIGURE 358. CAVITATION EFFECTS
70-01+P3 TURN-ON TRANSIENT
57 CIS 130°F

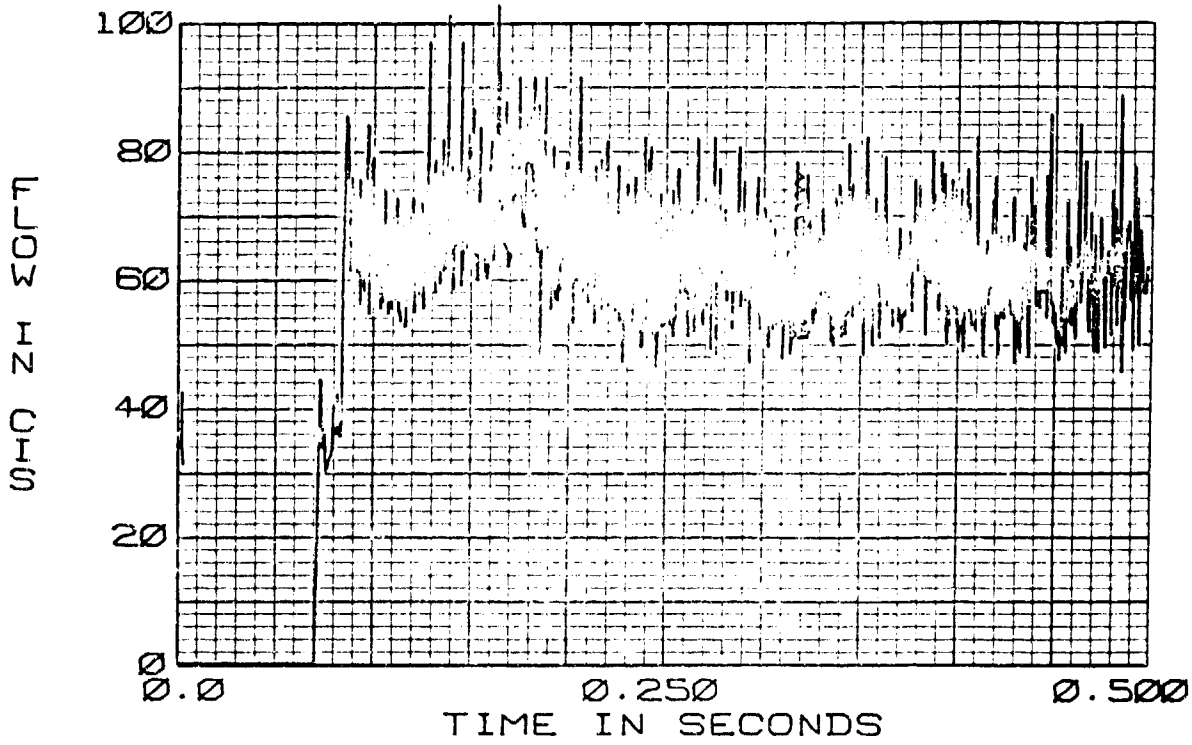

FIGURE 359. CAVITATION EFFECTS
70-01+Q3 TURN-ON TRANSIENT
57 CIS 130°F

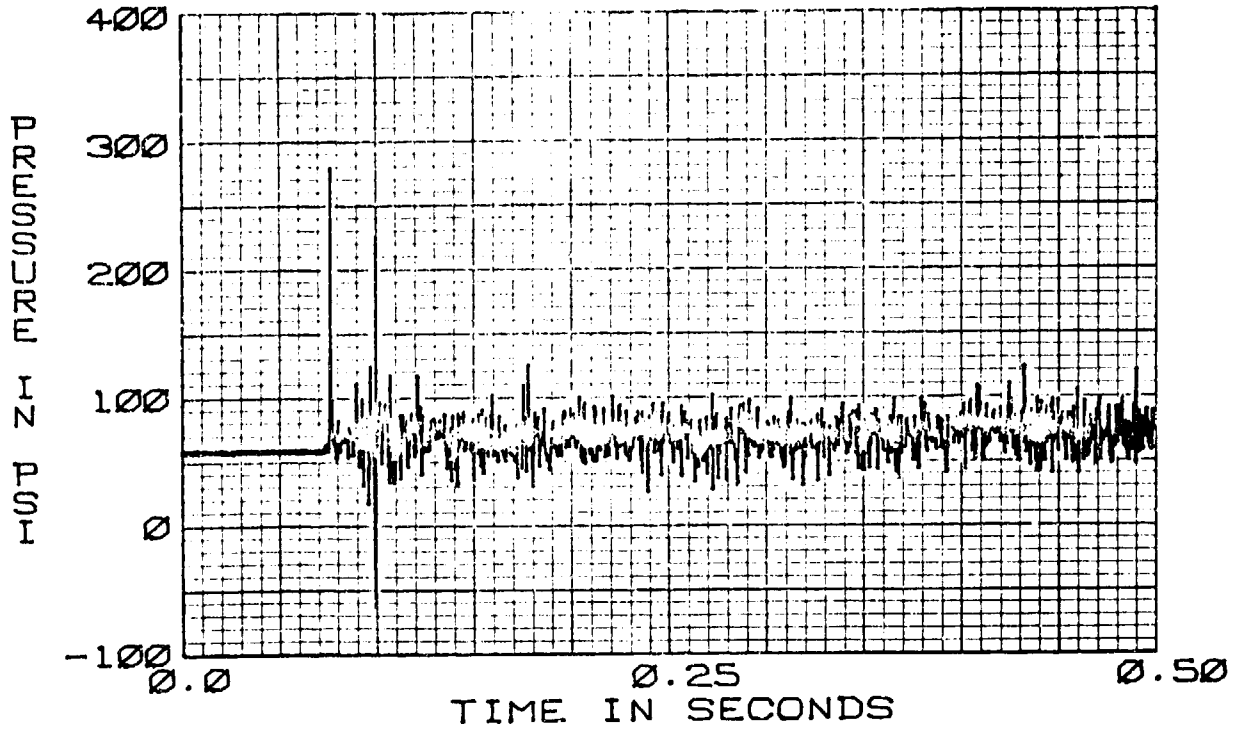

FIGURE 360. CAVITATION EFFECTS
70-01+P4 TURN-ON TRANSIENT
57 CIS 130°F

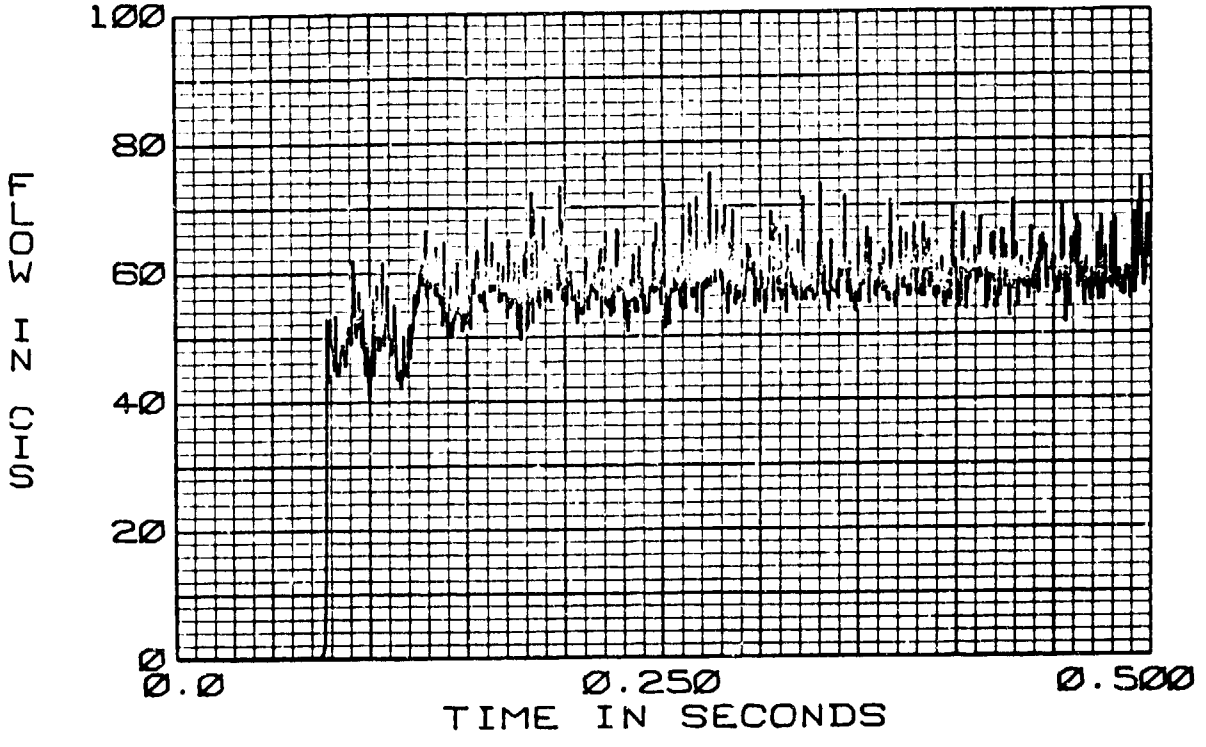

FIGURE 361. CAVITATION EFFECTS
70-01+Q4 TURN-ON TRANSIENT
57 CIS 130°F

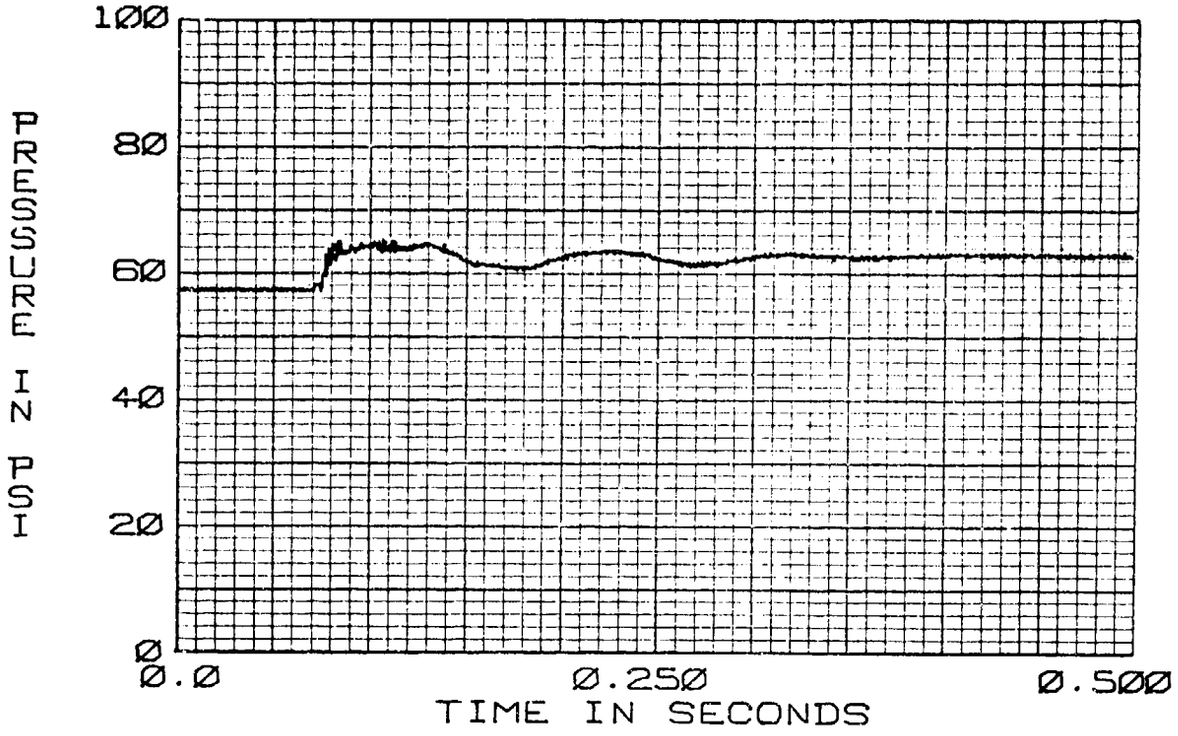

FIGURE 362. CAVITATION EFFECTS
70-01+P5 TURN-ON TRANSIENT
57 CIS 130°F

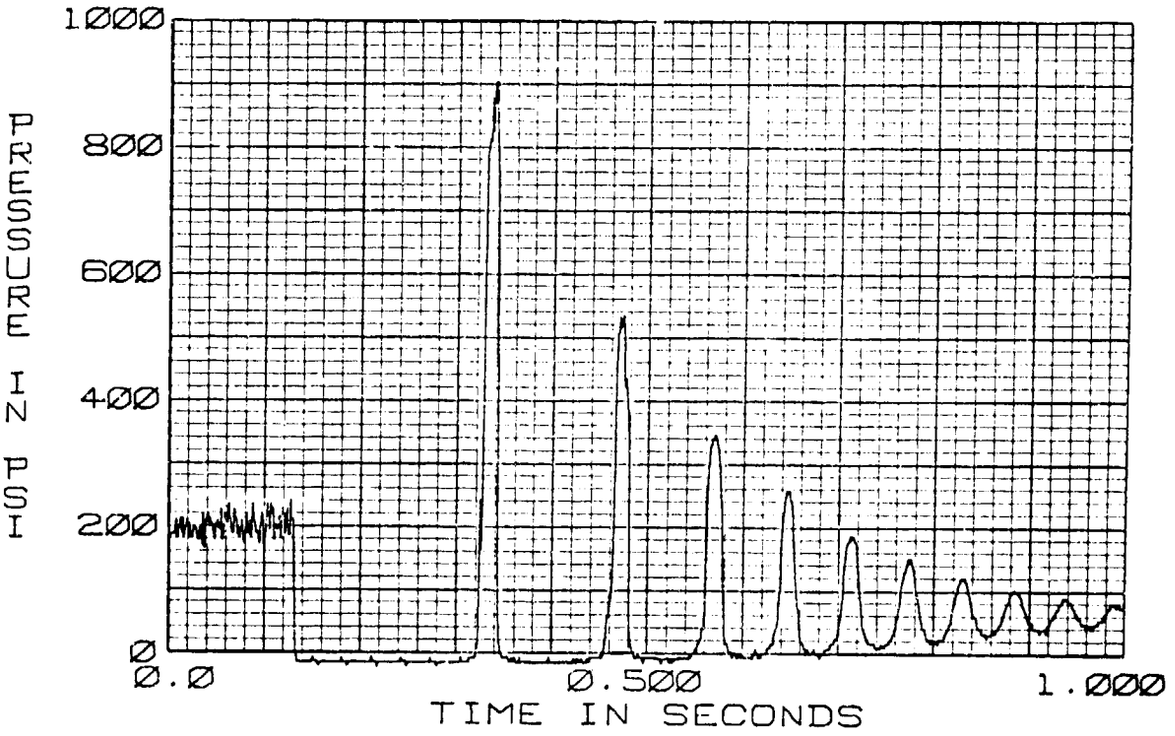

FIGURE 363. CAVITATION EFFECTS
70-05-P2 TURN-OFF TRANSIENT
57 CIS 130°F

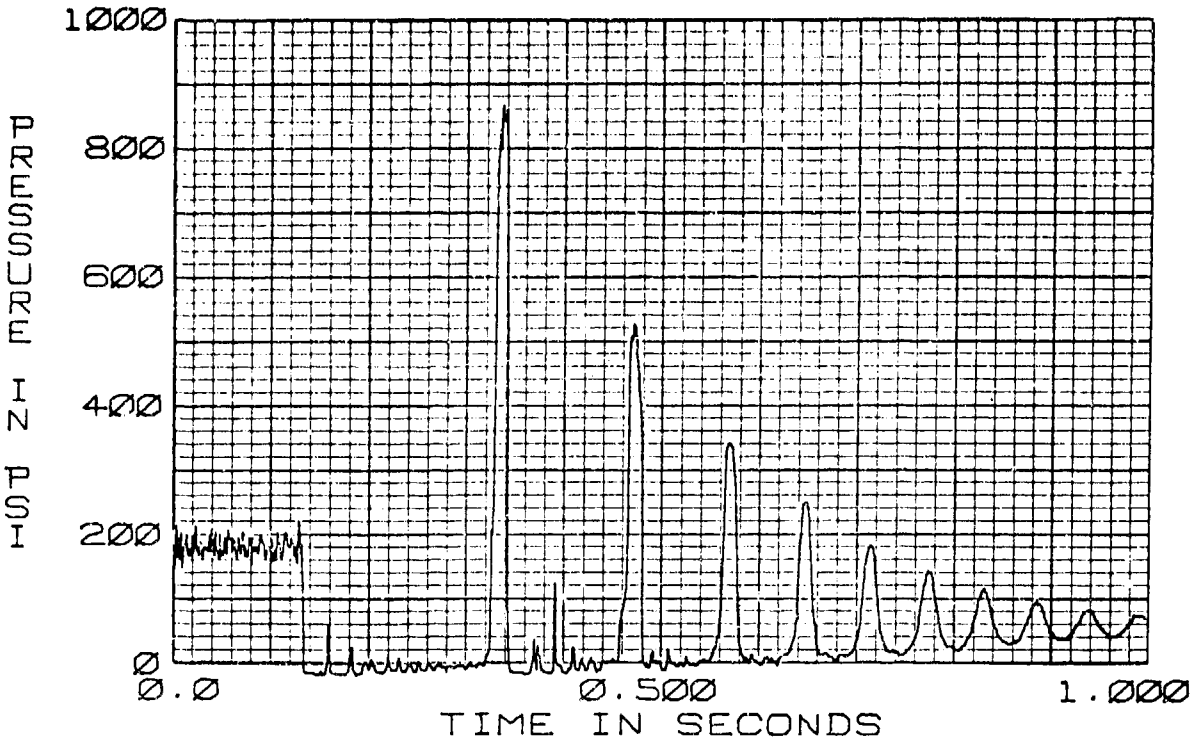

FIGURE 364. CAVITATION EFFECTS
70-05-P3 TURN-OFF TRANSIENT
57 CIS 130°F

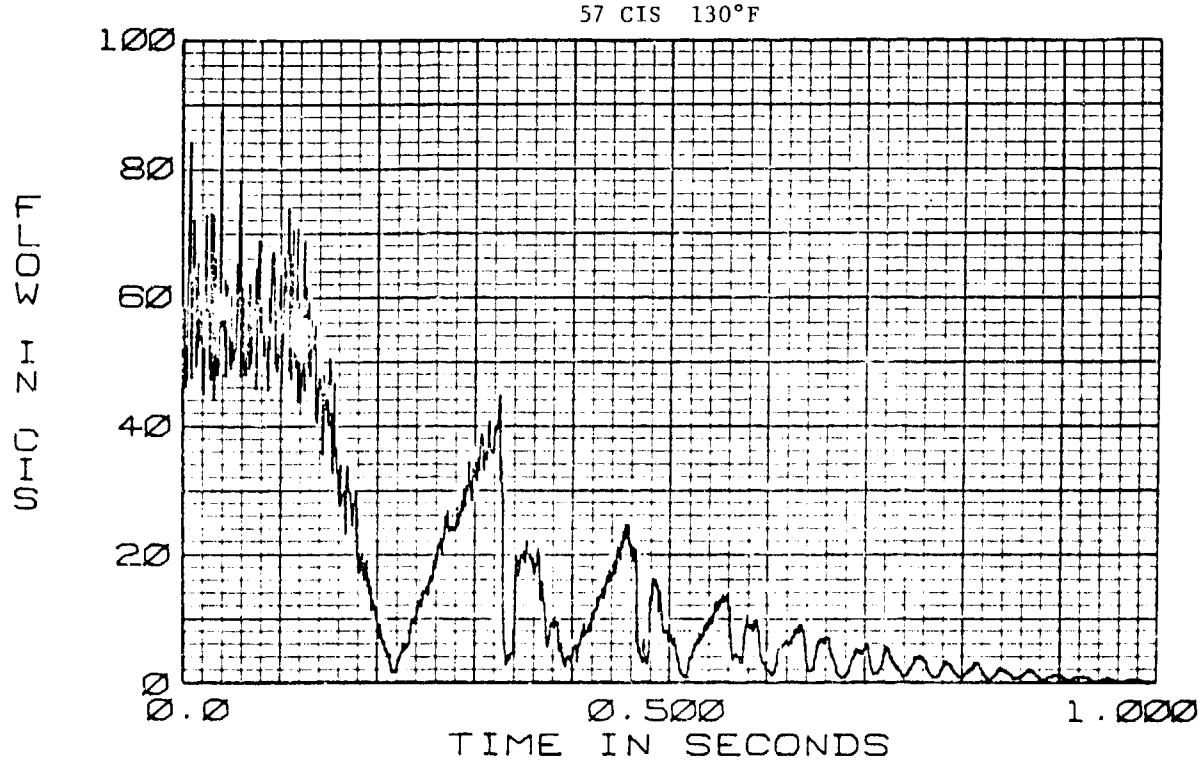

FIGURE 365. CAVITATION EFFECTS
70-05-03 TURN-OFF TRANSIENT
57 CIS 130°F

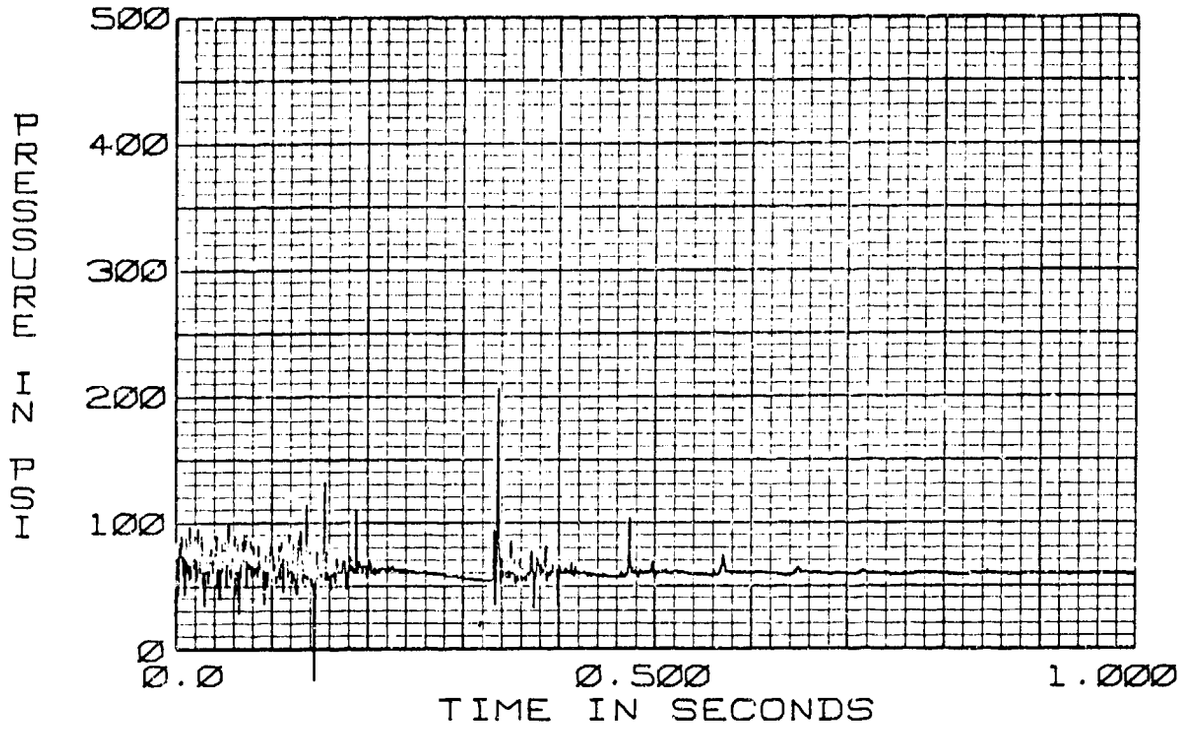

FIGURE 366. CAVITATION EFFECTS
70-05-P4 TURN-OFF TRANSIENT
57 CIS 130°F

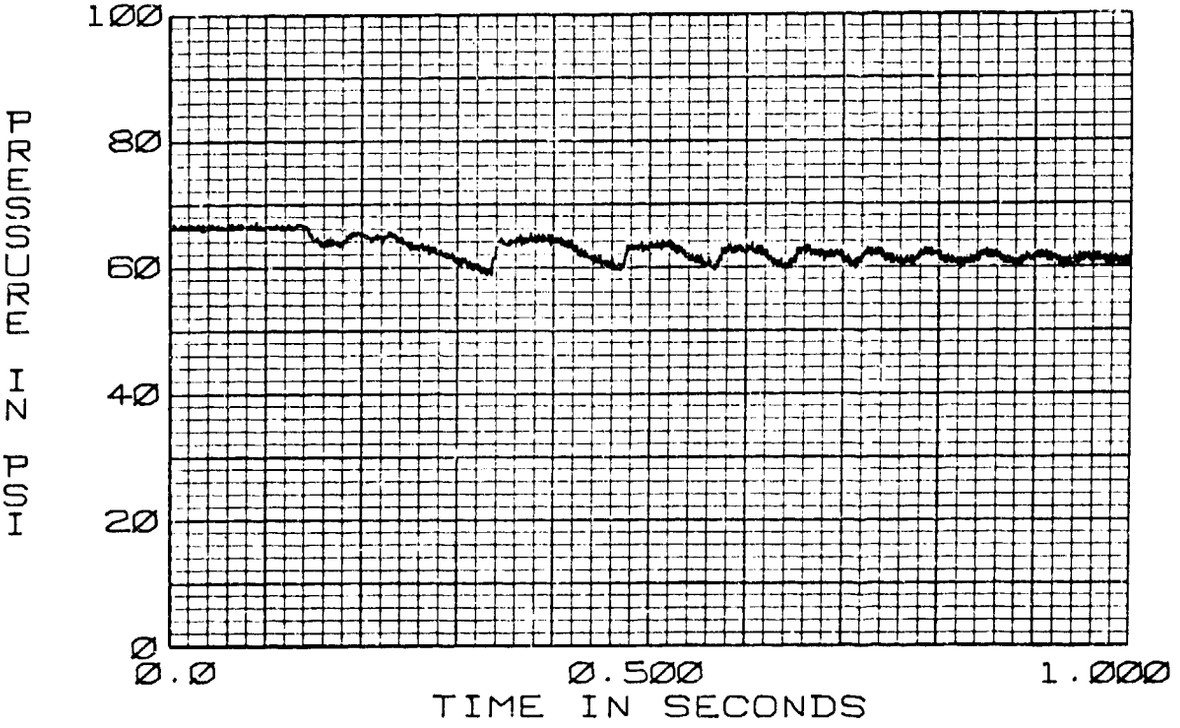

FIGURE 367. CAVITATION EFFECTS
70-05-P5 TURN-OFF TRANSIENT
57 CIS 130°F

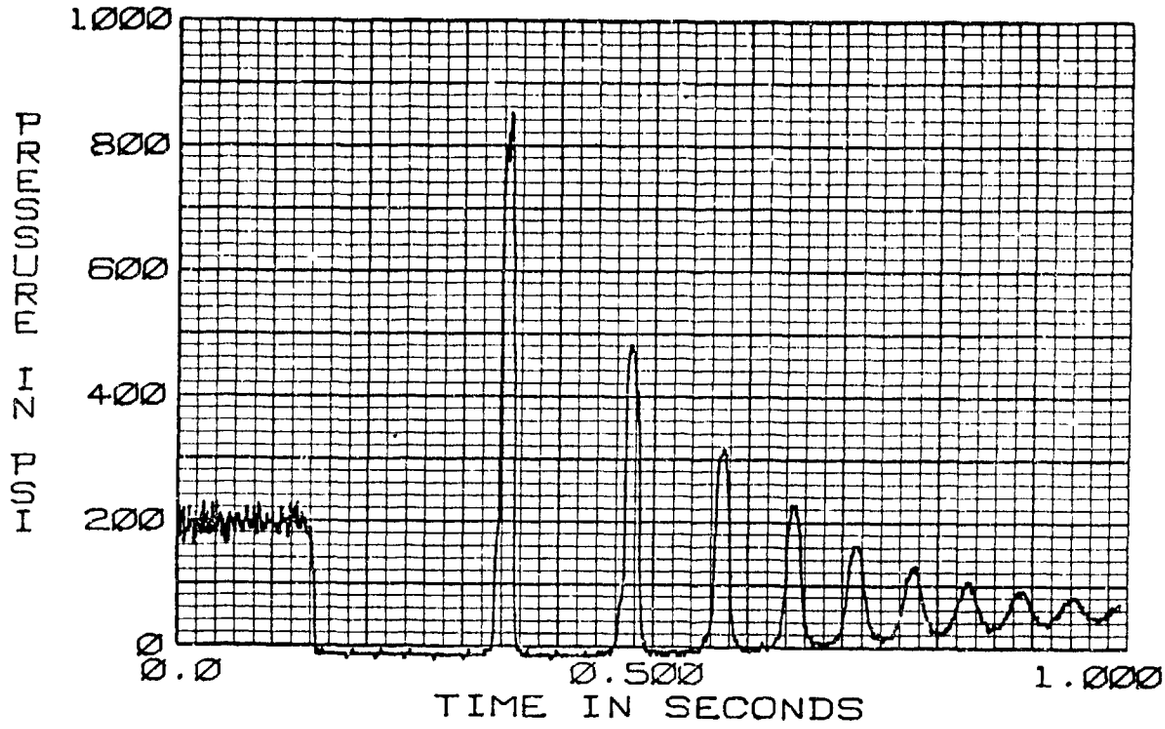

FIGURE 368. CAVITATION EFFECTS
70A05-P2 TURN-OFF TRANSIENT
57 CIS 130°F

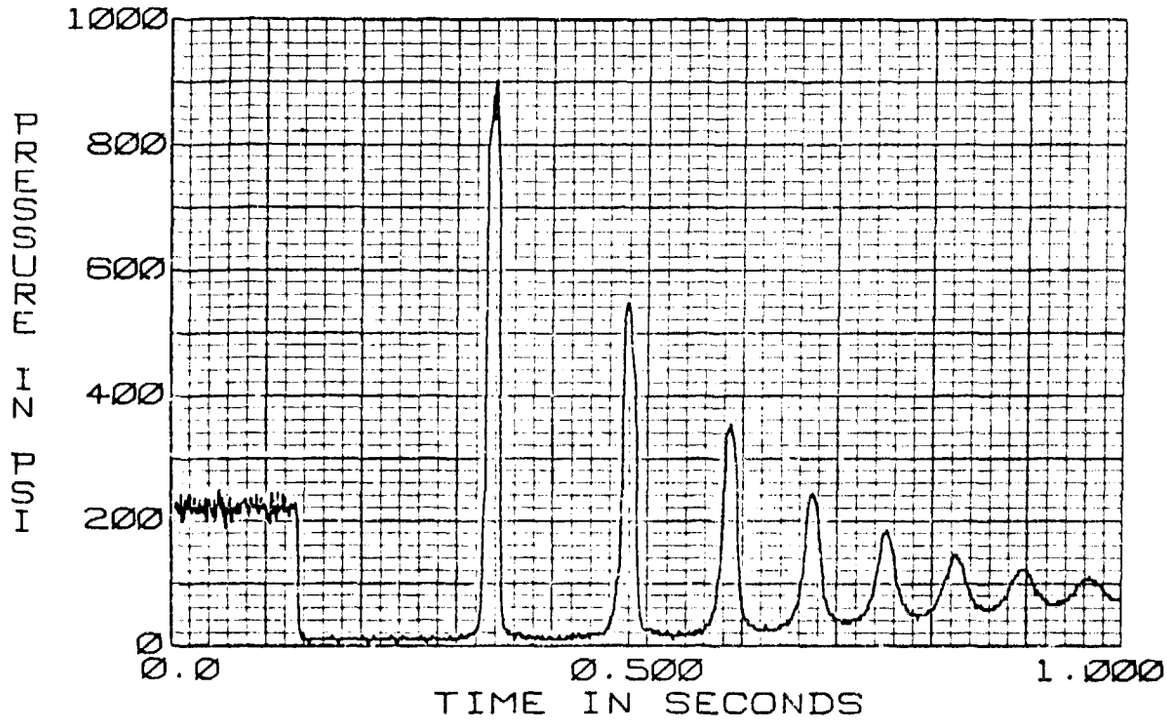

FIGURE 369. CAVITATION EFFECTS
70-11-P2 TURN-OFF TRANSIENT
57 CIS 130°F

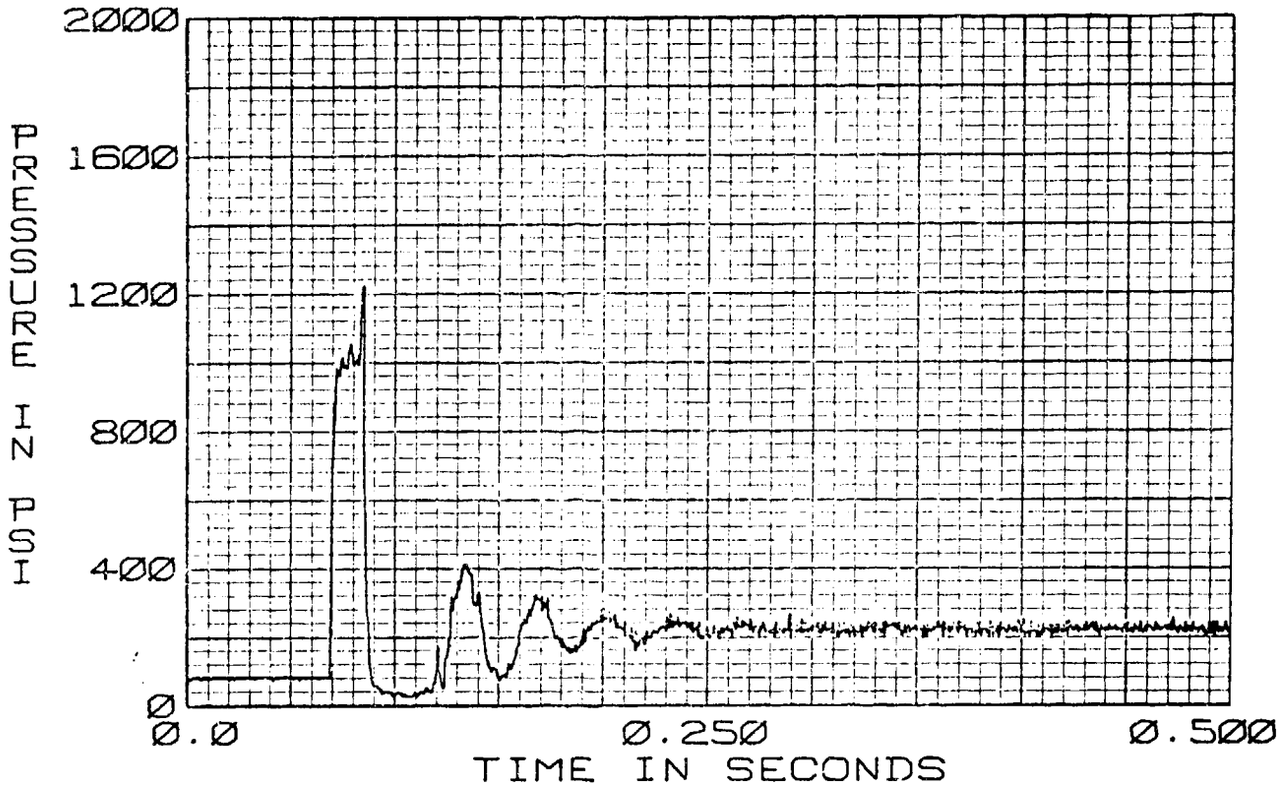

FIGURE 370. CAVITATION EFFECTS
70-11+P2 TURN-ON TRANSIENT
57 CIS 130°F

The main damping effect seen in the higher air content runs comes from air that has left solution due to the exposure of the oil to vapor pressure, since dissolved air does not alter the volume or compressibility of the oil. The addition of an air/volume accumulator slows and dampens the rate of change of pressure in the line. The more free air in the line the greater the effect.

Run numbers 70-13±XX, 70-15±XX and 70-17±XX are turn-on and turn-off transients at 30, 38 and 48 percent dissolved air contents. Each run shows how the higher air content level reduces the material frequency of the decaying pressure and flow waves. Figure 371 has 7 1/2 pressures peaks, Figure 372 has 7 and Figure 373 has 6.

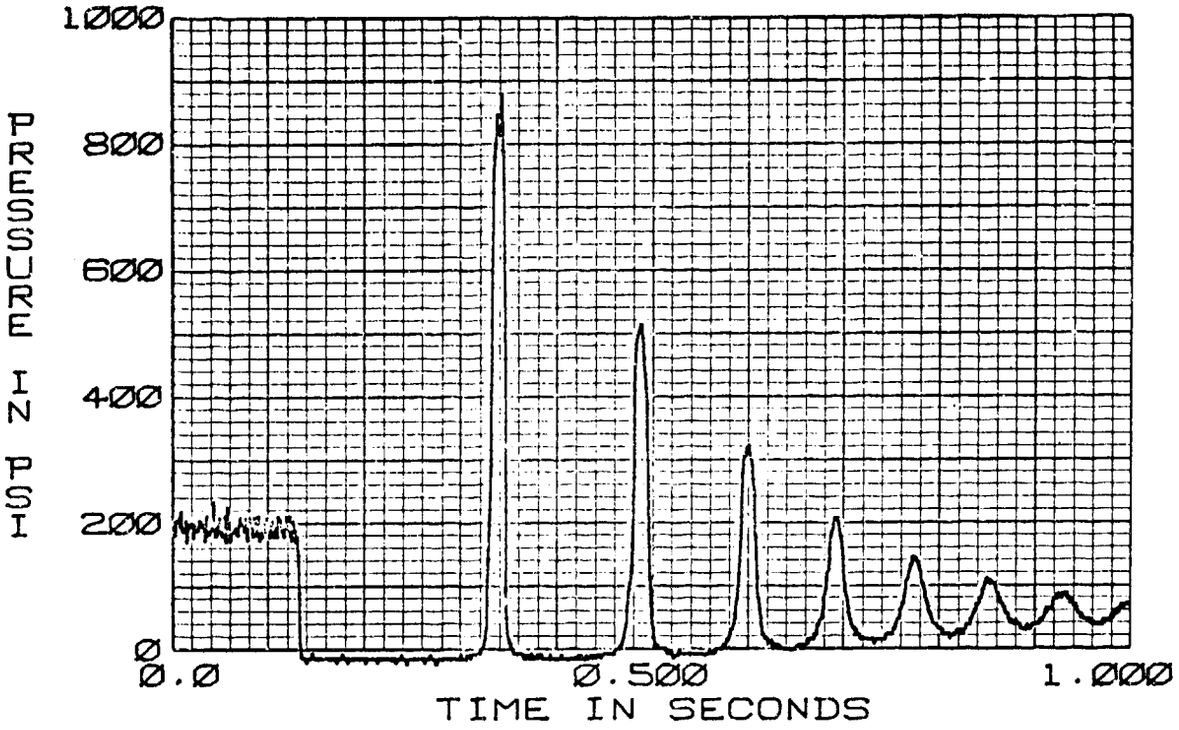

FIGURE 371. CAVITATION EFFECTS
70-13-P2 TURN-OFF TRANSIENT
57 CIS 130°F

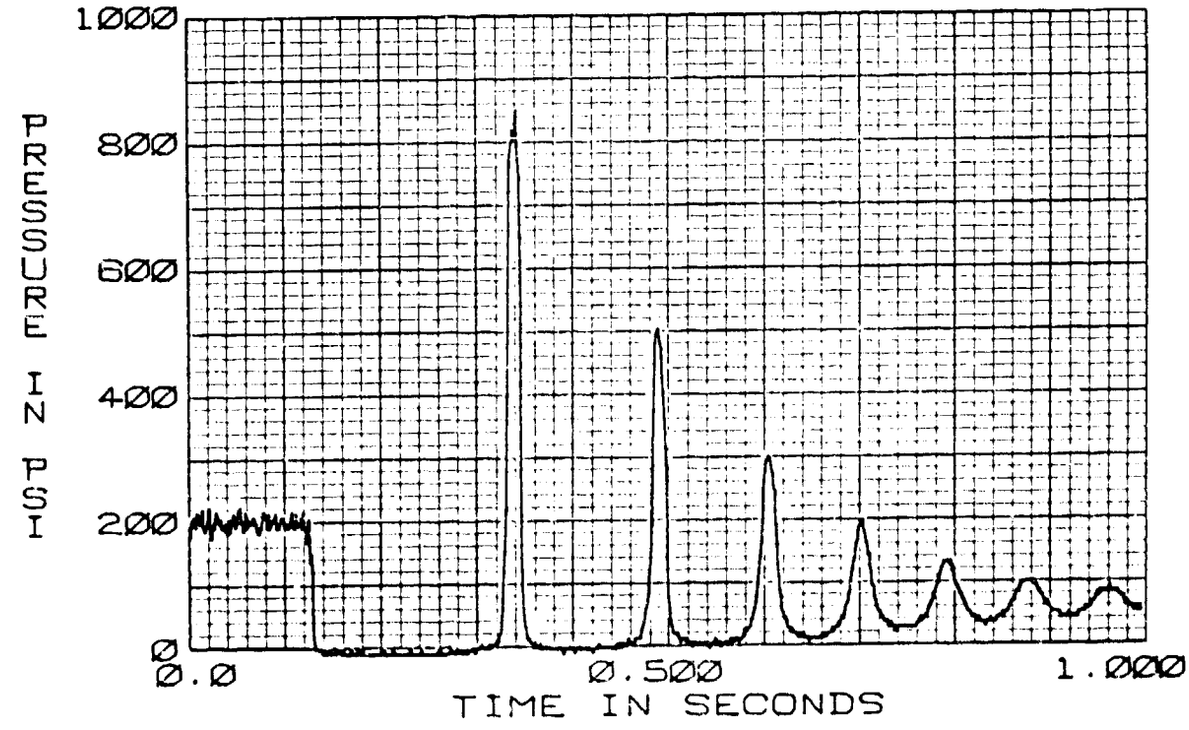

FIGURE 372. CAVITATION EFFECTS
70-15-P2 TURN-OFF TRANSIENT
57 CIS 130°F

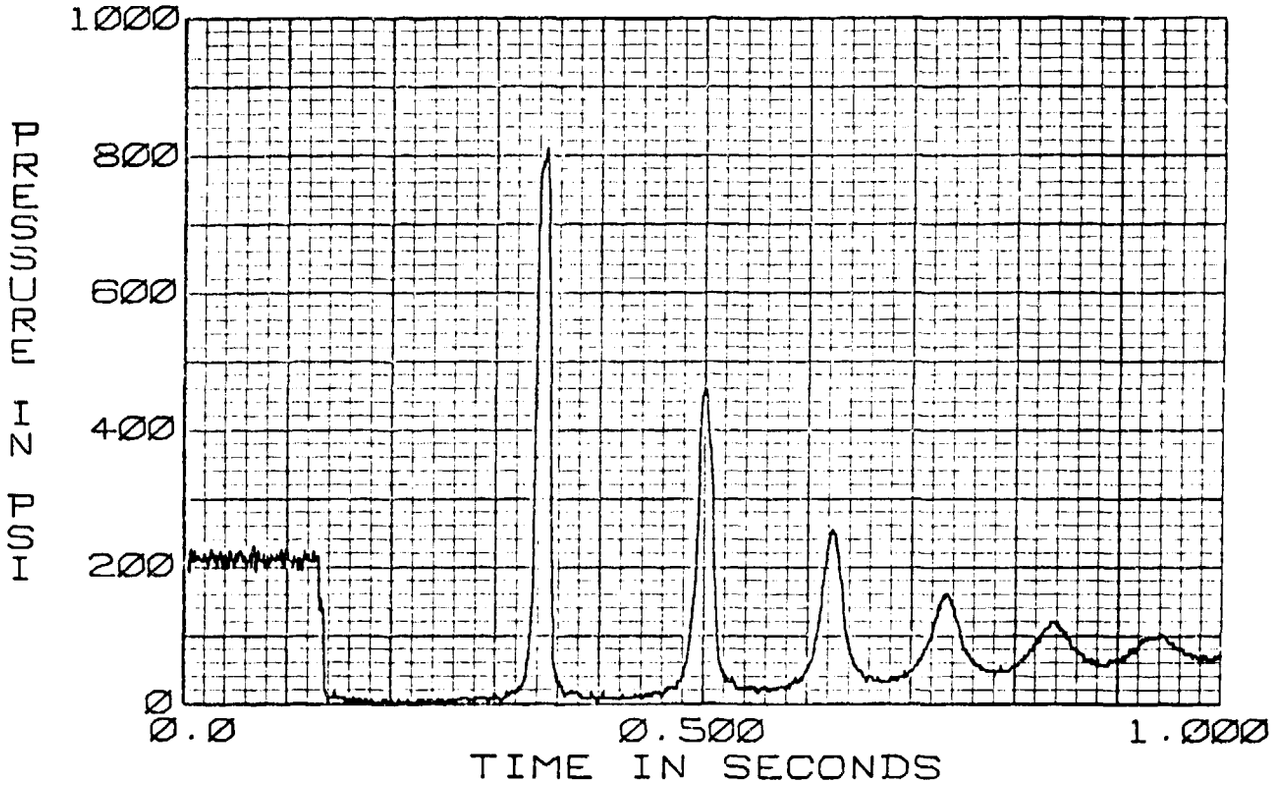

FIGURE 373. CAVITATION EFFECTS
70-17-P2 TURN-OFF TRANSIENT
57 CIS 130°F

b. Conclusions - Return system transients were generated in the lab by rapid opening and closing of a control valve. Air was added to the system and allowed to dissolve into the hydraulic fluid. As the system air content levels increased from 0.4% to 48% by volume, the transient

tests showed a significant decrease in the oscillating frequency of the pressure and flow waves following cavitation. This phenomena results from free air collecting in the return system downstream of the valve. The air came out of solution after the pressure drops to near zero which occurred when the control valve was either opened or closed. At higher dissolved air contents more air would leave the fluid given the same valve operating rate and system temperature and reservoir pressure. This free air would slow the rise and decay of the pressure and flow waves by providing an additional air/spring for these waves to travel through.

The testing indicates that at higher air contents the severity of return line pressure transients are reduced.

Unfortunately this was about the only benefit of dissolved air. From a total system viewpoint, large amounts of air may cause serious problems relating to system start-up and normal operation. Start-up problems include lack of pump prime (airlock), system damage due to transient air ingestion by the pump and excessive drop in reservoir level.

Currently the effects of air in hydraulic systems is not modeled in the HYTRAN computer program. Dissolved air does not alter the physical properties of the hydraulic fluid, but free air in the form of large or small bubbles in the fluid flow would drastically affect the component and line models. Predicting the occurrence of these air bubbles, their size and interactions with the fluid and components would be a prodigious task far beyond the scope of the present contract. The testing has provided basic data on how dissolved air affects hydraulic return system performance.

Since the .4% and 12% air content tests showed little change, and the existing HYTRAN cavitation model gives a reasonable cavitation simulation, as shown in Section V Paragraph 2 it is considered that the current model is adequate for most program needs.

12. VALVE CONTROLLED ACTUATOR MODEL VERIFICATION

The test results obtained on a modified F-15 stabilator servoactuator are compared to the HYTRAN valve controlled actuator model - subroutine ACT101. The testing with the servoactuator was performed on a 1/2 inch line system with MIL-H-83282 hydraulic fluid.

The ACT101 subroutine models a simple servoactuator with a mechanical unit connected to the servovalve, which operates open loop without feedback. The valve is assumed to have a linear square port configuration with zero overlap. The width of each port was input independently to allow the valve areas to be matched to the actuator piston areas. The measured time history of the valve position was used as the mechanical input to the computer program. The stabilator configuration and input data is shown in Figure 374.

The F-15 stabilator test series was run on the system configuration shown in Figure 375. The following parameters were recorded in the laboratory for the test runs: P1, P2, P3, P4 and P5 cylinder no. 1 pressure, P6 - cylinder no. 2 pressure, Xv - valve position and x - main ram position. The test runs are listed in Table 17.

TABLE 17

F-15 STABILATOR TEST SERIES

Test Conditions	Initial Control Valve Position (IN)	Run Number
Extend*	0.0	67-01
Retract*	0.0	67-02
Extend-Retract*	-3.93	67-03
Retract-Extend*	+3.93	67-04
Bottoming (Extend)*	0.0	67-05
Bottoming (Retract)*	0.0	67-06
Extend (.25 VDC step input)	0.0	67-07
Retract (.25 VDC step input)	0.0	67-08
Extend (.5 VDC step input)	0.0	67-09
Retract (.5 VDC step input)	0.0	67-10
Extend (1.0 VDC step input)	0.0	67-11
Retract (1.0 VDC step input)	0.0	67-12

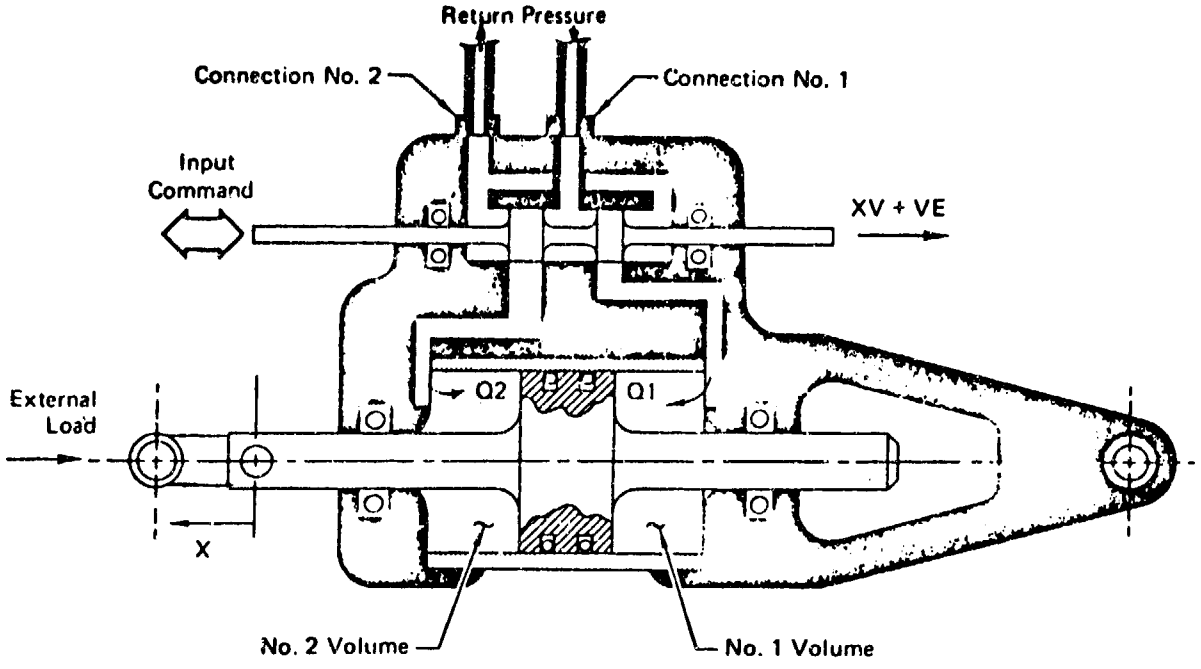

No. 1 Area	6.848 IN**2
No. 2 Area	6.848 IN**2
No. 1 Volume	28.00 IN**3
No. 2 Volume	28.00 IN**3
Stroke with Actuator Fully Retracted	3.93 IN
Stroke with Actuator Fully Extended	3.93 IN
Velocity Damping	.5 LB-SEC/IN
Load Mass	.0259 LB-SEC^2/IN
Slot Width Vol #1 to Con #1	0.3832 IN
Slot Width Vol #1 to Con #2	0.3832 IN
Slot Width Vol #2 to Con #1	0.3832 IN
Slot Width Vol #2 to Con #2	0.3832 IN
Compressive Load with Actuator Retracted	0.0 LBS
Compressive Load with Actuator Extended	0.0 LBS
Initial Actuator Position	DEPENDENT ON TEST THAT WAS RUN

FIGURE 374. F-15 STABILATOR INPUT DATA

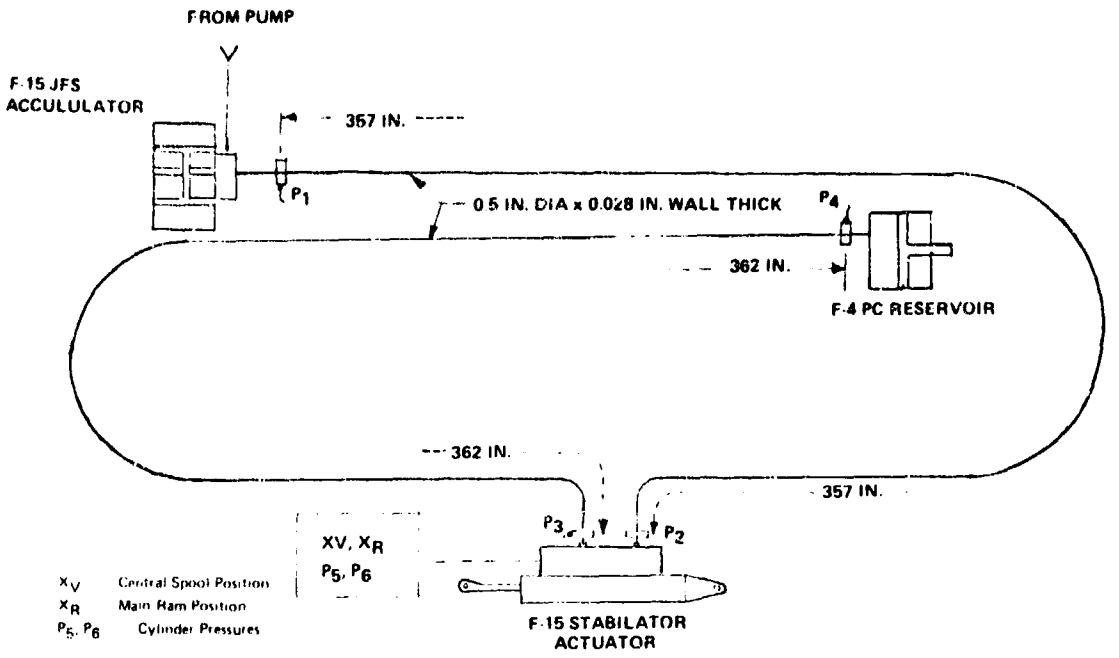

FIGURE 375. F-15 STABILATOR ACTUATOR TEST CONFIGURATION

The actuator subroutine was modified to accept the valve position commands at each calculation time step. Normally the command data is inserted for a few points and a linear interpolation is made to determine the valve position at any time step.

To closely approximate the operation of the actuator it was necessary to add a couloumb friction force in the computation of the main ram velocity. There was no load on the actuator but the weight of the main ram was input with the data shown in Figure 374.

a. Computer Simulation with the F-15 Stabilator Test Data - The computer simulation used the input data shown in Figure 376 along with the input boundary data in Figures 377, 378, and the control valve position in Figure 379. The control valve was moved from the null position to an extend direction at the maximum valve rate. The results of the simulation are shown in Figures 380, 381, 382, and 383. Figure 380 contains the pressure immediately upstream of the stabilator actuator. The computed data at 50 miliiseconds is about 400 psi below the actual results. The data measured downstream of the actuator in Figure 381 cavitates while the computed data only drops to the return pressure of 250 psi.

```
**** F-15 STABILATOR ACTUATOR - EXTENDING ****(STAB26)

THE TRANSIENT RESPONSE IS FROM T=0.0  TO T=  .200 SECONDS AT TIME INTERVALS OF DELT= .00020
WITH OUTPUT POINTS PLOTTED AT INTERVALS OF  ,  .00200  SECONDS

FLUID DATA FOR  MIL-H-83282 AT  3000.0 PSIG, -   90.0 PSIG AND 100.0 DEG F  IN  10.0 DEG F STEPS
                VISCOSITY    - .337E-01          .249E-01IN**2/SEC
                DENSITY      - .801E-04          .791E-04(LB-SEC**2)/IN**4
                BULK MODULUS - .244E+06          .209E+06PSI
                VAPOUR PRESS.- .200E+01 AT  100.0 DEG F

LINE DATA
LINE NO.    LENGTH      INTERNAL DIA   WALL THICKNESS   MODULUS OF ELASTICITY   DELX        CHARACTERISTIC IMPEDANCE   VELOCITY OF SOUND
   1        358.6000      .4440           .0280            .300E+08            10.5471          26.8478                 51912.4297
   2        362.0000      .4440           .0280            .300E+08            10.6471          26.8478                 51912.4297
  COMP#,  1 INTEGER DATA    1  91  0  -1   1  0  0  0  0  0  0  0  0  0  0  0  0  0
  COMP#,  2 INTEGER DATA    2  96  0   0   1  3  0  0  0  0  0  0  0  0  0  0  0  0
  COMP#,  3 INTEGER DATA    3 103  2   1  -2  0  0  0  0  0  0  0  0  0  0  0  0  0
REAL DATA CARD #  1   .6848E+01  .6848E+01  .2700E+02  .2700E+02  -.3930E+01  .3930E+01  .1000E+00  .2590E-01
REAL DATA CARD #  2   .6000E+00  .6000E+00  .6000E+00  .6000E+00  0.          0.         -.2900E+01  0.
  COMP#,  4 INTEGER DATA    4  91  0   2   1  0  0  0  0  0  0  0  0  0  0  0  0  0
```

FIGURE 376. RUN 67-11 HYTRAN INPUT DATA FOR ACTUATOR EXTENDING

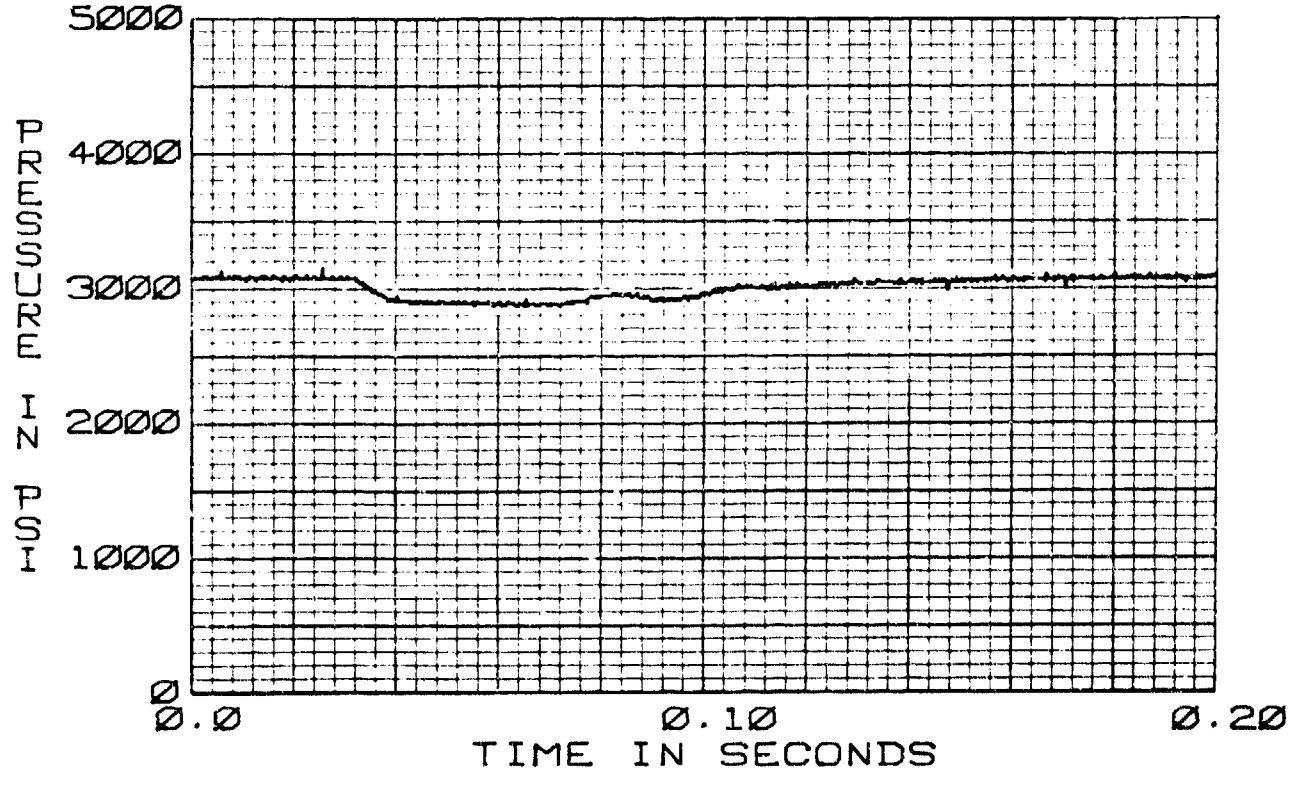

FIGURE 377. F-15 STABILATOR ACTUATOR 67-11-P1 STEP INPUT EXTEND 100°F

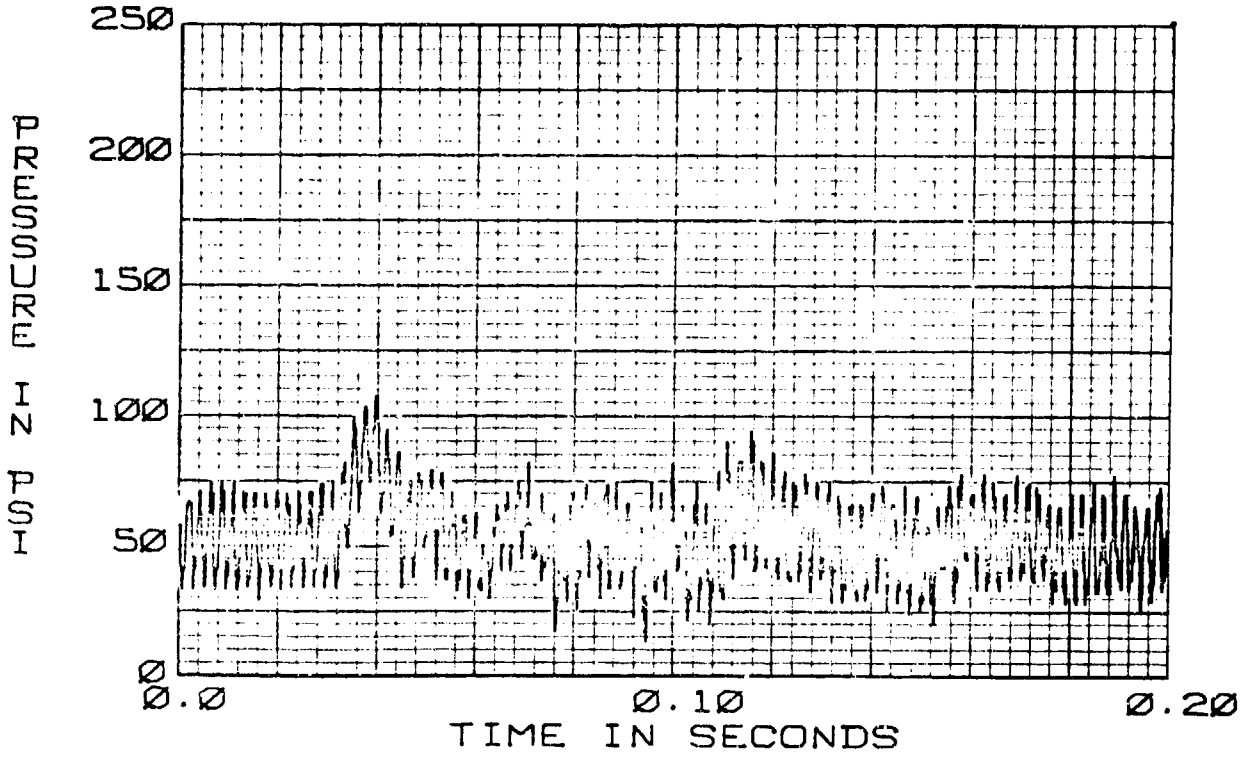

FIGURE 378. F-15 STABILATOR ACTUATOR 67-11-P4 STEP INPUT EXTEND 100°F

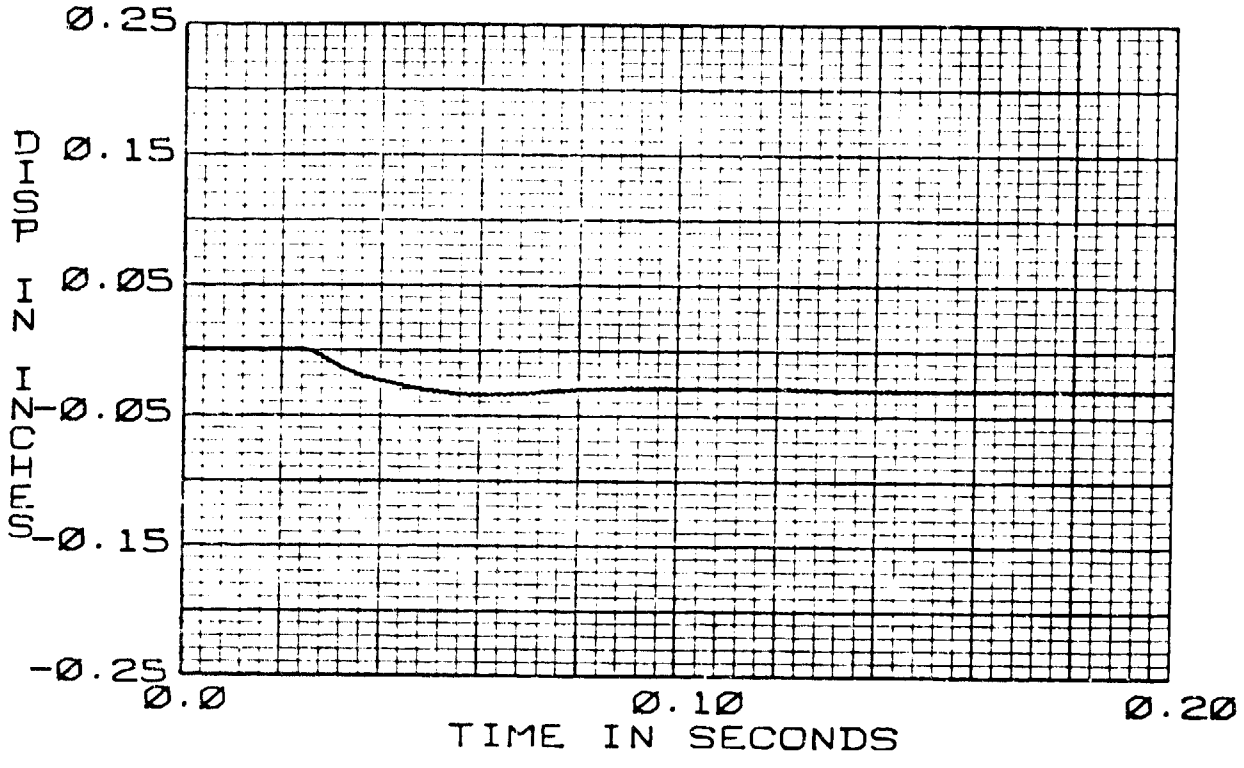

FIGURE 379. F-15 STABILATOR ACTUATOR 67-11-XC STEP INPUT EXTEND 100°F

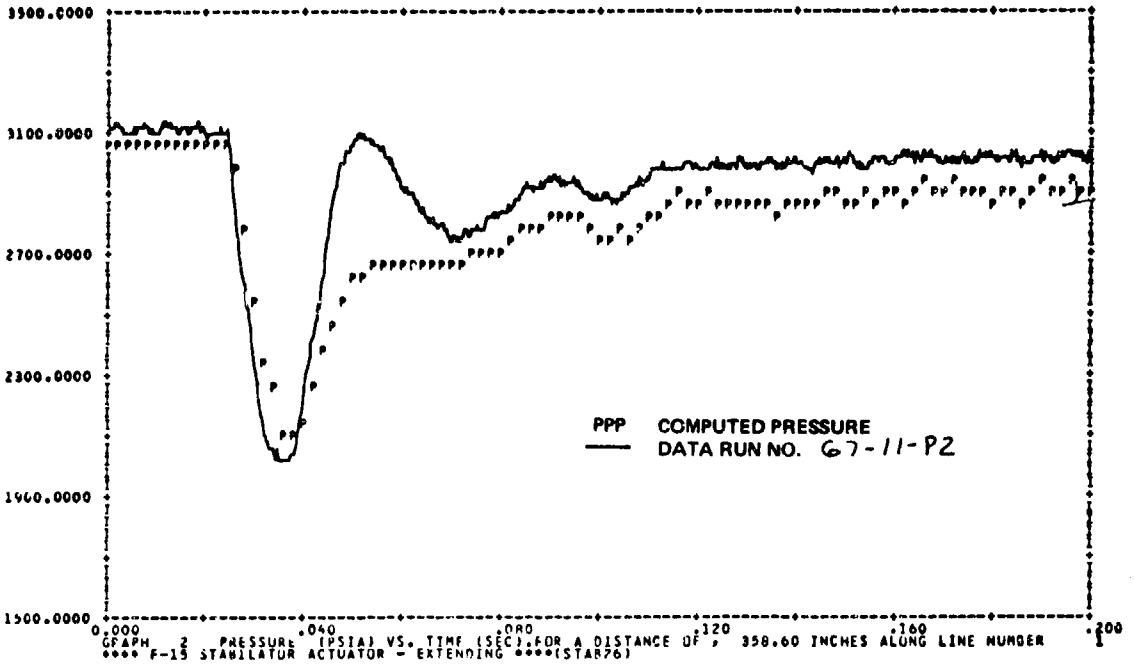

FIGURE 380. 67-11-P2 ACTUATOR EXTENDING

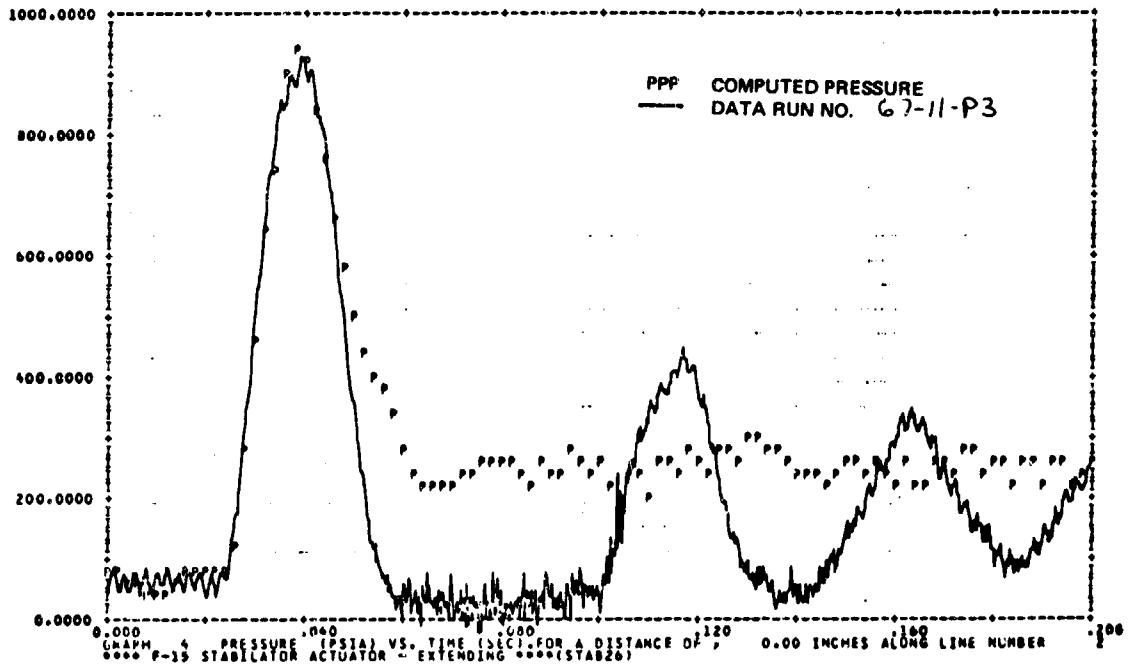

FIGURE 381. 67-11-P3 ACTUATOR EXTENDING

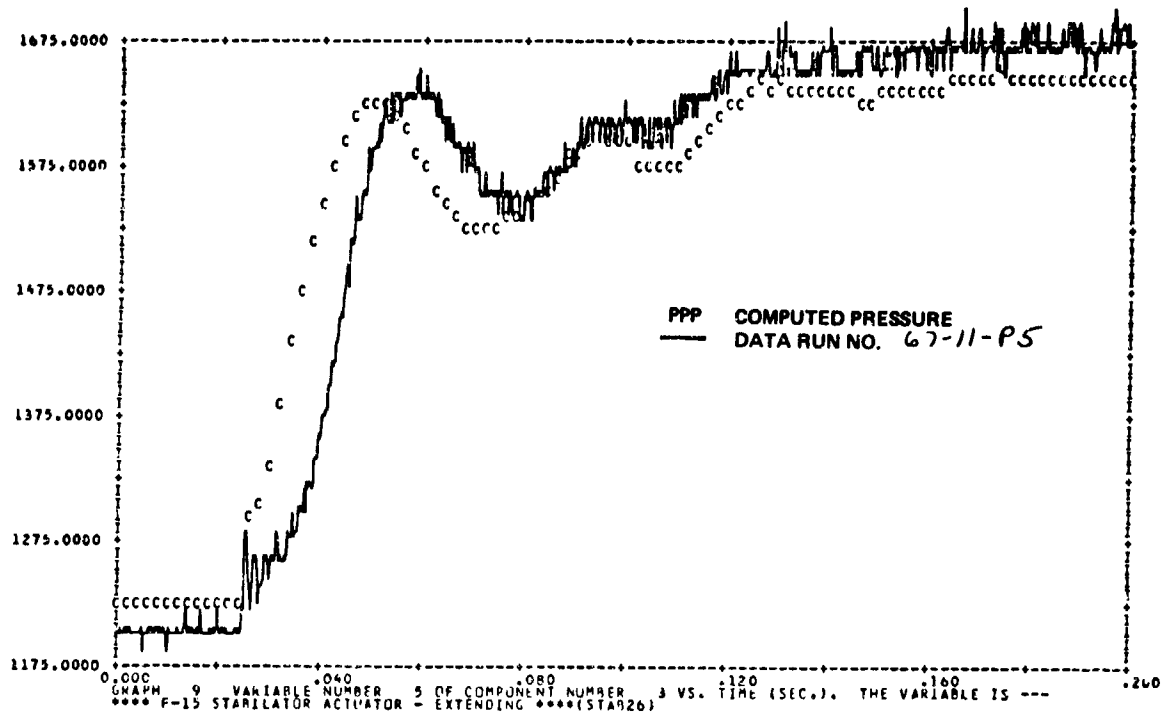

FIGURE 382. 67-11-P5 ACTUATOR EXTENDING

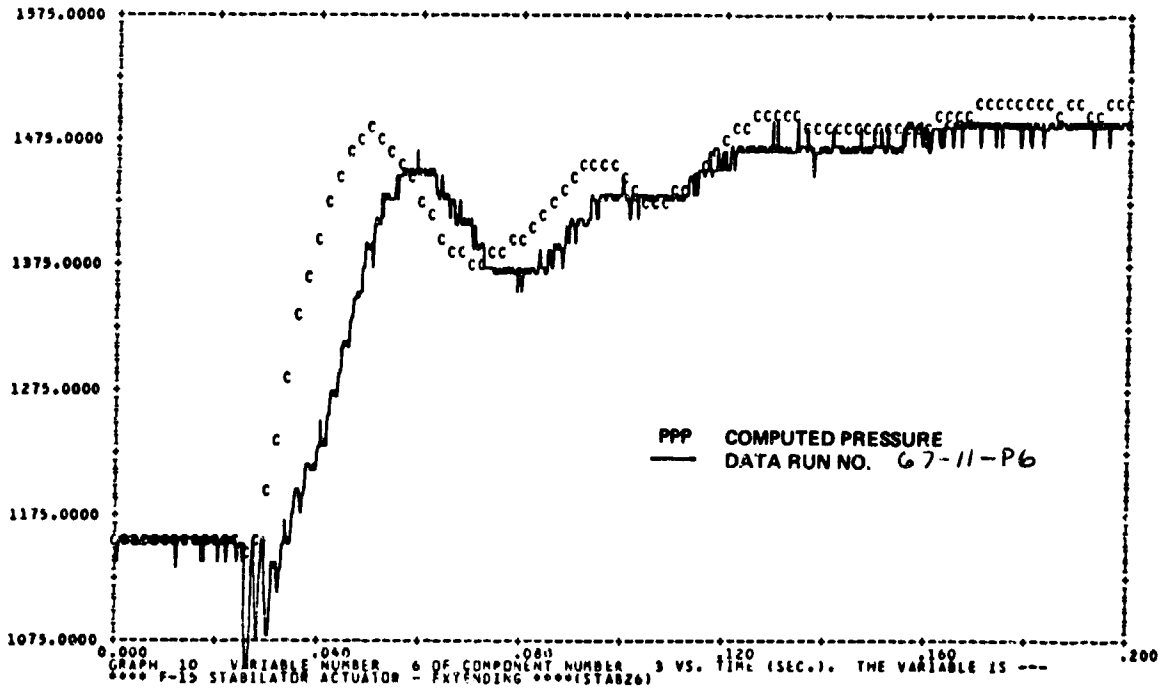

FIGURE 383. 67-11-P6 ACTUATOR EXTENDING

The computed cylinder pressures in Figures 382 and 383 do not show the 15 msec delay after the initial transient at 26 msec. Figure 384 is a plot of the valve reaction forces on the main control spool versus time. When the actuator is moved in the extend direction the initial transient valve reaction force is in the direction which tends to close the valve, however, the next transient reaction force is in the direction which tends to increase the valve opening. There is a net change of 3 lbs of force during this transient. The reason for the destabilizing effect is not thoroughly understood on the F-15 stabilator actuator. Perhaps the damper at the end of the valve is affecting the actual dynamics in this adverse manner. No attempt has been made to model the destabilizing effect in the program. Consequently the initial transient response in Figures 382 and 383 do not match the measured data. The remainder of the transient response is predicted adequately by the HYTRAN program.

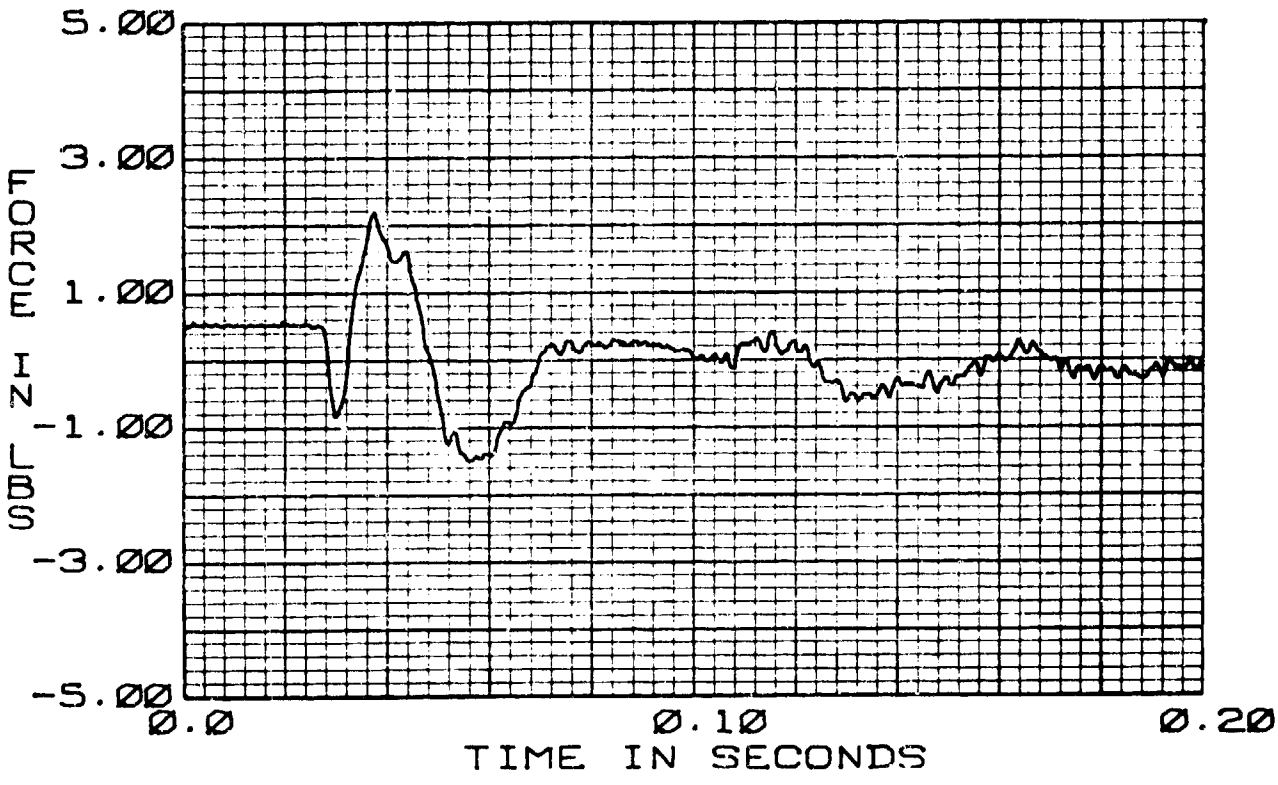

FIGURE 384. F-15 STABILATOR ACTUATOR 67-11-FF STEP INPUT EXTEND 100°F

b. Conclusions - The valve controlled actuator tested in the lab exhibited some destabilizing valve reaction forces. These may have accounted for the poor correlation with the initial transient. The addition of the stiction forces help with predicting the magnitude of the first transient spike, but it could not model the subsequent 15 msec delay before the rise of the cylinder pressures. The inclusion of a dynamic friction term assured that the cylinder pressures were of the proper magnitude.

The simple servoactuator model used in the HYTRAN program gives reasonable correlation with the lab test data and is considered a good subroutine for most applications.

13. SUBSYSTEM MODEL VERIFICATION

Transient testing was done on the F-15 Iron Bird utility speedbrake system. Figure 385 contains a schematic diagram of the test configuration and instrumentation. The tests that were run are listed in Table 18. Most of the verification work to this point has been accomplished for individual component models. The speedbrake tests represents the first HYTRAN computer verification for an entire subsystem. The models used in the simulation were a four way valve (subroutine VALV22), a utility actuator (subroutine ACT120), three orifice restrictors (subroutine REST41) and the branch and line component models.

TABLE 18

F-15 IRON BIRD

TRANSIENT TESTS ON SPEEDBRAKE SUBSYSTEM

RUN NO.	TEST CONDITION VALVE POSITION	TEMP UTILITY PUMP INLET (°F)
80-04	Hold - Extend	183
80-05	Hold - Ret	184
80-06	Ret-Ext-Ret	185
80A04	Hold-Ext	190
80B05	Hold-Ret	187
80A06	Ret-Ext-Ret	193
80-07	Ext-Ret-Ext	197
80-08	Ret → Ext	190
80-09	Ext → Ret	190
80-10	Ret to Ext Actuator Bottomed Ext	187
80-11	Hold to Ret Actuator Bottomed Ret	190

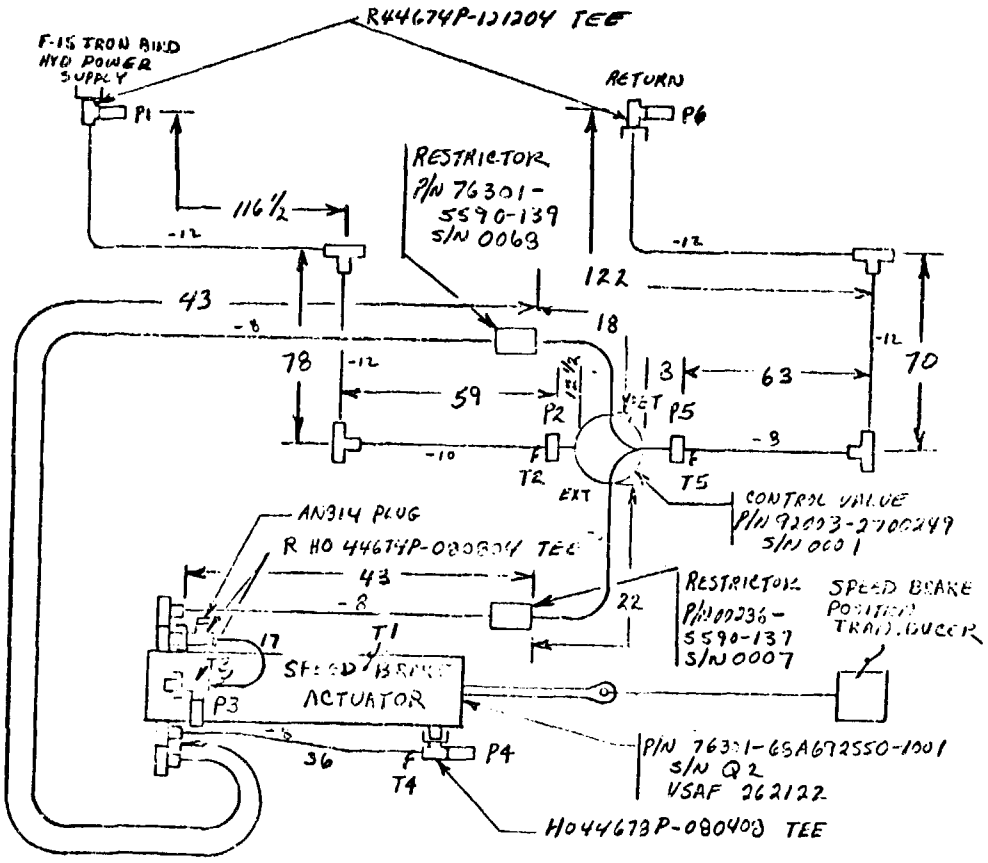

FIGURE 385. F-15 IRON BIRD SPEEDBRAKE SYSTEM CONFIGURATION

a. Computer Simulation With Test Data - A computer run extending the actuator was made with the system configuration data in Figure 386 and the pressure boundary conditions in Figures 387 and 388. The results of the simulation are shown in Figures 389, 390, 391, and 392 overplotted with the test data. The computed pressure correlates well with the measured values. The computer peak pressure in Figure 392 is 100 psi higher than the measured data. This occurs because the 4 way - 3 position control valve opened the actuator to return before the pressure side was opened. The peak pressure value could be lowered by adjusting the valve opening position in the data shown in Figure 386.

A change in the max opening position of the valve will alter the rate of decay characteristics of the transient which would change the computed points in Figures 390 and 391.

```
**** F-15 SPEED BRAKE SYSTEM - 80A04 EXTEND ****(DTS855)

THE TRANSIENT RESPONSE IS FROM T=0.0  TO T=   .200 SECONDS AT TIME INTERVALS OF DELT= .00020
        WITH OUTPUT POINTS PLOTTED AT INTERVALS OF  ,   .00200  SECONDS

FLUID DATA FOR  MIL-H-5606  AT  3000.0 PSIG, -    50.0 PSIG AND 193.0 DEG F  IN   10.0 DEG F STEPS
                VISCOSITY    -  .927E-02        .760E-02IN**2/SEC
                DENSITY      -  .795E-04        .786E-04(LB-SEC**2)/IN**4
                BULK MODULUS -  .182E+06        .146E+06PSI
                VAPOUR PRESS.-  .200E+01 AT  193.0 DEG F

LINE DATA
LINE NO.      LENGTH        INTERNAL DIA     WALL THICKNESS     MODULUS OF ELASTICITY     DELX          CHARACTERISTIC IMPEDANCE     VELOCITY OF SOUND
    1        194.5000          .6720             .0390              .150E+08              8.8409              9.7473              43480.3285
    2         71.5000          .5610             .0320              .150E+08              8.9375             13.9672              43421.5314
    3         22.0000          .4480             .0260              .150E+08             11.3000             21.9314              43480.3285
    4         60.0000          .4480             .0260              .150E+08             10.0000             21.9314              43480.3285
    5         79.0000          .4480             .0260              .150E+08              8.7778             21.9314              43480.3285
    6         18.0000          .4480             .0260              .150E+08              9.0000             21.9314              43480.3285
    7         51.0000          .4440             .0280              .100E+08              5.5000             21.6045              42070.6420
    8         21.0000          .4440             .0280              .100E+08             10.5000             21.6045              42070.6420
    9        192.0000          .6800             .0350              .100E+08              8.3478              9.0092              41190.2428
 COMP#,  1  INTEGER DATA     1  91   0  -1   1   0   0   0   0   0   0   0   0   0   0   0
 COMP#,  2  INTEGER DATA     2  11   0   1  -2   0   0   0   0   0   0   0   0   0   0   0
 COMP#,  3  INTEGER DATA     3  22   4   2  -3  -7   6   0   0   0   0   0   0   0   4   0
REAL DATA CARD #   1    .2500E-02   .1250E+00   .6200E-01   .3200E+02  -.2500E-02  -.1250E+00   .6300E-01   .3200E+02
REAL DATA CARD #   2    .2500E-02   .6200E-01   .6200E-01   .3200E+02  -.2500E-02  -.1250E+00   .6300E-01   .3200E+02
REAL DATA CARD #   3    0.          .2300E-01   .7300E-01   .2000E+00   0.          0.          0.          0.
REAL DATA CARD #   4    0.          0.          .1863E+00   .1863E+00   0.          0.          0.          0.
 COMP#,  4  INTEGER DATA     4  41   1   3  -4   0   0   0   0   0   0   0   0   0   0   0
REAL DATA CARD #   1    .4637E+00   .6500E+00   0.          0.          0.          0.          0.          0.
 COMP#,  5  INTEGER DATA     5 102   2   4  -5   0   0   0   0   0   0   0   0   0   0   0
REAL DATA CARD #   1    .8230E+01   .7040E+01   .1190E+01   .2418E+03   .1000E+00   .3412E+02   .1000E+00   .3880E-01
REAL DATA CARD #   2    0.          0.          .1000E-01   0.          0.          0.          0.          0.
 COMP#,  6  INTEGER DATA     6  41   1  -6   5   0   0   0   0   0   0   0   0   0   0   0
REAL DATA CARD #   1    .4637E+00   .6500E+00   0.          0.          0.          0.          0.          0.
 COMP#,  7  INTEGER DATA     7  41   1   7  -8   0   0   0   0   0   0   0   0   0   0   0
REAL DATA CARD #   1    .3310E+00   .6500E+00   0.          0.          0.          0.          0.          0.
 COMP#,  8  INTEGER DATA     8  11   0   8  -9   0   0   0   0   0   0   0   0   0   0   0
 COMP#,  9  INTEGER DATA     9  91   0   9   1   0   0   0   0   0   0   0   0   0   0   0
     CPU TIME IN SECONDS =    8.621

                                STEADY STATE INPUT DATA

        NUMBER OF NODES =  8     NUMBER OF LEGS =  8     NUMBER OF CONSTANT PRESSURE NODES =  0

                            LEG CONNECTION INPUT DATA

LEG NO    UPST NODE NO    DWST NODE NO    NO OF ELEMENTS    FLOW GUESS    UPST PRESS    DWST PRESS
   1            1               2               4          10.00000      0.00000       0.00000
   2            2               3               1          10.00000      0.00000       0.00000
   3            3               4               1          10.00000      0.00000       0.00000
   4            4               5               1          10.00000      0.00000       0.00000
   5            2               5               1          10.00000      0.00000       0.00000
   6            3               6               4          10.00000      0.00000       0.00000
   7            8               5               4          10.00000      0.00000       0.00000
   8            4               7               6          10.00000      0.00000       0.00000

LEG NO    ELEMENTS IN LEG----
   1    1 -- 1,  0 -- 1,  2 -- 1,  0 -- 2,
   2    3 -- 1,
   3    3 -- 2,
   4    3 -- 3,
   5    3 -- 4,
   6    0 -- 3,  4 -- 1,  0 -- 4,  5 -- 1,
   7    5 -- 2,  0 -- 3,  6 -- 2,  0 -- 6,
   8    0 -- 7,  7 -- 1,  8 -- 8,  8 -- 1,  0 -- 9,  9 -- 1,
```

FIGURE 386. RUN 80A04 HYTRAN INPUT DATA FOR SPEEDBRAKE EXTENDING

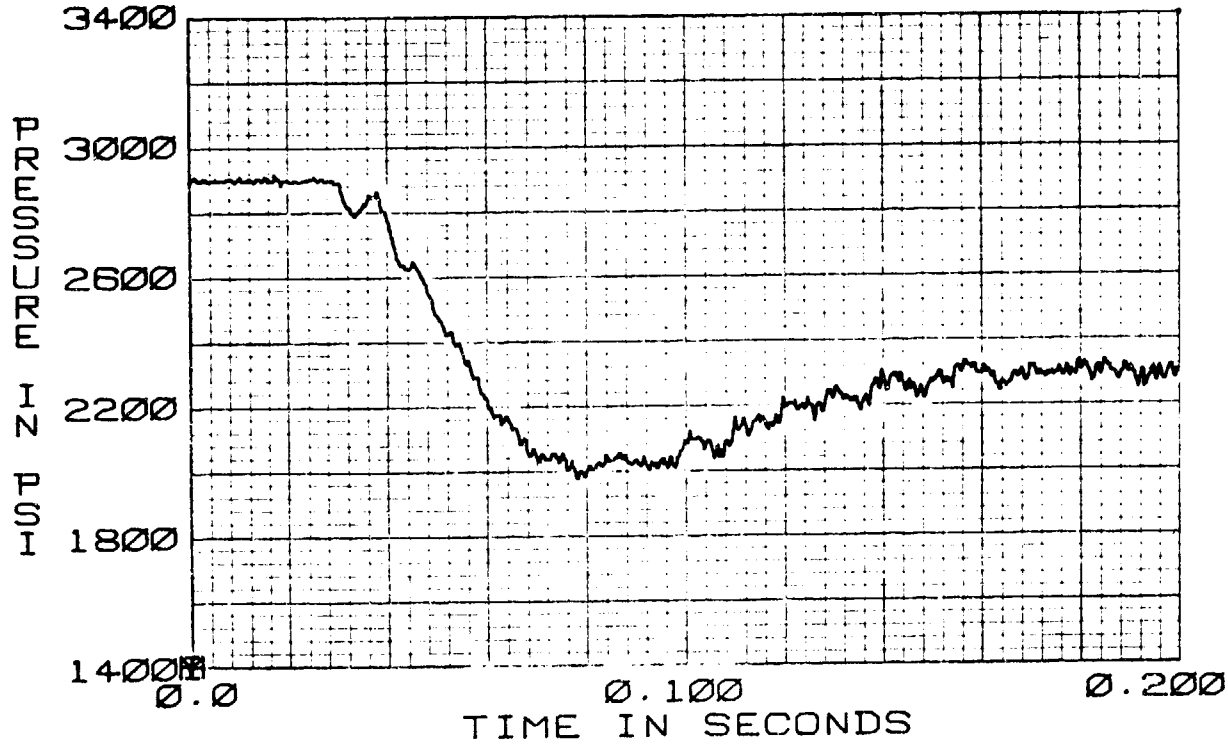

FIGURE 387. F-15 SPEEDBRAKE SYSTEM 80A04-P1 STEP INPUT EXTEND DIRECTION 190°F

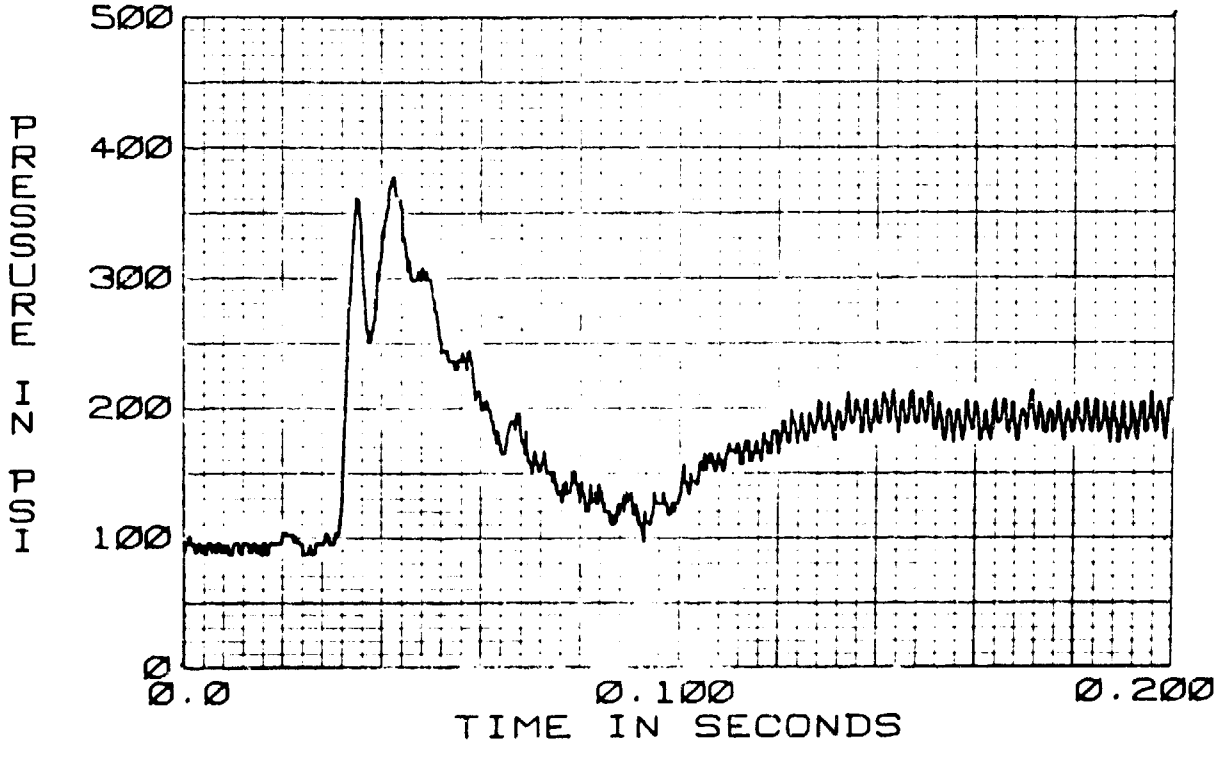

FIGURE 388. F-15 SPEEDBRAKE SYSTEM 80A04-P6 STEP INPUT EXTEND DIRECTION 190°F

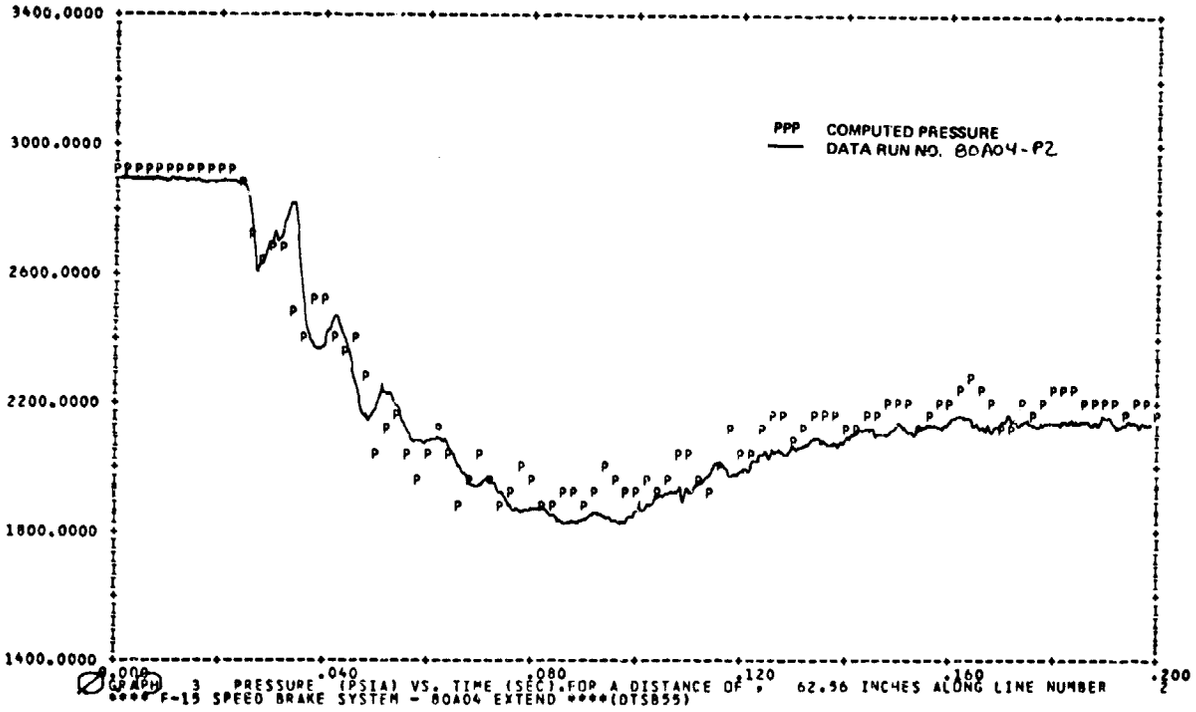

FIGURE 389. 80A04-P2 SPEEDBRAKE EXTENDING

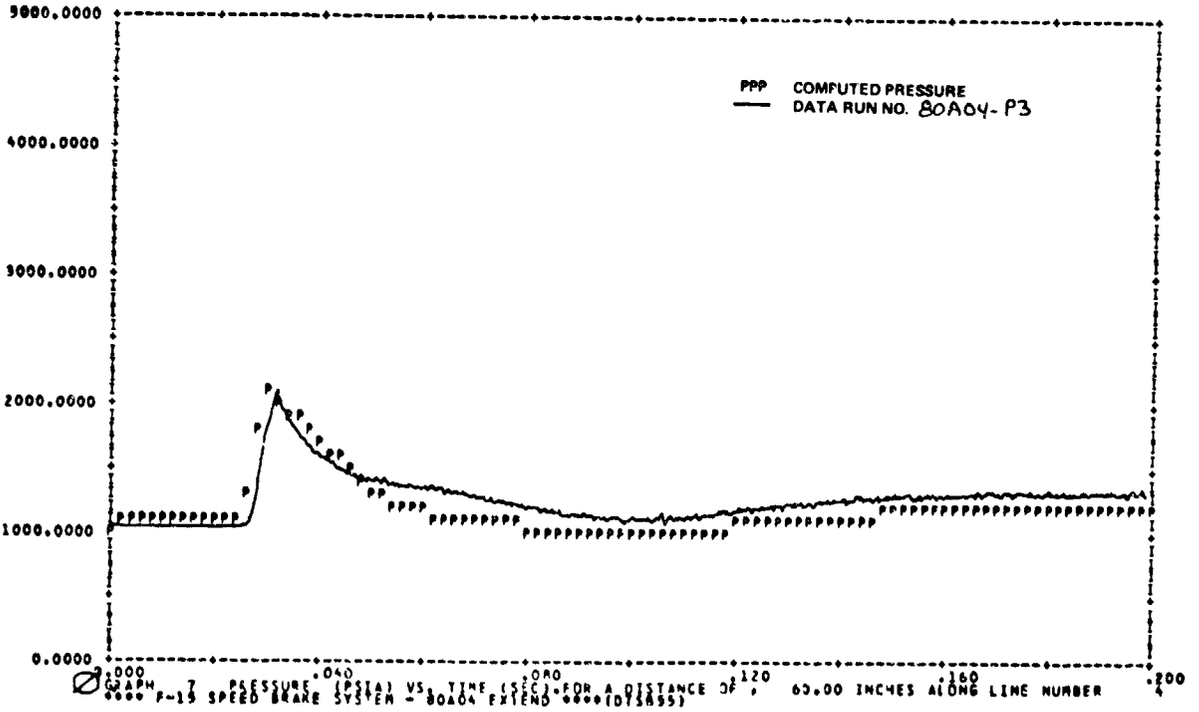

FIGURE 390. 80A04-P3 SPEEDBRAKE EXTENDING

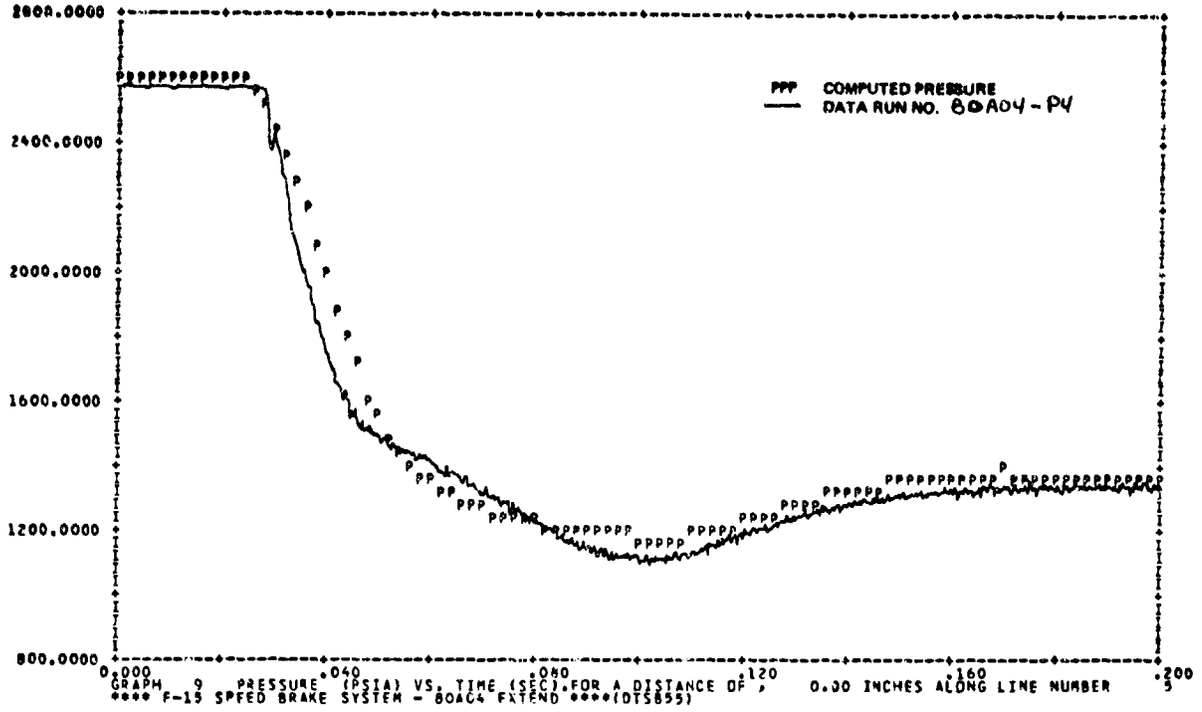

FIGURE 391. 80A04-P4 SPEEDBRAKE EXTENDING

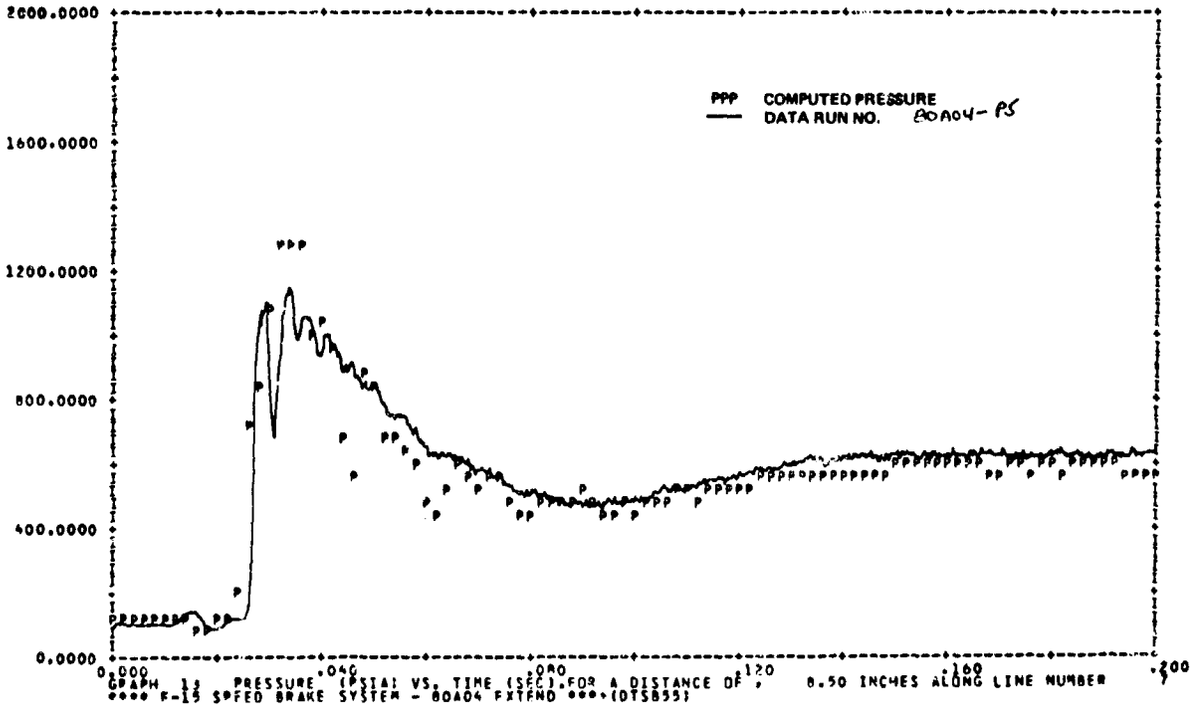

FIGURE 392. 80A04-P5 SPEEDBRAKE EXTENDING

b. Conclusions - Modeling of the speedbrake subsystem with the HYTRAN program went exceedingly well. This computer run showed that the component models do function properly in a system simulation, and for this basic system the HYTRAN program was able to calculate the proper pressures and flows.

14. TWO PUMP TESTING AND SYSTEM VERIFICATION

The test results obtained from the two pump testing are compared to the HYTRAN program computer simulation. The testing was done on a one inch line system with MIL-H-83282 hydraulic fluid. Test conditions were established to determine factors and pump modes affecting instability, and to examine changes in the pumps or system that would improve stability. Table 19 contains a list of the time domain tests that were made on the parallel pump setup. A simplified system schematic of the parallel pump test setup is shown in Figure 393.

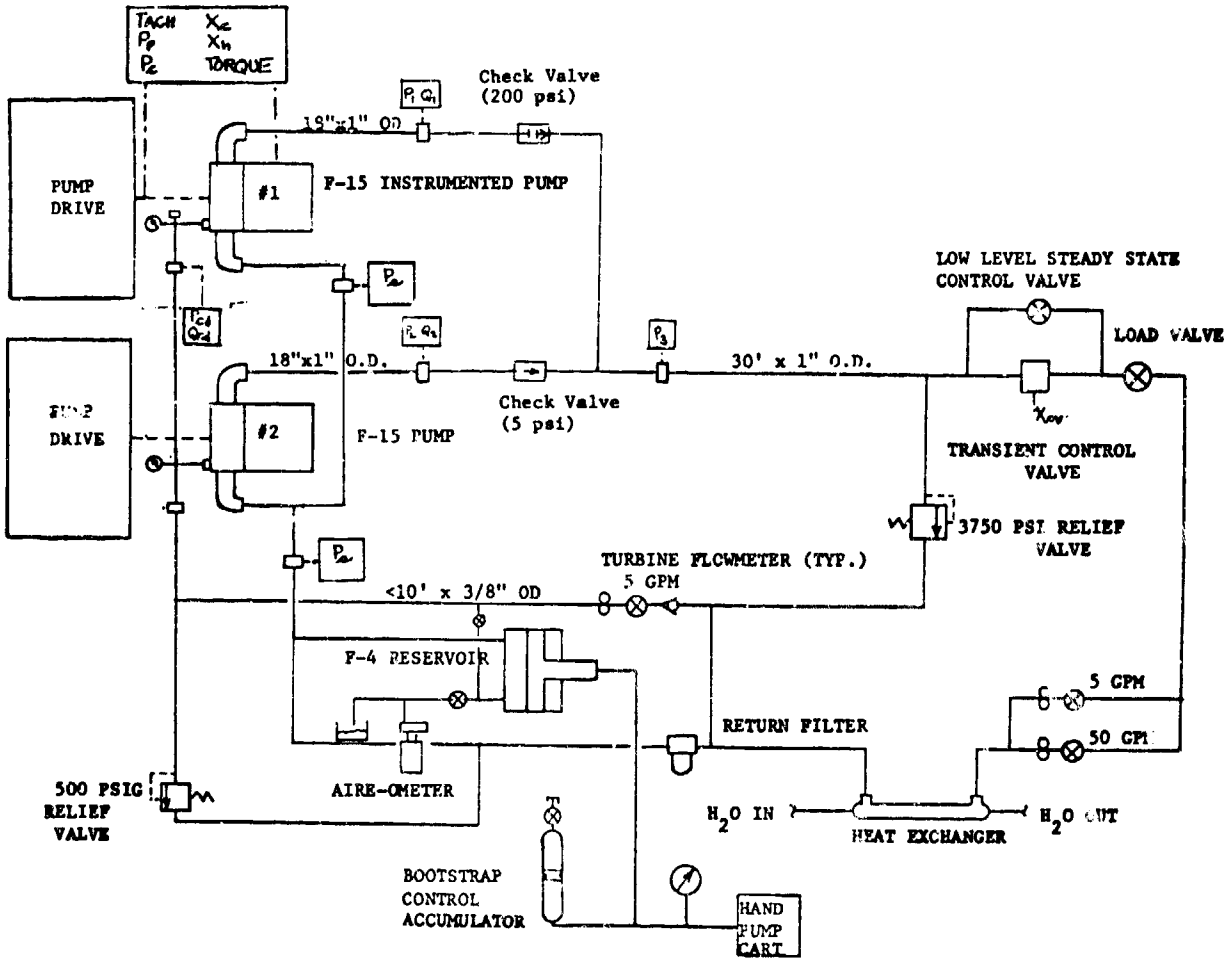

FIGURE 393. PARALLEL PUMP TEST SETUP

TABLE 19. PARALLEL PUMP OPERATION TEST

#1 Pump - 5 psi check valve - F-15 instrumented pump
#2 Pump - 225 psi check valve

Run No.	Test Condition	Drive Speed (RPM) 1	Drive Speed (RPM) 2	QCD (CPM) 1	QCD (CPM) 2	PS (psig)	PR (psig)	S.S. Flow(GPM)	Pump Inlet Temp (°F) 1	Pump Inlet Temp (°F) 2
69-01-XX	Turn-Off Transient 40 →0.5GPM	3585	3600	.60	1.33	41.7	49	40	124	124
69-01+XX	Turn-On Transient 0.5 →40GPM	3590	3600	.82	1.36	48.1	48.5	0.5	125	126
69-02-XX	Turn-Off Transient 47 →0.56GPM	3596	3573	.63	1.34	40.2	49	47	127	126
69-02+XX	Turn-On Transient 0.5 →47GPM	3596	3600	.88	1.35	47.2	48.5	0.5	128	128
69-03-XX	Turn-Off Transient 20 →0.5GPM	3596	3600	.67	1.34	43.3	51.	20	126	125
69-03+XX	Turn-On Transient 0.5 → 20GPM	3591	3600	.86	1.31	43.5	48.5	0.5	128	132
#1 Pump - 5 psi check valve #2 Pump - 225 psi check valve - F-15 instrumented pump										
69-04-XX	Turn-Off Transient 40 →0.5 GPM	3597	3600	.63	.27	39.1	49	40	126	134
69-04+XX	Turn-On Transient 0.5→ 40GPM	3601	3600	1.39	1.13	46	49	0.5	126	129
69-05-XX	Turn-Off Transient 47 →05.GPM	3605	3560	.53	.5	38	50.5	47	127	125
69-05+XX	Turn-On Transient 0.5 →47GPM	3598	3600	1.33	1.03	46.7	49	0.5	124	123
69-06-XX	Turn-Off Transient 20 →0.5GPM	3602	3600	.98	.89	45.5	50	20	130	128
69-06+XX	Turn-On Transient 0.5 →20GPM	3596	3600	1.40	1.04	46.8	50	0.5	128	143

TABLE 19. (CONT)

#1 Pump - 5 psi check
#2 Pump - 225 psi check - F-15 instrumented pump

Both pump compensators set for identical outlet pressure

69-07-XX	Turn-Off Transient 47 →0.5GPM	3599	3560	.55	.5	42.3	51	47	126	124
69-07+XX	Turn-On Transient 0.5→ 47GPM	3598	3600	1.36	1.0	50.6	49	0.5	128	132
69-08-XX	Turn-Off Transient 20 →0.5GPM	3598	3600	.98	.68	46.4	48.5	20	129	125
69-08+XX	Turn-On Transient 0.5 →20GPM	3590	3600	1.29	1.00	0.5	50.9	49	128	132

#1 Pump - 5 psi check valve
#2 Pump - 5 psi check valve - F-15 instrumented pump
Pump compensations set for same outlet pressure

69-09-XX	Turn-Off Transient 47 →0.5GPM	3594	3573	.64	.07	41.9	48.5	47	127	126
69-09+XX	Turn-On Transient 0.5 →47GPM	3595	3600	1.35	.81	52.5	50	0.5	128	126
69-10-XX	Turn-Off Transient 20 →0.5GPM	3592	3600	1.05	.57	-	49	20	133	123
69-10+XX	Turn-On Transient 0.5 →20GPM	3594	3600	1.36	.86	50.1	49.5	0.5	125	125
69-11-XX	Turn-Off Transient 47 →0.5GPM	3432	3573	.60	.50	38.2	50.5	47	129	130
69-11+XX	Turn-On Transient 0.5 →47GPM	3432	3600	1.31	.82	46.0	49.5	0.5	130	132
69A11-XX	Turn-Off Transient 47 →0.5GPM	3435	3560	.77	.50	41.4	49	47	126	127
69A11+XX	Turn-On Transient 0.5 →47GPM	3435	3600	1.36	.83	48.9	49	0.5	130	131
69-12-XX	Turn-Off Transient 20 →0.5GPM	3433	3537	1.09	.60	50.9	50	20	130	132
69-12+XX	Turn-On Transient 0.5 →20GPM	3435	3600	1.31	.87	51.2	49	0.5	129	132

a. Computer Simulation - A computer simulation of the two-pump system was made with the HYTRAN Program. The HYTRAN block diagram of the test system is shown in Figure 394. The complete test setup is modeled except for emergency relief path lines and components. The elements which make up the system are split into lines and components. The lines are numbered sequentially and have upstream and downstream ends. The components are also numbered in a separate sequence. Node numbers are assigned to the points at which the flow divides or combines under steady state flow conditions and leg numbers are labeled between two nodes.

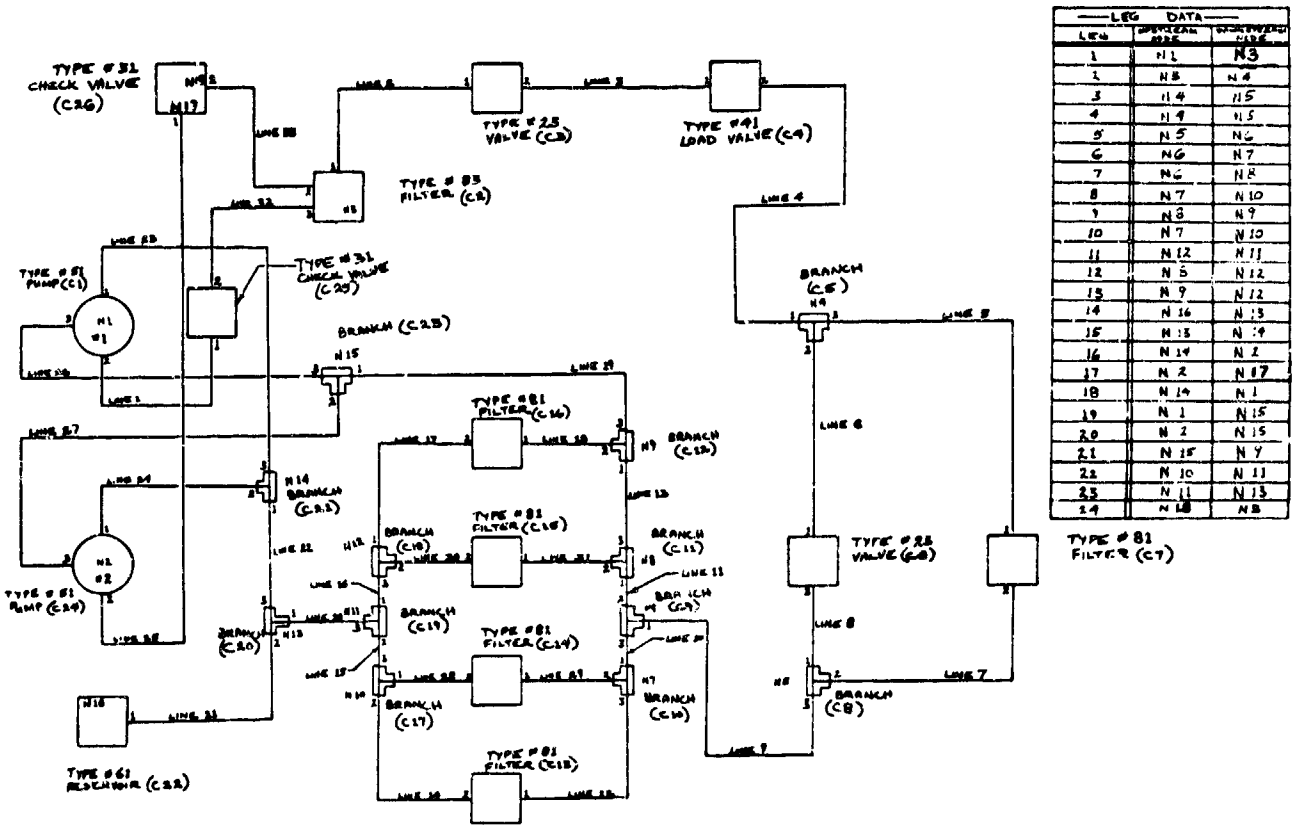

FIGURE 394. HYTRAN SCHEMATIC OF TWO PUMP TEST SYSTEM

The simulation consisted of running the HYTRAN Program under the same lab test conditions. Measured test data was not used as boundary conditions in the simulation. This was done to test the basic accuracy of the program without any external forcing factors. A turn-on transient was made with the test conditions similar to run number 69-07+XX.

The test data for run number 69-07+XX are presented in Figures 395 through 399 overplotted with the results from the computer program.

b. Conclusions - The HYTRAN simulation of the two pump test system indicated reasonably good correlation with the measured data. The initial response predictions were adequate but the final steady state operating pressures were not correct. Further work with the pump model should correct this situation.

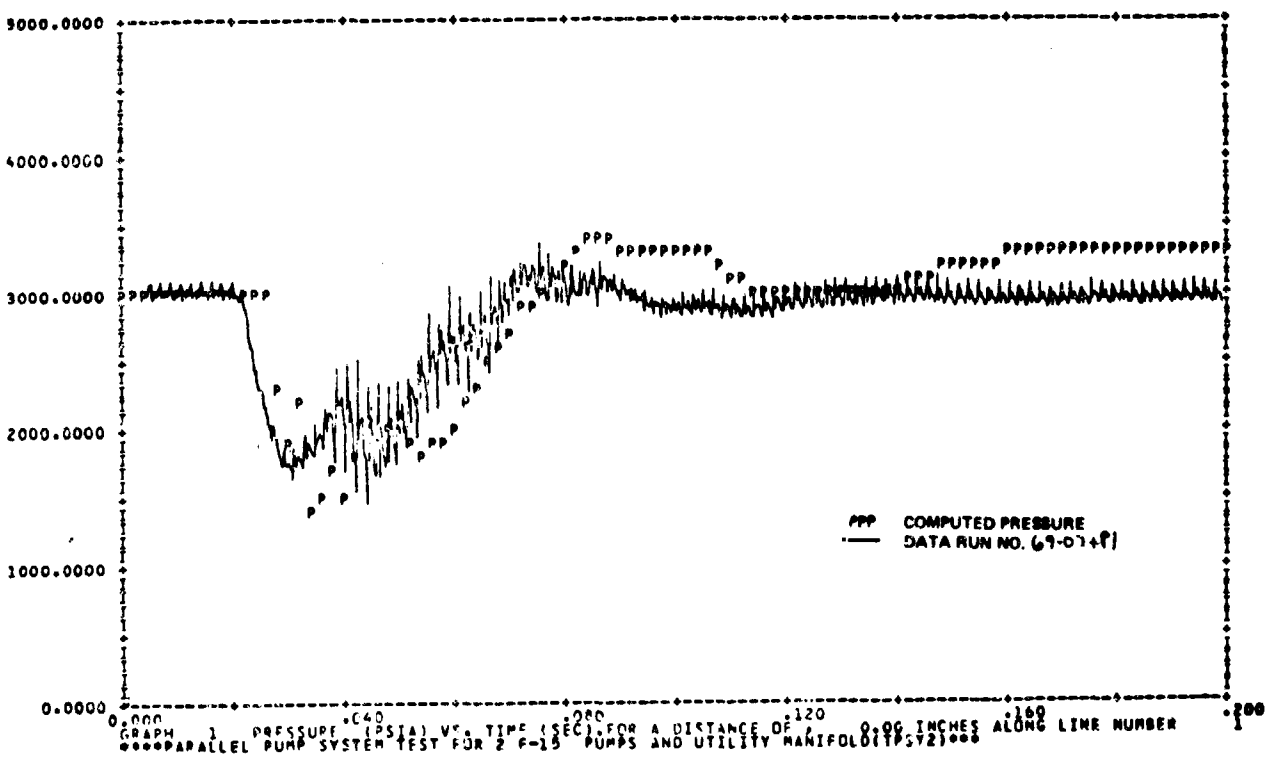

FIGURE 395. 69-07+P1 TURN-ON TRANSIENT

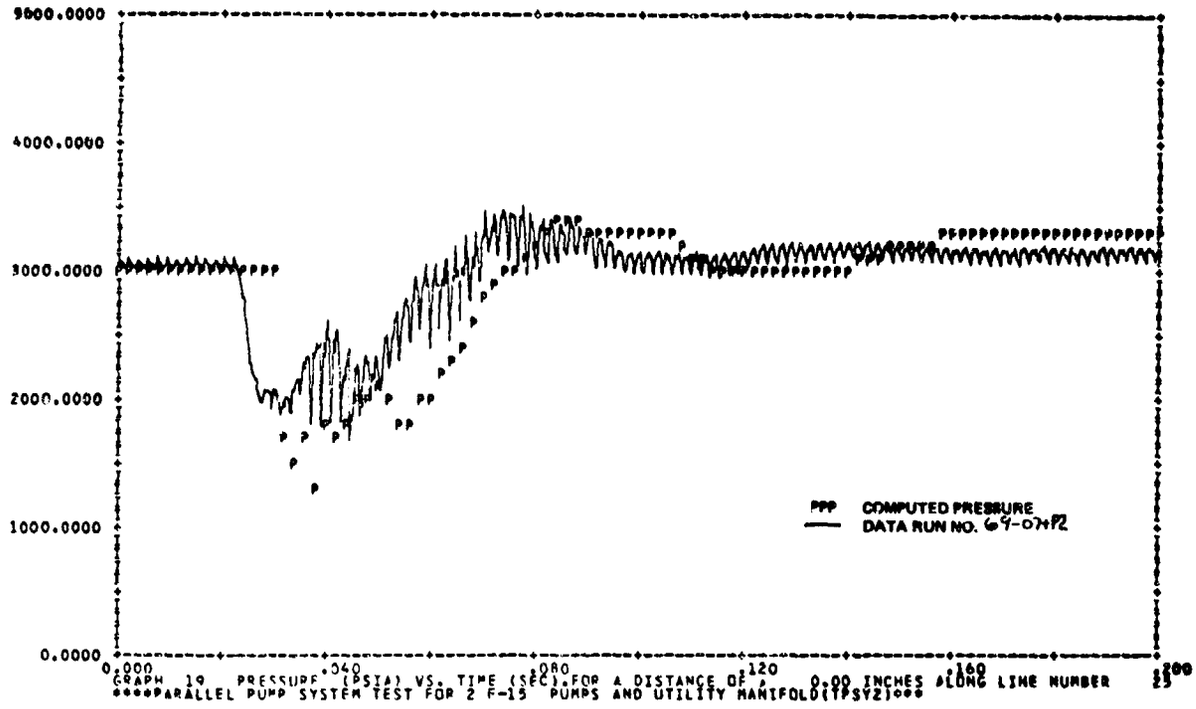

FIGURE 396. 69-07+P2 TURN-ON TRANSIENT

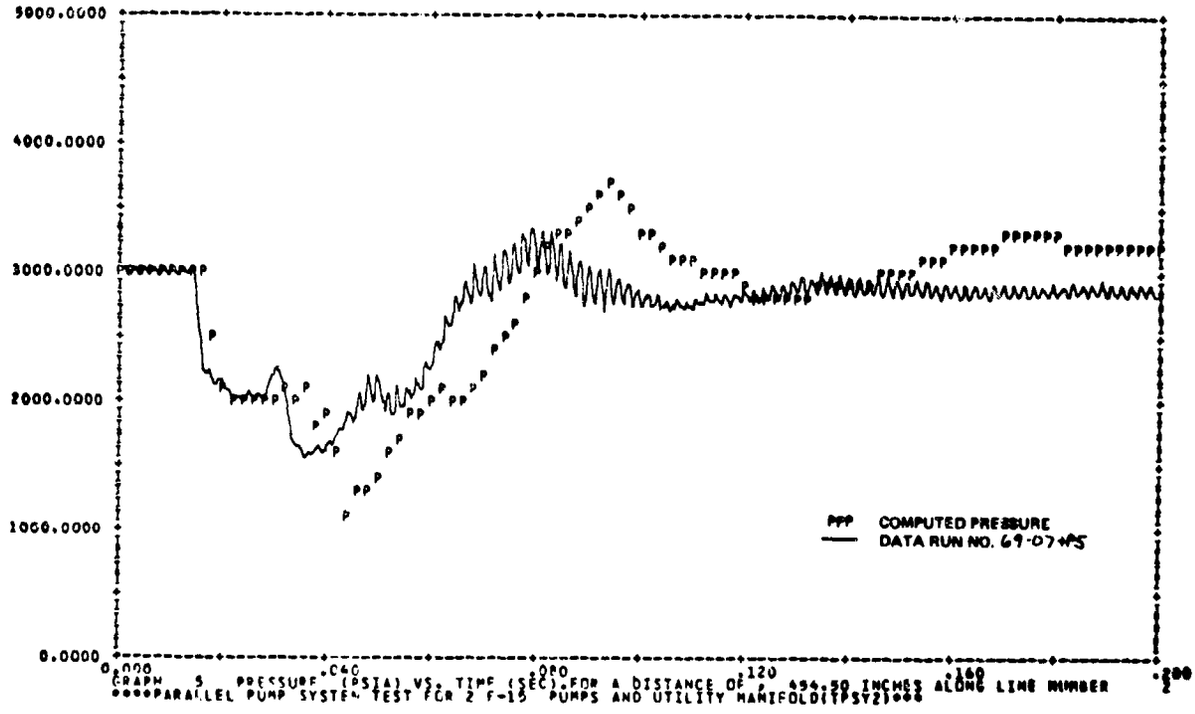

FIGURE 397. 69-07+P5 TURN-ON TRANSIENT

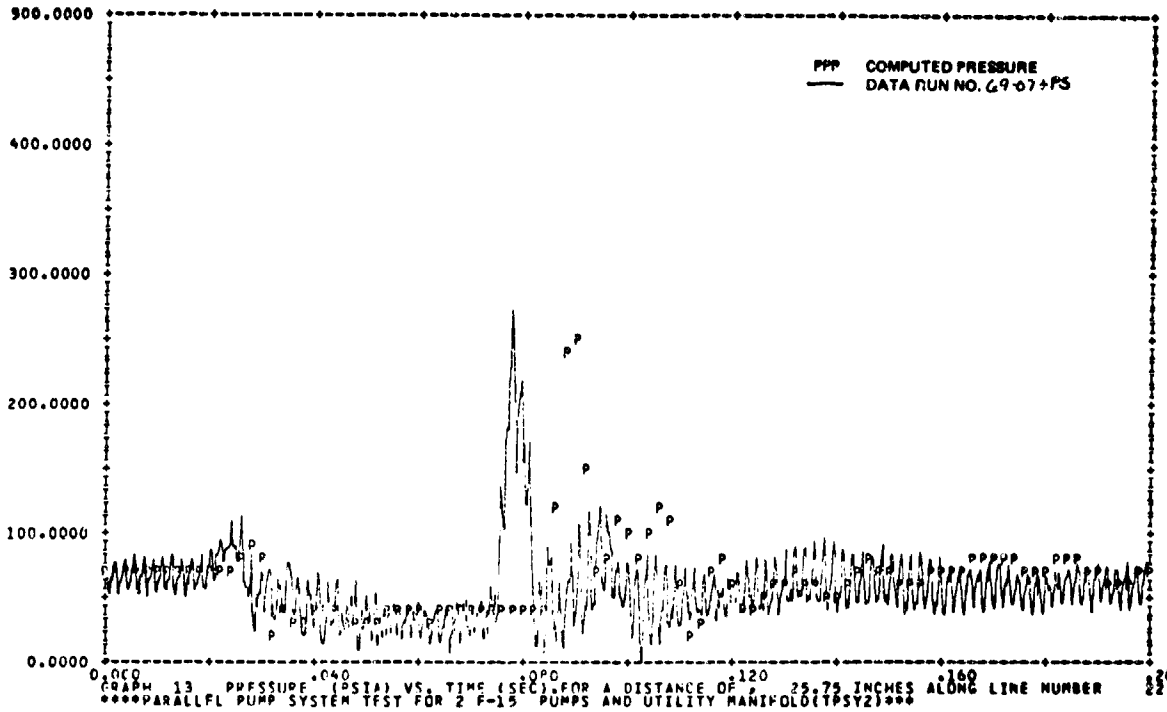

FIGURE 398. 69-07+P5 TURN-ON TRANSIENT

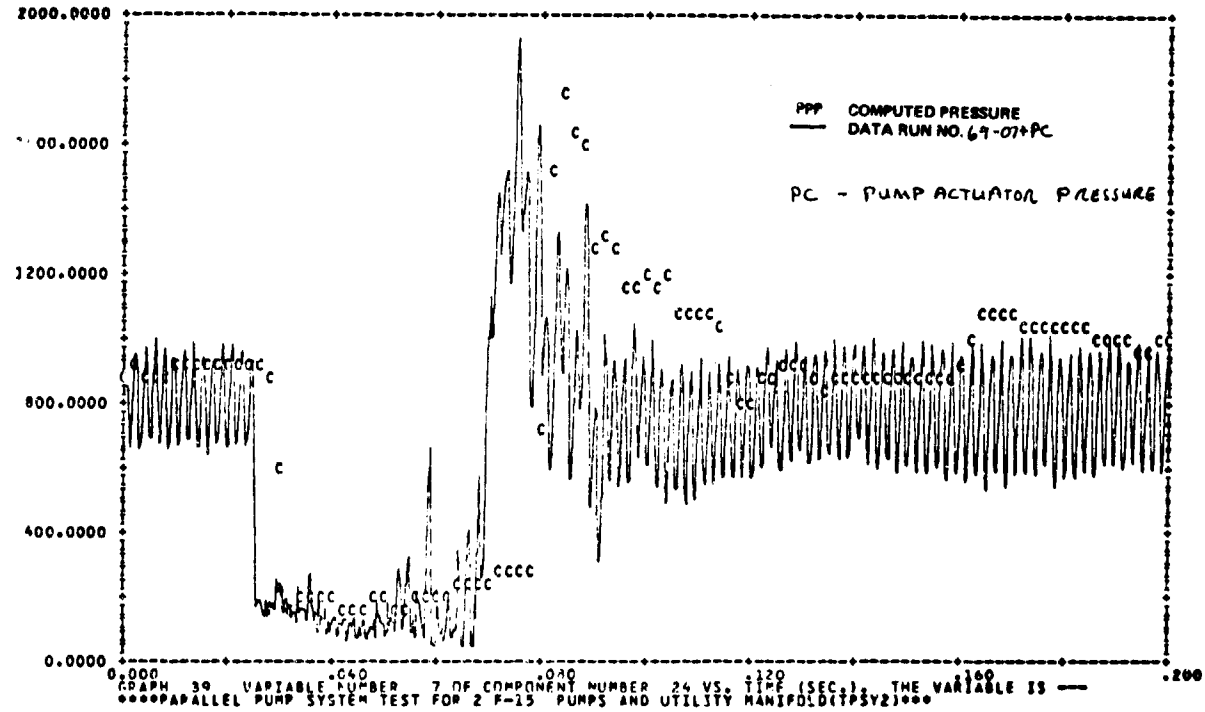

FIGURE 399. 69-07+PC TURN-ON TRANSIENT

15. F-15 COMPENSATED CHECK VALVE TESTING

Transients tests were performed on a compensated type check valve shown in Figure 400. The check valve is designed to trap a quantity of fluid which can be transferred back into a selector valve that contains a return pressure sensing (RPS) circuit. During operation of a subsystem the return oil decelerating when a valve is shut off causes momentary cavitation. With a standard type check valve this oil is prevented from returning to the cavitated valve and the RPS circuit shuts off the selector valve until sufficient pressure builds up on the return side through valve leakage. The volume of trapped oil (.5 in^3) in the compensated check valve can be immediately supplied to the cavitated line preventing RPS shut off. The reservoir back pressures supplies a sufficient force to transmit the trapped volume of oil to charge the RPS.

The transient tests were made to determine the dynamic effects of the compensated check valve in a return circuit. The test runs made with the check valve are shown in Table 20. The test configuration was the same as shown in Figure 233 in Section V, Paragraph 5. The compensated check valve was located in the same position as the test specimen.

Figures 401 and 402 are oscilloscope pictures of the transducer data for a 38.5 CIS turn-off transient. The P6 data shows a pressure spike occurring at 0.4 sec in the test run. The P6 transducer is located immediately

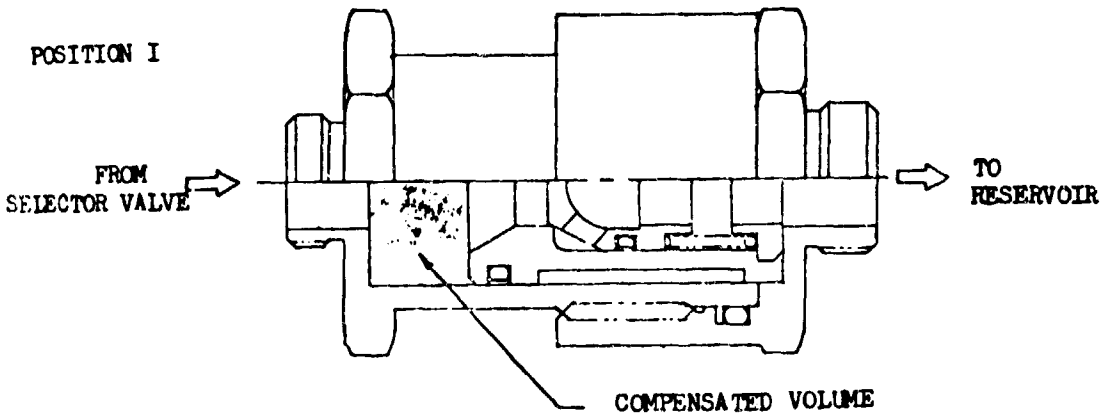

FIGURE 400. F-15 COMPENSATED CHECK VALVE

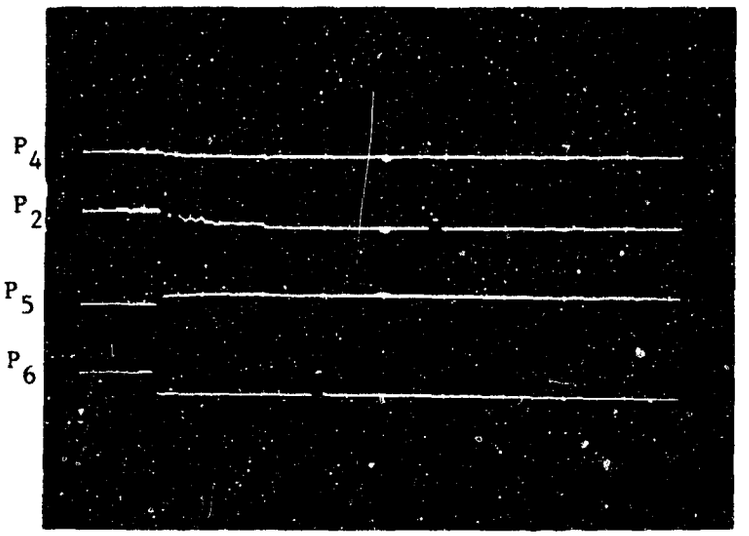

FIGURE 401
Run No. 61A07-XX
Flow 38.5 CIS
Sample Interval - 1 msec
Data Points - 1000
Temperature - 125°F
P4 & P2 - 500 psi/cm
P5 - 1300 psi/cm
P6 - 500 psi/cm

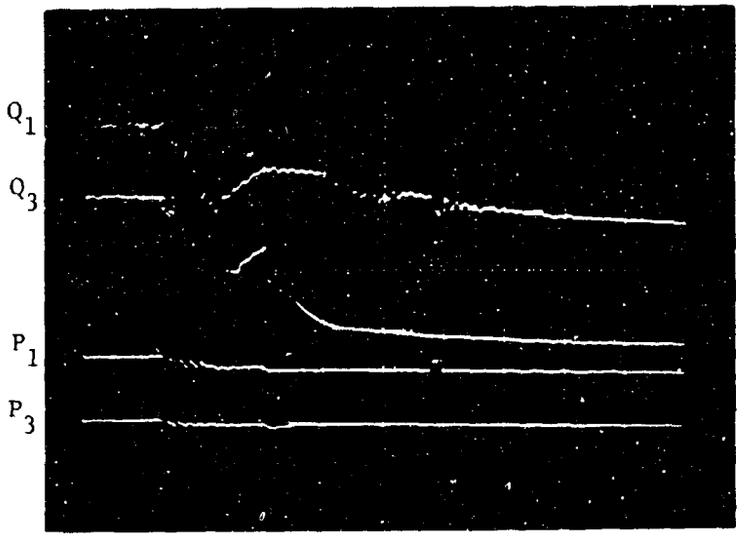

FIGURE 402
Run No. 61A07-XX
P1 & P3 - 500 psi/cm

TABLE 20. COMPENSATED CHECK VALVE TEST SERIES

Run Number	Test Condition	Flow Rate (CIS)	Temperature (°F)
61-07-XX*	Turn-Off	38.5	125
61-07+XX	Turn-On	38.5	125
61-08-XX	Turn-Off	11.55	125
61-08+XX	Turn-On	11.55	125
61-09-XX	Turn-Off	38.5	210
61-09+XX	Turn-On	38.5	210
61-10-XX	Turn-Off	11.55	210
61-10+XX	Turn-On	11.55	210

*XX-Denotes measured parameter

downstream of the control valve. The pressure spike results from the cavity collapsing with a zero flow rate. The pressure spike is close to the system return pressure. The affect of this compensated check with the oil volume in the line was to dampen the turn-off transient. The compensated check valve did not operate in the proper manner for these tests.

In the F-15 the compensated check valve is located three to four feet downstream of the valve. Within this distance the check valve is able to provide enough oil to prevent the RPS from triggering the valve. However, in the test set-up the compensated check valve was located thirty feet from the control valve. Therefore the check valve could not perform adequately. Consequently no computer analysis of these test results were made.

16. ACCUMULATOR TRANSIENT TEST DATA

Transient tests were performed on the F-15 Jet Fuel Starter (JFS) accumulator. A simplified schematic diagram of the test accumulator is shown in Figure 403. The accumulator is a self-displacing type with a normal operating pressure of 3000 psig. A thermocouple temperature probe was installed in the gas side so as to directly measure gas temperature.

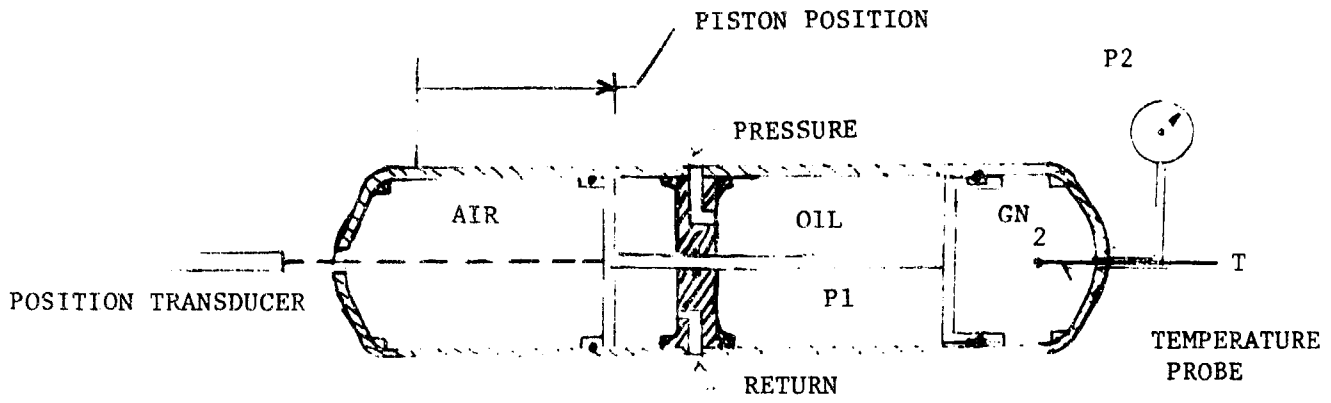

P1	Oil Pressure (psig)
P2	Gas Pressure (psig)
P	Piston Position (in)
T	Gas Temperature (°F)

Piston Area (gas side)	19.6 in^2
Rod Area	0.708 in^2
Max Oil Volume	140 in^3
Max Gas Volume	215 in^3
Operating Pressure	3000 to 3500 psig
Fluid	MIL-H-5606B
Gas	Nitrogen

FIGURE 403. JFS Accumulator

Testing consisted of precharing the gas side to either 1000 to 1720 psig then charging or discharging the accumulator at various rates. Data from test runs 3, 4, 6, 13 and 14 were analyzed to determine the polytropic specific heat ratio (n) of the nitrogen gas. Test runs and conditions are listed in Table 21 . The initial stabilized temperature of the accumulator was shop ambient (75 to 85°F) for all test runs.

Data plots for run number 3 are shown in Figures 404 through 407 for a 3 second charge-up transient. The specific heat ratio was computed at various time steps during the charging transient. Each value of n was computed using the initial state conditions at zero time, and the state condition at the elapsed time from the start of the transient. The specific heat ratio was determined using the pressure-volume relationship for a reversible polytropic process.

$$\frac{P_2}{P_1} = \left(\frac{V_1}{V_2}\right)^n$$

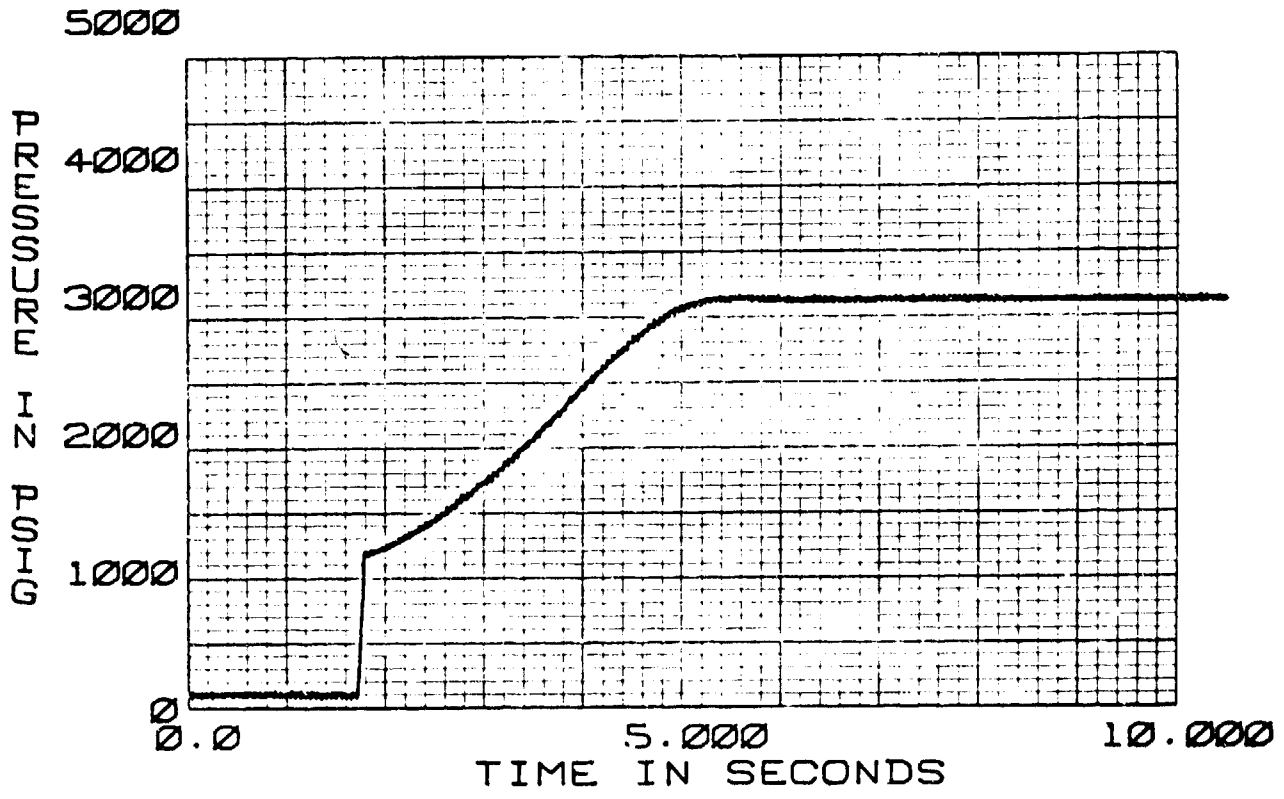

FIGURE 404. ACCUMULATOR ACC-3P1
P1 OIL PRESSURE
75°F CHARGE

TABLE 21. F-15 JFS ACCUMULATOR TESTS

Run Number	Test Condition	Charge or Discharge Time (Sec)	Gas Precharge (psig)
2	Discharge	10	1000
3	Charge	3	"
4	Discharge	5	"
5	Charge	30	"
6	Discharge	31	"
7	Charge	10	"
8	Discharge	16	"
9	Charge	15	"
10	Discharge	20	"
11	Charge	10	1720
12	Discharge	10	"
13	Charge	1	"
14	Discharge	2	"
15	Charge	25	"
16	Discharge	23	"
17	Charge	15	"
18	Discharge	15	"
19	Charge	32	"
20	Discharge	34	"

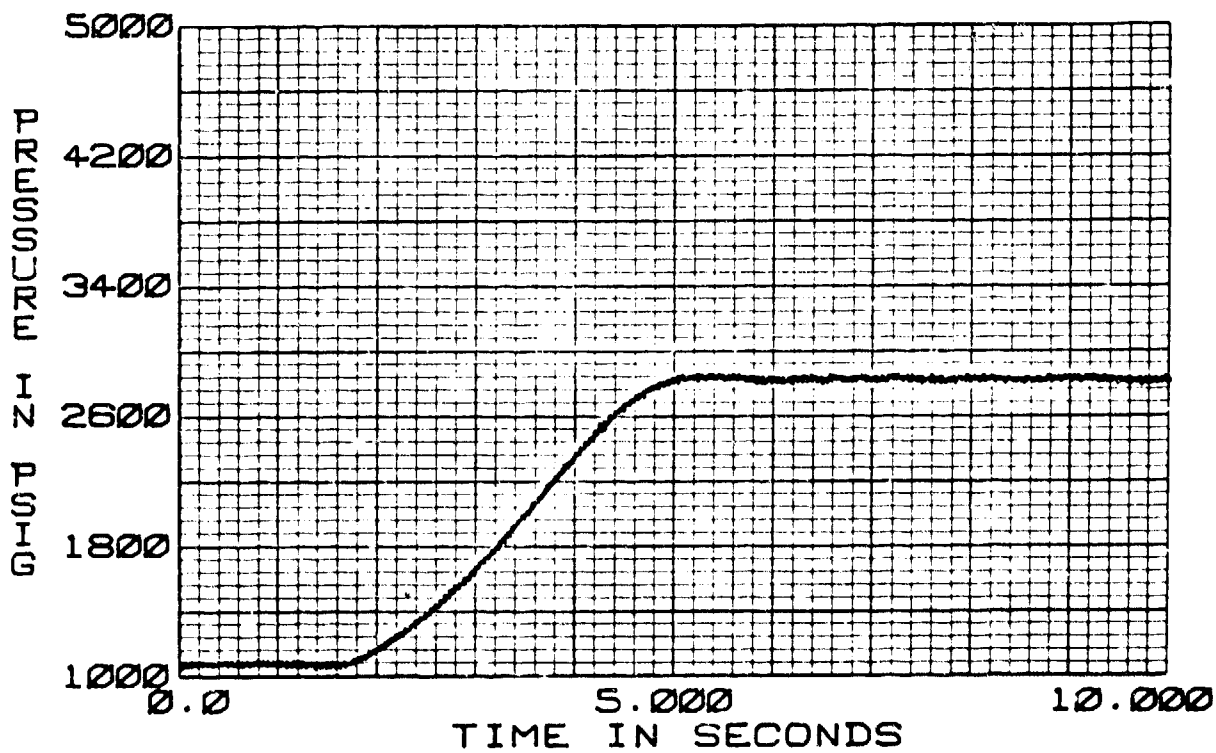

FIGURE 405. ACCUMULATOR ACC-3P2
P2 GAS PRESSURE
75°F CHARGE

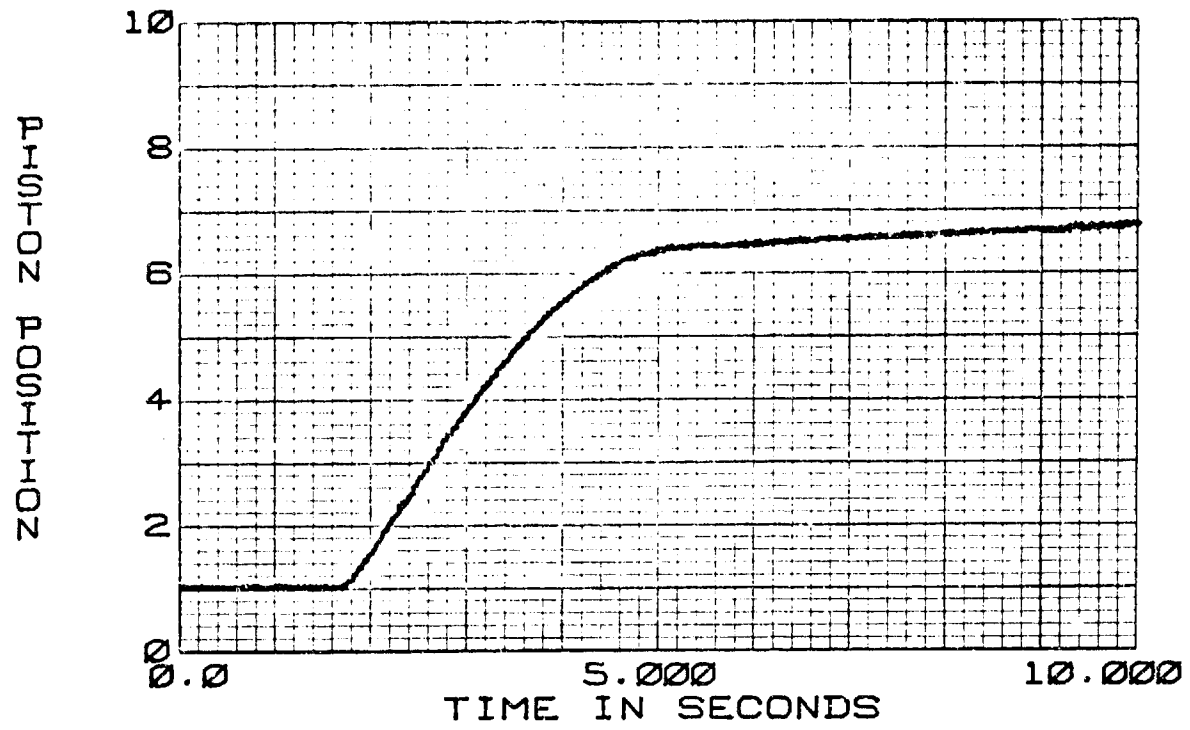

FIGURE 406. ACCUMULATOR ACC-3P
PISTON POSITION
75°F CHARGE

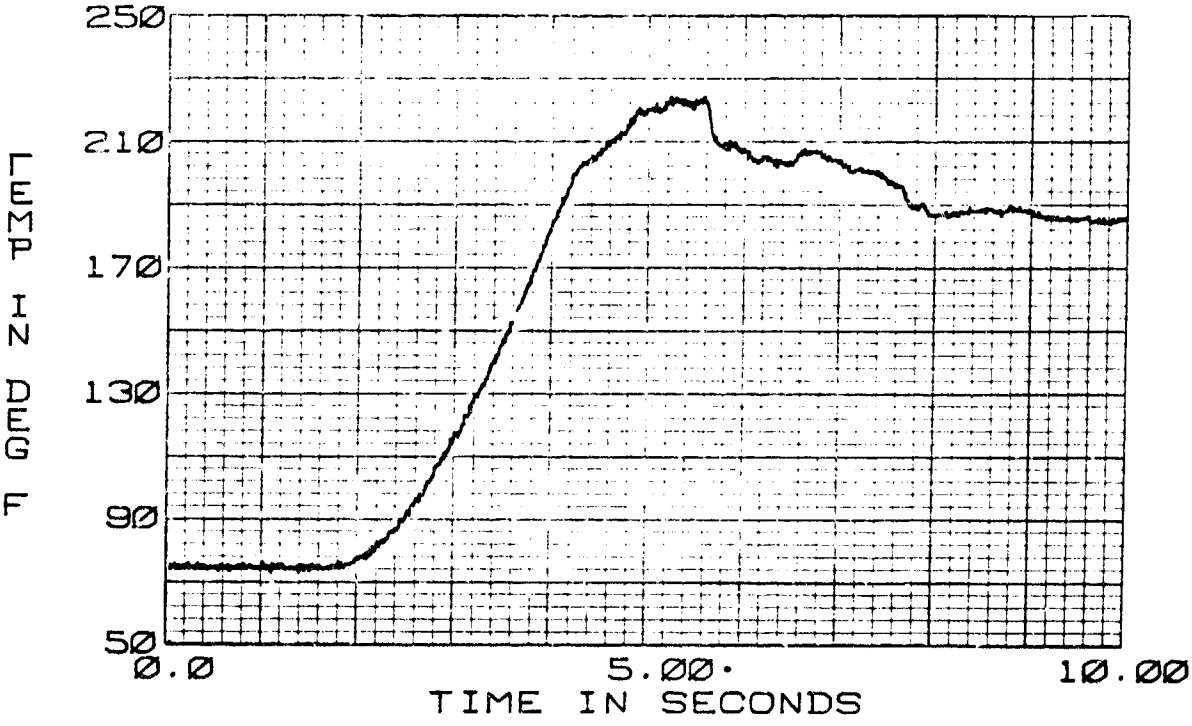

FIGURE 407. ACCUMULATOR ACC-3T
GAS TEMPERATURE
75°F CHARGE

Gas pressures (P2) were taken from Figure 405. Volumes were calculated from the change in piston position from Figure 406. A plot of n versus the time from the start of the transient is shown in Figure 408.

Calculated values of n for a 1 second charge up are shown in Figure 409 (Run 13). The computed value of n is slightly higher than the ideal gas value of 1.4 for an adiabatic process.

Run number 4 was a 5 second discharge transient. Results are shown in Figures 410 through 413. A plot of n vs time is contained in Figure 414, which also shows the specific heat ratio computed from pressure-temperature and volume-temperature relationships. Although the temperature probe response was relatively good the T - P and V - T values of n exhibit a different characteristic than the P - V values. The curves intersect at a value of n = 1.276 and a time of 2.58 seconds. The intersection indicates that the temperature probe provided an accurate reading of gas average temperature at this condition. The T - P and V - T values are lower initially. This occurs because of the time lag needed for the mass of the thermocouple to react to the rapid drop in the gas temperature at the probe, i.e. indicated temperature is higher than the average. After 2.58 seconds, the thermocouple output is still lagging local gas temperature, however, the gas is now receiving significant heat from the accumulator walls. The net effect is that the probe temperature is below the average gas temperature after 2.58 seconds.

The P - V relationship should be used in the computation of the ratio of the specific heats since the measurement of these parameters does not entail a significant response characteristic.

Figure 415 is a plot of the ratio of specific heats versus time for run number 6, a 31 second discharge transient. Heat transfer from the accumulator wall to the gas produces an average process value less than that for an isothermal process (n = 1).

Figure 416 shows values computed for a rapid discharge (2 seconds). Average specific heat ratios are well above the adiabatic ideal gas value of 1.4.

Discharge characteristics of the F-15 JFS accumulator are summarized in Figure 417. Average specific heat ratio is plotted vs total discharge time. Average specific heat ratio is based on end state conditions at the start of the transient and at the end when the accumulator is empty (bottomed on the

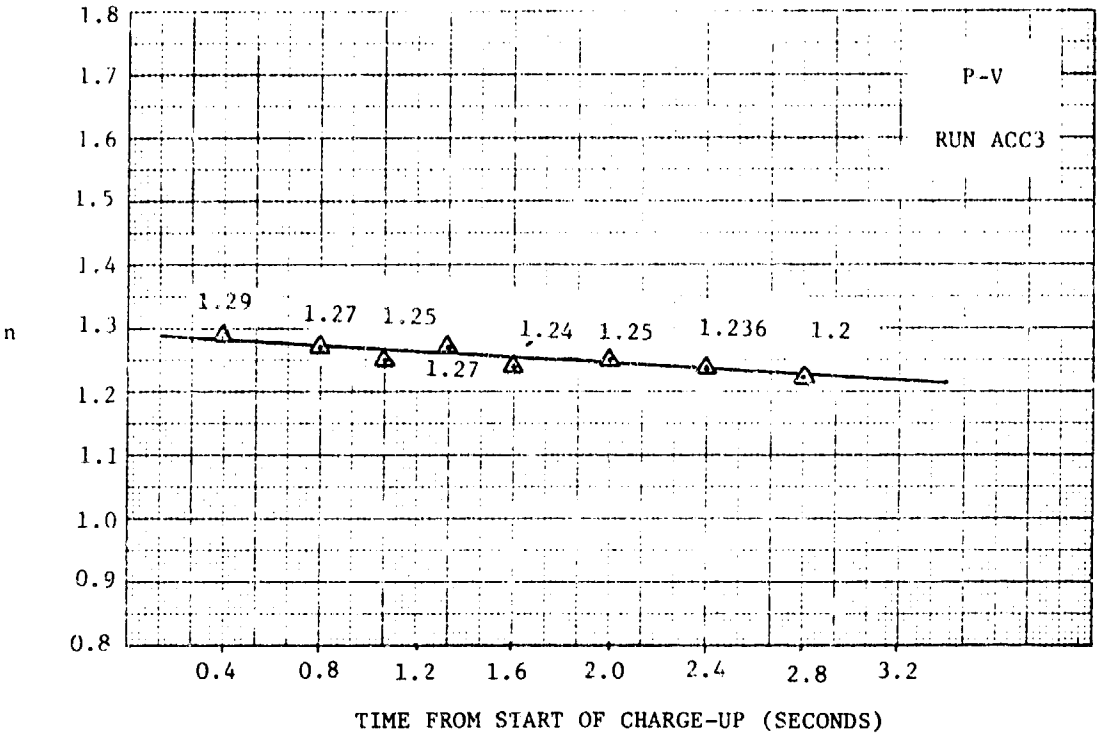

FIGURE 408. F-15 JFS ACCUMULATOR POLYTROPIC SPECIFIC HEAT RATIO (n) VS. TIME FROM START OF CHARGE-UP

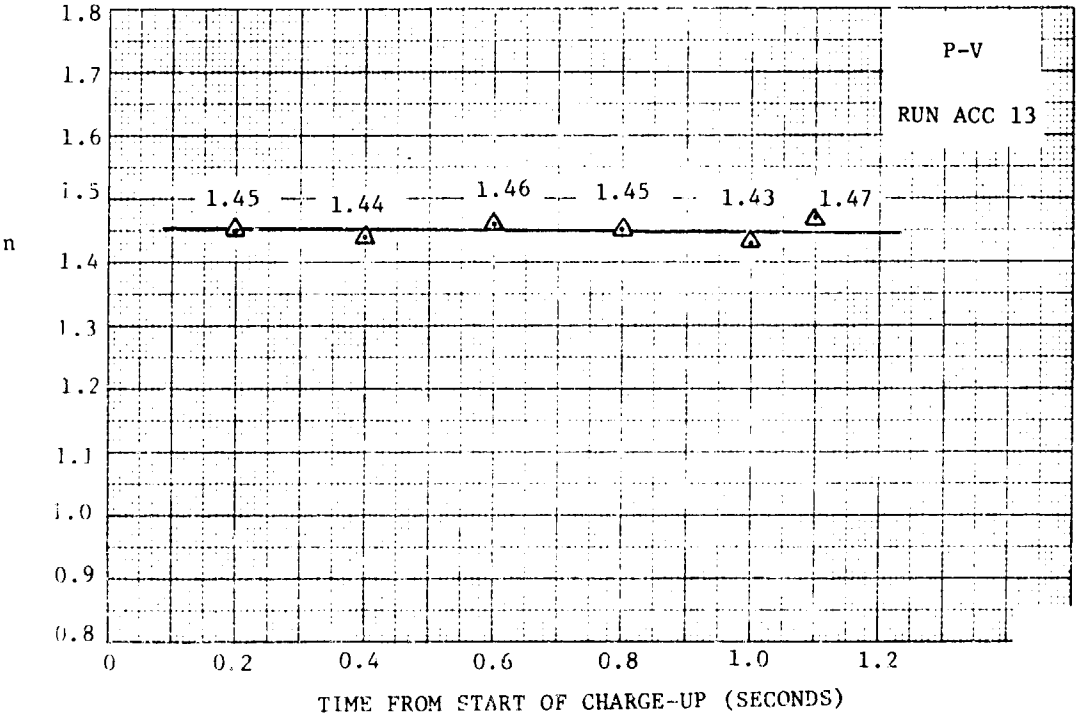

FIGURE 409. F-15 JFS ACCUMULATOR POLYTROPIC SPECIFIC HEAT RATIO (n) VS. TIME FROM START OF CHARGE-UP

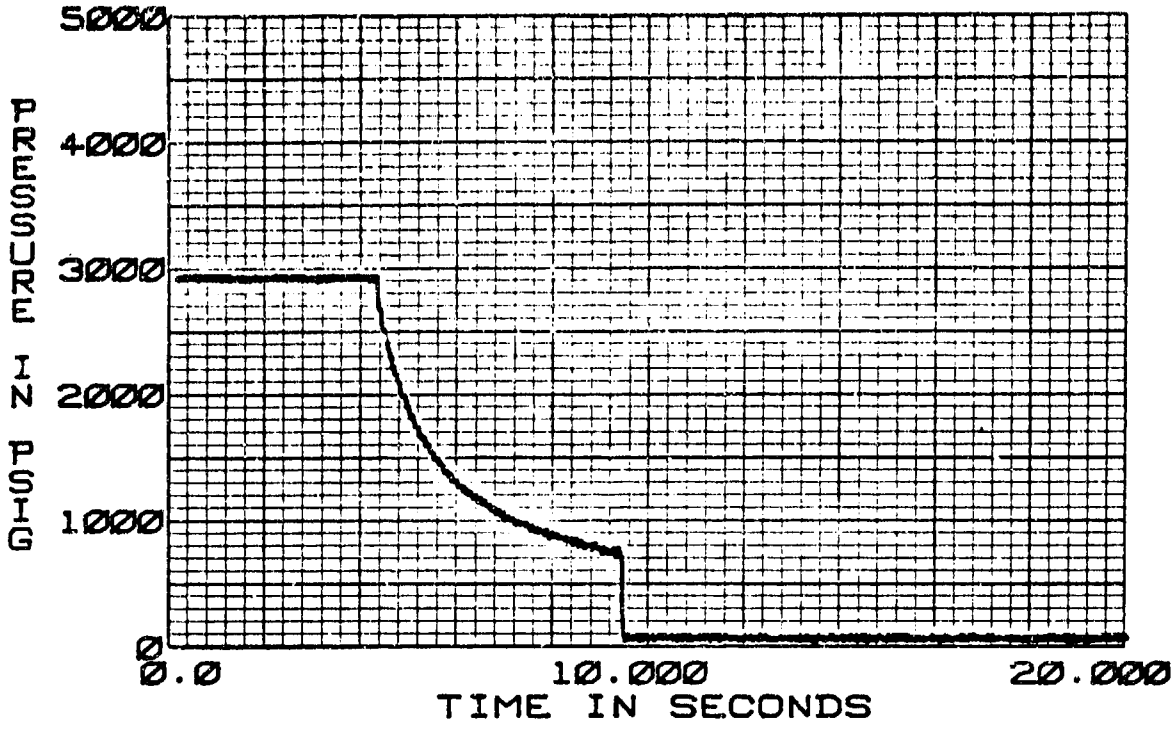

FIGURE 410. ACCUMULATOR ACC-4P1
P1 OIL PRESSURE
75°F DISCHARGE

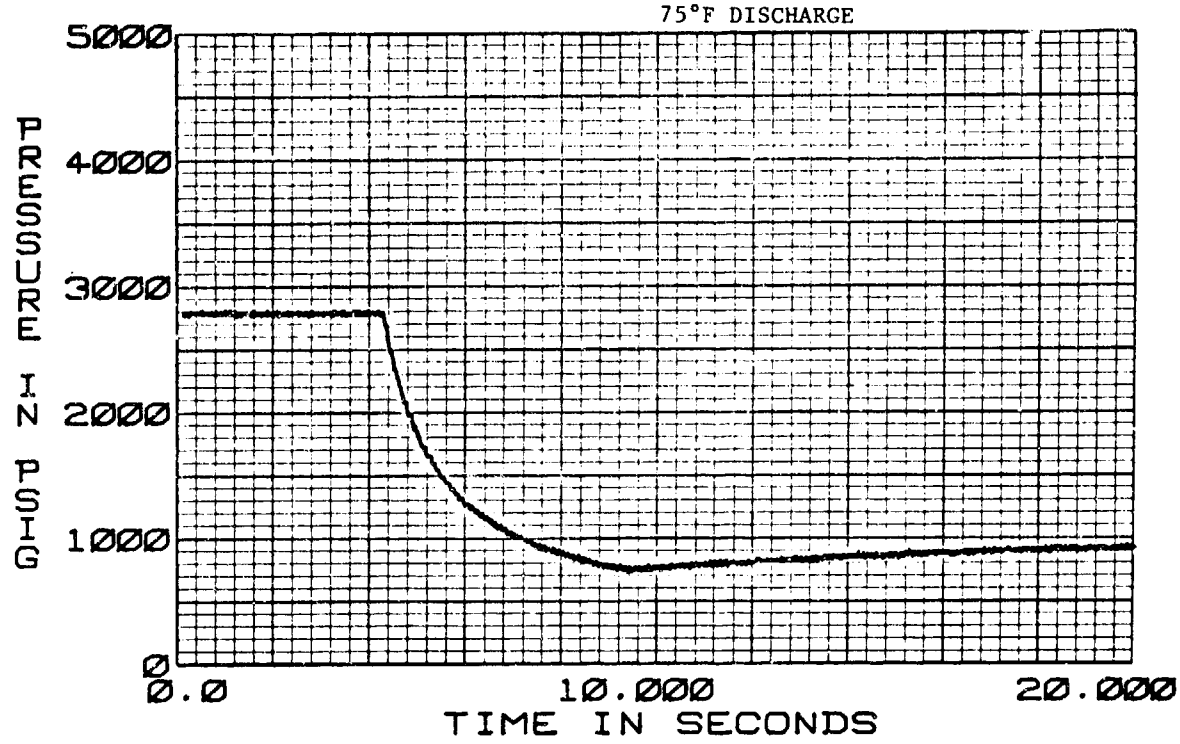

FIGURE 411. ACCUMULATOR ACC-4P2
P2 GAS PRESSURE
75°F DISCHARGE

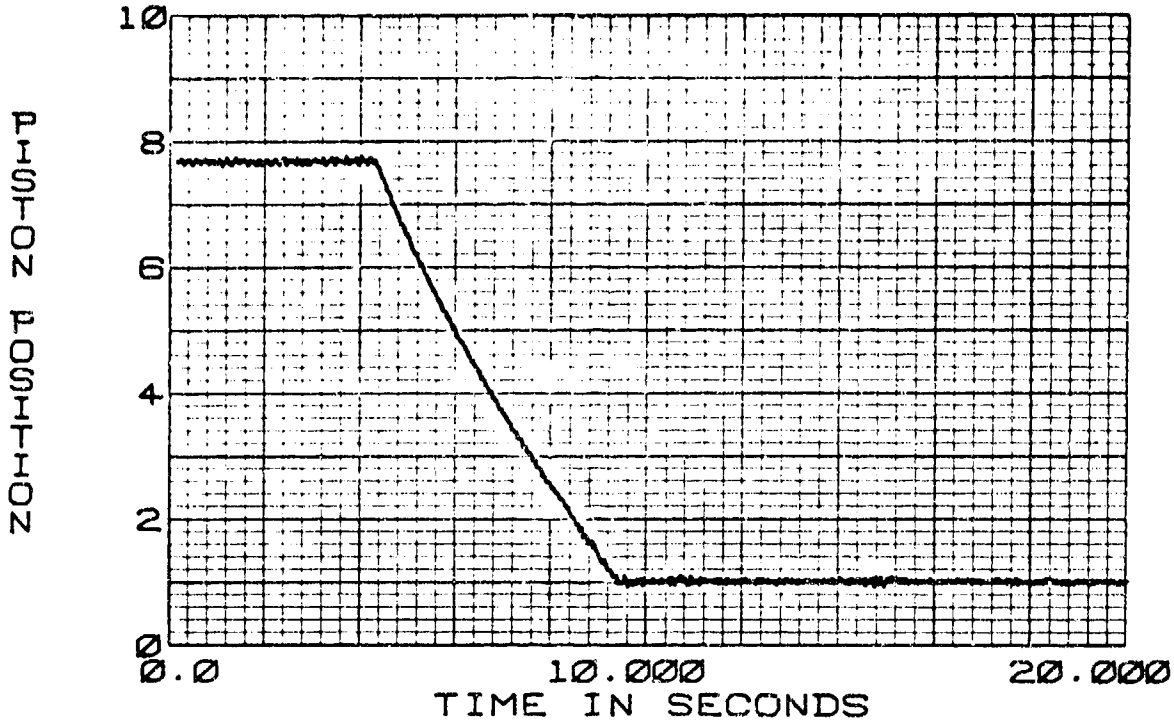

FIGURE 412. ACCUMULATOR ACC 4P
P PISTON POSITION
75°F DISCHARGE

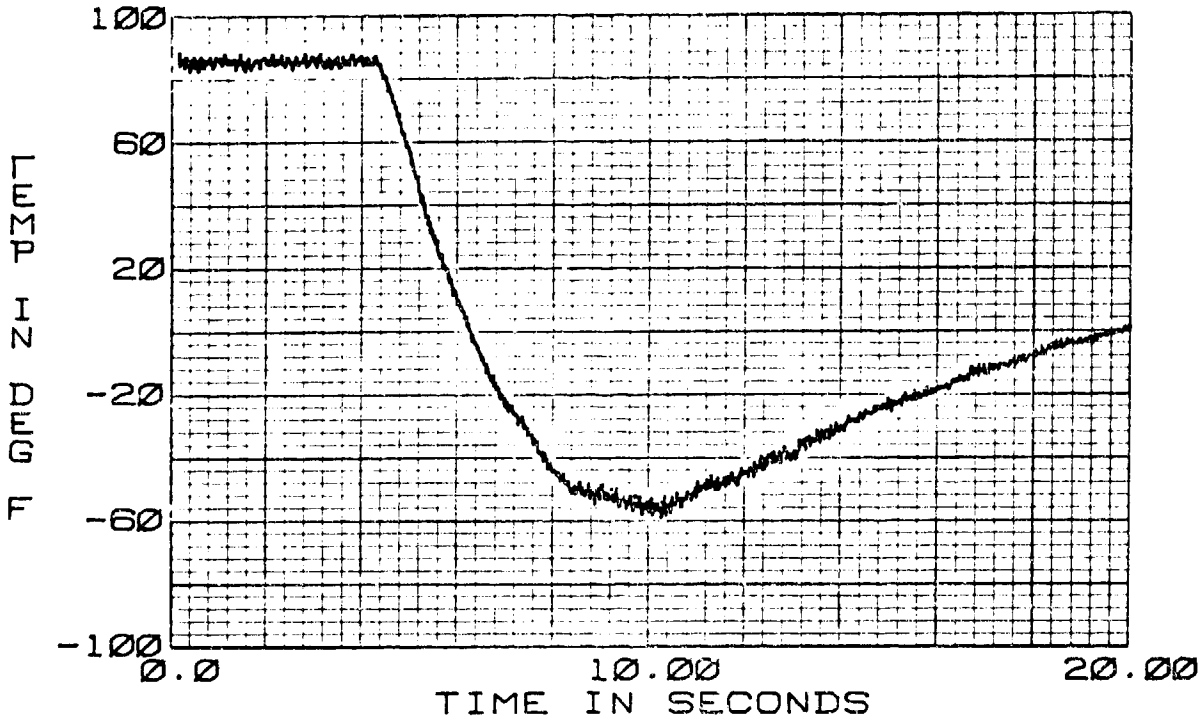

FIGURE 413. ACCUMULATOR ACC 4T
T GAS TEMPERATURE
75°F CHARGE

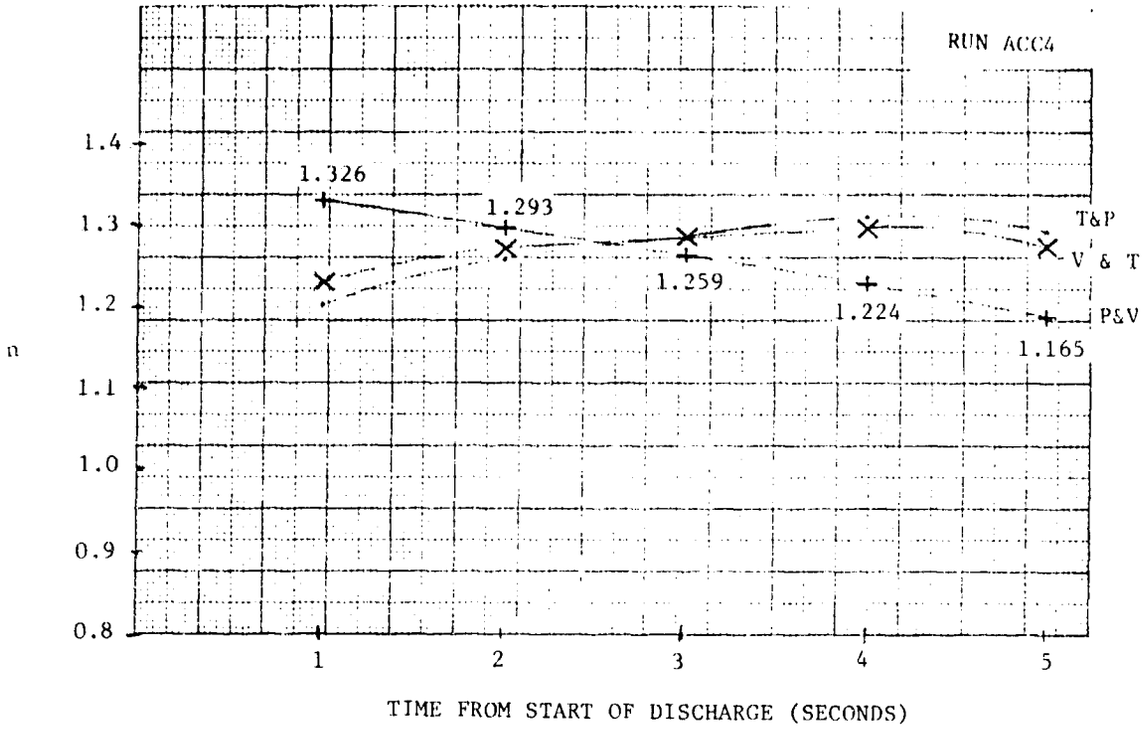

FIGURE 414. F-15 JFS ACCUMULATOR POLYTROPIC SPECIFIC HEAT RATIO (n) VS. TIME FROM START OF DISCHARGE

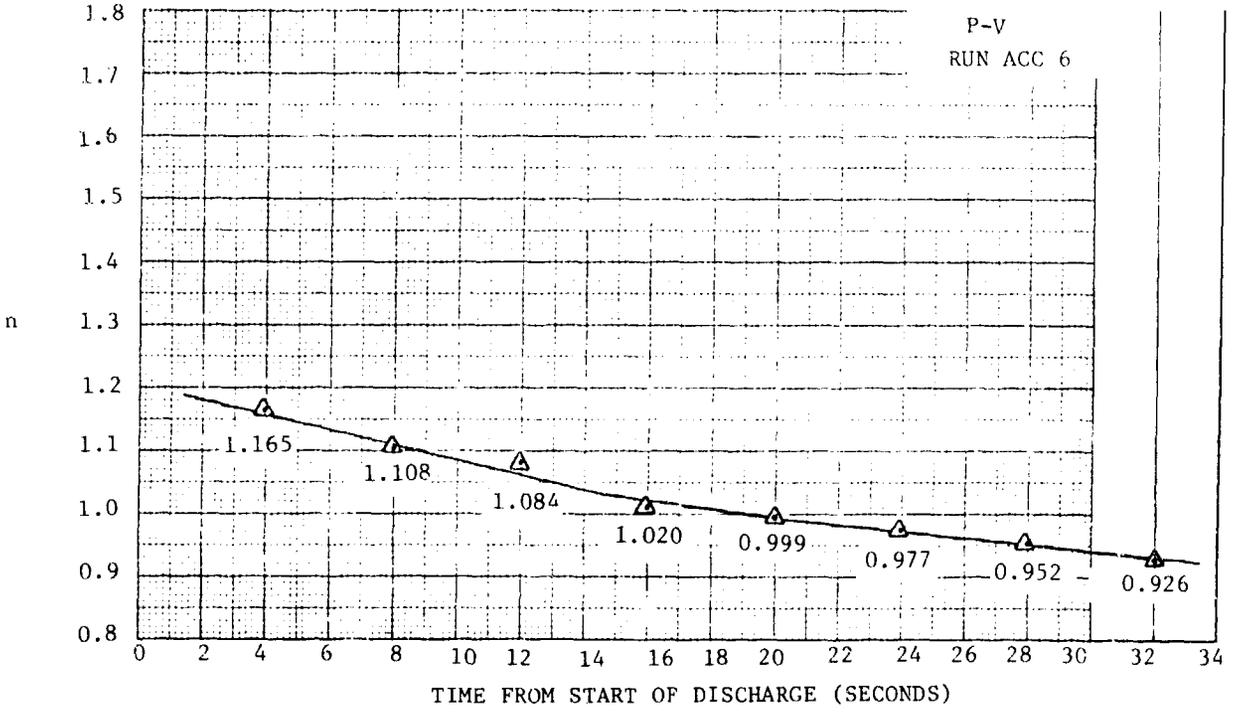

FIGURE 415. F-15 JFS ACCUMULATOR POLYTROPIC SPECIFIC HEAT RATIO (n) VS. TIME FROM START OF DISCHARGE

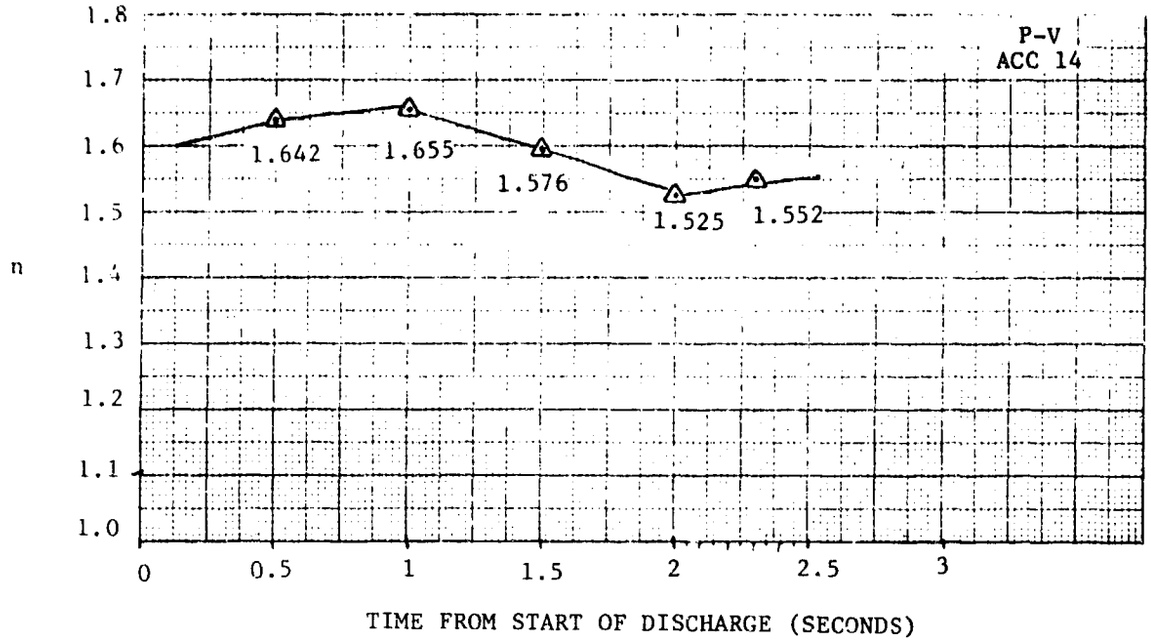

FIGURE 416. F-15 JFS ACCUMULATOR POLYTROPIC SPECIFIC HEAT RATIO (n) VS. TIME FROM START OF DISCHARGE

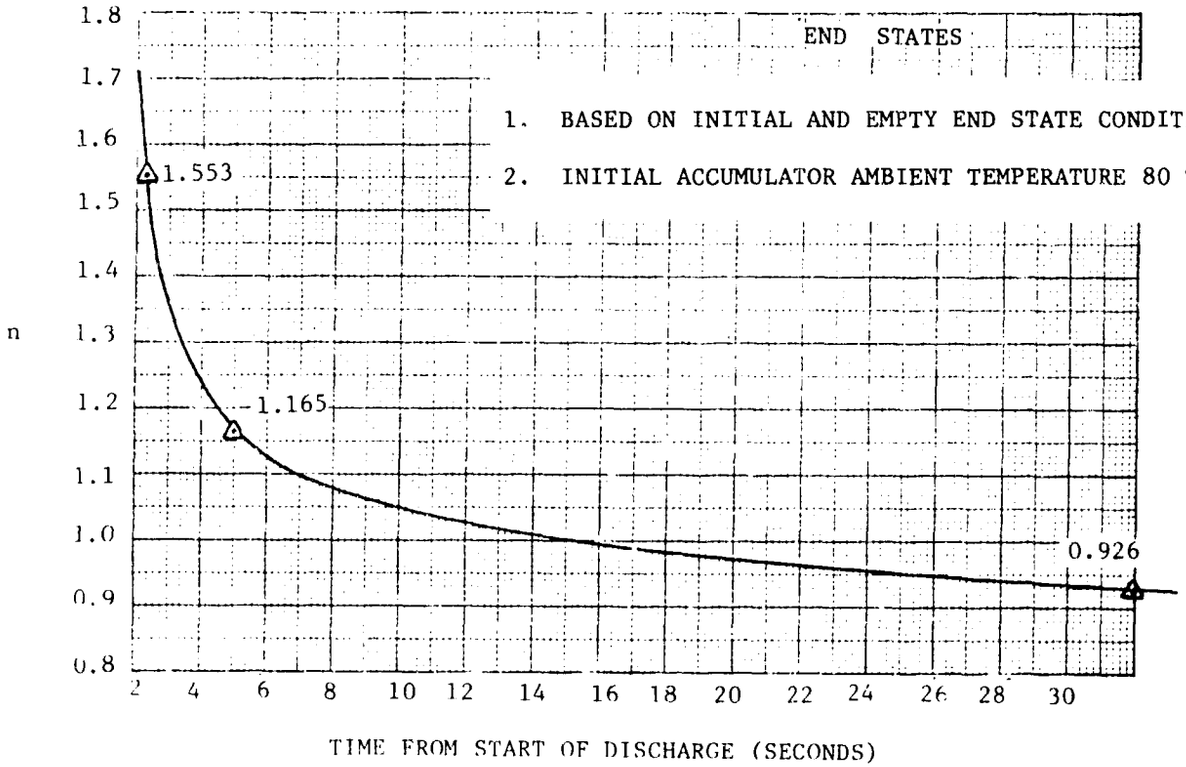

FIGURE 417. F-15 JFS ACCUMULATOR POLYTROPIC SPECIFIC HEAT RATIO (n) VS. TIME FROM START OF DISCHARGE

oil side). This plot provides good design values for sizing accumulators. A family of these curves exists for various initial JFS accumulator temperatures. Design values greater than 1.6 may be required for low initial temperatures.

a. Conclusions - The range of specific heat ratio during accumulator discharge (and charge) varies widely depending on the duration of the transient.

Discharge of the F-15 JFS accumulator from an initial shop ambient temperature condition produced the following specific heat (n) values for various discharge times.

Total Discharge Time (Sec)	Range of Specific Heat Ratio (GN_2) During Discharge
2.3	1.65 to 1.52
5.0	1.32 to 1.16
32.0	1.16 to .926

Higher specific heat ratios would be obtained for lower inital temperatures particularly for the longer discharge time. A specific heat ratio for sizing an accumulator should be chosen for the maximum discharge rate and lowest initial temperature expected in the applicable system.

Computer simulations which model rapid changes in accumulator pressure should use a high specific heat ratio, 1.4 to 1.6. The present HSFR program uses 1.4. The HYTRAN program accumulator model currently uses a specific heat ratio of 1.0, making no attempt to model the wide range of specific heat ratios possible for transient calculations. A constant specific heat ratio should be selected and used in the HYTRAN gas accumulator model to suit the type of application being analyzed. Choosing a good design value for specific heat is a significant factor when sizing 3000 psig accumulators such as those used in hydraulic start systems for engine start and auxiliary power systems. It will be even more important for sizing accumulators in high pressure (8000 psig) systems.

SECTION VI

STEADY STATE VERIFICATION TESTS

The essential components test plan originally contained a large variety of component types and sizes that were typical in aircraft hydraulic systems. Testing and model development of these elements was considered necessary before any meaningful pump/system verification could occur. Steady state tests were generally required on each test specimen. At least one specimen in each basic component group was tested to determine if further steady state tests were required. It was determined that the basic steady state data on line, unions, fittings, etc. were not necessary for proper model verification of the higher priority test specimens. Consequently the test plan was modified to define the minimum number of essential components types and sizes necessary to permit accurate modelings of all similar system essential components. Steady state test results for the essential test conditions are presented along with results from the supplemental test plan series. The steady state pump test results are also included.

1. ESSENTIAL COMPONENT TEST DATA

Table 22 contains a listing of the steady state data taken for the essential component test series. Figure 418 is a graph of flow vs ΔP for a 30 ft 1/4" x .020" stainless steel tube at 125°F. At 10 CIS the measured pressure drop is about 235 psi. The Reynolds number for this condition may be computed as

$$RE = \frac{Q}{\nu d} \tag{1}$$

where

ν = Fluid viscosity (in^2/sec)

d = Line I.D. (in)

Q = Flow rate (in^3/sec)

at 125°F

$$RE = \frac{10}{(.0198)(.21)} = 2400$$

Assuming a 1200 Reynolds transition point the flow is turbulent. The computed pressure drop in the line can then be found using the Darcy-Weisbach equation with a turbulent friction factor ($f = .316/RE^{.25}$)

$$\Delta P = .241 \quad \frac{\rho \nu^{.25} l Q^{1.75}}{d^{4.75}} \tag{2}$$

TABLE 22

ESSENTIAL COMPONENT STEADY STATE TESTS

Test Specimen	Temperature (Deg F)	Figure Number(s)
30 Ft, 1/4" x .020 304 S.S. Tube	125, 210	418, 419
30 Ft, 1/2" x .028 304 S.S. Tube	125, 210	420, 421
6 Ft, 1/2" x .028 304 S.S. Straight Tube	210	422
6 Ft, 1/2" x .028 304 S.S. Tube with 45° Bend	210	423
6 Ft, 1/2" x .028 304 S.S. Tube with 90° Bend	125	424
6 Ft., 1/2" x .028 304 S.S. Tube with Two 90° Bends	125	425
AN815-8J Union Drilled DU7 To = .444" I.D.	125, 210	426, 427
AN821-8J 90° Elbow	210	428
7M43-8D Nipple	125, 210	429, 430
AN824-8J Tee on the Side	125	431
AN824-8J Tee on the Run	125, 210	432, 433
ST7M229T8 Dynatube Nipple	125, 210	434, 435
ST7M203T8 Dynatube 90° Elbow	125, 210	436, 437
F4 PC Filter Housing (AC-900-6101)	125	438
F4 PC Filter with Element	125	439
Victor Solenoid Valve SV305-9053	125	440

substituting the appropriate conditions at 125°

$$\rho = .814 \text{ E-4 } \frac{\text{lb/sec}^2}{\text{in}^4}$$

$$\nu = .0198 \text{ in}^2/\text{sec} \quad \text{(Viscosity)}$$

$$l = 350 \text{ in}$$

$$Q = 10 \text{ in}^3/\text{sec}$$

$$d = .21 \text{ in}$$

$$\Delta P = 246 \text{ psi}$$

The pressure drop is 11 psi higher than the measured data giving an error of about 5% in the measurement. The same specimen at 210°F is shown in Figure 419.

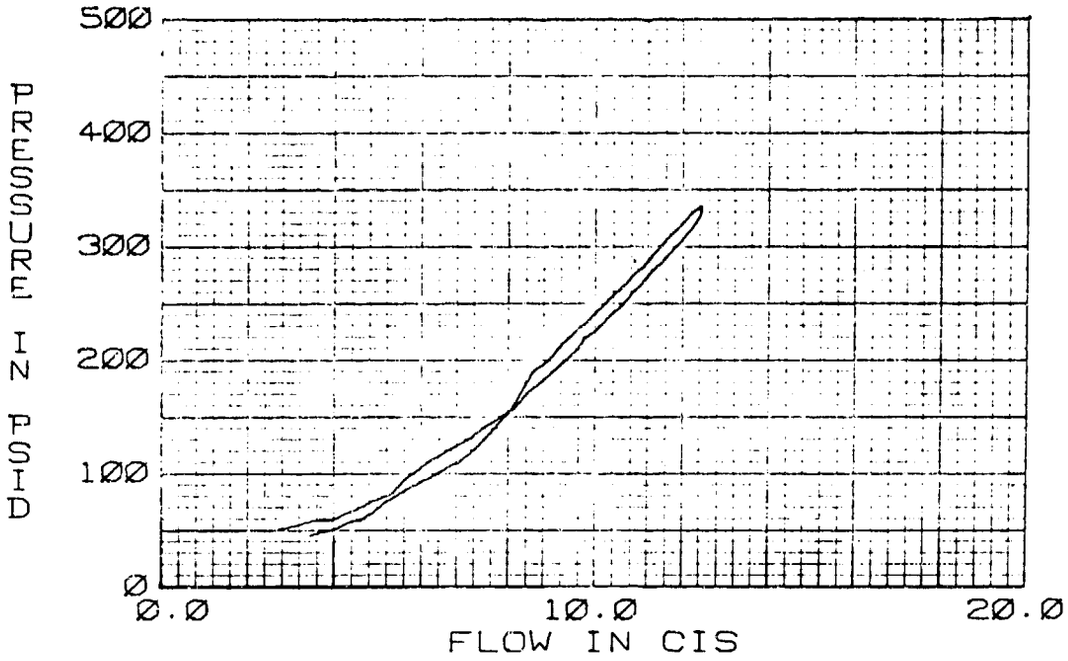

FIGURE 418 30 FT. 1/4 X .020 WALL 304 SS TUBE, 125°F

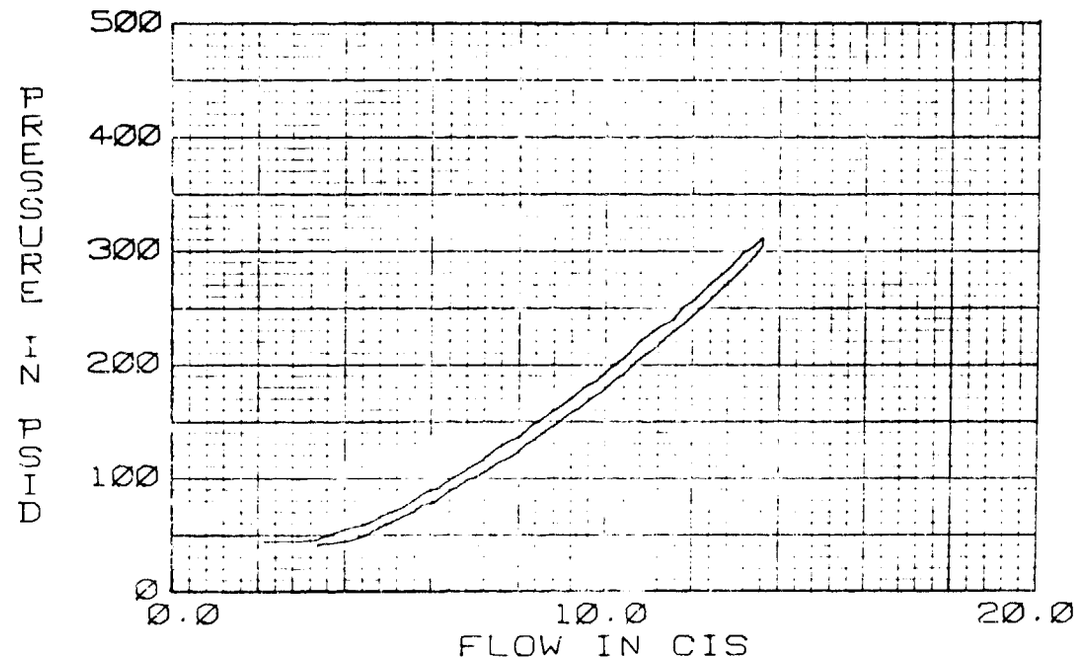

FIGURE 419 30 FT. 1/4 X .020 WALL 304 SS TUBE, 210°F

Flow vs. pressure drop for a 1/2" dia x .028 S.S. 30' tube is shown in Figures 420 and 421 respectively. The anamoly between 27 and 33 CIS results from mechanical vibration in the line system. The turbine flowmeter used in the test circuit was not loaded adequately to reject these mechanical signals generated between 27 and 33 CIS. Projecting a line through the data as shown in Figure 420 and 421 gives a good indication of the flow pressure drop characteristics of the line through this flow region. At 30 CIS in Figure 420 the computed ΔP using equation (2) is 48 psi. This compares to a projected measured value of 44 PSI.

At 5 CIS and 125°F the Reynolds number is

$$Re = \frac{5}{(.0198)(.444)} = 567$$

Using the Darcy-Weisbach formulation with a laminar flow friction factor ($f = 64/R_e$) results in Equation (3).

$$\Delta P = \frac{128\rho\nu l Q}{\pi d^4} \qquad (3)$$

Substituting the condition at 125° into equation (3) yields

$$\Delta P = \frac{128(.0198)(.814E-4)(360)(5)}{\pi(.444)^4} = 3.04 \text{ psi}$$

From Figure 420 at 5 CIS the ΔP was measured to be 4 psi.

Figures 422 through 425 contain test data for a 6 foot tube with various number of bends.

The straight tube in Figure 422 gives a ΔP of 5 psi at 25 CIS. At the same temperature and flow in Figure 423 the ΔP is 6.2 psi. The data in Figures 424 and 425 appear to be in error because at 25 CIS the pressure drop is higher in the tube with one ninety degree bend than the tube with two ninety degree bends.

Figures 426 through 437 contain steady state pressure drops versus flows for various simple hydraulic components.

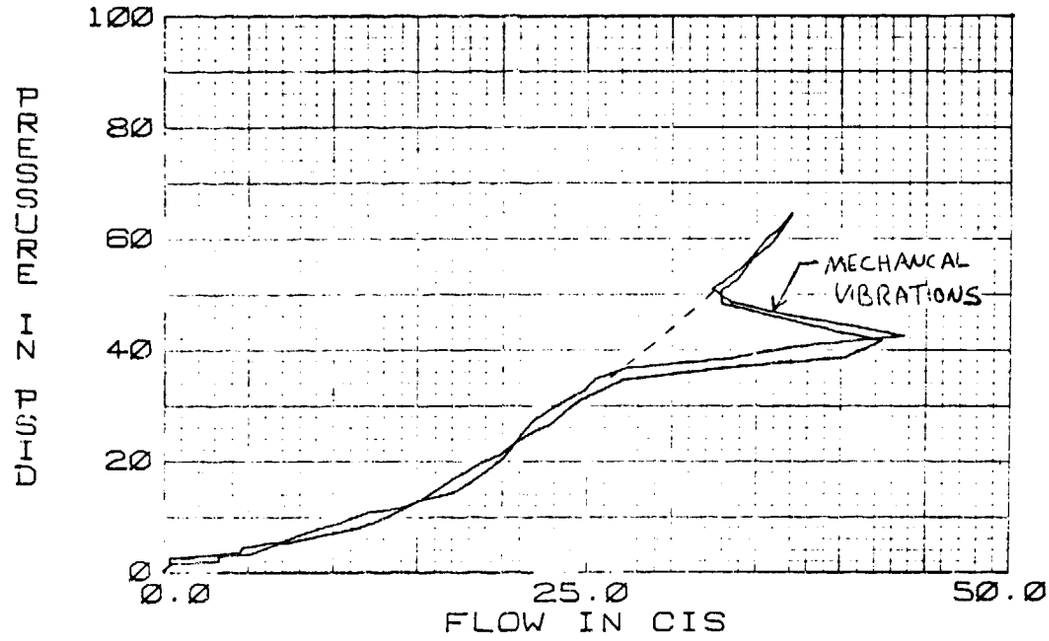

FIGURE 420 30 FT. 1/2 X .028 WALL 304 SS TUBE, SS, 1 125°F

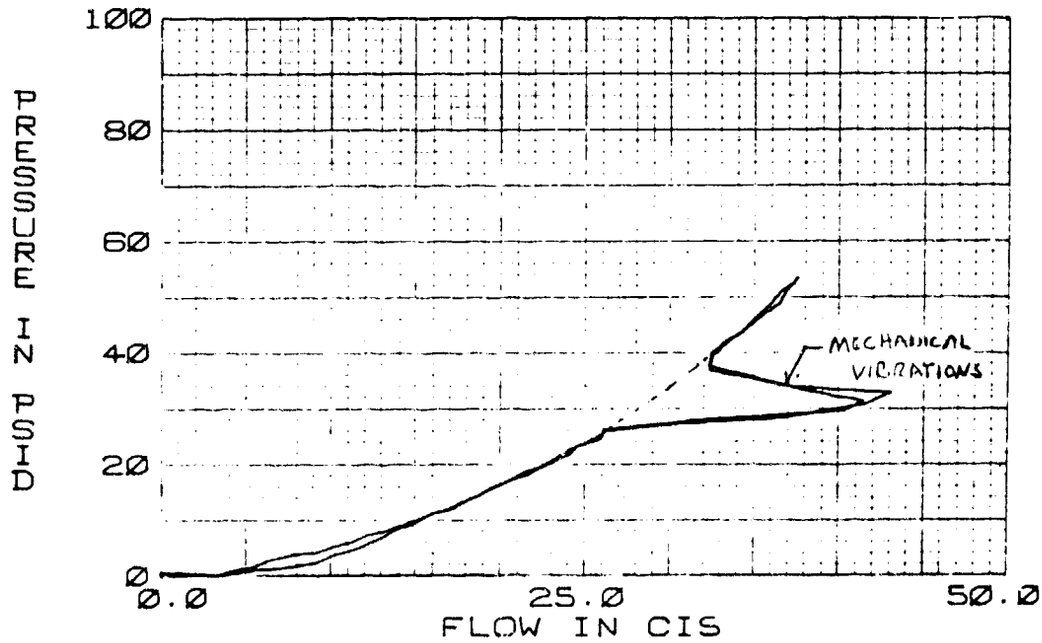

FIGURE 421 .5 IN. DIA X 30 FT. TUBE
FLOW DELTA P TEST
FL DP 210°F

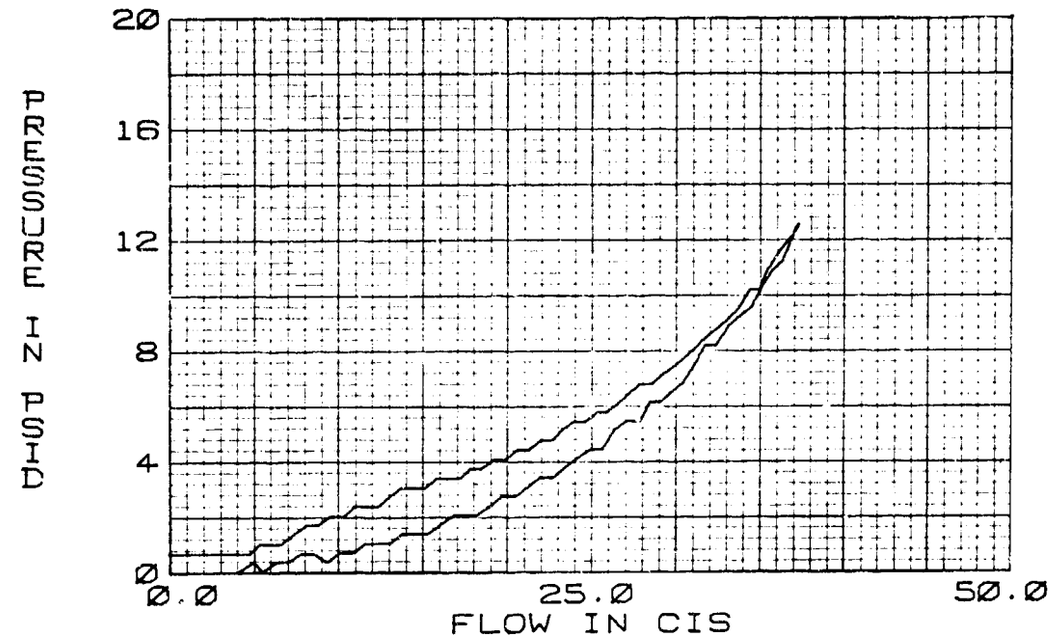

FIGURE 422 .5 IN DIA. 6 FT STRAIGHT TUBE
FLOW DELTA - P
FL DP 210°F

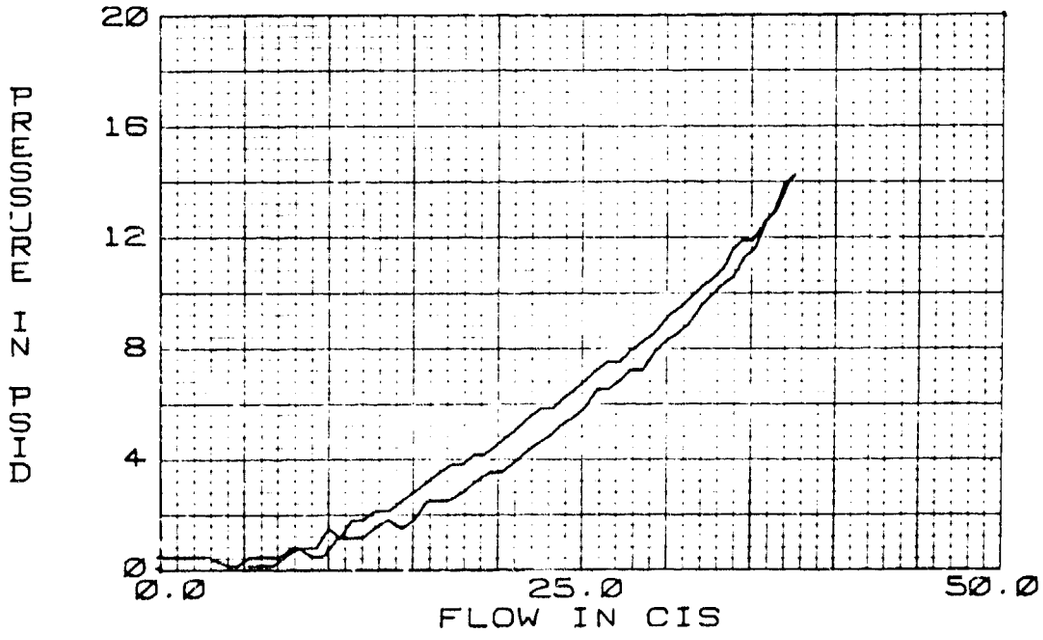

FIGURE 423 .5 IN DIA. TUBE X 6 FT. 45 DEG BEND
DELTA - P
FL DP 210°F

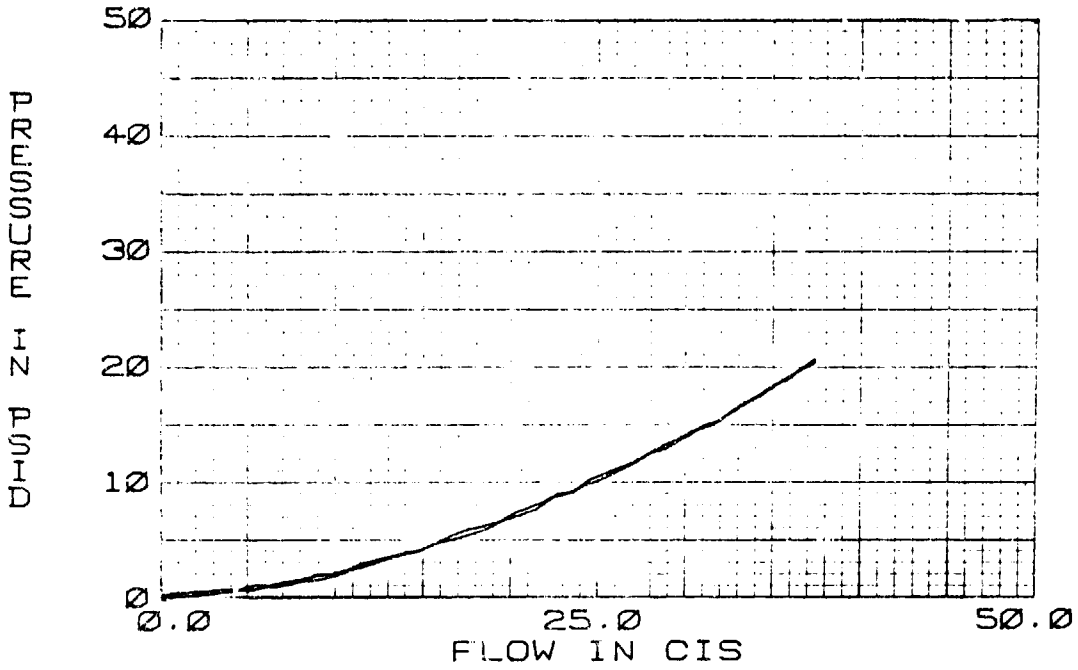

FIGURE 424 .500 IN DIA X 6 FT. TUBE WITH 90 DEG BEND
DP
FL DP 125°F

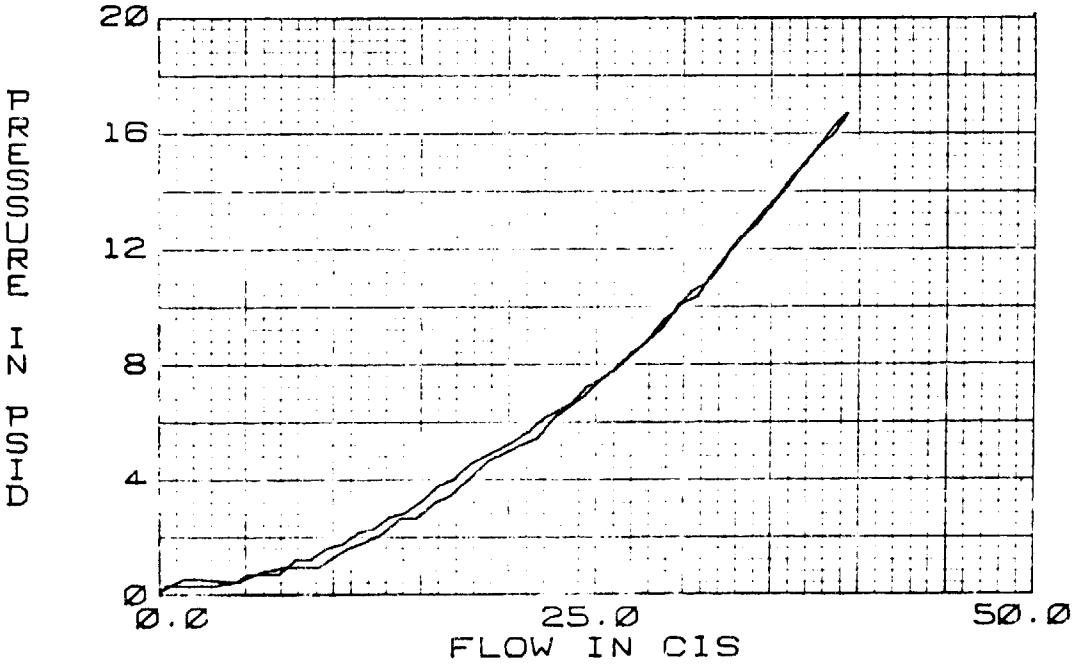

FIGURE 425 6 FT. TUBE WITH TWO 90 DEGREE BENDS
STEADY STATE
FL DP 125°F

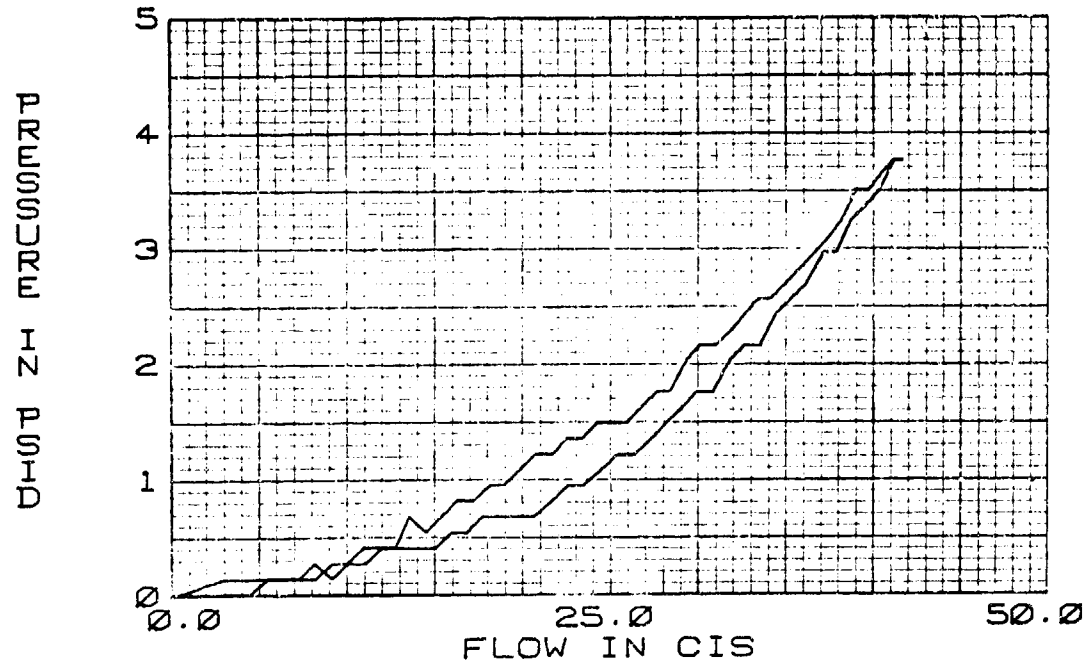

FIGURE 426 DRILLED OUT (.444 I.D.) AN815-8J UNION
30-03
FL DP 125

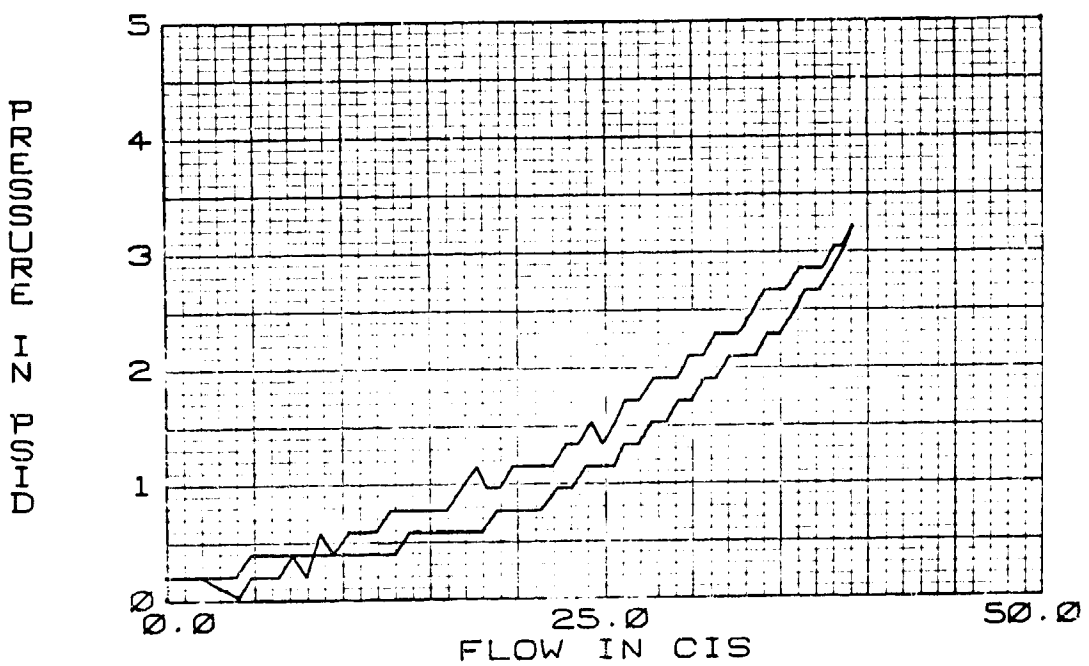

FIGURE 427 DRILLED OUT AN815-8J UNION
FLOW DELTA P
FL DP 210°F

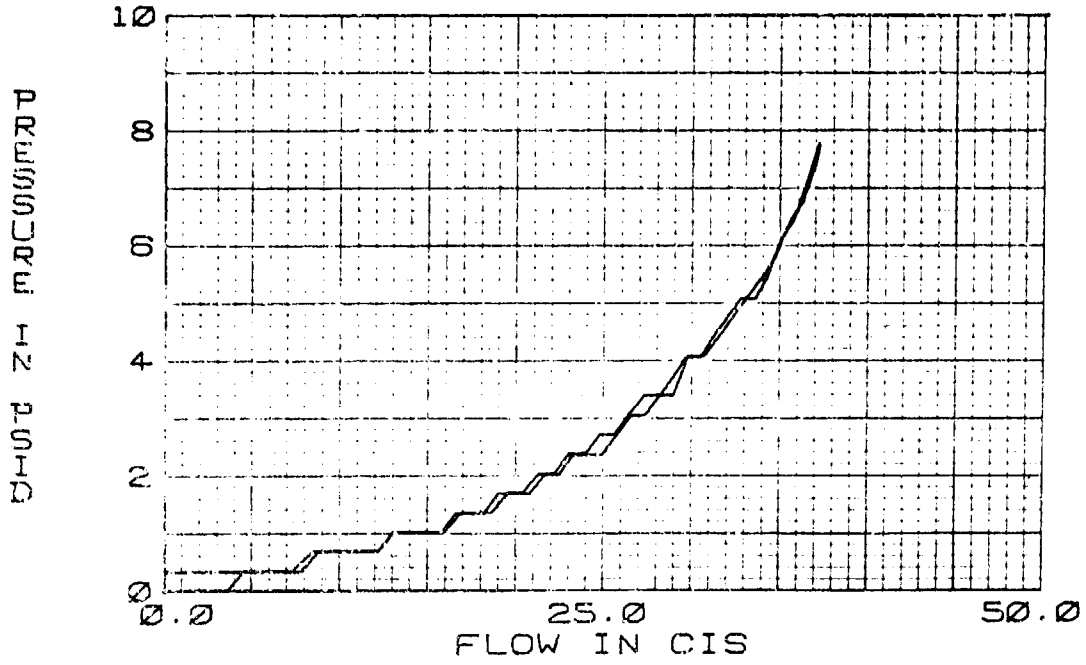

FIGURE 428 AN821-8J ELBOW
FLOW DELTA - P
210°F

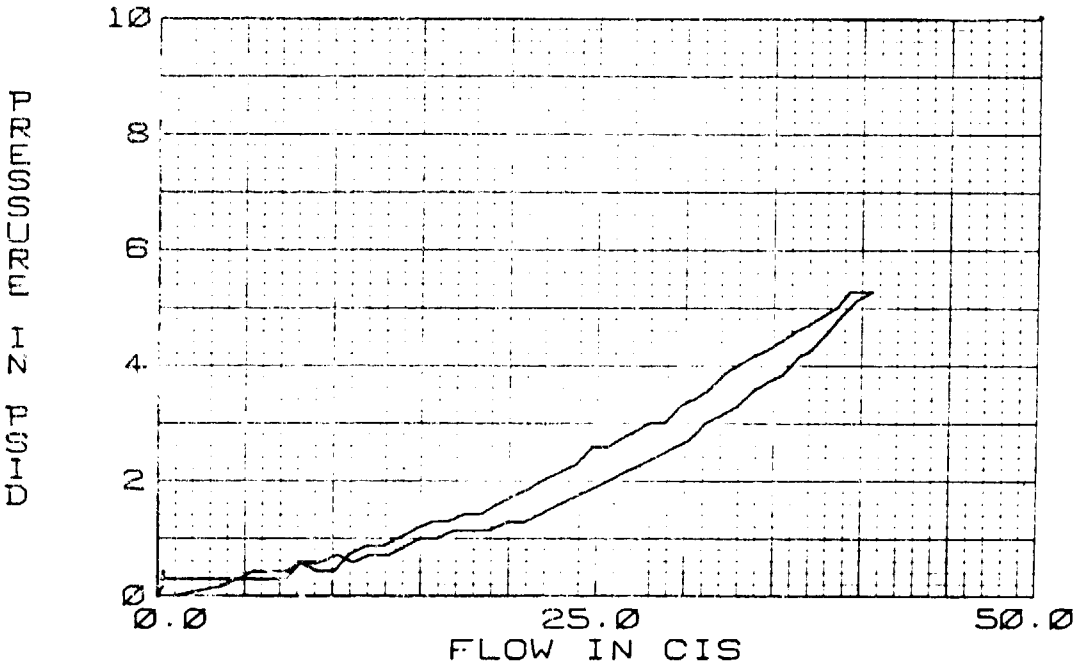

FIGURE 429 7M43-8D NIPPLE
32-03
FL DP 125°F

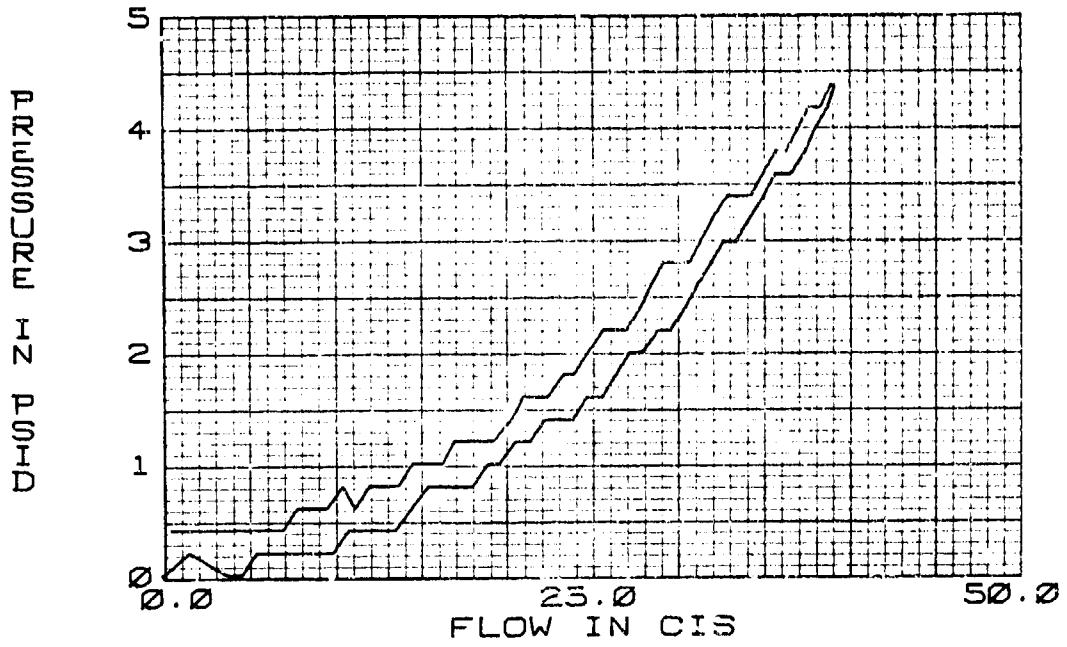

FIGURE 430 7M43-8D NIPPLE
FLOW DELTA P
FL DP 210°F

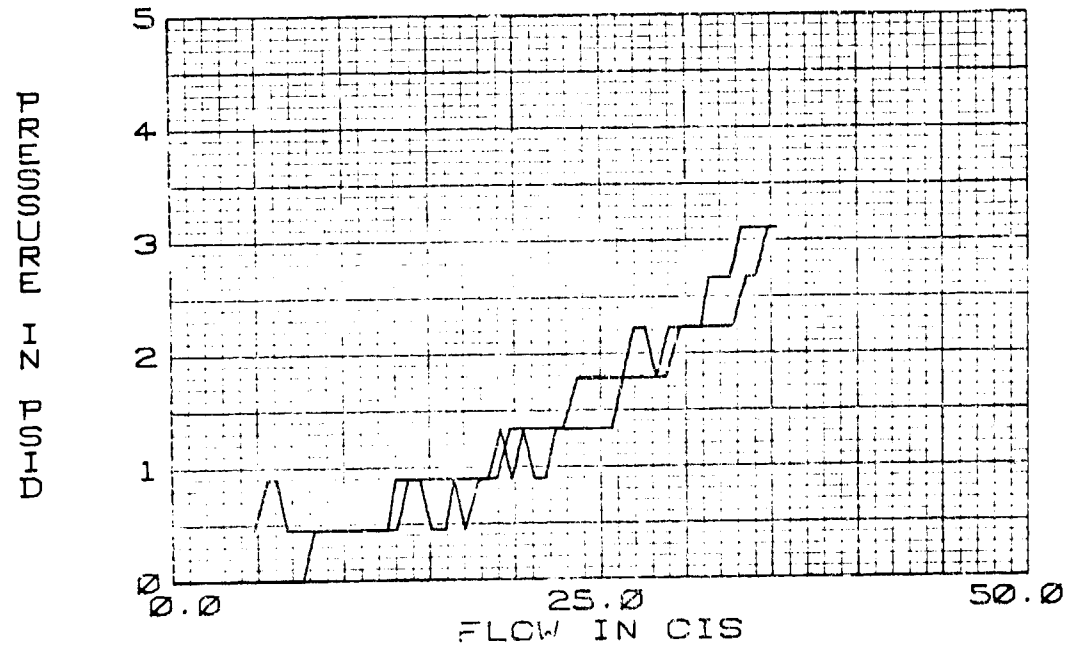

FIGURE 431 AN824-8J (TEE ON SIDE)
FLOW - DELTA P
125°F

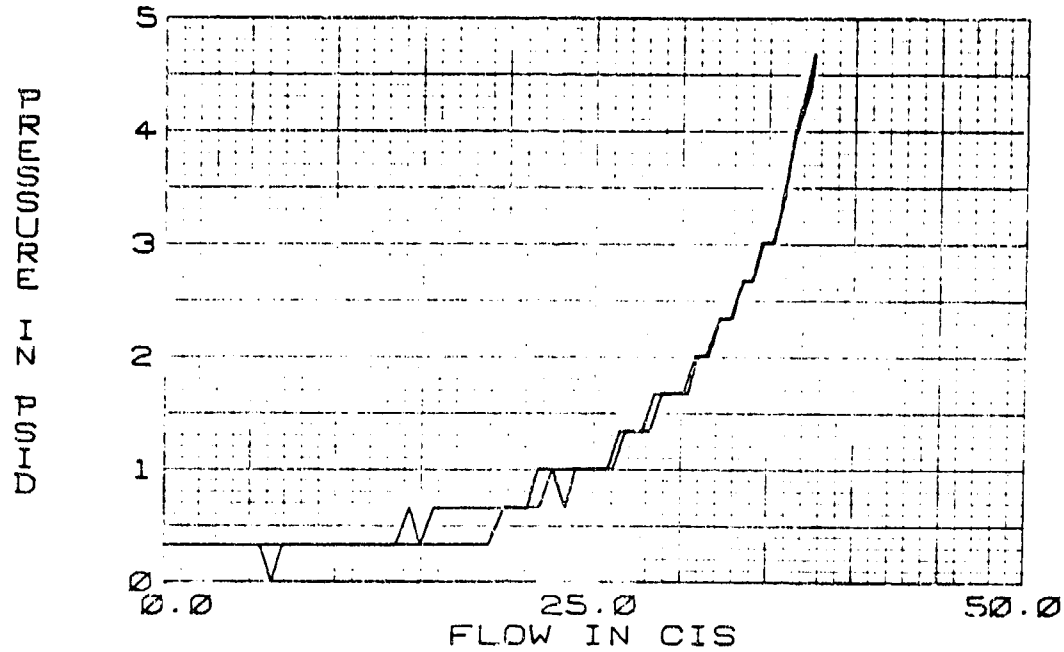

FIGURE 432 AN824-8J (TEE ON RUN)
125°F

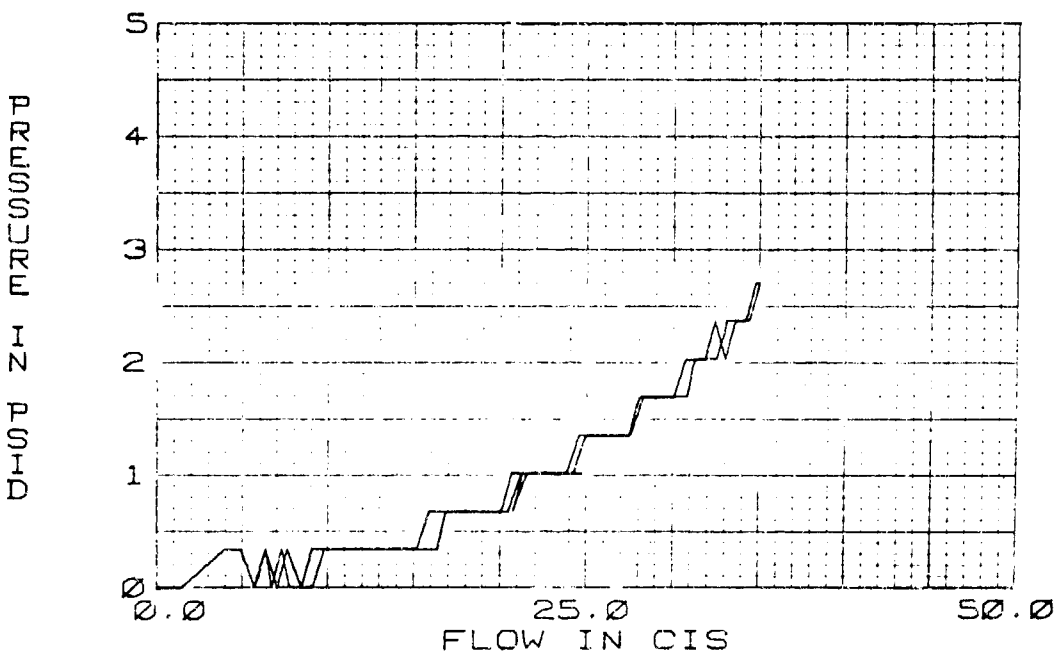

FIGURE 433 AN824-8J (TEE ON RUN)
FLOW DELTA - P TEST
FL DP 210°F

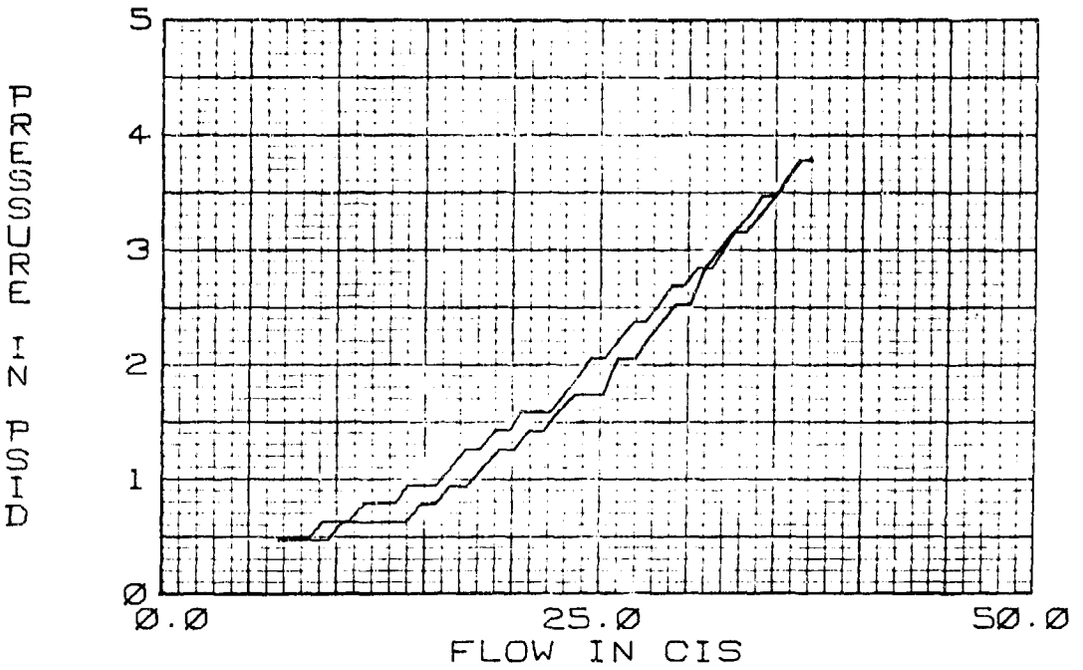

FIGURE 434 ST7M229T8 DYNATUBE NIPPLE
125°F

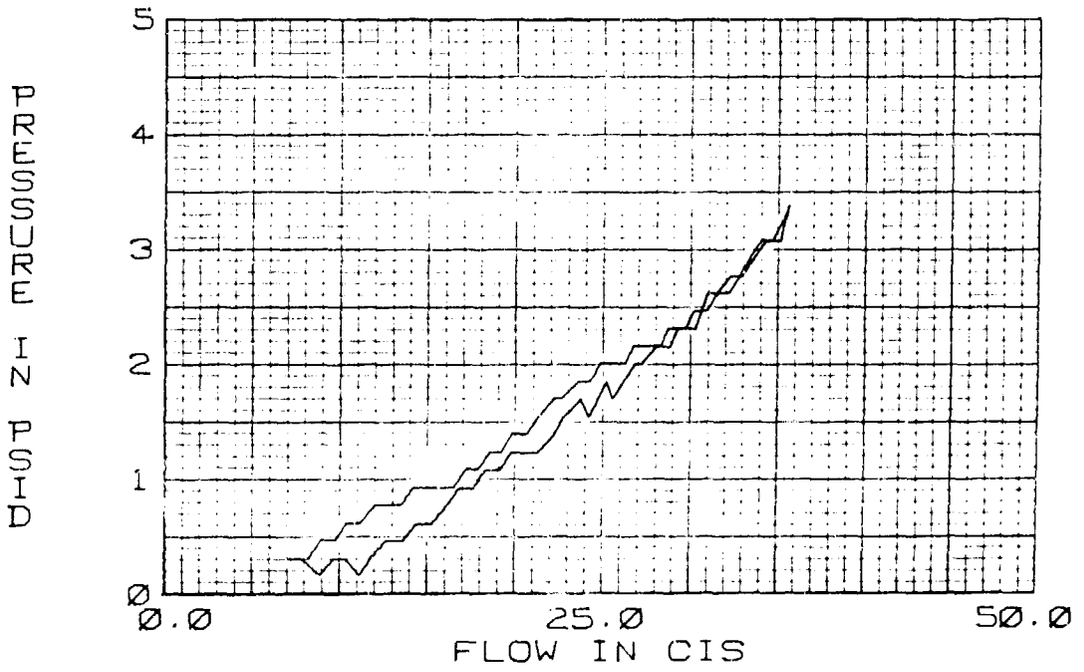

FIGURE 435 ST7M229T8 DYNATUBE NIPPLE
210°F

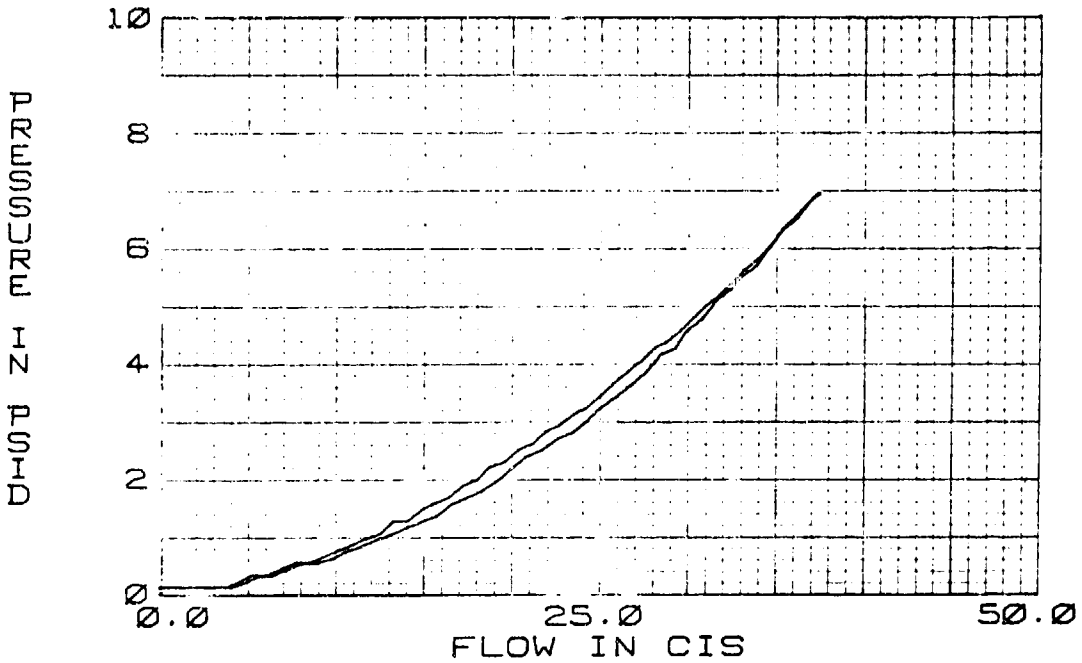

FIGURE 436 ST7M203T8 DYNATUBE (90° ELBOW)
FLOW DELTA P
FL DP 125°F

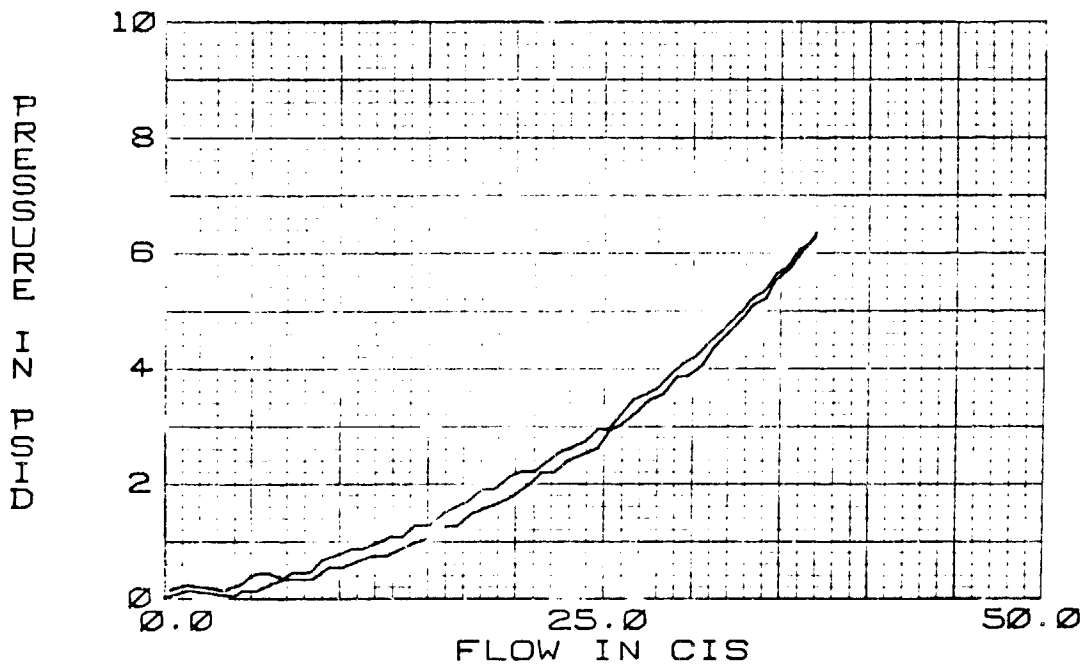

FIGURE 437 90° ELBOW
FLOW DELTA P
FL DP 210°F

The laminar and turbulent flow coefficients for the filter were determined experimentally from flow-pressure drop data. The data taken using MIL-H-5606B hydraulic oil at 125° and an inlet pressure of 3000 PSI resulted in the graphs of Figures 438 and 439. Figure 438 contains the steady state flow vs pressure drop data for the F-4 PC Filter Housing, and Figure 439 contains the data for the same component with a filter element. The coefficients were determined at 125°F and corrected to 100°F.

A value of 12 CIS was assumed to determine the laminar flow constant for the filter housing in Fugure 438. At 12 CIS the ΔP is approximately 6 PSI. The constant for laminar flow is determined from the relation

$$\Delta P = KQ \tag{4}$$

where $\Delta P = 6$ PSI

$Q = 12$ CIS

Thus K in the above equation is .5 at 125°F. The HYTRAN program specifies that K be determined at 100°F and 3000 PSI. Since the test was performed at 125°F, the K coefficient must be corrected. This may easily be accomplished by a direct ratio of viscosities and densities at the appropriate temperatures as given below:

$$K_{100} = \frac{(\text{Viscosity})_{100}(\text{Density})_{100}}{(\text{Viscosity})_{125}(\text{Density})_{125}} K_{125} \tag{5}$$

Where the subscrips denote the temperature in degrees F.
Substituting into equation (5)

$$K_{100}(\text{laminar}) = \frac{(.028\frac{in^2}{sec})\ (8.2E\text{-}5\frac{lb\text{-}sec^2}{in^4})}{(.0201\frac{in^2}{sec})\ (8.14E\text{-}5\frac{lb\text{-}sec^2}{in^4})} \quad (.5)$$

$$K_{100}(\text{laminr}) = .7$$

The turbulent coefficient was determined by equation 6.

$$\Delta P = K Q^2 \tag{6}$$

where

$Q = 30$ CIS

$\Delta P = 32$ PSI from Figure 439.

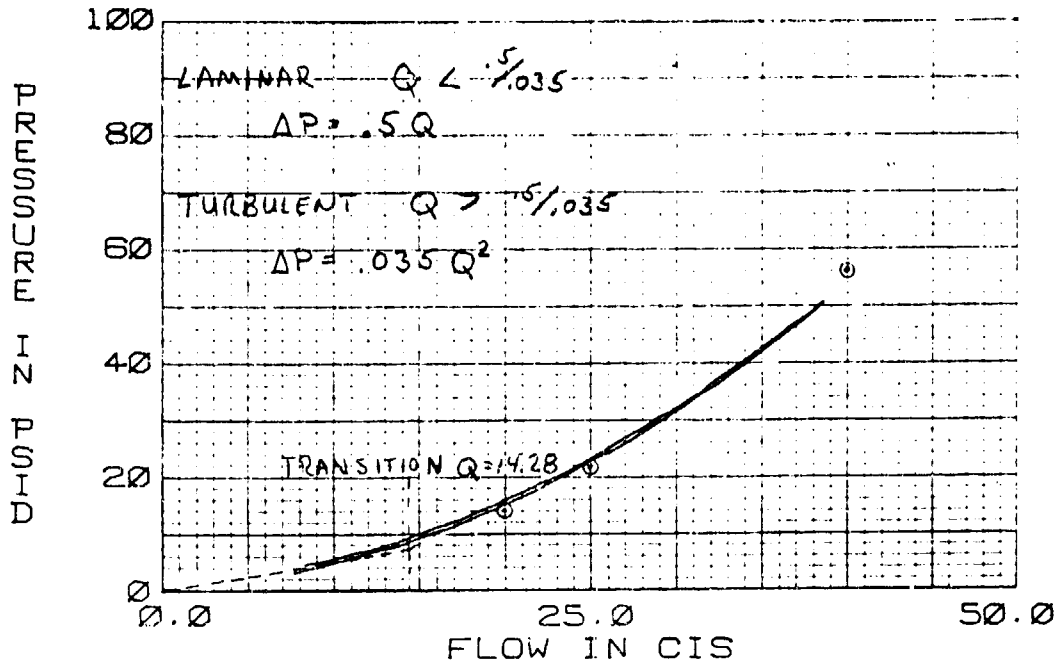

FIGURE 438 F4 PC FILTER WITH ELEMENT
125°F

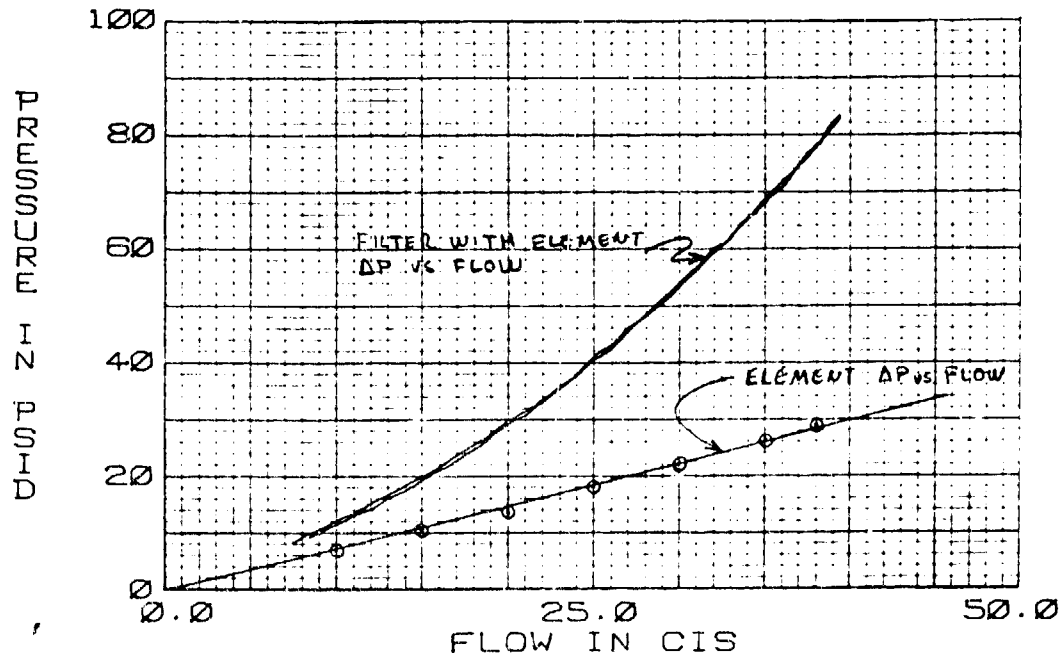

FIGURE 439 F4 PC FILTER WITH ELEMENT
125°F

Thus K at 125°F for turbulent flow is 0.025. Again using equation (5) except that viscosity must now be raised to the .25 power, the turbulent constant at 100 degrees is

$$K_{100}^{(\text{turbulent})} = \frac{(.028)^{.25}(8.2E\text{-}5)}{(.0201)^{.25}(8.14E\text{-}5)} \quad (.035) \qquad (7)$$

where $K_{100}^{(\text{turbulent})} = 0.038$

Table 23 is a listing of the laminar and turbulent flow constants for the computer input data. The losses were divided between the inlet and outlet conditions. From Figure 438 the transition flow is 14.28 CIS. The plotted points were determined by substituting Q into the turbulent flow equation $\Delta P = .035Q^2$. This square law relationship follows closely the measured data.

TABLE 23

LAMINAR AND TURBULENT FLOW
COEFFICIENTS FOR AC-900-61 OIL FILTER
WITHOUT AN ELEMENT

Total Losses		Inlet-Outlet Losses	Inlet-Outlet Losses	Temperature
Laminar	Turbulent	Laminar	Turbulent	°F
.5	.035			125
.7	.038	.35	.019	100

The element constant was found by subtracting the ΔP vs. flow curve of the filter with an element from the ΔP vs flow curve of the filter housing. The resultant values were plotted and a line was drawn through them on Figure 439 below the ΔP vs. flow curve. This line is the element pressure drop vs. flow curve and it is approximately a straight line. The slopes of this line gives the element constant, which is 0.7272 at 125°F. Correcting this element constant to a temperature of 100 degrees requires the use of equation (5)

$$K_{100}^{(\text{Element})} = \frac{(.028)(8.2E\text{-}5)}{(.0201)(8.14E\text{-}5)} \quad (.7272)$$

where $K_{100}(\text{Element}) = 1.02$

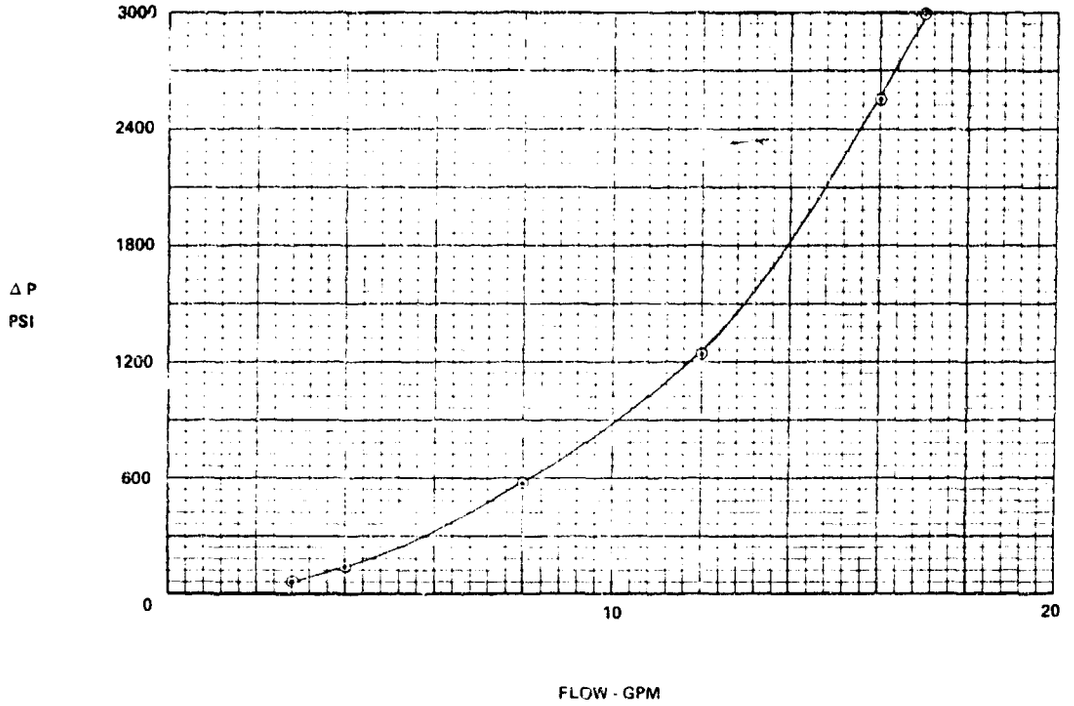

FIGURE 440 VICTOR SOLENOID VALVE MODEL
SV305-9053
NORMALLY CLOSED - 125°F

2. SUPPLEMENTAL COMPONENT TEST DATA

Steady state data was recorded for the following components: MCAIR miniature check valve, F-15 compensated check valve, teflon hoses (1/4 and 5/8 diameters), one-way restrictor, single orifice and stacked disc type orifices.

Figures 441 and 442 are the steady state flow vs. pressure drop curves for the MCAIR miniature check valve and F-15 compensated check valve respectively.

A set up was made to measure the change in volume due to pressure for a hose and oil system. The test configuration is shown in Figure 443.

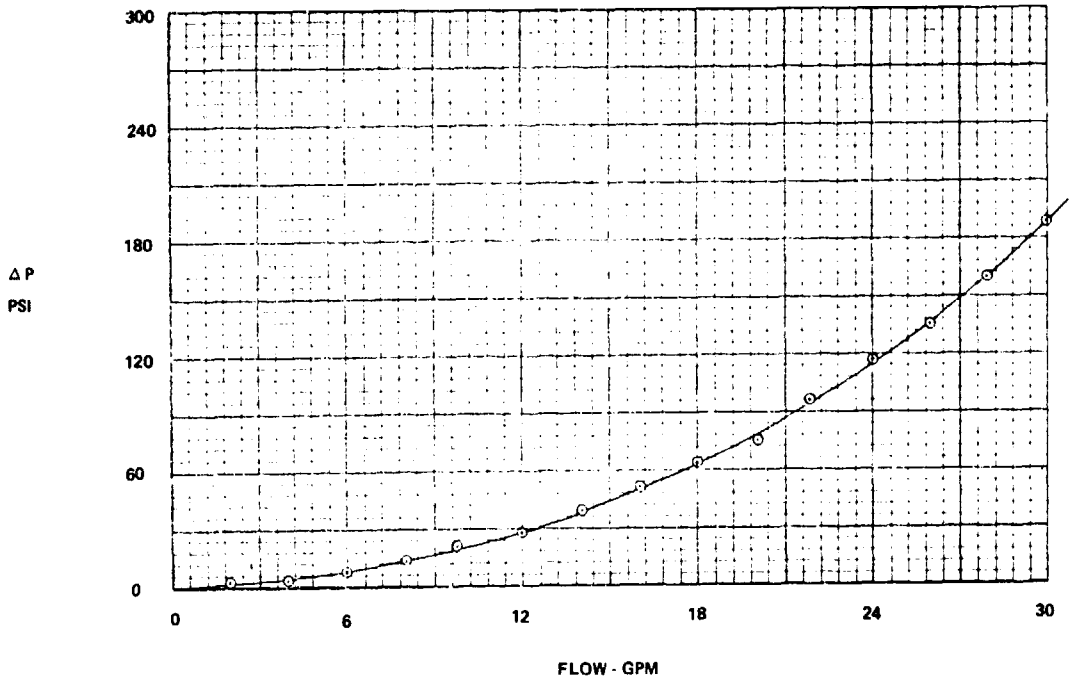

FIGURE 441 MCAIR MINIATURE CHECK VALVE

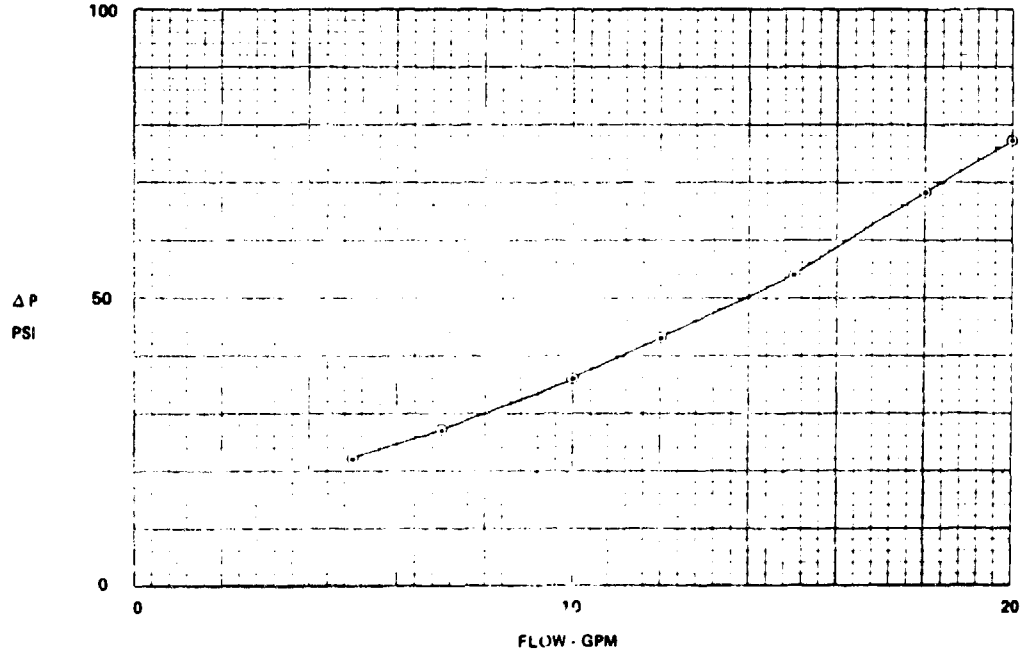

FIGURE 442 F-15 COMPENSATED CHECK VALVE
PN 6869022101-80°F

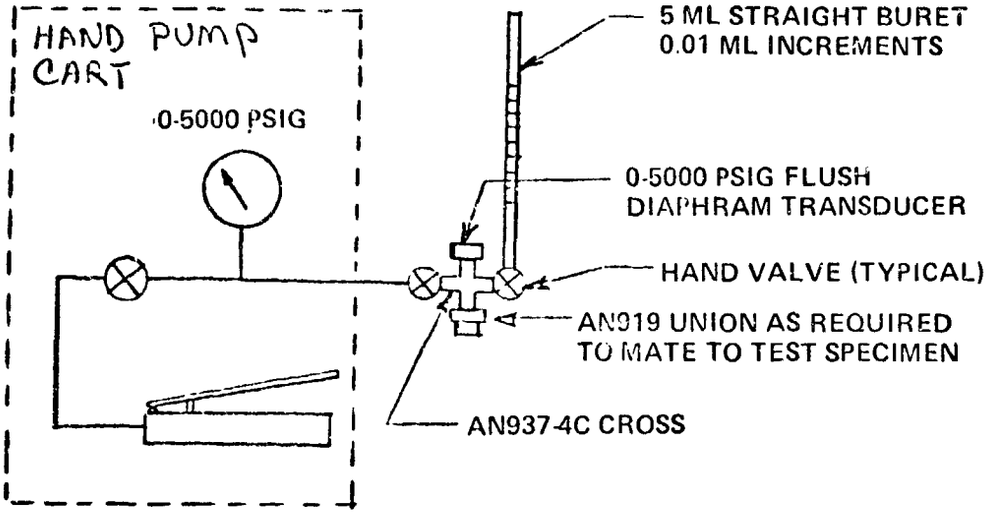

FIGURE 443 HOSE BULK MODULUS MEASUREMENT SETUP

After attaching the test specimen and removing all the air from the system, it was pumped to about 3500 psi. A value was measured on the buret, then the pressure was lowered by opening the hand valve allowing the fluid to go into the buret, and another reading was made. The temperature at each pressure was allowed to stabilize to 75°F for both tests. The procedure was repeated with a flat plug inserted into the union to obtain the tare volumes plotted in Figure 444. These values were subtracted from the hose data and the results are tabulated in Table 24 for a 5/8" and 1/4" steel braided hose.

TABLE 24

MEASURED VOLUME CHANGE (ΔV) FOR 5/8" AND 1/4" FLEXIBLE HOSES

5/8" HOSE P/N 730900-10-0240		1/4" HOSE P/N 730900-4-0240	
P (PSIG)	V(CC)	P (PSIG)	V(CC)
548	0.705	560	.135
1000	1.085	1000	.235
1500	1.540	1500	.350
2135	2.160	2000	.460
2580	2.545	2500	.565
3060	2.885	3000	.672
3735	3.380	3600	.775

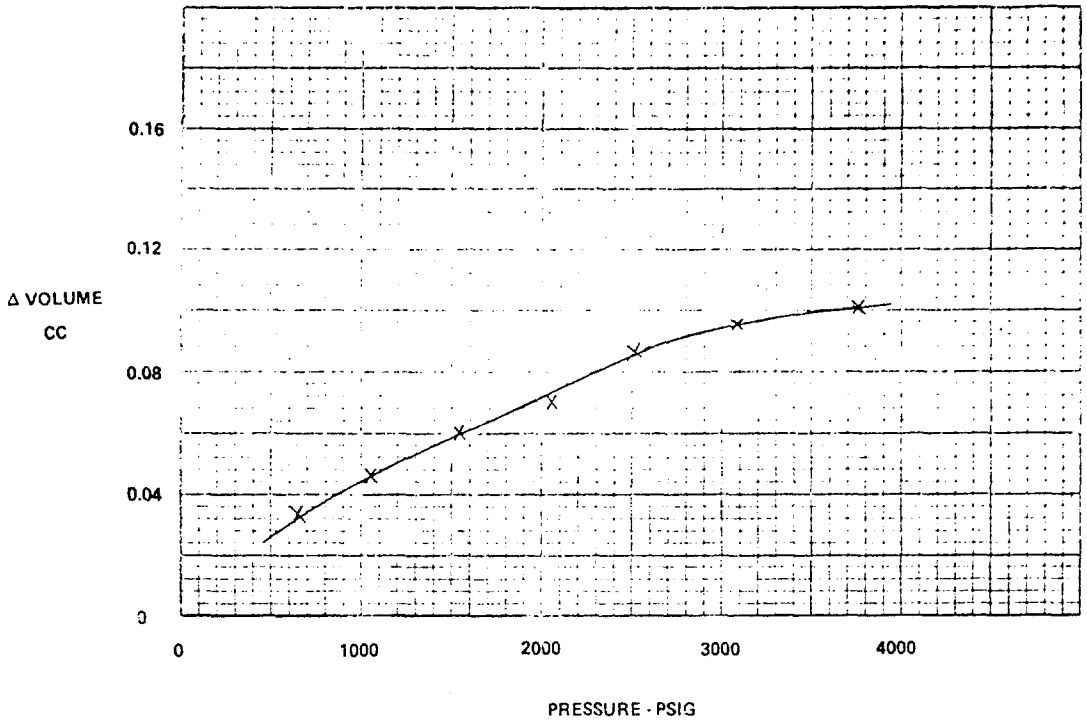

FIGURE 444 TARE DELTA V FOR HOSE BULK MODULUS
TEMP = 75°F

The volumes of the 5/8" and 1/4" hoses were 90cc and 10.5cc respectively. An effective isothermal tangent bulk modulus of the hose/oil system can be determined from the data in Table 24. This was done by drawing a tangent line to the data curve at the pressure point of interest. For the 1/4" hose in Figure 445 the tangent line was constructed at 3000 psig. The effective bulk modulus was determined from the following equation:

$$BULK_e = \frac{\Delta P}{\Delta V/V} \tag{8}$$

where ΔP = change in pressure = 3000 psi

V = volume of hose = 10.5cc

ΔV = change in volume = .54cc

$BULK_e$ = equivalent bulk modulus of the hose and fluid = 58333 psi

The effective bulk modulus is obtained by summing the reciprocals of the hose and oil bulk moduli.

$$\frac{1}{BULK_e} = \frac{1}{BULK_{hose}} + \frac{1}{BULK_{oil}} \tag{9}$$

Thus the bulk modulus of the hose is:

$$BULK_{hose} = \frac{BULK_e \; BULK_{oil}}{BULK_{oil} - BULK_e} \tag{10}$$

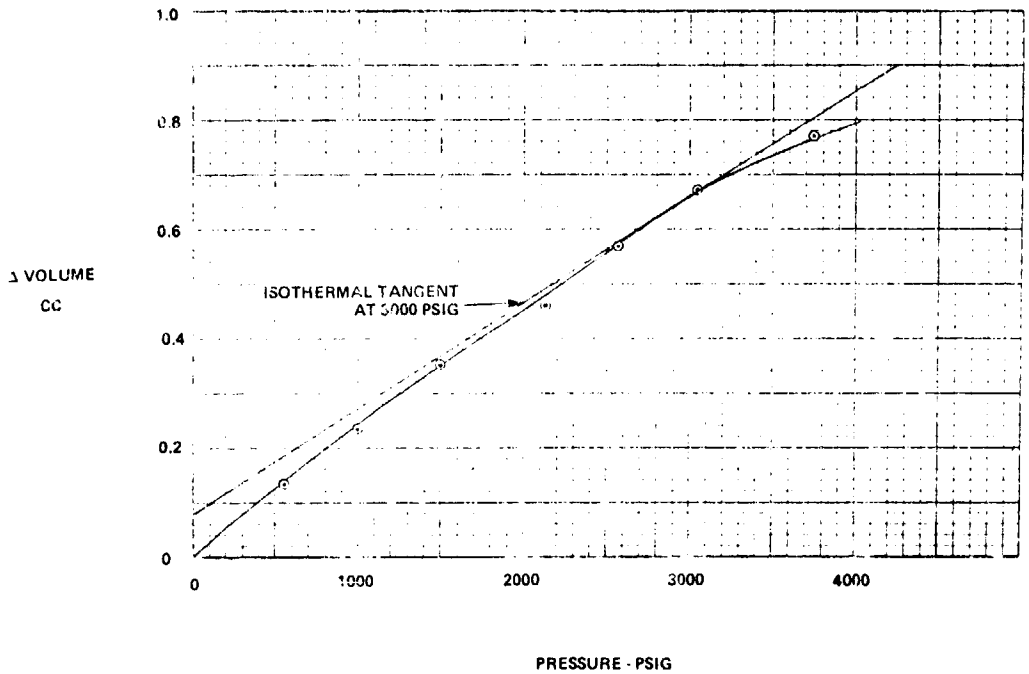

FIGURE 445 1/4" HOSE BULK MODULUS, 75°F

The value for the isothermal tangent bulk modulus of oil (MIL-H-5606B) at 75°F and 0 psig is 187551 psi. This $BULK_{oil}$ was then corrected to the steady state operating pressure.

$$BULK_{press} = BULK_0 + 12 * PRESS \qquad (11)$$

where $BULK_{press}$ = isothermal tangent bulk modulus at pressure (3000) = 223551 psi

$BULK_0$ = isothermal tangent bulk modulus at 0 psig = 187551 psi

The factor 12 is based on a bulk modulus versus pressure plot and is considered a good value for pressures up to 3000 or 4000 psig.

Substituting the appropriate values into equation (10), the hose isothermal tangent bulk modulus at 75° and 3000 psi is 78928 psi. This value was used as the 1/4" hose bulk modulus in the HYTRAN program.

The 5/8" hose data points from Table 24 are plotted in Figure 446. A tangent line was drawn at the 3000 psi pressure point. From Equation (8)

$$BULK_e = \frac{3000}{224/90} = 120536 \text{ psi}$$

substituting into equation (3)

$$BULK_{5/8" \text{ hose}} = \frac{(120536)(223551)}{223551-120536} = 261572 \text{ psi}$$

at 3000 psi and 75°F.

A steady state flow - ΔP test was made on the 1/4" flexible hose. The results are shown in Figure 447.

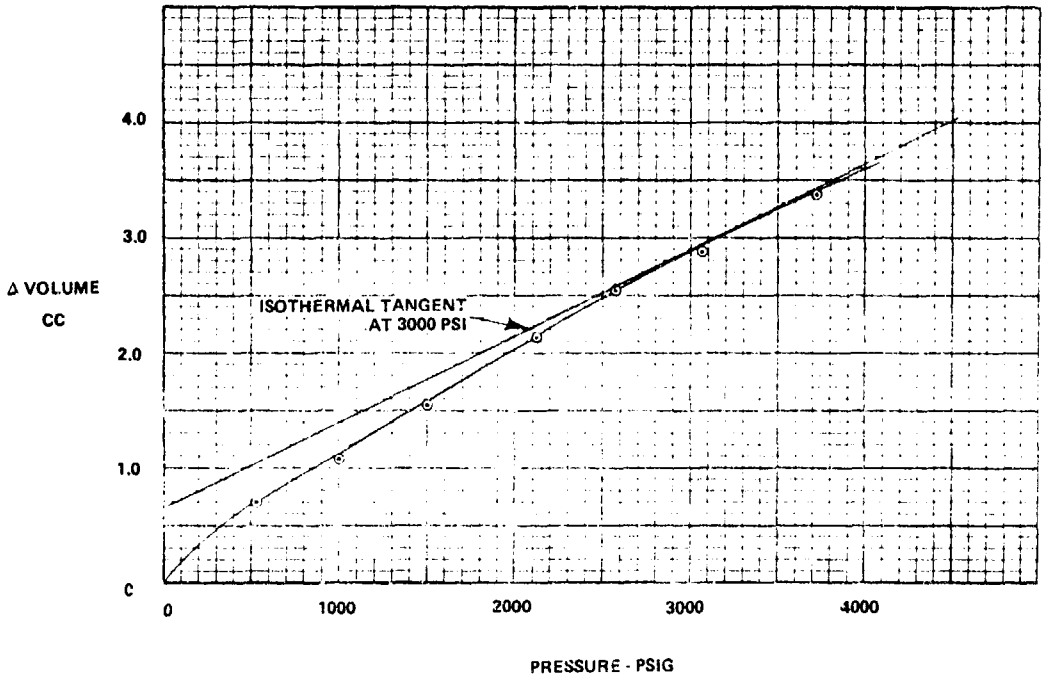

FIGURE 446 5/8" HOSE BULK MODULUS, 75°F

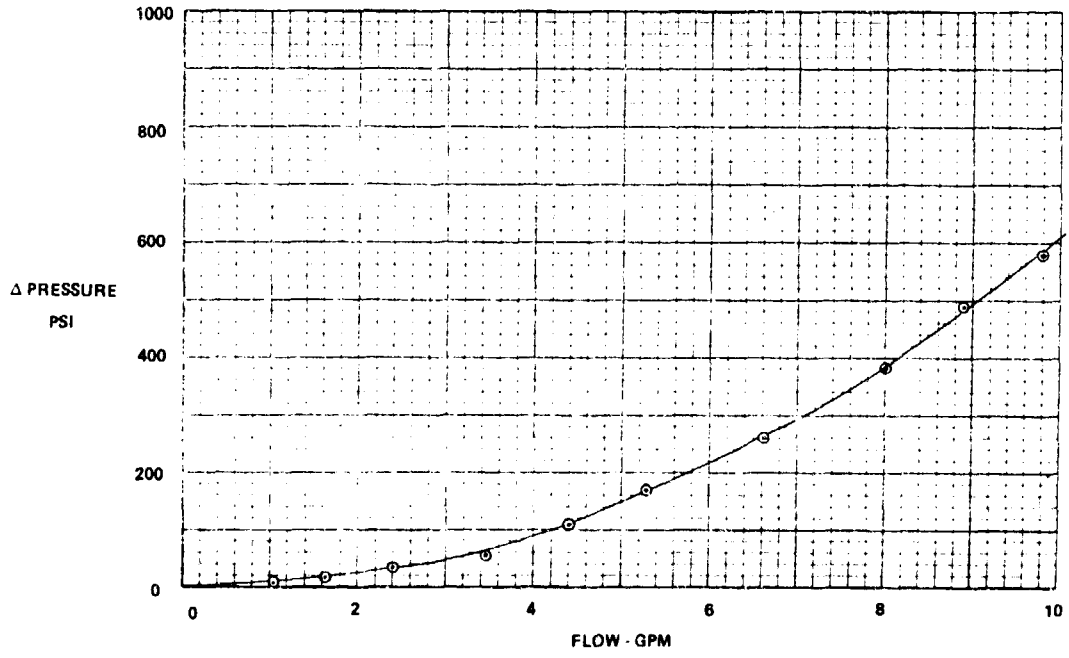

FIGURE 447 1/4" HOSE P/N 730900-4-0240, 116°F
WITH REDUCER FITTINGS - AN919-10C

The steady state pressure drop versus flow for both the free flow and restricted flow directions were measured for a Conair one-way restrictor. The results are plotted in Figures 448 and 449.

Steady state pressure drop versus flwo data were taken for both the Lee Jet and the Visco Jet. The results are shown in Table 25 and the normalized points at 100°F are plotted in Figures 450 and 451. A square law relationship is plotted in Figure 450 through the points from the formula $\Delta P = KQ^2$ where K was determined from the data in Table 25 at 100°F. For the Visco Jet in Figure 451 the equation was $\Delta P = KQ^{2.3}$. The K factor was determined from the data in Table 25 at 500 PSI pressure and .256 CIS flow.

The determination of the coefficient of discharge for the Lee Jet was made using the standard orifice equation:

$$C_d = \frac{Q}{A\left(\frac{2\Delta P}{\rho}\right)^{1/2}} \qquad (12)$$

where

C_d = discharge coefficient

Q = flow (CIS)

A = orifice area (in^2)

ΔP = pressure drop (psi)

ρ = mass density $\frac{lbs\text{-}sec^2}{in^4}$

The orifice diameter was measured to be .00945" giving an area of $7.0138 \times 10^{-5} in^2$.

The flow Q was normalized to 100°F at 1500 PSI mean pressure through the following equation:

$$Q_{100} = Q_{temp} \frac{RHO_{TEMP}}{RHO_{100}}^{1/2} \qquad (13)$$

where

Q_{100} = Flow at 100°F (CIS)

Q_{Temp} = Flow at temperature (CIS)

RHO_{100} = Density at 100°F $\frac{lbs\text{-}sec^2}{in^4}$

RHO_{Temp} = Density at Temp $\frac{lbs\text{-}sec^2}{in^4}$

The density was corrected to 1500 PSI mean pressure by using the expression

$$RHO_{Temp} = RHO_{Temp}\left(1 + \frac{Press}{250{,}000}\right) \frac{lbs\text{-}sec^2}{in^4} \qquad (14)$$

where 250,000 PSI is an average sealant bulk modulus at operating conditions for MIL-H-5606B hydraulic fluid.

The average discharge coefficient calculated from the seven pressure and flow values for the Lee Jet was approximately 0.9. The discharge coefficient is relatively large because the Lee Jet is not a true sharp edge orifice.

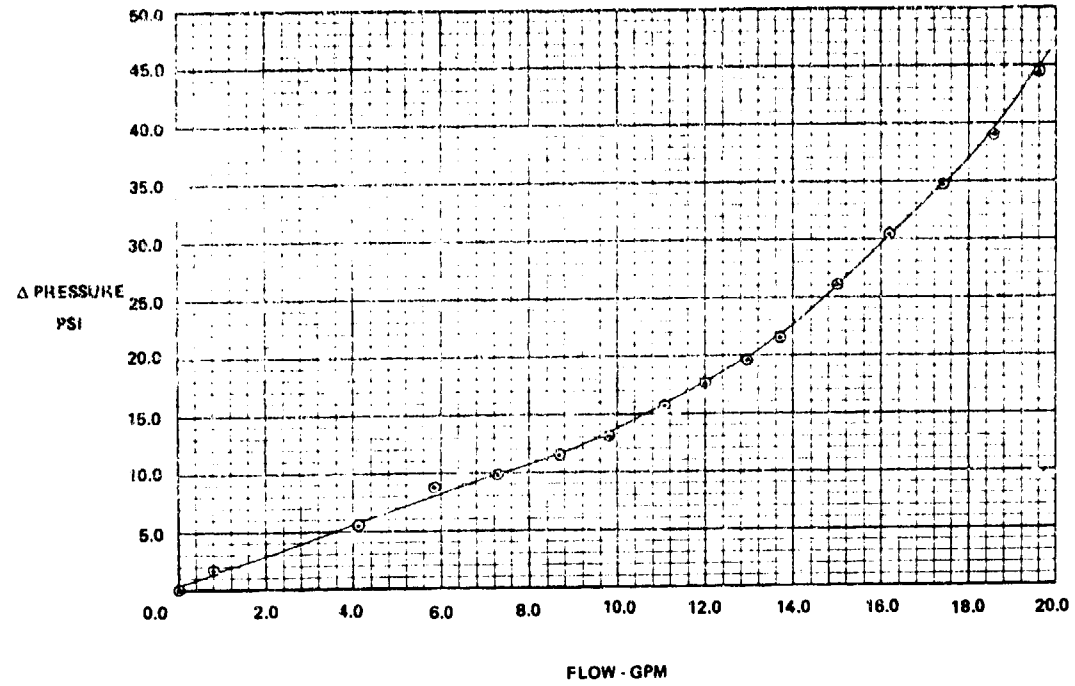

FIGURE 448 CONAIR 286-5590-105 RESTRICTOR
FREE FLOW DIRECTION

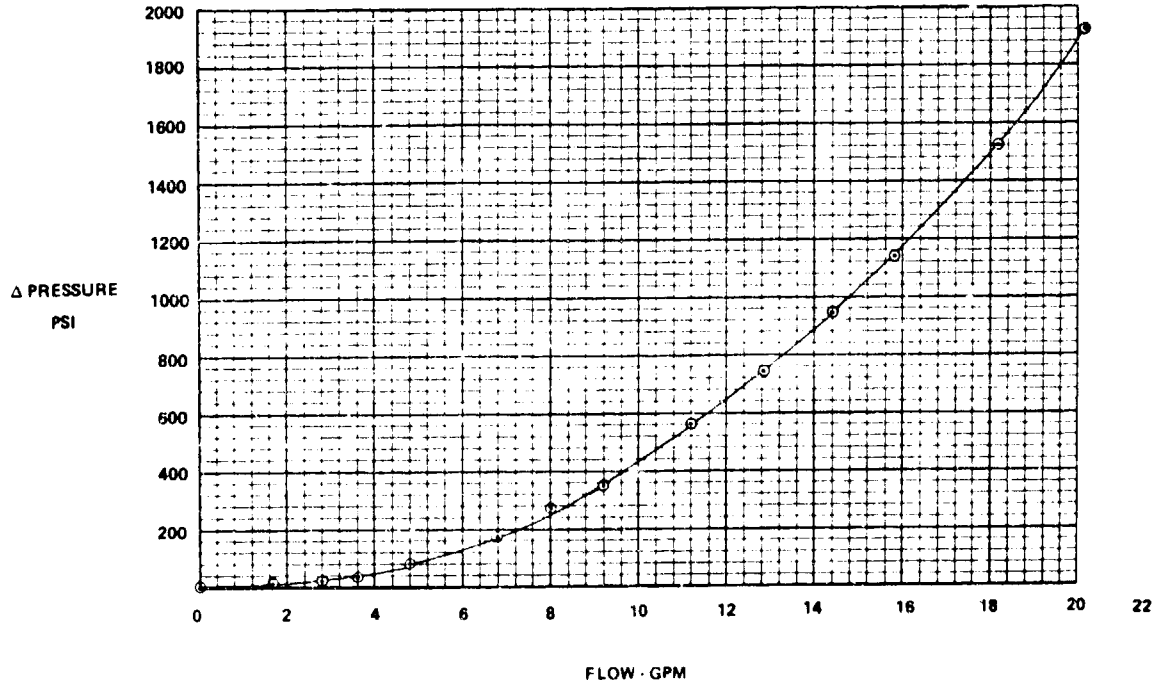

FIGURE 449 CONAIR 286-5596-105 RESTRICTOR
RESTRICTED FLOW

TABLE 25

LEE JET AND VISCO JET FLOW-PRESSURE DROP DATA

Lee Jet (.009 Dia)
JETA 1875850D

ΔP (psi)	FLOW (CIS)	FLOW (CIS) 100°F&1500PSI MEAN PRESSURE	TEMP (°F)	Cd DISCHARGE COEFFICIENT
500	.2135	.2137	95.0	.8697
504	.216	.2167	96.25	.8792
1000	.325	.325	97.5	.9361
1450	.3864	.3866	98.75	.9242
2000	.4475	.4475	100.0	.9114
2500	.480	.4796	102.5	.8738
3000	.541	.5401	105.0	.8982

Lee Visco Jet (.031 Dia)
VDLA 6810880D

ΔP (psi)	FLOW (CIS)	FLOW (CIS) 100°F & 1500PSI MEAN PRESSURE	TEMP (°F)
500	.255	.256	90.0
1000	.344	.345	90.0
1500	.412	.413	90.0
2000	.471	.472	95.0
2500	.510	.510	100.0
3000	.554	.553	105.0

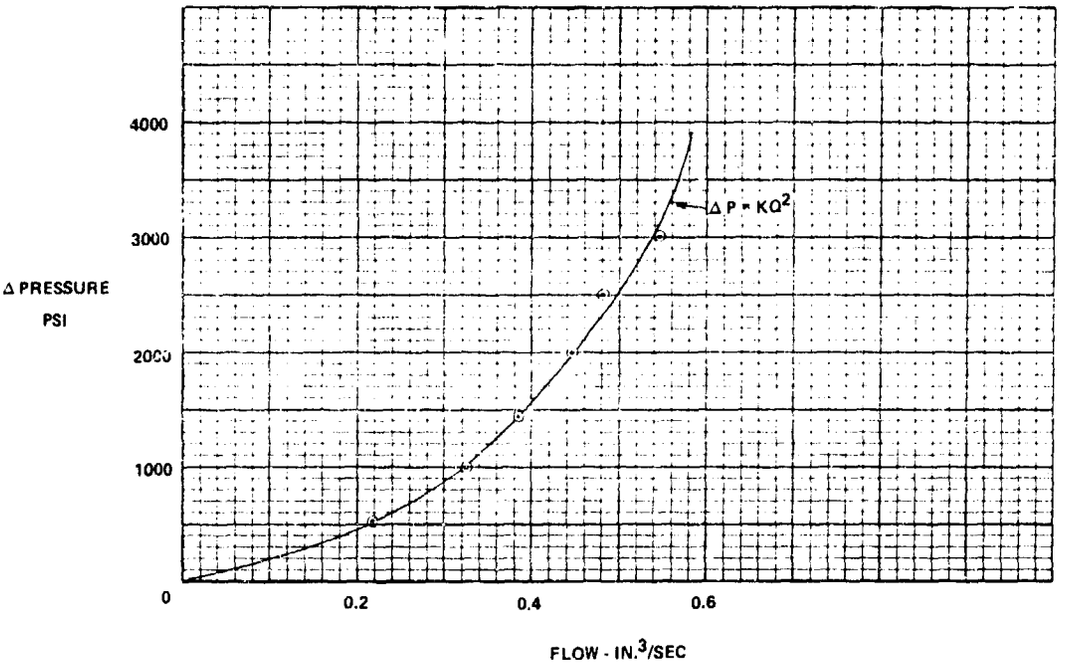

FIGURE 450 LEE JET JETA 1875850D

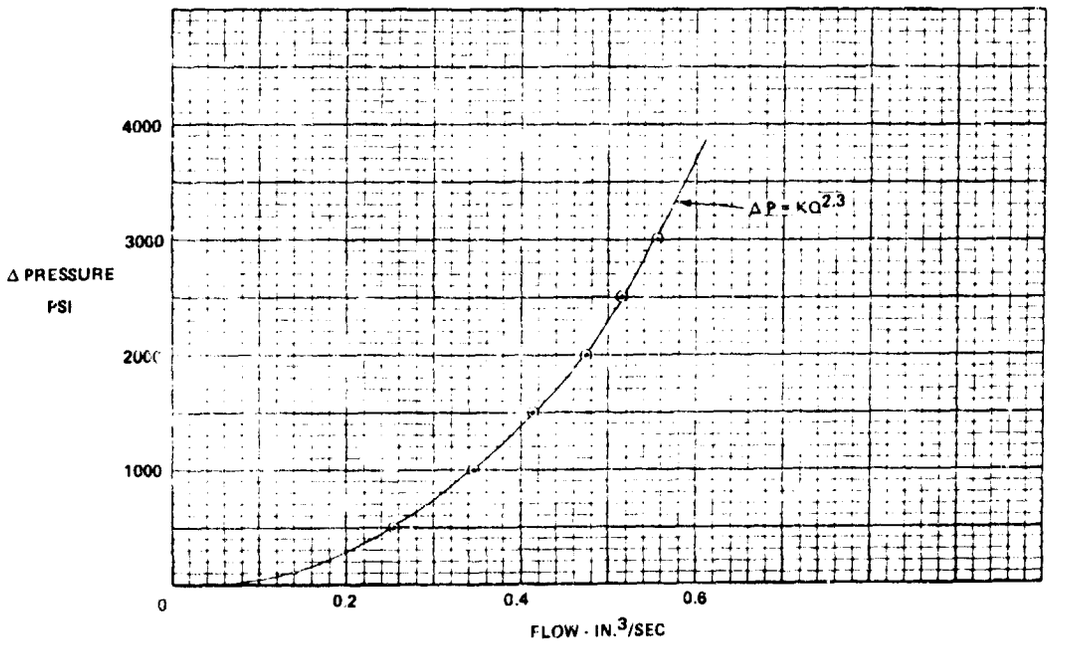

FIGURE 451 LEE VISCO JET VDLA 6810880D

3. STEADY STATE TESTING WITH THE F-15 INSTRUMENTED PUMP

The instrumented pump testing was accomplished with MIL-H-83282 and MIL-H-5606B hydraulic fluids. Steady state testing with both fluids yielded significantly different heat rejection and case drain flow characteristics. The Newtonian MIL-H-83282 vs. non-Newtonian MIL-H-5606B viscosity characteristics of the two fluids may account for the differences measured.

The effect of shear on Newtonian and non-Newtonian fluids is discussed in the following excerpt from the book "Fluid Power Control" edited by Blackburn.

"2.33. Effect of Shear

For a Newtonian fluid, the viscosity is independent of the rate of shear, and many liquids are almost perfectly Newtonian. Many others, however, are not, and among these are some of our most useful hydraulic fluids, especially those which contain appreciable amounts of compounds of high molecular weight. These compounds may be natural components of the fluid, or they may be additives, especially the viscosity-index improvers.

When a fluid of this type is subjected to shear, the effective viscosity decreases with increasing rate of shear. This increase appears to be instantaneously reversible for moderate shear rates and for most fluids. As the shear rate increases, however, the viscosity change also increases, and persists for a time after the flow ceases. At extremely high rates of shear the decrease of viscosity may be as much as 40 per cent, and part of this decrease is permanent.

One plausible explanation of these effects is that these three types of viscosity decrease are due respectively to increasing orientation of elongated molecules parallel to the flow lines, to uncoiling and orientation of coiled large molecules, and to actual fracturing of large molecules, accompanied by oxidation and other chemical reactions. This last explanation is supported by the fact that for some oils anti-oxidants help to increase the shear stability.

The rate of shear necessary to cause appreciable changes in viscosity, either transient or permanent, naturally varies with the liquid. Temporary changes may occur with many commercial hydraulic fluids and with many types of machines, such as positive-displacement pumps and motors, in piston or high-speed-bearing clearances. The higher shear stresses necessary to cause permanent viscosity changes are ordinarily attained only under conditions of extreme turbulence, as in throttling valves and orifices under high pressure drops. The effects are greater for oils containing high-polymer thickeners; this should be kept in mind when making detailed analyses of viscous-flow phenomena for such oils. The effective viscosities may be very different from those measured at low rates of shear in conventional viscometers.

The considerable changes in effective viscosity produced by shear, as well as by changes in temperature and pressure, the variability in the properties of commercial fluids as received by the user, and the effects of aging and contamination, suggest that there is really little point in trying to predict viscosity (or other properties) with high accuracy. This is true from a purely empirical standpoint, but there are two arguments against this point of view. One is that eventually we shall know more about all of these effects, and this greater knowledge will permit better control of the performance or our hydraulic systems.

The other argument is that the constant improvement in the fluids themselves, and still more in the quality of maintenance of the average hydraulic system, will greatly decrease the variability of the fluid properties. In any given case it is necessary for the engineer to decide for himself how much importance he must attach to the considerations that have been outlined here."

a. Comparison - Heat Rejection Characteristics - The data recorded during the verification program is presented in the following tables:

TABLE 26 - POWER LOSS COMPARISON

(OUTLET FLOW = 7.7 CIS COMPENSATOR SETTING - 2940 PSIG)

PUMP SPEED	INLET TEMP (°F)		POWER LOSS (HP)		
(RPM)	MIL-H-5606B	MIL-H-83282	MIL-H-5606B	MIL-H-83282	% INCREASE
3000	202	205	3.50	4.47	27.7%
3500	202	205	3.98	4.94	24.1%
4000	202	205	4.26	5.50	29.1%
4500	202	205	4.79	6.25	30.5%

The results in Table 26 show a 24.7% to 30.5% increase in heat rejection for MIL-H-83282 vs. MIL-H-5606B for the 3000 to 4500 rpm speed. The heat rejection at 4500 rpm was approximately 203 BTU/min. for 5606B vs. 265 BTU/min. for 83282.

TABLE 27 - POWER LOSS AT ZERO OUTLET

FLOW - MIL-H-83282 POWER LOSS (HP)

PUMP SPEED (RPM)	INLET = 88°F	INLET = 115°F	INLET = 200°F
1000	1.34	1.85	3.41
1500	1.71	2.09	3.76
2000	2.22	2.47	3.81
2500	2.74	2.77	3.84
3000	3.09	3.28	3.90
3500	3.66	3.77	4.44
4000	4.38	4.31	4.95
4500	4.99	4.99	5.35
5000	5.63	5.63	6.34

Table 27 presents the power loss with MIL-H-83282 at zero outlet flow for three inlet temperatures and speeds ranging from 1000 to 5000 rpm. The heat rejection at the 200°F inlet temperature was compared for the 3000 to 4500 rpm speed range for the zero outlet flow vs. the 7.7 cis outlet flow condition. The heat rejection for the 7.7 cis outlet flow condition ranged from 10 to 14.4% higher than for the identical zero outlet flow condition.

b. Comparison - Case Drain Flow Characteristics - The case drain pressure vs. flow characteristics of the F-15 pump with the two fluids are significantly different. The test setup provided for minimum case drain back pressure, no more than 5 psi at full flow. A manual valve was then used to gradually restrict case drain flow. Figures 452, 453, 454, and 455 show two lines resulting from first gradually closing the valve to complete case drain flow shutoff, then a gradual opening of the valve until it was completely open.

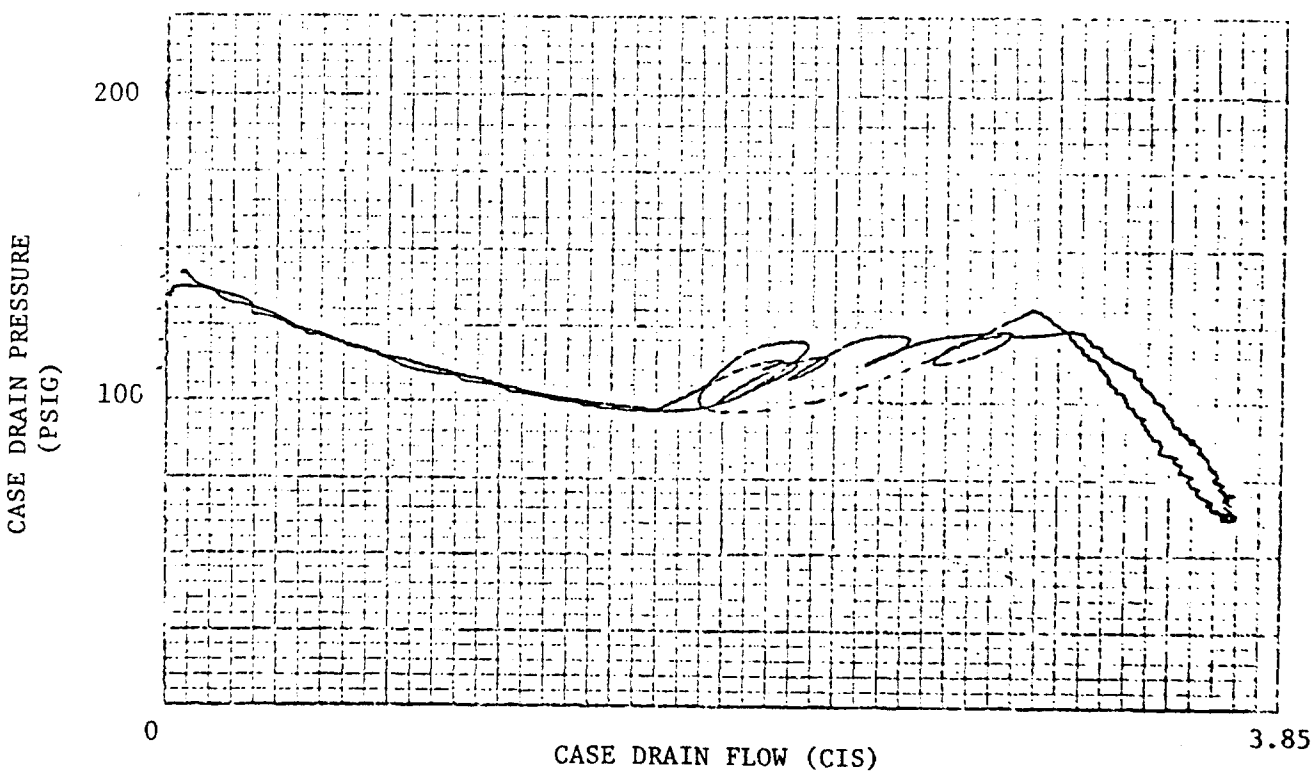

FIGURE 452. F-15 HYDRAULIC PUMP RUN E 7.7 CIS 91°F, MIL-H-5606B 4000 RPM

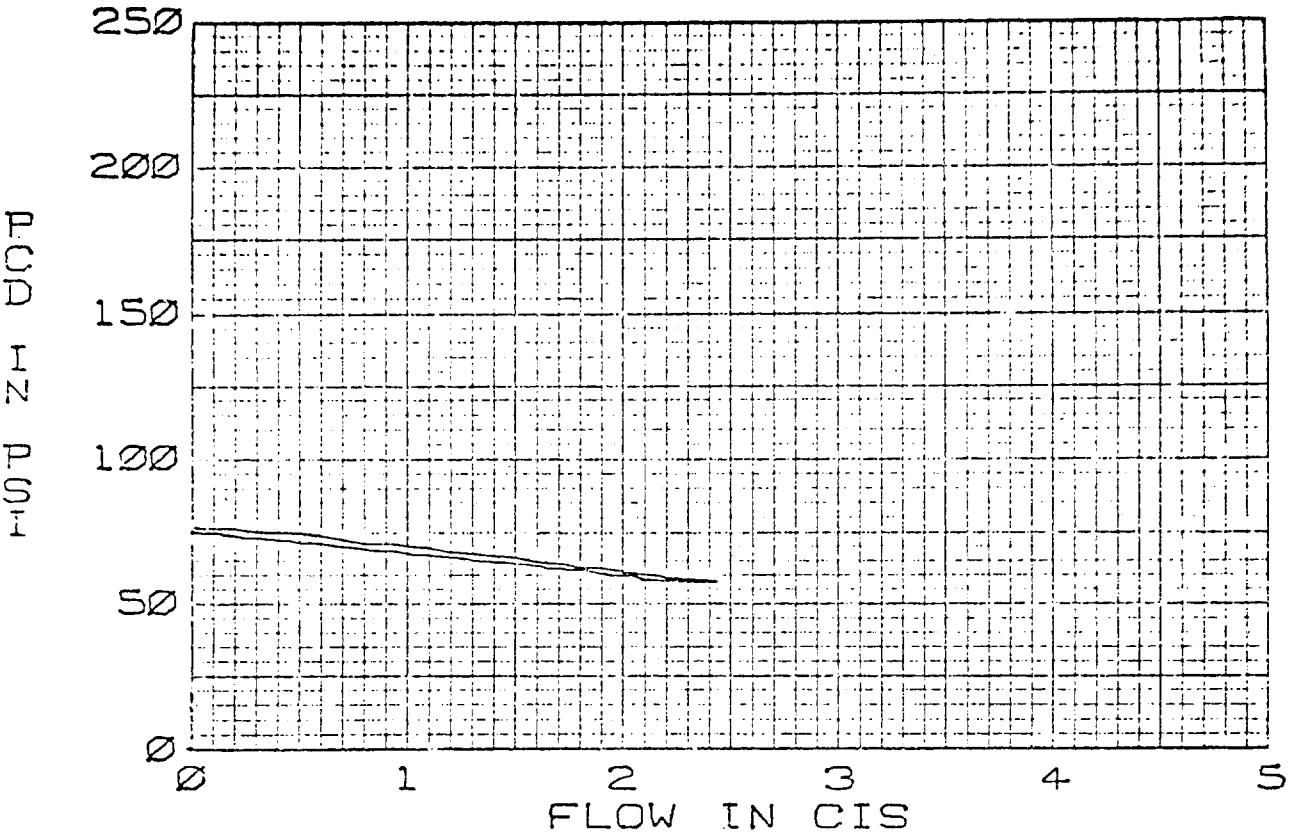

FIGURE 453. F-15 HYDRAULIC PUMP RUN 16 7.7 CIS 105°F, MIL-H-83282, 4000 RPM

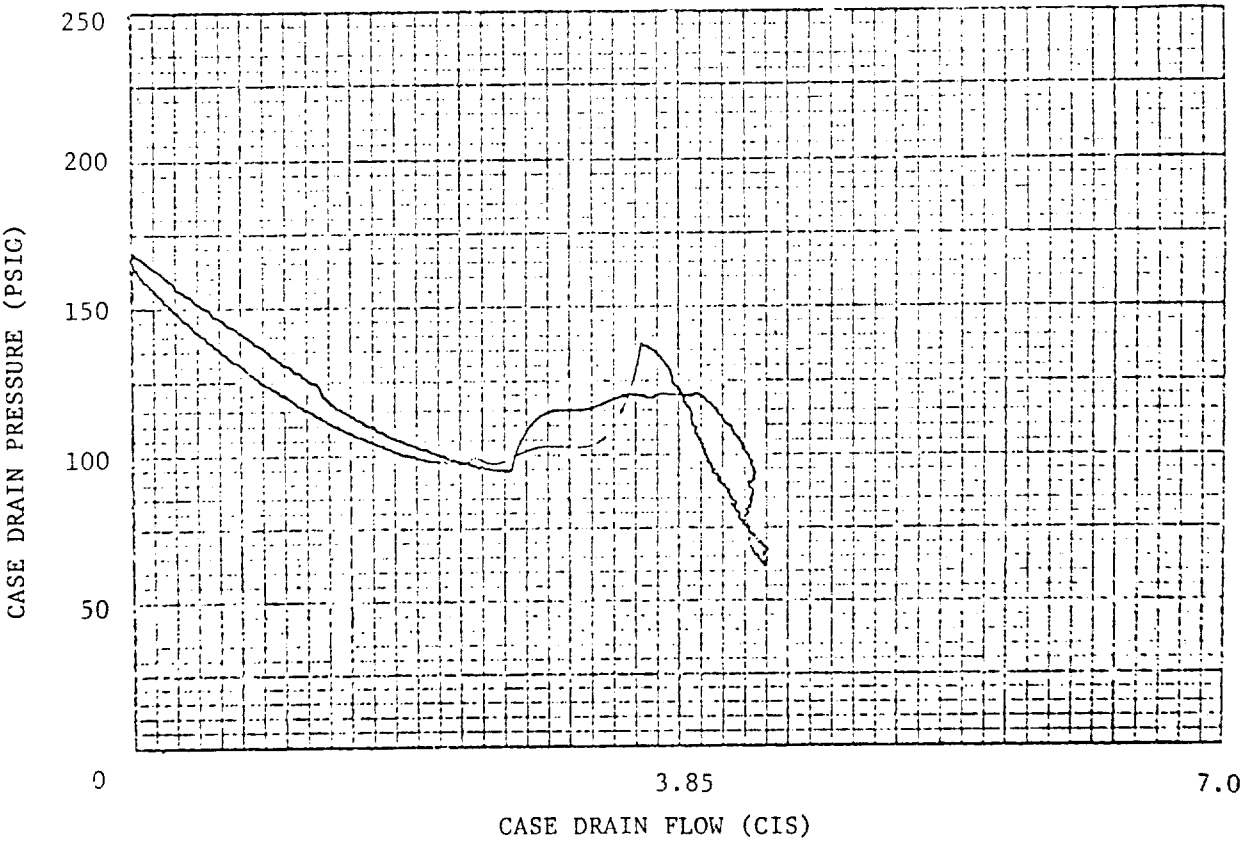

FIGURE 454. F-15 HYDRAULIC PUMP RUN 36 3.85 CIS, MIL-H-5606B, 4000 RPM

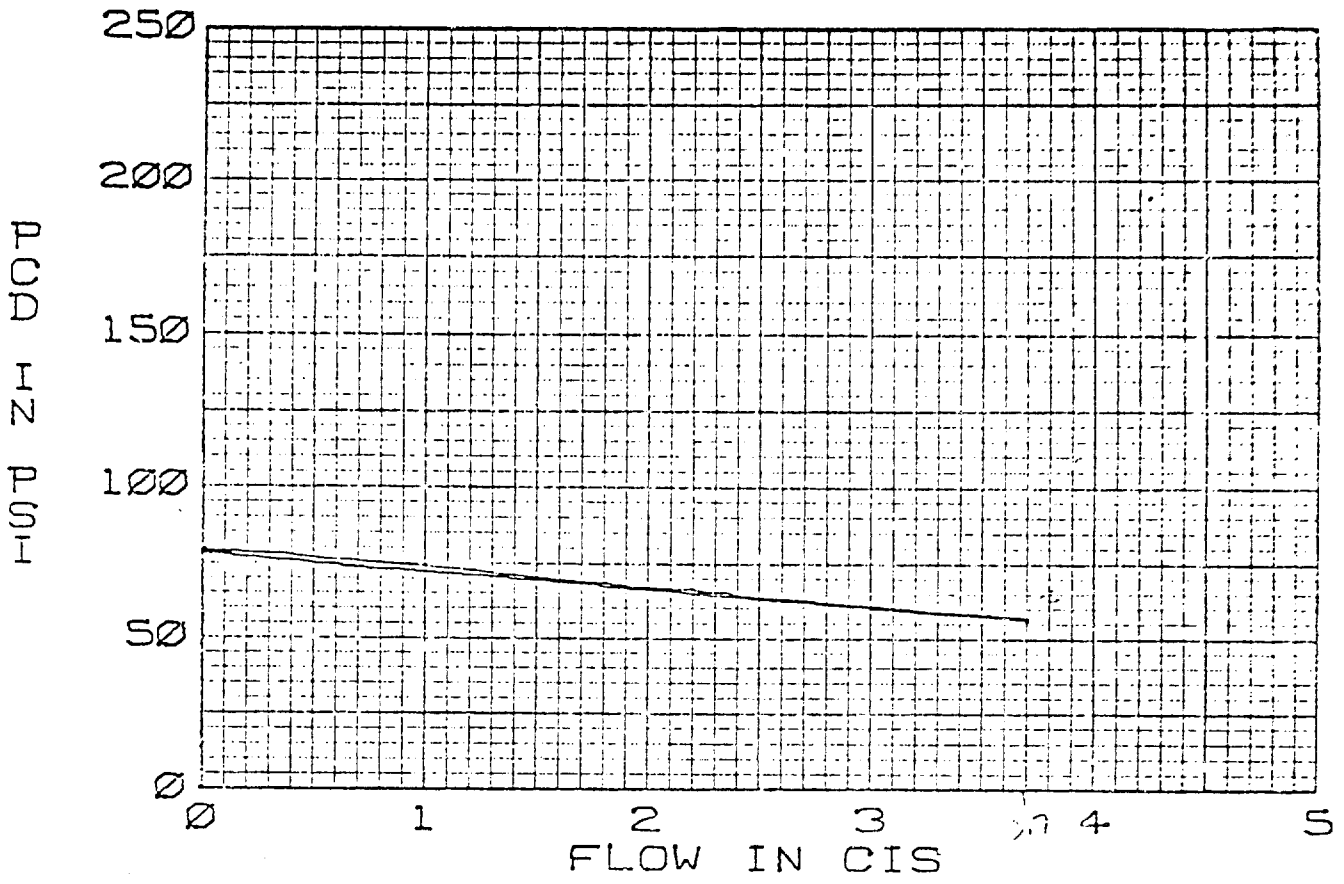

FIGURE 455. F-15 HYDRAULIC PUMP RUN 17 7.7 CIS 208°F, MIL-H-83282, 4000 RPM

There are two significant differences in comparing the performance characteristics of the two fluids. First, the unrestricted case drain flow was significantly reduced with the use of MIL-H-83282. Comparing Figure 452 and Figure 453 test results where the inlet temperatures are 91°F (5606) and 105°F (83282), the MIL-H-33282 flow was approximately 65% of the MIL-H-5606B fluid flow rate. This reduced flow characteristic also persists at higher inlet temperatures. A natural "fallout" of reduced case drain flow is reduced pressures at zero external case drain flow. In Figure 452 the case pressure developed when the case drain line was blocked with MIL-H-5606B is approximately 140 psi, approximately 90 psi above reservoir pressure. In Figure 453 the pressure chraacteristic noted with MIL-H-83282 was approximately 75 psi, approximately 25 psi above reservoir pressure. The MIL-H-83282 characteristics at 208°F inlet temp shown in 455 shows increased unrestricted flow without a significant increase in pressure at external zero case flow.

The second significant difference was the pump response to increasing case flow restriction. With MIL-H-83282 fluid the increase in pressure with decrease in flow was linear and stable. With the MIL-H-5606B the characteristic curve was very non-linear and there are indications of an instability. The instability and non-linearity may be a function of the increased pressure differentials in the pump adversely affected pump dynamic stability. Since the pressure increases with MIL-H-83282 fluid at restricted flows are relatively much lower it is likely this unstable condition caused by pressure was not reached.

c. Conclusions - The difference in case drain flow vs. pressure characteristics and heat rejection performance between MIL-H-5606B and MIL-H-83282 fluids is significant. The differences may be due to the non-Newtonian vs. Newtonian characteristics of the two fluids. Additional analysis and testing is required to confirm the assumption.

4. STEADY STATE TWO-PUMP SYSTEM VERIFICATION

The two-pump system simulated by HYTRAN in Section V Paragraph 14 was used as the basic system to verify the SSFAN Program. A simplified diagram of the parallel pump test setup is shown in Figure 394. The steady state test data was taken from run number 69-07-XX, a turn-off transient at 130°F. Both pump compensators were set for an identical outlet pressure. The drive speed for each unit was approximately 3600 RPM. The pumps were operating in a master-slave relationship, with the number one pump providing the flow. The steady state flow rate was established by a load restrictor downstream of the control valve. None of the emergency relief lines for the pressure and case drain lines were modeled in the simulation. The F-15 instrumented pump was the number two or slave pump in the test run.

a. Computer Simulation of the Two-Pump System - A schematic diagram of the SSFAN computer program representation of the two-pump system is shown in Figure 456. The F-15 utility filter manifold is simulated by two type 3 check valves and two special components and one inline filter. The special components provided the flow pressure drop characteristics for the two flow paths in the filter manifold. The control valve is a type 36 two-way-two-position valve, as is the thermal relief valve on the heat exchanger between junction numbers 200 and 205. For the computer run, the thermal valve was closed. The return filtration system modeled the actual test setup. There were four parallel inline filters with 10 micron elements.

SSFAN does not have a single line constant pressure reservoir. Instead a type 92 constant pressure reservoir was used with an extra leg that contained a 500 psi relief valve. Generally all the tube sizes and lengths represent the actual hardware. A type 23 reducer was included in the simulation in the case drain circuit of the number two pump. This was done to try to include as many of the SSFAN component models as possible in the verification run. (The location of the pressure instrumentation is shown in Figure 456).

Some modifications were made to the SSFAN program in order to simulate the parallel pump system.

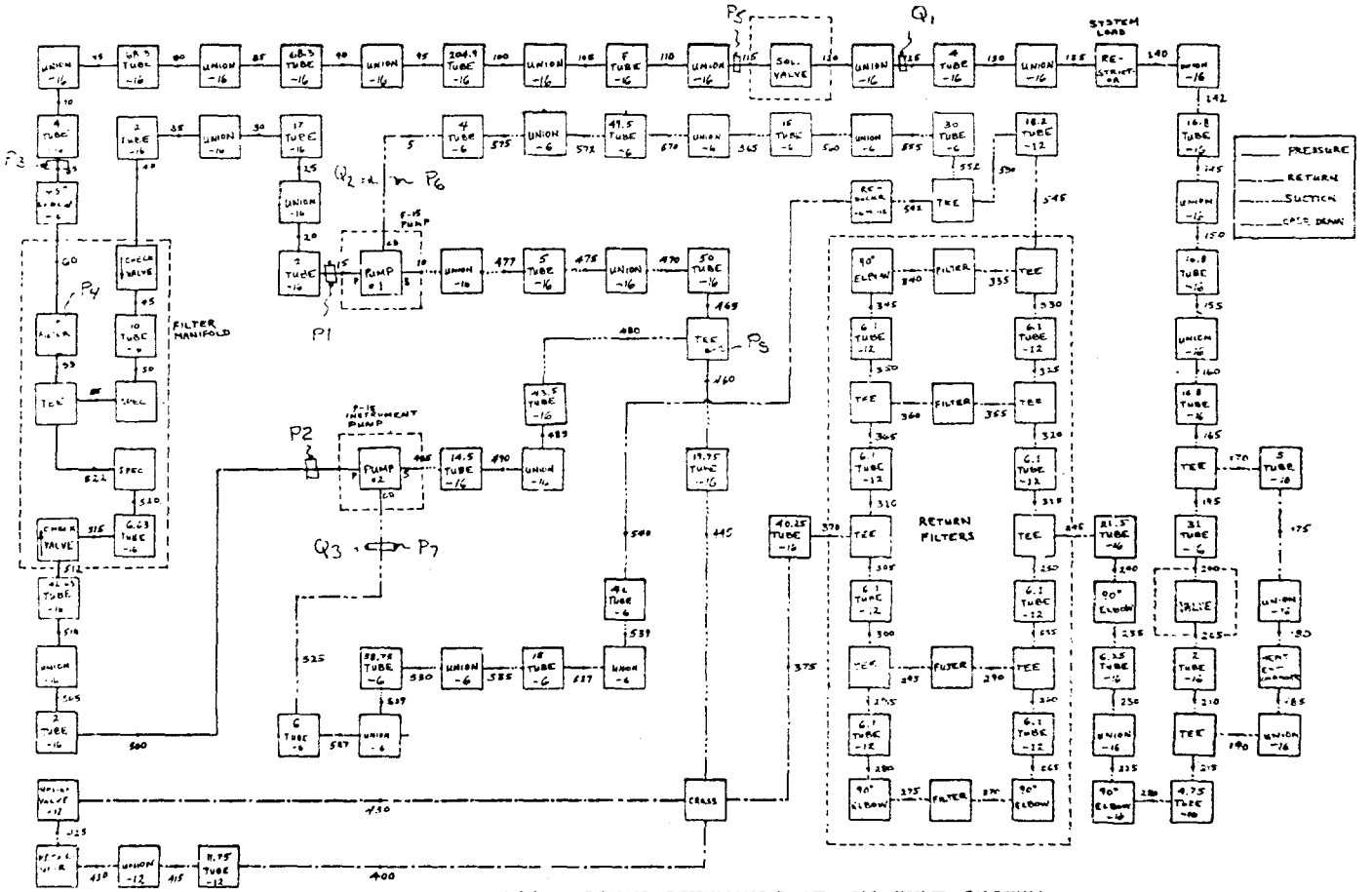

FIGURE 456. SSFAN SCHEMATIC OF TWO-PUMP SYSTEM

The SSFAN pump model fixes the outlet pressure for each iteration. For master-slave operation, the master pump fixed the outlet flow while the slave pump fixed the outlet pressure as boundary conditions. The pump subroutine updaced the outlet flow and pressure as the iteration proceeded.

Currently the pump model only fixes the outlet pressure. It is not capable of recognizing a master-slave relationship and adjusting the appropriate pump outlet parameter, however if the programmer is aware of this condition the actual changes to the pump subroutines are simple to make.

Figures 457 and 458 present some of the input data used in the simulation. The results of the computer run are shown in Figures 459, 460, and 461. Figure 459 is a type two output that gives the flows and pressure drops in all the legs of the two pump system. Some legs have negative flows, which correspond to flow in the opposite direction to the way the leg was assembled. All the junction pressures are listed in Figure 460 which is a type three output. The pump and reservoir data in Figure 461 is a type four SSFAN output. Actuator information would have also been included in this output if there had been an actuator in the system.

```
 SSSSS      SSSSS      FFFFFFFF      AAAAA      NN      NN
SSSSSSS    SSSSSSS     FFFFFFFF    AAAAAAA     NNN     NN
SS         SS          FF          AA   AA     NNNN    NN
SS         SS          FF          AA   AA     NN NN   NN
SSSSSS     SSSSSS      FFFFF       AAAAAAA     NN  NN  NN
 SSSSSS     SSSSSS     FFFFF       AAAAAAA     NN   NN NN
      SS         SS    FF          AA   AA     NN    NNNN
      SS         SS    FF          AA   AA     NN     NNN
SSSSSSS    SSSSSSS     FF          AA   AA     NN      NN
 SSSSS      SSSSS      FF          AA   AA     NN      NN

                STEADY STATE FLOW ANALYSIS


**** SSFAN PARALLEL PUMP TEST FOR 2 F-15 HYDRAULIC PUMPS AND UTILITY MANIFOLD **

FLUID TYPE = MIL-H-83282

FLUID VISCOSITY AT ATM PRESSURE =      9.860 CENTISTOKES

FLUID DENSITY AT ATM PRESSURE =   52.01176 LBS PER CU FT

TEMPERATURE =   130.00 DEG F

ALTITUDE =      0.00 FT

AMBIENT PRESSURE =    14.70 PSI
```

FIGURE 457. TYPE 1 SSFAN OUTPUT TITLE PAGE

**** SSFAN PARALLEL PUMP TEST FOR 2 F-15 HYDRAULIC PUMPS AND UTILITY MANIFOLD **

**** CHECK VALVE ARRAY-TYPE 3 ****

JCT1	JCT2	SIZE1	SIZE2	CRACKING P
40.000	45.000	16.000	16.000	5.000
512.000	515.000	16.000	16.000	225.000

**** PUMP ARRAY-TYPE 5 ****

JCT1S	JCT2P	JCT3CO	SIZE1	SIZE2	SIZE3	RPM	RRPM	RATED Q	P1	P2	PSMIN	RCDP	RCDL	PSET
10.00	15.00	5.00	16.00	16.00	6.00	3599.00	4600.00	57.00	3000.00	2970.00	42.00	200.00	1.00	42.00
495.00	500.00	525.00	16.00	16.00	6.00	3560.00	4600.00	57.00	3000.00	2970.00	42.00	200.00	1.00	42.00

**** FILTER ARRAY-TYPE 6 ****

JCT1	JCT2	SIZE1	SIZE2	FLUID VOL	RF ELEM	RDP ELEM	RVIS ELEM	CONTAM F	RELIEF DP	BYPASS DP-RF
335.000	340.000	12.000	12.000	8.055	10.000	8.500	14.600	0.000	0.000	0.000
355.000	360.000	12.000	12.000	8.055	10.000	8.500	14.600	0.000	0.000	0.000
290.000	295.000	12.000	12.000	8.055	10.000	8.500	14.600	0.000	0.000	0.000
270.000	275.000	12.000	12.000	8.055	10.000	8.500	14.600	0.000	0.000	0.000
59.000	60.000	16.000	16.000	12.816	104.000	35.000	14.600	0.000	0.000	0.000

**** BLEED AIR PRESSURIZED RESERVOIR ARRAY-TYPE 92 ****

JCT1	JCT2	SIZE1	SIZE2	PRESS
625.000	620.000	12.000	12.000	51.000

**** SPECIAL ARRAY-TYPE 10 ****

JCT1	JCT2	SIZE1	SIZE2	VISC	NPTS	DP1	DP2	DP3	DP4	DP5	DP6	Q1	Q2	Q3	Q4	Q5	Q6
50.	55.	16.000	16.000	14.60	3.	0.00	2.18	59.00	0.00	0.00	0.00	0.00	10.00	52.00	0.00	0.00	0.00
520.	522.	16.000	16.000	14.60	3.	0.00	2.44	66.00	0.00	0.00	0.00	0.00	10.00	52.00	0.00	0.00	0.00

FIGURE 458. TYPE 1 SSFAN OUTPUT

**** SSFAN PARALLEL PUMP TEST FOR 2 F-15 HYDRAULIC PUMPS AND UTILITY MANIFOLD **

LEG FLOW AND PRESSURE DROPS

JUNCTION NUMBERS AT LEG ENDS	PRESSURE DROP (PSIG)	FLOW (GPM)
15.- 55.	73.64	44.67
500.- 522.	232.44	2.93
59.- 115.	53.88	47.60
120.- 165.	24.39	47.60
170.- 190.	451.40	47.57
195.- 200.	.00	.02
205.- 210.	5.84	.02
215.- 245.	27.84	47.60
315.- 320.	11.73	31.89
290.- 295.	3.01	15.71
325.- 330.	4.94	16.97
355.- 360.	14.21	14.92
260.- 265.	6.51	7.03
290.- 295.	6.51	8.67
300.- 305.	16.77	15.71
310.- 305.	3.65	-32.89
370.- 375.	4.22	48.59
350.- 335.	9.27	-17.97
545.- 550.	3.74	-1.00
522.- 5.	.43	-.43
542.- 525.	.75	-.57
406.- 420.	.00	-.00
430.- 425.	.00	.00
445.- 460.	7.19	48.59
465.- 10.	6.69	45.10
490.- 495.	.06	3.50
115.- 170.	2167.55	47.60
200.- 205.	497.24	.02

FIGURE 459. TYPE 2 SSFAN OUTPUT

**** SSFAN PARALLEL PUMP TEST FOR 2 F-15 HYDRAULIC PUMPS AND UTILITY MANIFOLD **

PRESSURE POINT DATA

BRANCH/END POINT ELEMENT	JUNCTION NUMBERS	PRESSURE (PSIG)
PUMP	15.	2873.62
TEE	55.- 54.- 522.	2800.58
PUMP	500.	3033.02
VLV	115.	2746.70
VLV	120.	579.14
TEE	165.- 195.- 170.	554.75
TEE	190.- 210.- 215.	103.35
VLV	200.	554.75
VLV	205.	97.51
TEE	245.- 250.- 315.	75.51
TEE	320.- 355.- 325.	63.78
TEE	255.- 290.- 260.	72.50
TEE	330.- 335.- 545.	58.84
TEE	360.- 350.- 365.	49.57
TEE	285.- 295.- 300.	65.99
TEE	305.- 370.- 310.	55.22
CROSS	375.- 445.- 430.- 400.	51.00
TEE	550.- 542.- 552.	55.10
PUMP	5.	55.33
PUMP	525.	55.65
RESV	420.	51.00
RESV	425.	51.00
TEE	460.- 480.- 465.	43.81
PUMP	10.	37.12
PUMP	495.	43.75

FIGURE 460. TYPE 3 SSFAN OUTPUT

**** SSFAN PARALLEL PUMP TEST FOR 2 F-15 HYDRAULIC PUMPS AND UTILITY MANIFOLD **

PUMP AND RESERVOIR DATA

	PUMP						RESERVOIR		
	PRESSURE PORT		CASE DRAIN PORT		SUCTION PORT		RESERVOIR PRESSURES	RESERVOIR FLOWS	
PRESSURE PORT	PRESSURE (PSIG)	FLOW (GPM)	PRESSURE (PSIG)	FLOW (GPM)	PRESSURE (PSIG)	FLOW (GPM)	PRESSURE (PSIG)	FLOW-IN (GPM)	FLOW-OUT (GPM)
15.	2873.62	44.67	55.53	-.43	37.12	45.10	51.00	.00	-.00
500.	3033.02	2.93	55.85	-.07	43.75	3.50	51.00	.00	-.00

FIGURE 461. TYPE 4 SSFAN OUTPUT

Table 28 lists the comparison between the SSFAN simulation and the measured test data. The computer results indicate good correlation with the test data. However, the computed pump case pressures are about 25 psi lower than the measured data.

TABLE 28.
SSFAN TWO PUMP SYSTEM SIMULATION MEASURED VERSUS COMPUTED DATA

Parameter	Location	Measured	Computed
P1*	Pump #1 Outlet	2880	2873
P2	Pump #2 Outlet	3030	3033
P3	Downstream of Filter Manifold	2800	2800
P4	Filter Bowl	2820	2800
P5	Downstream of 30 Ft Tube	2760	2746
P6	Pump #1 Case Drain	80	55.53
P7	Pump #2 Case Drain	88	55.85
PS	Suction Pressure at Tee	42	43.81
PC	Pump #2 Actuator	750	-
PP	Pump #2 Manifold	3040	3033
Q_1	Downstream of Solenoid Valve	47	47.6
Q_2	Pump #1 Case Drain Flow	.55	.43
Q_3	Pump #2 Case Drain Flow	.5	.57

* NOTE: Pressures are in PSIG and flow in GPM

b. Conclusions - SSFAN simulation of the two pump test system correlated well with the test data. Some modifications were made to the pump model to handle the master-slave relationship. Although the changes had to be made by the user, they were relatively minor.

SECTION VII

THERMAL VERIFICATION TESTS

Thermal testing was performed on four elements and the F-15 iron bird utility speed brake system. The components test were the F-15 instrumented pump, a 1" dia x 30' line, a simple restrictor, and a F-4 utility heat exchanger. The test procedures, test bench set-up and computer verification are discussed in the following sections.

1. THERMAL LINE MODEL VERIFICATION

The line transient thermal tests were run on a one inch O.D. stainless steel tube approximately 380 inches long with eight thermocouples. T1 through T8 were taped with asbestos to the exterior of the line as shown in Figure 462. Two pressure transducers, P1 and P2 were located at either line end to record the upstream and downstream pressures for the computer simulation. An increase in the temperature measurement error resulted because the thermocouples were not welded to the line. Seven tests runs were made at various conditions, as indicated in Table 29. The tests were run to show the cooling down of the fluid and the amount of heat generation involved due to friction. Only two basic flow rates were used, 10 cis and 38.5 cis while the pressures remained constant and the inlet fluid temperatures, T1 from the data, to the system was varied to obtain the transient.

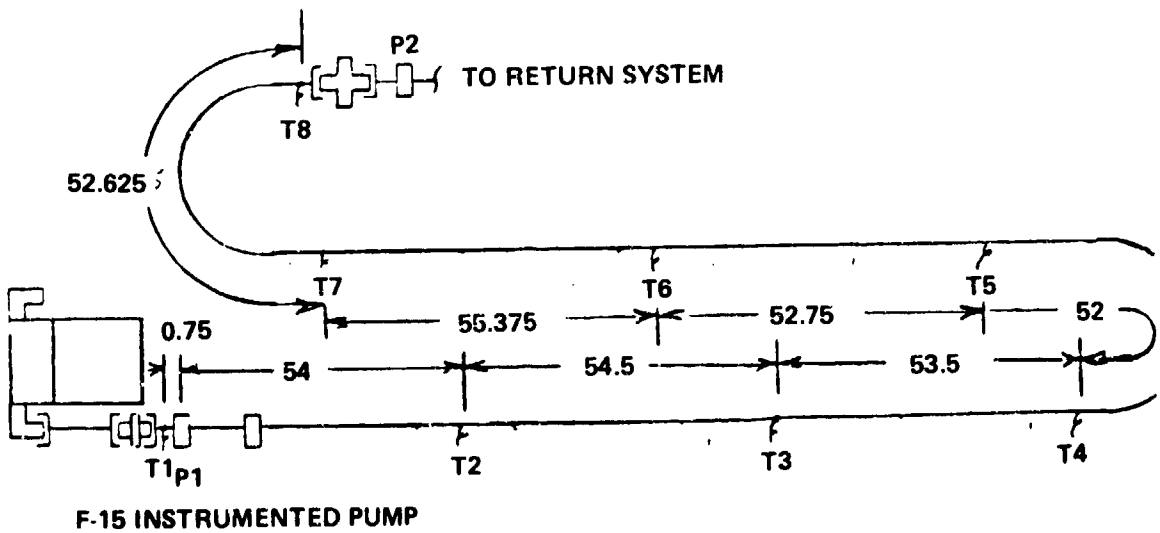

FIGURE 462. THERMAL LINE TEST CONFIGURATION

TABLE 29. THERMAL LINE TEST CONDITIONS

RUN NUMBER	TEST CONDITION	P1 PRESSURE (PSI)	P2 PRESSURE (PSI)	FLOW RATE (CIS)	AMBIENT TEMPERATURE (°F)
78-01-XX	Steady State	3004	3001	38.5	80
78-02-XX	Steady State	2996	2994	10	82
78-03-XX	Steady State	3007	3004	38.5	82
78-04-XX	Steady State	3006	3004	10	84
78-05-XX	Temp. Rise 80-120°F	3004	3001	38.5	82
78-06-XX	Temp. Rise 80-120°F	3004	3001	10	82
78-07-XX	Temp. Rise 80-120°F	3008	3005	38.5	85

XX - denotes recorded value

a. Computer Simulation with Line Test Data - The line was simulated in HYTTHA by the Subroutine TLINEA. In the program the pump was simulated by a constant pressure variable temperature component, TTEST91. At this point, upstream of the line, the fluid temperature transient from the data, T1, is input to the line. At the downstream point of the lines, the program uses a constant pressure, constant temperature reservoir, TRSVR61.

The actual areas, distances, heat transfer coefficients, etc., needed to be accurately measured for correct input in order to obtain an accurate computer model simulation, are shown in Figure 463.

Figure 464 shows the input test data, T1, (the solid line) that was input to the program.

Figure 465 compares the simulation of the data at location T2, with the temperature T2 data being the solid line. As shown the same computed slope occurs as T1 but the data reaches a higher end value. In comparing the T2 measured data with the input T1 data, a bad comparison is obtained. T2 shows the fluid increasing at least 7-8°F in approximately 50 inches of the line. This can't actually happen since there is no mechanism in the line to accomplish the temperature rise. The computed T2 temperature closely resembles the T1 data as it should. The T2 thermocouple therefore must be in error and the computed information looks correct.

RUN NUMBER 78-05

***** TEST OF THERMAL TRANSIENT PROGRAM ***** (DTTHERM)

THE THERMAL TRANSIENT RESPONSE IS FROM T=0.0 TO T= 200.000 SECONDS AT TIME INTERVALS OF DELT= .20300
WITH OUTPUT POINTS PLOTTED AT INTERVALS OF , 2.00000 SECONDS

FLUID DATA FOR FOR MIL-H-5606B WITH A VAPOR PRESSURE OF 2.0 PSI

LINE DATA LINE NO.	LENGTH	INTERNAL DIA	WALL THICKNESS	DELTAX	AMBIENT TEMP	STRUCTURE TEMP	FLUID TEMP	MATERIAL TYPE
1	400.0000	.HP40	.0500	100.0000	78.0000	78.0000	84.0000	9

COMP#, 1 INTEGER DATA	1	91	0	-1	1	0	0	0	0	0	0	0	0	0	0	0	0	
COMP#, 2 INTEGER DATA	2	61	1	1	0	0	0	0	0	0	0	0	0	0	0	0	0	

REAL DATA CARD # 1 .3000E+04 .8000E+02 .8000E+02 0. 0. 0. 0. 0.

FIGURE 463. RUN 78-05 HYTTHA INPUT DATA

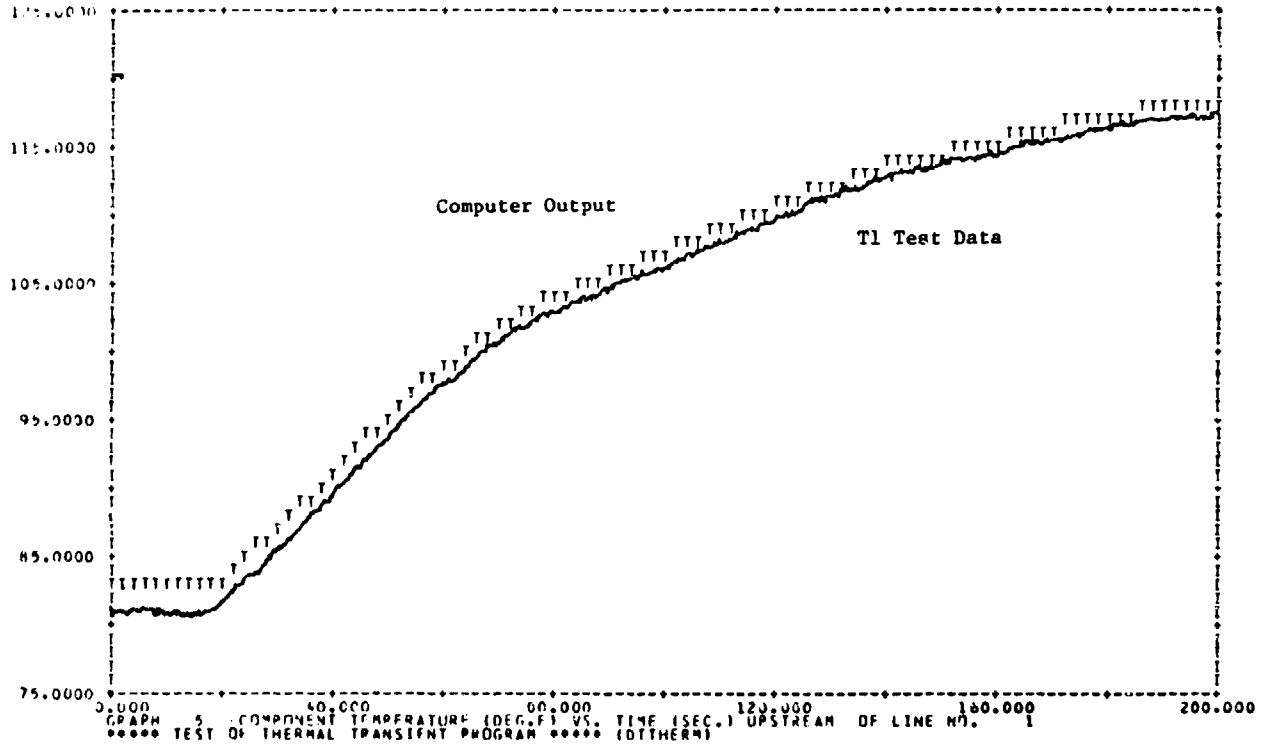

FIGURE 464. 78-05-T1 INPUT TEST DATA

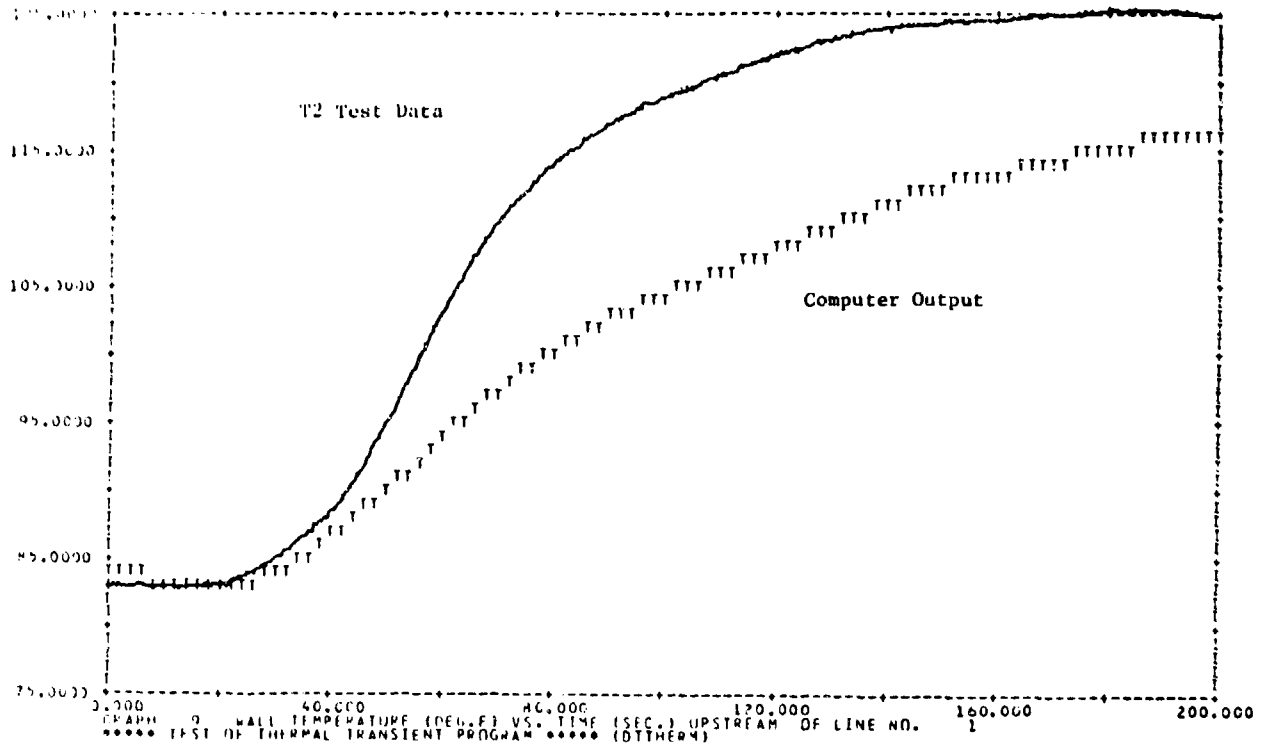

FIGURE 465. 78-05-T2 THERMAL TRANSIENT

Figures 466 and 467 show a comparison of the T7 location data temperature (solid lines) and the computed temperatures (the T's) at that same simulated location. Both the wall and fluid temperatures from the simulation (the T's) show good comparison to the data. These two temperatures may be a little low since the external temperature in the test was 78°F while the actual measured value was 82°F. The initial temperature is slightly above the input temperature with no measurable friction incurred and lower external temperatures. This seems to indicate a faulty thermocouple, making the data too high.

Reasonable results were obtained when considering the actual test conditions and comparing the calculated temperatures to input temperature.

For the next simulation, the computed input to HYTTHA is shown in Figure 468 with the test data in Figure 469.

Figures 470 and 471 compare the computer line simulation with the data at location T2, with the temperature data T2 being the solid line in each case. These two figures indicate that the wall and the fluid both respond similar to the data but at a slower rate and a lower final

temperature. Comparing the data in these two figures to the input data in Figure 469 there is no way the data in the later two (Figures 470 and 471) could reach 233°F when the input data only reaches 228°F and the external conditions are at 85°F (78°F in simulation). The error is in the measurement of the data, because no physical mechanism in the line can account for the 5°F temperature rise. The computer simulation is modeling the temperatures correctly.

In Figures 472 and 473 of the computed temperatures react somewhat slower and reach a lower final temperature than the measured data. The data for the line shows an increase from 228°F at t = 0 to 233°F at 375 seconds and down again to 228°F at the end. Since the beginning temperature is 228°F the final should be somewhat lower, nearer the calculated values. The overall response of the calculated line temperature values seem to be a good representation of the actual test conditions.

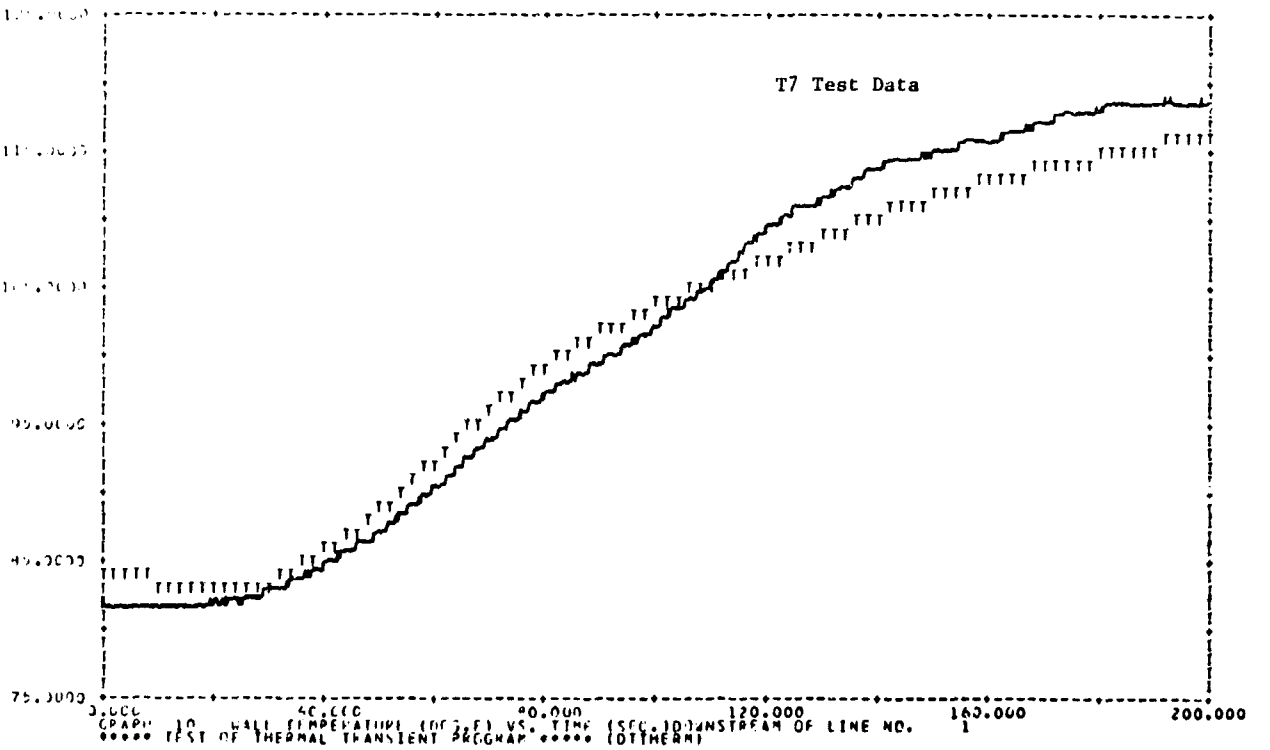

FIGURE 466. 78-05-T7 THERMAL TRANSIENT, WALL, TEMPERATURE

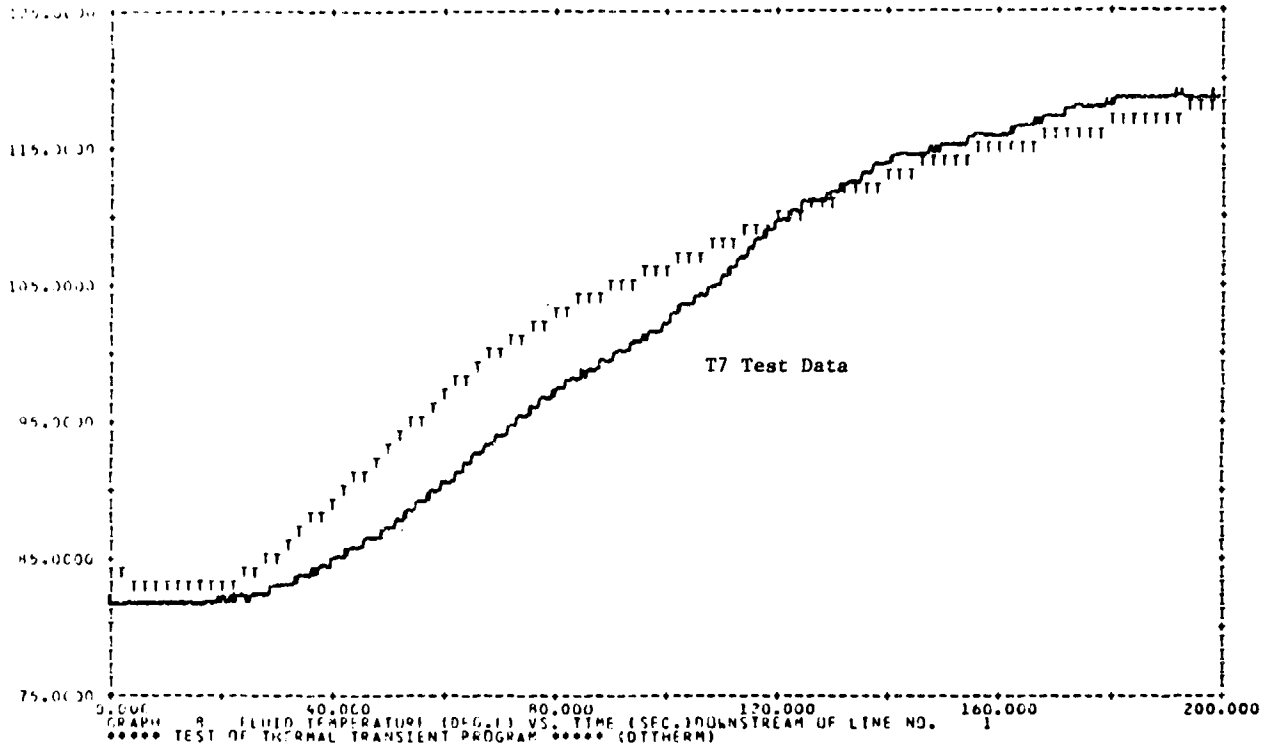

FIGURE 467. 78-C5-T7 THERMAL TRANSIENT, FLUID TEMPERATURE

RUN NUMBER 78-07

***** TEST OF THERMAL TRANSIENT PROGRAM ***** (DRTHERM)

THE THERMAL TRANSIENT RESPONSE IS FROM T=0.0 TO T= 500.000 SECONDS AT TIME INTERVALS OF DELT= .50000
WITH OUTPUT POINTS PLOTTED AT INTERVALS OF , 5.00000 SECONDS

FLUID DATA FOR MIL-H-5606B WITH A VAPOR PRESSURE OF 2.0 PSI

LINE DATA

LINE NO.	LENGTH	INTERNAL DIA	WALL THICKNESS	DELTAX	AMBIENT TEMP	STRUCTURE TEMP	FLUID TEMP	MATERIAL TYPE
1	400.0000	.4840	.0580	100.0000	76.0000	76.0000	84.0000	9

COMP= 1 INTEGER DATA 1 91 0 -1 1 0 0 0 0 0 0 0 0 0 0

COMP= 2 INTEGER DATA 2 61 1 1 0 0 0 0 0 0 0 0 0 0 0

REAL DATA CARD # 1 .3020E+04 .6000E+02 .4000E+02 0. 0. 0. 0. 0.

FIGURE 468. RUN 78-07 HYTTHA INPUT DATA

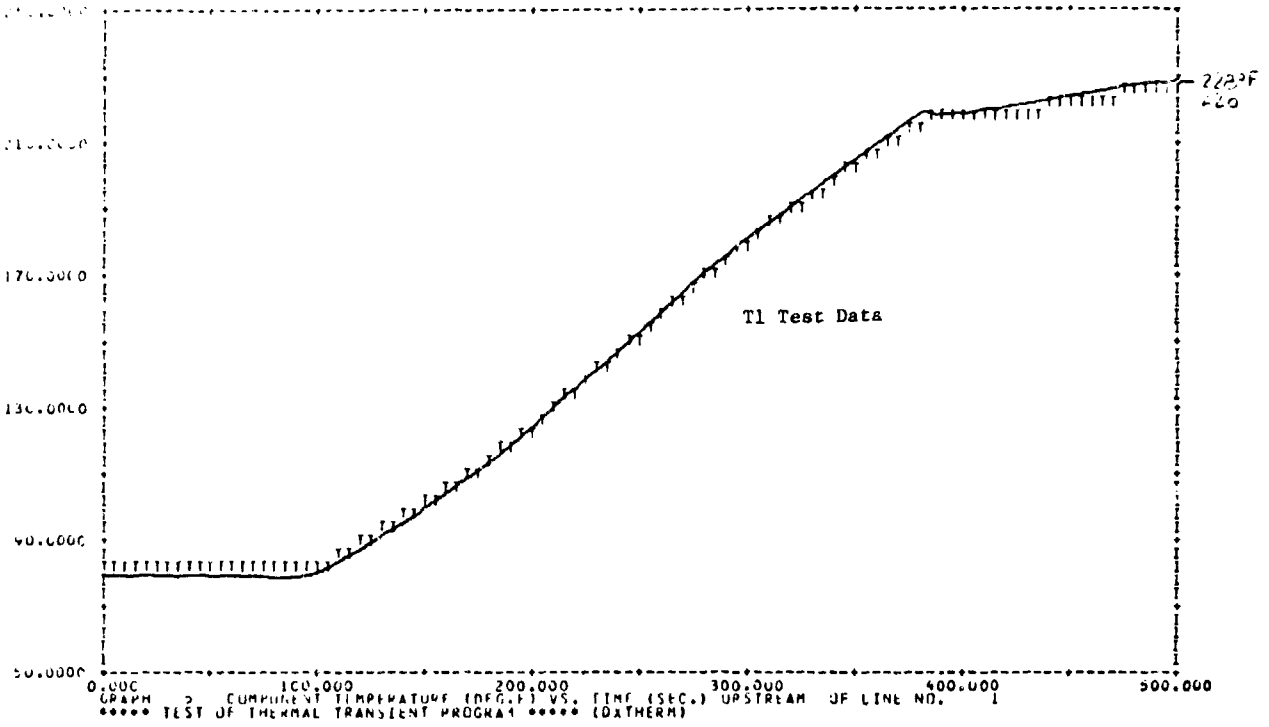

FIGURE 469. 78-07-T1 INPUT TEST DATA

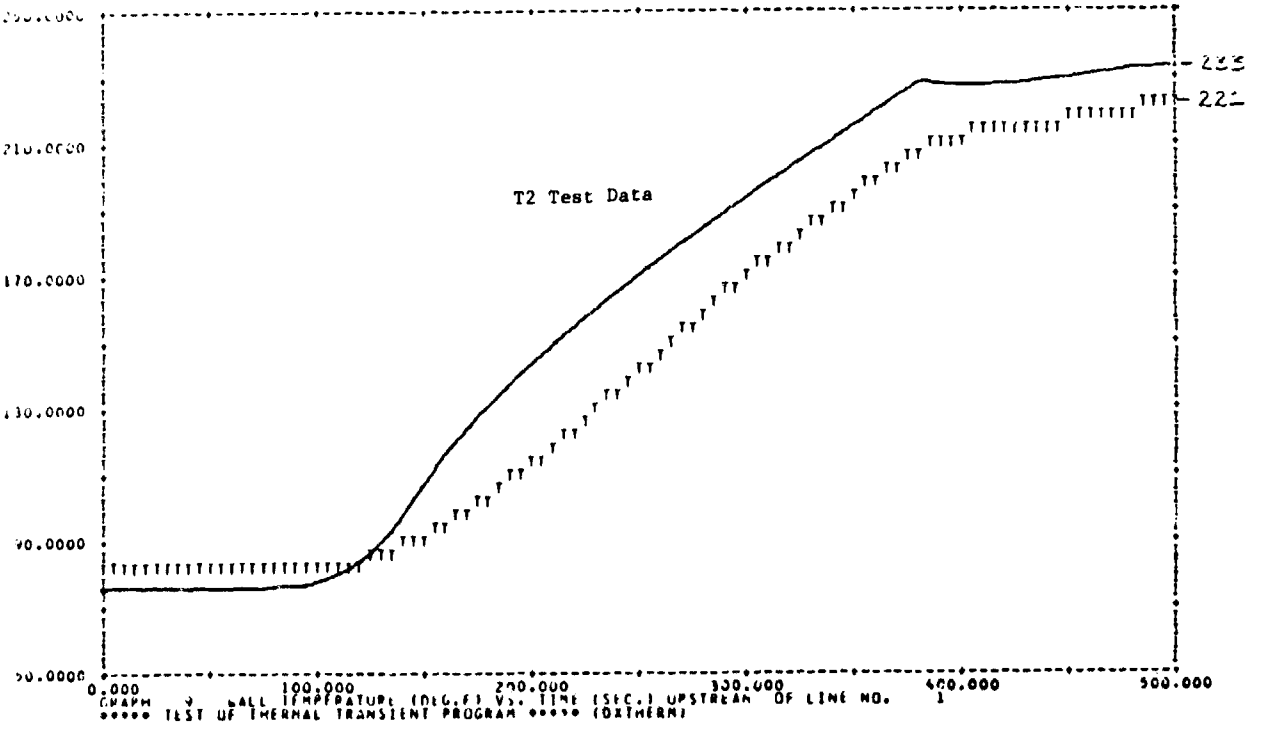

FIGURE 470. 78-07-T2 THERMAL TRANSIENT, WALL TEMPERATURE

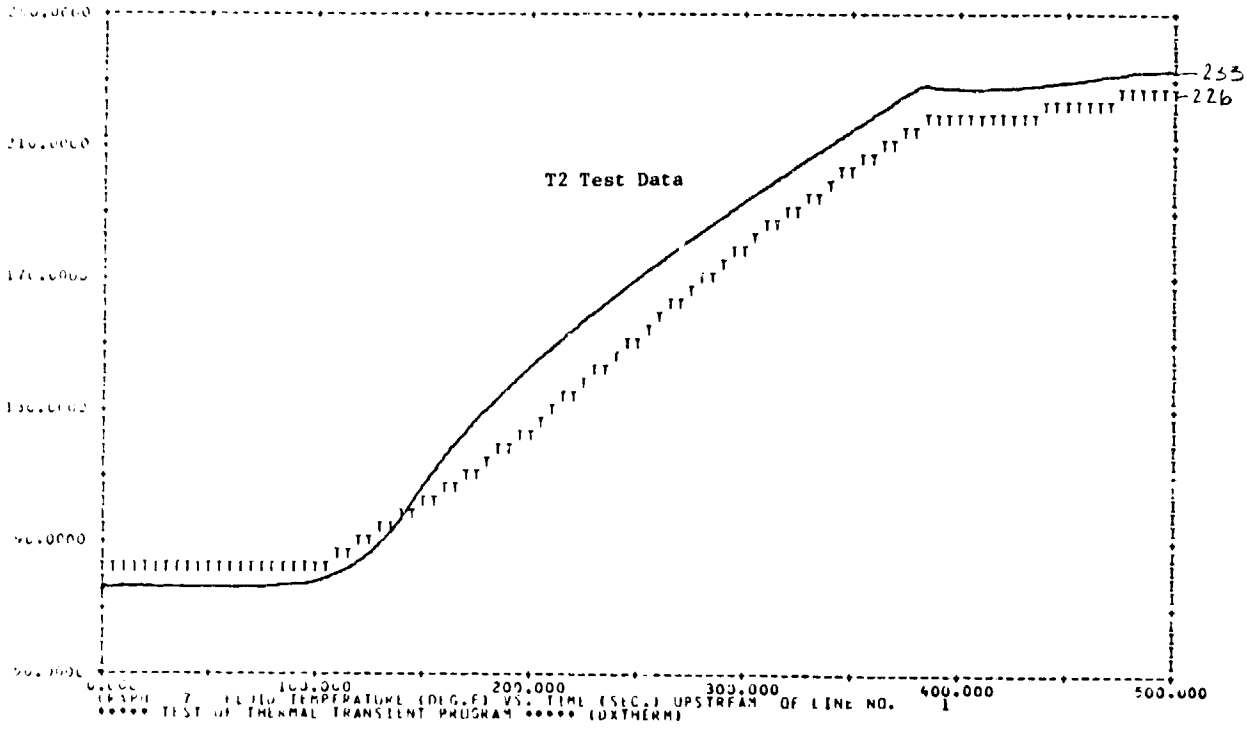

FIGURE 471. 78-07-T2 THERMAL TRANSIENT, FLUID TEMPERATURE

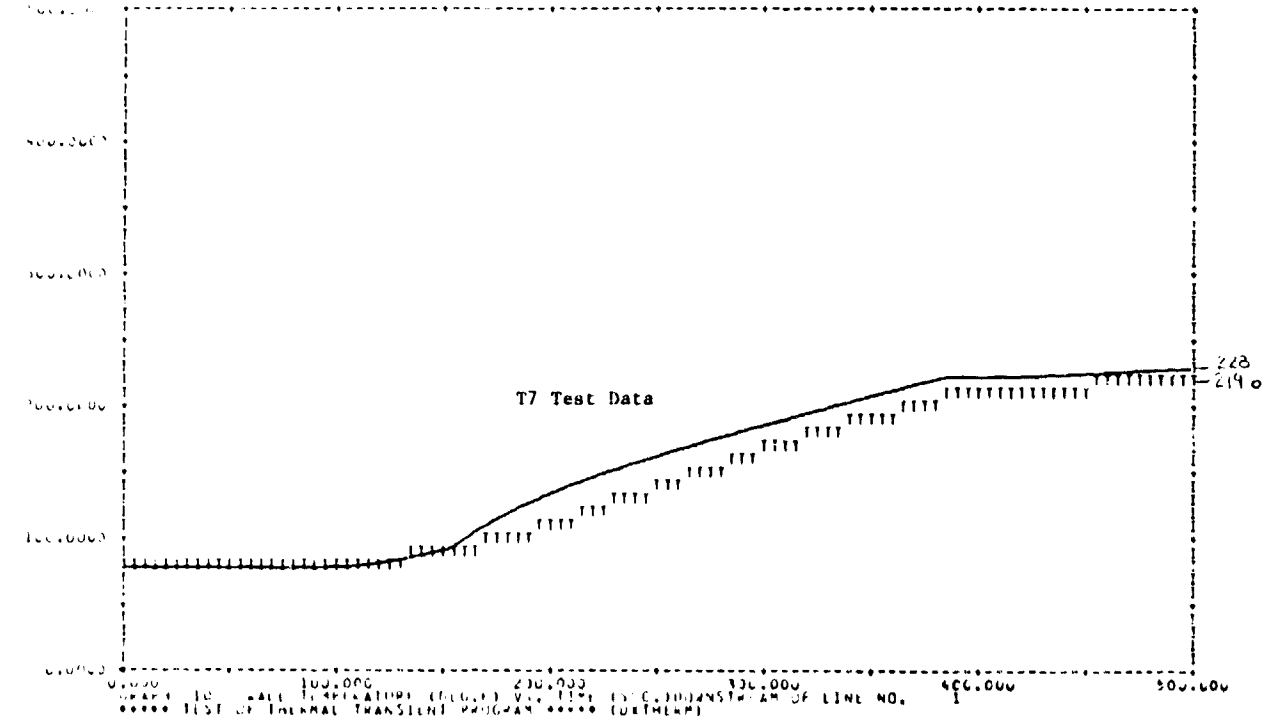

FIGURE 472. 78-07-T7 THERMAL TRANSIENT, WALL TEMPERATURE

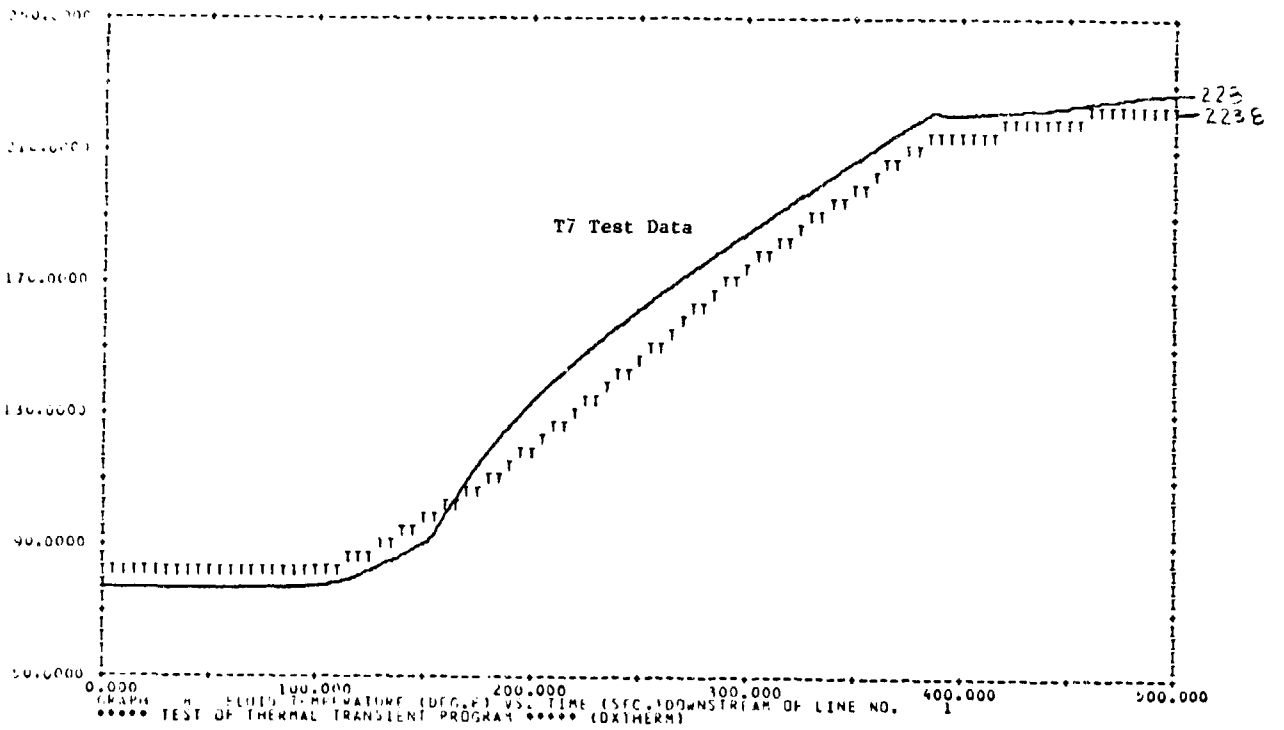

FIGURE 473. 78-07-T2 THERMAL TRANSIENT, FLUID TEMPERATURE

b. Conclusions - The thermal line model adequately predicted the temperature distribution in the tested line sections. Verification has been accomplished for the data presented in this report. Test data is not concurrently available to verify the line model over a wide range of temperature conditions.

2. THERMAL RESTRICTOR MODEL VERIFICATION

The restrictor thermal tests were run on 1/2 inch lines with a .094 inch diameter orifice restrictor between the two lines, as shown in Figure 474. Eight temperatures, T1 through T8, and three pressures, P1 through P3, were recorded during the tests and used for the computed simulation. The temperatures were recorded using thermocouples that were welded then covered with asbestos tape to their respective locations. Thermocouple No. T5 was inserted into the restrictor body and covered with the tape, as shown in Figures 474 and 475. The temperature transient was generated by cycling a thermal relief valve to a heat exchanger in the return system. The pressure source was the F-15 instrumented pump.

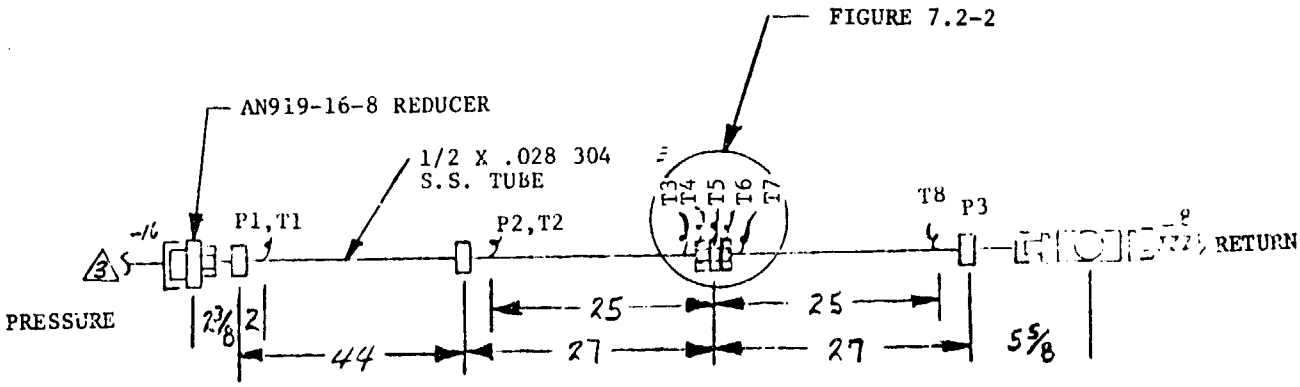

FIGURE 474. RESTRICTOR TEST CIRCUIT

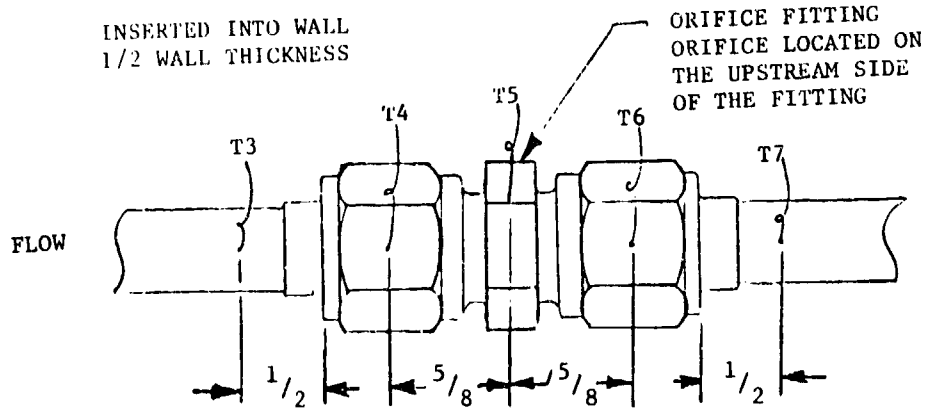

FIGURE 475. RESTRICTOR INSTRUMENTATION FOR THERMAL TESTS

TABLE 30.

RESTRICTOR TEMPERATURE EFFECTS TEST

RUN NUMBER	TEST CONDITION	PUMP PRESSURE	RESERVOIR PRESSURE	SYSTEM FLOW	EXTERNAL TEMPERATURES	INITIAL FLUID TEMPERATURES
87-01-XX	Steady State T1	2950	50	38.5CIS	78°F	85°F
87-02-XX	Temp Transient Amb 130°F T1	2950	50	38.5CIS	78°F	85°F
87-03-XX	Temp Transient Amb 210°F T1	2950	50	38.5CIS	76°F	84°F
87-04-XX	Temp Transient Amb 130°F T1	2950	50	38.5CIS	76°F	84°F
87-05-XX	Steady State T1	2900	110	36.5CIS	78°F	85°F
87-06-XX	Temp Transient Amb 130°F	2900	110	36.5CIS	78°F	85°F
87-07-XX	Temp Transient Amb 210°F T1	2850	60	36.5CIS	78°F	84°F

* - XX denotes measured data parameters

Table 30 contains an itemized account of the temperature, pressure and flow conditions for each of the restrictor tests. The test conditions at various steady state and warm up temperatures were established to look at the temperature response of different line and restrictor locations. The up and downstream pressure and flow rates were held between pressure differentials of 2900 and 3800 psi and flow rates of 38.5 and 36.5 cis. For the warm up tests the fluid temperature leaving the pump supplied the thermal transient to the line and restrictor system. The initial fluid temperatures started at atmospheric temperature.

a. Computer Simulation with Restrictor Test Data - The computer simulation of the test runs were done with the HYTTHA restrictor model, TREST41, and the line model (TLINEA). The upstream boundary conditions were input via the component TTEST91. The downstream

component was a constant pressure and temperature reservoir TRSVR61.

The computed input data to HYTTHA is shown in Figure 476 and 484 for two different simulations of the same data. The difference in the two simulations were external temperatures, initial temperatures, the mass of the restrictor was lowered by .01 pounds and the external heat transfer coefficient was changed from .0075 to .0069 WATTS/IN^2-°F. These were done to see what changes were most affecting the restrictor walls. Temperature T1 from the test data, in Figure 477, was used as the transient input to the system with the system configuration data in Figure 476.

The upstream line wall and fluid temperatures from the program very accurately simulate the actual T2 test data as shown in Figures 478, 479, 485 and 486. The computed wall temperatures are a little lower than the data (1-2°F) while the fluid is right on the data, as should be since in the test the thermocouples were insulated therefore measuring the fluid temperature.

The restrictor walls had several thermocouples installed to observe the temperature gradients in the walls. The computed program treated the restrictor walls as isothermal, and closely resembling the T5 location in the test the heat added to the fluid due to the pressure drop across the orifice was added to the fluid at location T5. The program adds it at location T4. So, as indicated in Figures 480 and 487, temperature T4 data is less than T5 calculated, as should be since T4 is upstream of the generation and only sees the cooler fluid. T4 heats up due to conduction back from T5, but at a slower rate than does T5.

The T5 data also shows a final lower temperature than the calculated temperatures at the same locations. The exterior heat transfer coefficient could be to low to reduce the end temperature, and this can be seen by comparing Figures 480 and 487. Figure 487 has a lower external temperature and a high external heat transfer coefficient therefore reducing the end calculated result.

In Figures 480, 481, 487 and 488 there is an initial lag for the calculated wall temperature versus the data. This may be caused from a high effective mass input, large external heat transfer coefficient or even a low computed calculated internal heat transfer coefficient. Figures 480 and 481 have a larger mass but smaller external heat transfer

coefficient than does the runs in Figures 487 and 488 and the first responds faster. Too large an external surface area could also cause this initial lag, convecting to much heat too fast.

In Figures 480 and 487 temperature T6 is a downstream wall temperature and follows that of T5 but a little lower since it is somewhat downstream of the generation, and has lost some heat to the external atmosphere.

The downstream line wall and fluid temperatures, correspond very well to the T8 data as shown in Figures 482, 483, 489 and 490. Not only does this verify the line subroutine but also helps verify the restrictor model. Since the downstream wall and fluid temperatures could not be correct unless given the correct upstream boundary temperatures; the upstream boundary conditions coming from the restrictor subroutine. So the fluid existing from the restrictor must be nearly correct or the downstream line fluid and wall calculations would differ from the data, which is not the case.

The temperature transient in Figure 491 was used as the input for two computer simulations.

***** TEST OF THERMAL TRANSIENT PROGRAM ***** (DRES761)

THE THERMAL TRANSIENT RESPONSE IS FROM T=0.0 TO T= 500.000 SECONDS AT TIME INTERVALS OF DELT= .50000
WITH OUTPUT POINTS PLOTTED AT INTERVALS OF , 5.00000 SECONDS

FLUID DATA FOR FOR MIL-H-5606B WITH A VAPOR PRESSURE OF 2.0 PSI

LINE DATA LINE NO.	LENGTH	INTERNAL DIA	WALL THICKNESS	DELTAX	AMBIENT TEMP	STRUCTURE TEMP	FLUID TEMP	MATERIAL TYPE
1	72.0000	.4480	.0260	36.0000	80.0000	80.0000	80.0000	9
2	32.0000	.4480	.0260	32.0000	80.0000	80.0000	80.0000	9

COMP#, 1 INTEGER DATA 1 91 0 -1 1 0 0 0 0 0 0 0 0 0 0 0 0

COMP#, 2 INTEGER DATA 2 41 2 1 -2 0 0 0 0 0 0 0 0 0 0 0 0

REAL DATA CARD # 1 .4000E+01 .4200E+00 .1700E+00 .1500F+01 .4500F+01 .6900E-02 .1000E+01 .8000E+02

REAL DATA CARD # 2 .8000E+02 .7200E+02 .7200E+02 .6500E+00 .9400E-01 0. 0. 0.

COMP#, 3 INTEGER DATA 3 61 1 2 0 0 0 0 0 0 0 0 0 0 0 0 0

REAL DATA CARD # 1 .1000E+03 .7800E+02 .7800E+02 0. 0. 0. 0. 0. 0.

38.5 CIS - Steady State Flow Rate

FIGURE 476. RUN 86-06 HYTTHA INPUT DATA, 0.5 SEC. TIME STEP

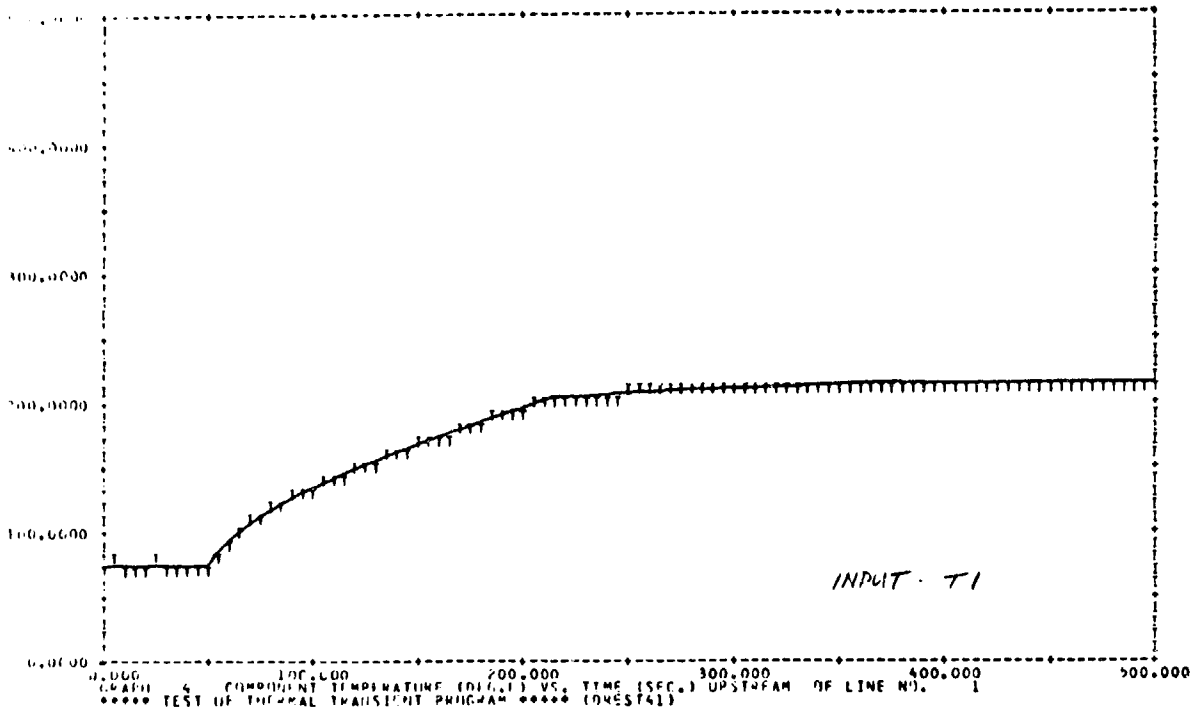

FIGURE 477. 87-06-T1 INPUT TEST DATA

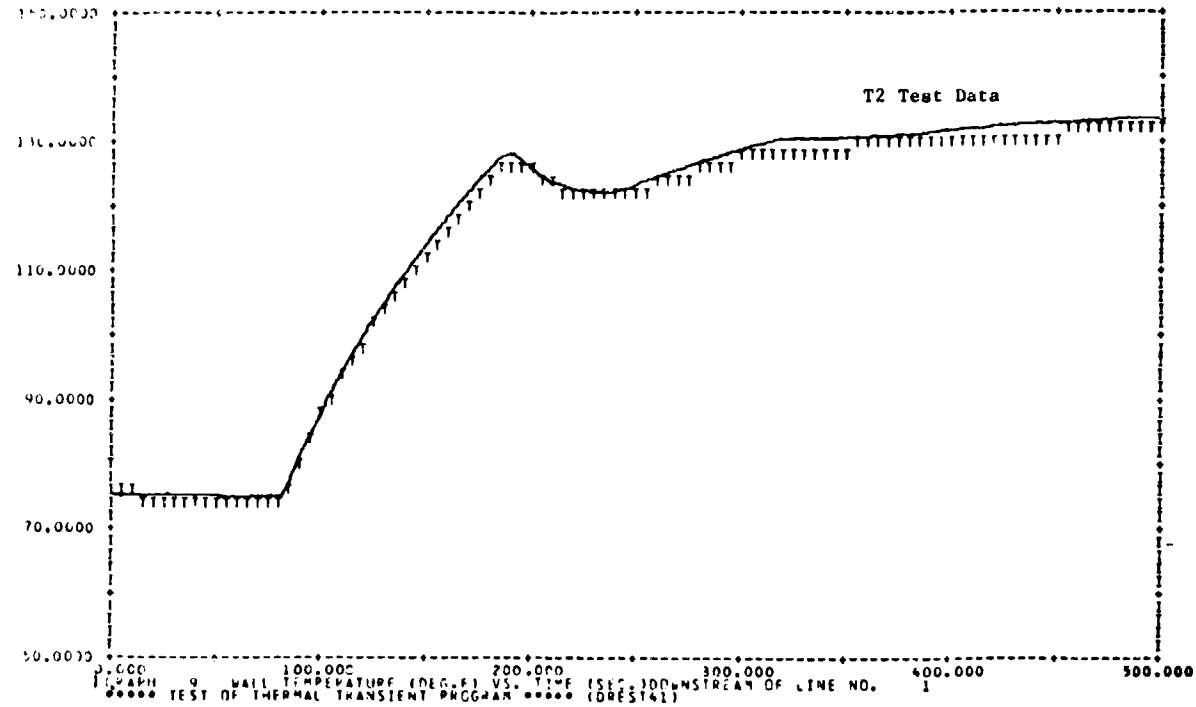

FIGURE 478. 86-06-T2 THERMAL TRANSIENT, WALL TEMPERATURE, 0.5 SEC. TIME STEP

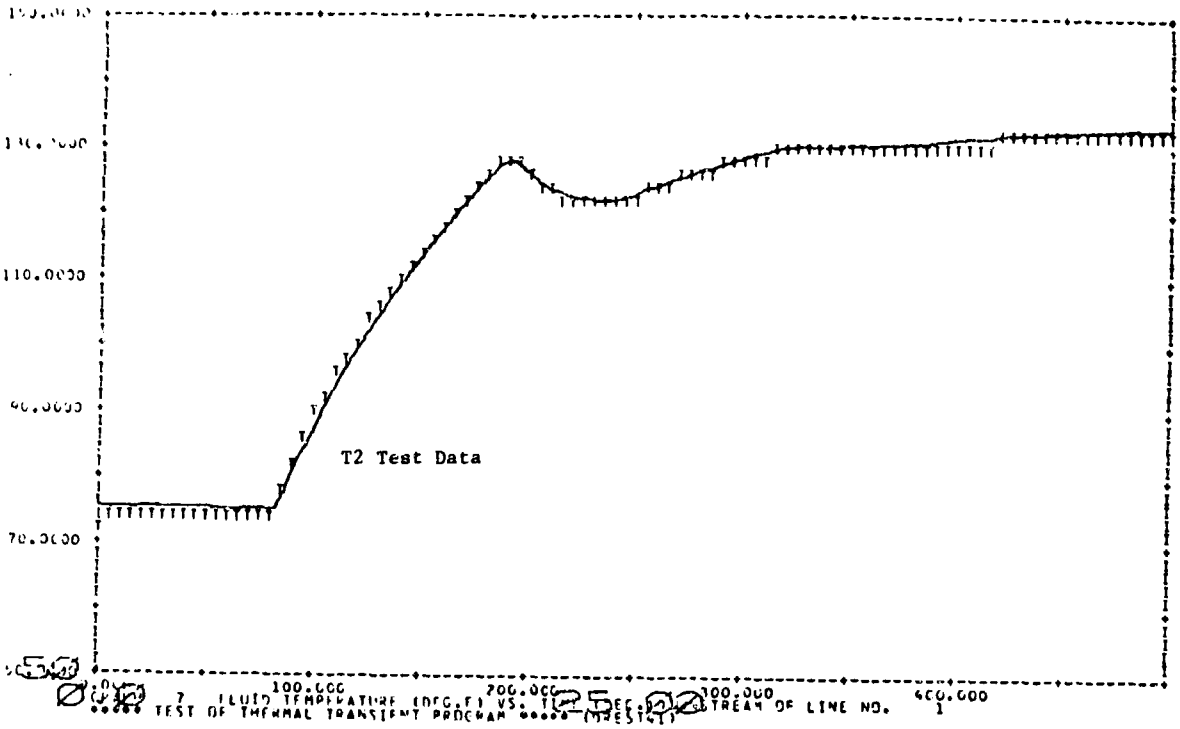

FIGURE 479. 86-06-T2 THERMAL TRANSIENT, FLUID TEMPERATURE, 0.5 SEC. TIME STEP

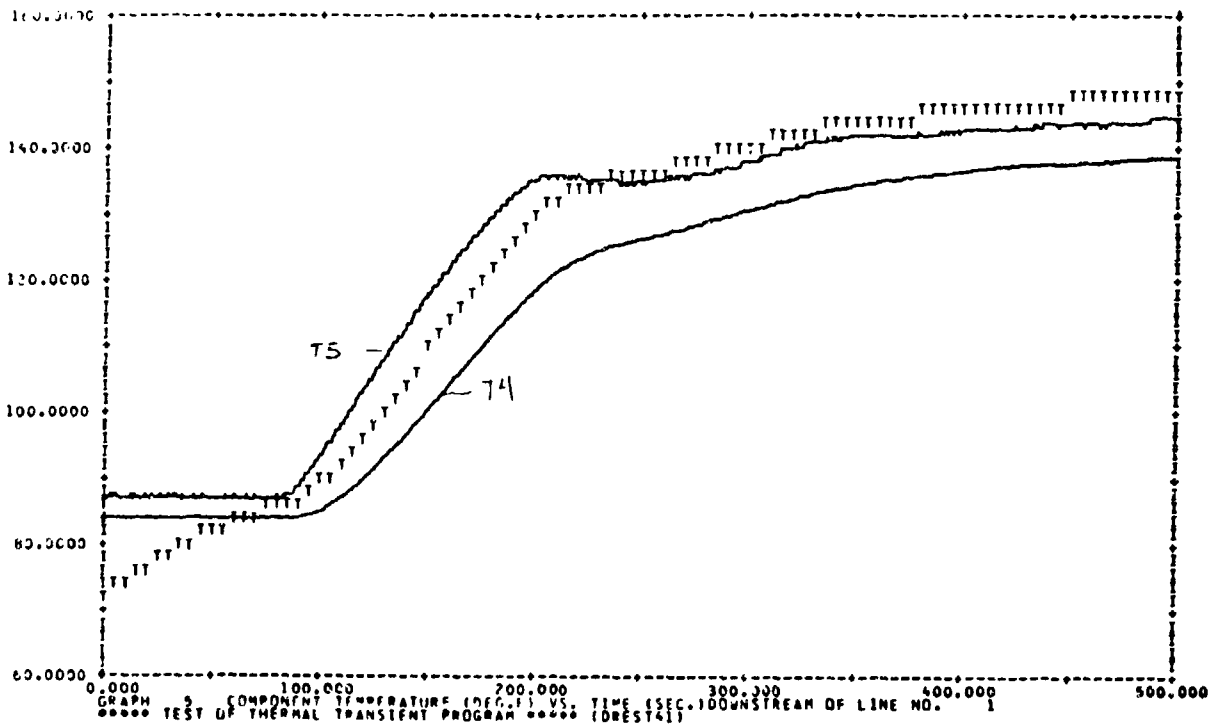

FIGURE 480. 87-06-T4 AND T5 THERMAL TRANSIENT, 0.5 SEC. TIME STEP

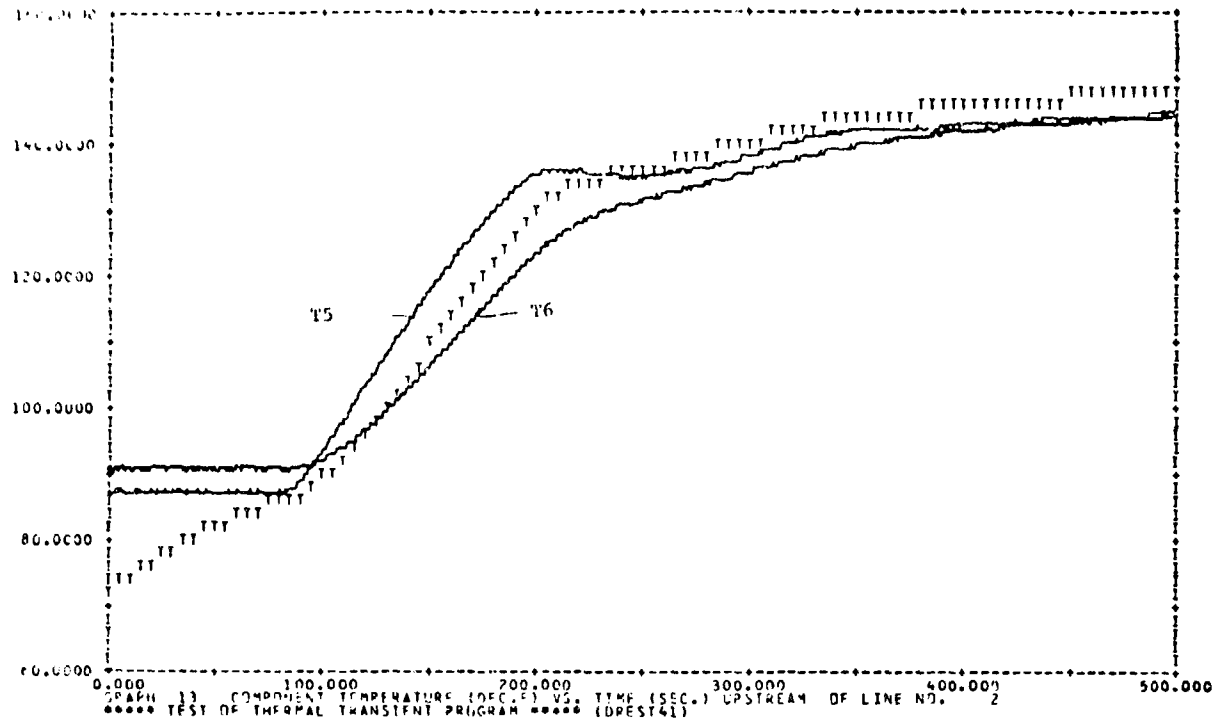

FIGURE 481. 86-06-T5 AND T6 THERMAL TRANSIENT, 0.5 SEC. TIME STEP

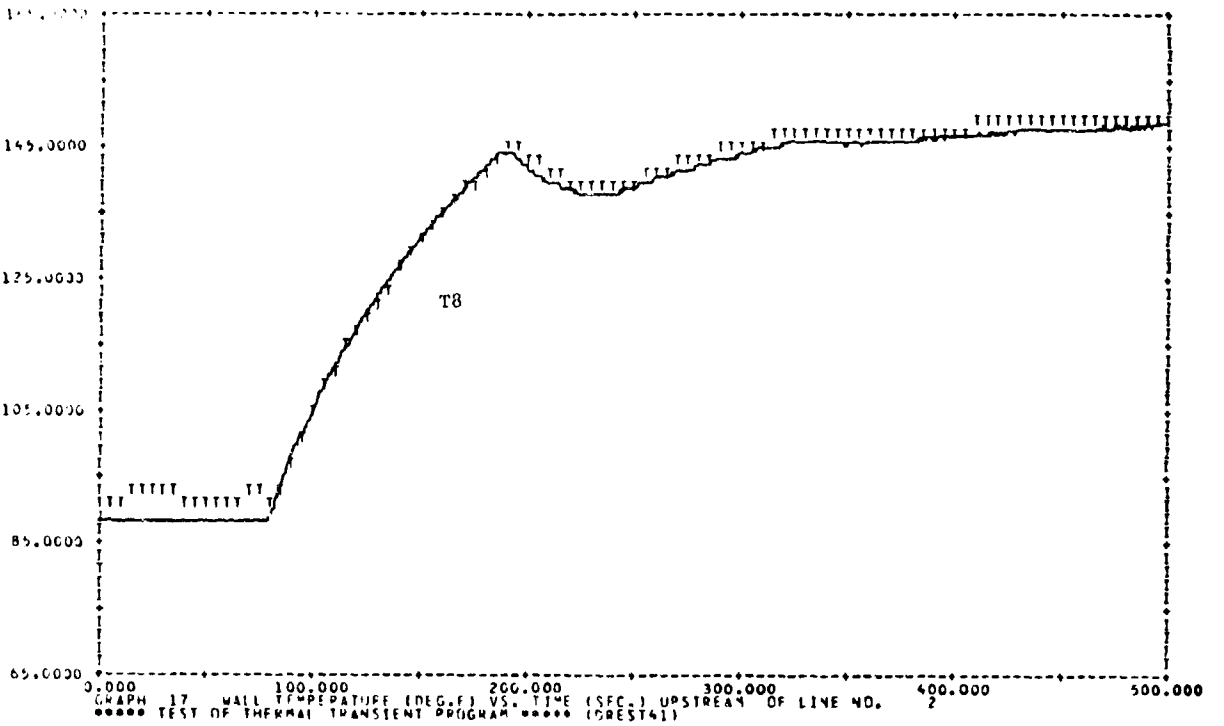

FIGURE 482. 86-06-T8 THERMAL TRANSIENT, WALL TEMPERATURE, 0.5 SEC. TIME STEP

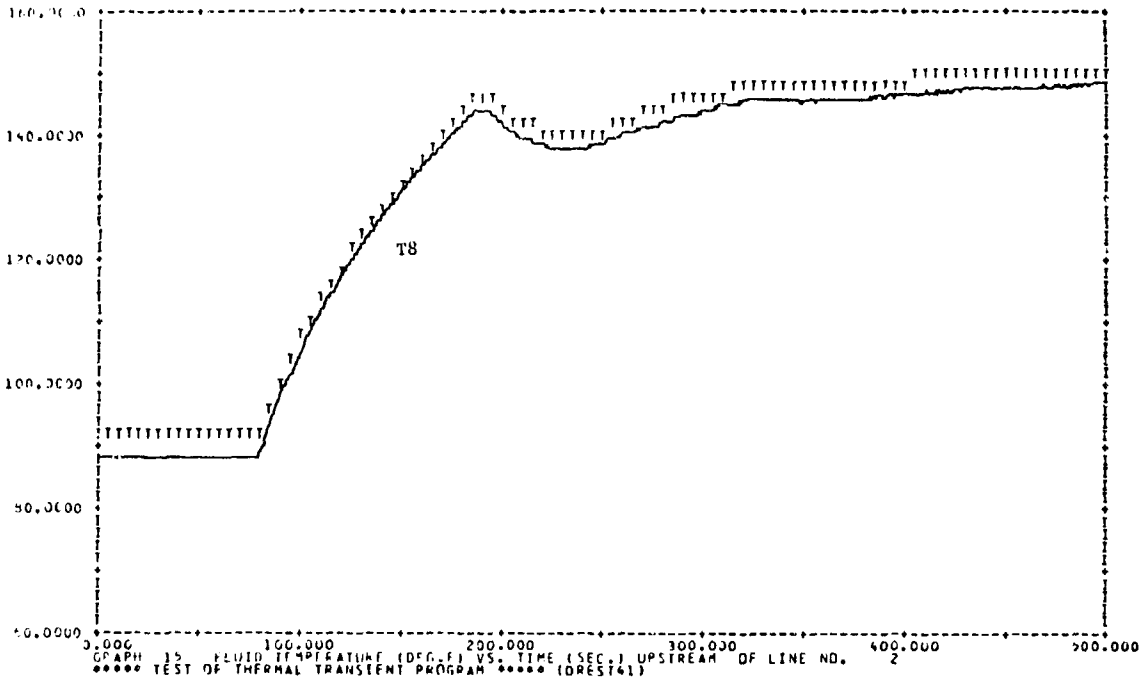

FIGURE 483. 87-06-T8 THERMAL TRANSIENT, FLUID TEMPERATURE, 0.5 SEC. TIME STEP

***** TEST OF THERMAL TRANSIENT PROGRAM ***** (DRES161)

THE THERMAL TRANSIENT RESPONSE IS FROM T=0.0 TO T= 200.000 SECONDS AT TIME INTERVALS OF DELT= .2000
WITH OUTPUT POINTS PLOTTED AT INTERVALS OF , 2.00000 SECONDS

FLUID DATA FOR FOR MIL-H-5606B WITH A VAPOR PRESSURE OF 2.0 PSI

LINE DATA LINE NO.	LENGTH	INTERNAL DIA	WALL THICKNESS	DELTAX	AMBIENT TEMP	STRUCTURE TEMP	FLUID TEMP	MATERIAL TYPE
1	72.0000	.4460	.0260	36.0000	70.0000	70.0000	70.0000	9
2	32.0000	.4460	.0260	32.0000	70.0000	70.0000	70.0000	9

COMP#, 1 INTEGER DATA 1 91 0 -1 1 0 0 0 0 0 0 0 0 0 0 0

COMP#, 2 INTEGER DATA 2 41 2 1 -2 0 0 0 0 0 0 0 0 0 0 0

REAL DATA CARD # 1 .4000E+01 .4160E+00 .1760E+00 .1500E+01 .4500E+01 .7500E-02 .1000E+01 .7600E+02

REAL DATA CARD # 2 .7600E+02 .8500E+02 .8500E+02 .8500E+00 .9400E-01 0. 0. 0.

COMP#, 3 INTEGER DATA 3 61 1 2 0 0 0 0 0 0 0 0 0 0 0 0

REAL DATA CARD # 1 .1100E+03 .7600E+02 .7600E+02 0. 0. 0. 0. 0.

FIGURE 484. RUN 86-06 HYTTHA INPUT DATA, 0.2 SECOND TIME STEP

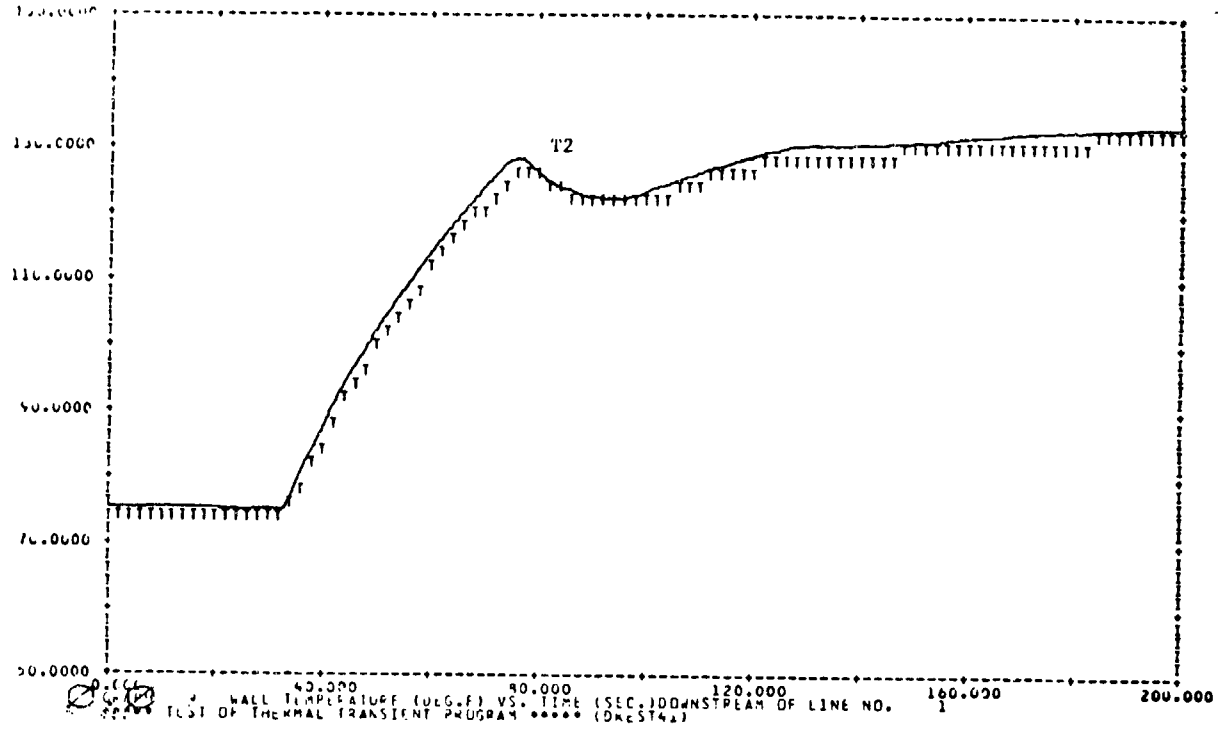

FIGURE 485. 87-06-T2 THERMAL TRANSIENT, WALL TEMPERATURE, 0.2 SEC. TIME STEP

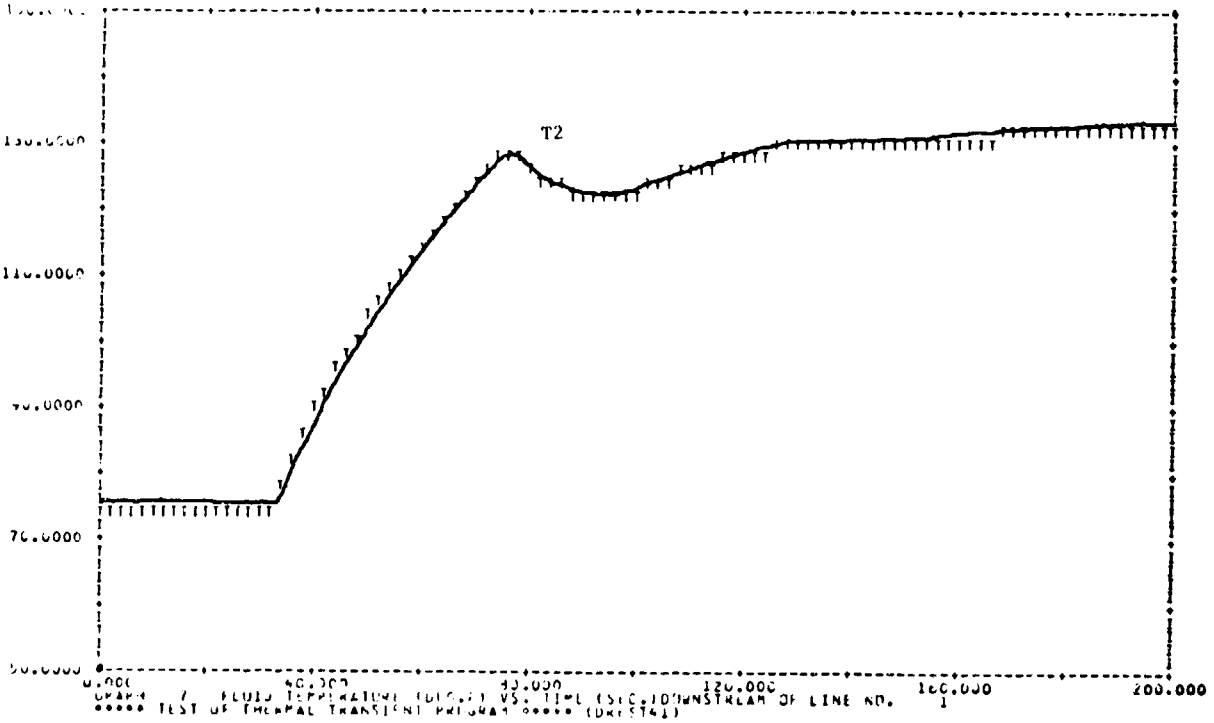

FIGURE 486. 86-06-T2 THERMAL TRANSIENT, FLUID TEMPERATURE, 0.2 SEC. TIME STEP

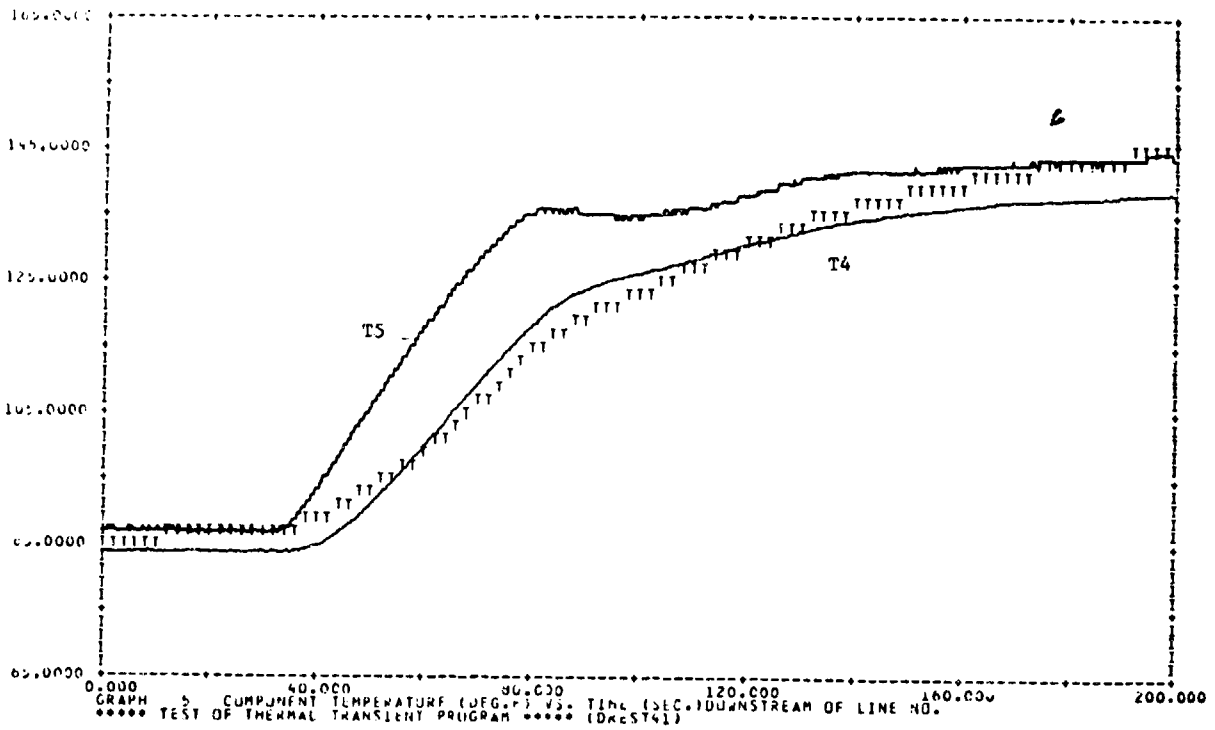

FIGURE 487. 87-06-T4 AND T5 THERMAL TRANSIENT, 0.2 SEC. TIME STEP

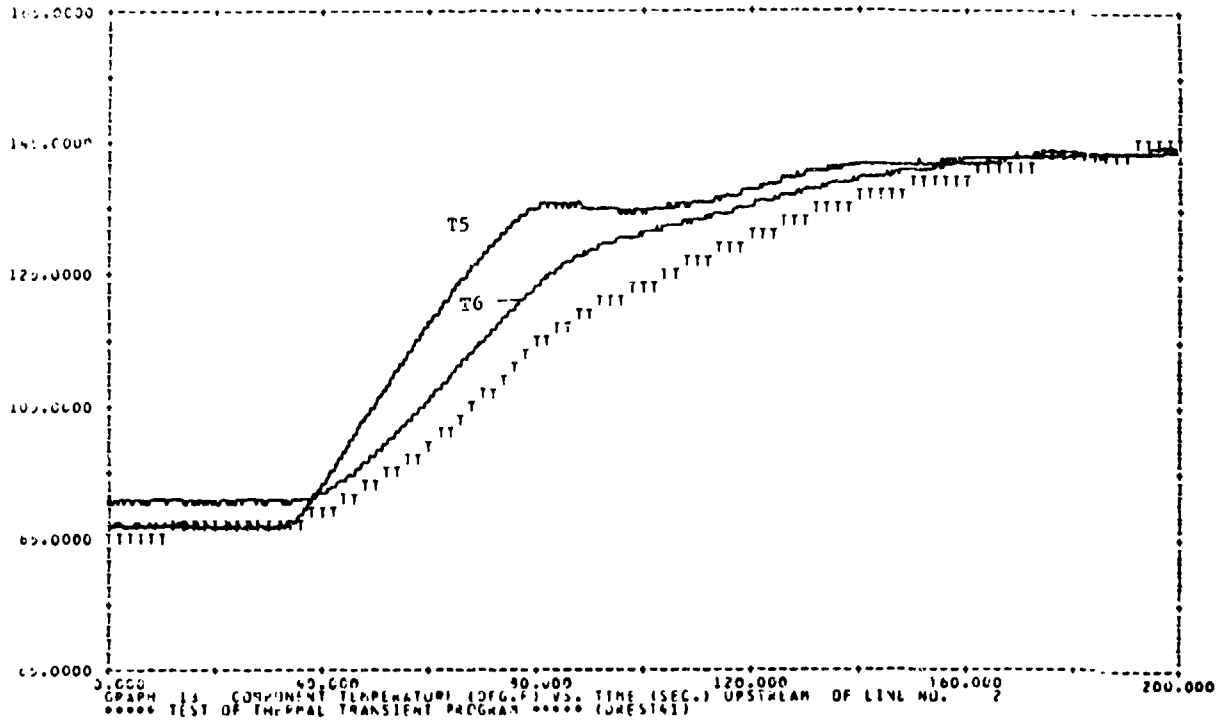

FIGURE 498. 87-06-T5 AND T6 THERMAL TRANSIENT, 0.2 SEC. TIME STEP

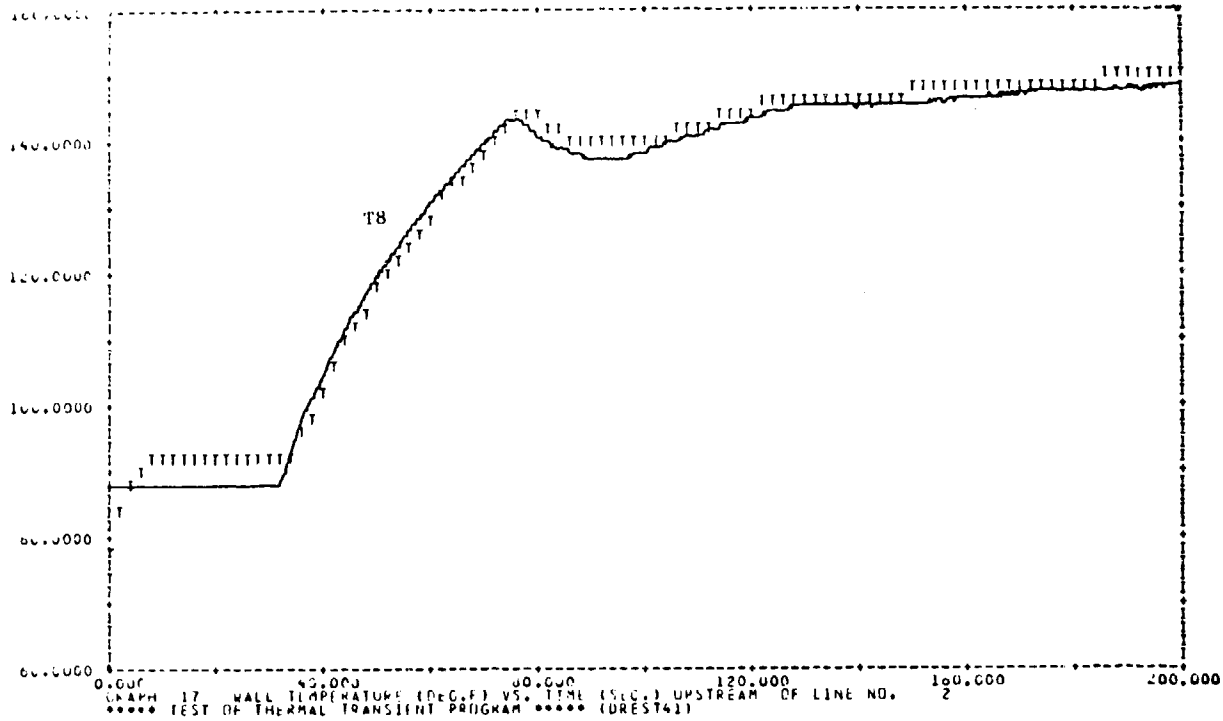

FIGURE 489. 87-06-T8 THERMAL TRANSIENT, WALL TEMPERATURE, 0.2 SEC. TIME STEP

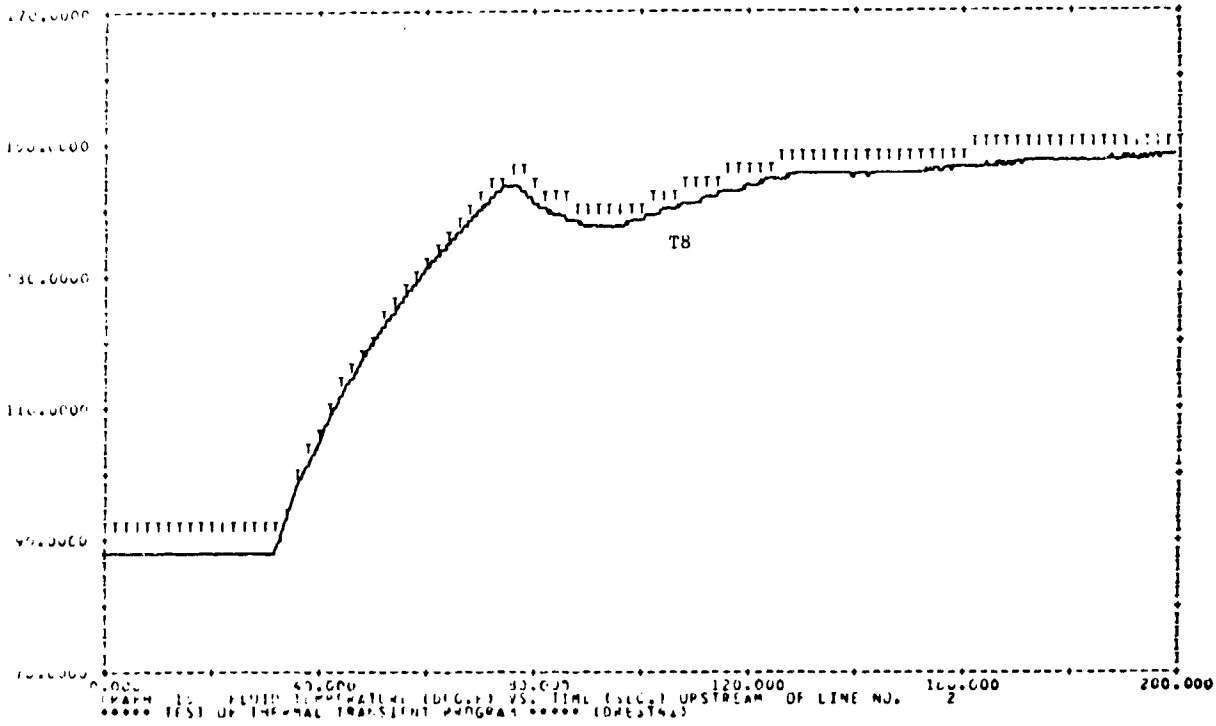

FIGURE 490. 86-06-T8 THERMAL TRANSIENT, FLUID TEMPERATURE, 0.2 SEC. TIME STEP

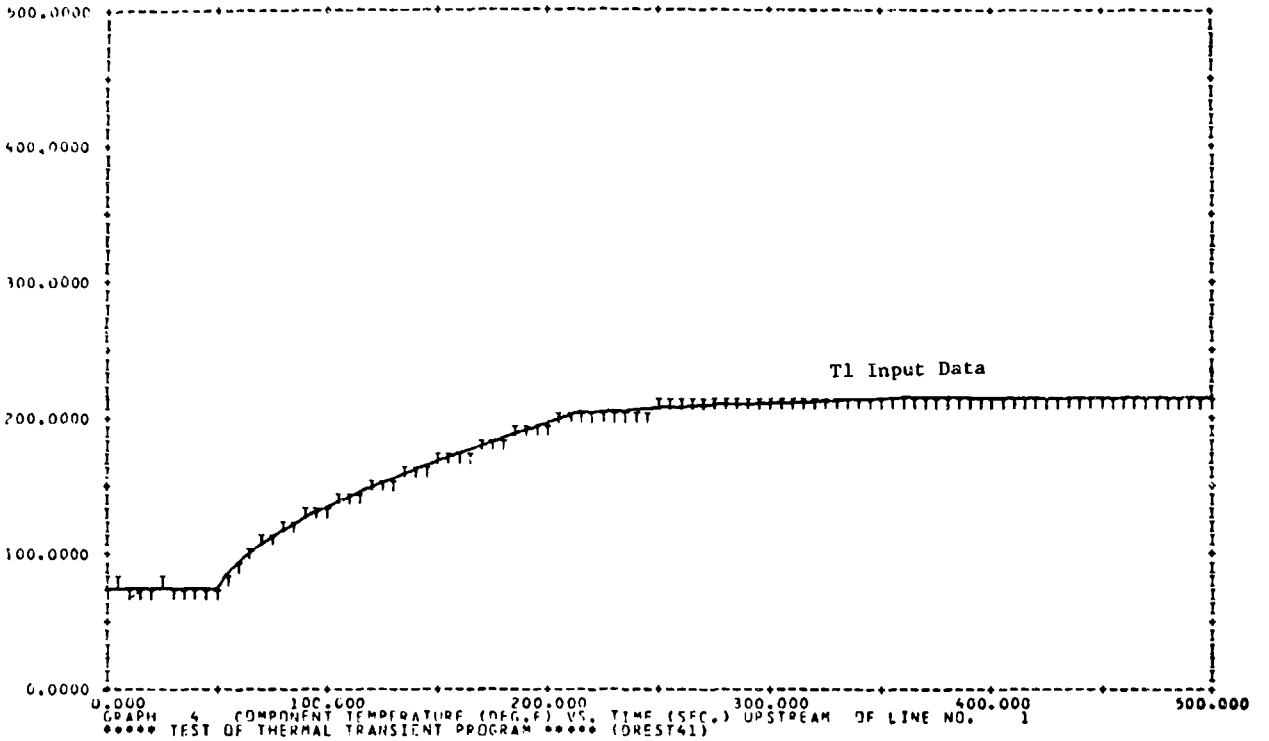

FIGURE 491. 87-07-T1 INPUT DATA

The difference in the two simulations (of the same test data), was that the mass of the restrictor walls has been decreased from .41 pounds to .387 pounds (to see if the wall temperature would respond faster) and the external heat transfer coefficient was increased from .0075 to .018 WATTS/IN^2-°F to try to lower the final temperature of the walls. The input data for the computed simulations are shown in Figures 492 and 499.

The upstream line and fluid temperatures from the program very accurately simulated the actual test data, T2, as shown in Figures 493, 494 and 500. A raise in the external heat transfer coefficients can lower the calculated temperatures including final temperature while increasing the wall mass increases the reaction time and total temperature of the walls, as seen when comparing Figures 495 to 501. Averaging the data temperatures, T4, T5 and T6 will bring the data closer to the calculated values from the program. The most accurate way to verify the restrictor model is to consider the wall as being isothermal as in the HYTTHA restrictor model.

The calculated downstream line wall and fluid temperature hit the data very accurately as shown in Figures 497, 498, 503 and 504 not only verifying

the line subroutine, TLINEA, but also verifying the restrictor subroutine, TREST41, since the upstream boundary condition for the line is the exit restrictor fluid temperature, so for the line to be correct the restrictor first must be correct.

Even though the restrictor wall does not respond as quickly as the data, it finally reaches the correct end temperature.

```
***** TEST OF THERMAL TRANSIENT PROGRAM ***** (TREST41)

THE THERMAL TRANSIENT RESPONSE IS FROM T=0.0 TO T= 900.000 SECONDS AT TIME INTERVALS OF DELT= .05000
          WITH OUTPUT POINTS PLOTTED AT INTERVALS OF  ,  5.00000  SECONDS

FLUID DATA FOR  FOR MIL-H-5606B          WITH A VAPOR PRESSURE OF      2.0 PSI

LINE DATA
LINE NO.     LENGTH      INTERNAL DIA      WALL THICKNESS      DELTAX      AMBIENT TEMP      STRUCTURE TEMP      FLUID TEMP      MATERIAL TYPE
    1        72.0000          .4480             .0260          36.0000          70.0000           70.0000          75.0000            9
    2        36.0000          .4480             .0260          36.0000          70.0000           70.0000          75.0000            9
 COMP#,  1  INTEGER DATA      1   91    0   -1    1    0    0    0    0    0    0    0    0    0    0    0
 COMP#,  2  INTEGER DATA      2   91    2    1   -2    0    0    0    0    0    0    0    0    0    0
REAL DATA CARD #    1     .9300E+01   .4160E+00   .1700E+00   .1500E+01   .4500E+01   .7500E-02   .1000E+01   .7800E+02
REAL DATA CARD #    2     .7800E+02   .8500E+02   .6500E+02   .6500E+00   .9400E-01   0.          0.          0.
 COMP#,  3  INTEGER DATA      3   61    1    2    0    0    0    0    0    0    0    0    0    0    0
REAL DATA CARD #    1     .6000E+02   .7800E+02   .7500E+02   0.          0.          0.          0.          0.
```

FIGURE 492. RUN 87-07 HYTTHA INPUT DATA

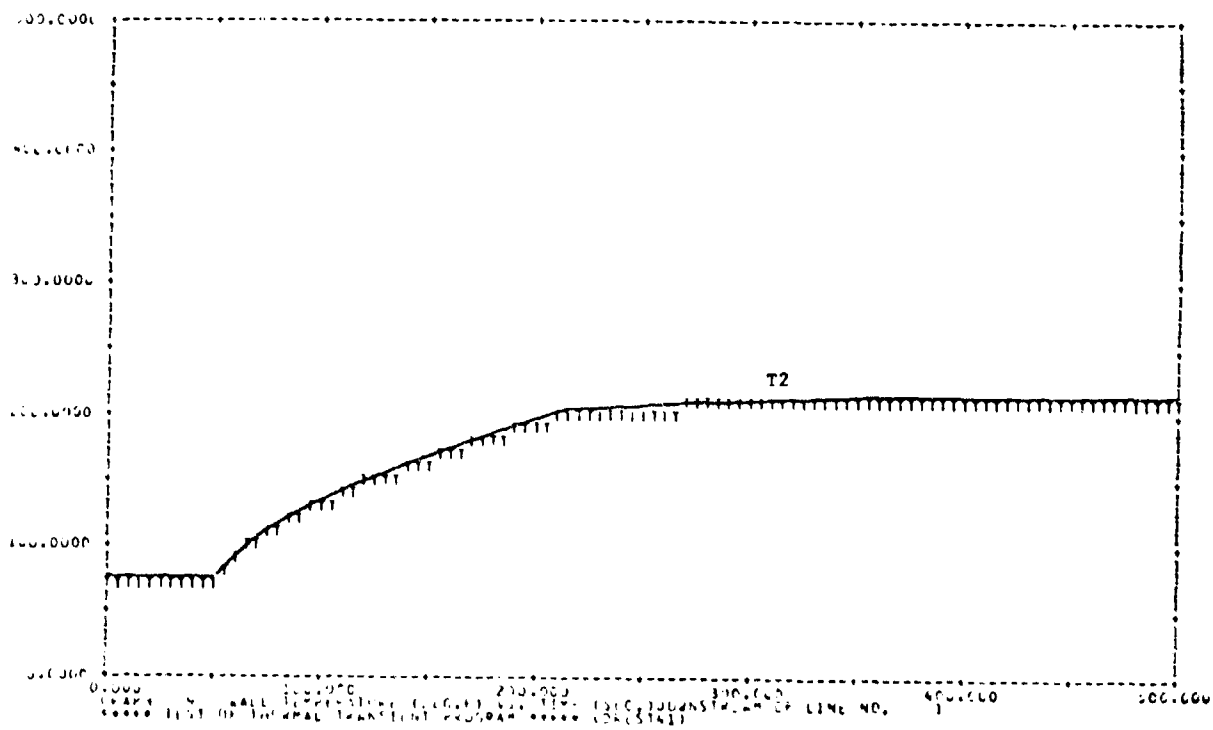

FIGURE 493. 87-07-T2 THERMAL TRANSIENT, WALL TEMPERATURE

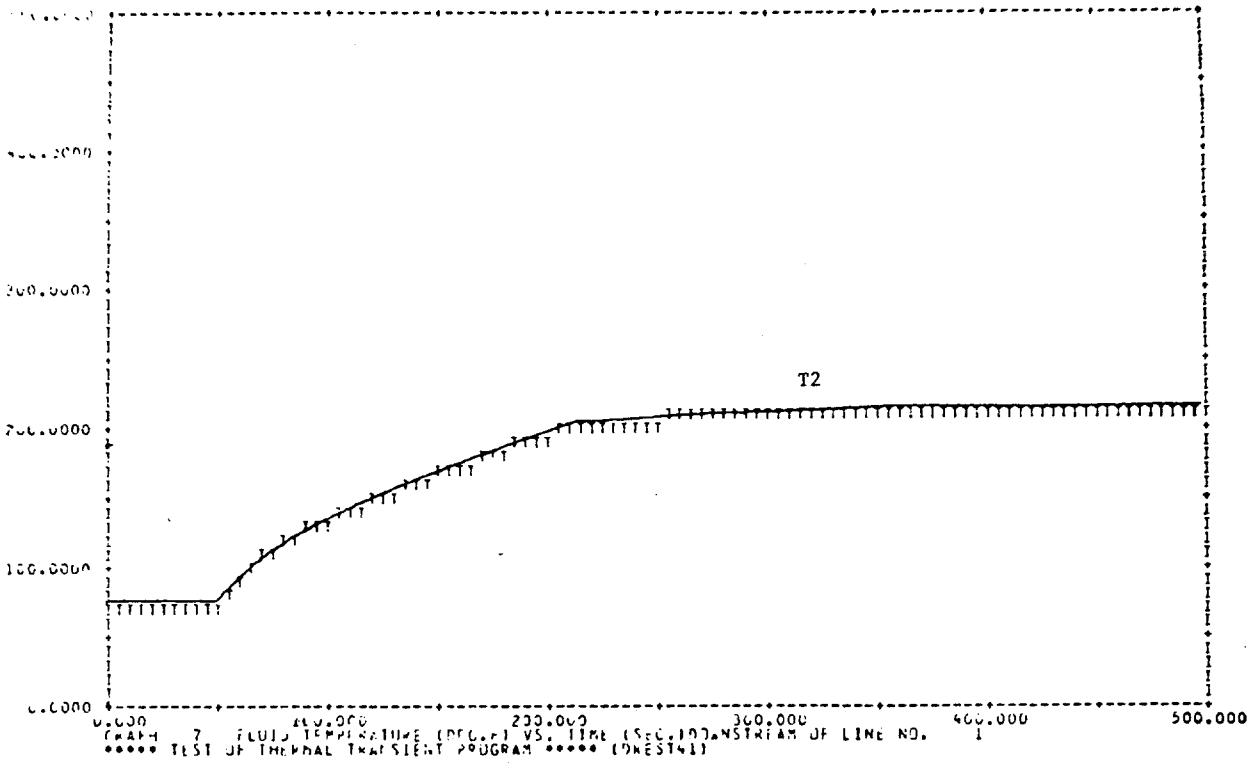

FIGURE 494. 87-07-T2 THERMAL TRANSIENT, FLUID TEMPERATURE

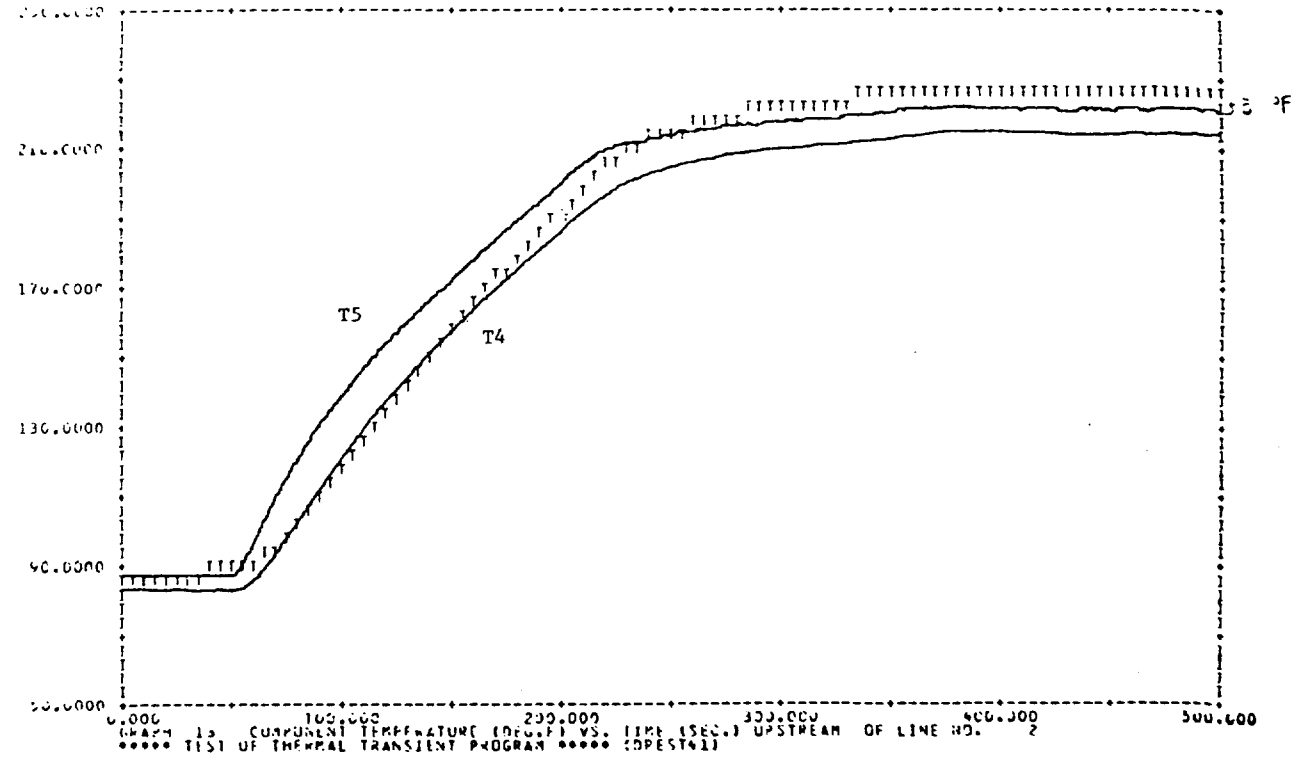

FIGURE 495. 87-07-T4 AND T5 THERMAL TRANSIENT

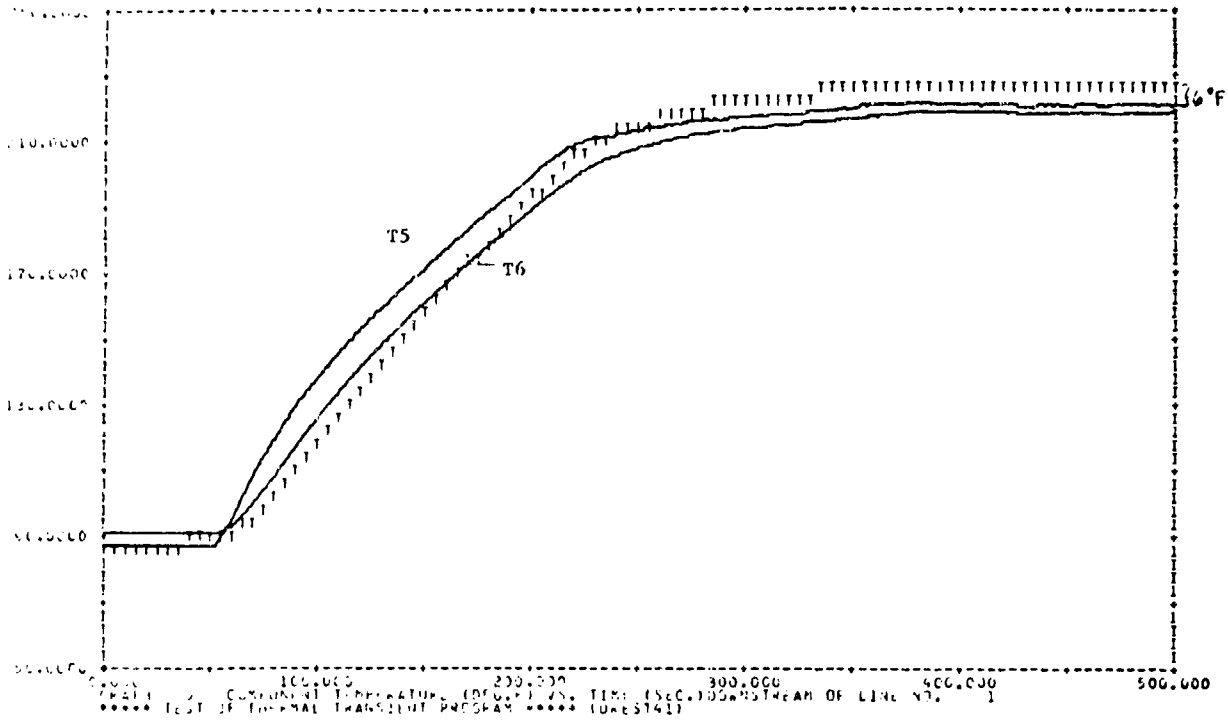

FIGURE 496. 87-07-T5 AND T6 THERMAL TRANSIENT

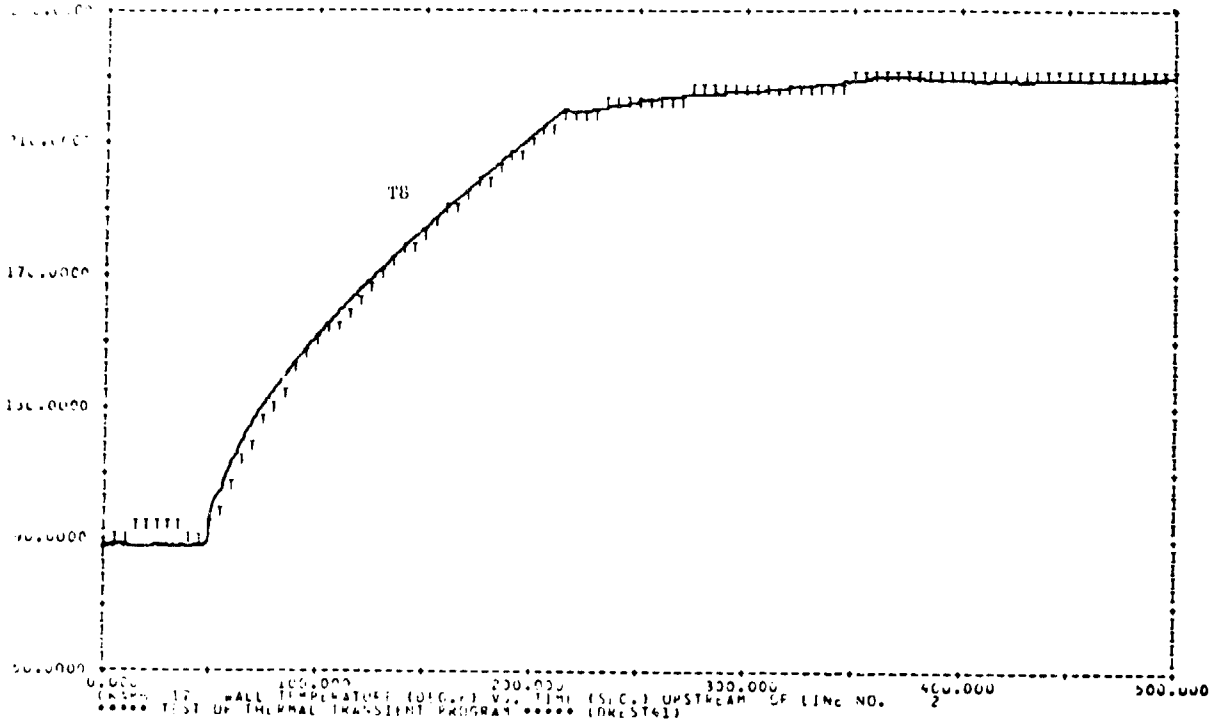

FIGURE 497. 87-07-T7 THERMAL TRANSIENT, WALL TEMPERATURE

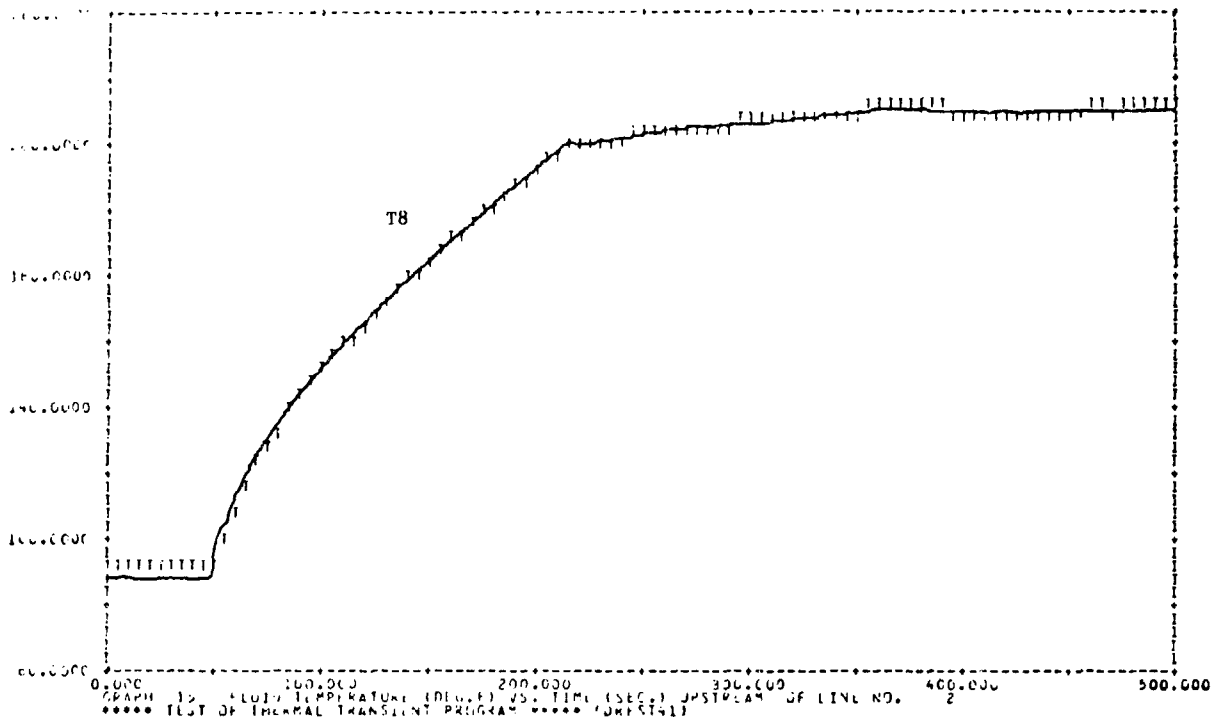

FIGURE 498. 87-07-T8 THERMAL TRANSIENT, FLUID TEMPERATURE

***** TEST OF THERMAL TRANSIENT PROGRAM ***** (DWEST41)

THE THERMAL TRANSIENT RESPONSE IS FROM T=0.0 TO T= 500.000 SECONDS AT TIME INTERVALS OF DELT= .50000
WITH OUTPUT POINTS PLOTTED AT INTERVALS OF = 5.00000 SECONDS

FLUID DATA FOR FOR MIL-H-5606A WITH A VAPOR PRESSURE OF 2.0 PSI

LINE DATA LINE NO.	LENGTH	INTERNAL DIA	WALL THICKNESS	DELTAX	AMBIENT TEMP	STRUCTURE TEMP	FLUID TEMP	MATERIAL TYPE
1	72.0000	.4480	.0260	36.0000	78.0000	78.0000	75.0000	9
2	32.0000	.4480	.0260	32.0000	78.0000	78.0000	75.0000	9

COMP#, 1 INTEGER DATA 1 91 0 -1 1 0 0 0 0 0 0 0 0 0 0 0

COMP#, 2 INTEGER DATA 2 41 2 1 -2 0 0 0 0 0 0 0 0 0 0 0

REAL DATA CARD # 1 .9000E+01 .3870E+00 .1600E+00 .1500E+01 .4500E+01 .1800E-01 .1000E+01 .7800E+02

REAL DATA CARD # 2 .7800E+02 .8500E+02 .9500E+02 .6500E+00 .9400E-01 0. 0. 0.

COMP#, 3 INTEGER DATA 3 61 1 2 0 0 0 0 0 0 0 0 0 0 0 0

REAL DATA CARD # 1 .5000E+02 .7900E+02 .7800E+02 0. 0. 0. 0. 0.

FIGURE 499. RUN 87-07 HYTTHA INPUT DATA WITH A LARGER HEAT TRANSFER COEFFICIENT

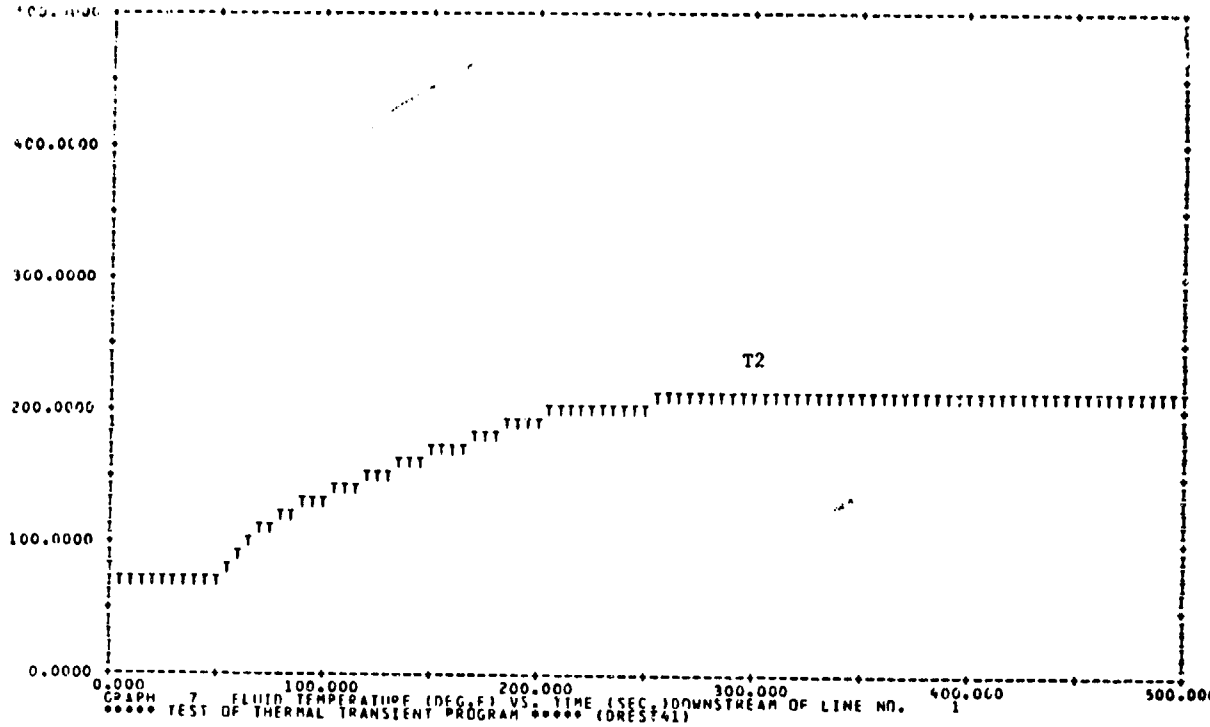

FIGURE 500. 87-07-T2 THERMAL TRANSIENT WITH A LARGER HEAT TRANSFER COEFFICIENT

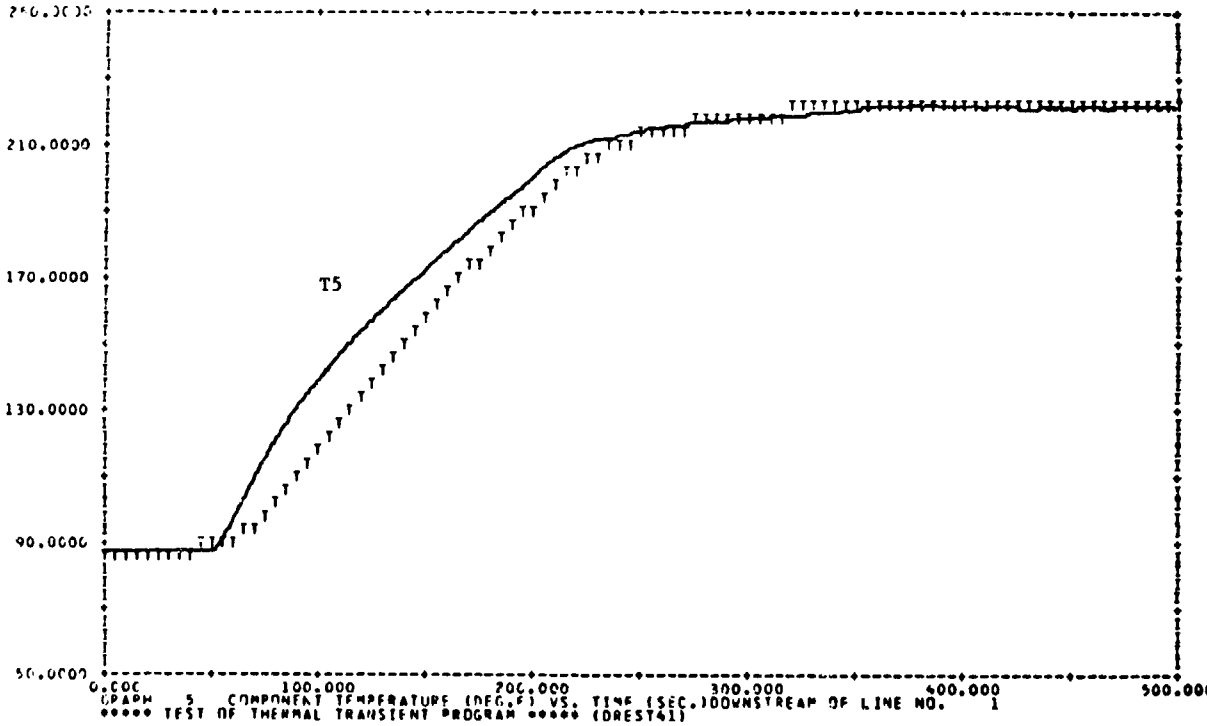

FIGURE 501. 87-07-T5 THERMAL TRANSIENT WITH A LARGER HEAT TRANSFER COEFFICIENT

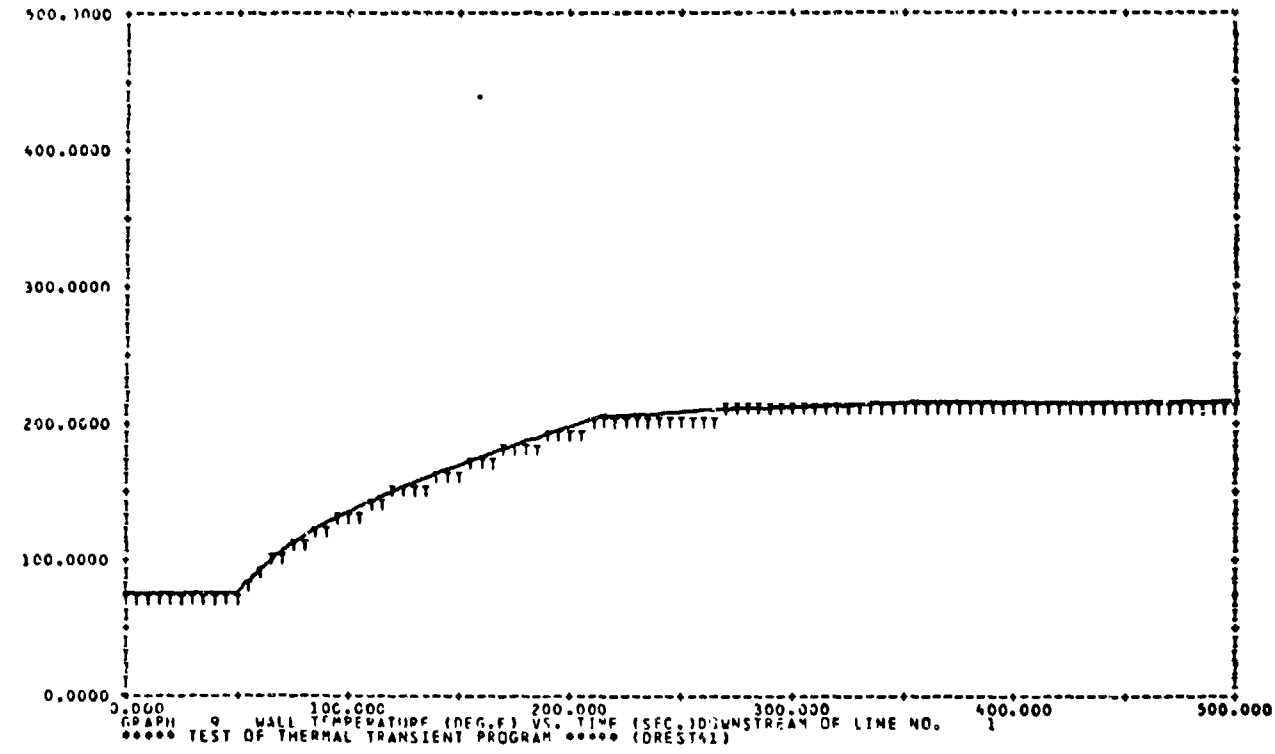

FIGURE 502. 87-07-T6 THERMAL TRANSIENT WITH A LARGER HEAT TRANSFER COEFFICIENT

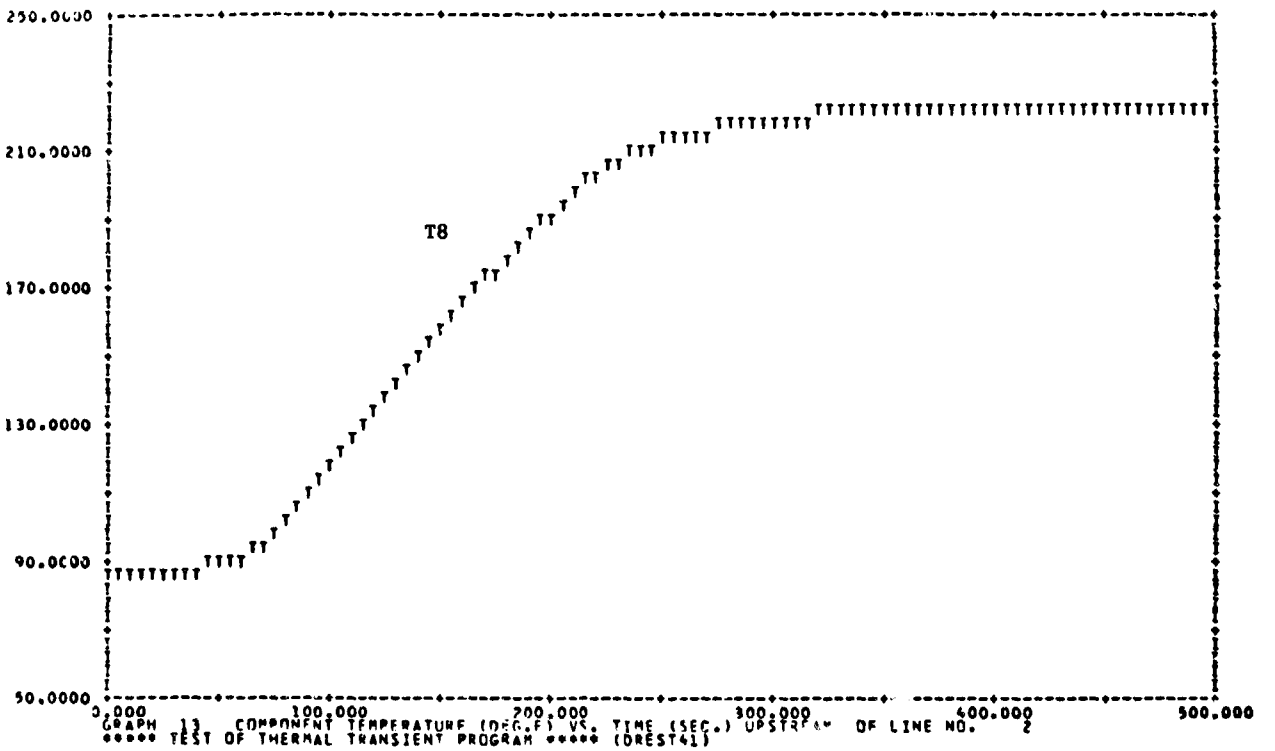

FIGURE 503. 87-07-T8 THERMAL TRANSIENT, COMPONENT TEMPERATURE WITH A LARGER HEAT TRANSFER COEFFICIENT

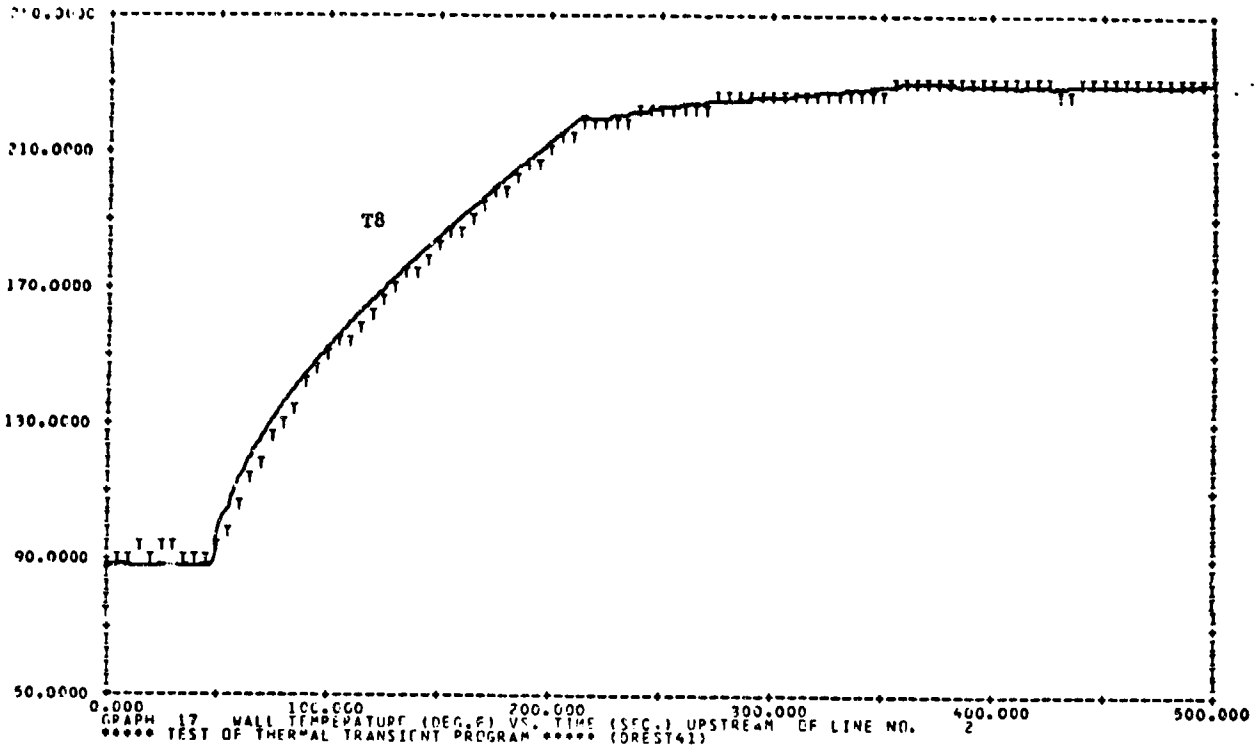

FIGURE 504. 87-07-T8 THERMAL TRANSIENT, WALL TEMPERATURE WITH A LARGER HEAT TRANSFER COEFFICIENT

b. Conclusions - The restrictor model computer runs correlate well with the test data measured in the laboratory. Some discrepancies exist in this model as noted in paragraph a. The model does provide adequate representation of the thermal effects of a simple restrictor in a line system.

3. PUMP MODEL VERIFICATION

The pump thermal tests were run on the configuration shown in Figure 505. Table 31 contains a listing of all the test conditions that were recorded. The thermocouples on the test stand were taped to the line. The drive torque, drive speed, pump pressures and flows were recorded for all test conditions.

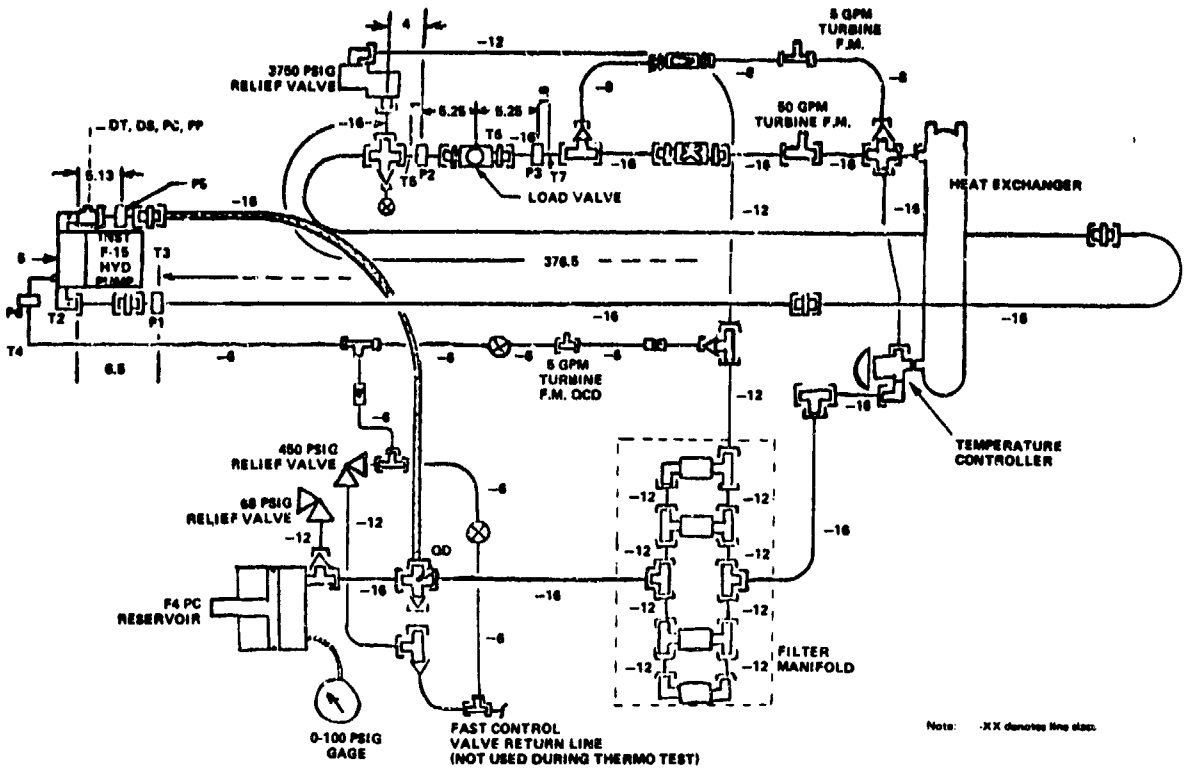

FIGURE 505 PUMP THERMAL TRANSIENT TEST CONFIGURATION

TABLE 31

CONDITIONS FOR THERMAL TEST - F-15 PUMP

Run Number	Steady State Flow (CIS)	Test Condition Pump Inlet Temperature	Drive Speed
77-01	38.5	120°F-Steady State	3000
77-02	10	120°F-Steady State	3000
77-03	38.5	210°F-Steady State	3000
77-04	10	210°F-Steady State	3000
77-05	10	77→ 121°F	3000
77-06	38.5	85→ 127°F	3003
77-07	38.5	80→ 218°F	3014
77-08	10	78→ 216°F	3022
77-09	38.5	91→ 122°F (Start-up)	3000
77-10	38.5	92→ 128°F (Start-up)	3508
77-11	38.5	92→ 119°F (Start-up)	4008
77-12	38.5	92→ 125°F (Start-up)	4501
77-13	10	87→ 117°F (Start-up)	3000
77-14	10	93→ 119°F (Start-up)	3500
77-15	10	94→ 121°F (Start-up)	4000

a. F-15 Instrumented Pump Test Data - Pump test data is presented for thermal transients generated by shutting off the heat exchanger bypass flow. Figures numbers 506, 507, 508, 509, 510 and 511 through 515 present temperature data for two thermal transients at 10 and 38.5 CIS pump outlet flow respectively. The pump compensator was set to 2940 psi for both test runs.

Shown in Figures 516 through 520 and 521 through 525 are start-up thermal transients. The pump was started and the temperatures were monitored until they reached a steady state condition.

b. Conclusions - No verification has been accomplished with the HYTTHA program pump model. The pressure data taken for each test oscillated and could not be used as boundary conditions in the simulation programs. Figures 526 and 527 contain typical pressure data taken in the thermal tests.

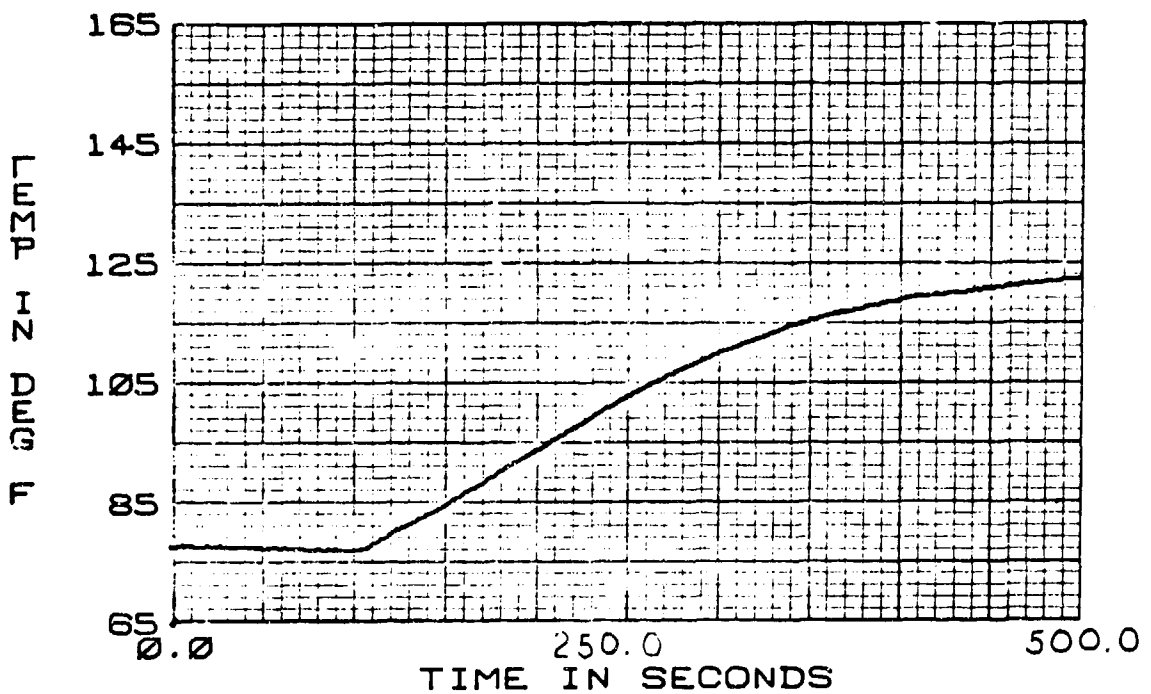

FIGURE 506 F-15 HYDRAULIC PUMP
77-05-T1 STEADY STATE
10 CIS 80-120°F

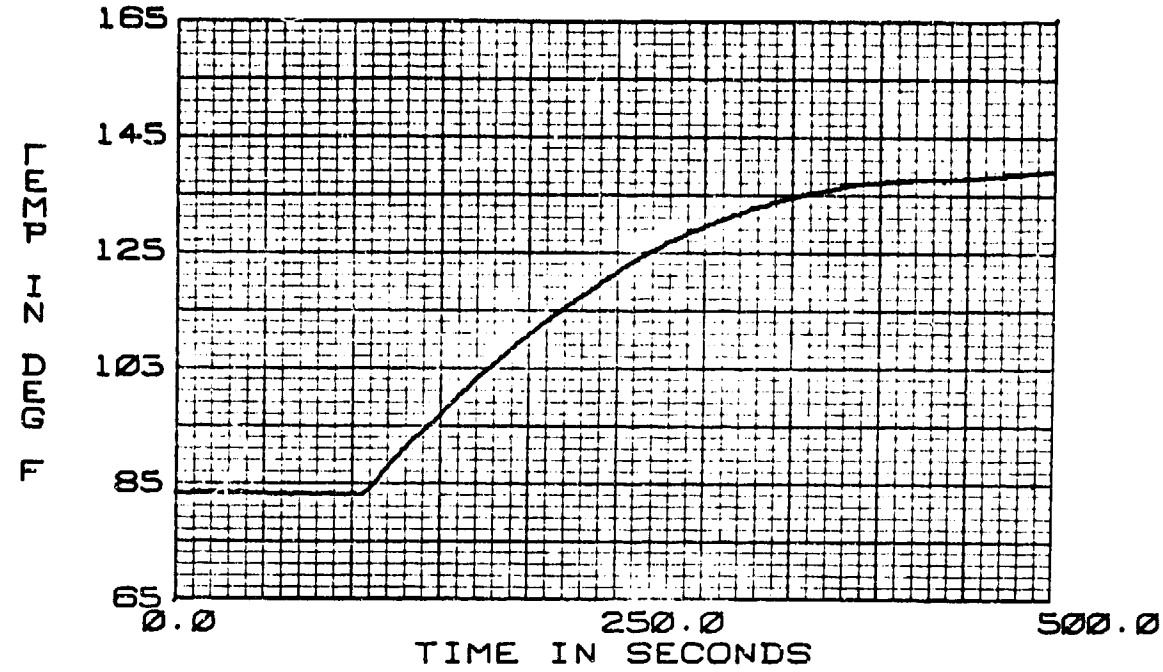

FIGURE 507 F-15 HYDRAULIC PUMP
77-05-T2 STEADY STATE
10 CIS 80-120°F

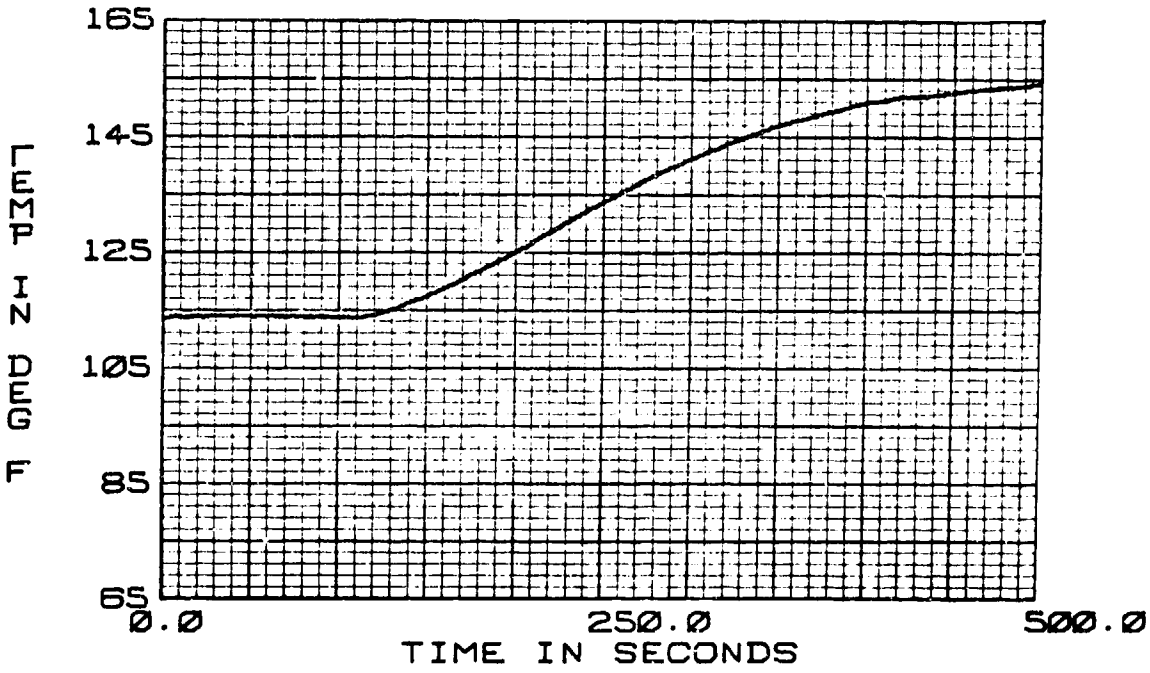

FIGURE 508 F-15 HYDRAULIC PUMP
77-05-T3 STEADY STATE
10 CIS 8-120°F

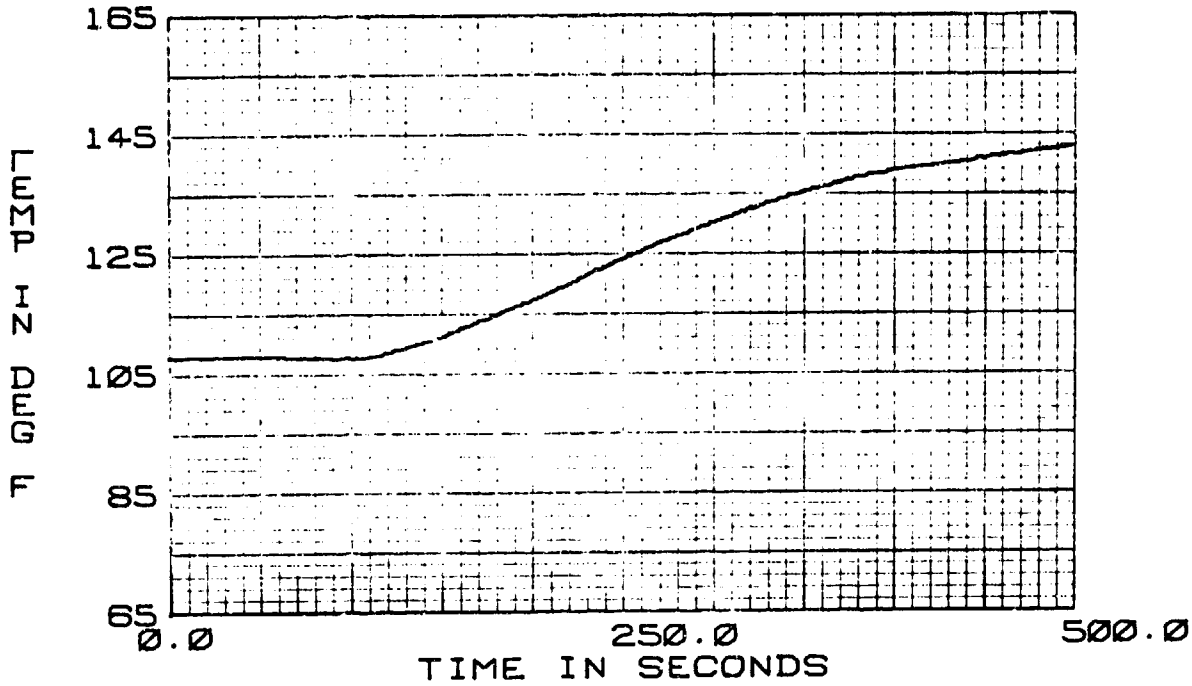

FIGURE 509 F-15 HYDRAULIC PUMP
77-05-T4 STEADY STATE
10 CIS 80-120°F

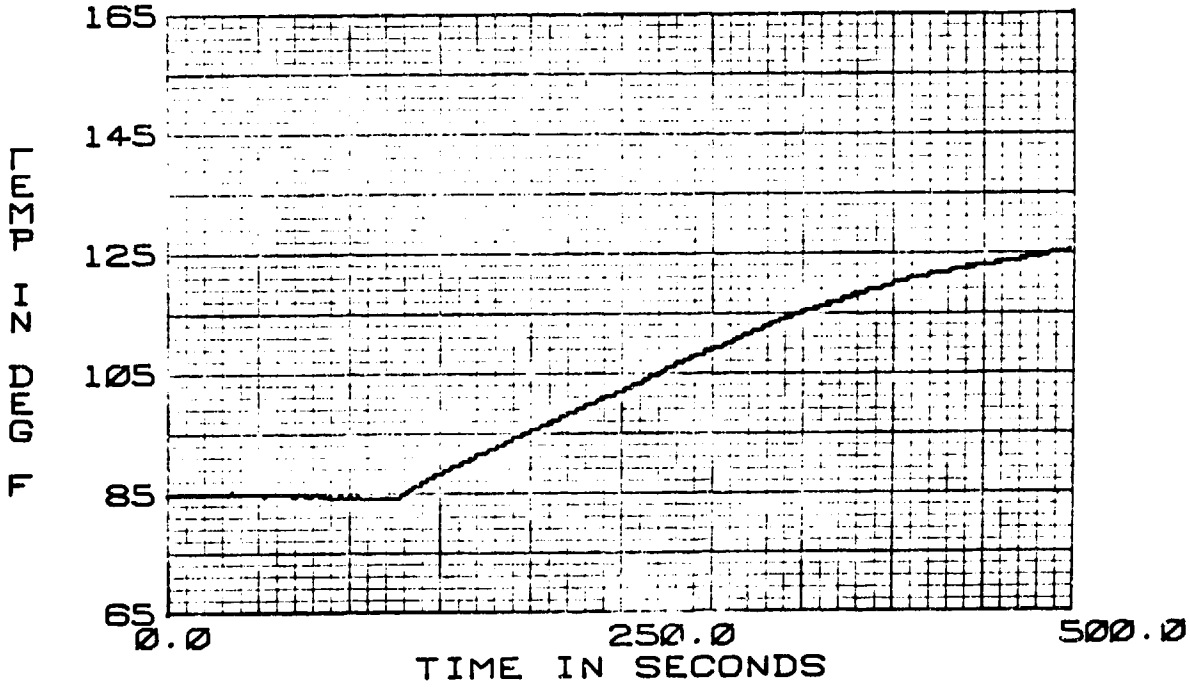

FIGURE 510 LOAD VALVE
77-05-T5 STEADY STATE
10 CIS 80-120°F

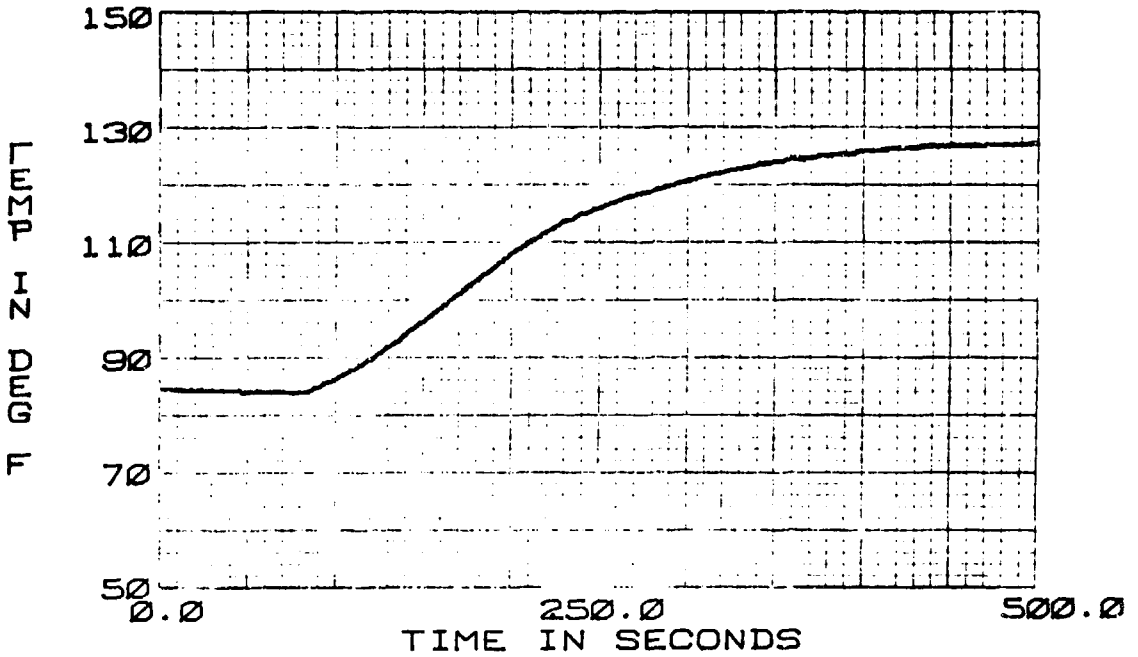

FIGURE 511 F-15 HYDRAULIC PUMP
77-06-T1 TEMPERATURE TRANSIENT
38.5 CIS 90 TO 120°F

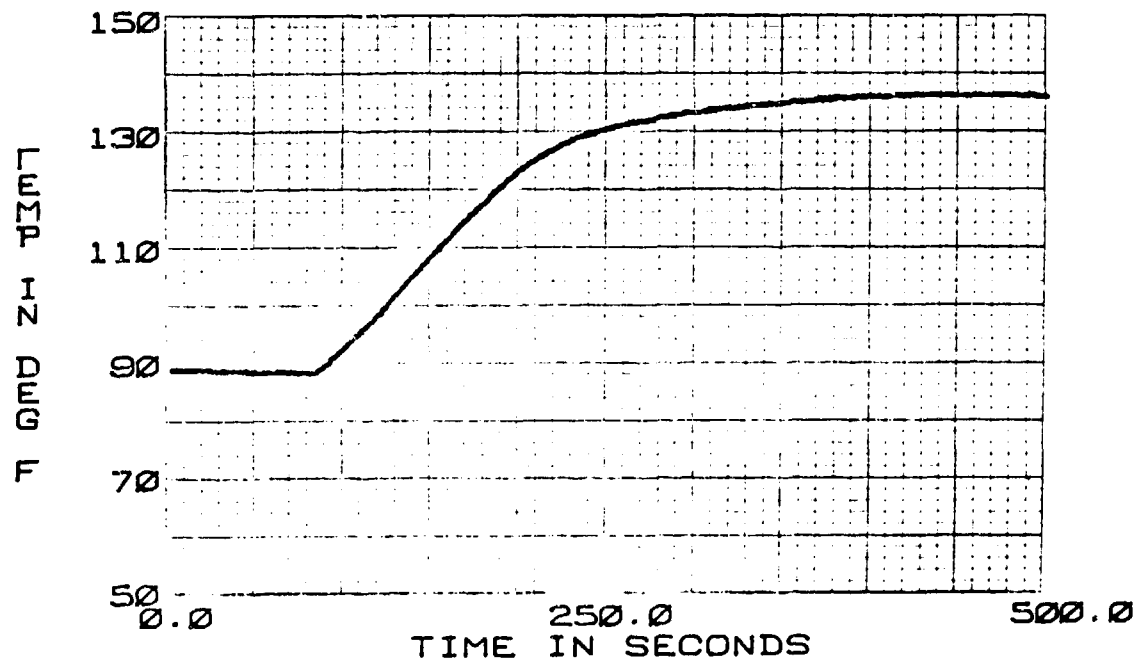

FIGURE 512 F-15 HYDRAULIC PUMP
77-06-T2 TEMPERATURE TRANSIENT
38.5 CIS 90 TO 120°F

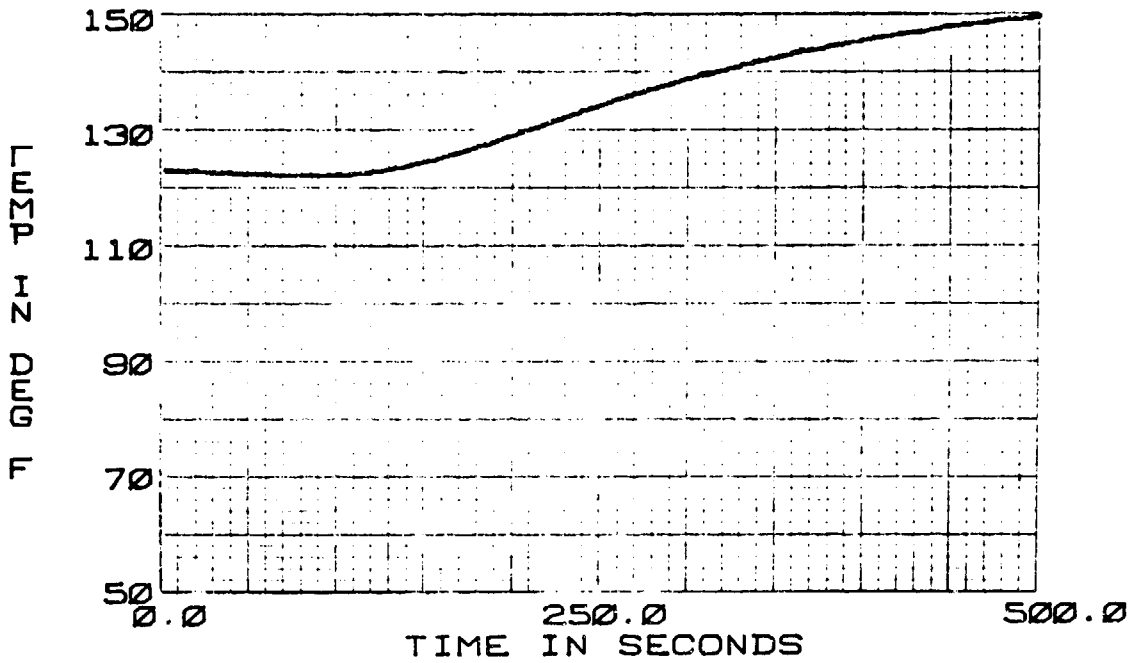

FIGURE 513 F-15 HYDRAULIC PUMP
77-06-T3 TEMPERATURE TRANSIENT
38.5 CIS 90 TO 120°F

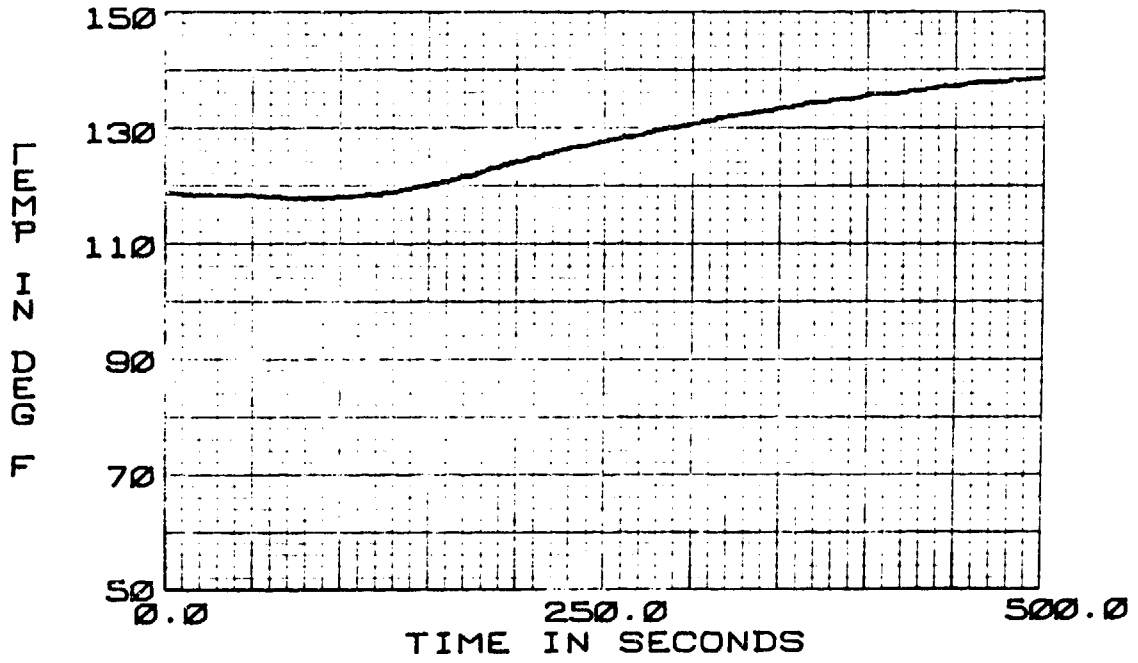

FIGURE 514 F-15 HYDRAULIC PUMP
77-06-T4 TEMPERATURE TRANSIENT
38.5 CIS 90 TO 120°F

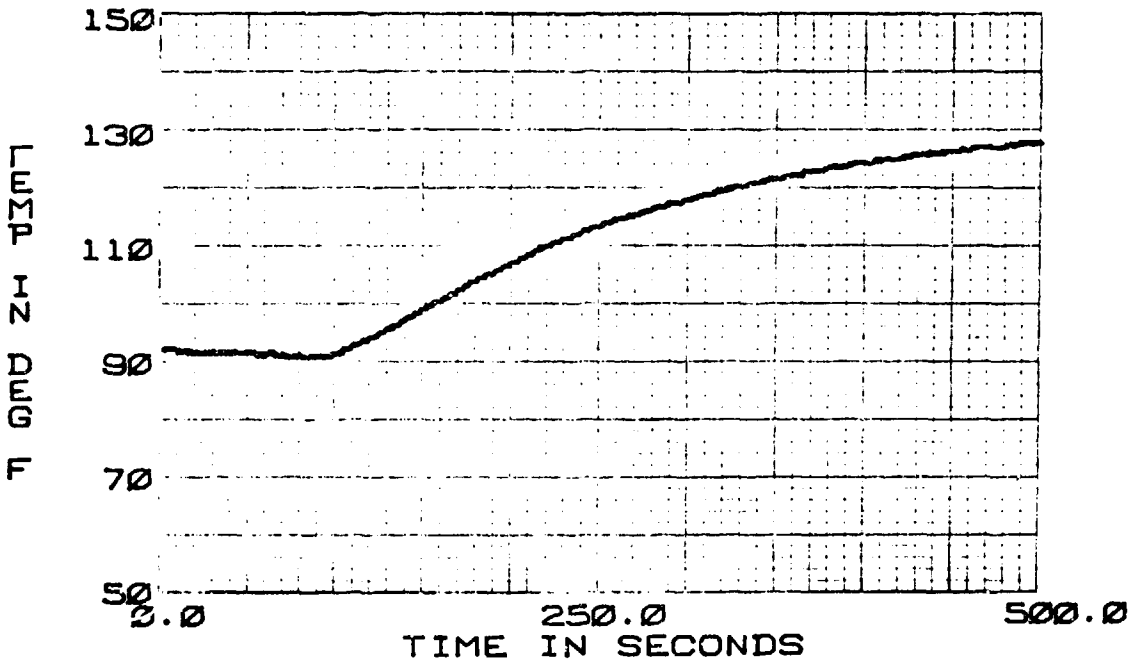

FIGURE 515 LOAD VALVE
77-06-T5 TEMPERATURE TRANSIENT
38.5 CIS 90 TO 120°F

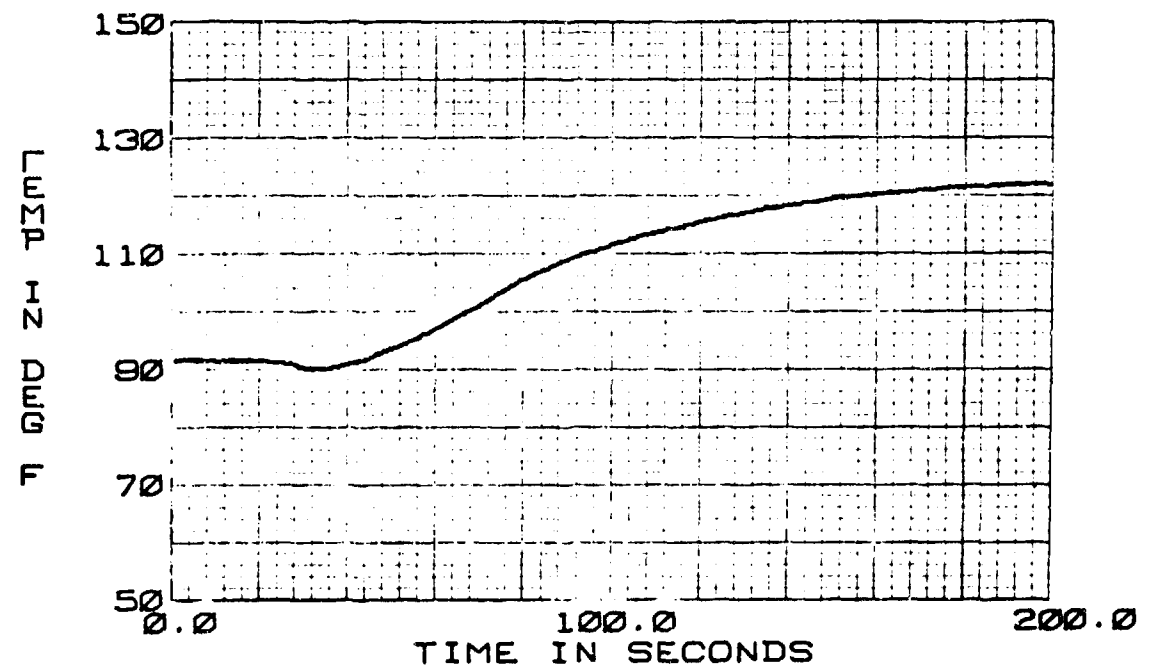

FIGURE 516 F-15 HYDRAULIC PUMP
77-09-T1 START UP
38.5 CIS 90-120°F

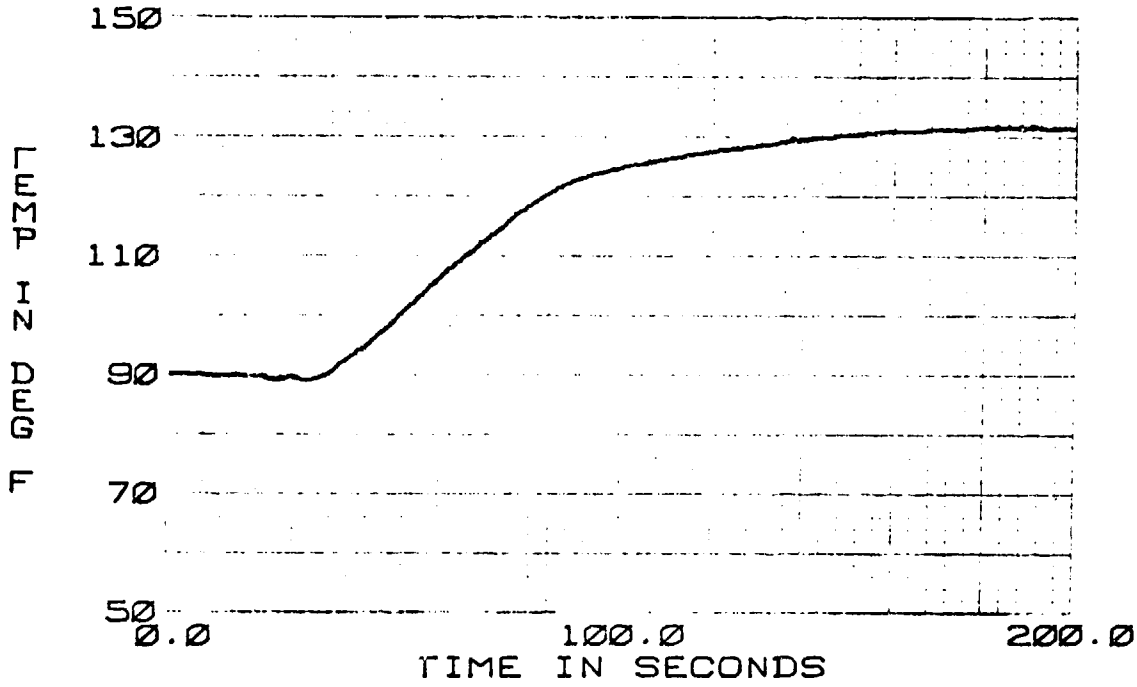

FIGURE 517 F-15 HYDRAULIC PUMP
77-09-T2 START UP
38.5 CIS 90-120°F

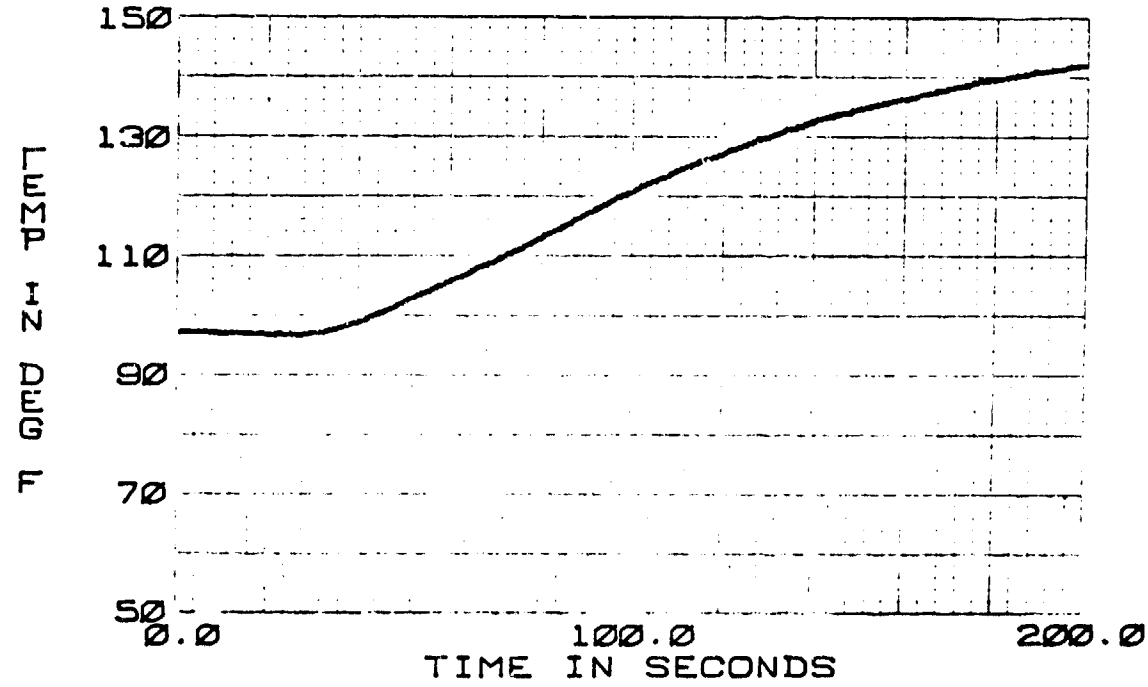

FIGURE 518 F-15 HYDRAULIC PUMP
77-09-T3 START UP
38.5 CIS 90-120°F

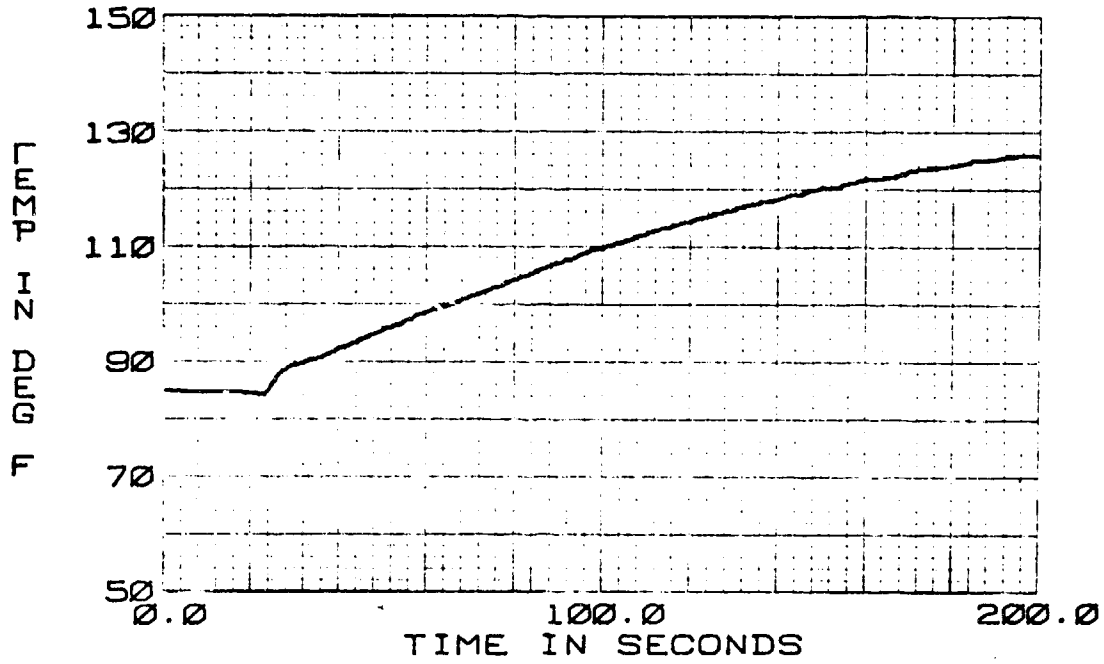

FIGURE 519 F-15 HYDRAULIC PUMP
77-09-T4 START UP
38.5 CIS 90-120°F

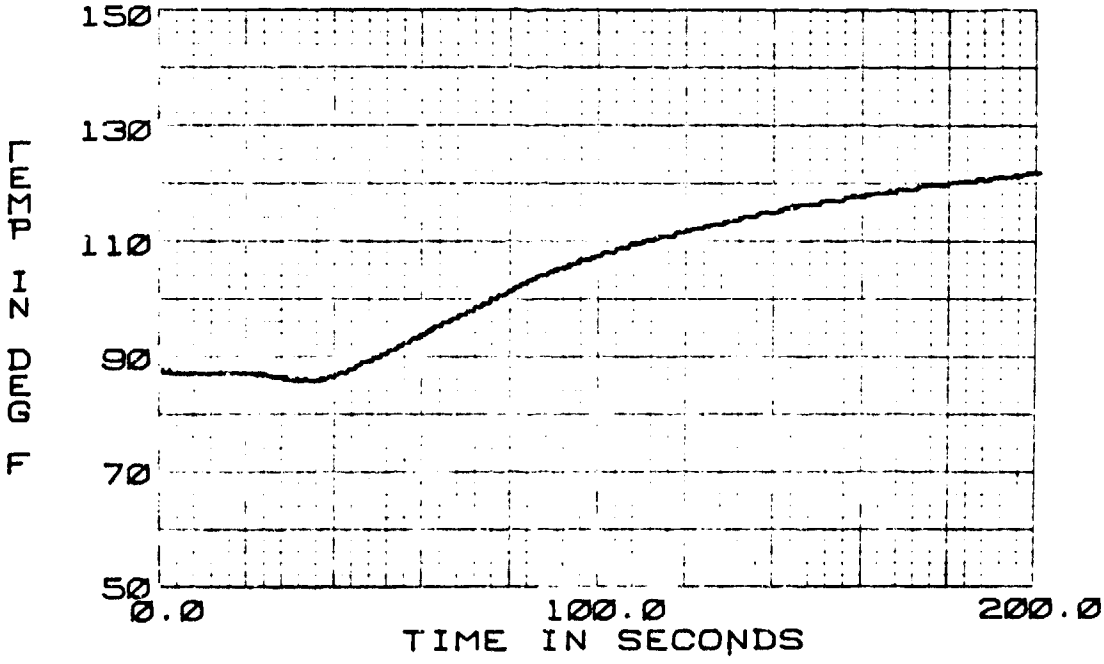

FIGURE 520 LOAD VALVE
77-09-T5 START UP
38.5 CIS 90-120°F

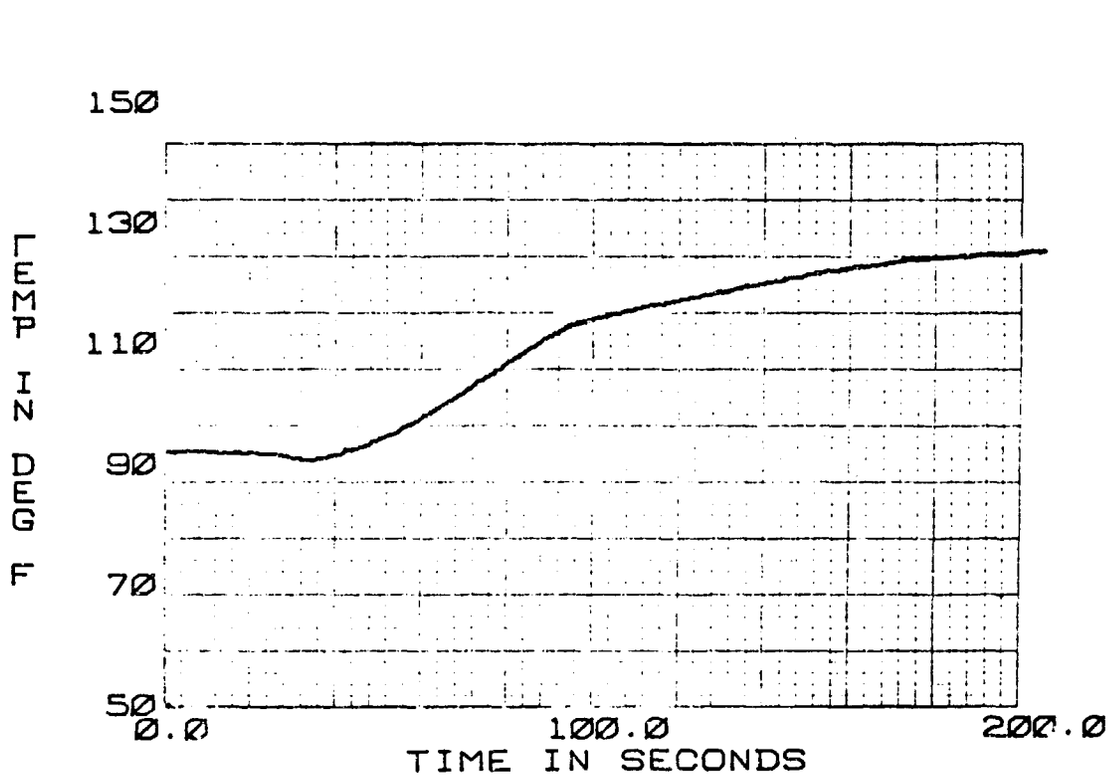

FIGURE 521 F-15 HYDRAULIC PUMP
77-12-T1 START UP
38.5 CIS 90-120°F

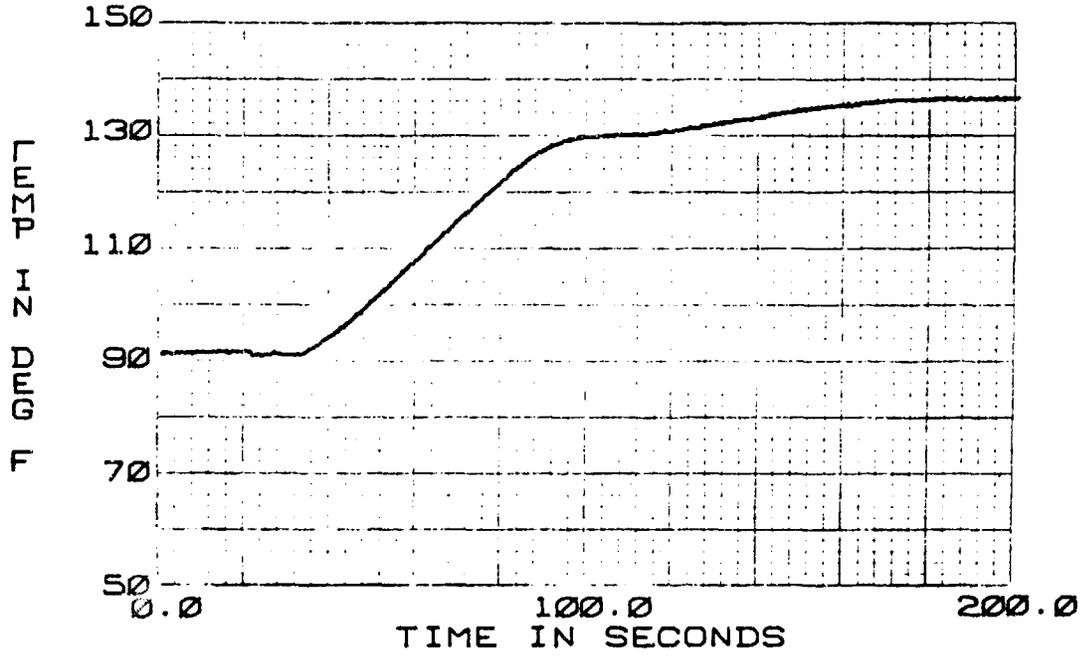

FIGURE 522 F-15 HYDRAULIC PUMP
77-12-T2 START UP
38.5 CIS 90-120°F

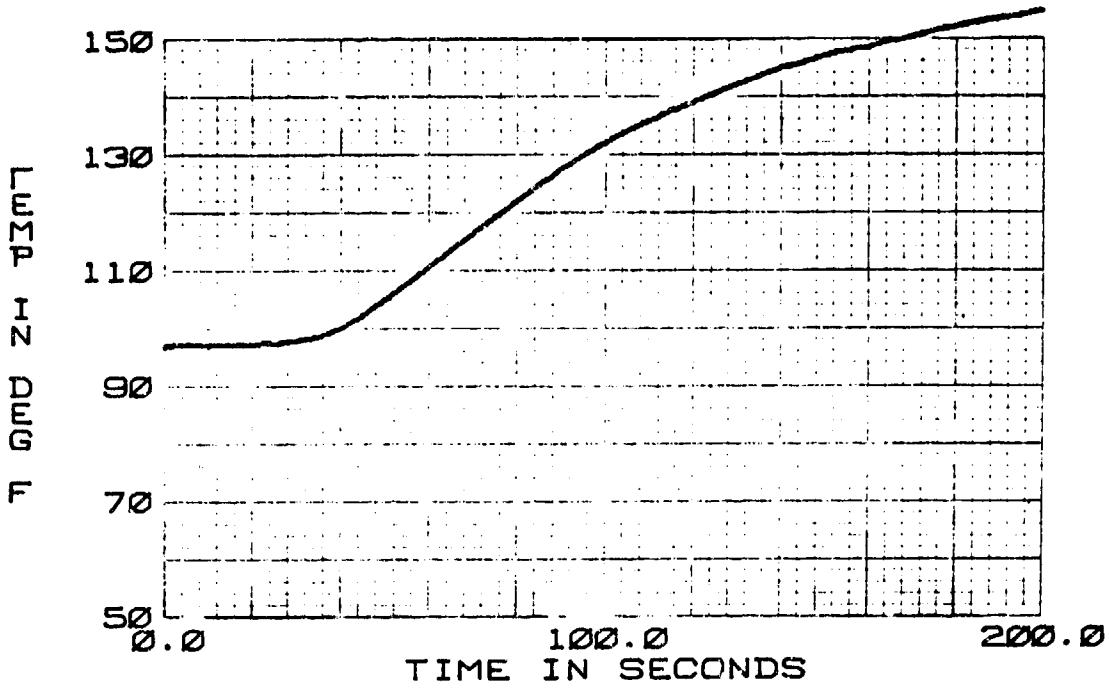

FIGURE 523 F-15 HYDRAULIC PUMP
77-12-T3 START UP
38.5 CIS 90-120°F

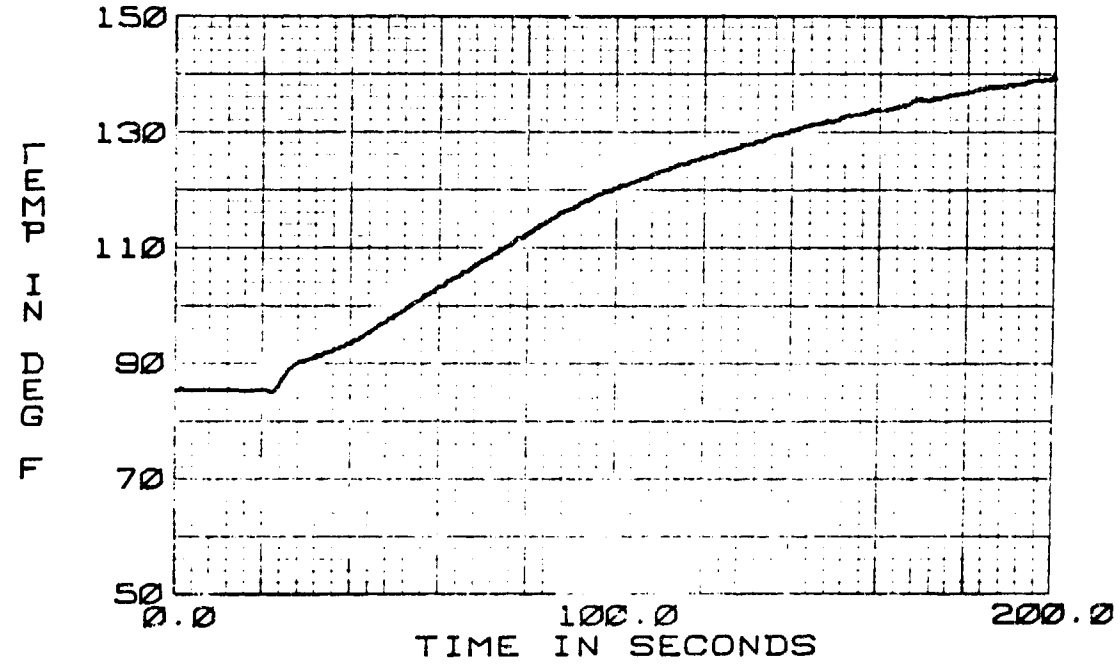

FIGURE 524 F-15 HYDRAULIC PUMP
77-12-T4 START UP
38.5 CIS 90-120°F

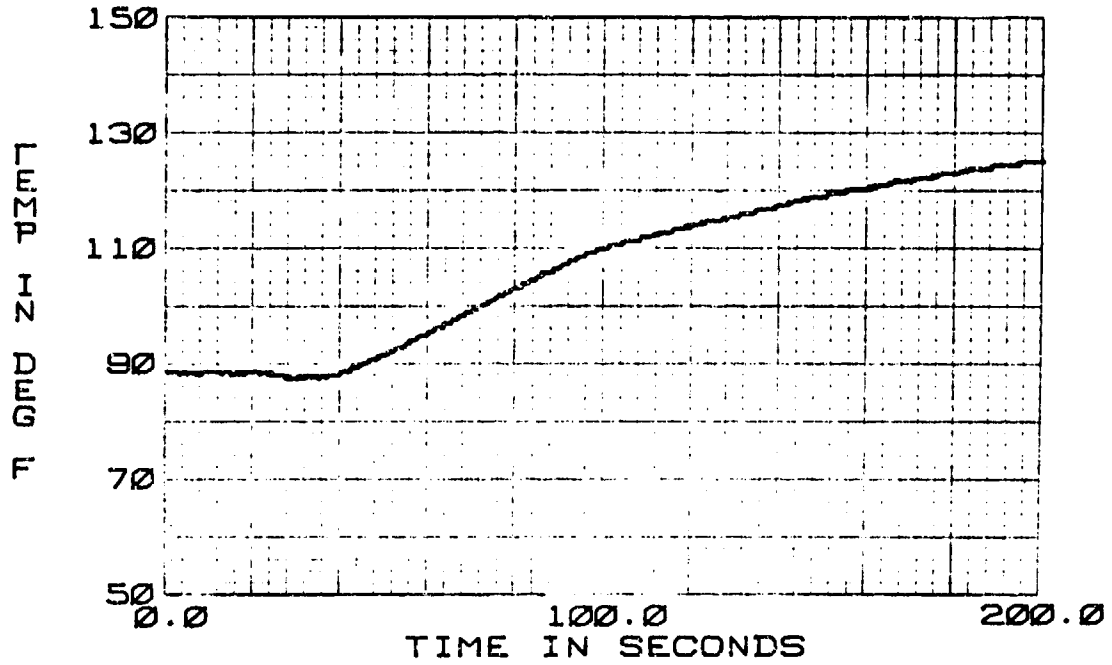

FIGURE 525 LOAD VALVE
77-12-T5 START UP
38.5 CIS 90-120°F

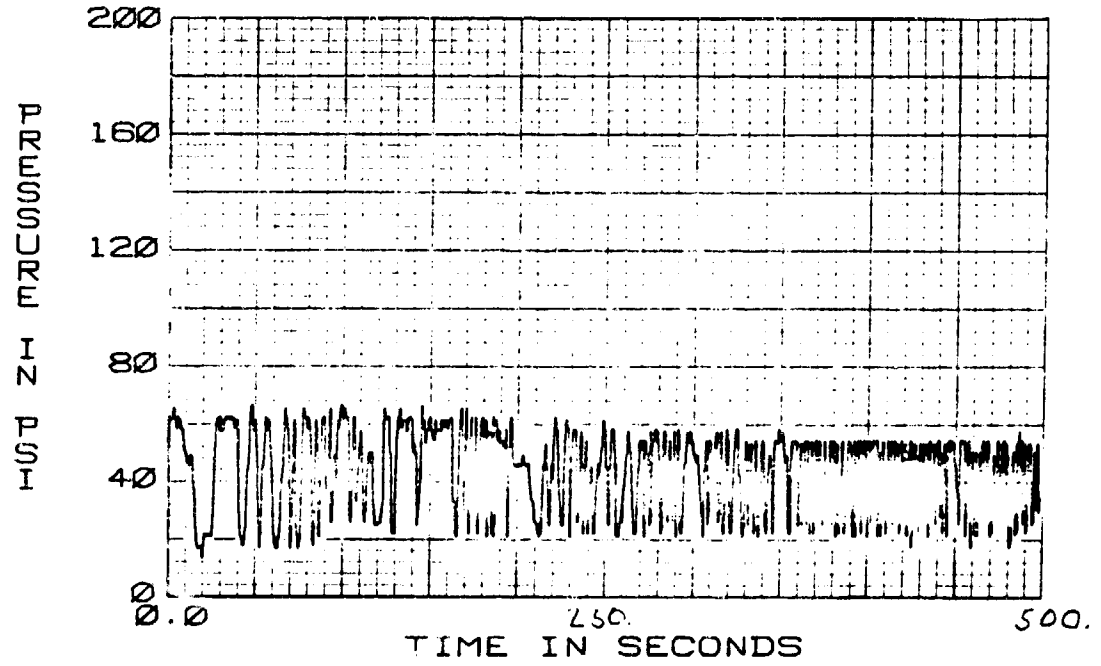

FIGURE 526 F-15 HYDRAULIC PUMP
77-05-PS TEMP TRANSIENT
10 CIS 77-120°F

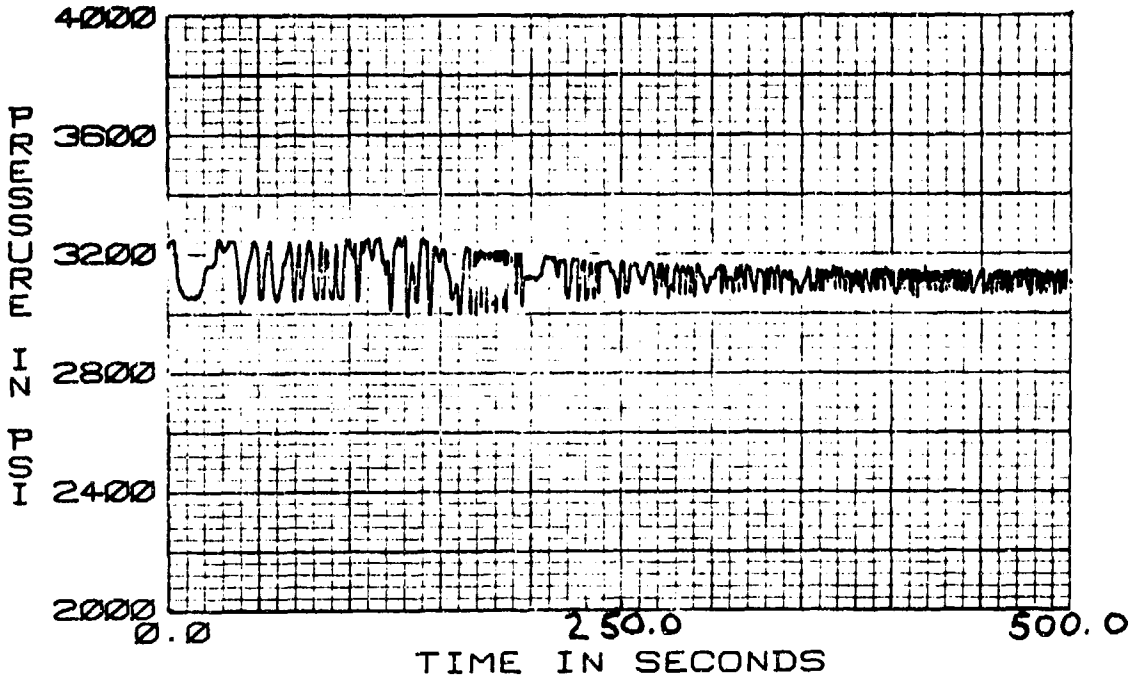

FIGURE 527 F-15 HYDRAULIC PUMP
77-05-P2 TEMP TRANSIENT
10 CIS 77-120°F

4. HEAT EXCHANGER MODEL VERIFICATION

The heat exchanger transient thermal tests were run on the system configuration shown in Figure 528. Table 32 contains a list of test conditions.

a. Computer Simulation with Heat Exchanger Test Data - The F-4 heat exchanger was simulated in HYTTHA by THEX69. In the program the pressure source was simulated by a constant pressure variable temperature component, TTEST91. The program uses a constant pressure, constant temperature reservoir, TRSVR61 as the downstream component. The actual areas, distances, volumes, heat transfer coefficients, etc., are shown in Figure 529.

A total of four runs were made at similar heat exchanger inlet pressures and various flow rates. The upstream hydraulic fluid temperature transient is the input to the system. In the tests the input cooling liquid, (water) was also varied, but in the THEX69 model the temperature of that liquid remained constant, at a representative value from the T1 temperature data.

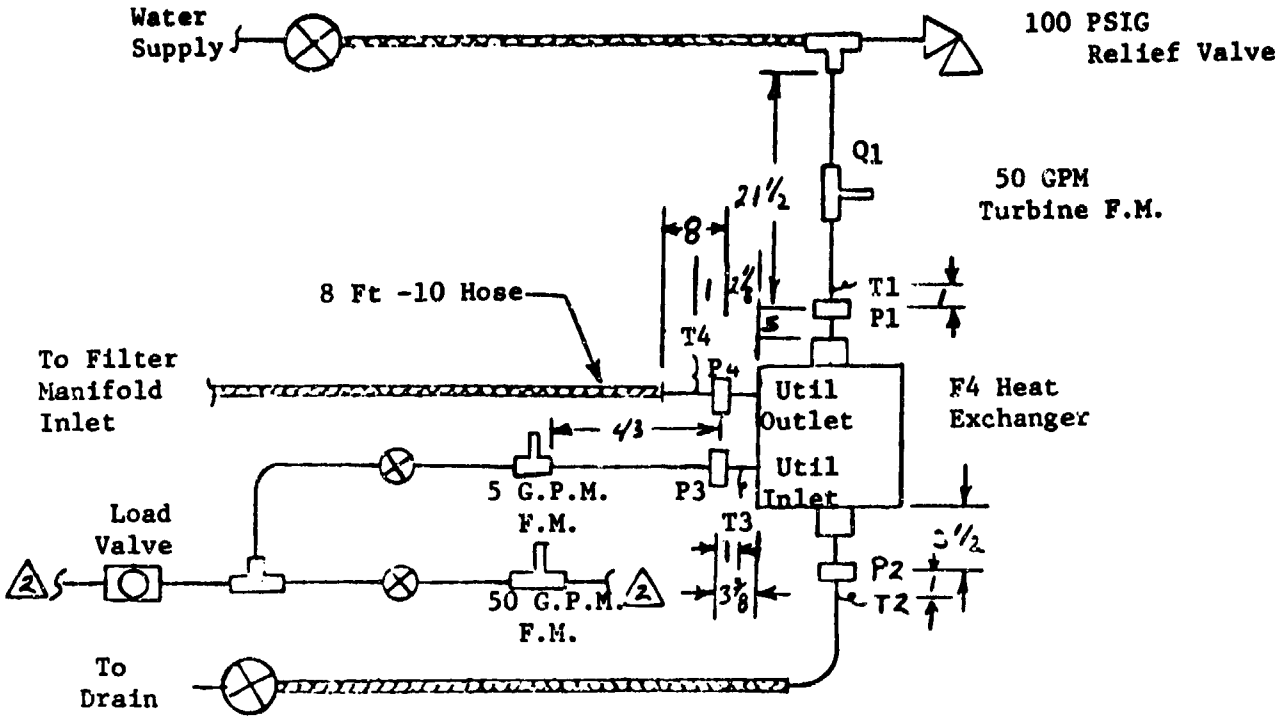

FIGURE 528 F-4 HEAT EXCHANGER THERMAL TEST CONFIGURATION

TABLE 32

HEAT EXCHANGER THERMAL TEST CONDITIONS

RUN NUMBER	TEST CONDITION	RETURN PRESSURE	FLUID FLOW	H_2O FLOW	AMBIENT TEMPERATURE	INITIAL SYSTEM TEMPERATURES
79-01-XX	Steady State	47	10 CIS	10.03 GPM	79	80
79-02-XX	Steady State	51	10 CIS	1.06 GPM	82	80
79-03-XX	Temp Transient 80-210	60	10 CIS	0.0 GPM	75-78	80
79-04-XX	Temp Transient 210-170	58.2	0 CIS	6.24 GPM	80	80,235

```
***** TEST OF THERMAL TRANSIENT PROGRAM ***** (OTHER69)

THE THERMAL TRANSIENT RESPONSE IS FROM T=0.0 TO T= 500.000 SECONDS AT TIME INTERVALS OF DELT= .50000
        WITH OUTPUT POINTS PLOTTED AT INTERVALS OF  =  5.00000  SECONDS

FLUID DATA FOR  FOR MIL-H-5606B          WITH A VAPOR PRESSURE OF      2.0 PSI

LINE DATA
LINE NO.*  LENGTH      INTERNAL DIA    WALL THICKNESS    DELTAX        AMBIENT TEMP    STRUCTURE TEMP    FLUID TEMP      MATERIAL TYPE
    1      36.0000       .4480           .0260          36.0000         80.0000          80.0000         80.0000            9
    2      32.0000       .4480           .0260          32.0000         80.0000          80.0000         80.0000            9
 COMP#,  1 INTEGER DATA      1  91   0  -1   1   0   0   0   0   0   0   0   0   0   0   0   0   0   0
 COMP#,  2 INTEGER DATA      2  69   3   1  -2   0   0   0   0   0   0   0   0   0   0   0   0   0   0
REAL DATA CARD #   1    .9000E+01  0.          .7800E+01  .5700E+01  .4665E+04  .9300E-01  .1200E+02  .3790E+02
REAL DATA CARD #   2    .8100E+02  .9480E+02  .1832E+04  .6900E-02  .6900E-01  .7300E-01  .3000E-01  .5800E+02
REAL DATA CARD #   3    .7800E+02  .7800E+02  .8000E+02  .8000E+02  .6000E+02  .1000E-01  0.            .3000E+02
 COMP#,  3 INTEGER DATA      3  61   1   2   0   0   0   0   0   0   0   0   0   0   0   0   0   0   0
REAL DATA CARD #   1    .9800E+02  .7800E+02  .7800E+02  0.          0.          0.          0.          0.
```

FIGURE 529 RUN 79-03 HYTTHA INPUT DATA

In run No. 79-03 temperature T3 in Figure 530 was used as the transient input to the system. There was no cooling flow through the heat exchanger. Figure 531 shows the existing fluid temperature. The predicted results responds very accurately to the data with the only variation at 1000 seconds with the two final temperatures differing by approximately 4°F. The calculated temperatures are high to begin with and low at the end. This is because the cooling liquid had an actual transient input from low to high and the program used a representative constant value, of 75.8°F for obtaining the result. Since there was very little cooling liquid flow this result was small, as Figure 531 indicates.

Figure 532 shows a plot of the cooling liquid output. The test data was recorded downstream where a large volume congregates while the calculated temperature (the T's) is inside the exchanger. So these two graphs aren't even at the same location. But looking at the calculated cooling liquid graph and comparing it to the existing fluid, it appears very reasonable answers. Since there is no liquid flow it should heat up considerably which it does, but at a slower rate than the fluid since its heat transfer coefficient with the pipes is very small. So this heating up transient correlates with the test data. Internal heat transfer coefficients are tricky and can be adjusted for closer results.

b. Conclusions - The heat exchanger was able to predict the test results for the range of temperatures that were tested.

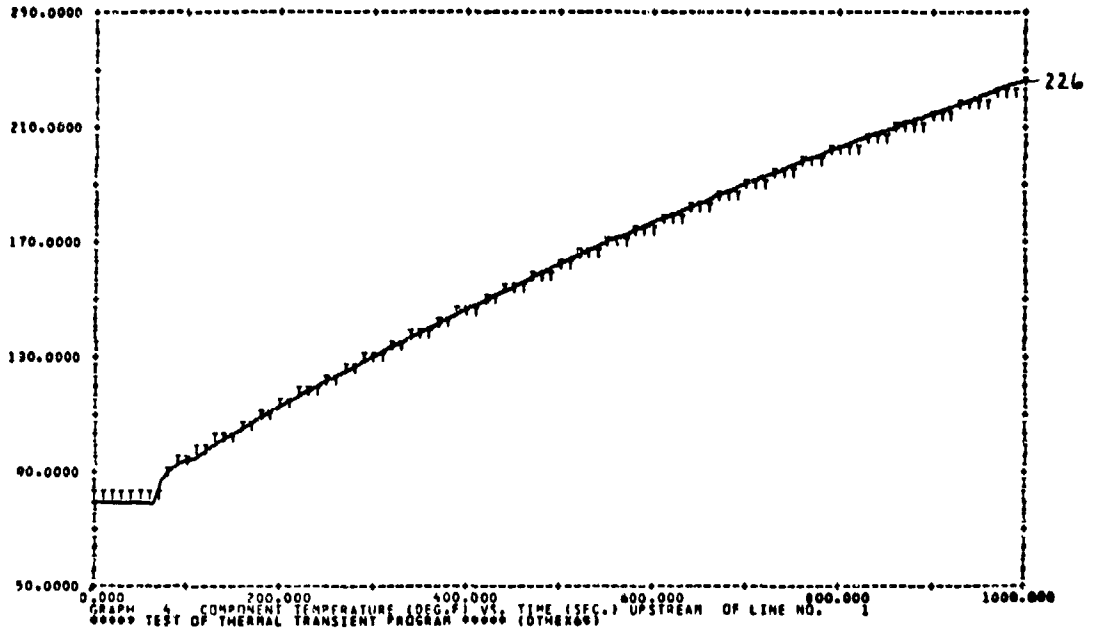

FIGURE 530 79-03-T3 INPUT DATA

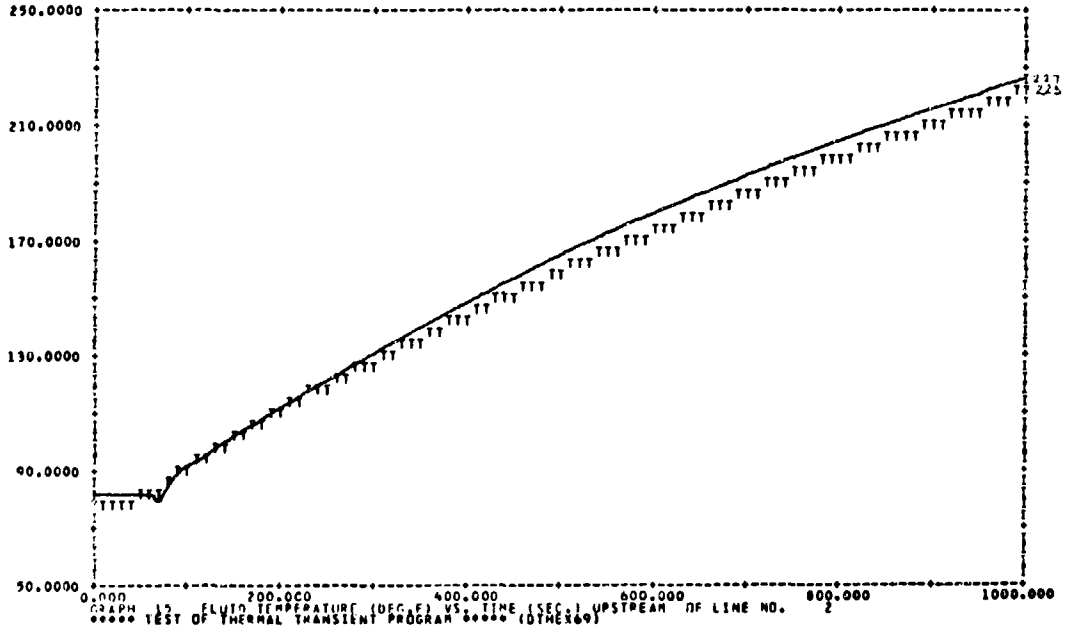

FIGURE 531 79-03-T4 THERMAL TRANSIENT

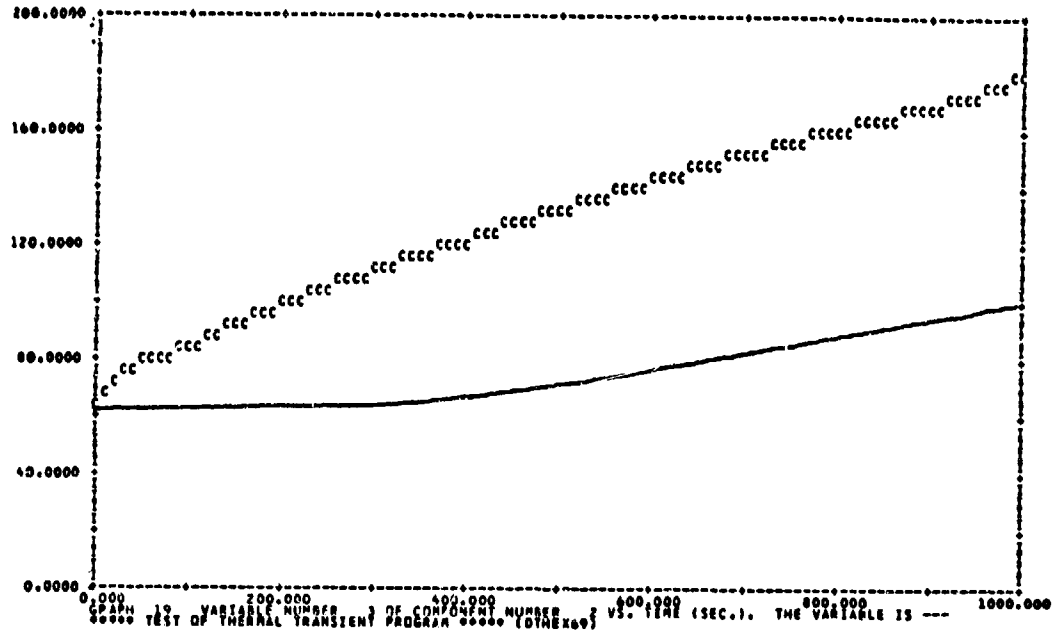

FIGURE 532 COOLING LIQUID OUTLET TEMPERATURE

5. F-15 SPEEDBRAKE THERMAL TESTS

The F-15 iron bird speedbrake test runs were made on the system configuration shown in Figure 533. A listing of the test runs is contained in Table 33. The utility system's oil was heated by cycling the system. The speedbrake solenoid selector valve was then operated to cycle the speedbrake. The hydraulic subsystem warmup characteristics from ambient temperature were measured. Data was then recorded for opening, closing and reversal transients while operating the speedbrake actuator with the solenoid selector valve.

a. Computer Simulation with Test Data - The HYTTHA computer program used the system configuration data in Figure 534 and the test data in Figure 535. The results of the simulation are shown in Figures 536, 537, 538 and 539. Figure 536 corresponds to the T4 thermocouple location in Figure 533. At 50 seconds the compute temperature is 10 degrees lower than the measured results. A graph of the computed actuator wall temperature is shown in Figure 537. The measured data corresponding to this temperature is in Figure 540. In the test data the actuator heats up 24°F above its initial temperature, but the computed output shows a 16°F rise in temperature.

The downstream thermocouple data which is Figure 541 for this retract run shows a slight increase in temperature. The computer predicted values in Figure 538 exhibit a completely different characteristic. The computed temperature at the T5 location in Figure 539 also does not correlate with the test data.

b. Conclusions - The test data on the speedbrake system does not correlate with the HYTTHA program predicted results. Further work on the subroutines must be done before adequate verification can be accomplished. The current limitations in the present contract prohibit further work on the development of these models.

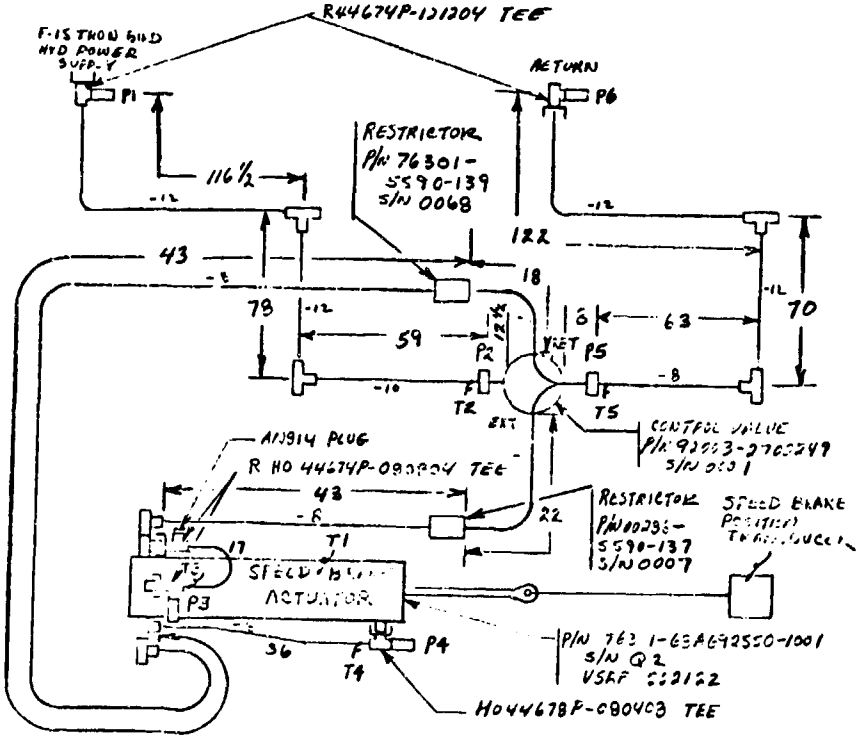

FIGURE 533 F-15 IRON BIRD SPEEDBRAKE SYSTEM CONFIGURATION

TABLE 33

THERMAL SPEEDBRAKE TESTS

RUN NUMBER	TEST CONDITION	AMBIENT TEMPERATURE (°F)	PUMP INLET TEMPERATURE (°F)	VALVE POSITION
80-01	Actuator Retract	75	193	Hold-Retract
80-02	Actuator Extend	74	190	Hold-Extend
80-03	Actuator Reversal	72	193	Hold-Retract-Extend
80-12	Actuator Reversal	70	195	Hold-Extend-Retract

TABLE 33 THERMAL SPEEDBRAKE TESTS

***** TEST OF THERMAL TRANSIENT PROGRAM ***** (80-01-HX)

THE THERMAL TRANSIENT RESPONSE IS FROM T=0.0 TO T= 90.000 SECONDS AT TIME INTERVALS OF DELT= .05000
WITH OUTPUT POINTS PLOTTED AT INTERVALS OF , .50000 SECONDS

FLUID DATA FOR FOR MIL-H-5606A WITH A VAPOR PRESSURE OF 2.0 PSI

LINE DATA LINE NO.	LENGTH	INTERNAL DIA	WALL THICKNESS	DELTAX	AMBIENT TEMP	STRUCTURE TEMP	FLUID TEMP	MATERIAL TYPE
1	52.0000	.5740	.0280	26.0000	75.0000	75.0000	84.0000	9
2	27.0000	.4440	.0280	27.0000	75.0000	75.0000	78.0000	9
3	54.0000	.4440	.0280	27.0000	76.0000	75.0000	84.0000	9
4	54.0000	.4440	.0280	27.0000	76.0000	76.0000	78.0000	9
5	27.0000	.4440	.0280	27.0000	75.0000	75.0000	78.0000	9
6	72.0000	.4440	.0280	36.0000	75.0000	75.0000	84.0000	9
7	126.0000	.6720	.0340	18.0000	75.0000	75.0000	84.0000	9

COMP#, 1 INTEGER DATA 1 91 0 -1 2 0 0 0 0 0 0 0 0 0 0

COMP#, 2 INTEGER DATA 2 22 6 1 -2 -5 5 6 0 0 0 0 0 0 0

REAL DATA CARD # 1	.2500E-02	.1250E+00	.6200E-01	.3200E+02	-.2500E-02	-.1250E+00	.6300E-01	.32[illegible]E+02
REAL DATA CARD # 2	.2500E-02	.1250E+00	.6200E-01	.3200E+02	-.2[illegible]E-02	-.1250E+00	.6300E-01	.32[illegible]E+02
REAL DATA CARD # 3	.9000E+01	.3000E+01	.3000E+01	.4500E+01	.1800E+02	.9000E+02	.6900E-02	.1000E+01
REAL DATA CARD # 4	.7500E+02	.7500E+02	.8000E+02	.8000E+02	.7500E-01	0.	0.	0.
REAL DATA CARD # 5	0.	.6100E+01	.8150E+01	.1210E+02	.1215E+02	.5100E+02	0.	0.
REAL DATA CARD # 6	0.	0.	-.1863E+00	-.1863E+00	0.	0.	0.	0.

COMP#, 3 INTEGER DATA 3 41 2 2 -3 0 0 0 0 0 0 0 0 0 0

REAL DATA CARD # 1	.9000E+01	.5000E+00	.2200E+00	.1600E+01	.6600E+01	.6600E-02	.1000E+01	.750[illegible]E+02
REAL DATA CARD # 2	.7500E+02	.8600E+02	.8600E+02	.6500E+00	.1325E+00	0.	0.	0.

COMP#, 4 INTEGER DATA 4 102 4 3 -4 0 0 0 0 0 0 0 0 0 0

REAL DATA CARD # 1	.1190E+01	.2410E+03	.8730E+01	.7040E+01	.9010E+01	.9000E+01	.3400E+02	.6400E-01
REAL DATA CARD # 2	.3840E+03	.3500E+01	.1600E+01	.5660E+00	.6000E+03	.6900E-02	.6000E-01	.900[illegible]E+02
REAL DATA CARD # 3	.9000E+02	.8000E+02	.8000E+02	.1000E+00	.3412E+02	.5000E+00	0.	0.
REAL DATA CARD # 4	.1320E+02	0.	0.	0.	0.	0.	0.	0.

COMP#, 5 INTEGER DATA 5 41 2 4 -5 0 0 0 0 0 0 0 0 0 0

REAL DATA CARD # 1	.9000E+00	.6900E+00	.2100E+00	.1600E+01	.6600E+01	.6900E-02	.1000E+01	.75[illegible]E+02
REAL DATA CARD # 2	.7500E+02	.8400E+02	.8600E+02	.6500E+00	.1222E+00	0.	0.	0.

COMP#, 6 INTEGER DATA 6 11 2 6 -7 0 0 0 0 0 0 0 0 0 0

REAL DATA CARD # 1	.9000E+01	.1000E+01	.1000E+01	.2000E+01	.9000E+01	.3000E+01	.6600E-02	.7[illegible]E+02
REAL DATA CARD # 2	.7400E+02	.8400E+02	.8400E+02	0.	0.	0.	0.	0.

COMP#, 7 INTEGER DATA 7 61 1 7 0 0 0 0 0 0 0 0 0 0 0

REAL DATA CARD # 1	.1000E+01	.9000E+02	.9000E+02	0.	0.	0.	0.	0.

FIGURE 534 RUN 80-01 HYTTHA INPUT DATA

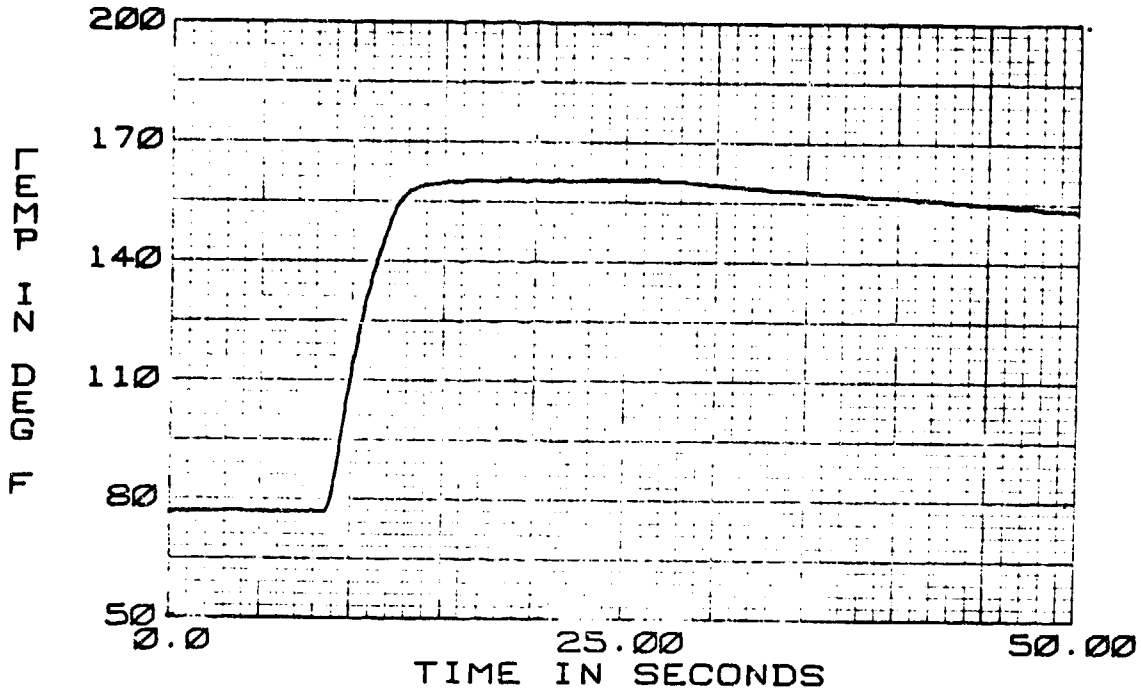

FIGURE 535 F-15 SPEEDBRAKE SYSTEM

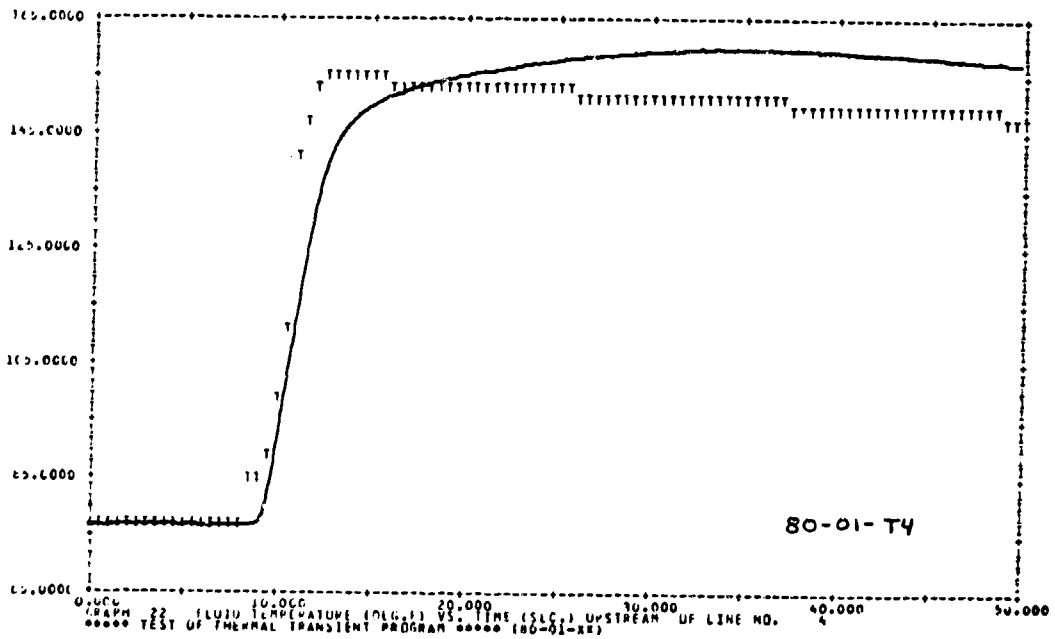

FIGURE 536 80-01-T4 FLUID TEMPERATURE

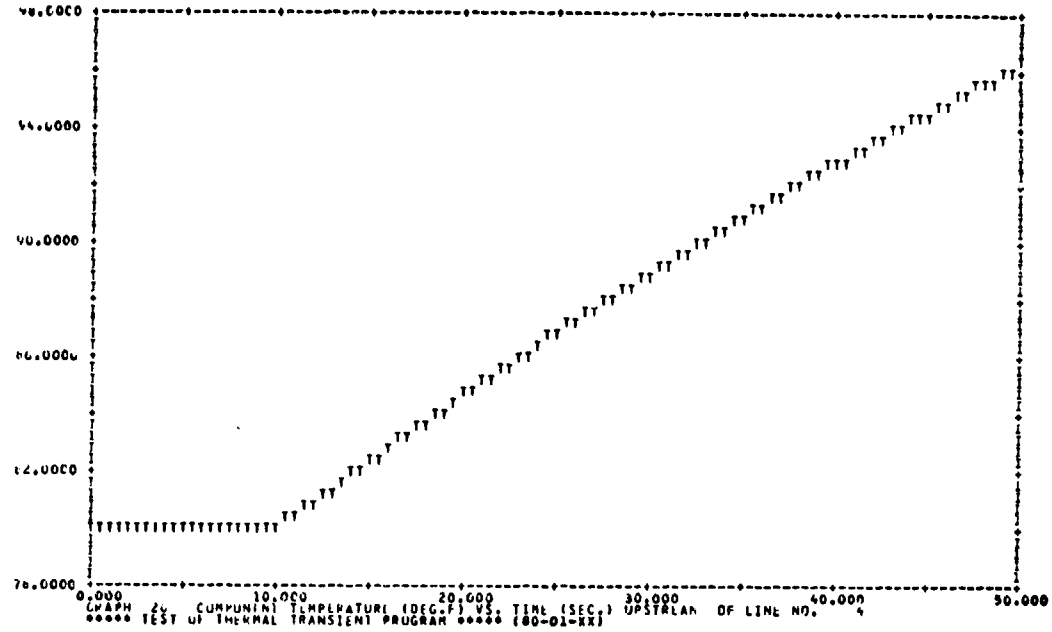

FIGURE 537 SPEEDBRAKE ACTUATOR WALL TEMPERATURE

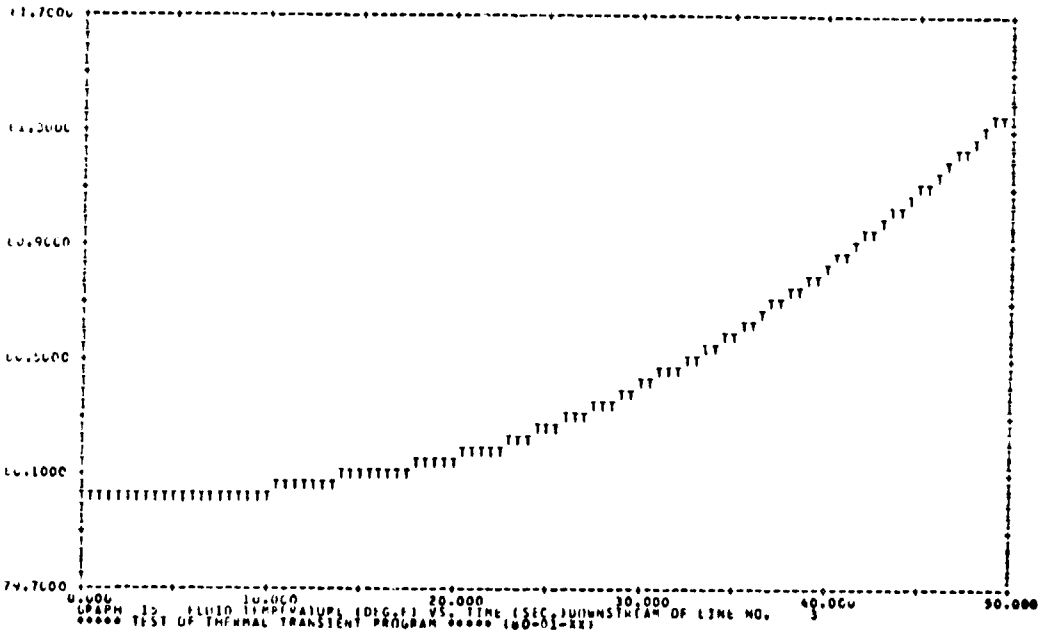

FIGURE 538 FLUID TEMPERATURE AT THE T1 LOCATION

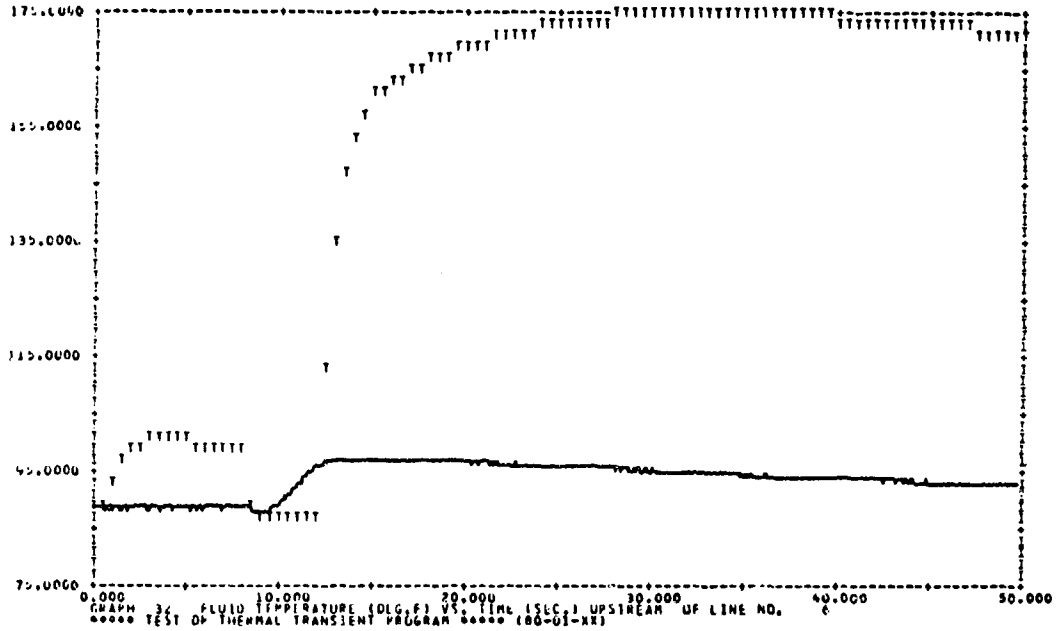

FIGURE 539 FLUID TEMPERATURE AT THE T3 LOCATION

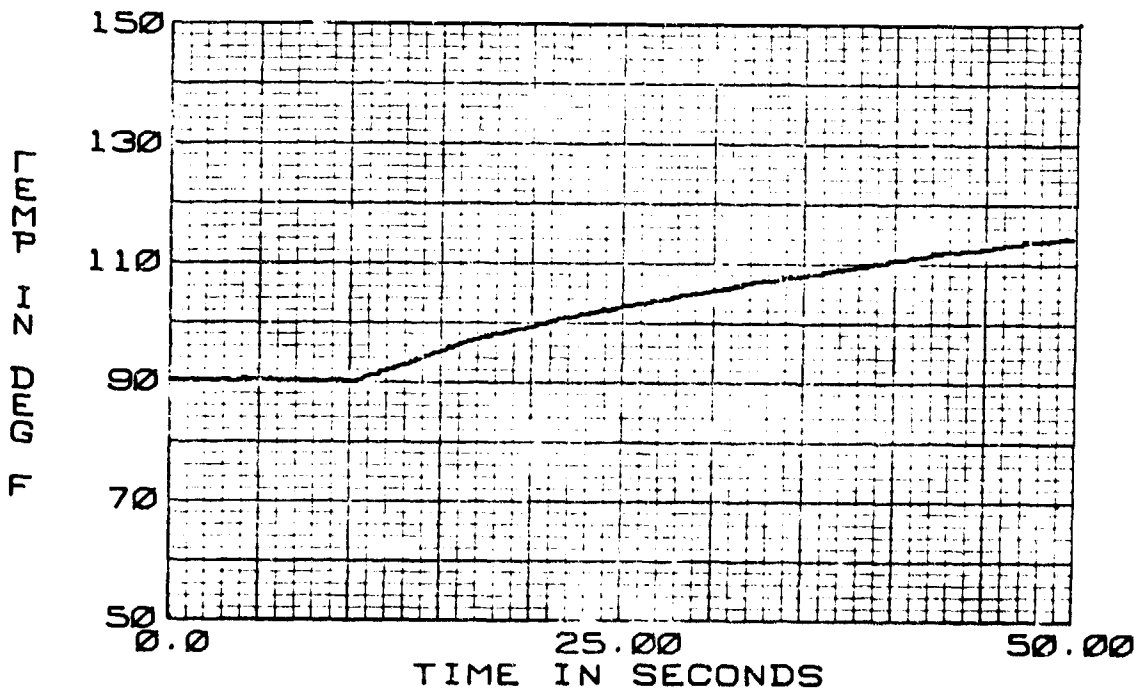

FIGURE 540 F-15 SPEEDBRAKE SYSTEM
80-01-T1 RETRACT DIRECTION

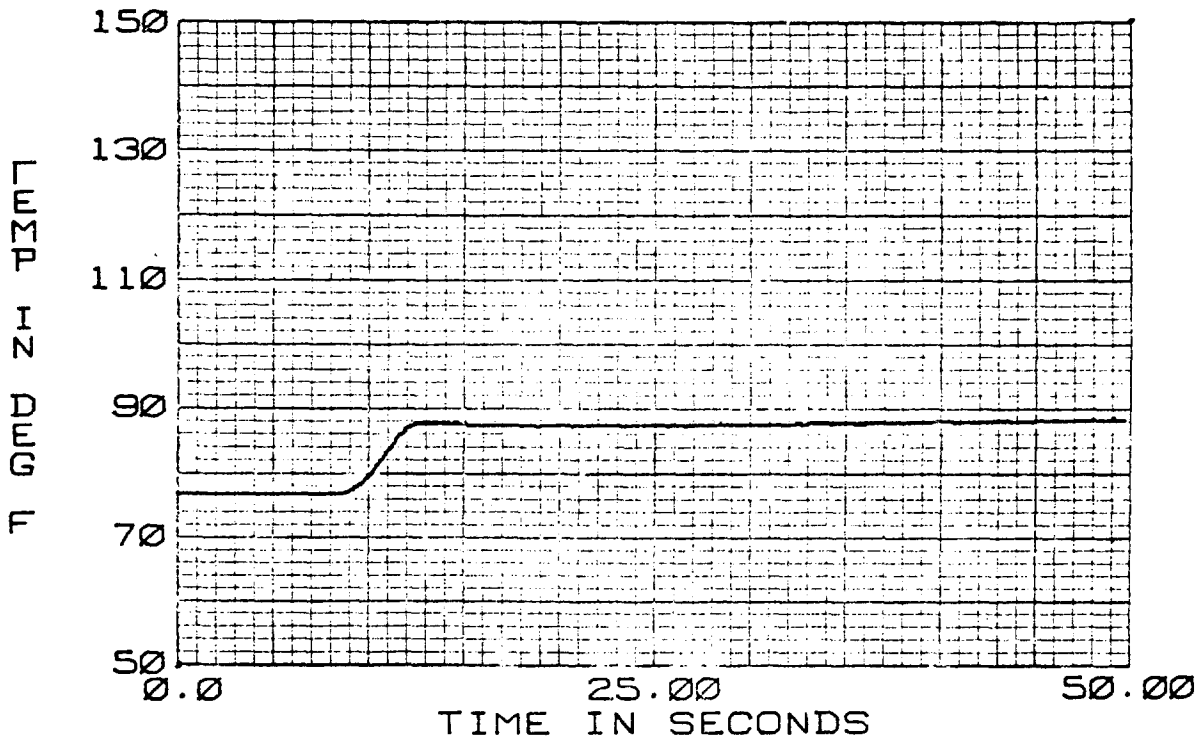

FIGURE 541 F-15 SPEEDBRAKE SYSTEM
80-01-T3 RETRACT DIRECTION

SECTION VIII

DISCUSSIONS AND CONCLUSIONS

1. AHSPA PROGRAM PHILOSOPHY AND EMPHASIS

Since 1970 MCAIR has been actively involved in developing and verifying effective computer programs for design and analysis of aircraft hydraulic systems. The AFAPL funded program has enabled MCAIR to significantly improve these programs and verify them through experimental tests. The resultant computer technology has been made available to all interested users and in addition all facets of the APL program, including testing and verification work, have been publicly presented and discussed during the contract period. This open give-and-take of information has been good for the computer programs because it provided a means by which the programs could be further verified by the experience of other users. The feedback from the varied backgrounds of academic, industrial and government users has been seriously studied and implemented wherever possible in the computer programs. MCAIR believes this rapport was necessary to provide viable and up-to-date computer programs that would be utilized.

The dynamics of aircraft hydraulic systems are complex. The rapid changes in flow demand, the influence of fluid friction, cavitation in return lines, the response characteristics of pressure compensated pumps and servo units, are all difficult to test and to analyze effectively using standard analytical techniques. The HYTRAN program was developed to simulate many of those phenomena. At the start of the contract there was no verification of the HYTRAN subroutines because of the lack of suitably instrumented tests. HYTRAN was the most complex of the programs and thus received much of the APL program funds for its development and verification. Continual attention was given to computation techniques so as to minimize the potentially high running costs of the transient program, while retaining useful but practical accuracy. MCAIR believes that these efforts have made HYTRAN a truely effective analysis tool in an area where proper analytic techniques were heretofore either cumbersome, time consuming, or not practical at all.

HSFR, SSFAN, and HYTRAN were originally developed separately with little commonality between the programs. The purpose was to obtain a wide variety of analytical techniques that would yield the best approaches to the varied problems encountered in hydraulic model and system simulation. As the contract progressed many of those techniques found their way into all three programs. This process however is not complete. The continuous evolution in program improvement and development is inherent, for example:

The SSFAN program benefited from the steady state portion of the HYTRAN program. Further work with improved numerical techniques enabled the HYTTHA program steady state section to be faster than HYTRAN. These changes have not been, but could be, incorporated in HYTRAN.

HYTRAN and HSFR are the most developed of the four computer programs because they received a majority of the test effort in the laboratory. However, the SSFAN program may be correlated to the steady state data taken for the HYTRAN tests on a subsystem level. The most pertinent and useful SSFAN verification is accomplished at low temperatures, which was outside the contract scope. Further work could be done in this area.

2. LABORATORY TEST PROGRAM EXPERIENCE

In a test program covering such a wide range of hydraulic components, systems, and operating conditions many problems were encountered. Much of the laboratory test effort has been documented in Section III of this report. The major areas of concern in the program were pressure instrumentation, adequate flow measurement of transient phenomena, proper component instrumentation, the ability to generate a reasonable system transient, and the need to remove unwanted mechanical and electronic noise.

a. Pressure Instrumentation - Strain gage and piezoelectric pressure instrumentation was used in the testing. The transducers were either split block, flush mounted, or clamp-on mounted to the lines. Resonances problems did occur for the split block mounting in areas where the column of oil exposed to the transducer surface would be excited by the pulsating flow in the line at critical pump speeds. Many of the transducers would drift with temperature and thus had to be recalibrated for each run. Normally the accuracy of the pressure transducers are within $\pm$0.5% of the rated pressure.

Flush mounting of fixed pressure transducers with the flow stream is recommended to avoid an extraneous signal from resonating liquid columns in short stub mounts. Roving clamp-on piezoelectric transducers are recommended for easy mapping of standing pressure waves.

b. Transient Flow Measurement - Hot film anemometers were used to measure transient flow in the test fixtures. The non-linear output of the transducers would drift with small changes in the system temperature. Thus calibration curves were generated for each temperature condition

that was run in the laboratory. Because of the non-directional characteristics of the hot film probe, care was needed in installation and proper data interpretation.

Although the anemometers were only capable of measuring local fluid velocity, they provided useful information for transient program verification.

c. F-15 Pump Instrumentation - The instrumentation on the pump worked well. The hanger position LVDT probe did lose contact with the rate piston during turn-on transients. A split block was added to the LVDT and nitrogen gas was used to load the probe shaft against the rate piston.

The proximity sensor used to measure compensator valve spool position had only a 0.050 inch linear range while the measured displacement on the test pump valve was 0.070 inch. This was not a serious shortcoming since spool position could be correlated to pump outlet pressure.

d. Transient Control Valve - Design and operation of the fast control valve presented many problems. A valve with an operating time of around 2 milliseconds and a maximum flow rate of 40 gpm was considered desirable. A commercial unit was extensively modified by the addition of a spring and a separately powered hydraulic servovalve/actuator to operate the valve poppet. Because of the valve design it was difficult to obtain any type of spool rate control over 10 milliseconds. The spool would frequently bounce during turn-on or turn-off transients causing the data run to be scrapped Also flow forces on the valve would sometimes cause it to close prematurely.

e. Mechanical and Electrical Noise - Lines on the test fixture were clamped according to standard aircraft procedures. Excessive line vibration did interfere with the transient component tests. When this occurred additional clamps and weights were added on to the system. A large commercial acoustic filter was used during many of the component transient tests to minimize pump pressure pulsations in the test section of the circuit.

Electronic filtering was required on the instrumentation to remove spurious signals caused by mechanical vibrations and excessive instrument sensitivity.

3. COMPUTER PROGRAM VERIFICATION AND STATUS

A brief synopsis of the status of each computer program and the results of the verification effort are presented in the following sections. The strengths and weaknesses of the programs are discussed along with areas of program usage and application. Observations are offered based on MCAIR's contract effort and other related efforts.

a. HSFR Computer Program - The present HSFR program can provide sufficiently reliable predictions of the resonant frequencies to permit useful design analysis of real hydraulic systems. MCAIR has used the program to advantage on the F-15 production power control (PC) systems, and the F-15 "Streak Eagle" DC motor-pump emergency hydraulic system. Preliminary analysis of the F-18 hydraulic systems has been done, and investigative modeling and testing have been done on the two-pump F-15 utility systems.

Usefulness of the current program is a function of system complexity and the number of continuous operation pump speeds. The HSFR program makes it possible to easily and quickly identify simple system changes or components which will relocate resonant frequencies away from continuous operating pump speeds. Simpler circuits and fewer continuous operating speeds allow more "room" in the operating pump speed range to accomplish safe relocation of resonances. The F-15 utility system is an example of an acoustically complex, two-pump, multi-branch system with numerous major resonant responses over the pump operating speed range. The F-15 PC systems are somewhat less complex with a single pump and fewer branch circuits.

Fortunately the accuracy of pulsation amplitude prediction is not critical. If resonance relocation can be accomplished, high pressure amplitudes can be tolerated since they are encountered only transiently during start/stop speed changes. If the circuit is too complex for resonance relocation, wide band attenuation over the entire operating speed range is probably required to solve pulsation related problems. In either case, close accuracy in predicting pressure pulsation amplitude is not required.

Amplitude predictions were good for the F-4 resonator test circuit. Fluid temperature and resonator location did not significantly effect the accuracy of the predicted amplitudes.

Predicted pulsation amplitudes are very high compared to test results for the filter circuit and hose circuit simulations. Further modeling and/or verification tests will be required to understand this phenomenon. No common factor is obvious. The filter and hose present an effect in the circuit which is not accurately modeled by the present HSFR program. Secondary resonances exist in the hose circuit indicating that the hose has a reflective characteristic which is not modeled.

The present HSFR program models one hydraulic acoustic source (pump). Accurate modeling of a two pump system is not practical unless the phasing between the two acoustic outputs is known. This requires phasing of the power source gear box and pump shafts with respect to pump cylinder barrel rotation angle. A two-pump system may be usefully analyzed by modeling each side as single pump independent system, particularly if pump to outlet junction lines are long. However, this remains a questionable technique due to the uncertainties of signal phasing and check valve effects in a master/slave pump arrangement.

The HSFR program can be used to study hydraulic return system resonance characteristics. The PUMP subroutine can be used to study pump hanger torque, port plate valve timing, and cylinder cavitation.

Use of adiabatic bulk modulus data for MIL-H-5606B hydraulic fluid is recommended when performing HSFR analysis of systems using MIL-H-83282A fluid. Test results have shown this to be more accurate than the available bulk modulus data for MIL-H-83282A. The FLUID subroutine is currently programmed in this manner.

A composite plot of the maximum standing wave pulsation level at each resonant pump speed should be used for showing and comparing the overall acoustic performance of a circuit. Standing pressure wave plots can be used for studying response at a single resonant frequency, and for evaluating pulsation amplitudes upstream and downstream of circuit reflection points and attenuators.

Sufficient measurements should be made to define the standing peak pressure wave, both upstream and downstream of attenuation devices, for effective evaluation of hydraulic system pressure pulsations. Line pressure measurements every 6 inches are sufficient with 9 piston pumps operating to 5000 rpm. This is particularly important for fully defining basic systems acoustics, and evaluating the net effect of circuit changes and attenuation devices.

The resonant frequency of a central hydraulic system between the pump and first major reflection point follows a half-wave characteristic ($f_M = \frac{C}{2L}$), even if the circuit has a closed-end. A closed end circuit branched off the main line exhibits a quarter-wave resonant frequency ($f_M = \frac{C}{4L}$).

Pressure service ports and pressure transmitters are sometimes located at the end of lines which branch off the central system. In a closed-end branch circuit a restrictor or check valve should be placed at the branch point, not at the terminating component, to protect the entire branch circuit from resonance damge.

b. HYTRAN Computer Program - The current version of the HYTRAN program can give useful predictions of peak waterhammer pressures and system response to changing flow demands. MCAIR is currently using this program to analyze the F-18 hydraulic systems and YAV-8B hydraulic systems. The HYTRAN program is also being used to simulate hydraulic systems on the space shuttle. The purpose of this study is to assure that the shuttle meets all the requirements for both normal and contingency operation during ascent and descent flight modes.

Many of the computer models have been adequately verified for HYTRAN. Simulation and testing of relatively complex hydraulic systems has shown the basic accuracy of the program. With simulation of more complicated systems, problems will undoubtedly be encountered. Modifications will have to be made to the subroutines to account for conditions not previously expected in the original development of the general models.

HYTRAN is an extremely complex program. A key to effective application and understanding of HYTRAN lies in the ability of the user to recognize bad computer output. This requires that the user be familiar with transient phenomena in hydraulic systems and know how to interpret the data provided by the program. Unacceptable program results may be due to inaccurate input data or unreal design conditions. Useful information can be obtained from HYTRAN because the effects of complex interrelationships between parameters may be easily observed and analyzed. HYTRAN, as with the other computer programs, is still in a development stage. As with all computer programming, the job for engineering design analysis is never finished. But HYTRAN general purpose models are adequately verified so that it may be used with confidence to analyze specific design and performance aspects of hydraulic systems.

When verifying the computer models, it was important to select adequate boundary conditions. Boundary conditions were located at dynamically quiet points in the hydraulic system. Reservoirs and accumulators provided such points. Excessively noisy data was filtered before data processing to remove the possibility of a mathematical instability arising in the simulation. Noisy data did result from numerous areas such as pump ripple, line vibration, or improper transducer mounting location.

Accurately defining the component input parameters was another key to proper computer model verification. Incorrect poppet mass on a check valve or fluid volume in a filter did drastically affect the computer simulations of these components. Care in measuring such parameters was important.

The computer program cannot give reasonable correlation unless test conditions are adequately measured. System air content, ambient temperature, and fluid properties were all important quantities that were recorded.

Evaluation of the data as testing progressed was important to proper computer simulation verification. Many problems encountered in the program verification effort were traced back to bad test data, or failure to properly interpret the data.

(1) Line Model - The line model has been verified between 0-3750 psi and at temperatures of 120 and 210°F. Turn-off transient correlation with pressure and flow data is good. For turn-on transients the computer program predicts typically 150-200 psi below the reflected pressure wave. Initial flow correlation is poor because the hot film anemometers were not capable of measuring mean flow, but only that flow based on a local velocity limited to a specific region close to the tube wall.

(2) Cavitation Model - The HYTRAN line model calculations of flow and pressures under transient cavitation conditions initially did not compare well with the test data. For turn-off transients reasonable correlation was obtained if the line dynamic friction was set to zero. DFRICD was zeroed whenever the pressure at either end point was equal to or less than the fluid vapor pressure.

The computer output results for cavitation during the turn-on transients also did not compare well with the data. The majority of the error may be attributed to the use of the turbulent friction term when the Reynolds number reaches the transition number, while in reality the line flow is still laminar.

(3) F-15 Pump Model - For the initial pump response, the PUMP51 subroutine adequately predicts the measured data. Since the initial transient is usually the most severe, the program results do reflect actual operating characteristics. However, subsequent oscillations as the transient dampened were not accurately computed. The PUMP51 subroutine calculations do reflect a stable prediction of transient dampening.

Errors in the subroutine may be attributable to a number of factors. Lack of cavitation effects caused by improper filling of the pistons, the effect of hanger angle and pump RPM, bulk modulus effects at different pressures and temperatures on piston hanger, and friction effects on the actuator and valve, are some of the factors not included in the pump model. Other sources of error exist in the model itself. Not adequately defining the flow forces on the valve, assuming linear leakage characteristics, and the treatment of hanger inertia could all introduce small errors into the simulation.

(4) Filter Model - The HYTRAN filter model calculations of flows and pressures compare reasonably well with the test data measured in the lab. Because of the small filter used there was little difference between the filter with and without an element. The filter supplied more attenuation to the pressure signal and slowed down the wave speed slightly as compared to the unobstructed line.

(5) Check Valve Model - The HYTRAN check valve model compares favorably to the test data measured in the lab. The majority of the model error can be attributed to the absence of adequate flow force effects on the poppet in the calculation. Flow forces are not well defined theoretically and really depend upon the actual valve geometry. Attempts to include axial flow forces in the calculations contributed some improvement for the 125°F and 210°F, 11.5 and 38.5 CIS turn-off transient calculations. Since the CVAL31 subroutine was written for a general check valve it appears that this model is adequate for what it was designed to accomplish.

(6) Restrictor Models - The HYTRAN restrictor model (REST41) and one-way restrictor model (CVAL33) calculations of pressures compare reasonably well with the test data measured in the lab. The verification results indicate that the restrictor models are relatively good.

(7) Hose Model - Hose model calculations of flows and pressures did not compare well with the test data. For the 1/4" hose the computer results predicted a lower damping frequency than was actually measured. However, the amplitudes on the computer pressures match well with the test results. The 5/8" hose computer results showed a higher frequency than the test data. Amplitude correlation with the computed pressures was good. In turn-on transients for both hoses the HYTRAN program consistently under predicted the maximum pressure amplitude of the test data.

(8) Two Stage Relief Valve Model - The malfunctioning control valve did not provide the necessary sharp turn-off transients in the test system, and prevented the direct verification of the two stage relief valve model. Computer runs made without the test data indicate that the relief valve model reasonably simulated the actual valve's operating characteristics.

(9) Air Effects Simulation - Return system transients were generated in the lab by rapid opening and closing of a control valve. Air was added to the system and allowed to dissolve into the hydraulic fluid. As the system dissolved air levels increased from 0.4% to 48% by volume, the transient tests showed a significant decrease in the oscillating frequency of the pressure and flow waves following cavitation. This phenomena results from free air collecting in the return system downstream of the valve. The air came out of solution after the pressure drops to near zero which occurred when the control valve was either opened or closed. At higher dissolved air contents more air would leave the fluid given the same valve operating rate and system temperature and reservoir pressure. This free air would slow the rise and decay of the pressure and flow waves by providing an additional air spring for these waves to travel through.

The testing indicates that at higher air contents the severity of return line pressure transients are reduced.

Unfortunately this was about the only benefit of dissolved air. From a total system viewpoint, large amounts of air may cause serious problems relating to system start-up and normal operation. Start up problems include lack of pump prime (airlock), system damage due to transient air ingestion by the pump, and excessive drop in reservoir level.

Currently, the effects of air in hydraulic systems is not modeled in the HYTRAN computer program. Dissolved air does not alter the physical properties of the hydraulic fluid, but free air in the form of large or small bubbles in the fluid would drastically affect the component and line models. Predicting the occurrence of these air bubbles, their size, and interactions with the fluid and components would be a task beyond the scope of the present contract. The testing has provided basic data on how dissolved air affects hydraulic return system performance.

Since the .4% and 12% air content tests showed little change, and the existing HYTRAN cavitation model gives a reasonable cavitation simulation, it is considered that the current model is adequate and representative of a well bled system.

(10) Valve Controlled Actuator Model - The valve controlled actuator tested in the lab exhibited some destabilizing valve reaction forces. These may have accounted for the poor correlation with the initial transient test data. The addition of the stiction forces helped with predicting the magnitude of the first transient spike, but it could not model the subsequent 15 msec delay before the rise of the cylinder pressures. The inclusion of a dynamic friction term assured that the cylinder pressures were of the proper magnitude.

The simple servoactuator model used in the HYTRAN program gives reasonable correlation with the lab test data and is considered a good subroutine for most applications.

(11) Accumulator Model - The range of specific heat ratio during accumulator discharge (and charge) varies widely depending on the duration of the transient.

Discharge of the F-15 JFS accumulator from an initial shop ambient temperature condition produced the following specific heat (n) values for various discharge times.

Total Discharge Time (Sec)	Range of Specific Heat Ratio (GN_2) During Discharge
2.3	1.65 to 1.52
5.0	1.32 to 1.16
32.0	1.16 to .926

Higher specific heat ratios would be obtained for lower initial temperatures, particularly for the longer discharge time. A specific heat ratio for sizing an accumulator should be chosen for the maximum discharge rate and lowest initial temperature expected in the applicable system.

Computer simulations which model rapid changes in accumulator pressure should use a high specific heat ratio, 1.4 to 1.6. The present HSFR program uses 1.4. The HYTRAN program accumulator model currently uses a specific heat ratio of 1.0, making no attempt to model the wide range of specific heat ratios possible for transient calculations. A constant specific heat ratio should be selected and used in the HYTRAN gas accumulator model to suit the type of application being analyzed. Choosing a good design value for specific heat is a significant factor when sizing 3000 psig accumulators such as those used in hydraulic start systems for engine start and auxiliary power systems.

(12) Subsystem Modeling - Modeling of the F-15 speedbrake subsystem with the HYTRAN program went exceedingly well. The computer run showed that the component models do function properly in a system simulation, and for this basic system the HYTRAN program was able to calculate the proper pressures and flows.

(13) Two Pump System Verification - The HYTRAN computer simulation of the two pump system indicated reasonably good correlation with the test data. The initial response predictions were adequate but the final steady state operating pressures were larger than actually measured.

c. SSFAN Computer Program Verification - The SSFAN computer program component models have been verified for many of the test conditions recorded in the lab. The basic techniques of linearizing the leg impedances and applying the continuity equation at branch points have been verified for use in SSFAN and the steady state portions of HYTRAN and HYTTHA.

The SSFAN program has been used to analyze the gun subsystem, the main and nose landing gear subsystems, the arresting gear damper precharge subsystem and the emergency brake/landing gear subsystems on the F-18. MCAIR has also used SSFAN to model the two hydraulic systems on the YAV-8B.

(1) Essential Components - Essential components were tested to determine their steady state flow vs pressure drop characteristics. It was determined that the basic data on lines, unions, fittings, etc., at ambient and high temperature test conditions were not necessary for adequate model verification of the higher priority HYTRAN test items. Line pressure drop equations used in SSFAN were verified by the test data.

(2) Supplemental Components - Steady state data was recorded for a check valve, 1/4" and 5/8" teflon hoses, one-way restrictor, single and stacked disc type orifices and a compensated check valve. The steady state portion of the HYTRAN program was verified for those components.

(3) Steady State F-15 Pump Testing - Steady state testing was accomplished on the F-15 instrumented pump with two hydraulic fluids. The difference in case drain flow vs pressure characteristics and heat

rejection performance between MIL-H-5606B and MIL-H-83282 fluids is significant. The difference may be due to the non-Newtonian vs Newtonian characteristics of the two fluids.

(4) Steady State Two-Pump System Verification - SSFAN simulation of a two pump test system correlated well with the test data. Modifications were made to the pump model to handle the master-slave relationship. Although the changes had to be made by the programmer, they were relatively minor.

d. HYTTHA Computer Program Verification - HYTTHA is the "junior" member of the four programs developed under the present APL contract. Many problems will be encountered by users as the complexity of the modeled systems increase. Every effort should be made to coordinate program changes with all the active program users.

(1) Line Model - The HYTTHA line model adequately predicted the temperature distribution in the tested line sections. Verification has been accomplished for the data presented in this report. Test data is not currently available to verify the line model over a wide range of temperature conditions.

(2) Restrictor Model - The restrictor model (TREST41) computer runs correlate well with the test data. The model does provide adequate representation of the thermal effects of a simple restrictor in a line system.

(3) Pump Model - No verification has been accomplished with the HYTTHA program pump model. The pressure data taken for each test oscillated and could not be used as boundary conditions in the simulation programs.

(4) Heat Exchanger Model - The heat exchanger model was able to predict the test results for the range of temperatures that were tested.

(5) Subsystem Model - Test data on the F-15 speedbrake system does not correlate with the HYTTHA program predicted results. Further work on the subroutines must be done before adequate verification can be accomplished.

SECTION IX

RECOMMENDATIONS

During the course of the Aircraft Hydraulic System Performance Analysis program a number of desirable additional efforts have identified themselves. Many of these are logical extensions of the current program; others lend themselves to independent investigation. The recommendations can be grouped into the following eight headings:

1) Improvement and extension of the existing computer programs (HSFR, HYTRAN, SSFAN, HYTTHA).
2) Development of a hydraulic line mechanical response (HLMR) computer program.
3) Verification of existing programs on a complete aircraft hydraulic system.
4) Adaptation of the existing programs to other aircraft fluid systems.
5) Evaluation of program correlation with user test data
6) Development of hardware for improved fluid system dynamics and testing.
7) Revisions and additional to military specifications.
8) Newtonian vs non-Newtonian fluid characteristics.

A summary of the recommendations developed is presented in Section 1, and the detailed discussion is presented in Section 3.

1. SUMMARY OF RECOMMENDATIONS

Recommendations for program improvements and areas of expansion are presented in Table 34. The activities included in the present one-year add-on contract are highlighted. Recommendations for areas of further study are listed in Table 35.

The higher priority recommendations are summarized in the next two sections. The distribution of funds into these areas would be cost effective because all program users could benefit from their implementation. These items will provide an immediate payoff to the engineer in solving practical design and analysis problems. They will also enhance and strengthen the capabilities of the computer programs.

a. Priority Recommendations for Future Computer Effort

The recommendations for future computer program work are presented in order of importance in Table 36. A specific discussion of each topic may be found in the referenced section.

b. Priority Recommendations for Complementary Effort - The items in Table 37 represent complementary efforts evolving from computer program verification and development work.

TABLE 34

AIRCRAFT HYDRAULIC SYSTEM PERFORMANCE ANALYSIS
RECOMMENDATIONS FOR IMPROVEMENT/EXPANSION OF COMPUTER PROGRAMS

	IMPROVEMENT	EXPANSION (NEW MODELS)
HSFR	o Increase program accuracy o Model pump compensator o Evaluate frequency dependent friction	Δ o Vane pump Δ o Axial piston Motor
HYTRAN	Δ o Further F-15 pump testing o Update bulk modulus	Δ o Vane pump Δ o Axial piston motor o Cavitating pump o Lossless line o Reservoir level sensing valve
SSFAN	o Verify at low temperature o Develop quasi-transient model o Simplify building routines o Analyze complex systems o Develop floating branch point o Modify special component model	o Flow regulator o Single node reservoir o Pressure regulator o Hydraulic motor o Constant displacement pump o Dynamic cross
HYTTHA	o Continued development and verification	

Δ Activity included in present one-year add-on contract

TABLE 35

AIRCRAFT HYDRAULIC SYSTEM PERFORMANCE ANALYSIS
AREAS RECOMMENDED FOR FURTHER STUDY

SUBJECT	COMPUTER PROGRAM APPLICABILITY AND AREAS OF STUDY
Δ Develop hydraulic line mechanical response program	New computer program to be verified with test data
Model and verify a complete aircraft hydraulic system to provide additional program development	Use HSFR, HYTRAN and SSFAN programs with verification from Iron Bird test data
Evaluate computer program correlation with user test data	Evaluate existing HSFR, HYTRAN, SSFAN and HYTTHA program models
Adapt existing programs to other fluid systems	Use HSFR, HYTRAN, SSFAN and HYTTHA for analysis of: 1. Fuel systems 2. Lubrication system 3. Electronic equipment liquid cooling systems
Develop hardware for improved fluid systems dynamics and testing	Develop 1. Wide band acoustic attenuator 2. Harmonic free hydraulic pulsation generator 3. Pump modifications to reduce acoustic energy 4. Dynamic flow measurement instrumentation
Revisions and additions to military specifications	1. Modify pump spec. (MIL-P-19692C) 2. Modify general spec. (MIL-H-5440) 3. Create new spec. which will provide computer program input information
Newtonian vs. non-Newtonian fluid characteristics	Conduct study, evaluation and tests to adequately understand the impact of Newtonian and non-Newtonian fluids in aircraft hydraulic systems

Δ Activity included in present one-year add-on contract

TABLE 36

AIRCRAFT HYDRAULIC SYSTEM PERFORMANCE ANALYSIS PRIORITY RECOMMENDATIONS FOR FUTURE COMPUTER PROGRAM EFFORT

Priority	Subject	Paragraph
1	Develop and verify hydraulic line mechanical response computer program	3.b.
2	Develop and verify vane pump model for HYTRAN and HSFR	3.a.(1)(a) 3.a.(2)(a)
3	Develop and verify axial piston motor model for HYTRAN and HSFR	3.a.(1)(b) 3.a.(2)(b)
4	Further data analysis and testing of the F-15 instrumented pump for HYTRAN	3.a.(2)(c)
5	Develop and verify SSFAN flow regulator model	3.a.(3)(a)
6	Verify SSFAN at low temperature	3.a.(3)(b)
7	Develop quasi-transient model for SSFAN	3.a.(3)(c)
8	Program User Experience Feed Back and Interchange	3.e
9	Verification of existing programs on complete aircraft hydraulic systems or subsystems	3.c
10	Develop and verify cavitating pump model for HYTRAN	3.a.(2)(d)
11	Develop and verify reservoir level sensing valve model for HYTRAN	3.a.(2)(e)
12	Adapt existing programs to fuel systems	3.d.

TABLE 37

AIRCRAFT HYDRAULIC SYSTEM PERFORMANCE ANALYSIS RECOMMENDATIONS FOR COMPLIMENTARY EFFORT

Priority	Subject	Paragraph
1	Further develop wide-band acoustic attenuators	3.f.(1)
2	Create new military spec. which will provide computer program input information	3.g.(3)
3	Study and evaluate Newtonian vs. non-Newtonian fluid characteristics	3.h.
4	Develop harmonic free hydraulic pulsation generator	3.f.(2)

2. SOURCE OF RECOMMENDATIONS

Development and test verification of the HSFR, HYTRAN, SSFAN, and HYTTHA computer programs has opened up new avenues for these analytical design tools. Upon verifying a component math model for a specific set of test conditions, there was a desire to see how well it would fit another set of test conditions. However, due to the limitations of time and money further inquiry was not permitted. Many recommendations for future computer program improvements have resulted.

Motivation for other computer program changes resulted from a desire to achieve greater utility by extending the program to cover additional requirements of the individual users. The changes include extensions to cover models of components not presently included and a sequence of programming steps to attain a specific type of output, require program modifications. The resulting capability will be beneficial enough to all program users to justify the efforts from a cost effectiveness standpoint.

Through the years, we have found that practical design experience shapes a computer program and recommendations based on application are the most useful. True design needs will dictate whether a change is ever implemented. In the final analysis, the users will have the responsibility of adapting the existing general purpose models to the analysis of design and performance aspects of their specific hydraulic/systems/subsystems. The vast scope and number of variables involved in these programs, particularly HYTRAN, make it unlikely that they could ever be so highly developed as to be effectively used by personnel totally inexperienced in computer technology and hydraulic system design and performance.

3. DETAILED RECOMMENDATIONS AND DISCUSSION

a. Additional Computer Program Work - The following recommendations cover areas for improvement in each of the four computer programs. These areas are judged worthy of additional development and test verification effort.

(1) HSFR Recommendations

(a) Vane Pump Model Development - Develop and verify a vane pump model to extend the HSFR program capability to simulate a typical pump used in many types of fluid systems.

(b) Axial Piston Motor Model - Develop and verify an axial piston hydraulic motor model. Frequency analysis capability in this area could be very helpful in understanding motor/system resonance problems.

(c) Improve Program Accuracy and Capability - Further develop the HSFR Program to increase the accuracy and capability of the program for analyzing the response of more complex hydraulic circuits. This capability will be useful for identifying the severity of resonant responses relative to operating conditions in hydraulic systems of low to moderate complexity. Determination of whether simple circuit changes, narrow band attenuators, or wide-band attenuators are needed can minimize systems cost, weight, and installation impact.

(d) Pump Compensator Valve Dynamics - Incorporate pump compensator valve dynamics in the pump model to allow the system designer to study the effects of system resonances which coincide with pump mechanical resonances.

(e) Frequency Dependent Friction Effects - Evaluate frequency dependent effects; these effects may be pertinent to existing errors in amplitude predictions. Laminar flow is the most pertinent mode for steady state conditions in aircraft hydraulic systems. (Turbulent flow is the predominant operating mode for gear box lubrication and electronic equipment cooling systems.)

(2) HYTRAN Recommendations

(a) Vane Pump Model - Develop and verify a variable displacement vane pump model for fuel system applications.

(b) Axial Piston Motor - Develop and verify a model for axial piston hydraulic motors. Successful integration of a hydraulic motor into system and load dynamics is a difficult task. Dynamic analysis capability in this area could be very fruitful.

(c) Further F-15 Pump Testing and Model Development - Extensive testing has been completed on the F-15 instrumented pump. Test conditions were established to try and reproduce many of the operating conditions that the pump encounters during its normal life. Actual pump operating time was approximately 150 hours during the test period. Obviously much more data was recorded

than could possibly be compared with the pump model. Because of the importance of the pump in its relation to the remainder of the system, a disproporationate number of manhours relative to other component models was spent on pump verification. The other demands of the contract did not allow time for a more thorough analysis of the pump model and further work on the pump model is essential. Some of the transient information that was recorded still needs to be analyzed. More testing with a case pressure transducer will also yield useful information.

(d) Cavitating Pump Model - Currently no provision is made in the pump subroutine for a cavitating pump. The development and verification of a model for HYTRAN, would be useful for suction system analysis.

(e) Reservoir Level Sensing Modification to the Reservoir Subroutine- F-15 and F-18 military aircraft use reservoir level sensing equipment. This function should be modeled and verified as part of the reservoir subroutine.

(f) Lossless Line Model - Experience on F-18 analysis has indicated a need for modeling two adjacent components without a line between them. A lossless line model should be developed for this application.

(g) Bulk Modulus Updated in the Line Subroutine - The bulk modulus is not entirely accurate in a transient simulation. Changes are necessary so that the values of bulk modulus can be updated based on the local fluid pressure in a line.

(3) SSFAN Recommendations

(a) Flow Regulator Model - In hydraulic system design it is necessary to size restrictors based on rate information. Develop a flow regulator model that would keep the flow in a leg constant while automatically computing the proper orifice size.

(b) Verify SSFAN at Low Temperature - Verification testing on the SSFAN program has been accomplished from 70 to 210°F. Operation rates at low temperature are often the critical factors determining a system configuration. Verification testing from -40°F to 70°F is recommended to further enhance the capabilities of the SSFAN program.

(c) SSFAN Quasi-Transient Model - Since SSFAN calculates the steady state flows and pressures of a system at a point in time, write a control program that will calculate a series of points starting at a fixed time and continuing for a long time period (10-20 seconds). This quasi-transient control program would integrate the system loads, actuator and accumulator pressures between the two time steps. The resultant solutions are based on the average flows in the system. Examples of data that may be derived from this addition are operating times for landing gear and flap subsystems, time to charge system accumulators on engine start-up and time to discharge the system accumulators.

(d) Single Node Constant Pressure Reservoir Model - The SSFAN program was written to solve closed loop hydraulic systems. Add a special component model to run open loop systems for subsystem work.

(e) Simplify the Building Routines - The building routines are complicated. Systems are assembled pressure side first followed by return then suction system. Simplification of the building routines are necessary to obtain a more efficient assembly method and reduce execution time and costs. The techniques could be applied to HYTRAN and HYTTHA.

(f) Complex Hydraulic System Analysis - The SSFAN program is capable of simulating many types of hydraulic systems. Every possible assembly combination of components in systems has not been verified and indeed the scope of the contract did not allow for such an effort. Consequently the programmer may run into situations in which the assembly phase may not function properly or the computation section of the program gives erroneous results. More effort is required to accommodate various types of systems.

(g) Floating Branch Point Model - Add a floating branch point, so the programmer can find the pressure at any location in the system.

(h) Constant Displacement Pump Model - Develop a constant displacement pump model. This may be constant flow type or constant pressure type. Versions may be written for closed and open loop applications.

(i) Pressure Regulator Model - Develop a pressure regulator model that would hold a constant pressure selected point anywhere in the system. This would be a two-port device different from the constant reservoir model.

(j) Hydraulic Motor Model - A hydraulic motor model to input load torque vs RPM should be developed.

(k) Modify the Special Component Model - Change the special element subroutine so that it will allow a single point input. A square law curve fit would then be used with the one data point. Currently this input allows for a minimum of two data points.

(l) Dynamic Cross Model - Develop dynamic cross model accounting for energy losses due to flow mixing.

(4) HYTTHA Recommendations

(a) Further HYTTHA Development and Verification - The HYTTHA computer program is used to calculate the transient thermal response of a hydraulic system. Detailed input data is needed to establish steady state pressure and flow rates to determine initial system temperatures. The interaction between components in a system and their environment represent a complex phenomena that in many instances is difficult to measure even in a controlled laboratory. The current version of HYTTHA may be applied to simple hydraulic systems with reasonable results. Larger more complex systems present many problems that are tedious and difficult to solve. HYTTHA was written to solve these problems but because of the intricate nature of temperature phenomena and lack of development, further work on the program is needed.

b. Recommended Development of a Hydraulic System Line Mechanical Response (HLMR) Computer Program - Hydraulic line vibrations due to exitation from pulsations generated by axial-type pumps can create serious problems in aircraft hydraulic system installations. During the transient test program excessive longitudinal vibrations were encountered in the laboratory that interfered with the data. The problem was solved by correctly clamping and weighing down the lines wherever necessary. An understanding of the behavior of the internal and external responses of the hydraulic system will lead to optimum, infinite fatigue life, configurations with minimum system weight. MCAIR has already undertaken the development of a computer program which will predict the mechanical response of a hydraulic line installation to pulsating external or internal forcing functions. The hydraulic system line mechanical response program (HLMR) needs to be further developed and verified before useful design data can be obtained.

c. Verification of Existing Programs on a Complete Aircraft Hydraulic System - The present computer programs should be applied to more complex aircraft hydraulic systems such as the F-15 with RLS, RPS and an intricate switching valve system. It is recommended that the programs be verified on a representative aircraft hydraulic system. Modeling specific subsystems and solving design problems yield information not obtained from general verification work. The modeling of a complete aircraft will greatly improve the capability of the computer programs.

d. Recommended Computer Program Development and Application - The existing computer program component models could be modified for fuel system applications. Similar changes could be made to make the programs capable for analyzing electronic equipment liquid loop heat transfer systems and lubrication systems.

e. Recommended Program User Experience Feedback and Interchange to be Implemented Through the APL - User test data should be employed for additional assessments of program correlation to reveal unidentified shortcomings and identify the areas of future work. This will continually improve and accelerate the development of the programs and help others in becoming more familiar with their application. Getting more people involved will further verify the programs and make them more useful in design and analytic studies.

f. Recommended Hardware Development Programs

(1) Wide-band Acoustic Attenuator - Design and develop small, low-cost, high-performance wide-band acoustic attenuators for aircraft hydraulic systems. The acoustic complexity of some aircraft hydraulic systems, line mechanical response, multiple pump operating speeds, and temperature shift effects render conventional narrow band techniques of questionable value. Application of wide-band attenuators is sometimes the cost effective approach for solving pulsation problems in acoustically complex systems. The HSFR Program would be used as a tool for designing and sizing the wide-band acoustic attenuators.

(2) Harmonic Free Hydraulic Pulsation Generator - Develop a harmonic-free hydraulic acoustic signal generator for general use in the industry. The power level and frequency range capability should be that normally encountered in aircraft hydraulic systems. Such a device would be useful for running qualification fatigue tests on equipment normally exposed to pulsating pressures or for model verification tests, and for checking the frequency response of hydraulic circuits.

(3) Dynamic Flow Measurement - Further develop dynamic flow measurement technology to permit accurate component level HSFR model verification. Accurate modeling of some components, e.g. filters and hoses, may depend on improved flow measurement technology.

(4) Pump Modifications to Reduce Acoustic Energy - Reduction of acoustic source energy by techniques integral to the hydraulic pump would reduce many hydraulic system dynamic problems at their source.

g. Recommended Military Specification Revisions and Additions

(1) MIL-P-1969C Hydraulic Pump Spec Modification - The MIL-P-19692C hydraulic pump specification pressure pulsation test data may be improved as follows:

1) It is imperative that the buyer specify the test hydraulic circuit to be as similar to the real system as possible.

2) Use a total pressure pulsation (peak or peak to peak) vs. pump speed data format during the specified speed sweep (50 to 125%) with 5% of maximum full flow to easily and accurately identify the most critical resonant speeds in the simulated hydraulic system.

3) Record 2) data long the line every 8 inches from the pump to identify a location in the line of the maximum standing wave pressure at each identified resonant speed.

4) Make measurement rpm sweeps over the full speed range at line locations identified for maximum resonant pressures rather than at the present arbitrarily specified 50, 75, and 100% speeds.

5) Apply the acceptance criteria to the maximum measured standing wave value at each resonant speed within the operating speed range.

6) Change acceptable pulsation level from $\pm$ 10% to $\pm$ 2.5% of rated outlet pressure.

(2) MIL-H-5440 General Spec Modification - The general MIL-Spec for nydraulic system performance should be modified to include analysis using the computer programs.

(3) MIL-Spec Specifying Component Data - All four computer programs require component data that is usually not readily available from the vendor. A military specification should be written that would call out the required data for each program by component. A MIL-Spec will provide the Government contractor with the information needed to routinely perform analysis of hydraulic systems. MCAIR has taken the initiative on this by requiring all F-18 vendors to supply specified computer input data for HSFR, HYTRAN, and SSFAN modeling.

h. Newtonian vs Non-Newtonian Fluid Characteristics- Component and system verification testing has been accomplished with Newtonian MIL-H-83282 and non-Newtonian MIL-H-5606B. Pump testing with the two fluids has shown significantly different heat rejection and case drain characteristics. In addition control valve leakage rates for the F-15 stabilator were not the same. The Newtonian characteristic differences between the two fluids apparently may account for most of the discrepencies. Confirmation of this assumption is subject to additional analysis and study. The results of this study would have an immediate impact on most component and system designs.

☆U.S.Government Printing Office: 1978 — 757-080/343